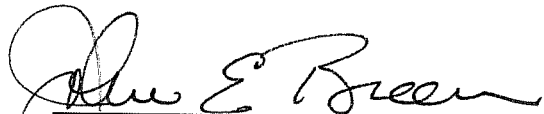



**ANCHORAGE ZONES IN POST-TENSIONED
CONCRETE STRUCTURES**

APPROVED BY

DISSERTATION COMMITTEE:




John E. Breen



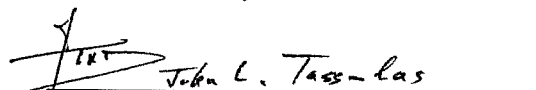
Eric B. Becker



Ned H. Burns



Michael E. Kreger



John L. Tassoulas

To Carin

**ANCHORAGE ZONES IN POST-TENSIONED
CONCRETE STRUCTURES**

by

Gregor Peter Wollmann, Dipl.-Ing., M.S.

DISSERTATION

Presented to the Faculty of the Graduate School of

The University of Texas at Austin

in Partial Fulfillment

of the Requirements

for the Degree of

DOCTOR OF PHILOSOPHY

THE UNIVERSITY OF TEXAS AT AUSTIN

May 1992

ACKNOWLEDGEMENTS

When I was approaching completion of my Master's degree here at the University of Texas at Austin some three years ago, it was with great sadness that I prepared to leave Texas. Fortunately, the encouragement of Dr. John E. Breen convinced me to enter the Ph.D. program at UT Austin, thus adding three years to a stay which was originally intended to last for only one. I have not regretted this decision. The stay in Austin and the work at the Phil M. Ferguson Laboratory was enjoyable and rewarding, not least due to the friendship of many wonderful people.

First I wish to thank my dissertation committee for their time and interest not only in my work but also in me as a person. Committee members were Drs. John E. Breen, Eric B. Becker, Ned H. Burns, Michael E. Kreger, and John L. Tassoulas. A special thank-you goes to my supervisor, Dr. Breen. His influence on me goes far beyond his technical advise. He has taught me the value of effective communication, the art of the compromise (I hope), and to keep the importance of my work in perspective. Dr. Breen will be a lasting example.

The help of the laboratory staff is gratefully acknowledged. Blake Stasney, Wayne Fontenot, Wayne Little, and Pat Ball assisted with the experimental work. Laurie Golding, Jean Gehrke, April Jenkins, and Sharon Cunningham carried me over administrative hurdles.

One of the most rewarding experiences was the interaction with so many fine fellow students from all parts of the world. They are too many to name them all, but I want to mention fellow anchorage zone researcher David Sanders. David and his wife Tina have been great friends.

I also wish to thank my American host family Fred, Carolyn, Aaron, and Ian Fasel. They made me a part of their family during many joyful activities, particularly on countless hikes through the beautiful Texas Hill Country.

I dedicate this dissertation to Carin Roberts, to thank her for all the fun and wonderful adventures we have had during the past three years.

Austin, Texas
February 1992

Gregor Wollmann

**ANCHORAGE ZONES IN POST-TENSIONED
CONCRETE STRUCTURES**

Publication No. _____

Gregor Peter Wollmann, Ph.D.
The University of Texas at Austin, 1992

Supervisor: John E. Breen

This study is the completion of a larger research project which was concerned with design and behavior of anchorage zones in post-tensioned concrete structures. Throughout the overall study a wide range of very different anchorage zone problems was investigated to create a base from which general and systematic design procedures could be derived.

The specific anchorage zone problems addressed in the present study included:

- end anchorages and the influence of reaction forces (three experimental tests);
- intermediate anchorages in blisters and ribs (eight experimental tests);
- anchorage of external tendons in diaphragms (three experimental tests).

All investigations were based on a combination of evaluation of state of the art, analytical procedures (finite element analysis and strut-and-tie models), and experimental tests. Particular emphasis was placed on the development and verification of strut-and-tie model procedures and the illustration of their use with numerous example problems. Strut-and-tie models may be considered lower bound solutions to a plastic limit load in the context of theory of plasticity. However, additional rules must be observed to arrive at useful design models. Such strut-and-tie models gave conservative predictions for the failure loads of the specimens tested in this study and in the overall study with sufficient accuracy for design. Significant conservatism was introduced by neglecting the concrete tensile strength and by the assumption of a linear-elastic stress distribution at the end of the anchorage zone even after concrete cracking.

The findings of the comprehensive investigations of this study and of its companion studies were basis for the development of general design procedures for anchorage zones in post-tensioned concrete structures and were implemented in a proposal for detailed code provisions suitable for inclusion in current AASHTO bridge specifications.

TABLE OF CONTENTS

1	INTRODUCTION	1
1.1	Anchorage Zones in Prestressed Concrete	1
1.2	Project NCHRP 10-29	2
1.3	Objectives	3
1.4	Scope	3
1.4.1	Scope of the Overall Project	3
1.4.2	Scope of this Dissertation	4
2	BACKGROUND INFORMATION	6
2.1	General	6
2.1.1	Flow of Forces in the Anchorage Zone	6
2.1.2	State of the Art	8
2.1.2.1	General	8
2.1.2.2	Literature	9
2.1.2.3	Code Provisions	13
2.1.2.4	User Survey	14
2.1.3	Anchorage Zone Problems	15
2.1.3.1	Damages and Failures	15
2.1.3.2	Unclear Responsibilities	16
2.1.3.3	Lack of Knowledge	17
2.1.4	Division into Local Zone and General Zone	17
2.1.4.1	General	17
2.1.4.2	Definitions	18
2.2	Design of the Local Zone	20
2.2.1	General	20
2.2.2	Experimental Study by Roberts	21
2.2.3	Basic Anchorage Devices	23
2.2.4	Special Anchorage Devices	24
2.3	Design of the General Zone	25

2.3.1	General	25
2.3.2	Strut-and-Tie Models	26
2.3.2.1	Introduction	26
2.3.2.2	Concrete Plasticity	27
2.3.2.3	Development of Strut-and-Tie Models	29
2.3.2.4	General Remarks	31
2.3.2.5	Experimental Studies by Sanders	32
2.3.3	Finite Element Analysis	34
2.3.3.1	Introduction	34
2.3.3.2	Analytical Study by Burdet	35
2.3.3.3	Approximate Equations	35
2.4	Multiple Slab Edge Anchorages	37
3	END ANCHORAGES AND THE INFLUENCE OF SUPPORT REACTIONS	39
3.1	Introduction	39
3.1.1	General	39
3.1.2	Objectives	39
3.1.3	Scope	39
3.2	Background Information	40
3.2.1	Literature	40
3.2.2	Companion Investigations	42
3.3	Finite Element Analysis	43
3.3.1	General	43
3.3.2	Analysis Results	45
3.3.3	Discussion	46
3.4	Development of Strut-and-Tie Models	47
3.4.1	General	47
3.4.2	Extent of the D-Region	48
3.4.3	Boundary Conditions	48
3.4.4	Location of the Bursting Tie	50
3.4.5	The Local Zone Node	51

3.4.5.1	General	51
3.4.5.2	Non-Hydrostatic Local Zone Node	52
3.4.5.3	Fan-Shaped Struts at the Local Zone Node	54
3.4.6	Member Capacities	55
3.4.7	Strut-and-Tie Model Solutions	56
3.4.7.1	Concentrically Loaded Rectangular Beam	56
3.4.7.2	Effect of a Reaction Force in the Anchorage Zone	59
3.4.8	Conclusions	62
3.5	Experimental Program	62
3.5.1	General	62
3.5.2	Materials and Fabrication	62
3.5.3	Specimen Design	64
3.5.4	Test Procedure and Measurements	65
3.6	Presentation of Test Results	68
3.6.1	Crack Development	68
3.6.2	Ultimate Loads and Failure Mode	69
3.6.3	Transvers Bursting Strains	72
3.6.4	Lateral Bursting Strains	80
3.6.5	Compressive Strains	80
3.7	Evaluation of Test Results	84
3.7.1	Finite Element Analysis Predictions	84
3.7.2	Strut-and-Tie Model Predictions	88
3.7.3	Approximate Equations	92
3.7.4	Comparison with Sanders' Test Results	93
3.7.5	Influence of a Reaction Force in the Anchorage Zone	94
3.8	Summary and Conclusions	94
3.8.1	Summary of Study	94
3.8.2	Behavior of Anchorage Zones for End Anchorages	95
3.8.3	Design Recommendations	96
3.8.4	Detailing Recommendations	97

4	INTERMEDIATE ANCHORAGES IN BLISTERS AND RIBS	99
4.1	Introduction	99
4.1.1	General	99
4.1.2	Objectives	99
4.1.3	Scope	99
4.2	Background Information	101
4.2.1	Literature	101
4.2.2	State of the Art	105
4.2.3	Typical Details	107
4.3	Slab Blisters	109
4.3.1	Introduction	109
4.3.2	Finite Element Analysis	111
4.3.2.1	Embedded Anchor	111
4.3.2.2	Isolated Slab Blister and Rib	115
4.3.2.3	Discussion	121
4.3.3	Development of Strut-and-Tie Models	123
4.3.3.1	Embedded Anchor	123
4.3.3.2	Isolated Slab Blister	124
4.3.3.3	Rib	132
4.3.4	Experimental Program	133
4.3.4.1	General	133
4.3.4.2	Specimen Design	135
4.3.4.3	Test Procedure and Measurements	143
4.3.5	Presentation of Test Results	146
4.3.5.1	Crack Development	146
4.3.5.2	Ultimate Loads and Failure Mode	148
4.3.5.3	Slab Bursting and Lateral Bending Strains	148
4.3.5.4	Blister Tie Strains	154
4.3.5.5	Strains Behind the Anchor	156
4.3.5.6	Local Bending Strains	158
4.3.6	Evaluation of Test Results	158

4.3.6.1	Finite Element Analysis Predictions	158
4.3.6.2	Strut-and-Tie Model Predictions	161
4.3.6.3	General	163
4.4	Corner Blisters	163
4.4.1	Introduction	163
4.4.2	Finite Element Analysis	163
4.4.2.1	Corner Blisters for Internal Tendons	163
4.4.2.2	Corner Blisters for External Tendons	166
4.4.2.3	Discussion	167
4.4.3	Development of Strut-and-Tie Models	170
4.4.3.1	Corner Blisters for Internal Tendons	170
4.4.3.2	Corner Blisters for External Tendons	172
4.4.4	Experimental Program	174
4.4.4.1	General	174
4.4.4.2	Design of Corner Blister Specimens With Internal Tendons	174
4.4.4.3	Design of Corner Blister Specimens With External Tendons	180
4.4.5	Presentation of Test Results	181
4.4.5.1	Crack Development	181
4.4.5.2	Ultimate Loads and Failure Mode	182
4.4.5.3	Reinforcement Strains	186
4.4.6	Evaluation of Test Results	191
4.5	Summary and Conclusions	191
4.5.1	Summary of Study	191
4.5.2	Behavior of Intermediate Anchorages in Blisters or Ribs	193
4.5.3	Design Recommendations	195
4.5.4	Detailing Recommendations	197
5	ANCHORAGE OF EXTERNAL	
	POST-TENSIONING TENDONS IN DIAPHRAGMS	199
5.1	Introduction	199
5.1.1	General	199

5.1.2	Objectives	199
5.2	Background Information	200
5.2.1	Literature	200
5.2.2	State of the Art	201
5.2.3	Typical Details	204
5.3	Finite Element Analysis	206
5.3.1	General	206
5.3.2	Analysis Results	207
5.3.3	Discussion	211
5.4	Development of Strut-and-Tie Models	211
5.4.1	General	211
5.4.2	The Tripod Model	212
5.4.3	Corbel Action	214
5.4.4	Frame Action	214
5.4.5	Extent of the D-Region	215
5.4.6	The Local Zone Node	215
5.4.7	Shear-Friction	217
5.4.8	Skew Reinforcement	218
5.4.9	Example	218
5.4.10	Discussion	226
5.5	Experimental Program	228
5.5.1	General	228
5.5.2	Specimen Design	230
5.5.3	Test Procedure and Measurements	235
5.6	Presentation of Test Results	236
5.6.1	General	236
5.6.2	Crack Development	238
5.6.3	Ultimate Loads and Failure Mode	239
5.6.4	Diaphragm Bending and Web Bursting Strains	245
5.6.5	Horizontal Bursting Strains	245
5.6.6	Flange Bursting Strains	250

5.6.7	Strains in Shear-Friction Reinforcement	251
5.6.8	Strut Bursting Reinforcement	251
5.6.9	Frame Action	251
5.6.10	Flange Compressive Strains	254
5.7	Evaluation of Test Results	255
5.7.1	Finite Element Analysis Predictions	255
5.7.2	Strut-and-Tie Model Predictions	256
5.7.3	General	257
5.8	Summary and Conclusions	258
5.8.1	Summary of Study	258
5.8.2	Behavior of Diaphragms for Anchorage of External Tendons	258
5.8.3	Design Recommendations	259
5.8.4	Detailing Recommendations	261
6	BEHAVIOR, DESIGN, AND DETAILING OF ANCHORAGE ZONES	262
6.1	Behavior of Anchorage Zones	262
6.1.1	Plain Concrete	262
6.1.2	Effect of Reinforcement	267
6.1.2.1	Confinement Reinforcement	267
6.1.2.2	Bursting Reinforcement	267
6.1.3	General	269
6.2	Design of Anchorage Zones	269
6.2.1	Limit States	269
6.2.1.1	Ultimate Limit State	269
6.2.1.2	Serviceability Limit State	271
6.2.2	Design of the Local Zone	272
6.2.2.1	Introduction	272
6.2.2.2	Basic Anchorage Devices	273
6.2.2.3	Special Anchorage Devices	274
6.2.2.4	Responsibilities	275
6.2.3	Design of the General Zone	276

6.2.3.1	Introduction	276
6.2.3.2	Elastic Analysis	276
6.2.3.3	Strut-and-Tie Models	277
6.2.3.4	Conclusions	282
6.3	Detailing of Anchorage Zones	283
6.3.1	Local Zone	283
6.3.2	General Zone	285
6.4	Design Example	285
6.4.1	Introduction	285
6.4.2	Local Zone Design	288
6.4.3	General Zone Design	293
6.4.4	Discussion	302
7	SUMMARY AND CONCLUSIONS	303
7.1	Summary of Overall Study	303
7.2	Local Zone and General Zone Concept	304
7.3	Use of Strut-and-Tie-Models for the Design of Anchorage Zones	305
7.4	Conclusions	306
7.4.1	General Conclusions	306
7.4.2	End Anchorages and the Influence of Support Reactions	308
7.4.3	Intermediate Anchorages in Blisters and Ribs	309
7.4.4	Diaphragms for the Anchorage of External Tendons	310
7.5	Proposed Anchorage Zone Specifications	311
7.5.1	General	311
7.5.2	Load and Resistance Factors	312
7.5.3	Definition of the Anchorage Zone Geometry	312
7.5.4	Responsibilities	312
7.5.5	Design of the General Zone	313
7.5.6	Design of the Local Zone	313
7.5.7	Special Anchorage Device Acceptance Test	313
7.6	Recommendations for Further Research	313

7.6.1	Variability of Concrete Strength	313
7.6.2	Local Zone-General Zone Interaction	314
7.6.3	Extent of Cracking in the Anchorage Zone	314
7.6.4	Effective Concrete Strength for Strut-and-Tie Models	314
7.6.5	Development of Interactive Design Programs for D-Regions	314
APPENDIX A	Proposed Post-Tensioned Anchorage Zone Provisions for Inclusion in the AASHTO Bridge Specifications	316
APPENDIX B	Commentary to the Proposed Anchorage Zone Specifications	339
REFERENCES	366

1 INTRODUCTION

1.1 Anchorage Zones in Prestressed Concrete

The performance of concrete structures can be dramatically improved by imposing a self-equilibrating state of stress that partially offsets the stresses due to external loads. This "prestressing" of the structure permits the construction of longer, more slender girders, allows better control of deflections, and delays cracking of the concrete. Because of these advantages, prestressed concrete has become a very popular construction material throughout the world.

Prestressing of concrete requires the introduction of large, concentrated tendon forces into the member. The dispersion of this tendon force induces tensile stresses over some distance ahead of and behind the anchorage. The region affected by the introduction of the tendon force is called the "**anchorage zone**". In pretensioned concrete structures the transfer of forces from the tendon onto the concrete occurs through bond stresses over the transfer length of the prestressing steel and is gradual. In post-tensioned concrete anchorage hardware is used and the transfer of the tendon force is very localized, causing high compressive stresses immediately ahead of the anchorage device and substantial tensile stresses normal to the tendon axis further ahead in the anchorage zone. Frequently, proprietary anchorage devices are used for anchorage of post-tensioning tendons which employ local confinement reinforcement to achieve higher bearing pressures than normally accepted for concrete. Use of such anchorage devices should be based on acceptance tests which have to prove that such high bearing pressures do not cause serviceability problems and that the anchor is capable of developing the full tendon force.

Pretensioned concrete has been used extensively in North America. Due to the repetitive, industrialized production of pretensioned concrete components, manufacturers are very experienced with this type of structure. In contrast, the use of post-tensioned concrete puts high demands on designer, anchorage device supplier, and constructor due to its greater versatility and the more concentrated stresses in the anchorage zone. Yet, there is a lack of general guidelines for the design of anchorage zones in post-tensioned concrete structures. Considerable confusion exists about the responsibilities of designer, anchorage device supplier, and constructor [44]. This has led to a wide range of problems.

At one extreme is the total absence of anchorage zone reinforcement, due to ignorance of the necessity for anchorage zone design or due to reliance on the other parties involved. At the other extreme are highly congested anchorage zone details resulting in poor concrete placement and compaction around the anchorage device. These problems have resulted in a number of actual failures and substantial delays and litigation [44].

A large number of studies of anchorage zone behavior and design have been conducted over more than 40 years, yet this abundance of information seems to have contributed to the confusion rather than alleviating it. While research has focused on a narrow range of special and often very idealized problems, the versatility of post-tensioned concrete requires a general and systematic procedure for anchorage zone design. Current US code provisions were developed with a very special application in mind and are not adequate to cover the wide range of anchorage zone problems encountered in modern post-tensioned concrete construction.

1.2 NCHRP Project 10-29

In recognition of the problems in the design of anchorage zones for post-tensioned concrete structures, the National Cooperative Highway Research Program (NCHRP) initiated Project 10-29 "Anchorage Zone Reinforcement for Post-Tensioned Concrete Girders" in 1986. The main objective of this five year program is to "develop design procedures for end and intermediate anchorage zones for post-tensioned girders and slabs" [6].

The project comprises two phases. Phase A is completed and included the following tasks:

- 1) A comprehensive literature review, user survey, and evaluation of the current state of the art [44];
- 2) An experimental study of the behavior of the region immediately surrounding the anchorage device [41];
- 3) An experimental study of anchorage zones at the end of members with various tendon configurations [44];
- 4) Linear-elastic 2D and 3D finite element analyses of basic anchorage zone problems [8].

This dissertation is part of Phase B which extends the study to include anchorage zone problems with more complicated geometries and to explore the use of non-linear finite element analyses. Phase B includes the following tasks:

- 1) Experimental study of multiple slab anchorages [17];
- 2) Experimental and analytical study of end anchors and the effect of reaction forces;
- 3) Experimental and analytical study of intermediate anchorages in blisters and ribs;
- 4) Experimental and analytical study of the anchorage of external tendons in diaphragms;
- 5) Exploration of the use of non-linear finite element analyses [25].

1.3 Objectives

The main objectives of the project are:

- 1) to develop general and systematic design procedures for anchorage zones in post-tensioned concrete;
- 2) to develop performance criteria and test procedures for the acceptance of anchorage devices;
- 3) to develop design and construction specifications for anchorage zones, including commentary, suitable for inclusion in the current AASHTO specifications [1].

1.4 Scope

1.4.1 *Scope of the Overall Project*

The approach taken to accomplish the ambitious and broad objectives of the overall project is based on a synthesis of

- 1) evaluation of existing literature, current state of the art, and industry input,
- 2) analyses of various anchorage zone problems at service load and ultimate load levels,
- 3) experimental investigations.

It was decided to minimize the number of repetitions of tests in the experimental program in favor of studying a larger number of different anchorage zone problems. The physical tests were not designed for the development of empirical expressions, but rather to supplement the information obtained from the analysis and from the review of the state-of-the-art portions of the project. All three approaches are equally important for the

accomplishment of the final objective of developing general design guidelines for anchorage zones.

The range of post-tensioned concrete applications is very large and many special anchorage zone problems were excluded from this study, for example problems associated with tendon coupling joints in post-tensioned construction [49] or splayed or looped dead end anchorages. The study is limited to post-tensioned concrete applications, although many of the findings could be adapted for pretensioned concrete. Despite these restrictions, the guidelines developed as a result of this project can be extended to most anchorage zone problems.

1.4.2 *Scope of this Dissertation*

This dissertation covers the investigation of end anchors and the effect of reaction forces (Chapter 3), intermediate anchorages in blisters and ribs (Chapter 4), and anchorage of external tendons in diaphragms (Chapter 5). The study of each of these problems includes:

- 1) Review of literature and state of the art;
- 2) Limited finite element analysis, to obtain information on the flow of forces prior to cracking and to identify critical regions in the anchorage zone;
- 3) Development of equilibrium based design models (strut-and-tie models);
- 4) A small series of verification test specimens;
- 5) Design and detailing recommendations.

Prior to the discussion of these special anchorage zone problems, Chapter 2 reviews two concepts which are the key to the development of general and systematic guidelines for anchorage zone design:

- 1) Division of the anchorage zone into a local zone and a general zone.
- 2) Equilibrium based design of concrete structures and strut-and-tie models.

Chapter 2 also includes a brief summary of the literature review conducted by Sanders [44] and of the companion investigation of multiple slab anchors by Falconer [17].

Chapter 6 is the conclusion of the overall project. Here the findings from all phases of the study are tied together to develop a general approach to anchorage zone design. It includes a discussion of the general behavior of anchorage zones, the development of a

consistent safety approach including load and resistance factors, a guideline for design, detailing recommendations, and a design example.

Chapter 7 presents a brief summary of the overall study and of the most important conclusions.

A proposal for post-tensioned anchorage zone provisions and a commentary, suitable for inclusion in the AASHTO bridge specifications, are included in Appendices A and B, respectively. These provisions are the outgrowth of the efforts of John E.Breen, Olivier L.Burdet, Carin L.Roberts, David H.Sanders, and Gregor P.Wollmann. They have been subjected to considerable industry and technical association review and comment.

2 BACKGROUND INFORMATION

2.1 General

2.1.1 Flow of Forces in the Anchorage Zone

The concentrated prestressing force is transferred through anchorage hardware from the tendon onto the concrete and then spreads out to reach a more nearly linear stress distribution over the cross section of the member at some distance from the anchor. Figure 2.1a illustrates this flow of forces for the case of a concentric end anchor. As the compressive stresses spread out, they have to deviate from the direction parallel to the load. This induces lateral compressive stresses immediately ahead of the anchor and then lateral tensile stresses which eventually diminish (Figure 2.1b). These lateral tensile stresses are usually referred to as "bursting stresses". The interaction between the deviation of the longitudinal compressive stresses and the lateral stresses can be readily visualized by the strut-and-tie model shown in Figure 2.1c.

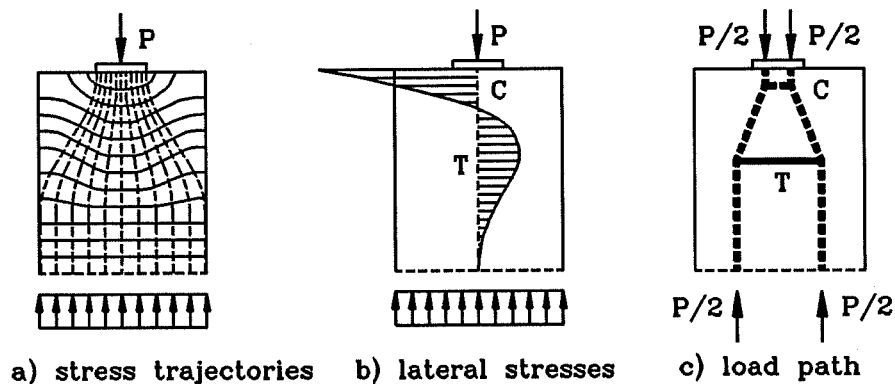


Figure 2.1 Flow of Forces in Concentrically Loaded Anchorage Zone (after [45])

Figure 2.2 shows contour plots for the principal tensile and compressive stresses for the same anchorage zone problem. Three critical regions can be identified:

- 1) The region immediately ahead of the load is subject to large bearing and compressive stresses.
- 2) The bursting zone extends over some distance ahead of the anchorage and is subject to lateral tensile stresses.
- 3) Very local tensile stress concentrations exist along the loaded edge of the member.

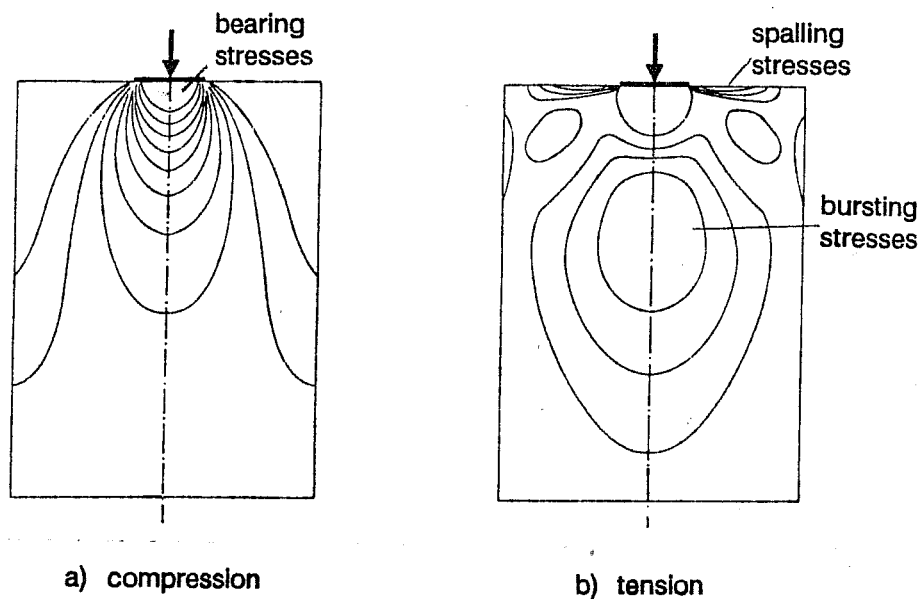


Figure 2.2 Stress Contours for Concentrically Loaded Anchorage Zone

The tensile stresses along the loaded edge have become known as "**spalling stresses**", despite the fact that they do not cause any spalling of the concrete.

At some distance away from the anchor, the longitudinal stresses on the cross section can be determined based on the assumption of a linear strain distribution over the cross section. On sections located closer than this distance the strain distribution is disturbed by the introduction of the concentrated anchorage force. The region affected by this disturbance is the "**anchorage zone**". The extent of this region is limited, as expressed by the **Principle of Saint-Venant**. In the formulation by Timoshenko [54] this principle states, that

if the forces acting on a small portion of the surface of an elastic body are replaced by another statically equivalent system of forces acting on the same portion of the surface, this redistribution of loading produces substantial changes locally but has a negligible effect on the stresses which are large in comparison with the linear dimensions of the surface on which the forces are changed.

For practical purposes the extent of the anchorage zone can be taken as equal to the largest cross sectional dimension of the girder [45](Figure 2.3). Timoshenko shows this approach to be correct within $\pm 3\%$ for the axial stresses at a distance equal to one beam

height ahead of a concentrated, concentric force acting on a rectangular member [54].

As indicated in Figure 2.2a, the magnitude of the compressive stresses is highest immediately ahead of the anchor, but decreases rapidly as the compression stresses spread out into the structure. For this reason, proprietary special anchorage devices are frequently used. They enhance the local compressive strength by some form of confinement and/or reduce the bearing pressure by distributing the anchorage force over a series of bearing plates or ribs (Figure 2.4). In many European countries the acceptance of such special anchorage devices is based on standardized acceptance tests [20, 41].

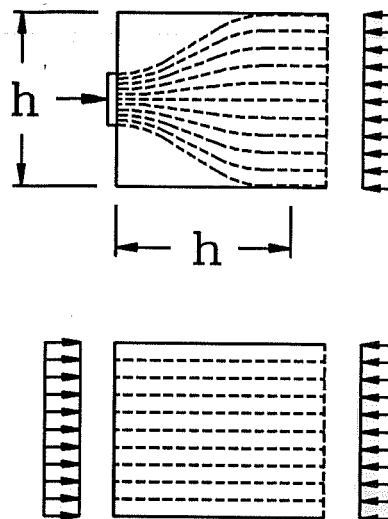


Fig. 2.3 Principle of Saint Vénant

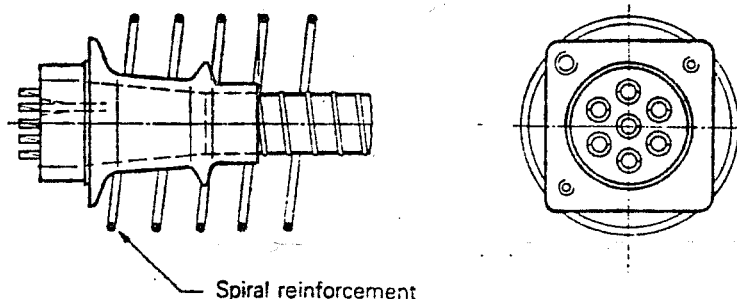


Figure 2.4 Special Anchorage Device (from [55])

2.1.2 State of the Art

2.1.2.1 General

Sanders (Reference 44) conducted a very comprehensive review of the state of the art of anchorage zone design which included a review of technical literature, product information, and current code provisions, as well as an industry wide user survey. Only a

brief summary of this review will be given here. More information can be found in References 6 and 44.

2.1.2.2 Literature

The problems associated with the introduction of concentrated loads into a structure have been studied for almost 70 years. In 1924 Mörsch introduced an equilibrium based model to visualize the load path in concentrically loaded members (Figure 2.5)[36]. Since then a large number of studies on anchorage zone problems have been conducted.

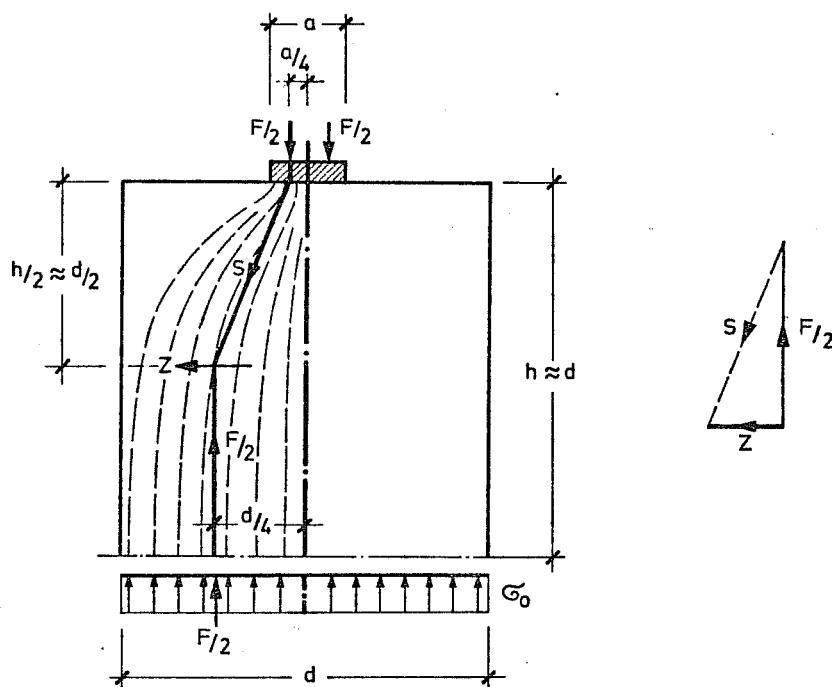


Figure 2.5 Mörsch's Load Path Model (from [29])

They include linear elastic studies, such as theory of elasticity, finite element analyses, and photoelastic investigations, nonlinear analyses, and experimental studies.

A classic solution based on theory of elasticity was presented by Guyon in 1953 and is still widely used today [22]. He determined the bursting stress distribution ahead of a concentric end anchor for different ratios of plate width to member width (Figure 2.6). Figure 2.7 shows the magnitude of the integrated bursting stresses and a comparison to

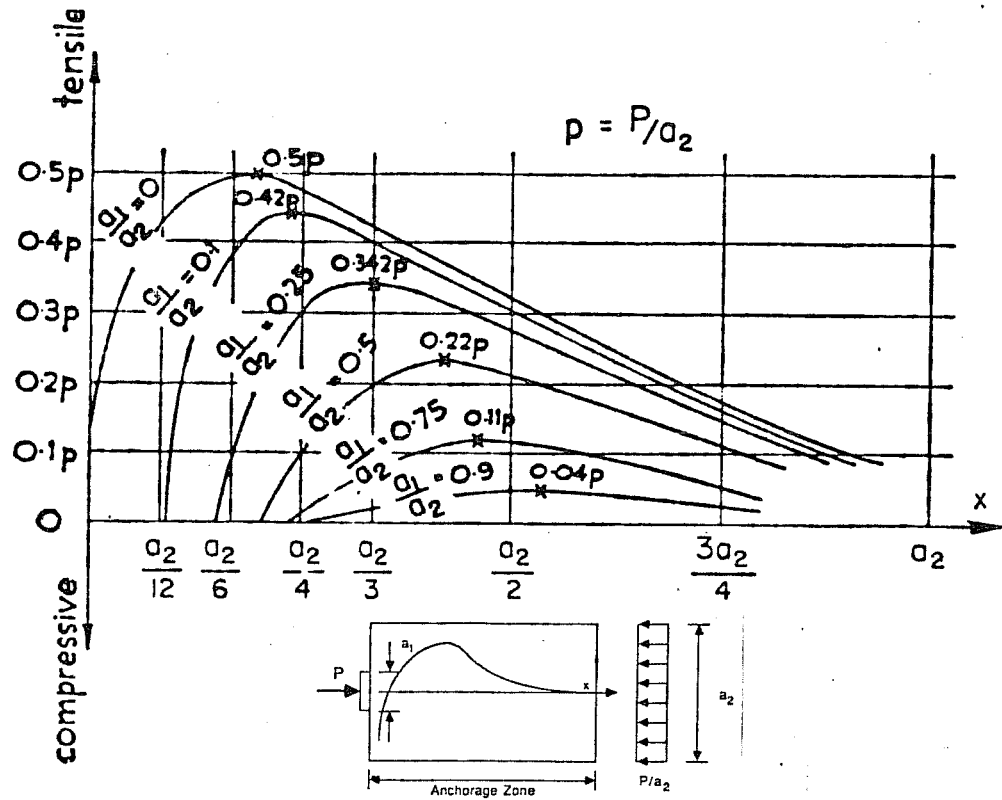


Figure 2.6 Guyon's Solution for the Bursting Stresses in Concentrically Loaded Anchorage Zones (from [22])

the bursting force obtained from Mörsh's simple truss solution. The agreement is remarkably good and many codes use some variation of Mörsh's equation even today. Guyon extended the application of his solution to eccentrically loaded anchorage zones by introducing the "symmetrical prism" approach (Figure 2.8).

A large number of linear elastic studies were conducted, all of which essentially confirm Guyon's solution, including the symmetrical prism approach. But they also revealed some of its limitations. For example:

- 1) Spalling stresses, which occur along the loaded edge in concentrically and eccentrically loaded anchorage zones and between multiple anchors, are not predicted.

- 2) Guyon's solution is only valid for members with rectangular cross section. The bursting force in I-sections, for example, is larger than that in beams with rectangular cross section.

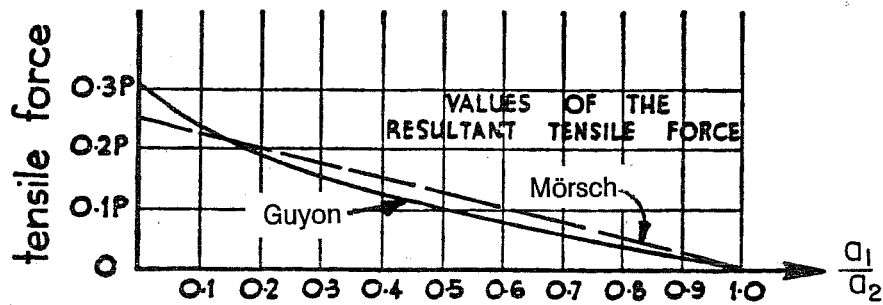


Figure 2.7 Magnitude of Bursting Force (adapted from [22])

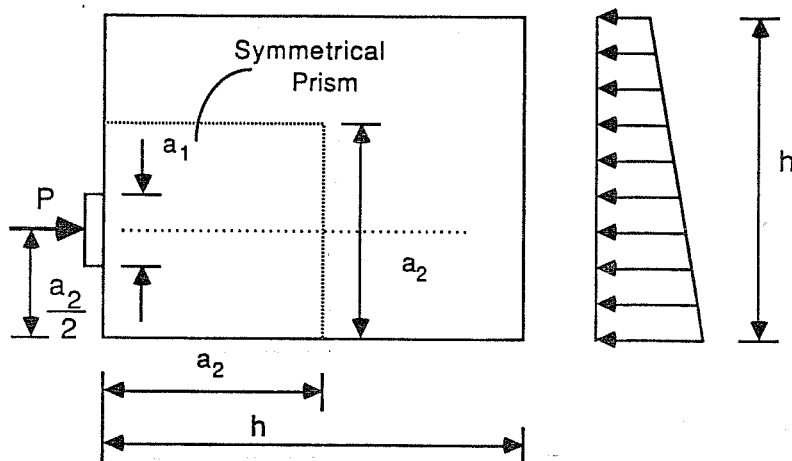


Figure 2.8 Guyon's Symmetrical Prism (from [6])

Adeghe and Collins conducted a nonlinear finite element study and pointed out, that a significant redistribution of stresses takes place after cracks have developed in the anchorage zone [4]. This redistribution causes the compressive stresses in the anchorage zone to spread out more slowly (Figure 2.9). Fenwick and Lee made the same observation in an experimental study and pointed out that the redistribution of stresses tends to reduce

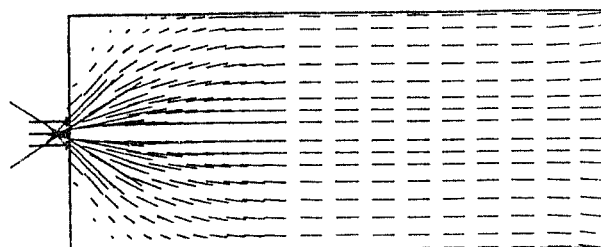
the bursting force [18]. They also confirmed the increase of the bursting force in members with I-sections.

Other experimental studies dealt with the effect of increasing tendon inclination and eccentricity, which tend to increase the tensile force along the loaded edge of the member. Guyon's symmetrical prism approach is found to be useful and safe for the determination of the bursting force within its range of applicability in many of these investigations.

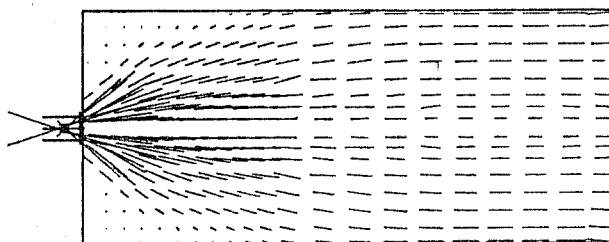
Stone and Breen conducted a comprehensive experimental and analytical study of single anchorages in

thin web members, which is frequently quoted by users and researchers [51, 52]. They developed empirical equations for cracking and ultimate load predictions, which take into account type of anchor, tendon eccentricity, tendon inclination, anchor plate size, section thickness, concrete strength, and type and amount of supplemental reinforcement (spiral, orthogonal reinforcement, lateral post-tensioning). The major difficulty with their recommendations appears to be that they are very conservative and are limited to anchorage zone problems not too different from those of their study.

A number of experimental studies were concerned with the bearing strength of concrete. The equations generally used today assume the bearing strength of concrete to be proportional to the cylinder strength and to the square root of the ratio of the supported area to the loaded area, where the supported area is geometrically similar to and concentric with the loaded area. The square root relationship was proposed by **Komendant** in 1952 and again by **Middendorf** in 1960. They based their recommendations on a large number



a) Compressive Stress Flow, Linear Elastic Analysis



b) Compressive Stress Flow, Nonlinear Analysis

Figure 2.9 Redistribution of Stresses after Cracking (from [4])

of tests on unreinforced concrete blocks and cylinders [41]. Figure 2.10 illustrates the definition of the supported area and shows Middendorf's proposal for the allowable bearing pressure.

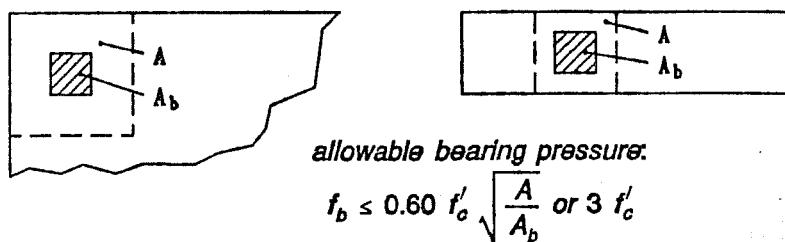


Figure 2.10 Middendorf's Bearing Pressure Equation (adapted from [41])

Hawkins conducted a study on the influence of the stiffness of the bearing plate [41]. Increase in thickness of the bearing plate increased the capacity of his specimens. However, beyond a certain thickness the bearing plate acted as a rigid plate and further increase in thickness was not effective.

2.1.2.3 Code Provisions

Current code provisions generally are concerned with limiting the bearing stress ahead of the anchorage, with the determination of the bursting force, and with arrangement of the bursting reinforcement. Some codes include provisions for spalling forces [44].

Limits on the bearing pressure generally are very similar to the equation recommended by Middendorf, with some variation on the multiplication factor and the maximum allowable bearing strength. One exception is the current **AASHTO** code, which prescribes a flat bearing stress limit of $0.9f'_c$, but not more than 3000 psi after seating of the tendon [1]. In the guide specifications by the **Post-Tensioning Institute** the following allowable bearing pressure limitations are recommended [38]:

$$\begin{aligned}
 \text{at stressing } f_b &\leq 0.8 f'_c \sqrt{A/A_b - 0.2} \quad \text{or } 1.25f'_c \\
 \text{after seating } f_b &\leq 0.6 f'_c \sqrt{A/A_b} \quad \text{or } 1.25f'_c
 \end{aligned}
 \tag{2.1}$$

These equations were adopted in the 1991 AASHTO interim specifications. In Europe many codes include provisions for special anchorage devices which are not subject to bearing pressure limitations, but have to pass a standardized acceptance test.

Determination of the bursting force is generally based on some variation of Morsch's expression or Guyon's solution for the concentrically loaded anchorage zone. Usually provisions for arrangement of the bursting reinforcement are also included. AASHTO does not give any recommendations on the determination of the bursting force, but requires a grid of horizontal and vertical reinforcement placed less than 1½ in. from the anchor bearing plate "to resist bursting stresses" [1]. The effectiveness of this reinforcement arrangement for the purpose of resisting bursting stresses must be questioned. Bursting stresses usually are critical significantly further ahead of the anchorage device than 1½ in. Probably this grid is intended to enhance the bearing strength of the concrete immediately ahead of the anchor. However, for this purpose spiral confinement reinforcement is more effective. This is reflected by the design codes used in Florida and North Carolina, which require the use of spirals and explicitly exclude the use of grids [44].

2.1.2.4 User Survey

Sanders [44] conducted an industry wide survey to obtain information on

- 1) commonly used anchorage zone configurations and reinforcing details,
- 2) problems encountered in design or checking of anchorage zones,
- 3) analysis procedures and references used,
- 4) specific failures or severe distress.

A questionnaire was sent out to researchers, designers, and to all bridge division members of AASHTO. Some of the conclusions of the survey results are listed below [44].

- 1) The reference and design methods most frequently used include the PTI recommendations [38], Guyon's symmetrical stress block [22], and recommendations by Leonhardt [28].

- 2) The empirical equations by Stone and Breen often are very conservative and require too much reinforcement and a very high concrete strength before stressing. This leads to congestion of the anchorage zone and slows down casting cycles.
- 3) The AASHTO provisions are either overconservative or non-existent. The grid of horizontal and vertical reinforcement close to the anchors is not effective, but leads to congestion and concrete consolidation problems.
- 4) A spiral is much more effective than the orthogonal reinforcement grid required by AASHTO. The spiral should be large enough to enclose the entire anchor bearing plate and its length should be at least one and one-half times the diameter of the spiral or twice the width of the bearing plate. One responder reported problems with concrete placement and consolidation with the typical spiral pitch of 1 in. to 1½ in. and recommended a spiral pitch of 2½ in. to 3½ in.
- 5) Congestion of reinforcement is a serious problem. Poor concrete consolidation due to congestion was the direct reason for a number of anchorage zone failures.

2.1.3 *Anchorage Zone Problems*

2.1.3.1 Damages and Failures

Most damages to anchorage zones in post-tensioned concrete structures occur during construction, when large tendon stressing forces are applied to usually very immature concrete. However, Libby describes an anchorage zone failure of a post-tensioned roof slab after five years of service [30]. He attributed the failure to the combined effect of anchorage zone stresses and cyclic flexural tensile stresses at a slab-column joint in close proximity to the anchorage.

Reinforcement congestion in the anchorage zone is a frequent cause for poor concrete consolidation, resulting in failures due to crushing of the concrete ahead of the anchor [31]. Congested anchorage zone details also complicate placing of the reinforcement. A respondent to Sanders' survey pointed out that special attention must be paid to placing confining spiral reinforcement coaxially with the tendon.

Another frequent problem in anchorage zones is cracking of the concrete, particularly along the tendon path. However, such cracking does not necessarily imply a structural deficiency. In fact, due to the presence of tensile stresses in the anchorage zone a limited amount of cracking should be expected. That makes it all the more necessary to

provide well detailed anchorage zone reinforcement to control cracking and to inhibit potential corrosion problems. A popular detail for anchorage zones in slabs does not provide any bursting reinforcement in the slab thickness direction and therefore relies completely on the concrete tensile strength (Figure 2.11). This may be acceptable for single, widely spaced strands in thin slabs, but problems are common for closely spaced anchors and anchors close to the side edge of the slab. Macchi describes explosive failures due to splitting of the slab, where closely spaced tendons caused large bursting stresses and at the same time created a weak plane in the slab [32].

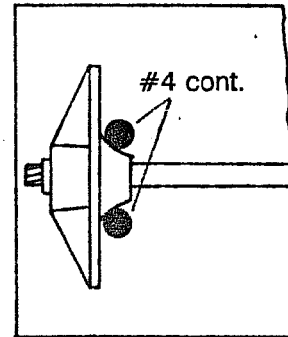


Figure 2.11 Typical Slab Anchorage Detail

Figure 2.12 shows how "unstressed corners" may cause severe cracking or even spalling. This does not affect the introduction of the tendon force into the structure, but certainly is unsightly and may also lead to corrosion problems. Other anchorage zone problems due to the effects of tendon curvature were reported, particularly where kinked tendons cause a concentrated deviation force [39, 56].

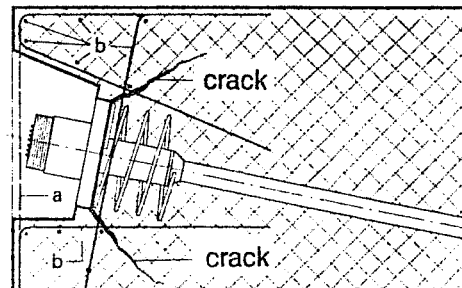


Figure 2.12 Unstressed Corner Cracking (from [24])

2.1.3.2 Unclear Responsibilities

In US practice contract drawings frequently do not include complete post-tensioning details. Rather, the contractor is expected to determine size, number, and location of the anchorage devices and to provide details for the anchorage zone [30]. The contractor in turn relies heavily on the anchorage device supplier to furnish the necessary information. This procedure has led to considerable confusion about the responsibilities of engineer of record, anchorage device supplier and constructor. This is not limited to the

design of the anchorage zone, but also includes confusion about who should furnish and pay for the anchorage zone reinforcement.

Another problem arising as a consequence of this method of practice is pointed out by Libby [30]. The contract drawings do not show anchorage zone details, while the shop drawings for the anchorage zone prepared by the constructor show anchorage details only, but none of the other reinforcement in the same region. This practice leaves congestion of the anchorage zone undetected, as well as physical conflicts between ordinary reinforcement, anchorage zone reinforcement, and tendon hardware. Often field changes are required to make reinforcement placement possible at all. Congestion of the anchorage zone is one of the major reasons for poor concrete consolidation and subsequent failures.

2.1.3.3 Lack of Knowledge

A wide range of technical literature on behavior and design of anchorage zones has been published. However, available information is limited to special applications and apparently lacks the generality required to address the wide variety of anchorage zone problems encountered in innovative post-tensioned concrete applications. Current AASHTO provisions were obviously developed with I-girders in mind and are very vague. The little specific guidance given in AASHTO is not applicable for a wide range of anchorage zone problems.

Another problem is the fact that education in the United States has not kept up with the dramatic increase in the use of prestressed concrete. Breen points out that many US universities do not offer prestressed concrete courses or limit access to graduate students [7], despite the fact that today 75% of new concrete bridges and 75% of new parking structures are built with prestressed concrete [7, 10].

2.1.4 *Local Zone and General Zone*

2.1.4.1 General

The main concerns in anchorage zone design are the high compressive stresses immediately ahead of the anchorage device and the tensile stresses in the remainder of the anchorage zone. Breen, et al. proposed to consider the anchorage zone as composed of two regions (Figure 2.13)[6]: The region of very high compressive stresses immediately ahead of the anchorage device is the **local zone**, and the region subjected to tensile

stresses due to spreading of the concentrated tendon force into the structure is the **general zone**.

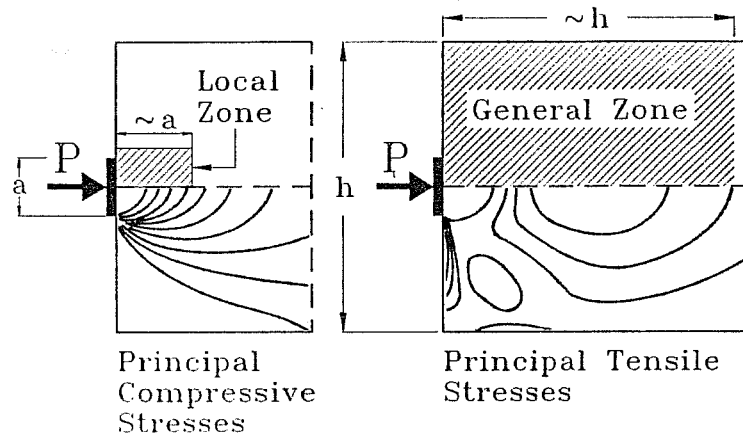


Figure 2.13 Local Zone and General Zone

This approach allows one to clearly delineate the responsibilities for the design of the anchorage zone. The main considerations in local zone design are the effects of the high bearing pressure and the adequacy of any confinement reinforcement provided to increase the bearing strength. Design of this region should be the primary responsibility of the anchorage device supplier. On the other hand, the main consideration in general zone design is to determine and provide for the flow of forces as the concentrated tendon force spreads into the structure. This includes the design of adequate reinforcement to resist tensile forces in the anchorage zone and to control cracking, and the check of compressive stresses at the interface with the local zone and at loading or geometry discontinuities. Design of the general zone should be the primary responsibility of the engineer of record.

2.1.4.2 Definitions

The division of the anchorage zone into a local zone and a general zone is a very useful concept to identify the different concerns in anchorage zone design. In order to develop code-language specifications it is essential to provide rather precise definitions. For this purpose it is more convenient to define local zone and general zone geometrically rather than by stress levels.

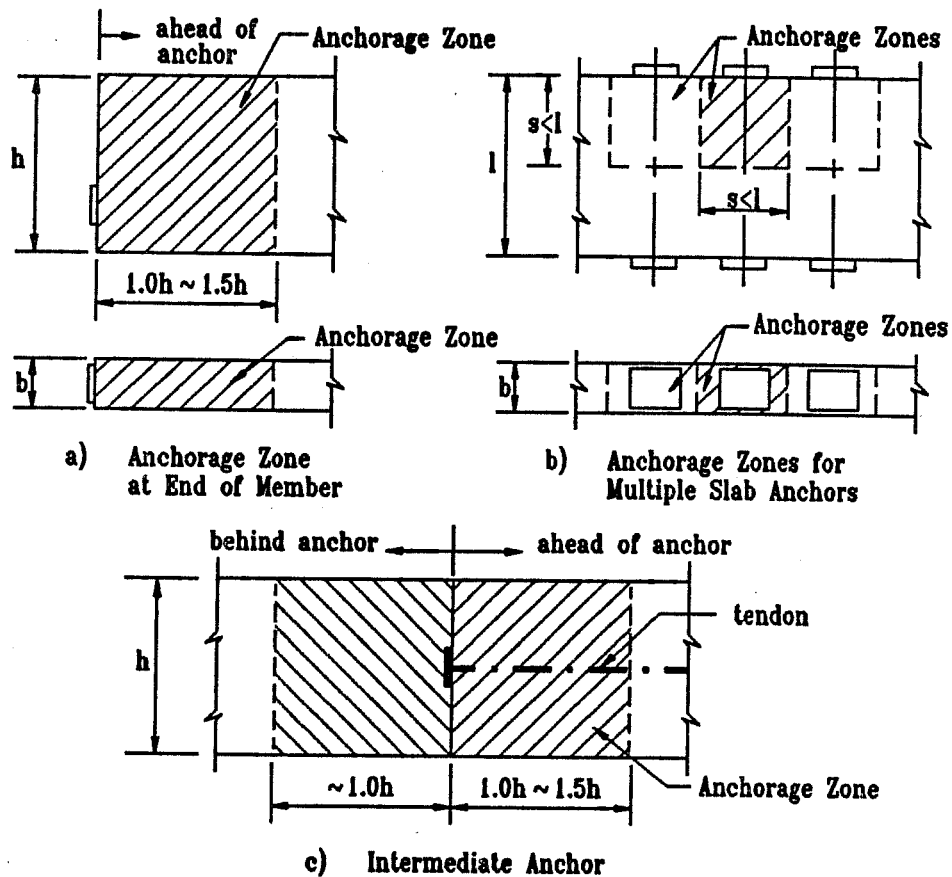


Figure 2.14 General Zone Dimensions

In the proposed anchorage zone provisions of this study, the geometric extent of the general zone is defined as being identical to that of the overall anchorage zone including the local zone (Appendix A, Section 9.21.2.1). This implies that the responsibility for the overall anchorage design, and particularly the integration of local zone details into the overall anchorage zone, remains with the designer of the general zone. The proposal includes definitions for the extent of the anchorage zone for end anchors, intermediate anchors, and multiple slab anchors (Figure 2.14). The definitions of the local zone were developed by Roberts and are based on the geometry of the anchorage device including any confining reinforcement, required concrete cover over reinforcement or anchorage

hardware, and manufacturer's recommendations on anchorage edge distance or spacing, if available (Figure 2.15)[41].

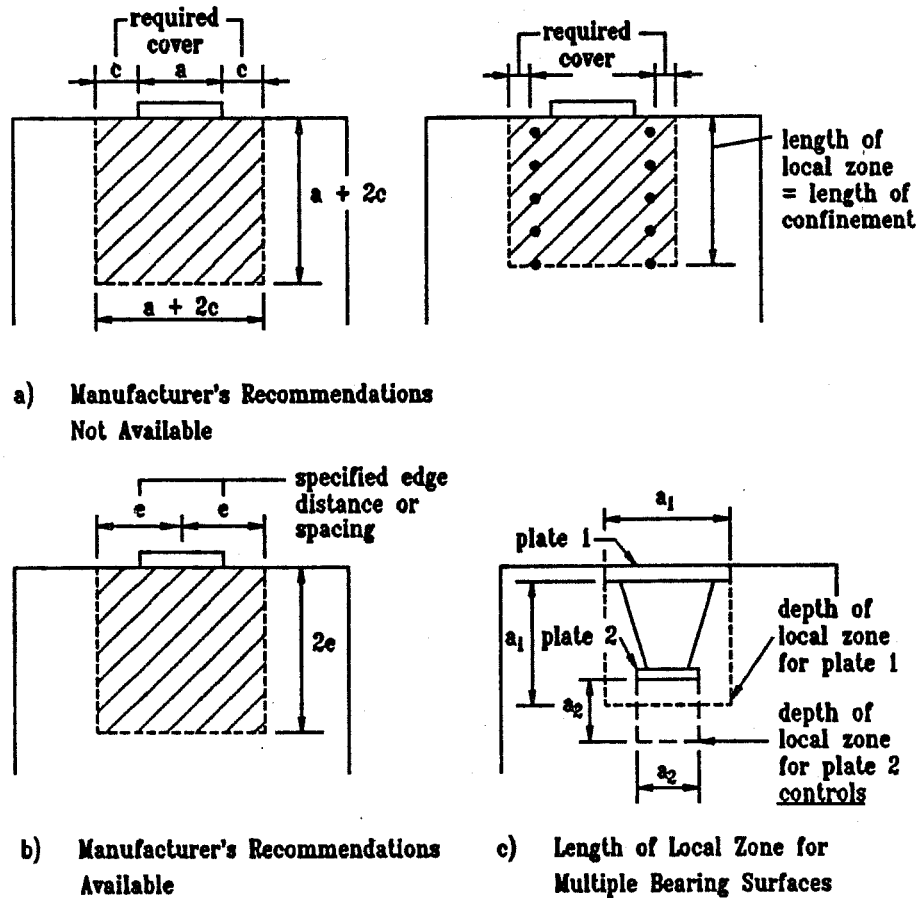


Figure 2.15 Local Zone Dimensions

2.2 Design of the Local Zone

2.2.1 General

For basic plate-type anchorage devices adequate performance of the local zone can generally be ensured by limiting the bearing pressure for that anchor. However, proprietary special anchorage devices with complex geometries and/or local confinement reinforcement are frequently used to increase the bearing strength of the concrete. Acceptance of such anchorage devices should be based on their performance in a

standardized acceptance test. Such a procedure is commonly used in Europe and is proposed in this study.

It is the responsibility of the anchorage device supplier to furnish hardware that can pass such an acceptance test. The anchorage device supplier also should submit all information concerning details required to ensure satisfactory performance of the local zone to the engineer of record and to the constructor. This includes records of the anchorage device acceptance test and information on required confinement and auxiliary reinforcement, minimum edge distance and anchor spacing, and minimum concrete strength at time of stressing.

The fact that an anchorage device has passed the acceptance test in a certain configuration should not discourage reasonable modifications reflecting the conditions in the actual structure, provided both engineer of record and anchorage device supplier agree to these modifications. For example, when an anchor is used in a member with a thickness somewhat larger than in the acceptance test, it is very advantageous to increase the diameter of the confining spiral accordingly.

2.2.2 *Experimental Study by Roberts*

Roberts conducted a study of behavior and design of the local zone as part of this project [41]. The study included a review of current test procedures for anchorage device acceptance tests, a comprehensive evaluation of previous local zone studies, and 28 physical tests. The variables investigated included edge distance, spiral parameters, auxiliary reinforcement, type of anchorage device, concrete strength, and interaction with the general zone. Based on this study Roberts developed recommendations for a test procedure for the acceptance test of special anchorage devices and an equation to predict the local zone capacity. Her recommendations are the basis for the provisions on local zone design and on the anchorage device acceptance test in the proposed code specifications (Appendix A).

Roberts found the following best fit equation for the prediction of local zone capacity of the tests included in her study:

$$P_n = 0.80 f'_{ci} \sqrt{\frac{A}{A_b}} (A_b) + 4.1 f_{lat} A_{core} \left(1 - \frac{s}{D}\right)^2 \leq 3 f'_{ci} A_b \quad (2.2)$$

$$\text{with } 0.80 f'_{ci} \sqrt{\frac{A}{A_b}} \leq 2 f'_{ci}$$

The terms in the equation are defined as follows:

- P_n is the nominal strength of the local zone;
- f'_{ci} is the concrete cylinder strength at time of loading;
- A is the area of supporting surface geometrically similar to the loaded area and concentric with it (Figure 2.10);
- A_b is the area of the bearing plate;
- f_{lat} is the lateral pressure provided by spiral or orthogonal reinforcement;
- A_{core} is the area confined by the spiral, based on the outside diameter of the spiral, or area confined by orthogonal ties;
- s is the spiral pitch or tie spacing;
- D is the outside spiral diameter or length of legs of orthogonal ties.

The lateral pressure f_{lat} is defined as:

$$f_{lat} = 2A_s \frac{f_y}{Ds} < 1.2 \text{ ksi for spirals} \quad (2.3)$$

$$f_{lat} = A_s \frac{f_y}{Ds} < 1.2 \text{ ksi for orthogonal ties}$$

where A_s is the cross sectional area of the spiral or tie reinforcement bars and f_y is their yield strength. The confining pressure f_{lat} is additive if both spiral and orthogonal ties are used, provided the length of the legs of the orthogonal ties is larger than the spiral diameter and at least three ties are present within the length of the spiral. The combined confining pressure cannot exceed 1.2 ksi, and A_{core} in Equation (2.2) is still based on the area confined by the spiral. It is noted that the limit on f_{lat} was not indicated by Roberts' test results, but was included based on earlier recommendations by Wurm and Dashner [41]. This limit reflects more the strength of the portion of the test block ahead of the local zone and should not be necessary if this portion is adequately reinforced.

Roberts recommends that the confinement reinforcement extend along the tendon axis at least as long as the largest side dimension of the anchor plate. The first turn of the spiral or the first orthogonal tie should not be further than 1 inch from the first bearing surface of the anchorage device. The spiral diameter should be at least as large as the larger side dimension of the anchorage device. Larger spirals perform better, but a maximum spiral diameter of no more than twice the side dimension of the anchorage plate is recommended.

In order to use the full bearing plate area A_b in Equation (2.2), the bearing plate has to be sufficiently stiff. Based on studies by Hawkins, Roberts proposed the following limit on the slenderness of the bearing plate:

$$\frac{n}{t} \leq 0.07 \sqrt[3]{\frac{E_b}{f_b}} \quad (2.4)$$

where

- n is the maximum distance from the edge of the loading punch (the stressing jack or the wedge plate of the anchorage device) to the outer edge of the bearing plate (Figure 2.16);
- t is the average thickness of the bearing plate;
- E_b is the modulus of elasticity of the bearing plate material;
- f_b is the bearing pressure.

For bearing pressures that do not meet this stiffness criterium an effective bearing area may be determined assuming a 45 degree dispersion of stresses within the anchor plate (Figure 2.16).

2.2.3 Basic Anchorage Devices

Based on the work by Roberts, anchorage devices are classified either as special anchorage devices or as basic anchorage device in the proposed specifications. Basic anchorage devices have to satisfy bearing strength limitations and stiffness requirements, but no acceptance test is necessary.

In the proposed specifications the first term of Equation (2.2) was adopted with some modifications. The factor 0.8 was reduced to 0.7, but the limit for this term was

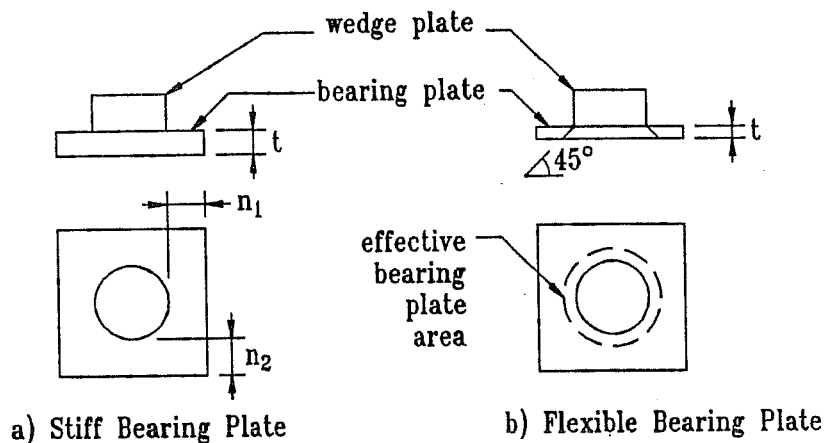


Figure 2.16 Stiffness Requirements for Anchor Plates

increased to $2.25 f_{ci}$. Anchorage devices that violate these limits and require confinement reinforcement were considered special anchorage devices. Therefore the second term of Robert's equation was not included in the definition of basic anchorage devices. Incidentally, the bearing pressure limit recommended by PTI is some 50% higher, depending on the choice of load and resistance factors (Equation (2.1)).

Because of evidence of satisfactory performance by some commercial anchors slightly more flexible than indicated by Equation (2.4), the stiffness requirements proposed by Roberts were somewhat relieved in the proposed anchorage zone specifications by increasing the factor 0.07 in Equation (2.4) to 0.08. In addition to the stiffness requirement, yielding of the plate material must also be checked.

2.2.4 Special Anchorage Devices

Anchorage devices that violate the bearing stress limitations and stiffness requirements to qualify as a basic anchorage device may still be acceptable if their performance can be proven by means of physical testing. This could be a test of a full scale model of the anchorage zone for a particular project. However, it is more conveniently done by a standardized acceptance test. In such tests, a certain anchorage system is evaluated under the most critical loading and geometry conditions. The criteria and test procedures for the acceptance test in the proposed anchorage zone provisions are based on the recommendations by Roberts and are summarized below.

The test block is a rectangular prism with its length equal to or larger than twice the larger cross-sectional dimension. The cross-sectional dimensions are selected such that the specimen can just accommodate the local zone, as defined in Section 2.1.4.2, for the particular anchorage system (Figure 2.17). The test block is reinforced with the local zone reinforcement as specified by the anchorage device supplier. In addition supplemental skin reinforcement may be provided throughout the specimen if desired by the manufacturer. The amount of this skin reinforcement is limited, and similar reinforcement has to be provided in the actual structure.

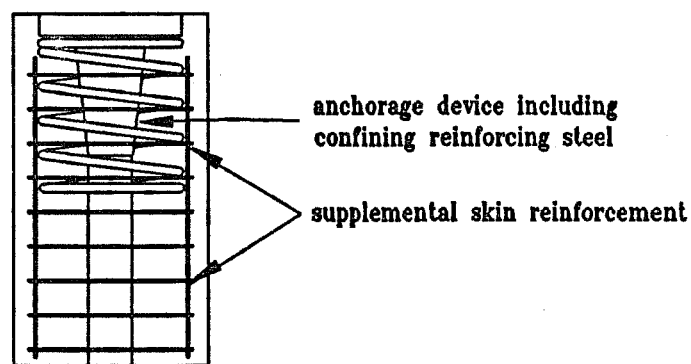


Figure 2.17 Anchorage Device Acceptance Test

Either of three test procedures is acceptable: monotonic loading, cyclic loading, or sustained loading. Crack widths and crack patterns have to be recorded at various stages of the test. The criteria for acceptance of an anchorage system include crack widths limitations and minimum failure loads. The criteria for the monotonic test are stricter in order to obtain results comparable to those of the more severe sustained and cyclic loading procedures.

2.3 Design of the General Zone

2.3.1 General

Frequently anchorage zones are designed on the basis of a linear elastic analysis, such as Guyon's solution or finite element results, by integrating the transverse tensile stresses along the tendon path. However, the applicability of Guyon's solution is limited and finite element analyses are involved and difficult to translate into reinforcement

arrangements. Linear elastic finite element computer programs are widely available today, but their application to the analysis of cracked concrete is not entirely satisfactory. For these reasons simple equilibrium based solutions are very appealing to the design engineer (Figure 2.18). Such methods have become known as strut-and-tie models and have received wide attention lately.

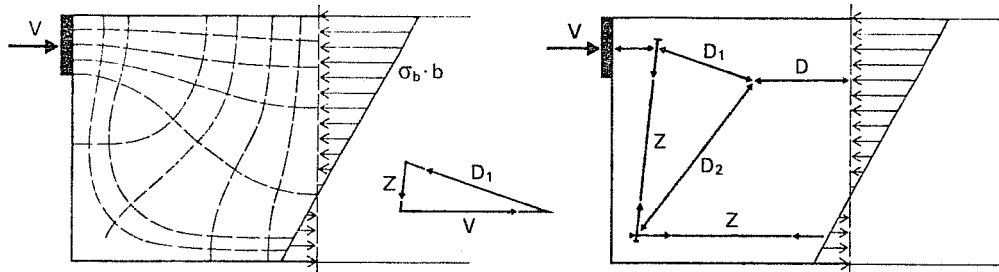


Figure 2.18 Flow of Forces in Anchorage Zone (from [24])

2.3.2 Strut-and-Tie Models

2.3.2.1 Introduction

Today's strut-and-tie model procedures have evolved from the truss model for shear design. Although the truss model was developed at the turn of this century, it is still a powerful concept and is

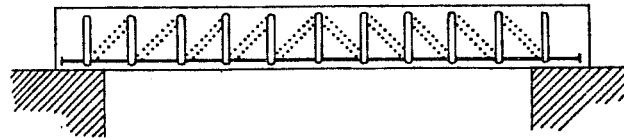


Figure 2.19 Ritter's Truss Model (from [10])

the basis for the code provisions for shear design in many countries (Figure 2.19). Schlaich, et al. proposed to generalize the truss model and to use it in the form of strut-and-tie models for the design of the disturbed regions of a structure in the vicinity of static or geometric discontinuities [45].

In strut-and-tie models the flow of forces in a structure is approximated by a system of compression members, the struts, and tension members, the ties, which intersect at nodes. The forces in the members are determined from equilibrium conditions and can then be used to evaluate compressive stresses in the concrete and to proportion the

reinforcement. Besides being an approximation to the state of stress in a structure, the strut-and-tie model can also be interpreted as a lower bound solution to a plastic limit load in the context of theory of plasticity.

2.3.2.2 Concrete Plasticity

Material models which assume perfect plasticity are commonly used in soil mechanics applications and efforts have been made to extend plastic analysis to structural concrete, particularly in Scandinavian countries [37] and Switzerland [53]. The stress-strain curve of a perfectly plastic material exhibits an unlimited horizontal yield plateau, so that arbitrarily

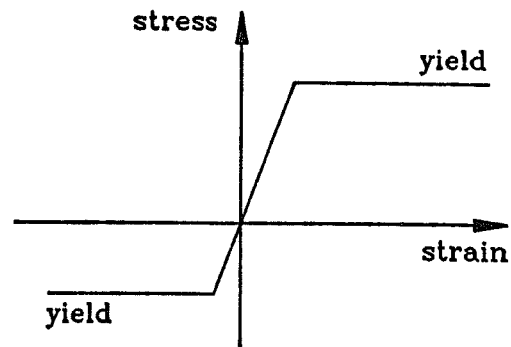


Figure 2.20 Elastic-Plastic Stress-Strain Curve

large strains without change of stress are possible after yielding (Figure 2.20). Collapse of a structure made of perfectly plastic material is characterized by the formation of a kinematic mechanism which allows unlimited deformations under constant stress. This collapse load or limit load can be bracketed by applying the lower bound theorem and the upper bound theorem, respectively. These limit theorems as stated by Drucker [12] and Chen [9] say:

Lower bound theorem: If an equilibrium distribution of stress can be found which balances the applied loads and is everywhere below yield or at yield, the structure will not collapse or will just be at the point of collapse.

Upper bound theorem: The structure will collapse if there is any compatible pattern of plastic deformation for which the rate of work of the external loads exceeds the rate of internal dissipation.

The assumption of perfect plasticity is not particularly good for the description of the behavior of plain concrete, due to the falling branch of its stress-strain curve and because of the limited ultimate strains. This is especially true for higher strength concrete (Figure 2.21). However, for reinforced concrete, and particularly for flexure of

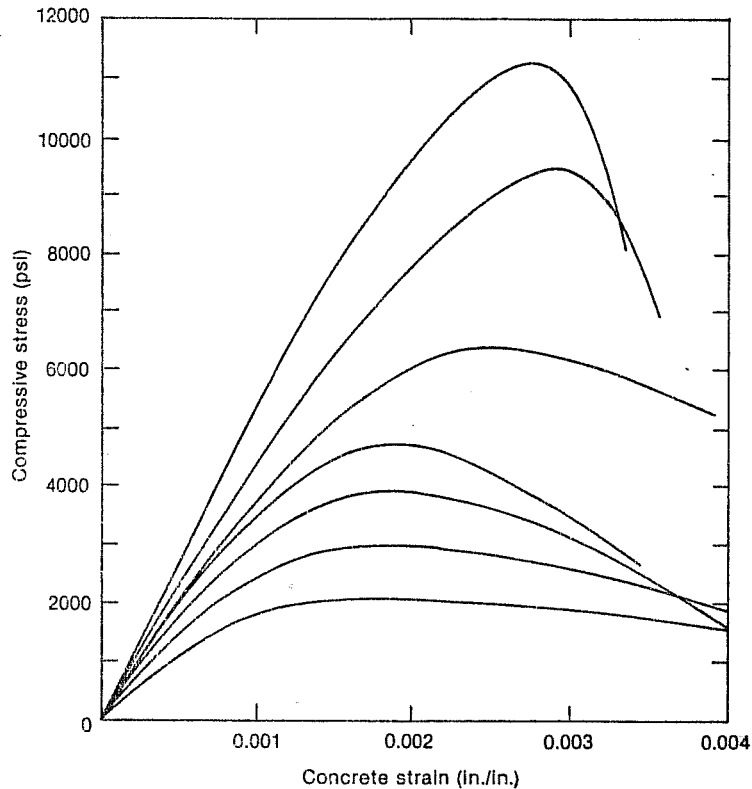


Figure 2.21 Stress-Strain Curves for Concrete (from [33])

underreinforced members, plastic analysis works very well. The strip design method for slabs is an example for the application of the lower bound theorem, while yield line analysis is based on the upper bound theorem. But even if the concrete strength has a stronger influence on the limit load, good correlation with test results can be achieved, when a reduced "effective concrete strength" is taken into account. The effectiveness factor depends on a wide range of variables, such as concrete strength, tensile strains perpendicular to the compressive stresses, cracking, and geometry of the structure. Therefore it has to be determined experimentally or estimated conservatively. Nielsen recommends as a lower bound for the effectiveness factor a value of approximately $24/\sqrt{f'_c}$ with f'_c in psi [37]. Collins and Mitchell developed a theory to account for the effect of lateral tensile strains on the effective concrete strength [10].

In practical applications of the upper bound theorem, failure surfaces are assumed so that the structure becomes kinematic. Examples for such failure surfaces are yield lines in slabs and plastic hinges in beams. The limit load for this assumed kinematic mechanism can then be determined by equating the work done by the external forces and the work done by the internal forces during a virtual displacement.

In the application of the lower bound theorem any state of stress in the structure is acceptable, as long as it is in equilibrium with the external forces and does not exceed the yield strength of the material anywhere. In particular, compatibility conditions do not have to be satisfied by this state of stress.

2.3.2.3 Development of Strut-and-Tie Models

A very good and practical paper on strut-and-tie modelling procedures with many example problems is presented in Reference 45. Additional information can be found in References 10, 23, 33, 34, 35, 42, 46, and 48.

Schlaich proposes to divide a structure into B-regions and D-regions [45]. In B-regions *beam* theory applies and traditional design and analysis methods may be used. D-regions are the *disturbed* regions in the vicinity of static or geometric discontinuities. The extent of these D-regions is approximately equal to the largest cross sectional dimension of the member. The forces acting on a D-region are the external loads and the internal forces at the boundaries between D-region and adjacent B-regions. The internal forces can be determined from simple beam theory (linear distribution of longitudinal strains).

In a next step the flow of forces in the D-region is approximated by a series of compression struts and tension ties, which are connected at nodes. This strut-and-tie model must establish a load path between the external and internal loads acting on the D-region and must satisfy equilibrium conditions. The ties represent the reinforcement in the structure. The struts represent compression stress fields.

Finally reinforcement is proportioned based on the tie forces obtained from the strut-and-tie model. Compressive stresses may be checked by assigning a width to the struts. The strut widths are controlled by the dimensions of bearing plates and by the reinforcement arrangement. All struts must fit within the boundaries of the overall D-region.

Figure 2.22 shows a strut-and-tie model for an eccentrically loaded anchorage zone. Reinforcement is visualized as being anchored through bearing plates. The strut widths

were selected such that all struts are stressed equally. This causes a hydrostatic state of stress in the nodes and is characterized by the node boundaries perpendicular to the struts. A non-hydrostatic state of stress in the nodes is acceptable if the ratio of stresses on adjacent edges of a node is not less than 0.5 or no more than 2 [45].

The state of stress in the struts is uniaxial and uniform over the strut width. The stresses are critical at nodal points where bottle necks in the compression fields occur. Schlaich recommends the following values for the nominal concrete strength, $f_c = v_e f'_c$, for struts:

- 0.85 f'_c for an undisturbed uniaxial state of stress;
- 0.68 f'_c if moderate cracking parallel to the strut may occur or in regions where reinforcement is anchored;
- 0.51 f'_c for skew cracking or skew reinforcement;
- 0.34 f'_c for skew cracking with large crack widths.

The lower bound for the effectiveness factor, $v_e = 0.34$, recommended by Schlaich agrees very well with Nielsen's recommendation (see Section 2.3.2.2) $v_e = 24/\sqrt{f'_c}$ which is 0.34 for 5000 psi concrete. Based on the evaluation of 122 tests reported in the literature, Bergmeister, et al. [5] propose an effectiveness factor of $v_e = 0.5 + 15/\sqrt{f'_c}$ which is 0.71 for 5000 psi concrete. A similar effectiveness factor ($v_e = 0.7$) is used in the proposed anchorage zone provisions (Appendix A) for all normal strength concrete.

There is no unique strut-and-tie model solution to a given problem. Rather, any strut-and-tie model that satisfies equilibrium and for which the effective concrete strength and the yield strength of the reinforcement are nowhere exceeded is a lower bound to the plastic limit load. Figure 2.23 shows an alternative load path for the eccentrically loaded anchorage zone discussed above. This model consists of a single strut that connects the applied load to a uniform stress distribution which extends only over a portion of the end of the anchorage zone. This is a perfectly acceptable lower bound solution, provided the

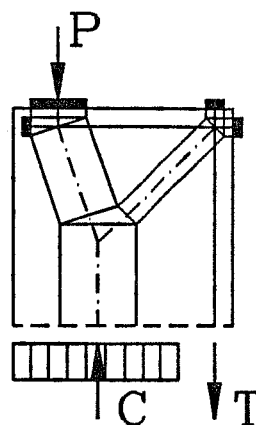


Figure 2.22 Strut-and-Tie Model for Eccentrically Loaded Anchorage Zone

concrete stresses in the strut do not exceed the effective concrete strength. However, this load path does not provide much guideline on the reinforcement requirements and should be eliminated.

This example illustrates that equilibrium conditions and material strength limitations alone are not sufficient to develop reasonable strut-and-tie models. Additional rules are needed to eliminate unsatisfactory solutions. The most important rule was already discussed: The internal forces at the boundaries of the D-region should be determined from simple beam theory. This requirement provides substantial additional information for the development of a strut-and-tie model, as can be seen by comparing Figure 2.23 to Figure 2.22. The enforcement of a simple beam theory stress distribution is equivalent to reintroducing compatibility conditions along the interface of the D-region and the adjacent B-region.

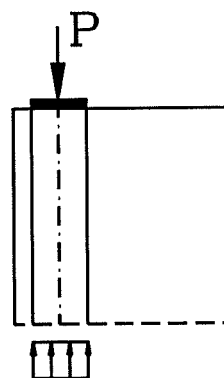


Figure 2.23 Direct Load Path in Eccentrically Loaded Anchorage Zone

There is still considerable freedom in the selection of the strut-and-tie model geometry, even with the restriction discussed above. Schlaich, et al. recommend the orientation of the strut-and-tie model according to the elastic stress trajectories with deviations up to 15 degrees as acceptable [45]. But even if results of an elastic stress analysis are not available the flow of the stress trajectories generally can be estimated using engineering judgement with sufficient accuracy for the development of a strut-and-tie model (Figure 2.18).

2.3.2.4 General Remarks

Obviously the approximation of the state of stress in a structure by strut-and-tie models is highly idealized. Therefore such models are not particularly useful as research models, where usually more accurate predictions are desired. However, strut-and-tie models are an excellent tool for ultimate load design. The designer is led to visualize a clear load path in the structure and attention is directed to global equilibrium. Furthermore, tie forces

can be translated directly into reinforcement requirements and the importance of well anchored reinforcement is emphasized by the nodal concept.

Strut-and-tie models have only a limited capability to detect compatibility and constraint induced stresses. However, such stresses disappear upon cracking of the concrete and reinforcement is required for crack control, but not for structural safety. This is well established for the case of compatibility torsion, for example. Consequently, crack control reinforcement should supplement the primary reinforcement determined from a strut-and-tie model. The regions where such crack control reinforcement is required can be determined from linear-elastic analysis, experience, and common sense. As long as adequate reinforcement is provided for the primary load path the amount of supplementary crack control reinforcement is not critical in terms of ultimate capacity.

For the designer unexperienced in the use of strut-and-tie models, most likely its biggest problem is the non-uniqueness of the solution. But in fact, to a certain degree a reinforced concrete structure can and will adjust to the load path envisioned by the designer. This adjustment does not even require a perfectly plastic material but is induced by the change of stiffness and by the stress redistributions that come with cracking of the concrete.

2.3.2.5 Experimental Study by Sanders

Part of Phase A of this project was an experimental study to evaluate the use of strut-and-tie models as a tool for the design of the general zone [44]. Sanders conducted 36 tests of anchorage zone specimens. In the tests the local zone was adequately confined to preclude failure in this region. Tendon configurations included concentric, eccentric, multiple, and curved and inclined tendons. Other variables were reinforcement distribution, presence of lateral post-tensioning, and concrete strength. All specimens had a rectangular cross section except one which had a T-section.

The primary conclusion of Sanders' study is that strut-and-tie models oriented on the elastic solution and neglecting concrete tensile strength are very conservative. This is due to two reasons. Before the bursting crack extends all the way to the base of the specimen, there is a considerable contribution of the concrete tensile strength of the remaining uncracked portion of the specimen. As the crack extends, the compression struts become steeper and a smaller tensile force is required to redirect the compression forces

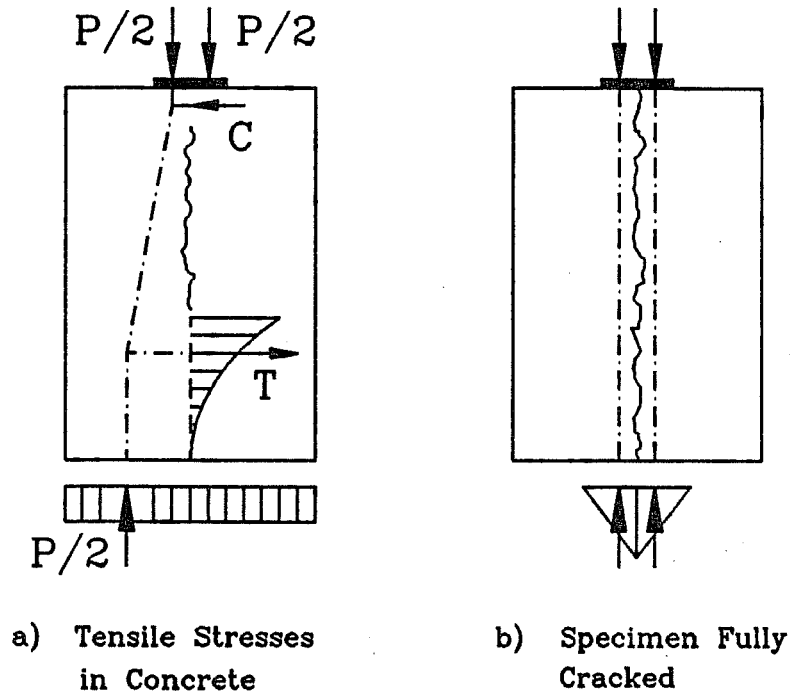


Figure 2.24 Effect of Bursting Crack

(Figure 2.24a). After the bursting crack has reached the base of the specimen a dramatic redistribution of stresses takes place. This can be well visualized by considering the limiting case of an unreinforced block (Figure 2.24b). The bursting crack splits the block into two separate eccentrically loaded portions. Since no tensile stresses can be transferred across the base of the specimen or across the bursting crack, the stress distribution at the base of each of the portions must be approximately triangular with the resultant force balancing the corresponding portion of the applied load. This in fact is the load path shown in Figure 2.23 that was so rashly discarded as unreasonable in Section 2.3.2.3.

If bursting reinforcement is present, some spreading of the compressive stresses in the anchorage zone will take place. The stresses in the reinforcement depend on the lateral stiffness provided by that reinforcement and are not easily calculated. However, even after the bursting reinforcement has reached its yield strength further increase of the applied load is possible. This causes the compression struts to become progressively steeper until

a compression failure occurs (Figure 2.25). In Sanders' tests this compression failure usually was located immediately ahead of the confined concrete of the local zone.

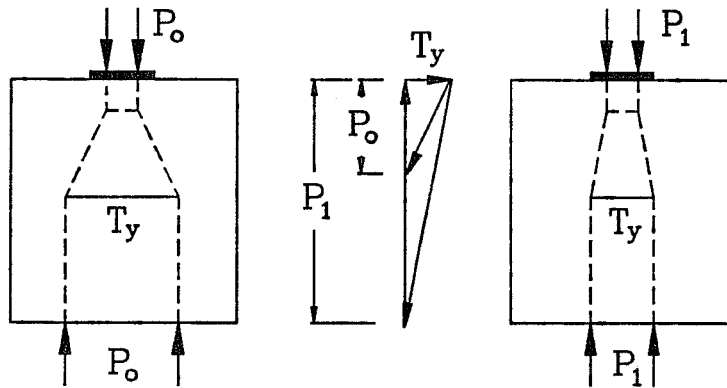


Figure 2.25 Increase of Load after Yielding of Bursting Reinforcement

Sanders confirmed the redistribution of stresses after full cracking of the specimen by an analytical model, where the separated portions of the cracked specimen were analyzed as beam columns on elastic foundation. He also developed modified strut-and-tie models which allowed deviation from the elastic stress distribution at the base of the specimens and was able to improve the ultimate load predictions for his tests significantly.

The important conclusion of Sanders' study is that stress redistributions after development of bursting cracks reduce the stresses in the bursting reinforcement but increase the compressive stresses in the anchorage zone. For design the basic strut-and-tie model approximating the elastic stress distribution is recommended.

2.3.3 *Finite Element Analysis*

2.3.3.1 Introduction

With the advance of inexpensive but powerful computers linear elastic finite element analysis has become quite feasible for design. Such analysis is appropriate in modelling the behavior of uncracked concrete and gives reasonable estimates for first cracking loads. Sanders pointed out that the concrete tensile capacity needs to be adjusted to account for

the two- or three- dimensional state of stress in the structure. He found an average effective concrete tensile strength of $4.2\sqrt{f'_{ci}}$ for his tests.

The prediction of first cracking loads using linear elastic finite element analysis becomes more unreliable when stress concentrations occur. This became particularly apparent for Sanders' concentric tendon test series. Although elastic analysis predicts very high spalling stresses (Figure 2.2) no corresponding cracks were detected in the specimens.

When linear analysis is used for design, the tensile stresses are usually integrated to obtain tensile forces and then reinforcement is provided accordingly. Although cracking of the structure induces significant stress redistributions, this procedure generally is safe.

2.3.3.2 Analytical Study by Burdet

As part of Phase A of this project Burdet conducted linear elastic finite element analyses of some basic anchorage zone configurations [8]. These analyses were to support the development of strut-and-tie models for Sanders specimens. Therefore the same anchorage zone configurations were investigated, that is concentric, eccentric, inclined, curved, and multiple tendons. Burdet also conducted parameter studies using finite element analysis and strut-and-tie models to extend the range of Sanders' experimental study.

Some of his major conclusions are:

- 1) Linear elastic finite element analysis is useful for prediction of first cracking loads.
- 2) Guyon's symmetrical prism gives a good estimate of the bursting force ahead of individual anchors.
- 3) Strut-and-tie models can be selected to give results very close to the elastic solution. Such models are recommended for design.
- 4) A diffusion angle of 26 degrees on either side of the tendon path may be assumed for the compression struts spreading from the concentrated tendon force.

2.3.3.3 Approximate Equations

Based on his finite element studies Burdet developed approximate equations for magnitude and location of the bursting force and for the critical compression stresses at the interface of local zone and general zone. These expressions are valid for rectangular sections with a single, straight, concentric or eccentric tendon, which may be inclined. The

expression for the critical compressive stresses is based on parameter studies of concentrically loaded anchorage zones. It should not be used for anchors with an edge distance of less than one and one-half plate widths, where the edge distance is measured to the center of the plate. The equations as developed by Burdet are:

$$T_{burst} = 0.25P_u \left(1 - \frac{a}{h}\right) + 0.5P_u \sin\alpha \quad (2.5)$$

$$d_{burst} = 0.5(h - 2e) + 5e \sin\alpha \quad (2.6)$$

$$f_{ca} = \frac{0.60P_u}{ab} \frac{1}{1 + a\left(\frac{1}{b} - \frac{1}{t}\right)} \leq \phi(0.75f'_c) \quad (2.7)$$

where

- T_{burst} is the bursting force;
- d_{burst} is the distance of bursting force from bearing plate;
- f_{ca} is the compressive stress at distance equal to a ahead of the bearing plate;
- P_u is the factored tendon force;
- a is the side length of the bearing plate in the long direction of the rectangular cross section;
- b is the side length of the bearing plate in the thin direction of the rectangular cross section;
- t is the thickness of the cross section;
- e is the eccentricity of the tendon force with respect to the centroid of the rectangular cross section;
- h is the larger side length of the rectangular cross section;
- α is the angle of inclination of the tendon force with respect to the center line of the anchorage zone, positive for concentric loading and if the tendon force points toward the centroid of the section, negative if it points away from the centroid of the section, with the limitation that $-5 \text{ degrees} \leq \alpha \leq 20 \text{ degrees}$.

Equation (2.7) is based on the assumption that confinement reinforcement is provided for the local zone and that this confinement reinforcement extends for a distance

at least equal to one plate width, a , ahead of the anchor plate. The concrete stresses are critical at this distance a if confinement of the local zone is adequate and must be checked. Burdet observed that these stresses are approximately 60 percent of the bearing stresses for a/h ratios less than 0.3. This observation is based on plane stress analysis. The second factor in Equation (2.7) accounts for the dispersion of the compressive stresses in the thin direction of the member. This factor is valid for t/b ratios not higher than three.

The approximate equations in the proposed code provisions are based on Burdet's recommendations with some modifications (Appendix A). Equation (2.7) was expanded to account for the bearing area of the locally confined concrete ahead of the anchorage device. The effective nominal concrete strength was reduced from $0.75 f_{ci}$ to $0.7 f_{ci}$.

2.4 Multiple Slab Edge Anchorages

Falconer conducted a study of multiple slab edge anchorages as part of Phase B of the overall project [17]. He tested six slabs with a total of 56 tendons. Variables included anchor orientation, anchor spacing, edge distance, stressing sequence, slab thickness, and reinforcement details. The tendons were perpendicular to the edge of the slab in all specimens but one, where they were inclined at an angle of approximately 17 degrees.

Falconer's primary conclusions are:

- 1) Anchor spacing and stressing sequence had little effect on vertical strains and failure loads for anchors spaced at a distance larger than two plate widths. Stressing of every second anchor caused the highest stresses in the horizontal bursting reinforcement. However, these stresses were not critical.
- 2) Edge distance and ratio of plate width, b , to slab thickness, t , determined the mode of failure. Interior anchors with ample edge distance and b/t ratios equal to 0.4 and b/t ratios equal to one, respectively, failed due to crushing of the concrete ahead of the anchor plate. Interior anchors with a b/t ratio of 0.2 failed due to splitting of the slab in its plane.
- 3) Anchors with an edge distance less than one slab thickness failed at significantly lower loads than the corresponding interior anchors. The failure mode changed from concrete crushing to horizontal or vertical splitting of the slab.

- 4) Vertical reinforcement in the form of ties or hairpins distributed over a distance equal to one slab thickness ahead of the anchor plate was most effective for increasing the ultimate load.

3 END ANCHORAGES AND THE INFLUENCE OF SUPPORT REACTIONS

3.1 Introduction

3.1.1 General

Most of the available solutions for anchorage zone problems focus on the effects of the concentrated prestressing force only. However, usually the tendon layout in a structure is selected to balance dead load and portions of the live load. During stressing of the tendons the member cambers upwards and off the supporting formwork. Consequently the anchorage zone may not only be subjected to the tendon stressing force but also to support reaction forces. Stresses due to the prestressing force are combined with stresses induced by the weight of the member. This raises the question of how a reaction force effects the behavior of the anchorage zone. On one hand the compressive stresses induced by the reaction force may reduce the bursting stresses, while on the other hand the additional shear force in the anchorage zone may increase them.

Another concern is how results from studies that are limited to the immediate anchorage zone relate to the behavior of an actual structure. Sanders observed considerable stress redistributions after full cracking of his limited length specimens [44]. However, in actual structures there is almost always some concrete available ahead of the bursting crack and the tensile strength of this concrete contributes significantly to carrying the bursting force.

3.1.2 Objectives

The main objectives of this portion of the study are:

- 1) To compare full beam specimens to Sanders' shorter anchorage zone specimens.
- 2) To evaluate the effect of shear forces and reaction forces in the anchorage zone.

3.1.3 Scope

This section is aimed at the verification and expansion of findings of phase A of the overall project for end anchors. Following the approach outlined in Section 1.4, the final recommendations are based on a tripod of literature review, analytical methods, and a

limited number of physical tests.

Available literature is reviewed in Section 3.2. The analytical methods investigated in this study are linear elastic finite element analysis (Section 3.3) and strut-and-tie models (Section 3.4). The experimental program and test results are presented in Sections 3.5 and 3.6, respectively. Evaluation of the test results and of the analytical methods is included in Section 3.7. Finally, Section 3.8 summarizes the results of this portion of the study with a discussion of the behavior of end anchorages and design and detailing recommendations.

3.2 Background Information

3.2.1 Literature

A good discussion of a photoelastic study on the effect of reaction forces in the anchorage zone by **Sargious** is included in Reference 28. Figure 3.1 shows the photoelastic solution for a concentric, slightly inclined tendon force, V , but without reaction force. Figure 3.2 shows Sargious' solutions for the same tendon force, V , and a reaction force, A , equal to 10% and 20% of the tendon force, respectively. Two

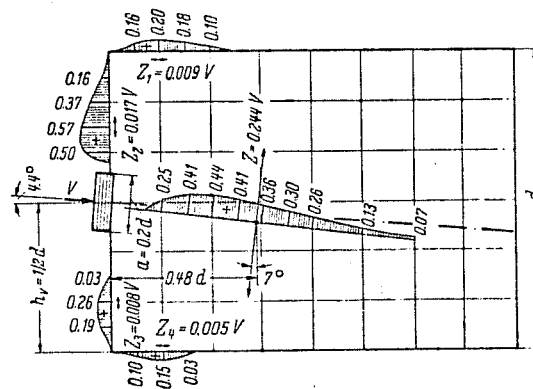


Figure 3.1 Sargious' Photoelastic Solution for Anchorage Zone without End Reaction (from [28])

different locations of the reaction force were investigated, $x_A = 1/3 d$ and $x_A = 1/6 d$. This comparison indicates that the reaction force has a beneficial effect on both bursting stresses and the resultant bursting force. It is interesting to note that doubling the reaction force from 10% to 20% of the tendon force has very little effect on bursting stresses and bursting force. However, the location of the reaction force has a significant influence.

Yong, et al. conducted three-dimensional, linear elastic finite element analyses and physical tests on beams with rectangular end blocks [58]. They found that the bursting stresses in the thin direction of the cross section (lateral stresses) are considerably larger than the transverse bursting stresses in the long direction of the cross section. A reaction force in the anchorage zone reduces the transverse stresses but has no effect on the lateral

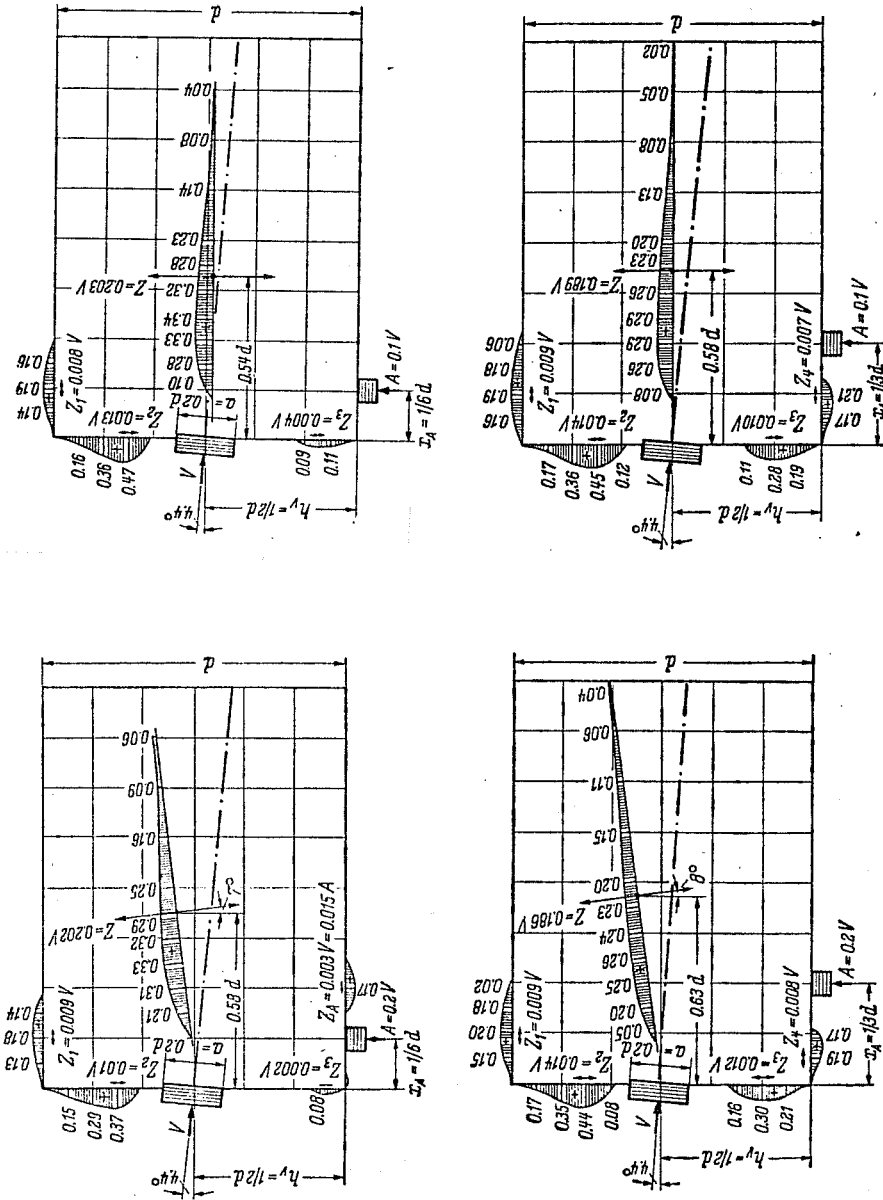


Figure 3.2 Sargious Photoelastic Solutions for Anchorage Zone with End Reactions (from [28])

stresses. In the experimental program strains were measured prior to cracking of the specimens and agreed reasonably well with the linear elastic predictions.

Schlaich discusses strut-and-tie models for anchorage zones including the effect of a reaction force in Reference 46. The basic strut-and-tie model shown in Figure 3.3a is inadequate to determine the bursting force and a more detailed model is needed (Figure 3.3b). Schlaich states that the bursting force determined from the more detailed model is not larger than the bursting force for an anchorage zone without reaction force and he concludes that neglecting the reaction force is conservative.

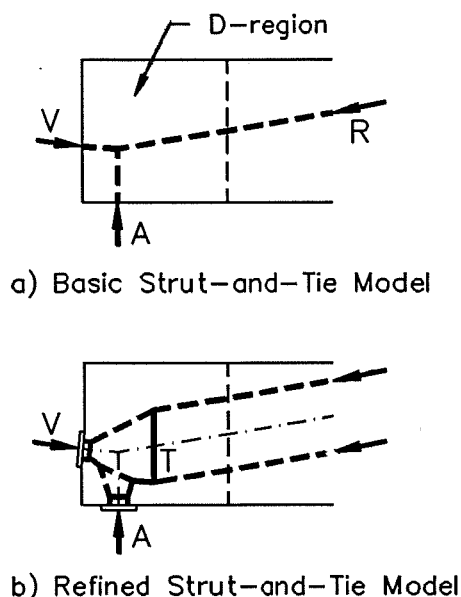


Figure 3.3 Strut-and-Tie Model (from [46])

3.2.2 Companion Investigations

3.2.2.1 Burdet's Linear-Elastic Finite Element Studies

Burdet conducted linear-elastic finite element studies on the effect of tendon inclination on the bursting stresses in the anchorage zone [8]. Although reaction forces in the anchorage zone were not included in this study the problems are related in-as-much as shear stresses at

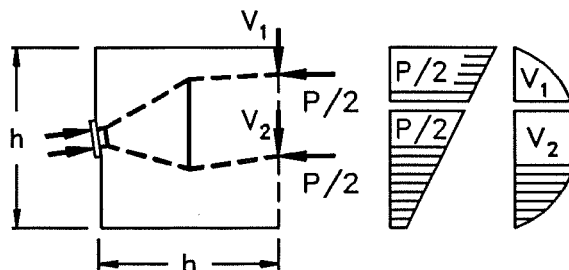


Figure 3.4 Location and Inclination of Struts

the end of the anchorage zone exist in both cases. Burdet found that the effect of increasing tendon eccentricity is to increase the magnitude of the transverse force in the anchorage zone (Equation (2.5)). The transverse force is the combined bursting and shear force in the anchorage zone. Strut-and-tie models give solutions in good agreement with the elastic solution if location and inclination of the struts intersecting the interface of the

anchorage zone with the adjacent B-region are based on simple beam theory (Figure 3.4).

3.2.2.2 Sanders' Experimental Study

As part of the experimental portion of Phase A of the overall project Sanders conducted tests of concentrically loaded anchorage zone specimens [44]. His specimen B3 had well distributed bursting reinforcement and was selected for comparison with a similar anchorage zone detail in a full beam to be tested in this study. Figure 3.5 shows dimensions and reinforcement arrangement for specimen B3. Mexican #2 bars with a yield strength of 44.9 ksi were used for the bursting reinforcement giving a bursting force capacity of 39.6

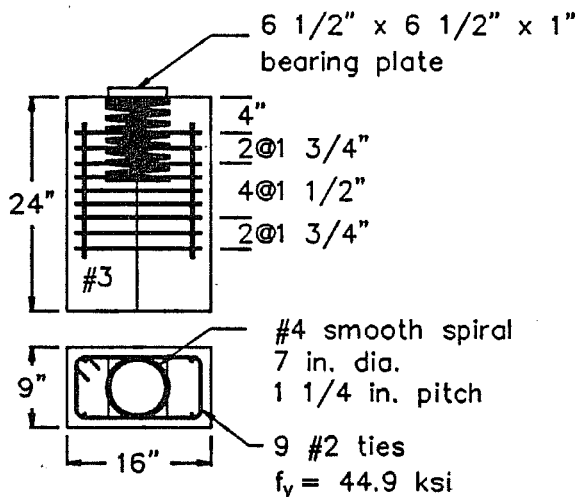


Figure 3.5 Specimen B3 Details (adapted from [44])

kips. The concrete compressive strength at time of testing was 5400 psi.

Figure 3.6 shows the measured strains in the bursting reinforcement. First cracking along the center line of the specimen was observed at a load of 217 kips. It was accompanied by a sudden increase of strains in the bursting reinforcement. All bursting reinforcement had yielded or was close to yielding at the ultimate load of 331 kips.

3.3 Finite Element Analysis

3.3.1 General

Linear-elastic, two-dimensional finite element analyses were conducted for a beam with a rectangular cross section subjected to a concentric tendon force, P , and a single vertical load, V (Figure 3.7). Variables were the shear span and the magnitude of the load V . V was selected such that the maximum bending moment in the beam was the same and equal to $Ph/3$ for all shear spans investigated. Poisson's ratio was taken as 0.16.

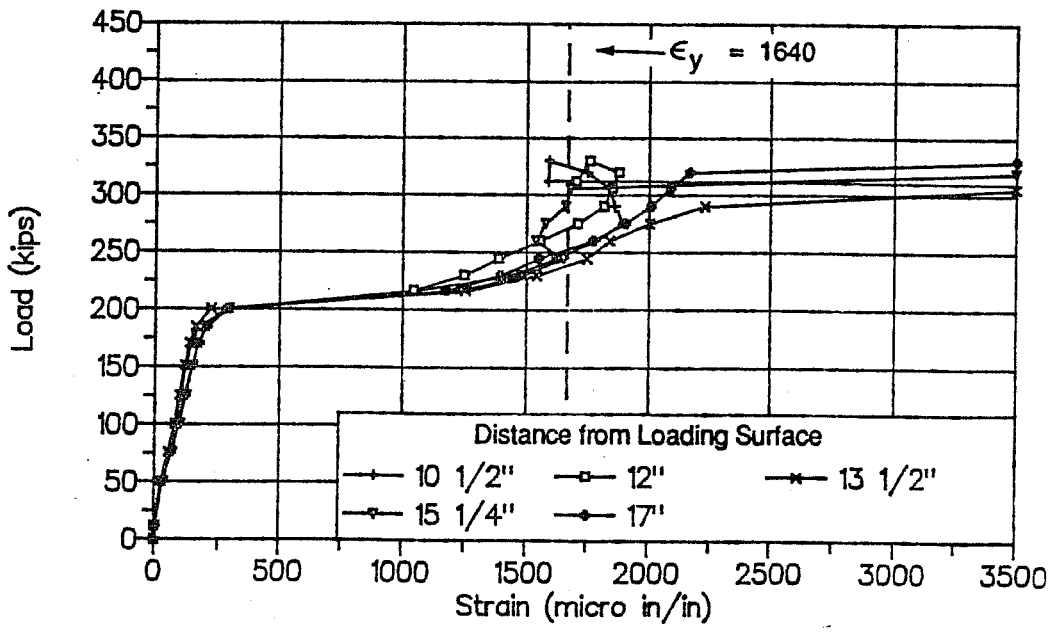
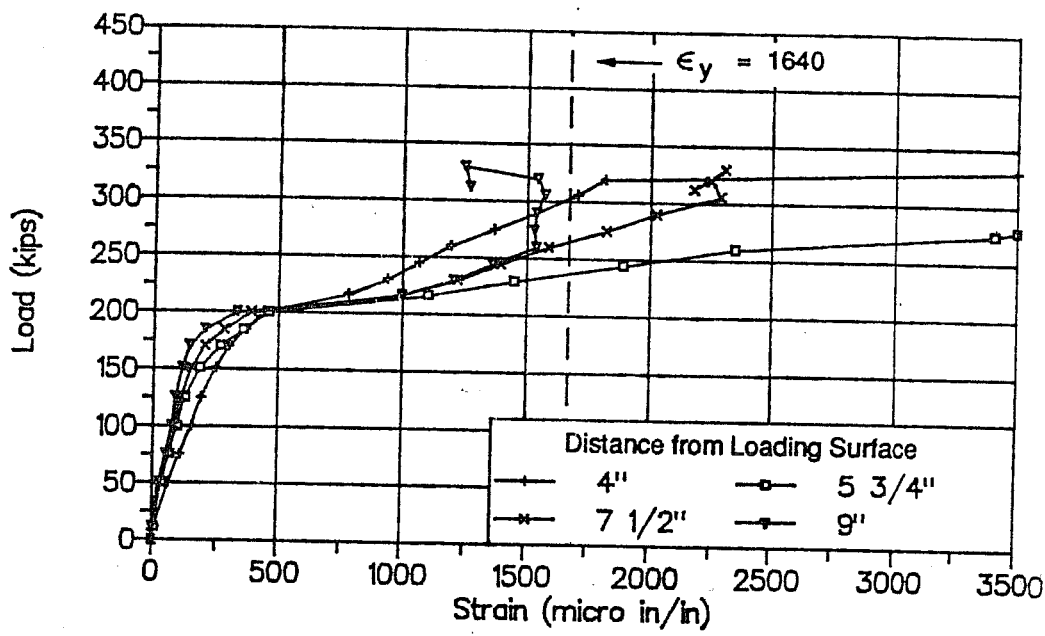


Figure 3.6 Specimen B3 Bursting Strains (from [44])

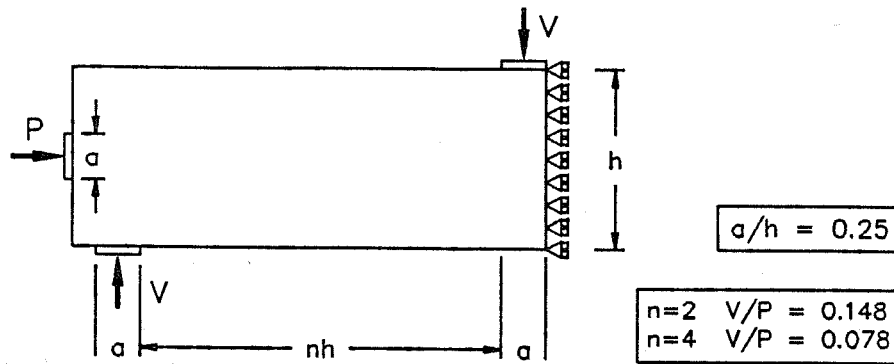


Figure 3.7 Parameters for Finite Element Analysis

3.3.2 Analysis Results

The maximum bursting stresses do not occur along the tendon path but are located along a main strut that is inclined due to the effect of the reaction force in the anchorage zone. This main strut approximately follows a line from the center of the anchor plate to the

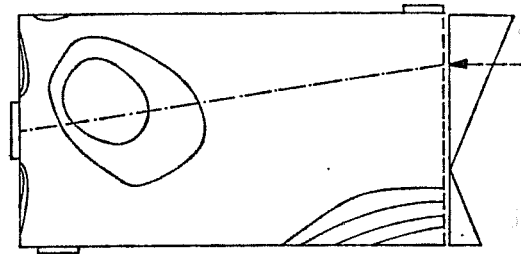


Figure 3.8 Main Compression Strut

centroid of the flexural compression force at the maximum moment section (Figure 3.8).

Figure 3.9 shows the relative tensile stresses perpendicular to the main strut for V/P ratios of 0, 0.078, and 0.148, respectively. These relative stresses were obtained by dividing the actual stresses by the average stress at the end of the anchorage zone. The relative magnitude and relative location of the resulting bursting forces are listed in Table 3.1. A reaction force in the anchorage zone tends to reduce the maximum bursting stress, but the effect on the resultant bursting force is very small. The beneficial effect on the maximum bursting stress is largely independent of the magnitude of the reaction force for the range of variables investigated.

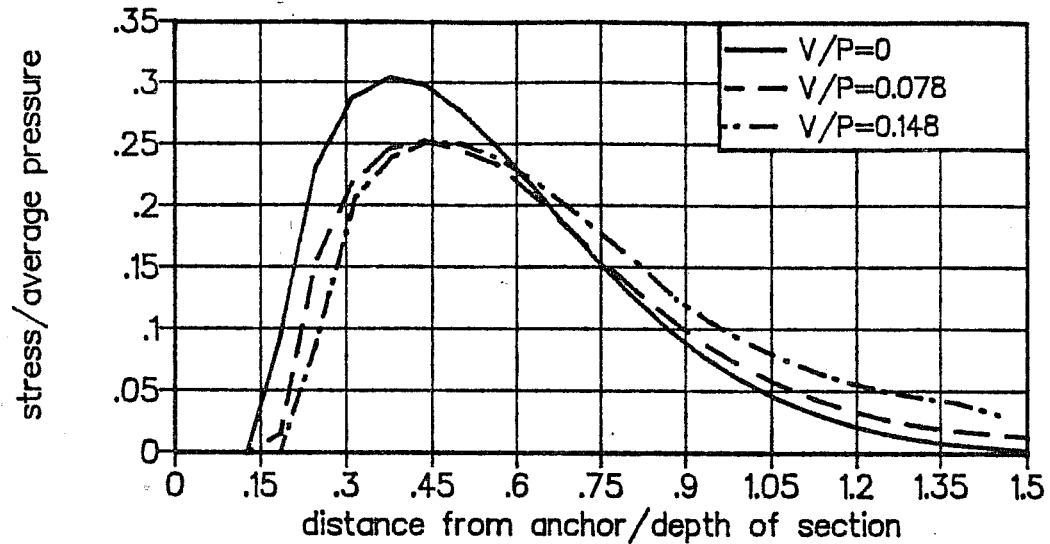


Figure 3.9 Tensile Stresses Perpendicular to Main Strut

3.3.3 Discussion

The finite element analyses confirm previous studies which found that a reaction force in the anchorage zone reduces the bursting stresses. This finding is in contradiction to Burdet's results, who observed that a shear force in the anchorage zone due to tendon inclination increases the bursting stresses and the resulting bursting force. This difference is explained in Figure 3.10 which shows two concentrically loaded anchorage zones. In Figure 3.10a

the tendon is inclined and the tendon force has a horizontal component P and a vertical component V . In Figure 3.10b the tendon is horizontal, but a vertical force V acts on the anchorage zone. The shear stresses and the flexural stresses at the end of the anchorage zone are identical for both cases. Considering equilibrium of vertical forces along a horizontal section in mid height of the beam reveals the difference between the two cases. For the anchorage zone with the inclined tendon, transverse tensile stresses are necessary

Table 3.1 Magnitude and Location of Bursting Force

V/P	T_{burst}/P	d_{burst}/h
0	0.173	0.56
0.078	0.159	0.62
0.148	0.169	0.68

to satisfy vertical equilibrium. Transverse compressive stresses are required for equilibrium when a reaction force is present in the anchorage zone.

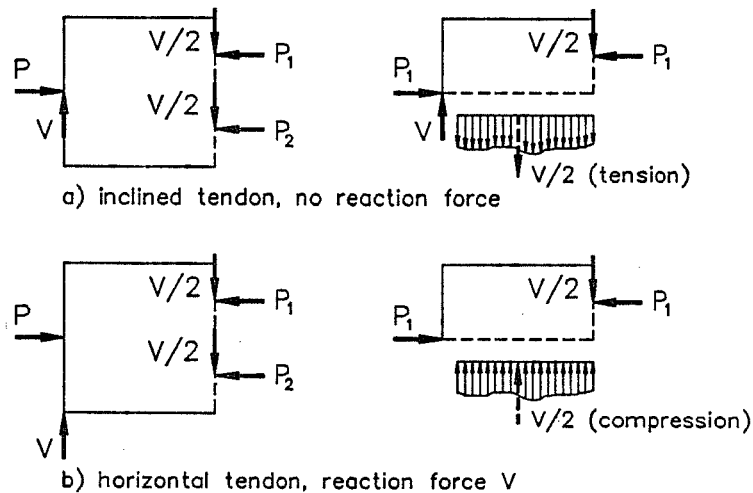


Figure 3.10 Effect of Tendon Inclination and of Reaction Force

3.4 Development of Strut-and-Tie Models

3.4.1 General

The development of a strut-and-tie model solution for a given problem is an iterative procedure that involves the following steps:

- 1) Estimate the extent of the D-region using Saint Vénant's Principle (see Section 2.1.1).
- 2) Determine the internal forces at the boundaries of the D-region using simple beam theory.
- 3) Select the geometry of the strut-and-tie model.
- 4) Determine the member forces.
- 5) Check the compressive stresses. If necessary, modify the geometry of the strut-and-tie model and repeat steps three to five.
- 6) Proportion the reinforcement.

Frequently the selected strut-and-tie model will be kinematically unstable and steps

three and four have to be considered simultaneously in order to satisfy equilibrium conditions. If truss analysis computer programs are used to determine the member forces, it is necessary to add a sufficient number of members to make the model statically determinate. The geometry can be selected such that the forces in the additional members become zero or very small.

Should the selected strut-and-tie model be statically indeterminate, the redundancy can be reduced by assuming tentative reinforcement proportions which in turn determine the forces in the corresponding tension ties. Another approach is to subdivide the indeterminate strut-and-tie model into determinate sub models and to assign a portion of the applied load to each of these sub models.

The member forces are quite sensitive to the selected geometry. Equilibrium conditions alone are not sufficient to find a satisfactory strut-and-tie model. Additional guidelines are needed and are discussed in the following sections.

3.4.2 Extent of the D-Region

The extent of the region where simple beam theory is not valid can be estimated using Saint Vénant's Principle. For rectangular beams with end anchors the D-region extends from the loaded face for a distance equal to approximately one member height (Figure 3.11a). However, a concentrated reaction force acting within the anchorage zone induces a larger disturbed region. For rectangular beams it extends from the end face of the beam to a distance equal to one member height measured from the reaction force (Figure 3.11b). For non-rectangular cross sections estimating the extent of the D-region is more difficult and some engineering judgement is required. The shorter the D-region is selected, the faster the concentrated tendon force has to spread out and the larger the bursting force becomes.

3.4.3 Boundary Conditions

The stresses at the end of the D-region can be determined from simple beam theory. These stresses are then integrated to find the resultant forces at the end of the D-Region. Frequently it is necessary to split a single resulting compression force into two or more individual forces (Figure 3.3).

Figure 3.12 shows how location and inclination of the struts at the end of the

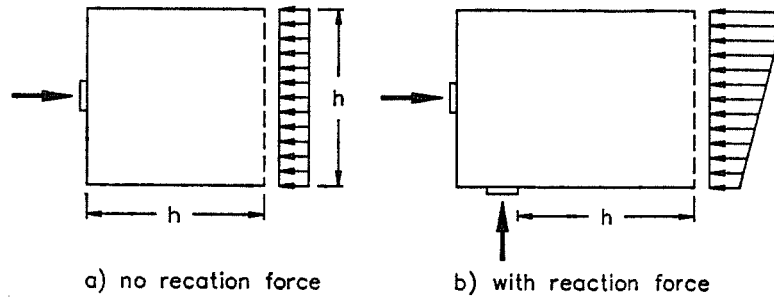


Figure 3.11 Extent of the D-Region

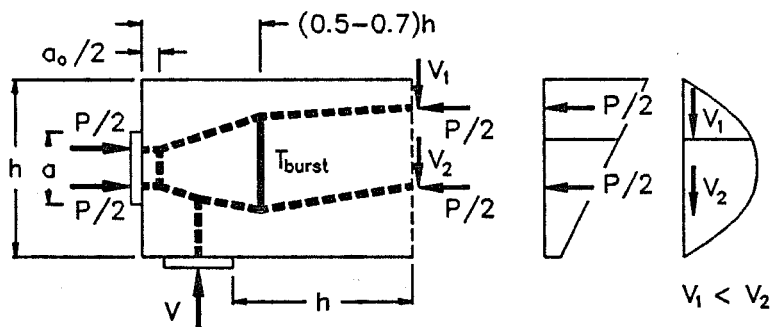


Figure 3.12 Strut-and-Tie Model for Uncracked Section

anchorage zone can be determined by integrating the flexural stresses and the corresponding shear stresses. If the section at the end of the anchorage zone may become cracked, a cracked section analysis should be used to determine the resulting forces. Depending on the level of concrete stresses, either linear elastic concrete behavior may be assumed or the rectangular stress block may be used (Figure 3.13). The location and direction of the flexural tensile force is determined by the reinforcement arrangement. The shear force is carried by the vertical components of the inclined compression struts. The angle between struts and ties should not be less than 25 to 30 degrees. Angles smaller than that lead to problems due to incompatibility of deformations of struts and ties and degrade the effective concrete strength.

The strut-and-tie model shown in Figure 3.13b evolved from the initial, simpler

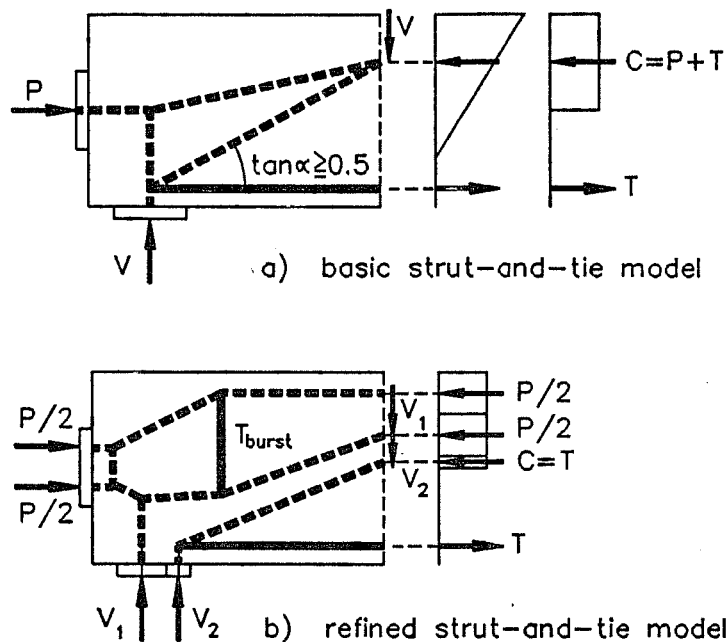


Figure 3.13 Strut-and-Tie Model for Cracked Section

model shown in Figure 3.13a. It is necessary to split the main bursting strut into two sub struts to obtain information on the bursting reinforcement requirement.

3.4.4 Location of the Bursting Tie

The bursting tie represents the resultant of the bursting reinforcement. The force in this member is quite sensitive to its distance from the anchor plate. Burdet gives information about the location of the centroid of the elastic bursting stresses for some special cases and recommends that the bursting reinforcement be centered around this location [8]. However, test results by Sanders indicate that significant deviations from this arrangement are possible without impairing the performance of the anchorage zone [44].

It appears reasonable to distribute the bursting reinforcement uniformly over the region subjected to bursting stresses. Non-linear finite element analysis results by Adeghe and Collins confirm the usefulness of this approach [4]. For concentrically loaded anchorage zones the bursting region extends approximately from $0.15h$ to $1.25h$, putting the centroid of the bursting reinforcement at a distance equal to $0.70h$ ahead of the anchor plate (Figure 3.9). For eccentric anchors Guyon's symmetrical prism may be used to

estimate the extent of the bursting region (Figure 2.8).

3.4.5 The Local Zone Node

3.4.5.1 General

The magnitude of the bursting force is not only determined by the distance of the bursting tie from the anchor plate but also by the location of the center of the local zone nodes (Figure 3.15). This location must be determined by considering the physical dimensions of the nodes. The smaller the local zone nodes, the larger the lever arm z and the smaller the bursting force T_{burst} become. The distance $a_o/2$ can be minimized by selecting a hydrostatic local zone node as shown in

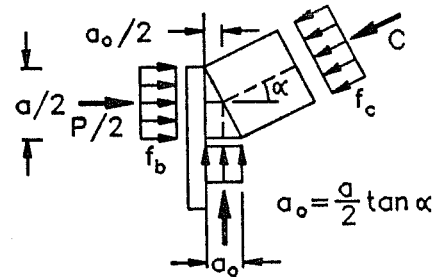


Figure 3.14 Hydrostatic Local Zone Node

Figure 3.14. The bearing pressure f_b and strut stresses f_c are identical. All stresses are perpendicular to their corresponding edge of the node. The depth of the node is labeled a_o . It depends on the width a of the bearing plate and on the inclination α of the struts. The intersection of the forces acting on the node is located at the distance $a_o/2$ ahead of the bearing plate.

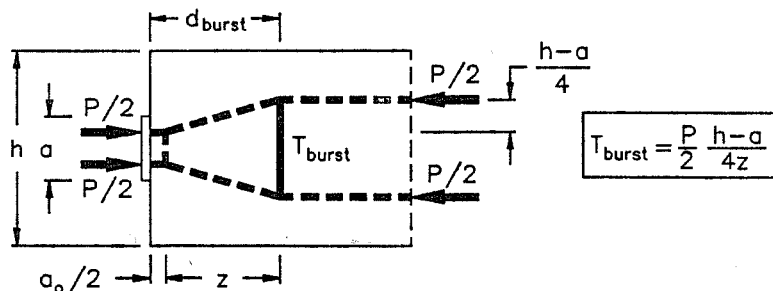


Figure 3.15 Effect of the Depth of the Local Zone Node on the Bursting Force

Frequently the bearing strength is increased due to the beneficial effect of confining concrete around the bearing plate (Figure 3.16). The same increase applies to the capacity of the struts joining at this node if $\tan \alpha$ is less than 0.5 (AASHTO, Section 8.16.7.3, [1]).

In this case a hydrostatic node can still be selected and will give the lowest bursting force. AASHTO limits the maximum useful $\sqrt{A/A_b}$ to 2. Based on Roberts' tests [41], in the proposed anchorage zone specifications this limit was increased to $2.25/0.7 = 3.2$, but the effective concrete strength was reduced from $0.85 f'_c$ to $0.7 f'_c$ (Figure 3.16 and Appendix A, Section 9.21.7.2.2).

The bearing capacity can be further increased by providing confinement reinforcement. In this case there are two options for the check of the compression stresses at the boundaries of the local zone node: Either a non-hydrostatic local zone node is necessary, or the struts joining at the local zone node have to be fan-shaped.

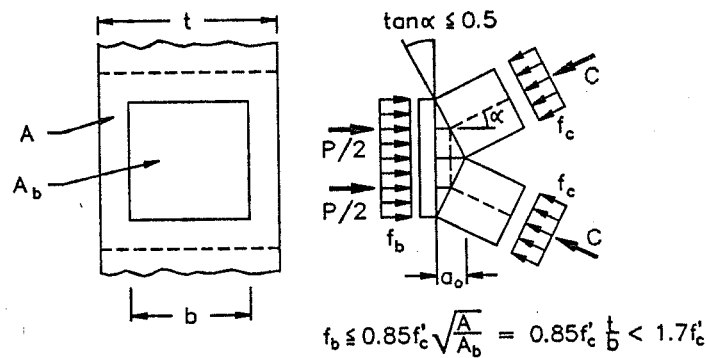


Figure 3.16 Effect of Confining Concrete

3.4.5.2 Non-Hydrostatic Local Zone Node

In a non-hydrostatic local zone node the depth a_o of the node is increased in order to reduce the stresses in the joining struts (Figure 3.17). Notice that this reduces the lever arm z (Figure 3.15) and thus increases the bursting force. The required depth of the local zone node depends on the bearing plate size, a , the inclination of the struts, α , and the ratio of bearing stress to strut

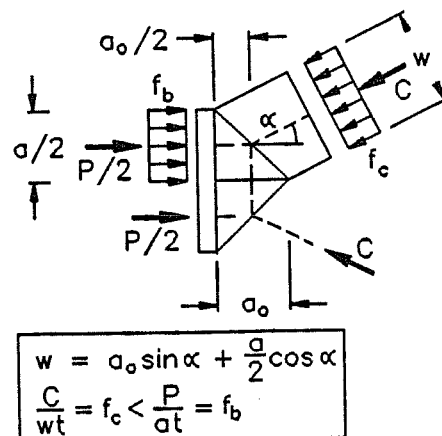


Figure 3.17 Non-Hydrostatic Local Zone Node

stress, f_b/f_c . For a symmetric local zone node, as shown in Figure 3.17, a_o can be determined from Equation (3.1).

$$\frac{a_o}{a} = \frac{f_b}{f_c} \frac{1}{2 \sin \alpha \cos \alpha} - \frac{1}{2 \tan \alpha} \quad (3.1)$$

$$\frac{f_b}{f_c} \leq 2$$

The limit on the f_b/f_c ratio is based on a recommendation by Schlaich that the ratio of stresses on adjacent sides of a node do not exceed a value of two [45]. However, for proprietary special anchorage devices where the tendon force is introduced through a series of bearing plates and ribs, this limit is frequently exceeded safely (Figure 2.4) [13, 55]. The optimum angle α resulting in the smallest a_o/a ratio for a given f_b/f_c ratio can be determined by differentiating Equation (3.1) with respect to α .

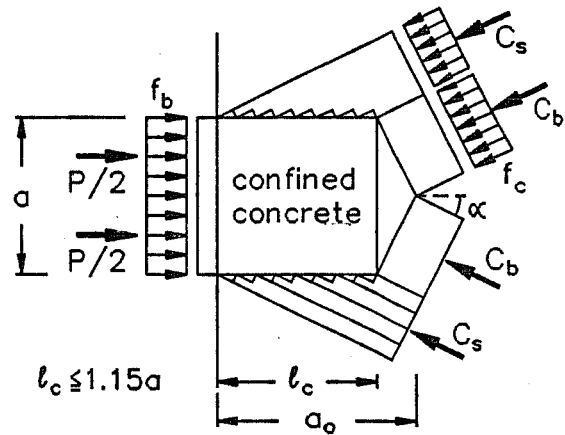


Figure 3.18 Local Zone Plug

The optimum angle α resulting in the smallest a_o/a ratio for a given f_b/f_c ratio can be determined by differentiating Equation (3.1) with respect to α .

$$\frac{\partial(a_o/a)}{\partial \alpha} = 0 \Rightarrow \tan^2 \alpha = 1 - \frac{f_c}{f_b} \quad (3.2)$$

With a non-hydrostatic local zone node, due to the presence of local confinement reinforcement the anchor capacity can be increased by a factor

$$\frac{P_{\text{confined}}}{P_{\text{unconfined}}} = 1 + 2 \frac{l_c}{a} \sin \alpha \cos \alpha \quad (3.3)$$

where l_c is the length of the confinement reinforcement. For $l_c = a$ and $\tan \alpha = 0.5$ this ratio is 1.8. Figure 3.18 illustrates the role of confinement reinforcement in the increase of

the depth of the local zone node. The confined concrete forms a highly stressed plug. Within this plug the transition from the lower general zone stresses to the higher bearing stresses takes place. Stresses are transferred by "skin friction" (struts C_s in Figure 3.18) and by "end bearing" (struts C_b), similar to a pile foundation. The effective length of the confinement, l_c , should be limited to avoid progressive collapse of the struts. A maximum value for l_c equal to 1.15 times the width of the confined plug is suggested but needs experimental verification.

3.4.5.3 Fan-Shaped Struts at the Local Zone Node

A hydrostatic local zone node can be maintained, if the struts joining at the node are fan-shaped (Figure 3.19). Inside the confined region the concrete stresses may exceed the effective concrete strength f_c . However, at the boundaries of the confined region all stresses are limited to f_c . As shown in Figure 3.19, the extreme fiber of the strut exits the confined region immediately ahead of the bearing plate. Hence the fiber

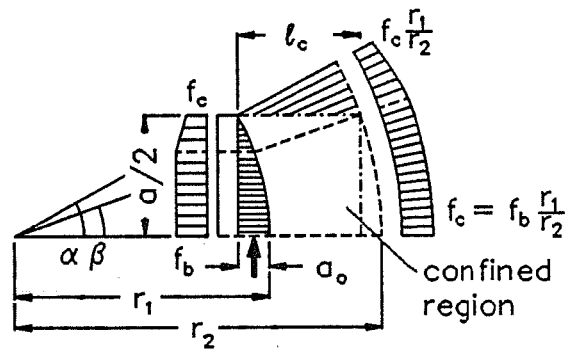


Figure 3.19 Fan-Shaped Struts at Local Zone Node

stress is limited to f_c at this location. By the time the fiber has reached the critical section at the end of the confined region (dashed line in Figure 3.19) the strut width has increased and the fiber stress is correspondingly smaller. As indicated in the figure, the consequence of using fan-shaped struts with local confinement is a non-uniform stress distribution for both bearing pressure and strut stresses at the critical section. The increase of anchor capacity for a symmetric local zone node is given by Equation (3.4).

$$\frac{P_{confined}}{P_{unconfined}} = 1 + \frac{1}{2} \left(\frac{\sin \alpha}{\sin \beta} - \frac{\sin \beta}{\sin \alpha} \right) \quad (3.4)$$

$$\text{with } \tan \beta = \frac{1}{\cot \alpha + 2 \ell_c / a}$$

For $\ell_c = a$ and $\tan \alpha = 0.5$ this ratio is 1.65.

The procedure recommended in the proposed anchorage zone specifications (Appendix A, Section 9.21.4.3) is a combination of a non-hydrostatic local zone node with fan-shaped struts. It is discussed in more detail in Section 3.7.3.

3.4.6 Member Capacities

After selection of the initial geometry of the strut-and-tie model and determination of the member forces, strut widths are selected to check the compressive stresses. The strut widths have to be large enough to accommodate the member forces without exceeding the effective concrete strength. After checking the compressive stresses adjustment of the strut-and-tie model geometry and a new iteration may be necessary.

The effective concrete strength is not the same throughout the D-region. Rather it depends on the state of stress in the nodes where strut and ties join and on the extent of cracking. In addition ϕ -factors are different for shear, flexure, bearing, and axial loads, which complicates the selection of the proper ϕ -factor for anchorage zone problems where all these actions occur simultaneously.

Several authors have given recommendations on effective concrete strengths and on ϕ -factors for design using the strut-and-tie model [10, 33, 45]. The recommendations vary somewhat but seem to converge at the following values:

CCC nodes:	$0.85 f'_c$	$\phi = 0.9$ for steel
CTC nodes:	$0.65 f'_c$	$\phi = 0.7$ for concrete
CTT nodes:	$0.50 f'_c$	

struts with skew, wide cracks: $0.35 f'_c$

C and T stand for "compression" and "tension", respectively. A CCC node is a node where three compression struts join.

The differentiation of ϕ -factors for concrete and for steel is incompatible with current US procedures. In US practice frequently the ϕ -factor is applied on the load side, and

nominal material strengths are used. Therefore the same ϕ -factor is used for both steel and concrete. In the proposed anchorage zone provisions (Appendix A) a single ϕ -factor of 0.85 is specified for the design of anchorage zones. Furthermore, the effectiveness factor for the effective concrete strength is taken uniformly as 0.7, independent from the type of node. This simplification gave conservative results in this and related studies [44].

3.4.7 *Strut-and-Tie Model Solutions*

3.4.7.1 Concentrically Loaded Rectangular Beam

As first example for the application of strut-and-tie model procedures the capacity of specimen Beam1 of the experimental portion of this study is determined. This specimen is patterned after Sanders' specimen B3 (see Section 3.2.2.2). The bursting reinforcement for specimen Beam1 provides a bursting force capacity, $A_s f_y$, of 44.4 kips (Figure 3.22). The centroid of the bursting reinforcement is located 10.5 inch ahead of the anchor plate. The concrete strength at time of testing was 5300 psi. A ϕ -factor of 1.0 will be used in order to be able to compare the strut-and-tie model prediction to the test result.

Figure 3.20 shows a strut-and-tie model for specimen Beam1. The struts at the end of the anchorage zone each carry half of the tendon force and are located at the quarter points of the section. The following steps lead through the procedure for the determination of the capacity predicted by this strut-and-tie model.

1. Make an initial guess for the depth of the local zone node.

As an initial assumption a_o is taken as half the plate width:

$$a_o = 0.5a = 0.5 \times 6.5" = 3.25"$$

2. Determine lever arm z and strut inclination α .

$$z = 10.5" - a_o/2 = 8.875"$$

$$\tan \alpha = 2.375"/z = 0.268 \Rightarrow \alpha = 15.0^\circ$$

3. Calculate the ultimate load, P_u , from the given tie capacity, $T_{burst,1}$.

$$P_u = 2T_{burst,1}/\tan \alpha = 2 \times 44.4/0.268 = 331.8 \text{ kips}$$

4. Check the compressive stresses at the local zone node.

$$\text{The bearing pressure is } f_b = P_u/(ab) = 331.8/(6.5 \times 6.5) = 7.85 \text{ ksi.}$$

Using an effectiveness factor of 0.85 for this CCC node and taking advantage of the surrounding confining concrete (see Figure 3.16) the effective concrete strength is

$$f_c = 0.85 f'_c t/b = 0.85 \times 5.3 \times 9/6.5 = 6.24 \text{ ksi.}$$

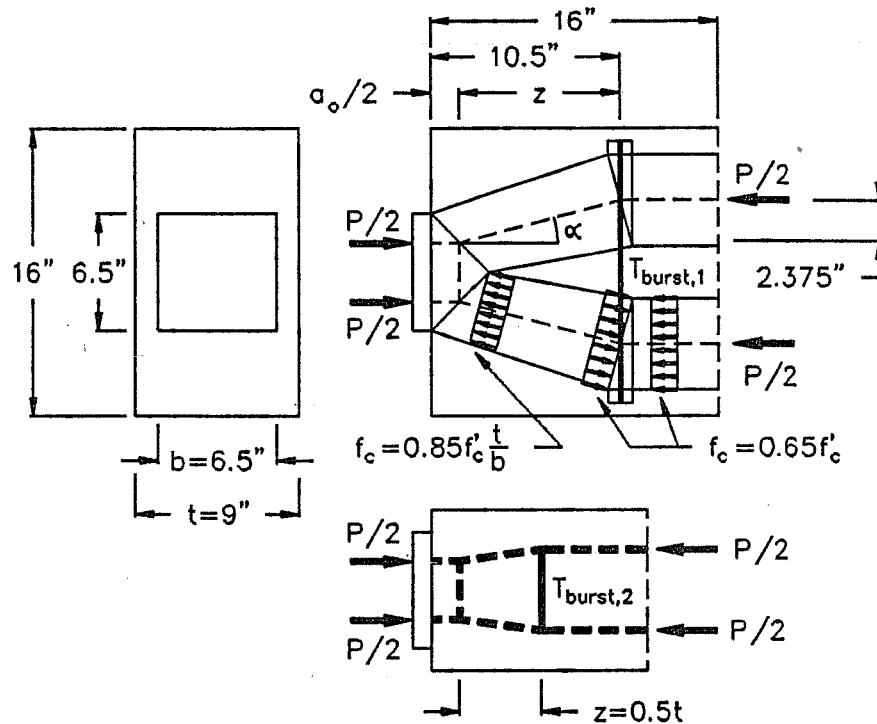


Figure 3.20 Strut-and-Tie Model for Specimen Beam1

Since the bearing pressure is larger than the effective concrete strength local confinement reinforcement is required to enhance the bearing strength. Design of this reinforcement is discussed in Step 7.

Using a non-hydrostatic local zone node (Section 3.4.5.2), the required depth of the node can be determined from Equation (3.1):

$$\begin{aligned} \text{required}(a_o/a) &= (f_b/f_c)/(2\sin \alpha \cos \alpha) - 1/(2\tan \alpha) = 7.85/6.24 \times 2.00 - 1.87 \\ &= 0.65 > 0.50. \end{aligned}$$

This is significantly higher than the initial assumption of $a_o/a = 0.50$ and a new iteration is required.

5. Repeat steps one through four.

$$\text{New assumption } a_o = 0.58a = 0.58 \times 6.5 = 3.77''$$

$$z = 10.5 - a_o/2 = 8.615''$$

$$\tan \alpha = 2.375/z = 0.276 \Rightarrow \alpha = 15.4^\circ$$

$$P_u = 2T_{\text{burst},1}/\tan \alpha = 2 \times 44.4/0.276 = 322.1 \text{ kips}$$

$$f_b = P_u/(ab) = 322.1/(6.5 \times 6.5) = 7.62 \text{ ksi}$$

$$\begin{aligned} \text{required}(a_o/a) &= (f_b/f_c)/(2\sin \alpha \cos \alpha) - 1/(2\tan \alpha) = 7.62/6.24 \times 1.95 - 1.81 \\ &= 0.57. \end{aligned}$$

This is close enough to the initial assumption and $P_u = 322$ kips.

6. Check the compressive stresses at the other nodes in the anchorage zone.

The remaining nodes in the anchorage zone are CTC nodes. The effective concrete strength at such nodes is taken as $f_c = 0.65 f'_c = 0.65 \times 5.3 = 3.45$ ksi. Therefore the minimum strut width is $P_u/(2f_c) = 322/(2 \times 9 \times 3.45) = 5.2$ in. This can be easily accommodated by the available width of 8 in. As shown in Figure 3.20 the inclined compression struts have to fan out slightly because the effective concrete strength is smaller at the CTC node than at the CCC node.

7. Design the local zone reinforcement.

Since the bearing pressure exceeds the effective concrete strength confining local zone reinforcement is required. This reinforcement will be designed using Robert's recommendations (Equations (2.2) and (2.3)).

$$P_n = 0.80 f'_c (A/A_b)^{1/2} A_b + 4.1 f_{lat} A_{core} (1 - s/D)^2$$

$$\text{required } P_n = 322 \text{ kips}$$

$$0.80 \times 5.3 \times (9/6.5) \times 6.5^2 = 248 \text{ kips} < 2f'_c A_b = 448 \text{ kips}$$

Therefore

$$4.1 f_{lat} A_{core} (1 - s/D)^2 \geq 322 - 248 = 74 \text{ kips.}$$

The largest spiral that can be accommodated in the cross section with 1 in. cover is $D = 7$ in. Choosing a #3 bar for the spiral and a pitch of $s = 1.25$ in the confining pressure becomes

$$f_{lat} = 2A_s f_y / (Ds) = 2 \times 0.11 \times 60 / (7 \times 1.25) = 1.51 \text{ ksi.}$$

This is larger than the maximum recommended value of 1.2 ksi and $f_{lat} = 1.2$ ksi will be used for subsequent calculations.

The enhanced bearing capacity is

$$\begin{aligned} P_n &= 248 + 4.1 \times 1.2 \times 7^2 \pi / 4 (1 - 1.25/7)^2 \\ &= 248 + 128 = 376 \text{ kips} < 3f'_c A_b = 672 \text{ kips.} \end{aligned}$$

This bearing capacity is well above the required capacity of 322 kips. The stiffness of the bearing plate need not be checked because the applied load is distributed over the full anchor plate. \therefore USE #3 spiral, $D = 7$ in., $s = 1\frac{1}{4}$ in.

8. Design the bursting reinforcement in the thin direction of the beam.

Bursting stresses also occur in the thin direction of the member (Figure 3.20). The magnitude of the bursting force is estimated using Equation (2.5).

$$T_{burst,2} = \frac{1}{4}P (1 - b/t) = 322/4 (1 - 6.5/9) = 22.4 \text{ kips}$$

The resistance provided per turn of the spiral in the local zone is

$$2 \times A_s f_y = 2 \times 0.11 \times 60 = 13.2 \text{ kips.}$$

Hence bursting force $T_{burst,2}$ can be easily accommodated by two turns of the spiral. For this purpose the length of the spiral should be at least equal to the thickness of the section, that is $\ell_c = t = 9$ in.

This completes the analysis and design for specimen Beam1. The predicted ultimate capacity based on the strut-and-tie model shown in Figure 3.20 is $P_u = 322$ kips.

The bursting reinforcement requirements become significantly higher if ϕ -factors are included in the calculations. The bursting reinforcement is affected directly by the ϕ -factor for steel and indirectly by the ϕ -factor for concrete. A lower ϕ -factor requires a deeper local zone node and thus reduces the lever arm z . For example, a ϕ -factor of 0.8 for both concrete and steel applied to the example discussed above increases the a_o/a ratio from 0.58 to 1.04. The bursting force increases from 44.4 kips to 53.9 kips for the same ultimate load $P_u = 322$ kips. Hence the bursting reinforcement requirement is increased by a factor of $(53.9/0.8)/44.4 = 1.52$. This problem does not occur with fan-shaped struts joining at the local zone node, because in that case the depth of the node is fixed by the dimensions of the bearing plate and by the rate of spreading of the compression stresses (Figure 3.19).

3.4.7.2 Effect of a Reaction Force in the Anchorage Zone

In this example the effect of a reaction force in the anchorage zone is investigated. The bursting force is calculated for the same beam as in the previous example. External loads on the anchorage zone are the tendon force $P_u = 322$ kips and a reaction force, V , equal to 10% of the tendon force acting at a distance of 5 in. from the loaded face. As in the previous example the concrete strength is 5300 psi and the centroid of the bursting reinforcement is located 10½ in. ahead of the anchor plate (Figure 3.21).

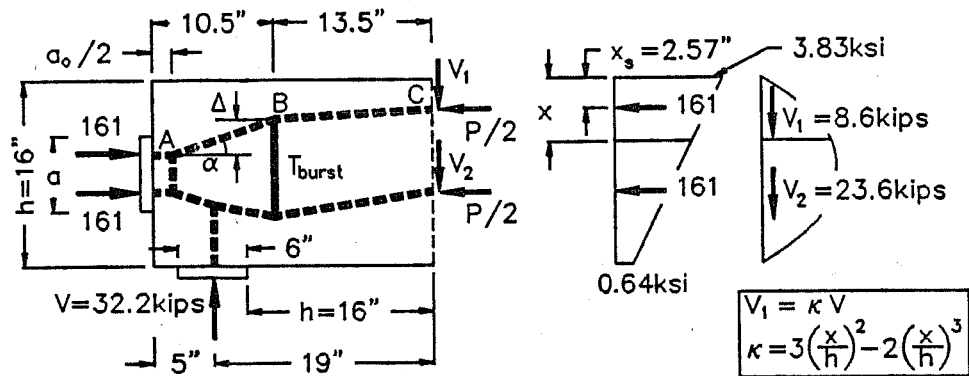


Figure 3.21 Strut-and-Tie Model for Anchorage Zone With Reaction Force

1. Determine the extent of the D-region.

The region affected by the introduction of the tendon force and of the reaction force extends for a distance equal to one beam height from the end of the bearing plate for the reaction force (Figure 3.21).

2. Determine the internal stresses and the resultant forces at the end of the D-Region.

The bending moment at the end of the D-region is $M = V \times 19 \text{ in.} = 32.2 \times 19 = 611.8 \text{ in.-kip}$. The normal force is $N = P_u = 322 \text{ kips}$. The flexural stresses can be determined from simple beam theory:

$$f = -N/A \pm M/S$$

With $A = 9 \times 16 = 144 \text{ in}^2$ and $S = 9 \times 16^2 = 384 \text{ in}^3$ the extreme fiber stresses are

$$f_{\text{top}} = -322/144 - 611.8/384 = -3.83 \text{ ksi}$$

$$f_{\text{bot}} = -322/144 + 611.8/384 = -0.64 \text{ ksi}$$

Next, the flexural stresses are integrated into two resultant compressive forces each carrying $P_u/2 = 161 \text{ kips}$. Solving a quadratic equation the distance x is found to be $x = 5.44 \text{ in.}$ The two struts pass through the centroids of the stress trapezoids. The inclination of the struts is found by assigning the corresponding portion of the shear force to each strut (Figure 3.21).

3. Select the location of the bursting tie.

The bursting tie is located at the same distance from the end face of the beam as in the previous example, which is $10\frac{1}{2} \text{ in.}$ or $0.66h$. It would also be acceptable to place the

bursting tie midway in the disturbed region at a distance of 12 in. or 0.75h from the end face.

4. Make an initial guess for the depth of the local zone node.

As a first guess the depth of the local zone node is taken as $a_o = 0.55a = 3.58$ in.

5. Determine the lever arm z and the strut inclination α .

The geometry of struts A-B-C is now fully determined and the strut angle α can be readily determined (Figure 3.21).

$$z = 10.5 - a_o/2 = 10.5 - 3.58/2 = 8.713''$$

$$\Delta = (h/2 - x_s - V_1/(P_u/2) \times 13.5) - a/4 = 3.08''$$

$$\tan \alpha = \Delta/z = 0.354 \Rightarrow \alpha = 19.5^\circ$$

6. Determine the required depth of the local zone node.

As in the previous example the bearing pressure is $f_b = 7.62$ ksi and the effective concrete strength at the local zone node is $f_c = 6.24$ ksi. As before, local zone reinforcement is required to enhance the bearing strength of the concrete. From Equation (3.1) the required depth of the local zone node is found.

$$a_o/a = (f_b/f_c)/(2\sin \alpha \cos \alpha) - 1/(2\tan \alpha) = 7.62/6.24 \times 1.59 - 1.41 = 0.53$$

This required a_o/a is smaller than the initially assumed value, hence the solution is safe. Further iteration through steps three to five to reduce the depth of the local zone is optional. If the calculated a_o/a ratio is larger than the initially assumed value the solution is unsafe and further iteration is necessary.

The local zone node is the most critical node in the anchorage zone. The next critical location is at node B (Figure 3.21). Strut BC carries a compressive force of 161.2 kips. With the effective concrete strength $f_c = 0.65 f'_c = 0.65 \times 5.3 = 3.45$ ksi and the member thickness $t = 9$ in., the required strut width at this node is $w = 161.2/(9 \times 3.45) = 5.2$ in. which can be easily accommodated within the boundaries of the structure.

7. Calculate the bursting force.

Once the angle α is established, the bursting force can be readily calculated from equilibrium conditions at node B.

$$T_{burst} = P_u/2 \tan \alpha - V_1 = 161 \times 0.354 - 8.61 = 48.4 \text{ kips}$$

This is about 10% higher than the bursting force in the previous example where no reaction force was present in the anchorage zone. However, if the location of the bursting tie is selected midway in the disturbed region, that is 12 in. ahead of the bearing plate, similar

calculations as above lead to a bursting force of 41.4 kips. This is about 8% lower than the bursting force calculated when no reaction force is present.

Design of the local zone reinforcement and of the bursting reinforcement in the thin direction of the member is exactly the same as in the previous example.

3.4.8 *Conclusions*

The discussions and examples in the foregoing sections illustrate the sensitivity of the magnitude of the bursting force to the geometry of the strut-and-tie model. The most efficient geometry has the local zone nodes as close as possible to the anchor plate and the bursting tie as far removed as possible. The location of the center of the local zone nodes is determined by the effective concrete strength, the size of the anchor plate, and the inclination of the joining struts. A limit should be placed on the distance of the bursting tie from the anchor plate. This limitation is motivated by the need to place bursting reinforcement where cracking initiates in order to minimize stress redistributions and crack widths. A uniform arrangement of the bursting reinforcement between a distance of $0.15h'$ and $1.25h'$ ahead of the anchor plate is suggested, where h' is the width of Guyon's symmetrical prism. For the range of variables investigated, the effect of a reaction force in the anchorage zone was not very significant and can be ignored safely.

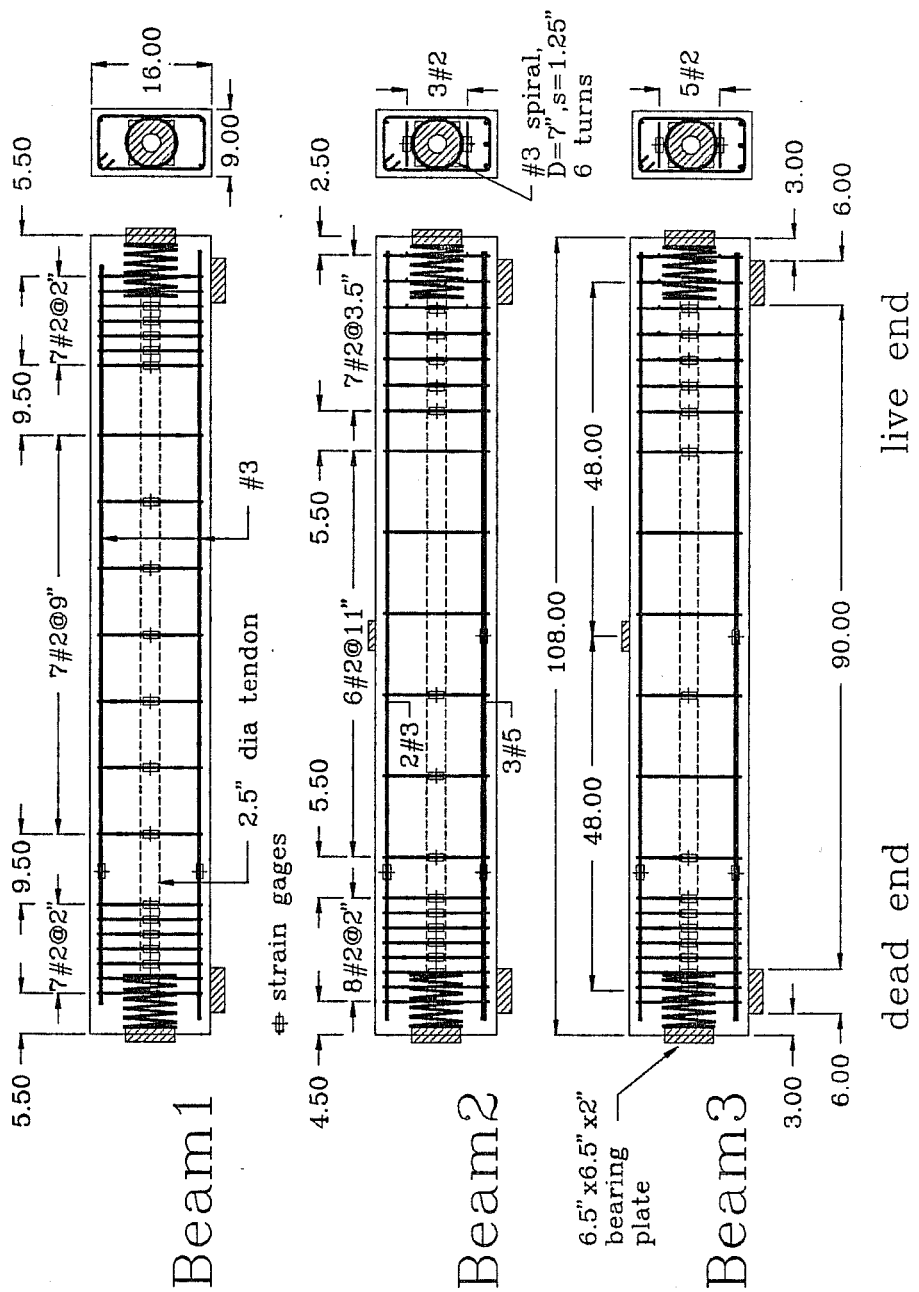
3.5 **Experimental Program**

3.5.1 *General*

The experimental program included three specimens, labeled Beam1, Beam2, and Beam3. These specimens were patterned after Sanders' specimen B3 described in Section 3.2.2.2. Dimensions and details are shown in Figure 3.22. Specimen Beam1 was subjected to a concentrated tendon force only. Specimens Beam2 and Beam3 were designed to investigate the effect of a reaction force in the anchorage zone. Therefore, in addition to the tendon force a vertical concentrated load was applied at midspan (Figure 3.23). The shear span for these beams was 48 in. or three times the depth of the cross section.

3.5.2 *Materials and Fabrication*

All specimens were fabricated in the laboratory. Concrete was delivered from a local ready-mix plant. The concrete strength was monitored periodically until the desired strength



all dimensions in inches

Figure 3.22 Dimensions and Details for Beam Specimens

for testing was reached. Table 3.2 lists the concrete cylinder compressive strengths at the day of testing. Specimen Beam3 was added to the experimental program after specimen Beam2 developed an excessively high concrete strength. Reinforcement sizes #3 and larger were standard ASTM A615 GR60 steel. Instead of #2 bars Swedish reinforcement bars with 6 mm diameter, an area of 0.044 in^2 , and a yield strength of 72 ksi were used. Sanders used Mexican 6 mm diameter bars with a measured yield strength of 44.9 ksi in specimen B3.

Table 3.2 Concrete Strengths of Beam Specimens

specimen	f'_{cl} (psi)
B3*	5400
Beam1	5300
Beam2	7500
Beam3	5100

*) specimen tested by Sanders [44]

2-5/8 in. diameter corrugated steel duct was used for the tendons, which allowed a maximum of 12 tightly packed 1/2 in. prestressing strands to be inserted. A straight tendon layout was chosen to minimize friction losses between live and dead end. However, in specimen Beam1 the tendon duct deflected upwards about one inch during concrete casting causing a slight tendon curvature. Friction losses due to this curvature were estimated to be around 5% of the stressing force. In specimens Beam2 and Beam3 deflection of the duct was prevented by inserting a stiff steel pipe during casting.

3.5.3 Specimen Design

The design axial load, F_{pu} , was 284 kips for all specimens. This load is approximately equal to the breaking strength of a 7-1/2 in. strand tendon, GR 270. The design vertical load for specimens Beam2 and Beam3 was 56.8 kips, which results in a reaction force equal to 10% of the axial load at each support. Design of the bursting reinforcement was based on simple strut-and-tie models and on Equation (2.5). In these early applications of strut-and-tie modelling techniques the location of the local zone node was not optimized and hence the selected bursting reinforcement is conservative. Table 3.3 shows magnitude and location of the bursting force used for proportioning and arranging the reinforcement.

Two different bursting reinforcement arrangements were tested (Table 3.3, Figure 3.22). One arrangement had a bursting force capacity T_{burst} equal to 50.7 kips and

the centroid of the bursting reinforcement was located 10½ in. ahead of the end face of the bearing plate. In the other arrangement the bursting force was located further ahead of the bearing plate at a distance of 12 in. A smaller bursting force, T_{burst} equal to 44.4 kips, is sufficient to achieve approximately the same ultimate load capacity (Table 3.7). Outside the bursting regions minimum shear or tie reinforcement was provided.

The spirals used in the local zones of the specimens had the same dimensions as the spiral used by Sanders in specimen B3 except for the bar size which was reduced from a #4 bar to a #3 bar. The reduction in bar size was motivated by Robert's recommendation to limit the lateral pressure provided by the confinement reinforcement, f_{lat} , to 1.2 ksi, which can be easily accomplished with a #3 bar (Sections 2.2.2 and 3.4.7). In specimen Beam1 and in one end of specimens Beam2 and Beam3 the spiral was relied on to carry the lateral bursting force in the thin direction of the beam. In the other anchorage zones lateral bursting reinforcement was provided. Specimen Beam2 had six lateral ties and specimen Beam3 had ten lateral ties (Figure 3.22).

Four #3 bars, one in each corner, were provided as longitudinal reinforcement in specimen Beam1. In specimens Beam2 and Beam3 the bottom bars were three #5 bars to preclude failure in midspan.

3.5.4 Test Procedure and Measurements

All specimens were loaded axially through the tendon. The vertical load in specimens Beam2 and Beam3 was applied with a 60 ton hydraulic ram. Figure 3.23 and Figure 3.24 show the test set-up for the vertically loaded specimens.

Specimen Beam2 was initially loaded at a V/P ratio between 0.05 and 0.06, where

Table 3.3 Magnitude and Location of the Design Bursting Forces

Specimen	T_{burst} (kips)	d^*_{burst} (in)
B3**	39.6	10.5
Beam1	44.4	10.5
Beam2 (LE)	44.4	12
Beam2 (DE)	50.7	10.5
Beam3 (LE)	44.4	12
Beam3 (DE)	50.7	10.5

*) measured from embedded face of bearing plate

**) from Reference 44

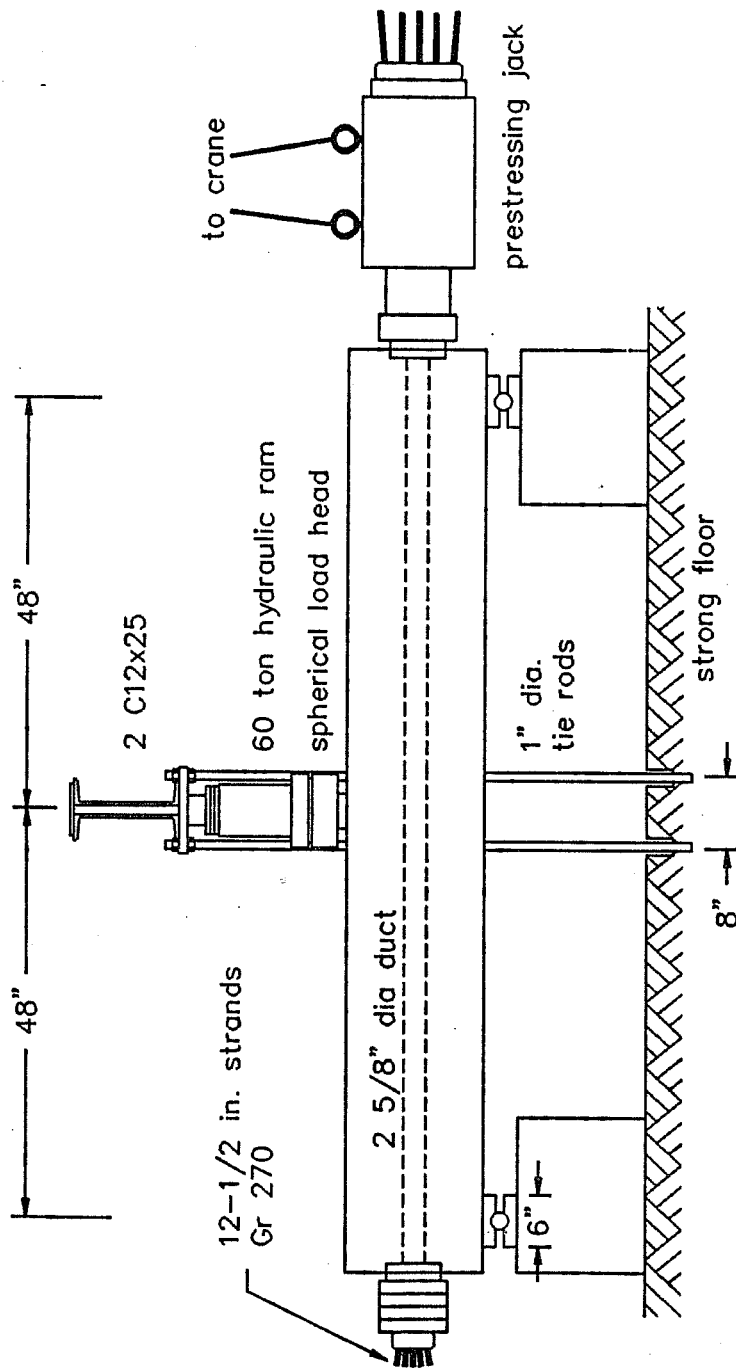
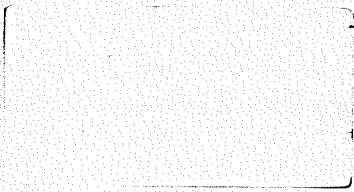
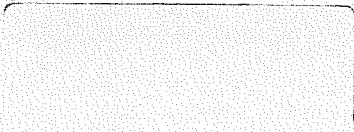


Figure 3.23 Test Set-Up for Beam Specimens



All Run

23 Texas Seals, Signs & Symbols (cont.) XXV



B-650



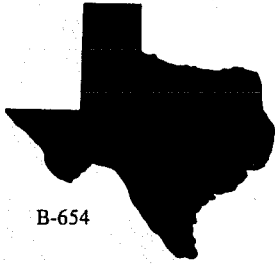
B-651



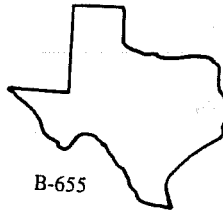
B-652



B-653



B-654



B-655



B-656



B-657

24

Maps & Globes



C-200



C-201



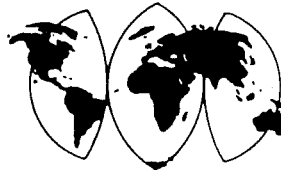
B-658



B-659



B-660



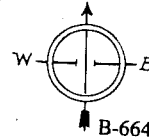
B-661



B-662



B-663



B-664

25

Sunsets, Vistas, Stars & Planets



B-665



C-202



B-666



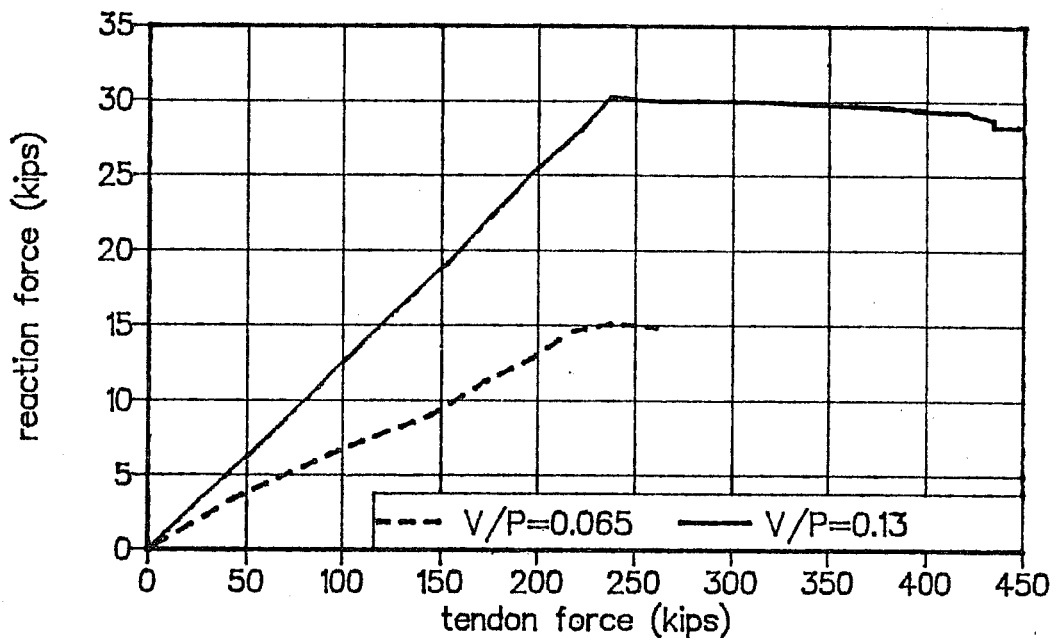


Figure 3.25 Load History for Specimen Beam2

3.6 Presentation of Test Results

3.6.1 Crack Development

Table 3.4 lists first cracking, first yield, and ultimate loads for Sanders' specimen B3 and for the beam specimens of this series. All loads are expressed in terms of the design load, F_{pu} . The higher values for specimen Beam2 are due to its significantly higher concrete strength (Table 3.2). The lower first yield load in Sanders' specimen B3 is due to the use of Mexican #2 bars with a lower yield stress (45 ksi) in this specimen. Except for Sanders' isolated anchorage zone specimen none of the specimens experienced cracking under service loads ($0.8 F_{pu}$).

Figures 3.26, 3.27, and 3.28 show crack development and final crack pattern for specimens Beam1, Beam2, and Beam3, respectively. For all specimens anchorage zone cracking initiated at some distance ahead of the anchor plate and propagated in both directions towards and away from the anchor plate. First cracking loads are listed in Table 3.4. The bursting cracks extended as far as 26 in. or approximately one and one-half times the height of the beam ahead of the anchor plate prior to failure.

The crack pattern at the dead end side of specimen Beam1 which had no vertical

Table 3.4 First Cracking, First Yield and Ultimate Loads for Beam Specimens

specimen	F_{pu} (kips)	1 st cracking load (% F_{pu})	1 st yield load (% F_{pu})	ultimate load (% F_{pu})
B3 *	284	0.76	0.83	1.17
Beam1 (LE)	284	0.88	1.04	1.11
Beam1 (DE)	284	0.88	-	-
Beam2 (LE)	284	1.13	1.57	-
Beam2 (DE)	284	1.06	1.38	1.57
Beam3 (LE)	284	0.84	1.25	1.34
Beam3 (DE)	284	0.99	-	-

*) Reference 44

load applied was symmetric with respect to the tendon axis (Figure 3.26). Cracking of the live end anchorage zone was unsymmetric. The crack pattern seems to be influenced by a weak layer of concrete at the top of the beam or by an accidental loading eccentricity or tendon inclination. In specimens Beam2 (Figure 3.27) and Beam3 (Figure 3.28) the bursting cracks were inclined due to the influence of the reaction force in the anchorage zone. In specimen Beam3 additional cracking occurred at the end faces of the beam at about 85% of the failure load.

Figure 3.29 shows the development of maximum crack widths. In specimen Beam2 the crack widths on the left and right side of both anchorage zones started to diverge at approximately 85% of the failure load. Maximum crack widths remained below 0.03 in. in all specimens.

3.6.2 Ultimate Loads and Failure Mode

Specimens Beam1 and Beam3 failed at the live end while specimen Beam2 failed at the dead end. The relative tendon loads at failure are listed in Table 3.4. In specimens Beam2 and Beam3 a vertical load of approximately 60 kips acted simultaneously with the tendon load at failure. The failure mode was identical for all three specimens. The concrete outside the ties and the spiral in the anchorage zone spalled off (Figure 3.30) and the

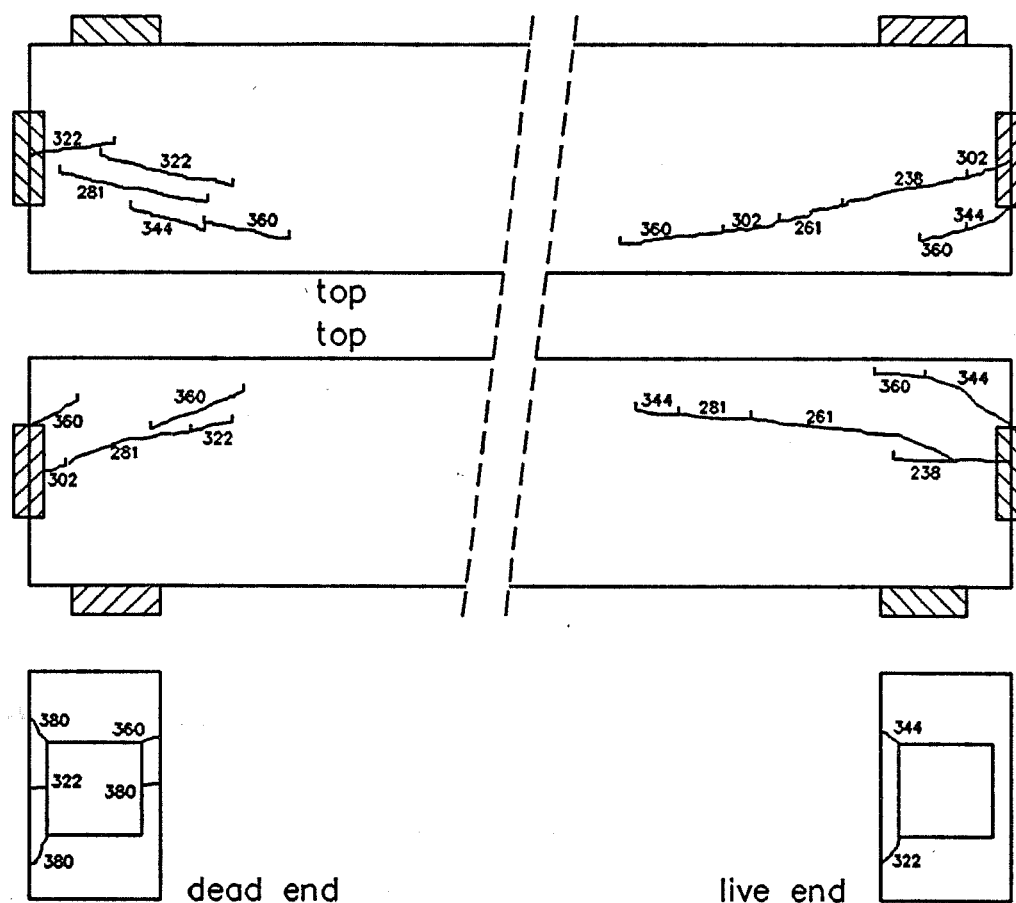


Figure 3.28 Crack Pattern for Specimen Beam3

concrete ahead of the spiral was crushed completely (Figure 3.31). The concrete confined by the spiral formed a plug which punched in up to two inches at failure. The plug completely separated from the surrounding material and a thin layer of pulverized concrete was noticed on the skin of this plug (Figure 3.32). Removal of all loose concrete revealed a cone ahead of the spiral typical for compression failures of unconfined concrete (Figure 3.33). The concrete within the plug was in good condition and plug and cone could be removed easily from the specimen (Figure 3.34).

Failures occurred with little warning and were explosive, particularly for specimen Beam2 with its high concrete strength (Figure 3.35). One of the concrete pieces ejected from specimen Beam2 had a weight of 10 lbs. and was thrown for a distance of 18 feet. As seen in Figure 3.29 most anchorage zone cracks remained smaller than 0.02 in. prior to

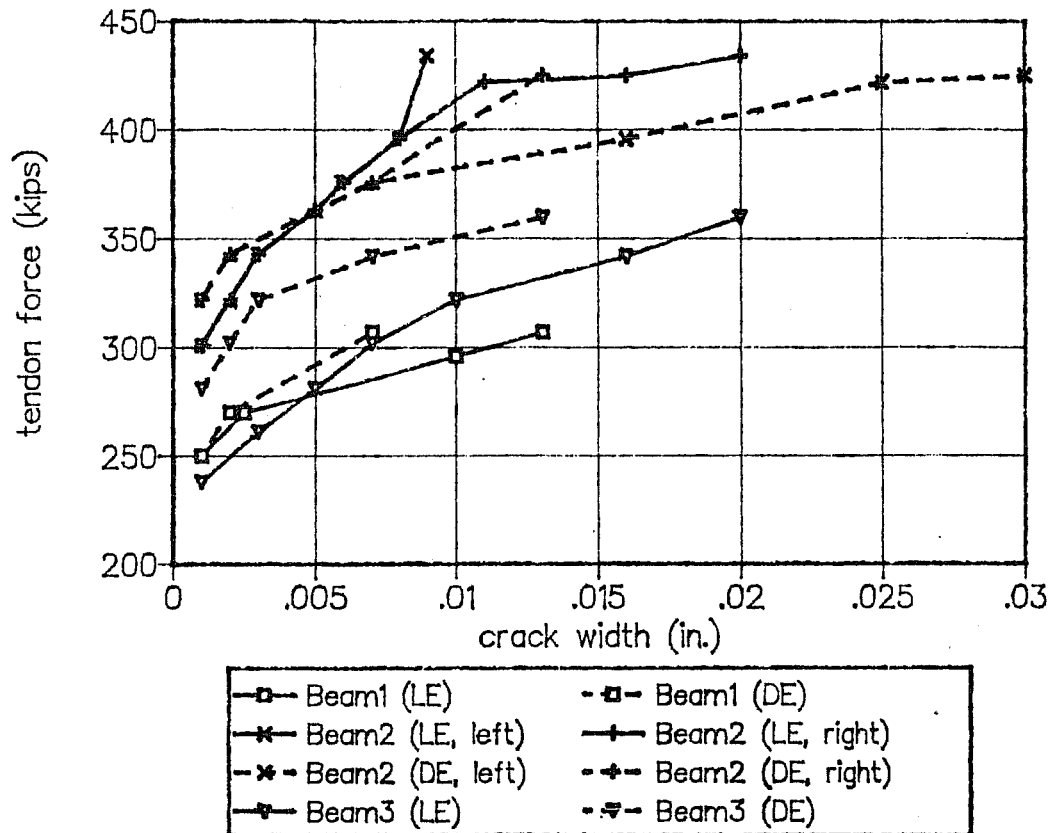


Figure 3.29 Crack Width Development in Beam Specimens

failure. Figure 3.36 shows load-bearing plate displacement curves for specimens Beam2 and Beam3. Prior to failure the bearing plates had punched into the beams less than 1/10 of one inch.

3.6.3 Transverse Bursting Strains

Figures 3.37 and 3.38 show the development of the vertical or transverse bursting strains at live and dead end of specimen Beam1. First cracking in specimen Beam1 occurred at both ends at a tendon force of 250 kips and was associated with a sudden jump of bursting strains at the dead end side (Figure 3.38). However, at the live end side the increase was gradual and did not occur until a tendon load of 300 kips, that is 95% of the failure load, was applied (Figure 3.37). This is due to the fact that the strain gages were arranged along the tendon path, whereas the bursting cracks at the live end side were

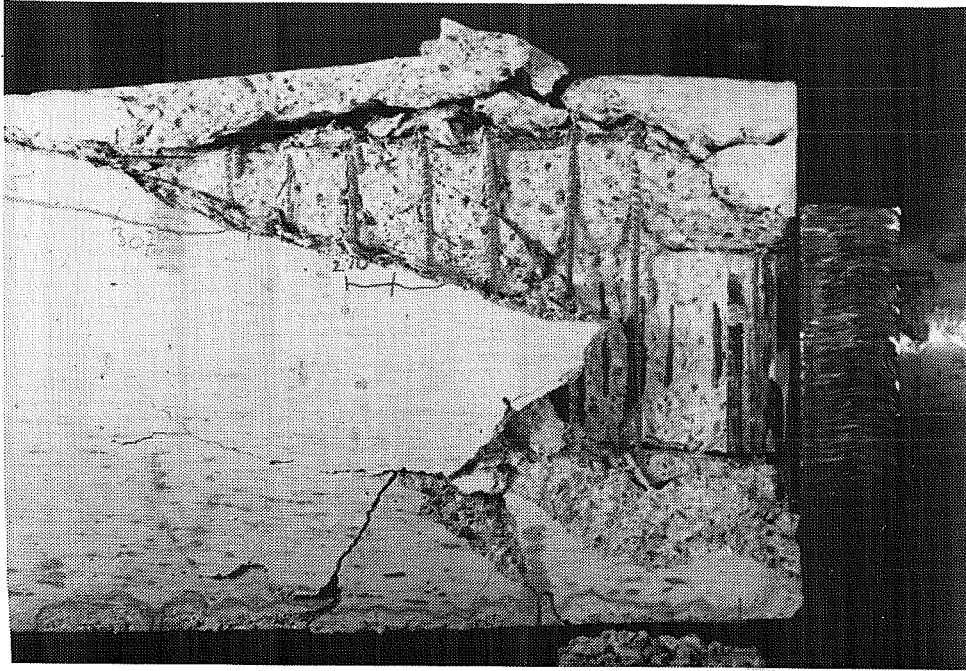


Figure 3.30 Spalling of Concrete Cover (Specimen Beam1)



Figure 3.31 Crushing of Concrete Around the Spiral (Specimen Beam2)

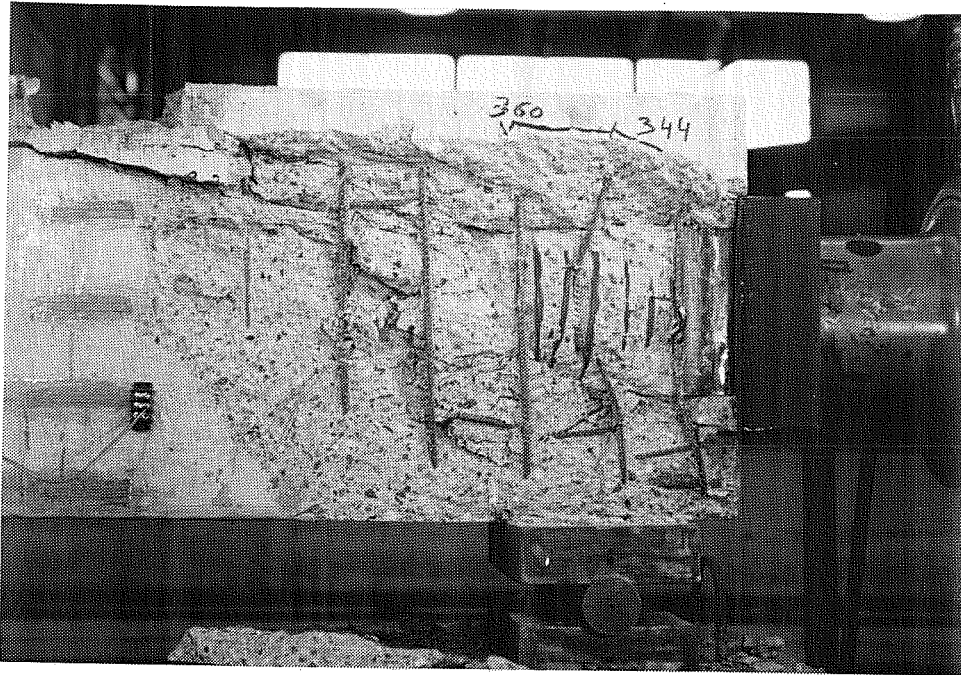


Figure 3.32 Concrete Plug Punched into Beam (Specimen Beam3)

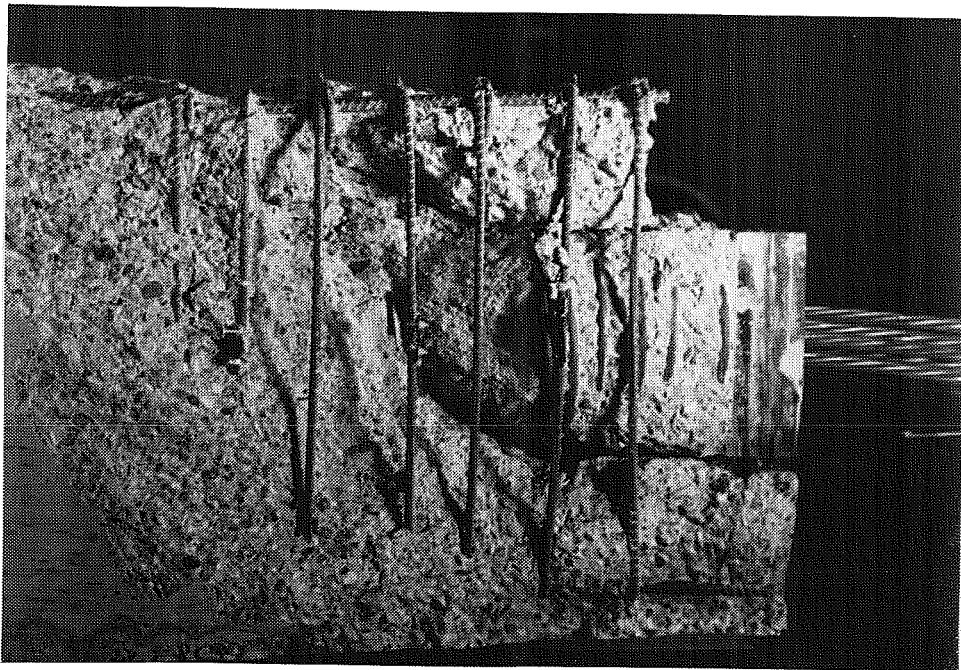


Figure 3.33 Failure Cone ahead of Spiral (Specimen Beam1)

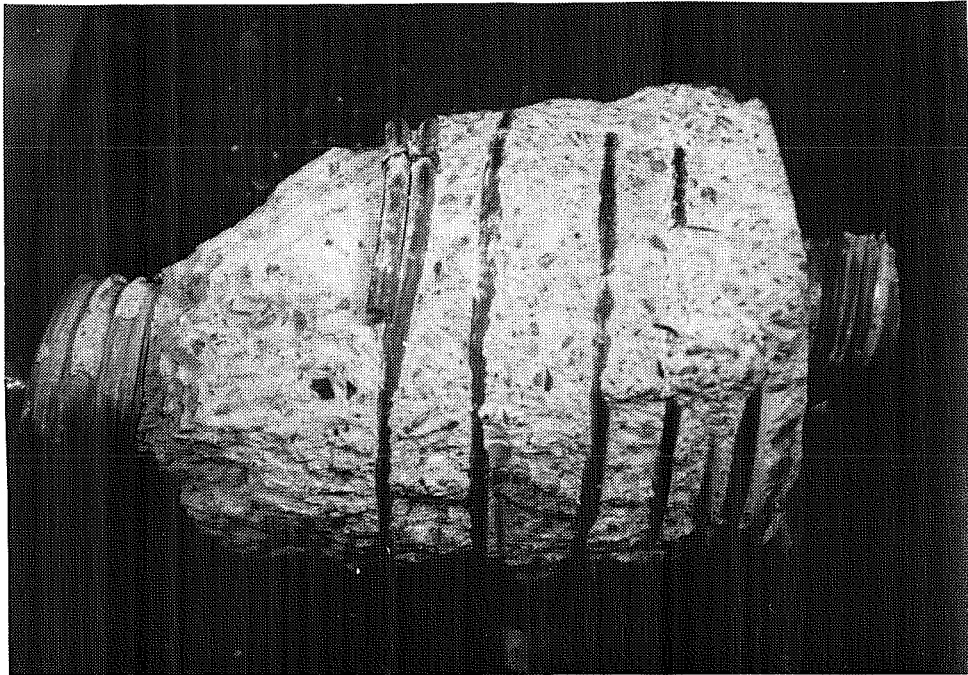
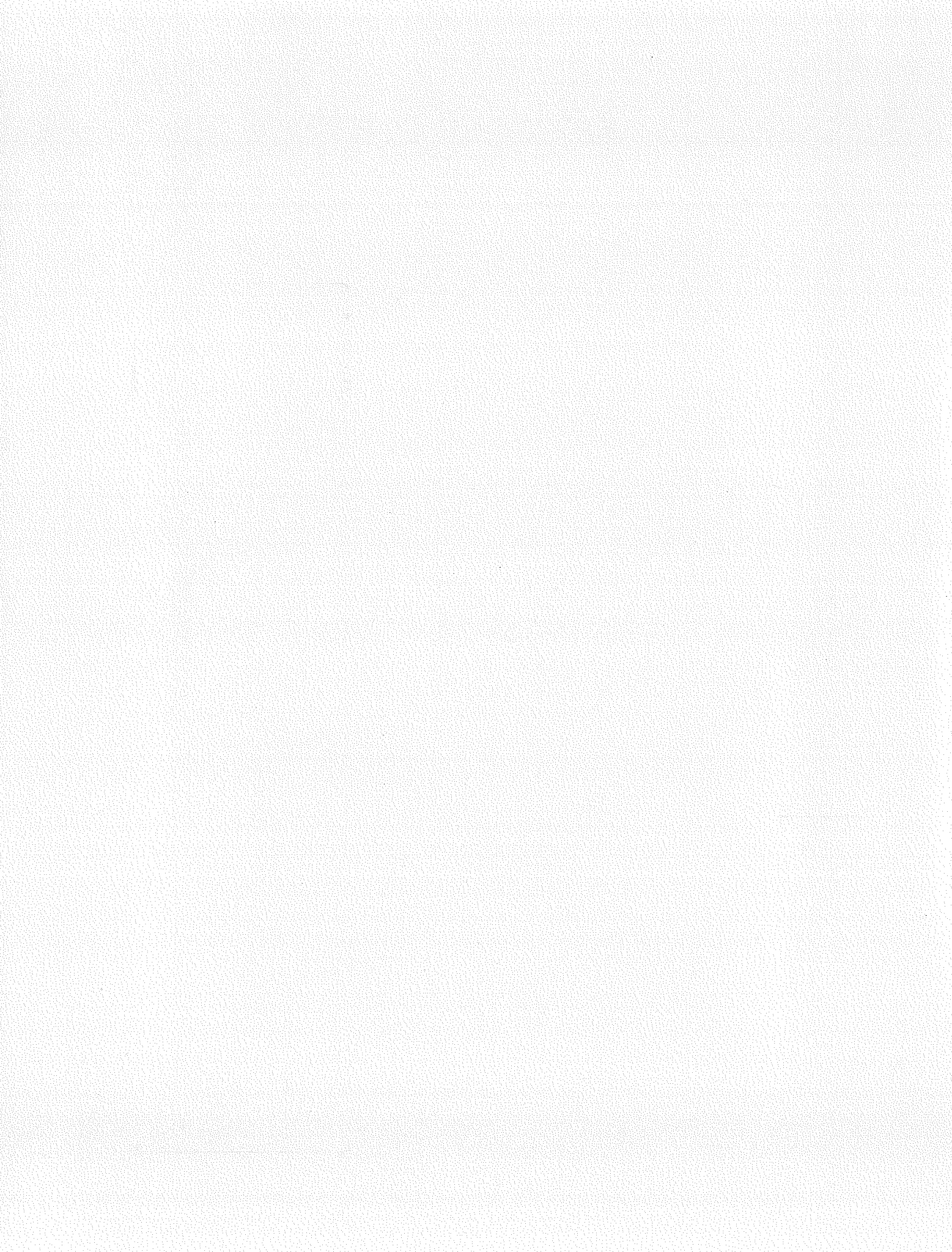


Figure 3.34 Concrete Plug Removed from Specimen Beam3



Figure 3.35 Explosive Failure of Specimen Beam2



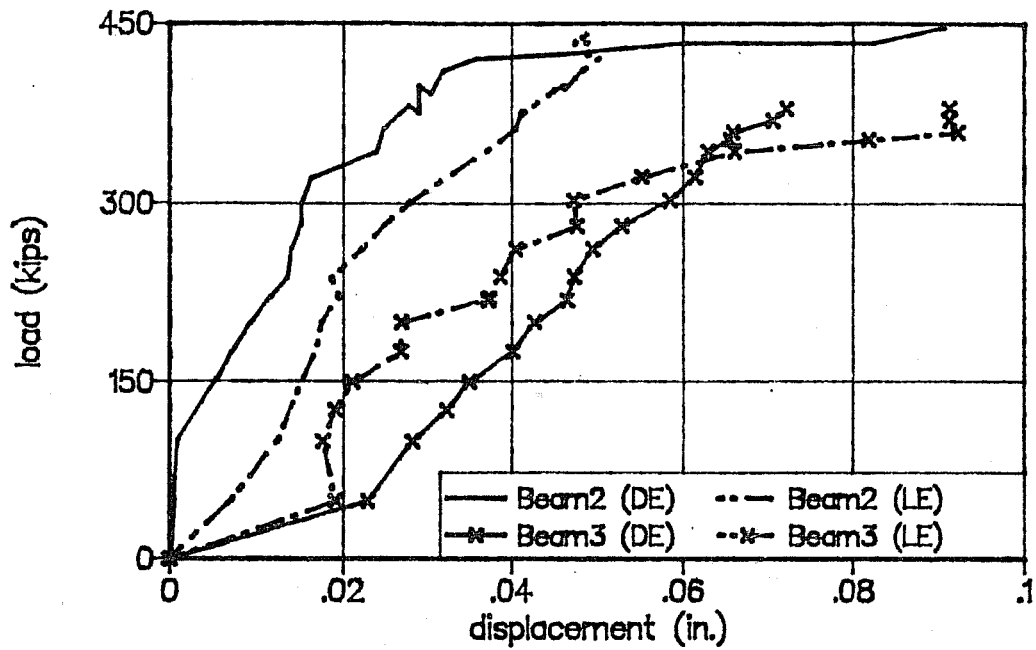


Figure 3.36 Load-Bearing Plate Displacement Curves for Specimens Beam2 and Beam3

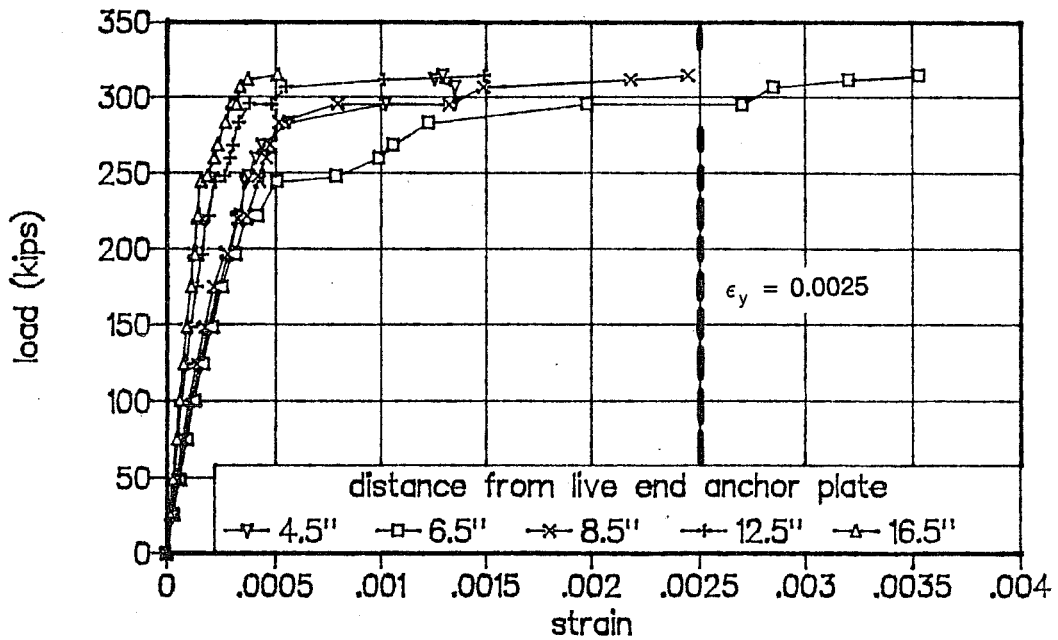


Figure 3.37 Live End Bursting Strains in Specimen Beam1

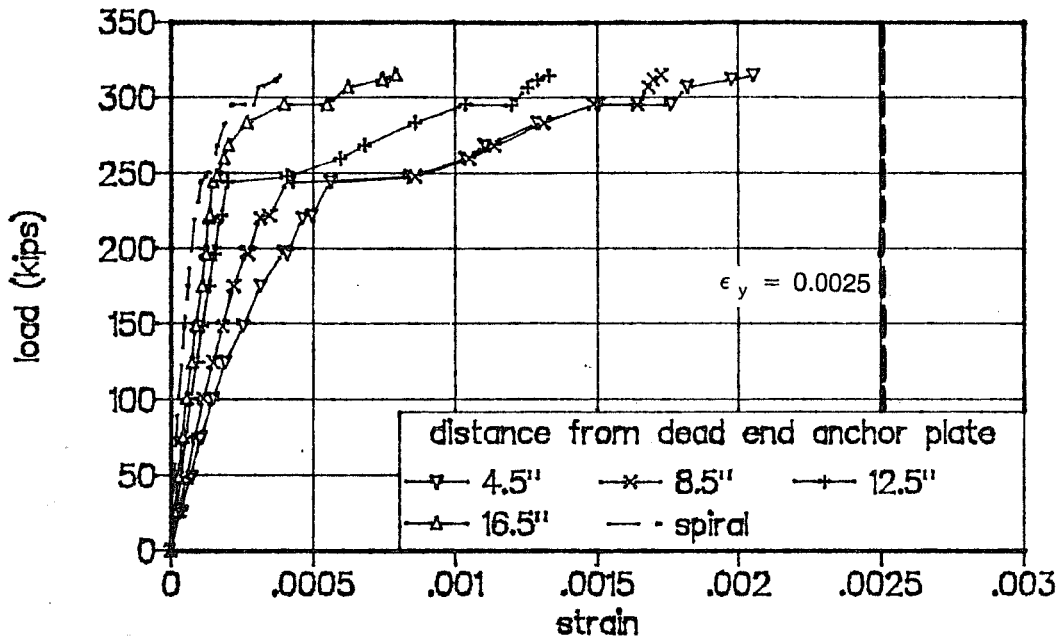


Figure 3.38 Dead End Bursting Strains in Specimen Beam 1

inclined and hence did not pass through the location of strain gages. A similar observation was made for specimens Beam 2 and Beam 3 which had inclined anchorage zone cracking due to the presence of the reaction force. Increase of the bursting reinforcement strain rate initiated at 90% to 95% of the failure load.

Figures 3.39, 3.40, and 3.41 show the measured tie strains throughout the specimens at various load stages. The region affected by the introduction of the tendon force extends for about 16 in. or a distance equal to the height of the beam for specimen Beam 1. This distance was 24 in. or one and one-half times the beam height for specimens Beam 2 and Beam 3 where a reaction force was present in the anchorage zone. First yielding of the bursting ties occurred at 85% to 95% of the failure load (Table 3.4). Associated crack widths were 0.01 in. to 0.02 in. Peak strains were measured 4 in. to 8 in. ahead of the bearing plates and diminished rapidly with the distance from the anchor. Only one or two bursting ties in the anchorage zone yielded prior to failure. In contrast, in Sanders' isolated anchorage zone specimen B3 all of the bursting reinforcement had yielded or was close to yielding at ultimate load (Section 3.2.2). Figure 3.42 illustrates this more clearly with a comparison of the bursting ties strains in the live end anchorage zone of specimen Beam 1

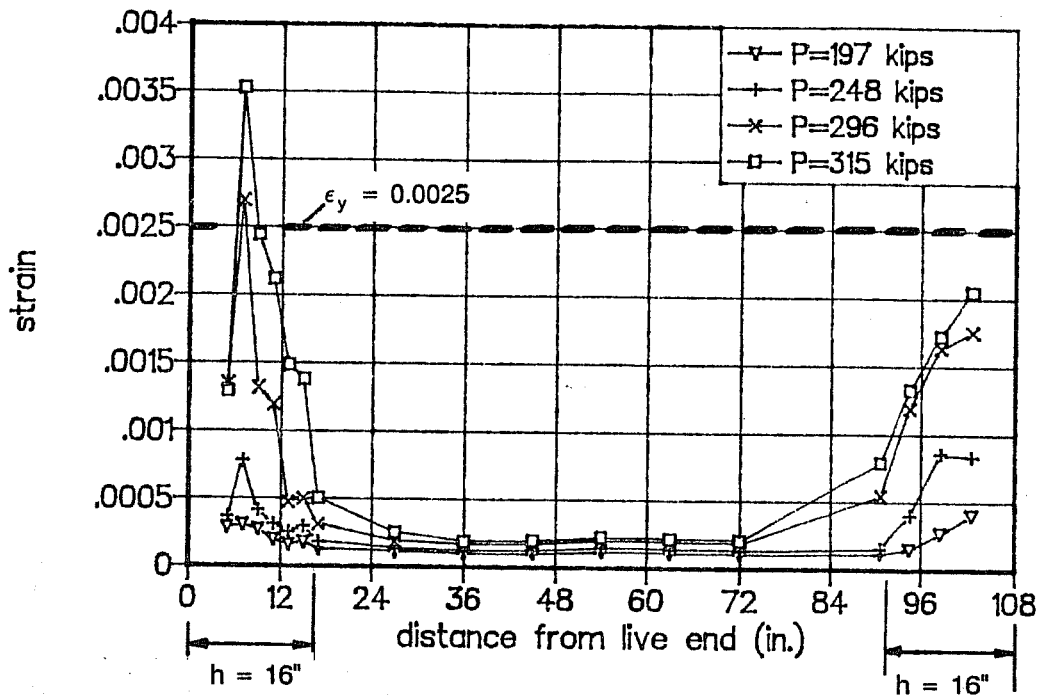


Figure 3.39 Tie Strains in Specimen Beam 1

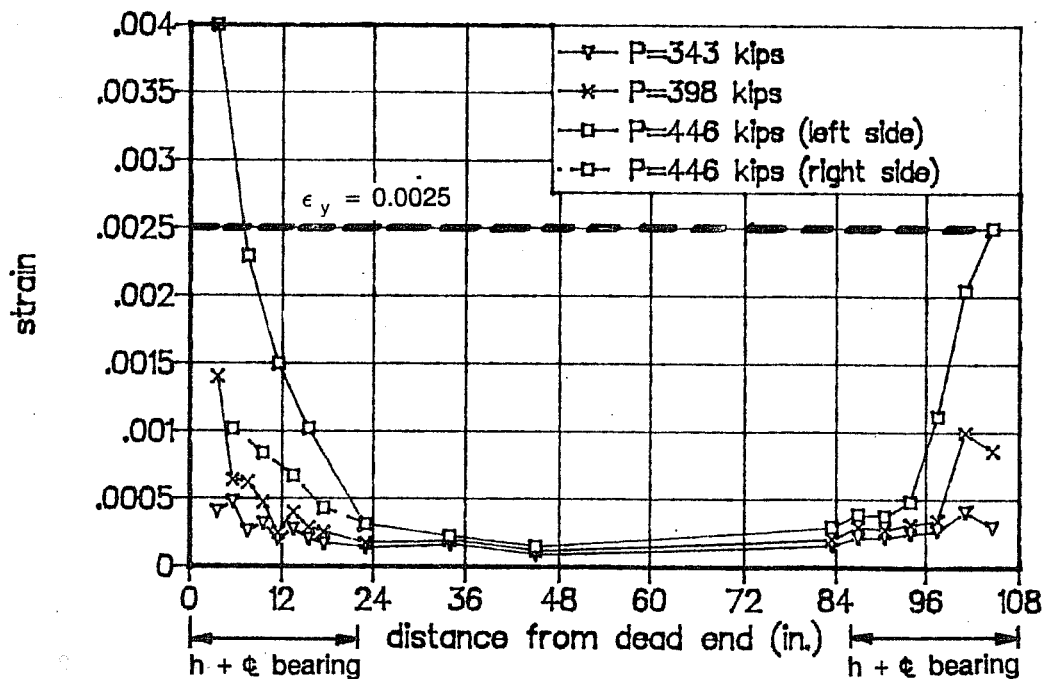


Figure 3.40 Tie Strains in Specimen Beam 2

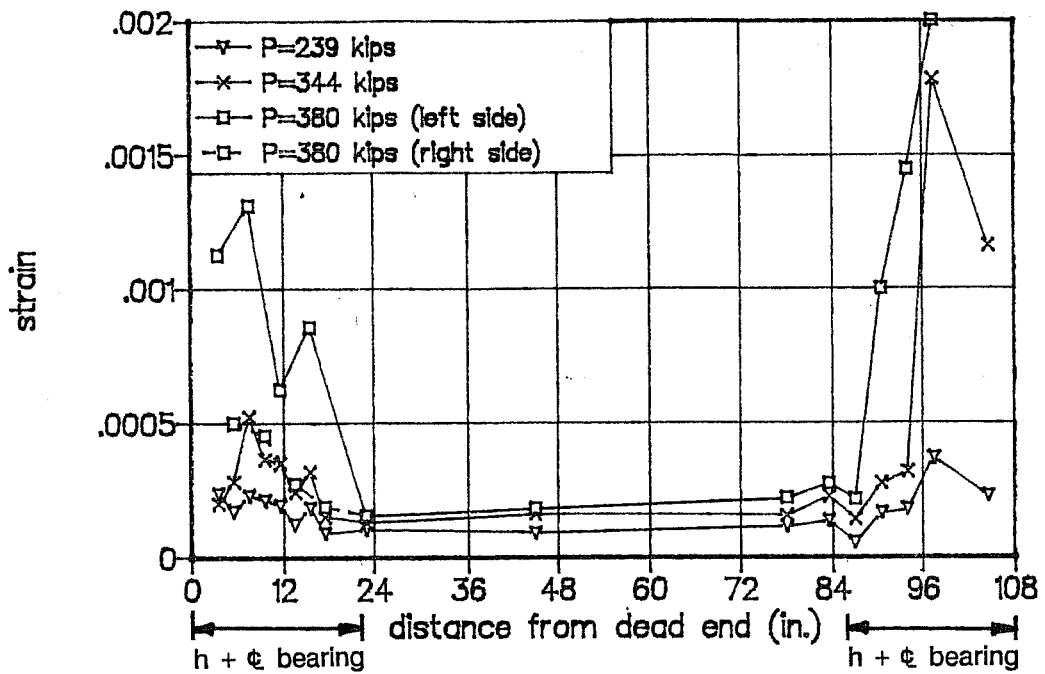


Figure 3.41 Tie Strains in Specimen Beam3

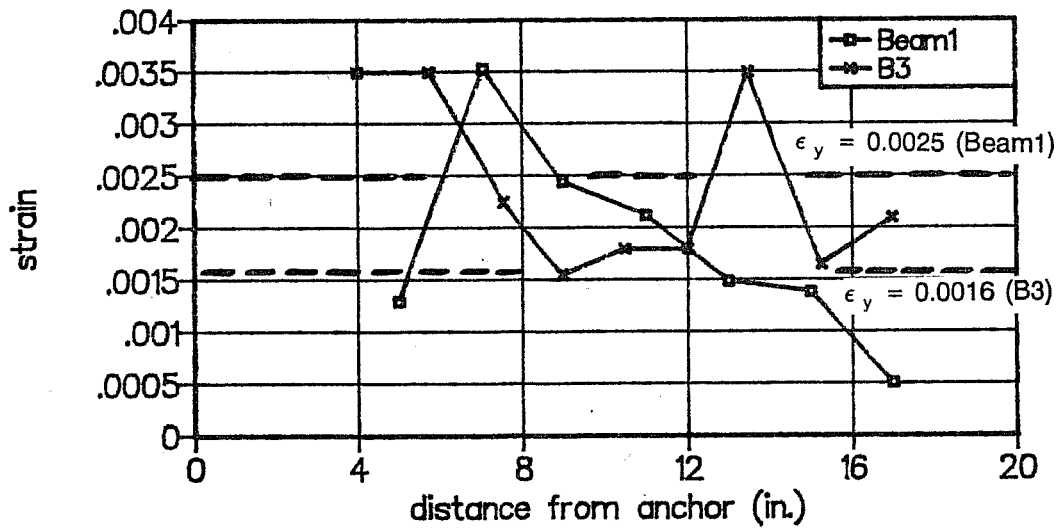


Figure 3.42 Comparison of Bursting Strains in Specimens Beam1 and B3

and in specimen B3 at a tendon force of 315 kips. The lower first yield load in specimen B3 is due to the use of Mexican #2 bars with a lower yield strength of 45 ksi, where the beam specimens had 72 ksi Swedish reinforcement.

The next series of figures illustrates the influence of a reaction force in the anchorage zone. Figure 3.43 shows the tie strains in Beam2 at a tendon load of 237 kips and two different reaction forces. Doubling the reaction force reduces the tie strains marginally. Figure 3.44 shows a comparison of the tie strains in specimens Beam1 and Beam3 at roughly the same tendon force. No reaction force was present in specimen Beam1. The figure indicates a beneficial effect of the reaction force. However, if load stages relative to the failure load are compared, rather than absolute values, this influence is less obvious (Figure 3.45).

3.6.4 *Lateral Bursting Strains*

In Figure 3.46 the lateral bursting strains in the thin direction of the member just prior to failure are plotted for specimens Beam2 and Beam3. The strains remained small within the region of the spiral reinforcement, but reached about half the yield strain immediately ahead of the spiral. The spiral strains never exceeded 500 micro strains (25% of yield) in any specimen.

3.6.5 *Compressive Strains*

Figure 3.47 shows the measured strain distribution over the height of the beam 24 in. (one and one-half times the height of the beam) ahead of the live end anchor in specimen Beam2 at a load of 398 kips (90% of the failure load). The calculated strain distribution, shown as dash-dot line, is based on simple beam theory and assuming a modulus of elasticity equal to $57\sqrt{f'_c} = 4940$ ksi. Agreement is good. The compressive strain distribution 24 in. ahead of the dead end anchor shows a discrepancy between the strains on the left-hand side and on the right-hand side of the beam, indicating a lateral eccentricity of the tendon force (Figure 3.48). An eccentricity of $\frac{1}{4}$ in. is sufficient to cause this difference in strains. Eccentricities of such small magnitude are extremely difficult to avoid but affect the behavior of the anchorage zone adversely. Similar measurements for specimen Beam3 confirm that simple beam theory is valid at a distance equal to one and one-half beam heights, even if bursting cracks have propagated for the same distance.

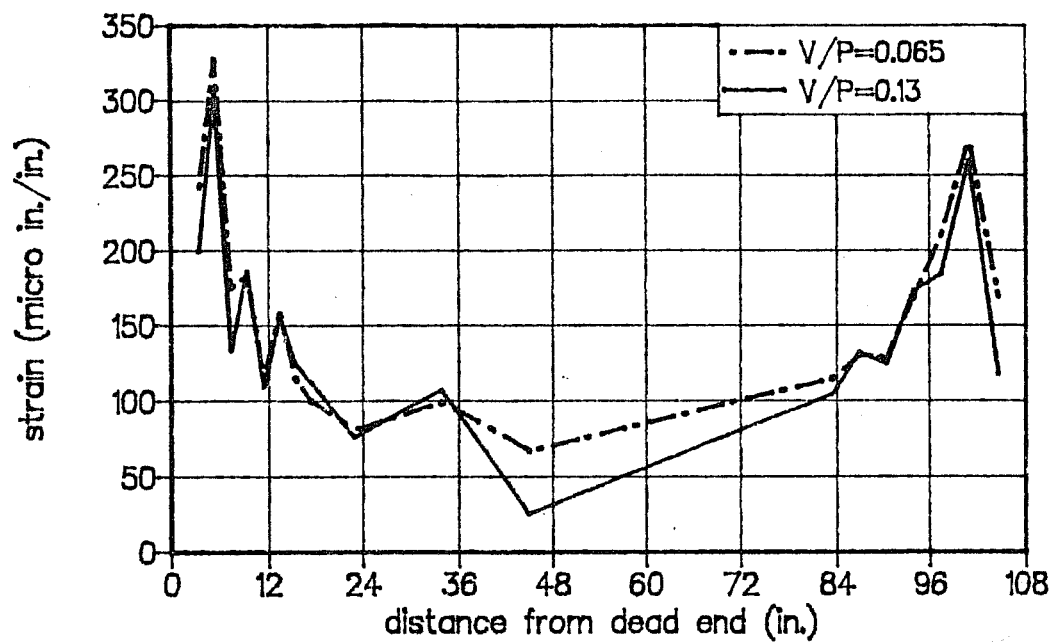


Figure 3.43 Comparison of Tie Strains in Specimen Beam2

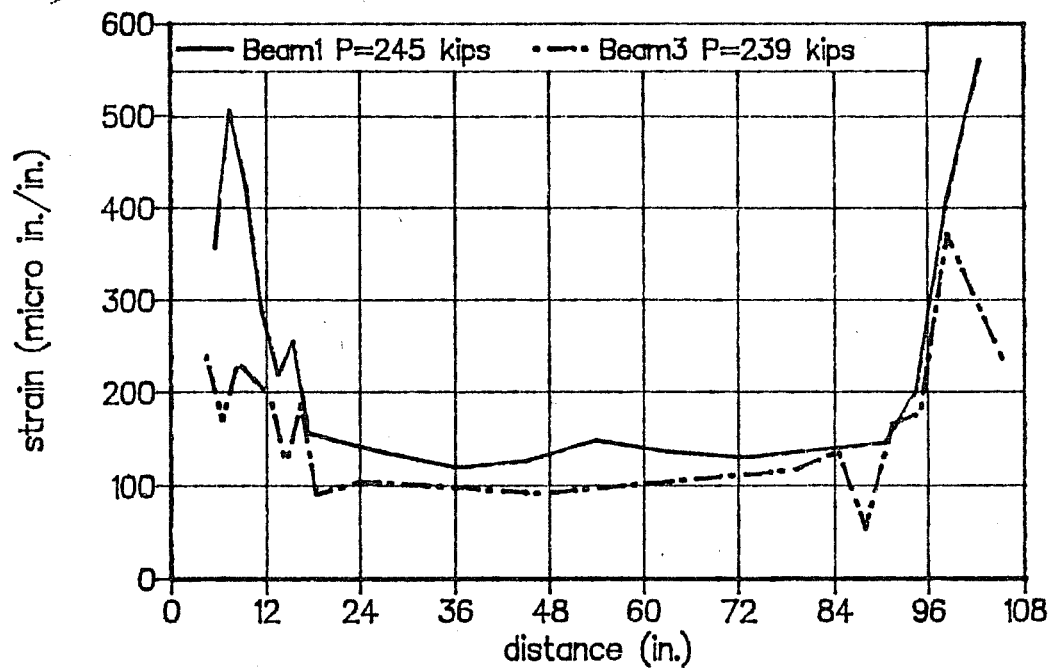


Figure 3.44 Comparison of Tie Strains in Specimens Beam1 and Beam3

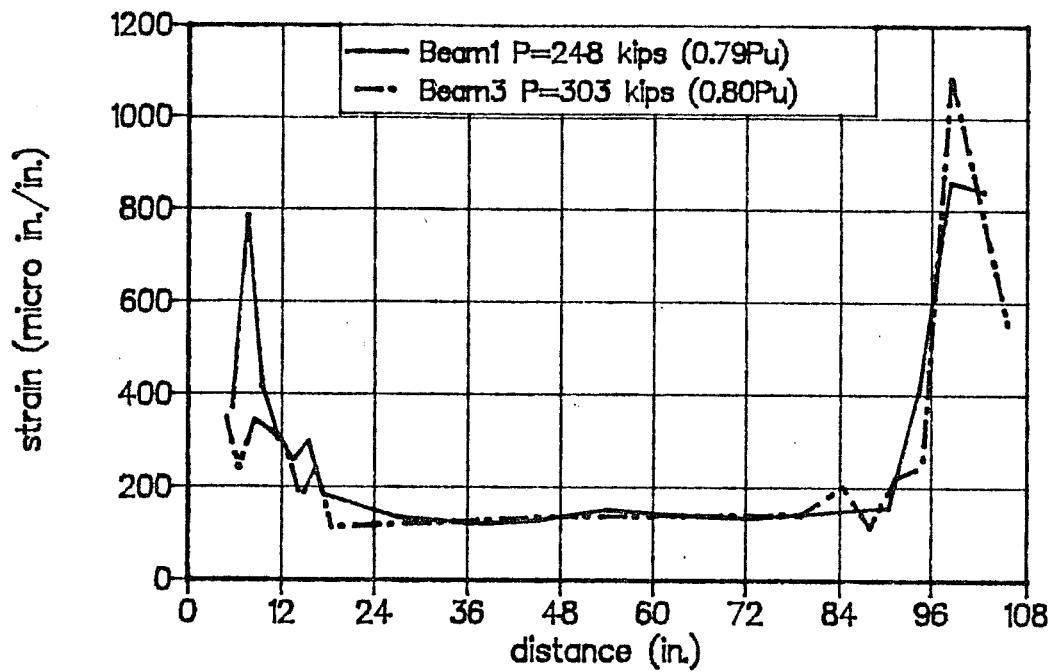


Figure 3.45 Comparison of Tie Strains in Specimen Beam1 and Beam3

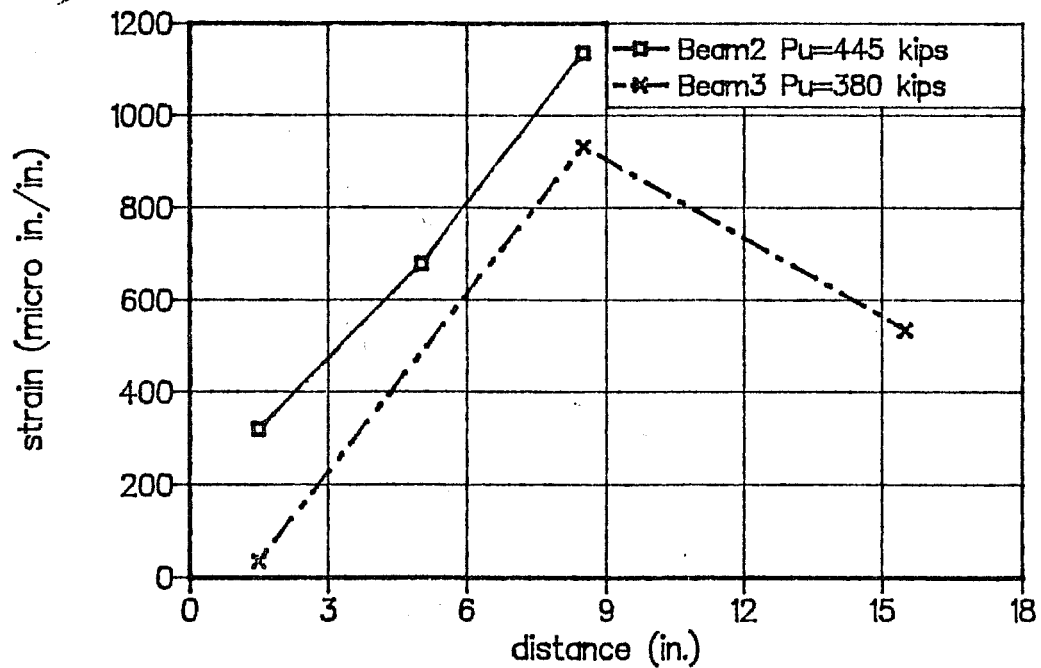


Figure 3.46 Lateral Tie Strains in Specimens Beam2 and Beam3

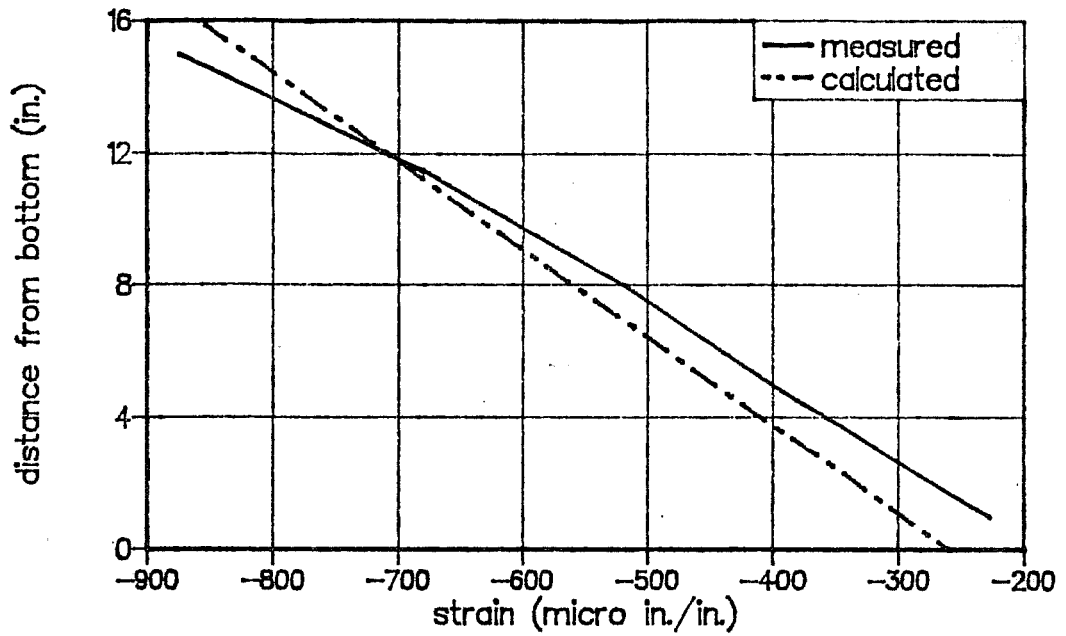


Figure 3.47 Compressive Strains 24 in. ahead of Live End Anchor in Specimen Beam2

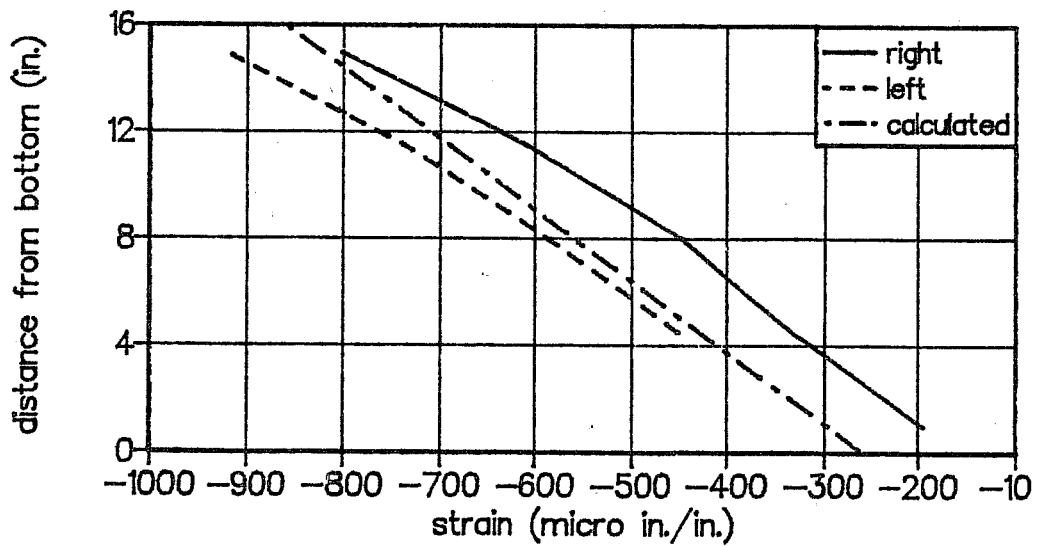


Figure 3.48 Compressive Strains 24 in. ahead of Dead End Anchor in Specimen Beam2

3.7 Evaluation of Test Results

3.7.1 *Finite Element Analysis Predictions*

Proportioning of the bursting reinforcement based on the results of a linear-elastic finite element analysis is a popular design method. Burdet confirmed this approach and also developed recommendations to check the concrete compressive stresses in the anchorage zone [8]. These recommendations were adopted in the proposed anchorage zone specifications (Appendix A, Section 9.21.5).

Location and magnitude of the bursting force are determined by integrating the elastic bursting stresses. Reinforcement is provided accordingly. In the proposed specifications the full yield strength of the reinforcement may be taken into account, but a relatively low ϕ -factor of 0.85 is applied.

The concrete compressive stresses are critical immediately ahead of the anchor plate if no local confinement reinforcement is present. They can be checked using bearing pressure limitations similar to Equation (2.1) or (2.2). If well designed local confinement reinforcement is used to enhance the bearing capacity, the concrete compressive stresses are also critical immediately ahead of that confinement reinforcement. Therefore, in the proposed anchorage zone provisions a check of the concrete stresses at some distance ahead of the anchor plate is required. This distance is not to exceed the smaller of the length of the local confinement reinforcement and the smaller lateral dimension of the bearing plate (Appendix A, Section 9.21.3.4.2). The concrete stresses at this location may be determined from a linear-elastic finite element analysis and must not exceed $\phi(0.7f'_{ci})$. Local stress maxima may be averaged over an area equal to the bearing area of the anchorage device to reflect the non-linear behavior of concrete at higher stresses (Appendix A, Section 9.21.5.2).

The finite element solutions discussed in Section 3.3 can be used to compare the loads predicted by this method to the actual failure loads. Since the finite element analysis was conducted for an a/h ratio of 0.25 and assuming a plane state of stress, some modifications are required to account for three-dimensional effects, presence of a tendon duct, and the actual a/h ratio of 0.40 in the test specimens of this series.

The critical section for the check of the compressive stresses is one plate width or $6\frac{1}{2}$ in. ahead of the anchor plate. The finite element results for the a/h ratio of 0.25 can be used. According to finite element analysis results by Burdet [8], at a distance equal to $0.40h$

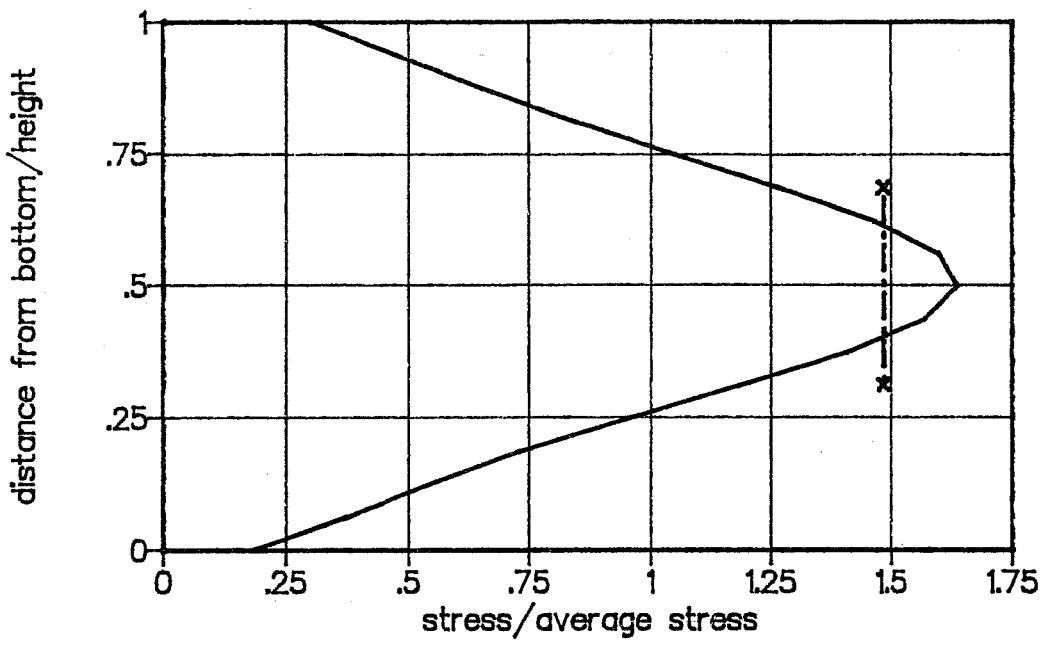


Figure 3.49 Elastic Compressive Stresses at Critical Section

the peak compressive stresses are approximately equal for $a/h=0.25$ and $a/h=0.40$. Figure 3.49 shows the distribution of elastic compressive stresses for $V/P=0.078$ at the critical section. Local peak stresses can be averaged over an area equal to the bearing area of the anchor plate as indicated by the dash-dot line. The ratio of this critical stress to the average stress on the cross section (P/A) is 1.48.

For thin members spreading of stresses in the thin direction can be approximated by considering an effective thickness that increases linearly with the distance from the bearing plate (Figure 3.50)[8]. This approach is valid for t/b ratios not larger than three.

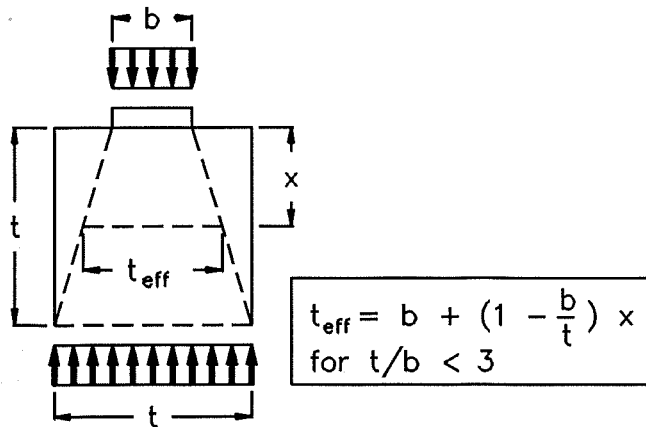


Figure 3.50 Effective Thickness in Thin Members (adapted from [8])

For the specimens of this series with $b=x=6\frac{1}{2}$ in. and $t=9$ in., the effective width at the critical section is 8.31 in. Hence, the compressive stresses obtained from the plane stress finite element analysis have to be multiplied by a factor of $9/8.31 = 1.08$ to account for this three-dimensional effect. With this adjustment the calculated stress at the critical section becomes $1.48 \times 1.08 = 1.60$ times the average stress at the end of the anchorage zone (Figure 3.49). The ultimate load prediction, assuming compression controls and with $\phi = 1.0$ for comparison with tests, can be estimated using Equation (3.5).

$$1.60 \frac{P}{ht} \leq 0.7f'_c \quad (3.5)$$

A further reduction may be necessary if the tendon duct is very large. The effect of the tendon duct is estimated by multiplying the left-hand side of Equation (3.5) with the ratio of gross bearing plate area to net bearing plate area. With a $6\frac{1}{2}$ in. x $6\frac{1}{2}$ in. bearing plate and a $2\text{-}5/8$ in. duct this ratio is 1.15. The ultimate load for a compression failure is then predicted by Equation (3.6).

$$1.83 \frac{P}{ht} \leq 0.7f'_c \quad (3.6)$$

The capacity of the local zone is checked using Roberts' equation (Equation (2.2)) which is restated below.

$$P_n = 0.80 f'_c \sqrt{\frac{A}{A_b}} A_b + 4.1 f_{lat} A_{core} \left(1 - \frac{s}{D}\right)^2 \quad (3.7)$$

The elastic analysis prediction assuming that the bursting tie capacity controls will be based on Guyon's solution for the concentrically loaded anchorage zone (Figure 2.7). For an a/h ratio of 0.4 the magnitude of the bursting force T_{burst} is $0.13P$ and the centroid of the bursting reinforcement is located at $d_{burst} \sim 0.63h$. The predictions must be adjusted to account for the difference between the actual location of the centroid of the bursting reinforcement and the location indicated by the elastic solution, as shown in Equation (3.8).

$$P_{calc} = \frac{T_{burst}}{0.13} \frac{d_{burst}}{0.63h} \quad (3.8)$$

where T_{burst} is the capacity of the bursting reinforcement;

d_{burst} is the distance of the centroid of the bursting reinforcement from the anchor;

h is the height of the girder ($h = 16$ in.).

Table 3.5 shows a comparison of the actual failure loads to the predictions of the finite element analysis and to the local zone capacities, assuming a ϕ -factor of 1.0. The predictions are either controlled by the limit on the compressive stresses at the critical section ahead of the confined region (local zone - general zone interface) or by the capacity of the bursting reinforcement, if the concrete tensile strength is neglected. The governing prediction is underlined. The agreement between calculated and actual capacities is excellent in most cases. For specimen Beam3 the calculated capacity is conservative.

Table 3.5 Finite Element Analysis Predictions for Beam Specimen

specimen	P_{test} (kips)	local zone (kips)	interface (kips) (Equation (3.4))	bursting (kips)	P_{calc} (kips)	P_{test}/P_{calc}
B3*	331	602	340	<u>317</u>	317	1.04
Beam1	315	379	<u>292</u>	355	292	1.08
Beam2	445	470	413	<u>406</u>	406	1.10
Beam3	380	370	<u>281</u>	406	281	1.36
*) Sanders' isolated anchorage zone specimen [44]				average		1.15
				standard deviation		0.13

It is pointed out that the predictions based on the capacity of the bursting reinforcement do not reflect the actual failure mode. In the beam specimens only a few ties yielded, while the calculations are based on the assumption that all ties reach yield and ignore the tensile strength of the concrete. As illustrated in Figure 2.25 further load increase is possible, even after yielding of all the bursting ties, due to stress redistributions in the anchorage zone. This is reflected in Table 3.6 which shows a comparison of the actual failure loads to the predictions based on the check of compression stresses at the local

zone-general zone interface and ignores the limiting capacity of the bursting reinforcement. These predictions are just as good as the predictions shown in Table 3.5.

Based on these observations and the discussions in the preceding sections it is concluded that the critical failure mode in thin sections is a compressive failure within or ahead of the local zone reinforcement. The results in Table 3.6 indicate that a simple check of the compressive stresses at a critical section is quite adequate to predict the ultimate load, provided well distributed bursting reinforcement is present in the anchorage zone. The location and amount of this bursting reinforcement can be conservatively based on the results of a linear-elastic finite element analysis.

Table 3.6 Finite Element Analysis Predictions for Beam Specimens Assuming Compression Controls

specimen	P_{test} (kips)	P_{calc} (kips)	P_{test}/P_{calc}	
B3*	331	340	0.97	
Beam1	315	292	1.08	
Beam2	445	413	1.08	
Beam3	380	281	1.35	
*) Reference [44]			average	1.12
			standard deviation	0.14

3.7.2 Strut-and-Tie Model Predictions

The proposed anchorage zone specifications include provisions for the application of strut-and-tie models to the design of anchorage zones (Appendix A, Section 9.21.4, Appendix B, Section C.9.21.4). These provisions differ from the procedure discussed in Section 3.4 in the following points:

- 1) The effective concrete strength for unconfined concrete is $0.7f_{ci}$ throughout the anchorage zone.
- 2) The local zone nodes may be placed at a depth of $a/4$ ahead of the anchor plate, independent of the state of stress at the node (Appendix B, Section C.9.21.4.2). If local confinement reinforcement is present, the compressive stresses may be

checked at some distance from the node assuming a linear increase of the width of the strut with the distance from the node (Figure 3.51). The critical section is defined as that section whose extension intersects the axis of the tendon at a depth equal to the lateral dimension of the anchorage device (Appendix A, Section 9.21.4.3.2).

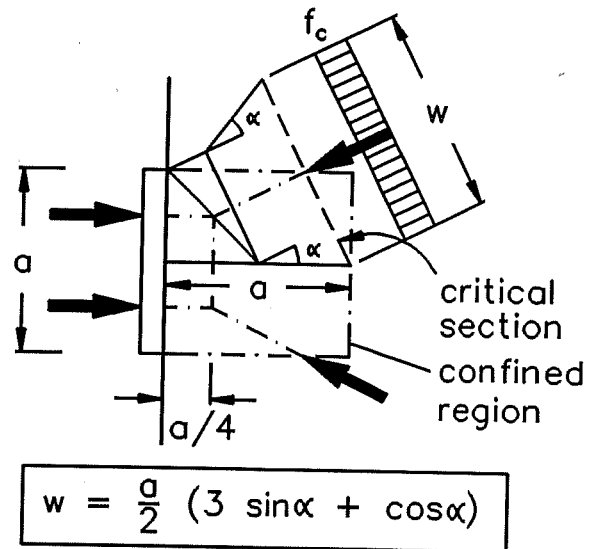


Figure 3.51 Critical Section for Confined Local Zone Nodes

- 3) For thin members with a ratio of member thickness to anchor plate width of no more than three, an effective strut width in the thin direction of the member is determined by assuming a linear increase of the strut width with the distance from the anchor (Figure 3.50) (Appendix A, Section 9.21.4.3.3).

As shown in Figure 3.51 the code procedure leads to a local zone node which is a combination of a non-hydrostatic node (Section 3.4.5.2) with fan-shaped struts (Section 3.4.5.3). Strictly speaking, a non-uniform stress distribution would be required over the critical section in order to not exceed the effective concrete strength in the unconfined portions of the strut. For simplicity this requirement is ignored in the proposed specifications. With this type of node the increase of anchor capacity due to the presence of confinement reinforcement is given by Equation (3.9), provided the node is symmetric and the critical section is located one plate width ahead of the anchor.

$$\frac{P_{\text{confined}}}{P_{\text{unconfined}}} = 3 \sin \alpha \cos \alpha + \cos^2 \alpha \quad (3.9)$$

For $\tan \alpha = 0.5$ this ratio is 2.0

Point 3 of the list above also merits further discussion. An effective strut width t_{eff} in the thin direction of the member is defined. Since this effective strut width is less than the thickness of the member, confining concrete is available. It appears reasonable to increase the effective concrete strength, similarly to the increase of the bearing strength when confining concrete is present. As illustrated in Figure 3.52 in many cases it is equivalent but simpler to use the full member thickness with the basic concrete strength,

rather than the effective thickness with the enhanced concrete strength, to check the compressive stresses. However, the proposed anchorage zone specifications do not provide for this increase of the effective concrete strength due to the presence of confining concrete.

Table 3.7 shows a comparison of both strut-and-tie model procedures to the test results for the specimens of this series. The capacity of the local zone (see Table 3.5) did not control in any case and is not shown. Table 3.7 also includes information on the level of the compressive stresses at the critical section for the strut-and-tie model predictions based on the proposed code procedure (method A). The maximum stress at the critical section is limited to $\max f_c = 0.7 f'_c$. In the strut-and-tie model procedure of Section 3.4 (method B) the depth of the local zone node a_o is selected such that the concrete stresses at the local zone node are just at their limit strength ($f_c = 0.85 f'_c$). Table 3.7 lists the relative depth of the local zone nodes, a_o/a , determined by this procedure. The distance of the center of the local zone nodes from the bearing plate is $a/4$ for method A and is $a_o/2$ for method B.

The comparison of calculated to maximum compressive stress at the critical section

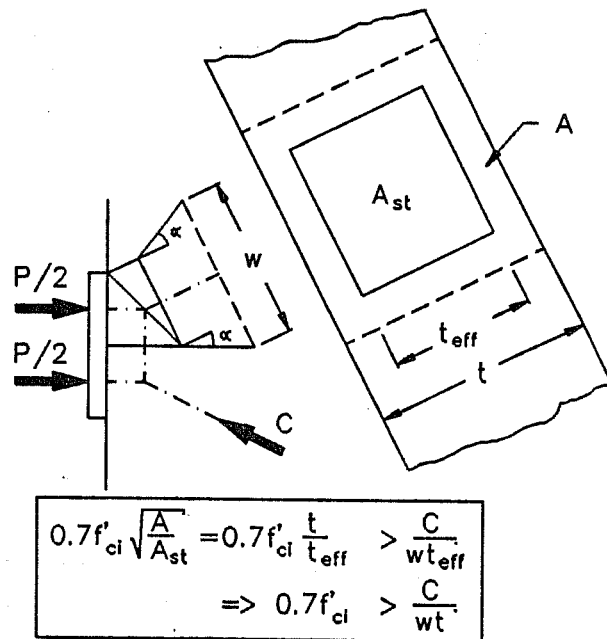


Figure 3.52 Confinement of Struts

Table 3.7 Strut-and-Tie Model Predictions for Beam Specimens

specimen	P_{test} (kips)	A strut-and-tie model (code procedure)			B strut-and-tie model (Section 3.4)		
		$\text{calc } f_c /$ $\text{max } f_c$	P_{calc} (kips)	$P_{test} /$ P_{calc}	a_o / a	P_{calc} (kips)	$P_{test} /$ P_{calc}
B3	335	0.80	296	1.13	0.41	306	1.09
Beam1	315	0.91	332	0.95	0.58	322	0.98
Beam2 (LE)	-	0.71	373	-	0.30	405	-
Beam2 (DE)	445	0.66	363	1.23	0.29	401	1.11
Beam3 (LE)	380	1.00	359	1.06	0.72	336	1.13
Beam3 (DE)	-	0.97	363	-	0.67	332	-
average				1.09	average		1.08
standard dev.				0.10	standard dev.		0.06

In Table 3.7 shows that the load predictions of the code procedure are controlled by the capacity of the bursting tie in most cases. The only exception is the live end side of specimen Beam3 where the strut capacity is slightly below the tie capacity. The predictions of method B are a function of both tie capacity and concrete strength and assume that tie and struts reach their limit strength simultaneously.

With the exception of the live end side of specimen Beam3, the difference in the predictions of the two methods is entirely due to the different local zone node locations (Figure 3.15). In method A the location of the local zone nodes is fixed at $a/4$ ahead of the anchor plate, whereas in method B its location depends on the state of stress at the node. Method B predicts higher than method A if the a_o/a ratio is less than 0.5 and predicts lower if that ratio is larger than 0.5.

Both methods give predictions within 15% of the actual failure load in most cases. (Table 3.7). However, it should be noted that all predictions (except the method A prediction

for the live end side of specimen B3) assume yielding of all bursting ties in the anchorage zone. In the beam tests much of the bursting reinforcement did not yield due to the contribution of uncracked concrete in tension. As shown in Sections 3.7.1 and 3.7.3, procedures that consider only the compressive stresses and ignore capacity and arrangement of the bursting reinforcement are just as accurate.

3.7.3 Approximate Equations

The proposed anchorage zone provisions include approximate procedures which may be used for rectangular members (Appendix A, Section 9.21.6). The provisions include simple equations to check the compressive stresses ahead of the local zone confining reinforcement and to determine magnitude and location of the bursting reinforcement. These equations are based on linear-elastic finite element studies by Burdet [8].

The check of compressive stresses is based on the simple observation that the elastic compressive stresses at a distance equal to the bearing plate width ahead of the anchor are not higher than 60% of the bearing pressure, provided the edge distance of the anchor is larger than one and one-half times the corresponding bearing plate width. This result applies to plane stress analysis. Spreading of stresses in the thin direction of the member is approximated by the assumed dispersion of stresses shown in Figure 3.50.

Table 3.8 shows the ultimate load predictions based on the checks of the compressive stresses only (Appendix A, Section 9.21.6.2). Not surprisingly, the results are very similar to the finite element predictions (Table 3.6) and are very good in most cases. Ignoring the influence of amount and arrangement of the bursting reinforcement does not affect the quality of the prediction. The actual location of the centroid of the bursting

Table 3.8 Approximate Equations

specimen	P_{calc} (kips)	P_{test} (kips)	$\frac{P_{test}}{P_{calc}}$
B3	351	335	0.95
Beam1	301	315	1.05
Beam2	426	445	1.04
Beam3	290	380	1.31
	average		1.09
	standard deviation		0.13

reinforcement in the specimens of this series was quite a bit different from what would be required by the approximate equations. For a concentric anchor the approximate equations

place the centroid of the bursting reinforcement at $d_{burst} = \frac{1}{2}h$. The actual location was $0.65h$ and $0.75h$, without adverse effect on the performance of the respective anchorage zones. Linear elastic finite element analysis indicates a d_{burst} of $0.45h$ to $0.63h$ depending on the a/h ratio (Figure 3.53).

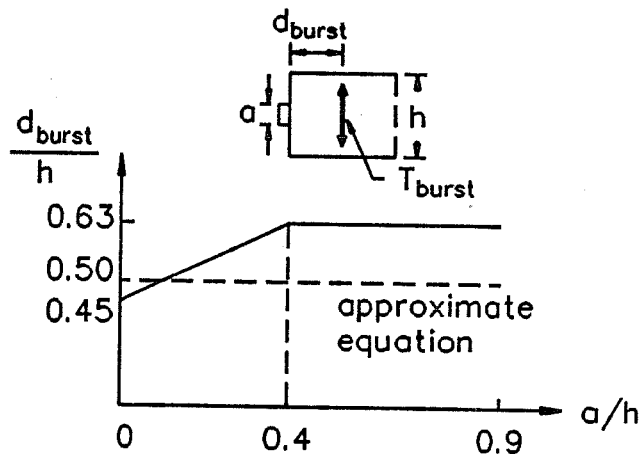


Figure 3.53 Location of Centroid of Elastic Bursting Stresses (adapted from [8])

3.7.4 Comparison with Sanders' Test Results

Comparison of Sanders' isolated anchorage zone specimen B3 and the beam specimens of this series yielded the following observations:

1.) Peak tie bursting strains were limited to a small region in the beam specimens and only a few ties yielded prior to failure. For example, in specimen Beam1 peak bursting strains occurred in the ties located $4\frac{1}{2}$ in. to $8\frac{1}{2}$ in. ($0.3h$ to $0.5h$) ahead of the anchor plate. At larger distances the tie strains diminished rapidly (Figure 3.42). In contrast, in Sanders' specimen B3 the tie strains became more uniform after the bursting crack had reached the base of the specimen. The tie strains did not decrease with the distance from the anchor plate. All ties had yielded or were close to yield at failure.

2.) The first cracking load for specimen Beam1 was some 15% higher than for specimen B3 (Table 3.4), although the concrete strength was very similar in both cases (5300 psi and 5400 psi, respectively).

3.) The first yield load for specimen B3 was much lower than for the beam specimens. However, this is a function of the lower yield strength of the reinforcement used in specimen B3 and direct comparisons are not meaningful.

4.) All specimens experienced a compression failure of the concrete outside the local zone spiral reinforcement. The failure loads for specimens B3 and Beam1 are almost identical (within 5%).

Based on this limited comparison it is concluded that isolated anchorage zone

specimens are a conservative method to investigate anchorage zone behavior. However, it should be kept in mind that concrete tensile strength and stress redistributions affect short anchorage zone specimens and actual girders differently. If possible, anchorage zone specimens should be dimensioned such, that bursting cracks do not extend all the way to the end of the specimen.

3.7.5 Influence of a Reaction Force in the Anchorage Zone

Due to the wide scatter of the concrete tensile strength it is difficult to isolate the influence of a reaction force in the anchorage zone on the first cracking load. Judging from the linear-elastic finite element analysis results, a slightly increased first cracking load should be expected with the presence of a reaction force (Figure 3.9). However, this increase is not significant compared to the variability of the concrete tensile strength and hence the test results are inconclusive (Table 3.4).

The direct comparison of tie strains at different vertical loads in Figure 3.43 shows that the presence of a reaction force in the anchorage zone has a slight effect on the bursting strains. The failure mode is more a function of the concrete strains in the thin direction of the girder was not affected by the presence of the reaction force in the anchorage zone.

Based on the finite element studies, strut and tie model considerations, and the test results, it appears to be safe to ignore the effect of a reaction force in the anchorage zone, provided the eccentricity of the anchor is small and no flexural tension stresses exist at the end of the anchorage zone.

3.8 Summary and Conclusions

3.8.1 Summary of Study

Linear-elastic finite element analysis, strut-and-tie model procedures, and a small series of physical tests were employed to investigate the behavior of anchorage zones in thin rectangular members and the effect of reaction forces in this region. The ratio of section thickness to corresponding bearing plate width was 1.38 for all specimens. The analysis and test results were evaluated with view to the proposed anchorage zone specifications (Appendix A). This chapter also includes detailed guidelines for the development of strut-and-tie models and two examples for their application.

3.8.2 Behavior of Anchorage Zones for End Anchors

Anchorage zones are subjected to high bearing and compressive stresses immediately ahead of the anchorage device and to tensile stresses due to spreading of the concentrated tendon force over the cross section.

Tensile bursting stresses cause cracking roughly parallel to the tendon force. Such cracking can be controlled but not avoided by well distributed and closely spaced bursting reinforcement. If bursting cracks must be avoided, transverse prestressing should be considered. In the physical test series of this study first cracking occurred at 65% to 80% of the failure loads. The bursting cracks extended as far as a distance equal to one and one-half beam heights ahead of the anchor. Crack widths remained below 0.03 in. throughout the tests. Bursting cracks reduce the tensile stiffness of the member in the direction perpendicular to the crack. Consequently, stress redistributions occur which cause the compressive stresses to spread out at a flatter angle from the anchor. Hence, bursting cracking reduces the magnitude of the bursting force but also hampers the dispersal of the concentrated compressive stresses ahead of the anchorage device.

Spirals or closely spaced, closed tie reinforcement are very effective to increase the bearing strength of concrete. The concrete confined by this reinforcement forms a highly stressed plug. The anchorage force is resisted

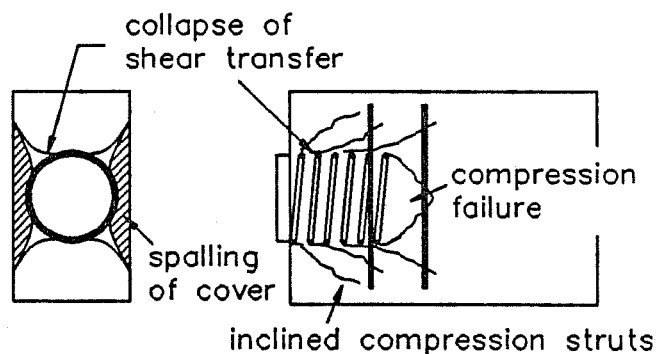


Figure 3.54 Failure of Concrete Surrounding the Confined Plug

by bearing stresses at the end face of this plug and by shear stresses along its skin. In this study failure of all specimens was initiated by the collapse of this shear transfer and subsequently a compression failure of the unconfined concrete ahead of the local confinement reinforcement occurred. Figure 3.54 illustrates this failure mode and also shows that concrete tensile stresses or reinforcement is required to tie back the inclined compression struts that originate along the skin of the plug. Based on shear-friction theory and on the crack patterns observed in the tests, the inclination of these struts is approximately 35 to

45 degrees (Figure 3.30).

3.8.3 Design Recommendations

Strut-and-tie model procedures provide a versatile and logical approach to the design of the primary anchorage zone reinforcement and to checking of critical compressive stresses. Strut-and-tie models based on a distribution of forces at the far end of the anchorage zone which satisfies simple beam theory are recommended. This procedure is conservative for design of the bursting reinforcement but may underestimate the compressive stresses ahead of local zone reinforcement. If well detailed bursting reinforcement is provided throughout the anchorage zone, the effect of bursting cracks on the compressive stresses is not critical.

The strut-and-tie model solution is sensitive to the location of the bursting tie. The bursting tie becomes more effective if located further away from the anchor plate. However, reinforcement should be provided throughout the bursting region. This requirement limits the distance of the bursting tie from the anchor plate. For concentric end anchors this distance should not exceed a value equal to 70% of the height of the girder. In view of the shear transfer through the skin of the confined plug in the local zone, a refined strut-and-tie model with two bursting ties could be considered (Figure 3.55). However, generally a simpler model with a single bursting tie is sufficient.

Linear-elastic finite element analysis is acceptable for anchorage zone design and gave conservative ultimate load predictions for the specimens studied in this chapter. Magnitude and location of the bursting force can be estimated by integrating the bursting stresses. Compressive stresses should also be checked. The main advantage of this approach is the better approximation of the state-of-stress in the structure prior to cracking. Disadvantages are the difficulty of translating the elastic stress distribution into a suitable reinforcement arrangement and the emphasis on local stresses rather than overall load paths.

The approximate equations in the proposed anchorage zone specifications give

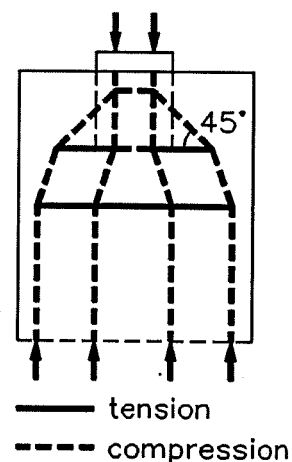


**Figure 3.55 Refined
Strut-and-Tie Model**

good results for thin, rectangular members. However, it should be kept in mind that the use of these equations is very restricted. In particular the bursting reinforcement requirements apply to rectangular sections only. Presence of flanges increases the bursting force. The restriction on the approximate equations to check the compressive stresses is not as severe. Use of these equations can be safely extended to non-rectangular sections, provided the edge distance of the anchor is larger than one and one-half times the corresponding bearing plate width.

In general, the effect of a reaction force should be considered in the design of an anchorage zone. This effect may be neglected only for concentric anchors or anchors with small eccentricity, and only if no tensile stresses due to the combined effect of reaction and tendon force exist at the end of the anchorage zone. Care must be taken when applying the approximate equations to eccentric anchors when a reaction force is present. The expressions for location and magnitude of the bursting force give misleading results in this case (Figure 3.56).

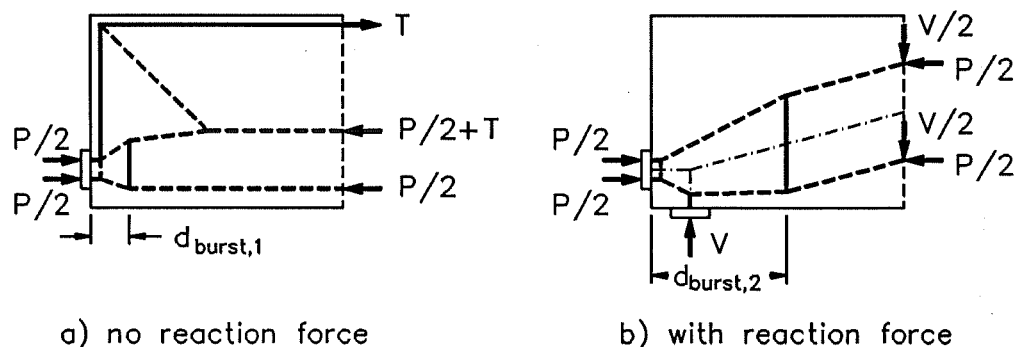


Figure 3.56 Strut-and-Tie Models for Eccentric Anchor Without and With Reaction Force in the Anchorage Zone

3.8.4 Detailing Recommendations

Well detailed bursting reinforcement is essential for the satisfactory behavior of the anchorage zone. Bursting reinforcement should be provided throughout the region where bursting stresses occur. Results of a linear elastic analysis may provide useful guidelines where such reinforcement is required.

Bursting reinforcement is also necessary for the shear transfer through the skin of

the confined plug in the local zone. Care should be taken that the first bursting ties are close enough to the local zone to facilitate this shear transfer. Ties are also necessary in the thin direction of the member unless the concrete tensile capacity can be relied on. In thin members this lateral tie requirement may lead to congestion of the local zone. This congestion can be relieved by replacing the confining spiral reinforcement by closed ties which perform a double function as confinement and as bursting reinforcement. However, it should not be overlooked that ties are roughly only half as effective as spirals as confinement reinforcement (Equation (2.3))[41].

Congestion of the anchorage zone is one of the leading causes for anchorage zone problems and must be avoided. For this reason overconservative design is just as harmful as inadequate reinforcement proportions. Space requirements to accommodate the maximum aggregate size and to facilitate proper concrete compaction must be considered when detailing the anchorage zone reinforcement.

In addition to the primary bursting reinforcement, supplementary reinforcement should be provided to control cracks induced by compatibility stresses. This includes spalling reinforcement along the loaded edge of the member and tie back reinforcement to control cracking and spalling of unstressed corners (Figure 2.12).

4 INTERMEDIATE ANCHORAGES IN BLISTERS AND RIBS

4.1 Introduction

4.1.1 General

In post-tensioned concrete bridges frequently it is desirable or necessary to use tendons that do not extend over the full length of the bridge. Such tendons have to be anchored at intermediate locations along the girder rather than at the end faces. These anchorages may be in the form of embedded anchors or may be located in recess pockets, blisters, or ribs (Figure 4.1). At intermediate anchorages compatibility requirements for the deformations ahead of and behind the anchor generate large tensile stresses behind the anchor which often cause cracking at this location. Such cracking may propagate to the webs and is potentially detrimental to the shear strength of the girder [39].

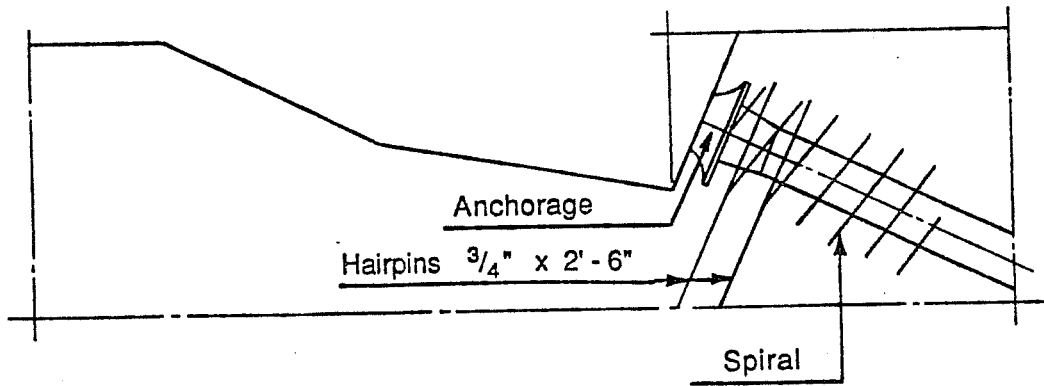
The problem of cracking behind intermediate anchorages has been subject to a large number of studies. It is well understood that mild reinforcement or permanent compression across the critical section are effective in controlling such cracking. However, there are still questions about the amount of reinforcement required for crack control behind the anchor. Furthermore, most previous studies were concerned with embedded anchors and did not consider the additional effects due to bending and shear transfer with blisters and ribs.

4.1.2 Objectives

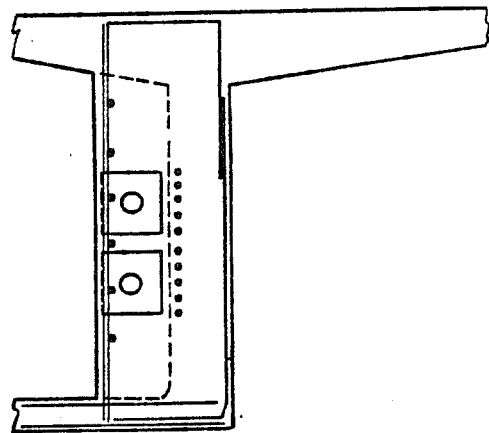
The objectives of this section are to document the behavior of intermediate anchorages in blisters and ribs and to develop design recommendations suitable for inclusion in the AASHTO specifications. Particular emphasis is placed on the development and discussion of strut-and-tie models and their verification with a limited number of tests.

4.1.3 Scope

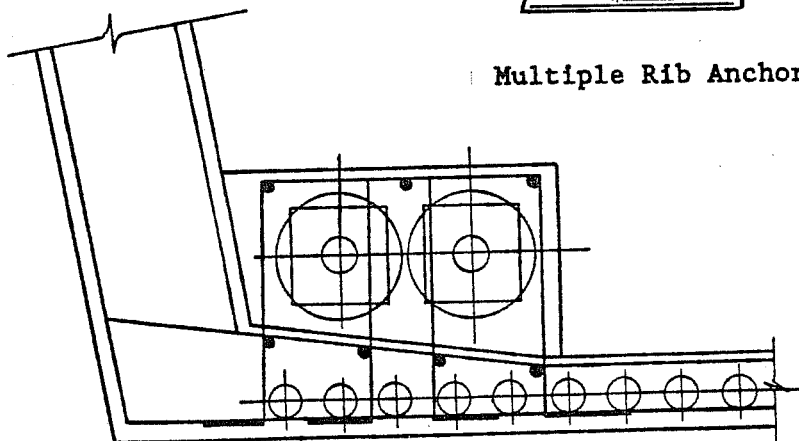
Linear-elastic finite element analysis is employed to gain insight into the stress distribution around intermediate anchorages prior to cracking. The analysis results indicate critical regions and, together with a review of the pertinent literature, provide the basis for the development of strut-and-tie models for the design of intermediate anchorages.



Recessed Deck Pocket



Multiple Rib Anchorage



Corner Blister

Figure 4.1 Intermediate Anchorages (from [44])

For greater clarity two types of intermediate anchorages are discussed separately. Section 4.3 treats isolated slab blisters and ribs for anchors located at some distance from a web-flange joint. Anchors in corner blisters for internal and external tendons are addressed in Section 4.4. Each section includes a discussion of finite element analysis results, development of suitable strut-and-tie models, and a presentation of the experimental test results. Figure 4.2 gives an overview of the anchorage zone specimens of this study and further illustrates various types of intermediate anchorages.

Prior to these discussions, Section 4.2 presents background information including previous research, code provisions, and typical details. Section 4.5 gives overall conclusions from the intermediate anchorage study.

4.2 Background Information

4.2.1 Literature

A comprehensive analytical and experimental study of intermediate, embedded anchorages was conducted by **Eibl and Iványi** in 1973 [14, 15]. Reference 14 includes a good review of earlier analytical and photoelastic studies. Such elastic solutions indicate that large tensile stresses exist behind the anchor. The resultant of these calculated tensile stresses can reach a magnitude equal to 50% of the applied tendon force for large slab width to anchor plate width ratios. This is in agreement with recommendations by **Leonhardt** [28] to tie back at least 50% of the tendon force into the portion of the slab behind the anchorage. However, Eibl's and Iványi's study showed that tie-back reinforcement for 25% of the anchor force is adequate. In their tests cracking was not critical behind the anchor but rather right at the anchor plate where the presence of the plate weakened the concrete section and caused stress concentrations. Crack widths stayed below 0.008 in. under service loads for single anchors. For multiple tendons anchored in the same section, crack widths exceeded 0.008 in. To avoid problems with multiple anchors the authors recommend staggering of such anchorages by a distance at least equal to one and one-half times the anchor spacing. Recommended measures to control cracking at the anchor include precompressing the critical section, provision of a closely spaced grid of reinforcement at the anchorage, and provision of concrete cover over the anchor plate not smaller than 70% of the plate width.

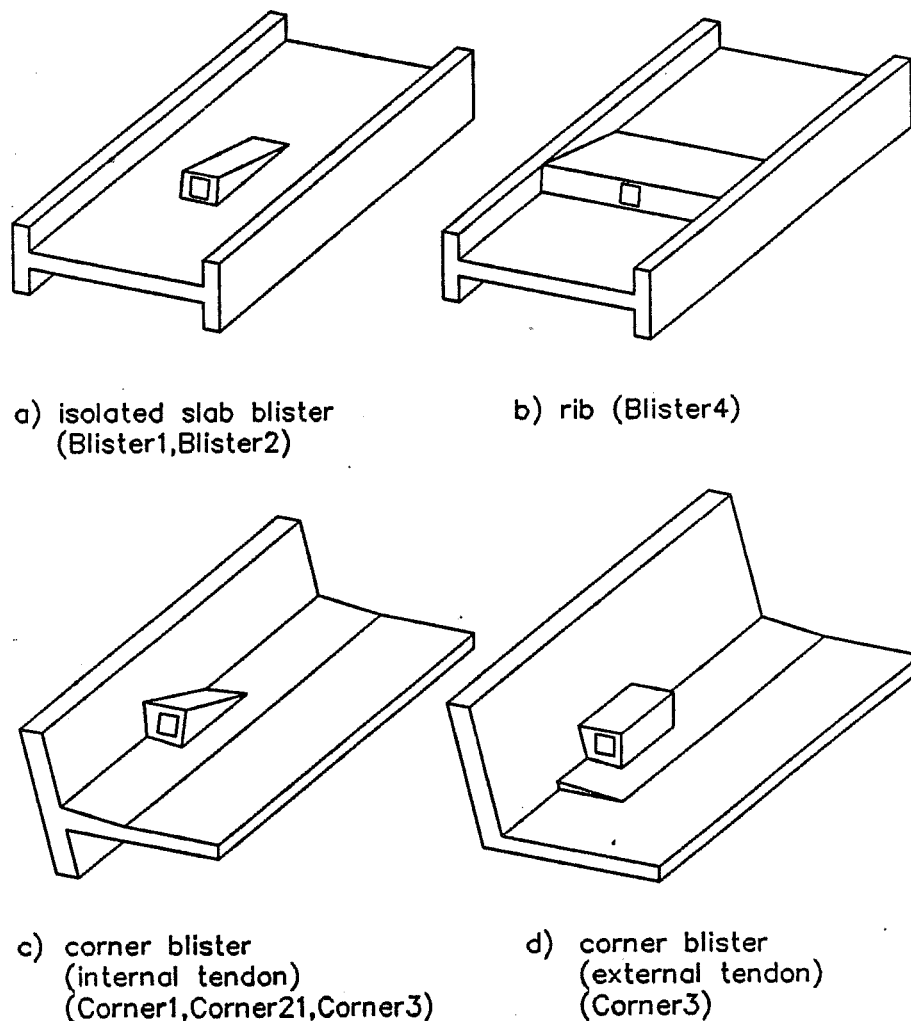


Figure 4.2 Intermediate Anchorage Specimens

Fujii, et al. used finite element analysis methods to investigate the effectiveness of reinforcement for crack control behind blisters and recess pockets [21]. Cracking was modelled by introducing an assumed crack in the finite element mesh. The orientation of this crack was based on the direction of the principal tensile stresses computed for the uncracked structure. Figure 4.3 shows their results for the blister analysis. Cracking reduces the computed tensile stresses behind the anchor significantly. Reinforcement for crack

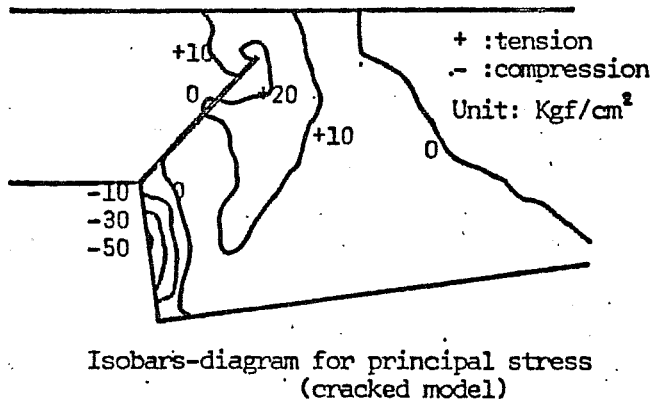
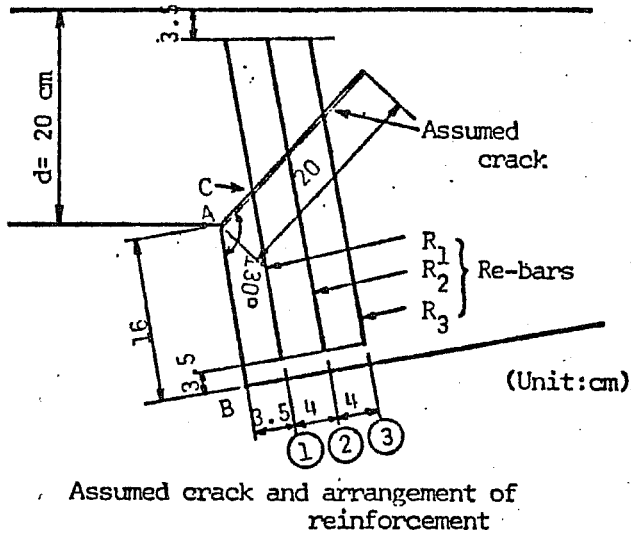
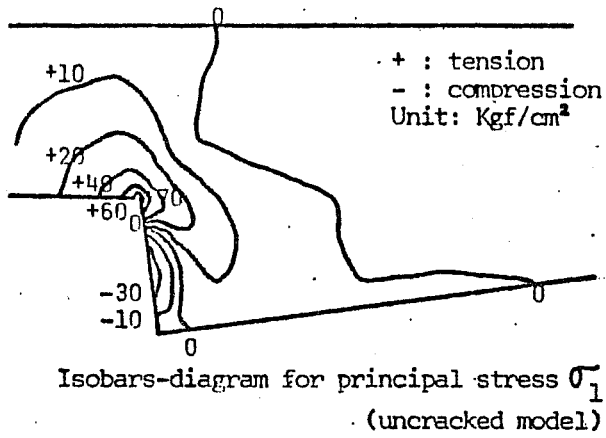


Figure 4.3 Analytical Blister Analysis by Fujii, et al. (from [21])

control is arranged parallel to the loaded face of the blister. The bar closest to this face is most effective. The resultant force in this reinforcement is dependent on the angle of the tendon force with respect to the slab, but never exceeded 25% of the anchor force for the range of variables investigated. Calculated stresses in the reinforcement were between 20 and 40 ksi and the predicted crack widths stayed below 0.004 in. at this level.

In Reference 39 **Podolny** describes a number of problems that have occurred in the vicinity of intermediate anchorages. Cracking behind the anchors or segment joint opening are frequent problems. Podolny points out that these cracks may propagate to the webs and then weaken the shear strength of the girder (Figure 4.4). He describes a case where cracks behind intermediate anchors in the top and bottom flange of a structure joined in the web and created an "inverted key stone" (Figure 4.5). Such cracking may potentially cause collapse of a structure. However, the problem appears to be caused to a greater extent by the insufficient overlap of the tendons rather than the presence of intermediate anchors.

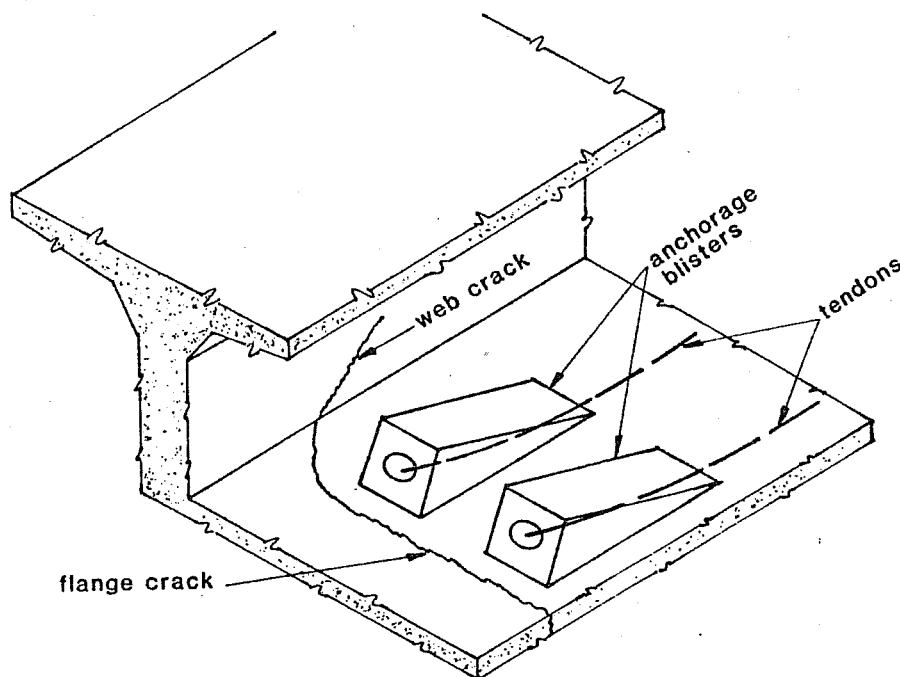


Figure 4.4 Cracking Behind Intermediate Anchor (from [39])

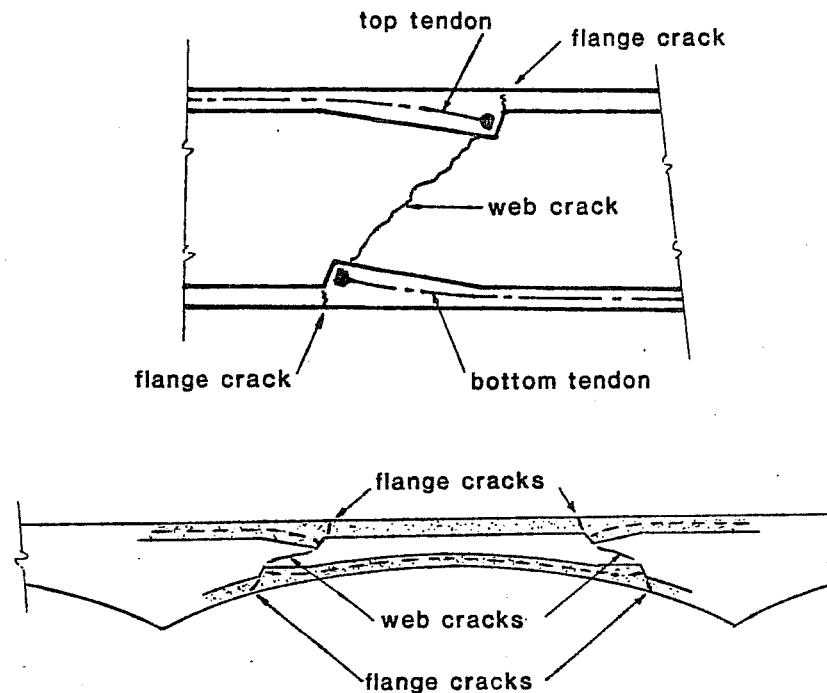


Figure 4.5 Inverted "Key Stone" (from [39])

Another critical location in blisters is the region of tendon curvature, where the tendon is deviated to enter the blister (Figure 4.6). In this region reinforcement is required to tie back the tendon deviation force. The problem is aggravated if the tendon is kinked at the toe of the blister concentrating the entire tendon deviation force at this location.

4.2.2 State of the Art

The AASHTO "Guide Specifications for Design and Construction of Segmental Concrete Bridges" [2] includes information on "anchorage in special blisters". They recommend that design of such blisters be based on the rules for shear-friction and corbels or on strut-and-tie model procedures. The designer is alerted to the presence of localized bending stresses at such blisters. 25 to 50% of the tendon force must be tied back into the concrete behind the anchor, based on an "evaluation of the compressive stress level due to other tendons or loads in the area behind the anchor". The allowable tensile stresses in the tie-back reinforcement under maximum jacking force are limited to 60% of its yield

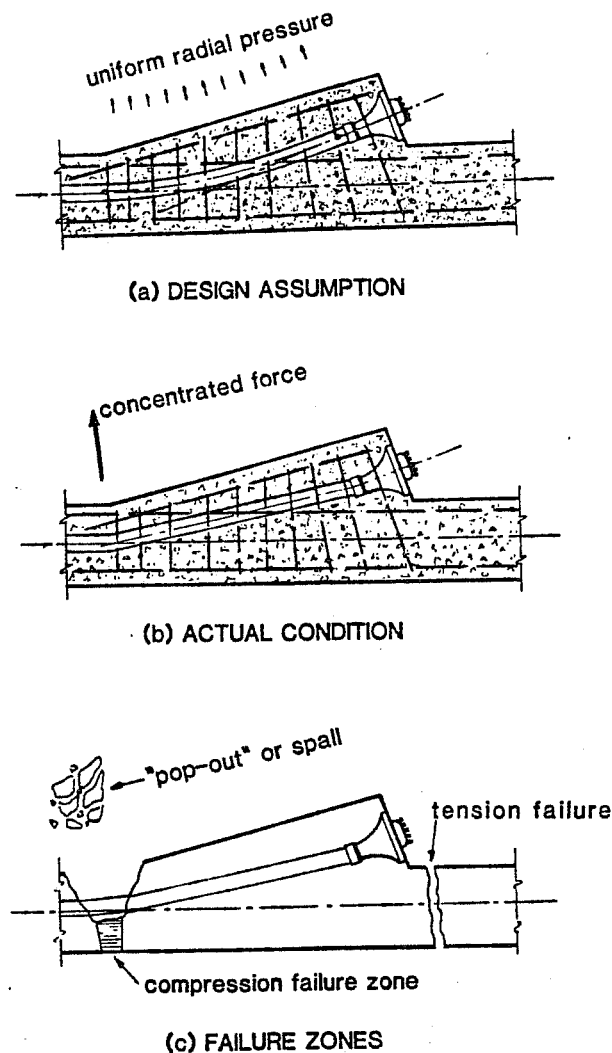


Figure 4.6 Tendon Pull-Out Due to Tendon Deviation Force (from [39])

strength but not more than 36 ksi.

The German code for prestressed concrete structures with bonded tendons, DIN 4227/1 [11], is more specific with regard to the amount of tie-back reinforcement required at intermediate anchorages. The DIN code calls for tie-back reinforcement for 25% of the tendon force. This reinforcement must be placed no further than $1.5\sqrt{A_g}$ from the tendon axis, where A_g is the area of the anchor bearing plate. Allowable stresses in mild tie-back reinforcement are limited to 57% of its yield strength. Reserve strength in bonded prestressed reinforcement may also be counted towards the tie-back reinforcement

requirement, but additional stresses are limited to 35 ksi. If compressive stresses, σ , act on the critical section behind the anchor the tie-back force may be reduced by an amount equal to $5A_g\sigma$.

A number of publications are available from anchorage device suppliers and specialty post-tensioning contractors. **Schneider and Kammenhuber** point out in Reference 24 that in rib anchorages lateral bending moments are generated at the region of tendon curvature. The concentrated tendon deviation force is balanced by distributed deviation forces due to redirection of the compression stresses, which induces this lateral bending moment (Figure 4.7). Local bending moments also occur due to tendon eccentricity with respect to the slab.

The use of strut-and-tie models for the design of blister and rib anchorages is discussed by **Rogowsky and Marti** in Reference 43 and by **Schlaich** in Reference 47. Figure 4.8 is adapted from Schlaich's recommendations for a strut-and-tie model for tendon anchorage in a rib. Two D-regions are identified: The region adjacent to the loaded face of the blister and the region where the tendon is curved. Simple beam theory may be used to determine the boundary conditions for these D-regions. The isolation of D-regions as shown in Figure 4.8 is valid only if the problem considered is two dimensional, that is either a plane stress or a plane strain problem. For the isolated slab blisters and corner blisters discussed in this chapter the state of stress is three dimensional and the D-region is much larger. It includes all of the blister and portions of the slab ahead of and behind the blister.

4.2.3 *Typical Details*

In response to Sanders' survey [44] a large number of drawings of anchorage zone details were received. Two of these details, one for an isolated slab blister (Figure 4.9) and one for a corner blister (Figure 4.10), served as prototypes for the anchorage zone specimens of this study.

Review of typical corner blister details revealed a wide variety of arrangements for the ties from the blister into adjacent slab and flanges (Figure 4.11). However, most details reflected the need for local zone reinforcement immediately ahead of the anchor and for tie-back reinforcement in the region of tendon curvature.

Corner blisters for the anchorage of external tendons were used in the Long Key Bridge in Florida (Reference 19, Figure 4.12). Such applications are fairly rare and more

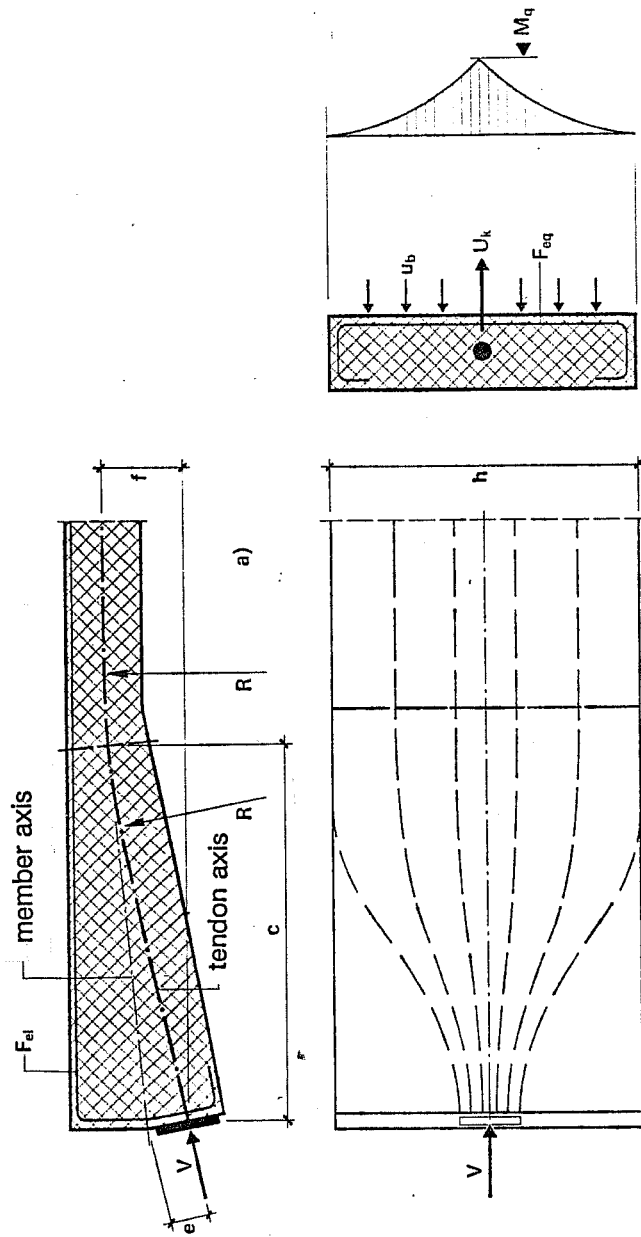
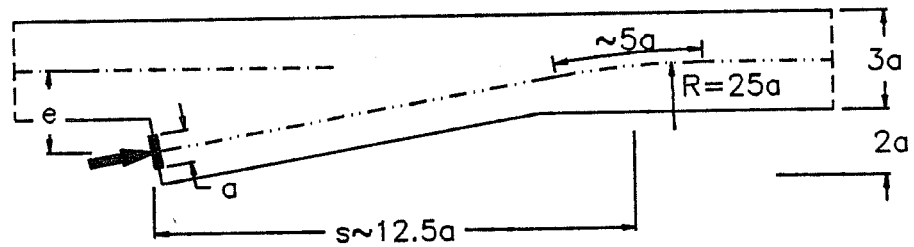
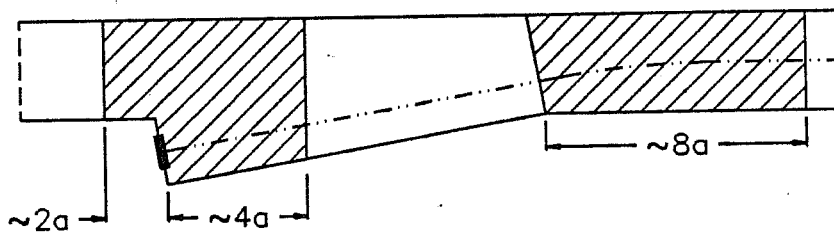


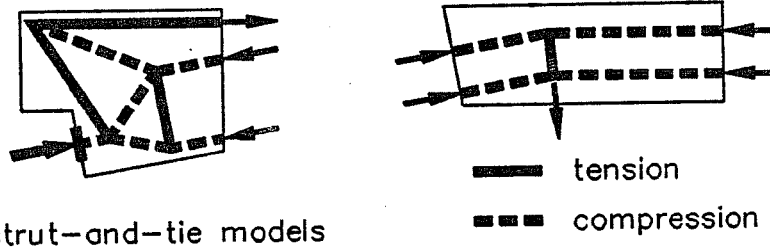
Figure 4.7 Lateral Bending Due to Tendon Deviation (from [24])



a) geometry



b) D-regions



c) strut-and-tie models

Fig. 4.8 **Strut-and-Tie Model for Tendon Anchorage in Rib (adapted from [47])**

frequently external tendons are anchored in diaphragms to minimize local bending effects (see Chapter 5). However, externally post-tensioned bridges are gaining more and more acceptance in the United States and hence the problem of anchorage of external tendons in corner blisters was included in the study.

4.3 Slab Blisters

4.3.1 Introduction

This section discusses intermediate anchorages located away from the web-flange joint of the cross section. Such anchorages may be embedded in the slab, or the tendons

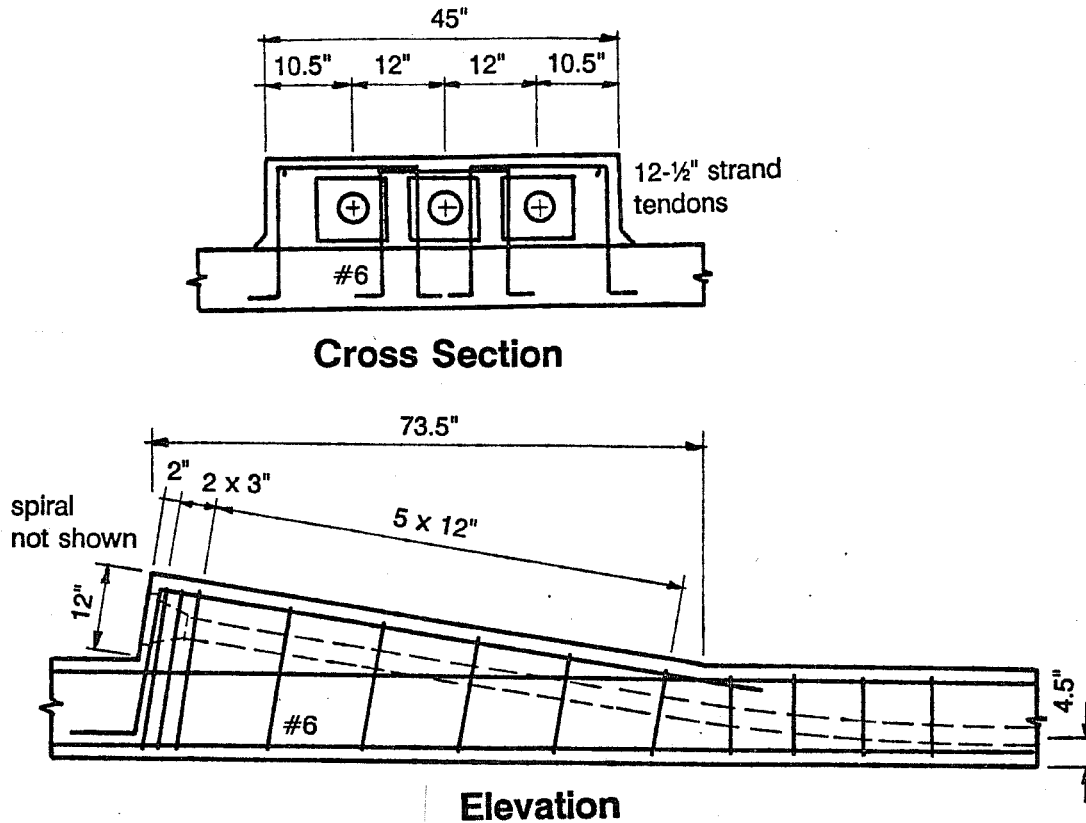


Figure 4.9 Typical Detail for Slab Blister

may be anchored in an isolated slab blister or in a rib extending over the full slab width. Many designers and codes discourage isolated slab blisters to avoid local bending moments induced around such anchorages. The AASHTO Guide Specifications for Segmental Bridges [2] recommend restriction of anchorage in blisters to "small tendons and bars". In the commentary a small tendon is specified as a 12-1/2 in. strand tendon, GR270, for a slab thickness from 5 to 9 in.

The analytical portion of this study on slab blisters included finite element analysis (Section 4.3.2) and development of strut-and-tie models (Section 4.3.3) for embedded anchors, isolated slab blisters, and ribs. The experimental program included three half-scale isolated slab blister specimens and one half-scale rib specimen (Sections 4.3.4, 4.3.5, and 4.3.6).

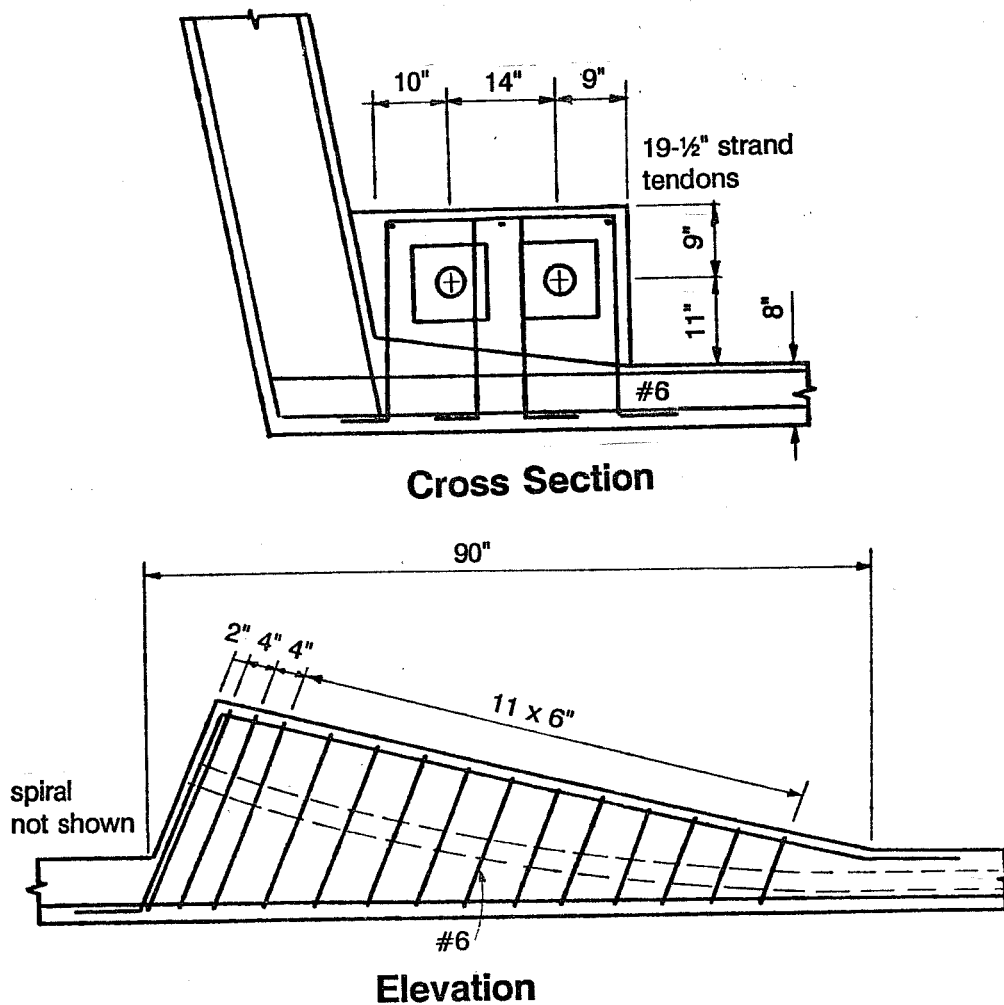


Figure 4.10 Typical Detail for Corner Blister

4.3.2 Finite Element Analysis

4.3.2.1 Embedded Anchor

Figure 4.13 shows the results of a linear-elastic finite element analysis for a plane slab with an intermediate anchor force. The distribution of bursting stresses ahead of the anchor is very similar in shape to the stress distribution for end anchors. However, the magnitude of peak tensile stress and of the resulting bursting force are smaller. For example, for a plate width to slab width ratio, a/h , of 0.25, the magnitude of the bursting force ahead of the anchor is about 18% of the anchor force, P , with an end anchor

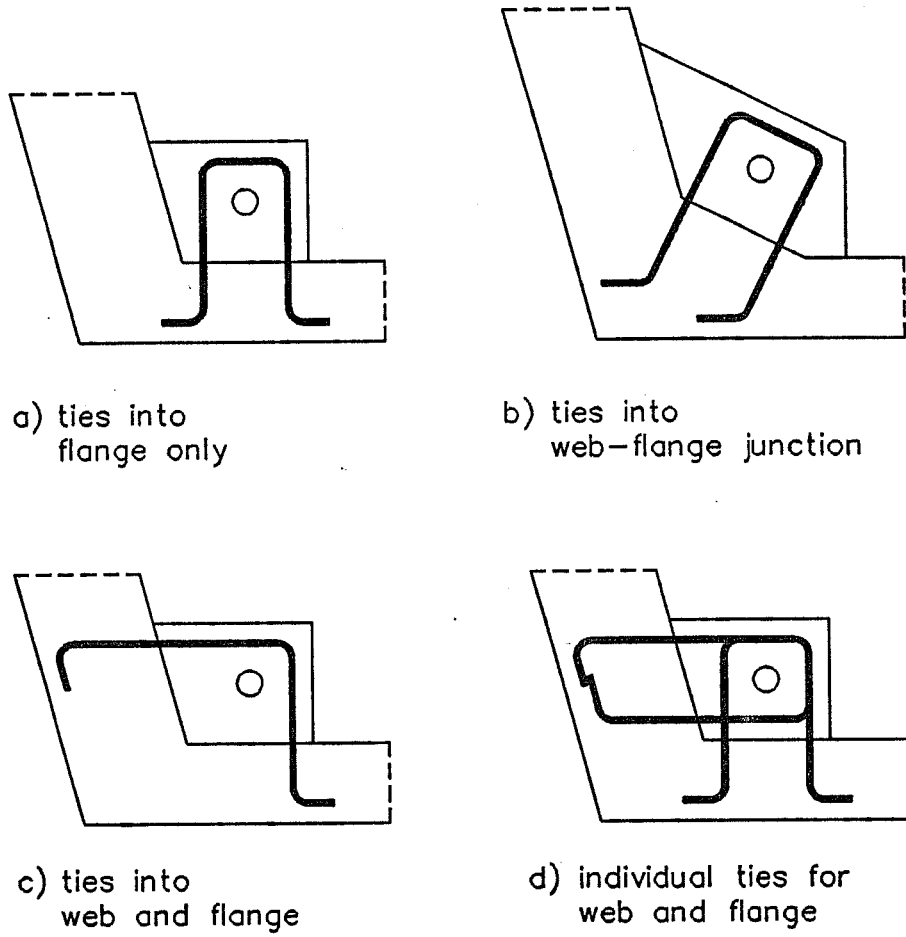


Figure 4.11 Typical Details for Ties in Corner Blisters

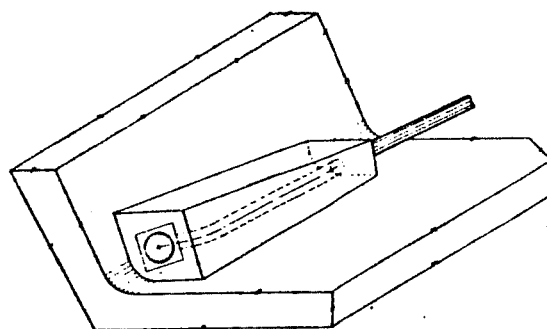
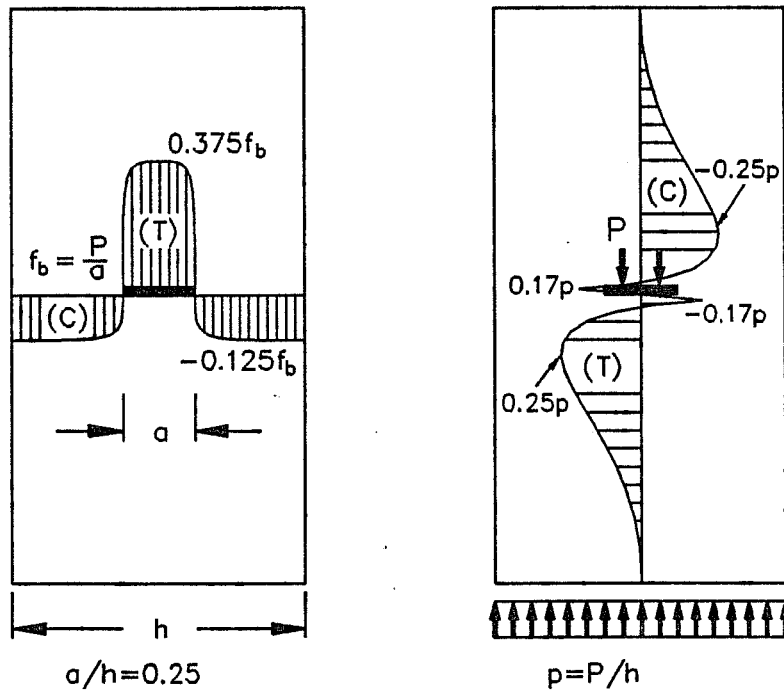


Figure 4.12 Corner Blister for External Tendon (from [19])



a) longitudinal stresses in section immediately behind anchor b) transverse stresses along plane of symmetry

Figure 4.13 Stresses at an Intermediate Anchorage

(Figure 2.7), but only 12% with an intermediate anchor. The peak bursting stress is about 25% smaller for the intermediate anchorage.

Additional tensile stresses exist locally behind intermediate anchors, both parallel and perpendicular to the tendon axis. In a section immediately behind the anchor the longitudinal tensile stresses have the same extent as the anchor plate (Figure 4.13a). Outside this region compressive stresses balance the tensile stresses so that there is no resultant longitudinal force behind the anchor. The portion of the anchor force carried in tension back into the portion of the slab behind the intermediate anchor becomes larger with increasing ratio of slab width to bearing plate width. Based on linear-elastic finite element analysis parameter studies this relation is quantified in Equation 4.1 and further illustrated in Figure 4.14.

$$\sigma_T = \frac{1}{2} f_b \left(1 - \frac{a}{h}\right) \quad (4.1)$$

$$T_{ia} = \frac{1}{2} P \left(1 - \frac{a}{h}\right)$$

where σ_T is the longitudinal tensile stress behind the anchor;
 f_b is the anchor bearing pressure;
 a is the anchor plate width;
 h is the slab width;
 T_{ia} is the resultant tie-back tension force at the intermediate anchorage;
 P is the tendon force.

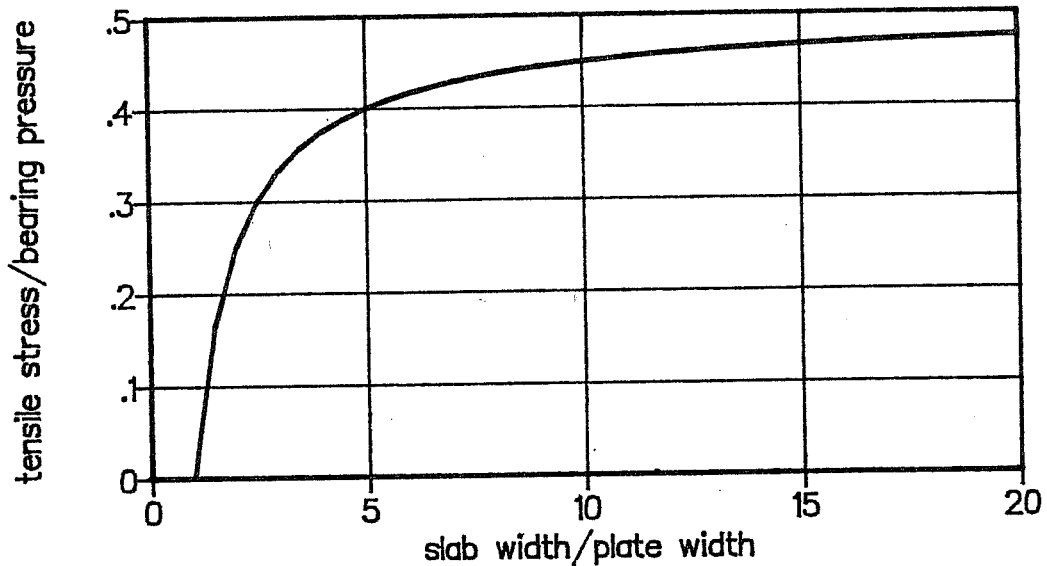


Figure 4.14 Tensile Stresses Behind Anchor

For slab width to anchor plate width ratios larger than five, 40 to 50 percent of the anchor force is indicated as tied back into the portion of the slab behind the anchor. For a typical bearing pressure of 3000 psi the calculated longitudinal tensile stresses behind the anchor can easily reach 1500 psi, which would definitely cause cracking. Such cracking is not detrimental to the strength of the structure since the direct load path in compression is available ahead of the anchor. However, it should not be overlooked that the loss of the load path in tension behind the anchor causes a significant increase of bursting stresses and of the resulting bursting force ahead of the anchor.

4.3.2.2 Isolated Slab Blister and Rib

Figures 4.15 and 4.16 show geometry, loading conditions, and the 3-D finite element mesh for the linear-elastic analysis of a half-scale model of an isolated slab blister. The anchor force of 124 kips corresponds to the breaking strength of a 12-½ in. strand tendon in the full-scale structure. In the finite element analysis all loads were applied as concentrated nodal forces.

A number of different boundary conditions were investigated and are summarized in Table 4.1. In

case (1) the portion of the slab behind the anchor was not included, so that an end

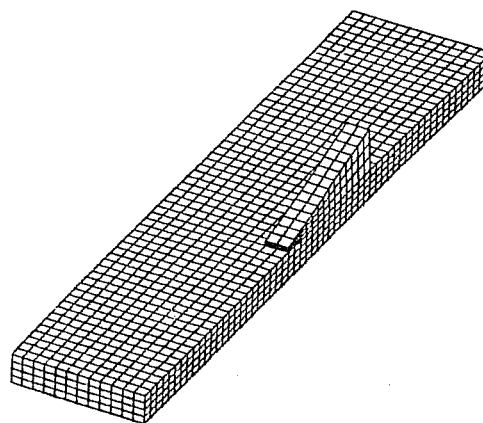


Figure 4.15 Finite Element Mesh for Isolated Slab Blister

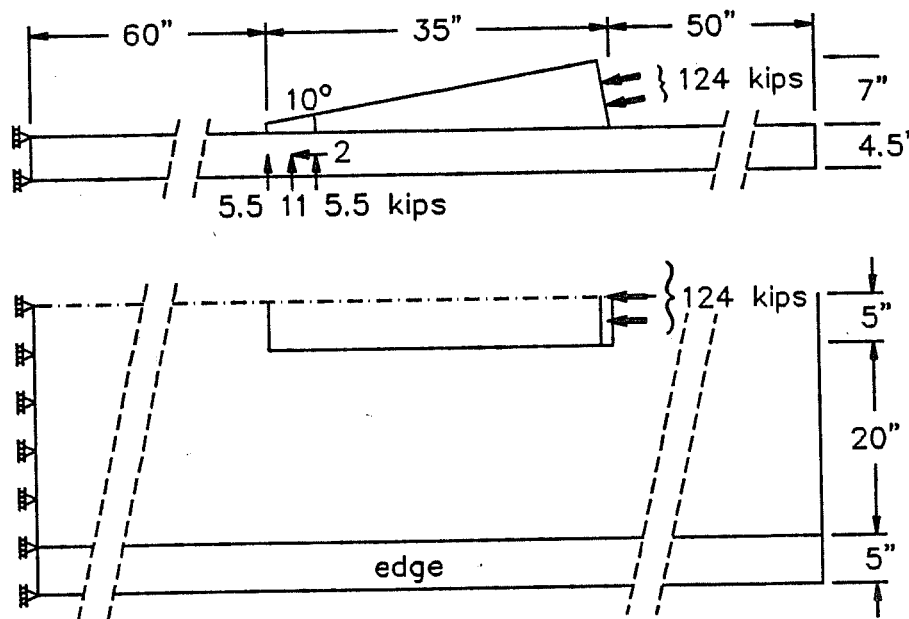


Figure 4.16 Dimensions and Loading Conditions for Isolated Slab Blister Finite Element Model

Table 4.1 **Finite Element Analysis Runs**

case	description	boundary conditions along edge	
		vertical support	stiffener
1	end blister, single anchor	free	no
2	intermediate blister, single anchor	free	no
3	intermediate blister, single anchor	fixed	no
4	intermediate blister, single anchor	fixed	yes
5	intermediate blister, two anchors	fixed	yes
6	rib, single anchor	fixed	yes

anchorage rather than an intermediate anchorage was modelled. In case (2) the portion of the slab behind the anchor was added. In actual bridge structures the slab with the blister would probably be part of a box girder. To model the restraints provided by the adjacent webs or flanges vertical displacements along the edge of the slab were locked in case (3). In the experimental portion of the study thin edge beams were provided to ensure stability during the test set-up and to model the webs of a box girder (Figure 4.30). In the finite element model the edge beams were modelled by increasing the modulus of elasticity of the corresponding portions of the slab and by locking the vertical displacements along the edges (case (4)). Although these boundary conditions are not entirely representative of the conditions for the test specimen, they are close enough to gain insight into the behavior of the specimens prior to cracking. In case (5) the width of the blister was doubled from 10 in. to 20 in. Two 62 kip loads were applied, one on either side of the center line at a distance of 5 in. In case (6) the blister extended over the full width of the slab to form a rib. A single, concentric 124 kip load was applied.

The general form of the distribution of principal tensile and compressive stresses in the plane of symmetry is quite similar for all cases (Figures 4.17 and 4.18). Critical regions with large tensile stresses exist behind the anchor, particularly at the reentrant

corner, and at the toe of the blister, where the tendon is deviated to enter the blister. The effects of tendon curvature include radial tensile stresses in the plane of curvature and stresses due to lateral bending perpendicular to the plane of curvature. The lateral bending stresses are tensile inside the tendon curvature (Figure 4.17) and compressive outside the curvature (Figure 4.18). Additional tensile stresses occur close to the bottom of the slab due to the eccentricity of the tendon ("local bending"). Compressive stresses are largest immediately ahead of the anchor. They remain significant within the blister region before dissipating into the slab.

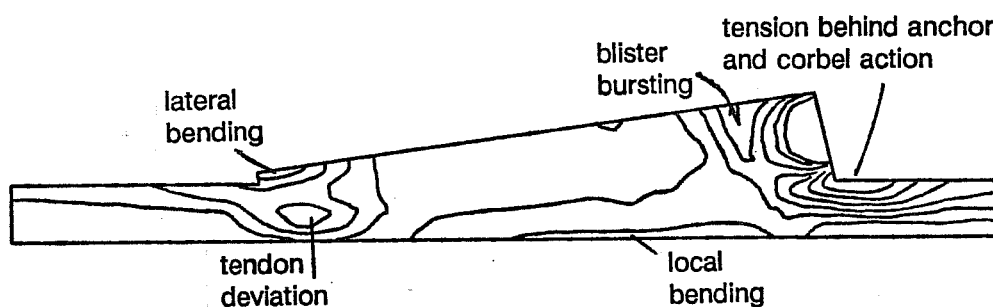


Figure 4.17 Principal Tensile Stresses in Plane of Symmetry

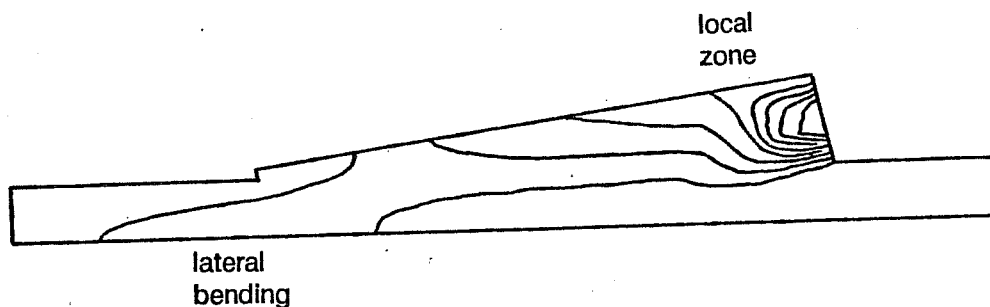


Figure 4.18 Principal Compressive Stresses in Plane of Symmetry

In Table 4.2 the magnitude of the resultant transverse tensile force was obtained by summing up the reaction forces in the plane of symmetry of the finite element models. Where possible, a rough break-down into slab bursting force, T_{slab} , blister bursting force, T_{blis} , and tensile force due to lateral bending, T_{lat} , is given. All forces are expressed as percentage of the total applied tendon load, P . The distance of the slab bursting force from the anchor is also indicated in the table.

Table 4.2 Resultant Transverse Tensile Forces

case	description	T_{slab}/P [%]	T_{blis}/P [%]	T_{lat}/P [%]	T_{total}/P [%]
1	end blister	18.5 @ 40.7"	8.3	3.8	30.6
2	free edge, no stiffener	18.3 @ 32.7"	7.6	3.6	29.5
3	edge fixed, no stiffener	22.0 @ 29.8"	7.3	3.5	32.7
4	edge fixed and stiffened	24.3 @ 32.3"	7.3	3.5	35.0
5	double blister	17.0 @ 40.1"	1.7 ¹	5.5	24.2
6	rib	26.4 @ 30.0"	14.2 ² @ 19.5"		40.5 @ 26.4"

¹) tie force between anchors at loaded face of blister

²) total transverse tension force in rib portion

There is not much difference in the magnitude of the slab bursting force between the end blister and the intermediate blister (cases (1) and (2)). However, for the end blister the resultant slab bursting force is located further ahead of the anchor. Comparison of cases (2) and (3) shows that locking the vertical displacements along the long edge of the slab increases the magnitude of the slab bursting force by 20% from 0.18P to 0.22P (Table 4.2). This is due to the fact that a portion of the vertical tendon component and of the tendon deviation force, respectively, is carried to the edge supports by lateral bending action. In case (3) roughly one third of the vertical forces is transferred to the edge supports.

Adding longitudinal stiffness to the edges further increases the slab bursting force (case (4)). The stiffened edges resist a larger portion of the applied tendon load, hence the compressive stresses have to spread out more, requiring larger transverse tension and compression forces. On the other hand, in case (5) the two applied loads are distributed over a larger portion of the slab and consequently the slab bursting force is smaller.

Case (6) indicates that for anchorage in a rib the total transverse tensile force is roughly 15% larger than for the corresponding isolated slab blister (case (6) versus

case (4)). In rib anchorages the compressive stresses spread out immediately ahead of the anchor. In contrast, in isolated slab blisters the compressive stresses first are gradually transferred from the blister into the slab before they can spread out. The more concentrated introduction of the tendon force and the larger lateral bending effect due to tendon curvature are responsible for the increase of the transverse tension force in rib anchorages. As a rule of thumb, it is noted that the slab bursting force, T_{slab} , is generally less or close to 25% of the tendon force.

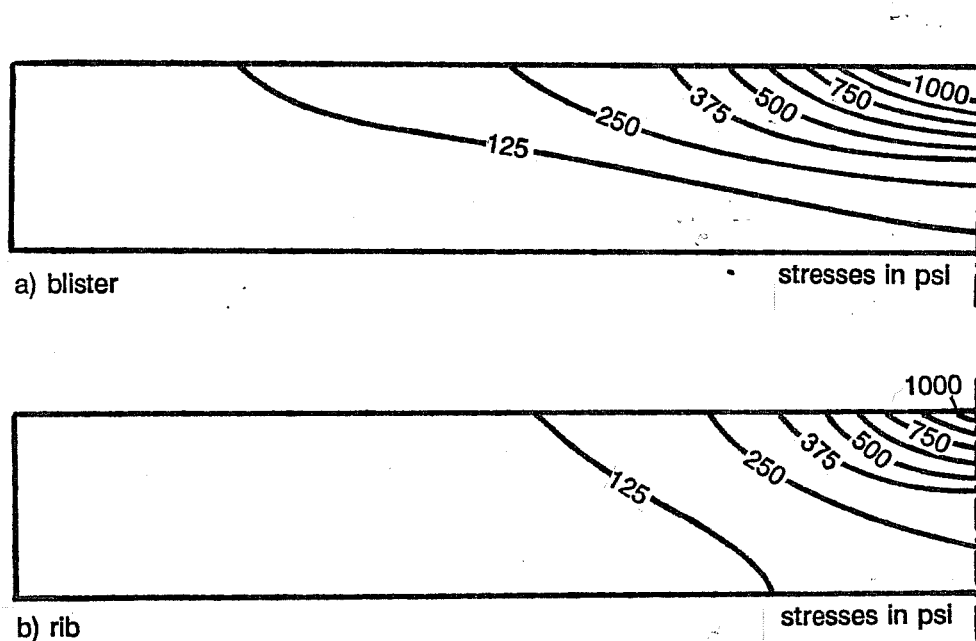


Figure 4.19 Comparison of Principal Tensile Stresses in Section Immediately Behind Anchor

Figures 4.19 through 4.22 further illustrate the difference between isolated slab blister and rib. Figure 4.20 compares principal tensile stress contours in the plane of symmetry. The tensile stresses behind the anchor are smaller for the rib anchorage, but the lateral bending stresses are larger and extend over a bigger region. This is also confirmed by Figures 4.19 and 4.21 which show principal tensile stresses in sections perpendicular to

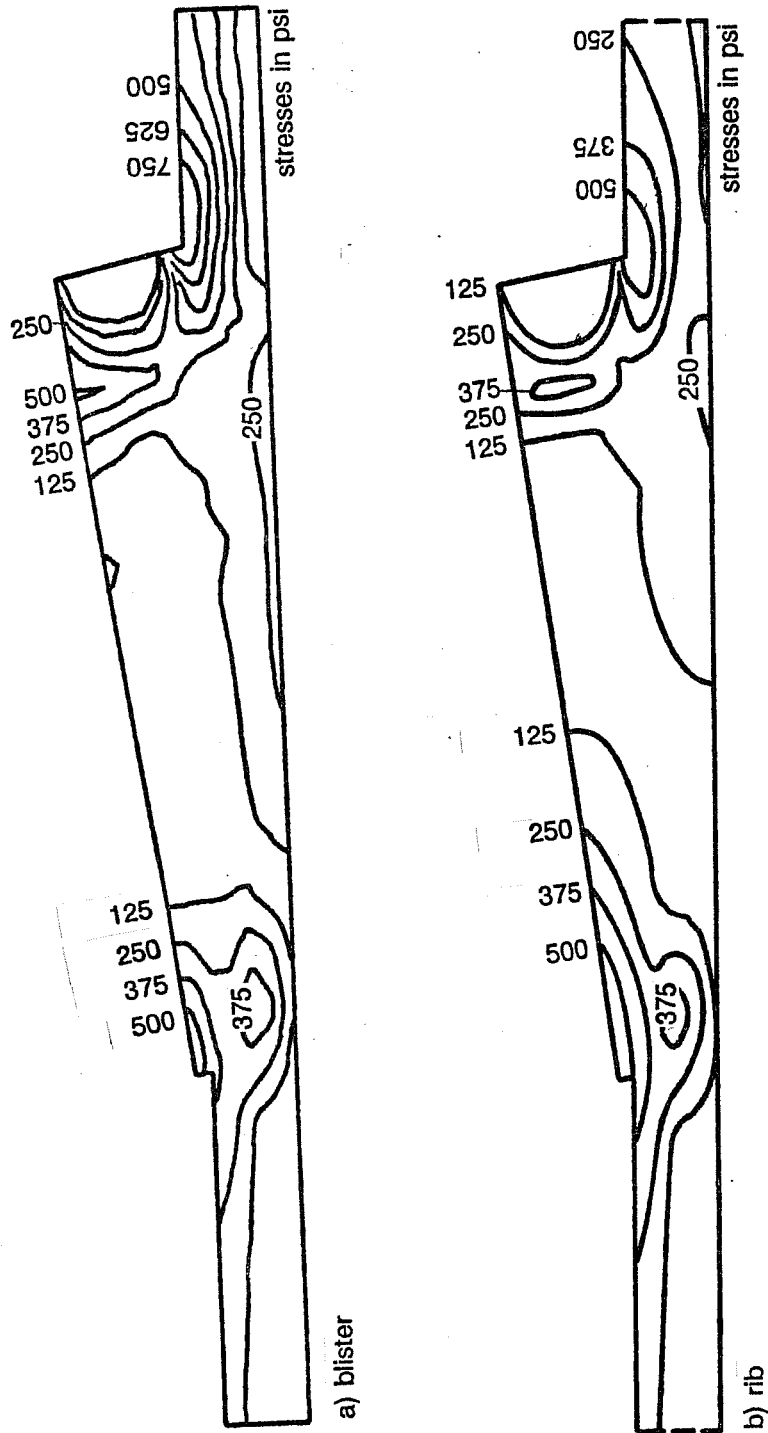


Figure 4.20 Comparison of Principal Tensile Stresses in Plane of Symmetry

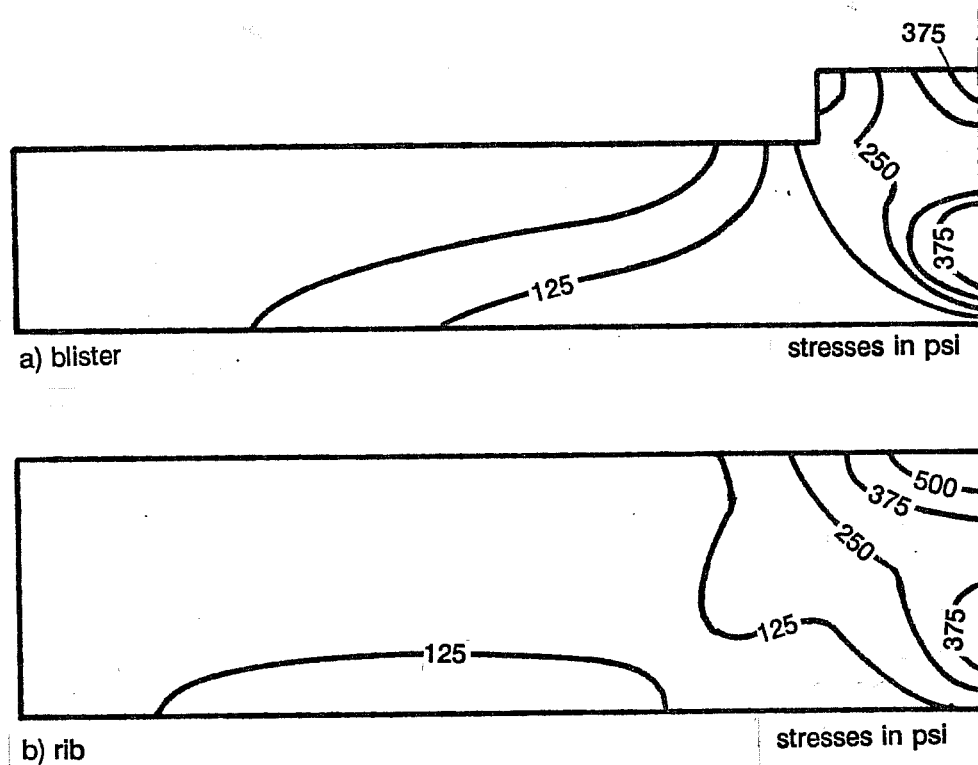


Figure 4.21 Comparison of Principal Tensile Stresses in Section at Toe of Blister

the tendon immediately behind the anchor and at the toe of the blister, respectively.

Comparison of principal compressive stresses in the plane of symmetry shows, that the compressive stresses disperse much faster for anchorages in ribs than for isolated slab blisters (Figure 4.22).

4.3.2.3 Discussion

In both blister and rib critical regions are located immediately ahead of the anchor where large compressive stresses occur. Tensile stresses are critical in the reentrant corner immediately behind the anchor, in the blister bursting region ahead of the anchor, and in the region of tendon curvature.

A rib allows for more rapid dispersal of the concentrated compressive stresses introduced by the anchor and reduces the tensile stresses behind the anchor. In isolated slab blisters the concrete compressive stresses are channeled in the blister. This increases

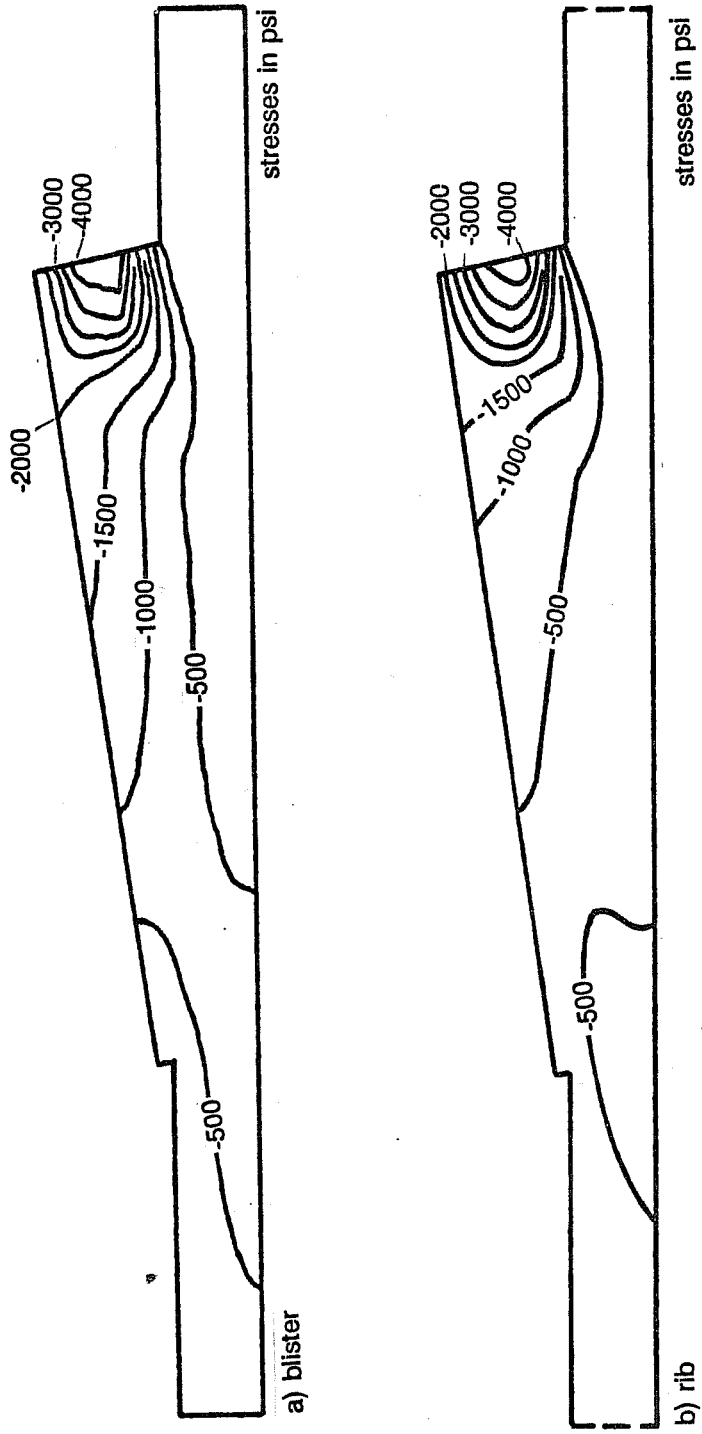


Figure 4.22 Comparison of Principal Compressive Stresses in Plane of Symmetry

the level of compressive stresses but also allows a more gradual transfer of the anchor force into the slab, which reduces the slab bursting force and the lateral bending moment due to tendon curvature. In either case tensile stresses behind the anchor and at the toe of the blister exceed typical concrete tensile strengths by far and cracking must be expected in these regions.

Cracking behind the anchor is not detrimental to the strength of the structure, since a more direct load path in compression is available. On the other hand, the region of tendon curvature requires careful attention to avoid premature failures.

4.3.3 Development of Strut-and-Tie Models

4.3.3.1 Embedded Anchor

Figure 4.23 shows a strut-and-tie model that closely approximates the stress trajectories of the elastic solution for the intermediate anchorage in a plane slab. For this simple case it is relatively easy to select the geometry of the strut-and-tie model such that the member forces match the corresponding resultant forces of the finite element solution exactly. Practically such close agreement is difficult to achieve other than for the most basic problems. However, considering the non-linear behavior of reinforced concrete, particularly after cracking, a solution in strict agreement with the linear-elastic solution is certainly not required.

Figure 4.23 shows that two load paths are available at the intermediate anchorage. One of them involves compression ahead of the anchor and transverse tensile forces due to spreading of the compression stresses. This load path is identical to that in end anchors (see Chapter 3). In the other load path, part of the anchor force is tied back into the portion of the slab behind the anchor. Since strut-and-tie model procedures have only a limited capability to detect compatibility requirements they cannot provide any guidance on the

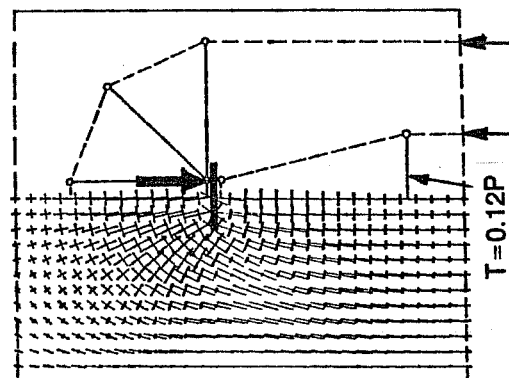


Figure 4.23 Stress Trajectories and Strut-and-Tie Model for Embedded Intermediate Anchorage

distribution of the anchor force to these two load paths. The linear-elastic solution indicates that up to 50% of the anchor force is carried by the tie-back path. However, in the finite element analysis the same material stiffness and unlimited strength was used for both tension and compression. In reality, large tensile stresses will cause early cracking behind the anchor plate which greatly reduces the stiffness of the tie-back path. Hence, only a small portion of the anchor load is carried in tension behind the anchor, depending on the amount of reinforcement present. A pragmatic, practical approach is to ignore this load path in the development of the strut-and-tie model and to provide nominal reinforcement behind the anchor for crack control. Then the bursting force ahead of the anchor can be determined from the same strut-and-tie model procedures as used for end anchors.

4.3.3.2 Isolated Slab Blister

For analysis and design of the blister problem three-dimensional analysis is required. This introduces considerable complexity and makes it more difficult to find a precise match of finite element solution and strut-and-tie model solution. However, strut-and-tie models can be found which capture all essential characteristics of the load path in blisters. Design of the reinforcement based on such load paths is actually easier than using finite element analysis results, because the interpretation of a three-dimensional stress distribution and its translation into reinforcement requirements are quite difficult.

Figure 4.24 illustrates development and successive refinement of a strut-and-tie model for an isolated slab blister. The procedure is discussed below step by step.

1. Concentrated strut model

In Figure 4.24a the anchor force, P , is carried by a concentrated compression strut. This strut is deflected by the tendon deviation force, D , in the region of tendon curvature. No concrete tensile force is required for this load path. Although it represents a valid equilibrium solution, it is not useful for determining the reinforcement requirements.

2. Split strut model

In Figure 4.24b the strut and tie model is refined by splitting the concentrated compression strut of Figure 4.24a into two struts. This step reveals the presence of a blister bursting force, T_1 , and of a tendon deviation force T_2 . The magnitude of the blister bursting force is very sensitive to the location of the local zone nodes, a , and to the distance of the blister bursting reinforcement from the anchor. Guyon's symmetrical prism approach is

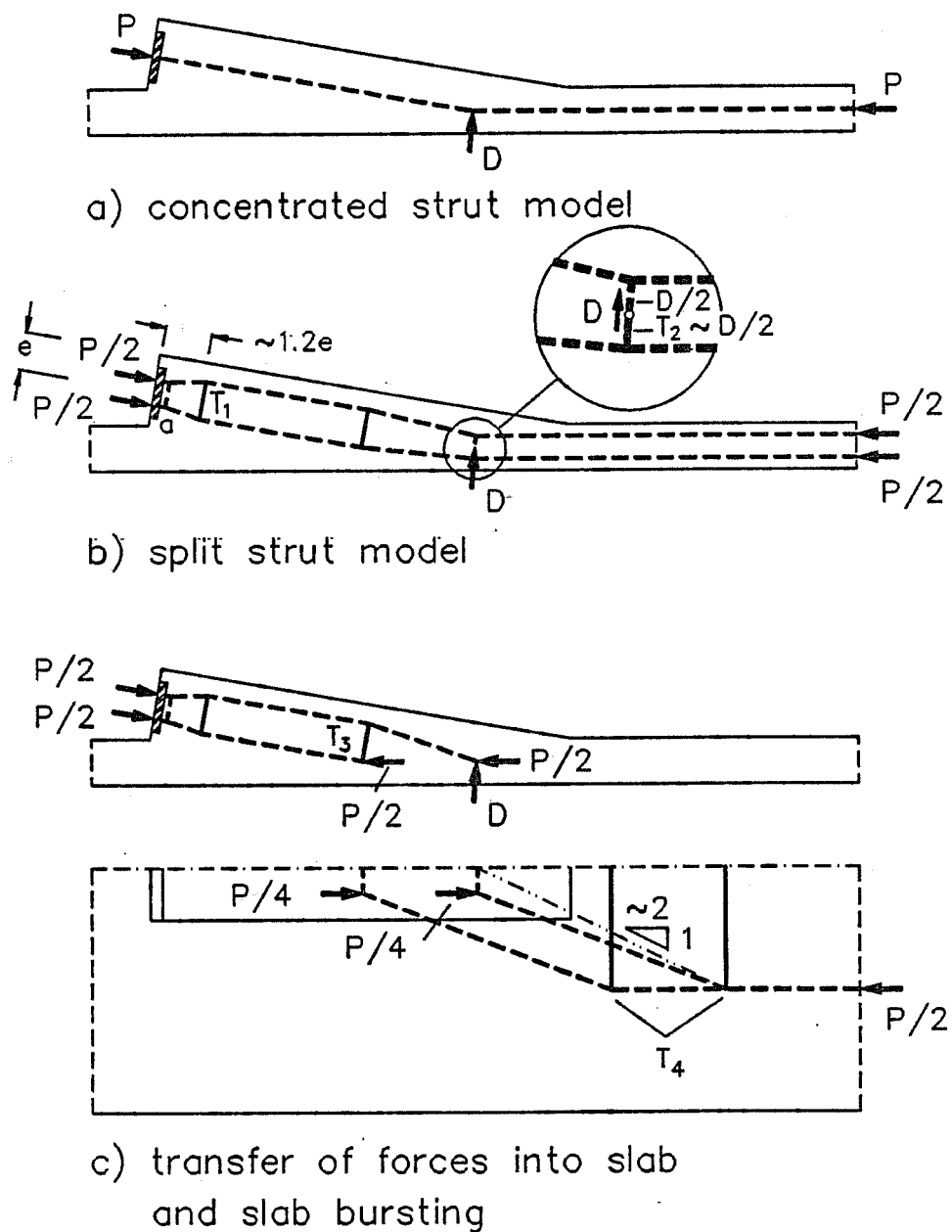


Figure 4.24 Development of Strut-and-Tie Model for an Isolated Slab Blister

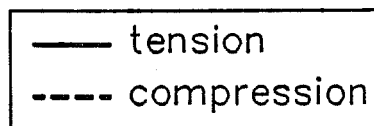
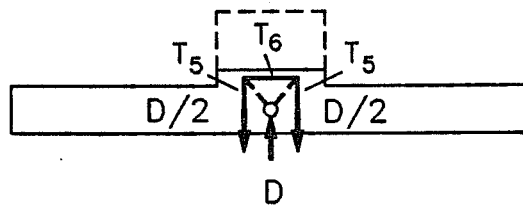
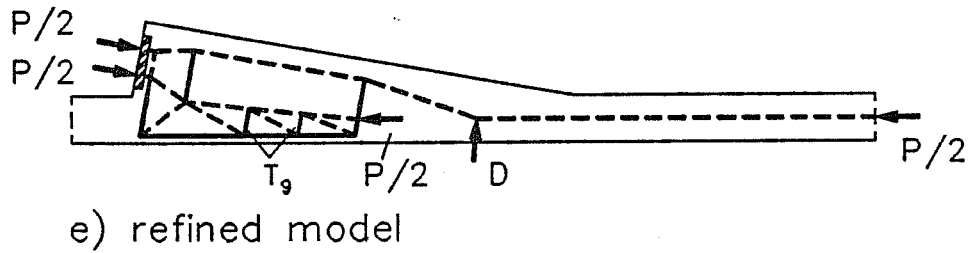
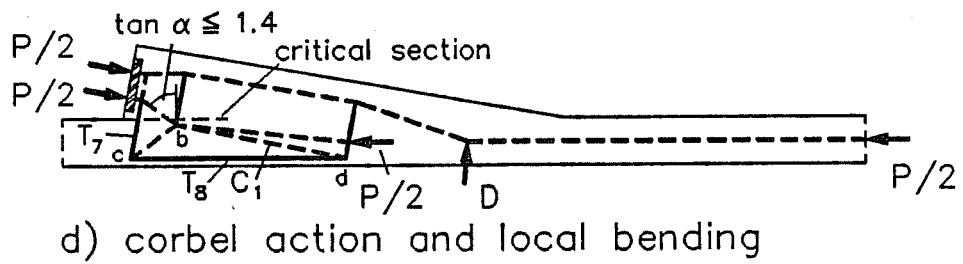


Figure 4.24 (cont.) Development of Strut-and-Tie Model for an Isolated Slab Blister

useful to estimate the magnitude of force T_1 . Generally the blister bursting force is fairly small and reinforcement requirements for confinement of the highly compressed local zone will control. Frequently a spiral is provided for confinement, and tie reinforcement is added to carry the blister bursting force. As an alternative solution the need for a spiral in the local zone may be eliminated by increasing the amount of tie reinforcement in this region [43]. Such a detail is advantageous in-as-much as it may reduce congestion in the local zone region.

The enlarged detail in Figure 4.24b indicates that only half the tendon deviation force needs to be tied back. The remainder is balanced by the compression forces on the inside of the curvature. Practically it is better to tie back the full tendon deviation force because this region is very sensitive to construction inaccuracies.

3. Transfer of forces into slab

In the previous two models spreading of the forces in the plane of the slab was ignored. In reality the compressive stresses will disperse as soon as they have reached the slab. This consideration is reflected in the load path shown in Figure 4.24c. Half of the anchor force is resisted at an intermediate location of the blister while the remainder is resisted close to the end of the blister. Figure 4.24c also shows the flow of forces in the slab to the end of the anchorage zone.

With this load path the vertical shear force stays inside the blister region and is balanced by the tendon deviation force. Figure 4.24f illustrates the tie-back reinforcement (force T_5) and lateral bursting reinforcement (force T_6) requirements in the region of tendon curvature.

4. Corbel action and local bending

In Figure 4.24d the lower compression strut is pulled down into the slab by the corbel action force, T_7 . Equilibrium at node c requires a local bending force, T_8 . The upper strut remains unchanged and consequently the blister bursting force, T_1 , is not affected by corbel action and local bending. The magnitude of forces T_7 and T_8 can be arbitrarily selected by the choice of the node b location. Some guidance for the location of node b can be obtained from shear-friction reinforcement requirements. To consider shear-friction in the development of strut-and-tie models, the angle α between compression struts and the direction normal to the critical section must be limited to values corresponding to the available coefficient of friction, μ (see Section 5.4.7 for a more detailed explanation). For

monolithically placed concrete $\mu = 1.4$. With these considerations the location of node b is determined. The load paths in the slab (Figure 4.24c) and at the toe of the blister (Figure 4.24f) are not affected by corbel action and local bending.

It is pointed out that forces T_7 and T_8 are not essential for equilibrium, since an alternate load path without these forces exist (Figure 4.24c). Force T_7 is not a true corbel action force but is induced by compatibility requirements of deformations between blister and slab. In contrast, in a true corbel loss of the corbel action force would lead to collapse of the member (Figure 4.25).

5. Refined Model

In Figure 4.24d tensile force T_8 and strut C_1 meet at a very acute angle at node d. To avoid compatibility problems it is recommended to make the angles between struts and ties not smaller than 25 degrees. Figure 4.24e shows the final model where strut C_1 is replaced by a system of strut and ties.

In Figure 4.26 the member forces are calculated for the refined model using a numerical problem corresponding to the finite element analysis of case (2) in Section 4.3.2. All forces are expressed as a fraction of the applied tendon force, P . Comparison with the results in Table 4.2 shows that the strut-and-tie model results are close to but consistently higher than the finite element analysis results.

6. Proportioning and arrangement of the reinforcement

Once the member forces are determined proportioning of the reinforcement is straight forward. Reinforcement should be arranged corresponding to the orientation of the ties in the strut-and-tie model. Figure 4.27 shows a schematic reinforcement arrangement for the isolated slab blister example of Figure 4.26. The indices in the reinforcement labels correspond to the tie forces in Figures 4.24 and 4.26. Besides the reinforcement determined from the strut-and-tie model additional longitudinal reinforcement is provided for crack control behind the blister. This load path could have been easily included in the strut-and-tie model, but it is simpler and safe to ignore it and to provide a nominal amount of reinforcement instead.

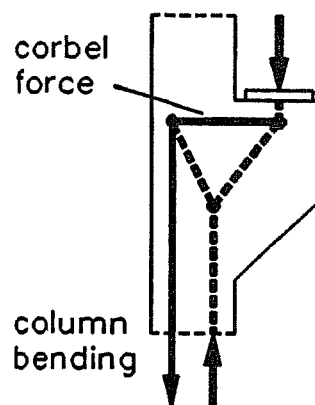


Fig. 4.25 Load Path in Corbel

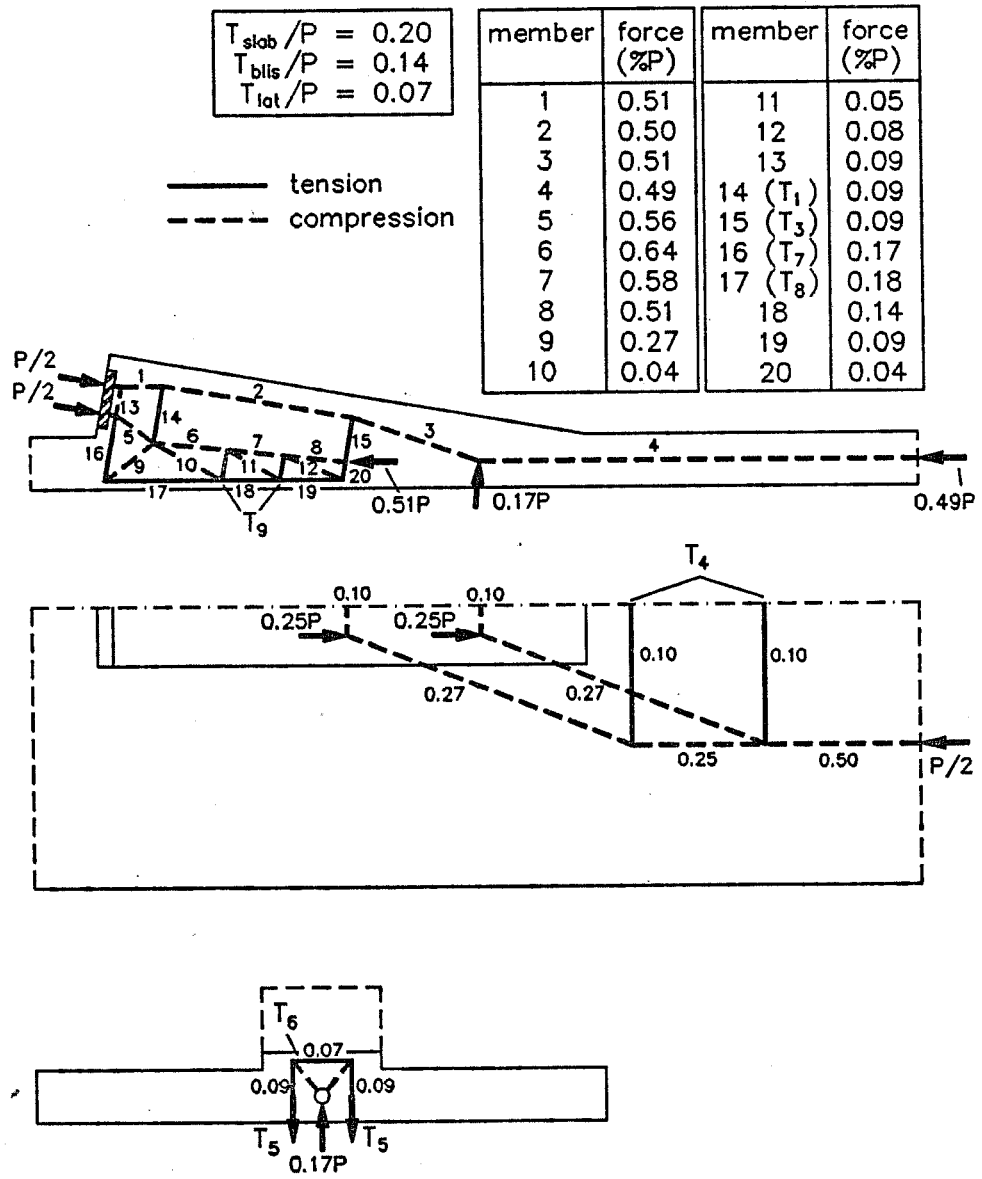


Figure 4.26 Member Forces

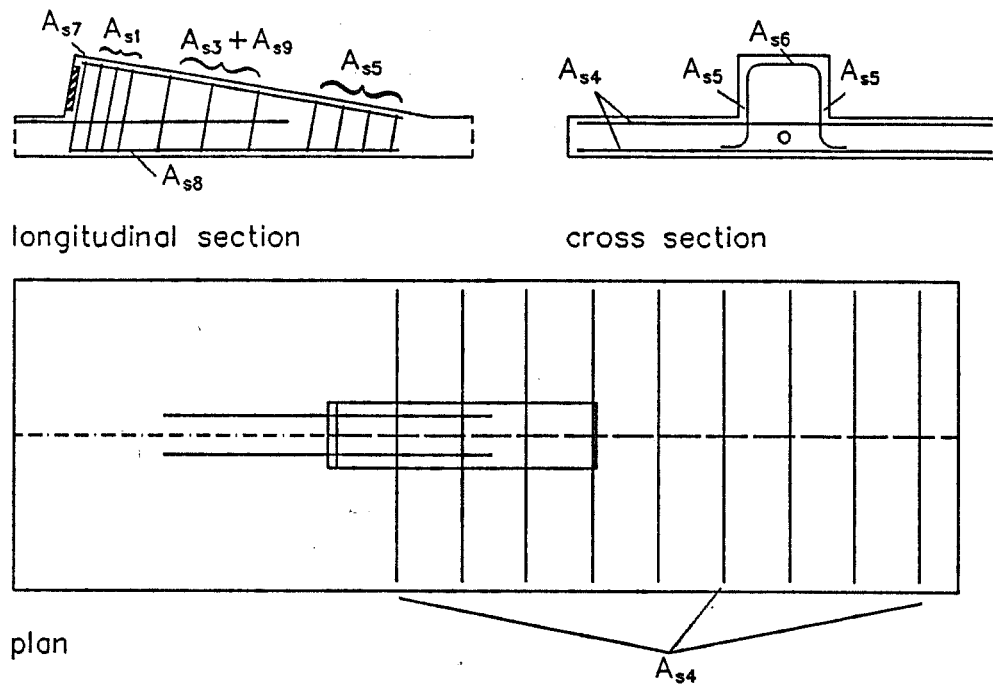


Figure 4.27 Reinforcement Arrangement

Attention must be paid to proper detailing. In particular, the blister tie reinforcement should be fully developed at the interface between slab and blister. In thin slabs this can be achieved by bending the legs of the ties around reinforcement in the slab.

7. Check of compression stresses

The check of concrete compressive stresses is more involved than proportioning the reinforcement. The basic procedure is to determine the minimum cross sectional area for each member to accommodate its force without exceeding the effective concrete compressive strength. In this way the members of the strut-and-tie model receive a physical dimension. If these members can be accommodated within the boundaries of the structure and if they do not overlap, the concrete compression stresses are safe.

Figure 4.28 shows the strut-and-tie model for the isolated slab blister example including minimum member dimensions. All struts are located within the boundaries of the structure and failure should be governed by the capacity of the reinforcement. Analysis of the nodes in this model is quite cumbersome and is practical only for the most critical struts. In Reference 48 procedures for the construction of nodes are presented which are

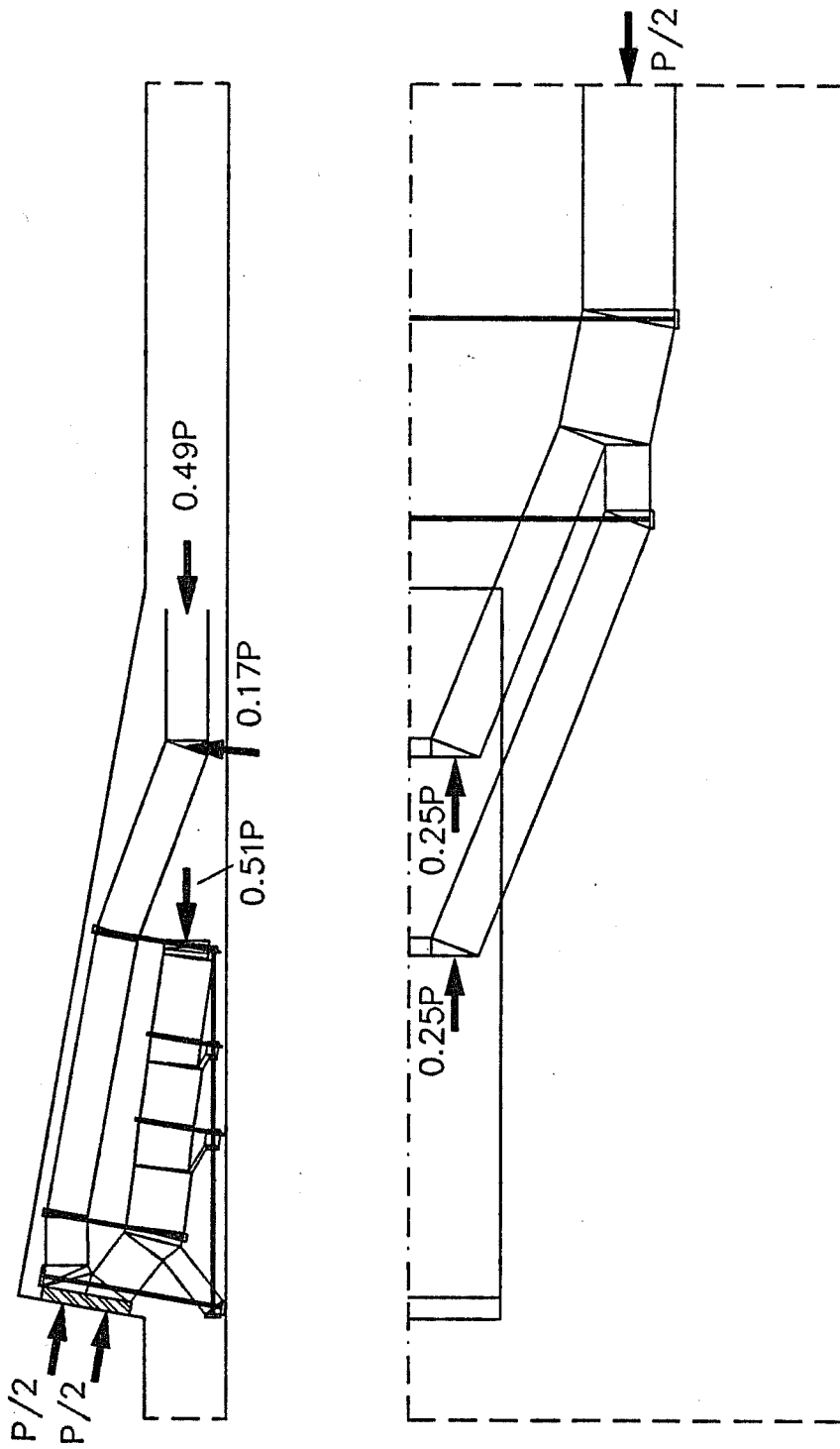
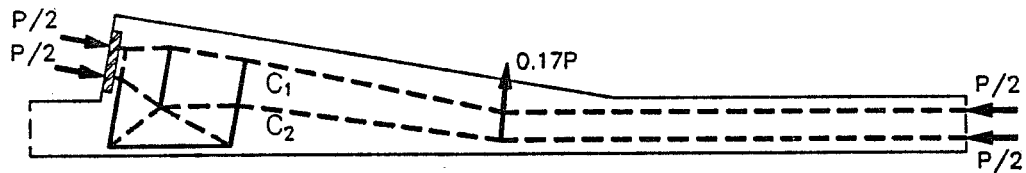


Figure 4.28 Strut-and-Tie Model With Minimum Member Dimensions

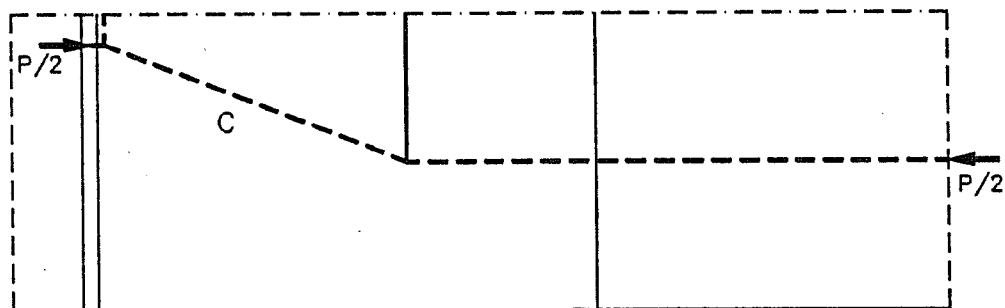
suitable for implementation in a computer program. Computer aided design procedures based on strut-and-tie models hold great promise for future developments [48].

4.3.3.3 Rib

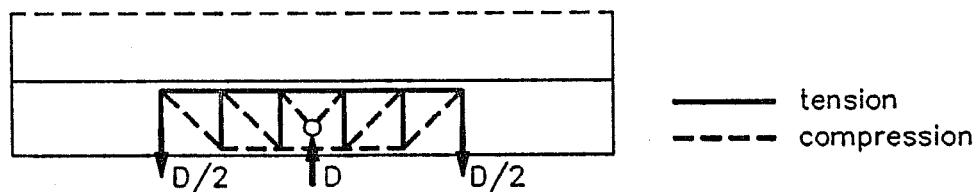
In isolated slab blisters the compressive stresses first must be transferred from the blister to the slab before they can disperse in the slab. In contrast, in ribs the compressive stresses can spread out immediately. Thus anchorage in a rib is not unlike anchorage in a rectangular member. However, additional considerations for corbel action, local bending and lateral bending are required.



a) longitudinal section



b) plan



c) cross section

Figure 4.29 Strut-and-Tie Model for a Rib Anchorage

Figure 4.29 shows a possible strut-and-tie model solution for the anchorage of a single concentric tendon in a rib. As for the isolated slab blister, the load path in tension behind the anchor is not included in the model. The plan view in Figure 4.29b shows how the compressive forces spread immediately ahead of the anchor. Compression strut C in this view represents the more complex system of struts and ties shown in the longitudinal section (4.29a). Figure 4.29c shows a cross section at the tendon deviation point. Lateral bending is required to balance the vertical components, $D/2$, of the inclined compression struts (C_1 and C_2) and the tendon deviation force, D .

Principally, the strut-and-tie model developed in the previous section for the isolated slab blister would also be a valid equilibrium solution for the rib. It is typical for strut-and-tie models that the solution to a given problem is usually not unique. This poses a considerable challenge to the design engineer, since judgement is required to select the "best" solution. Of course, from a limit state design standpoint all equilibrium solutions that do not exceed the effective material strengths are equally valid lower bounds to the actual plastic limit load.

4.3.4 *Experimental Program*

4.3.4.1 General

The experimental portion of the study included four half-scale specimens. Specimens Blister1 and Blister2 modelled isolated concentric slab blisters with a single anchor (Figure 4.2a), while specimen Blister3 had two anchors. Specimen Blister4 had a rib extending over the full slab width and anchored a single concentric tendon (Figure 4.2b).

Figure 4.30 shows geometry and dimensions of all specimens. The flanges along the edges of the slab were added to provide stability during test set-up and to model the webs of a box girder section. The lengths of the portions of the slab ahead of and behind the blister were determined by the need to model the entire region affected by the introduction of the anchor force. According to the principle of Saint Vénant this region extends for a distance approximately equal to the width of the slab ahead of and behind the anchor.

Table 4.3 lists the concrete cylinder compressive strengths at time of testing. Reinforcement included Swedish and Mexican #2 bars and ASTM A615 GR60 #3 bars. The Swedish #2 reinforcement were actually 6 mm diameter bars with an area of 0.044 in^2 and a yield strength of 72 ksi. The Mexican #2 bars had an area of 0.05 in^2 and a yield strength

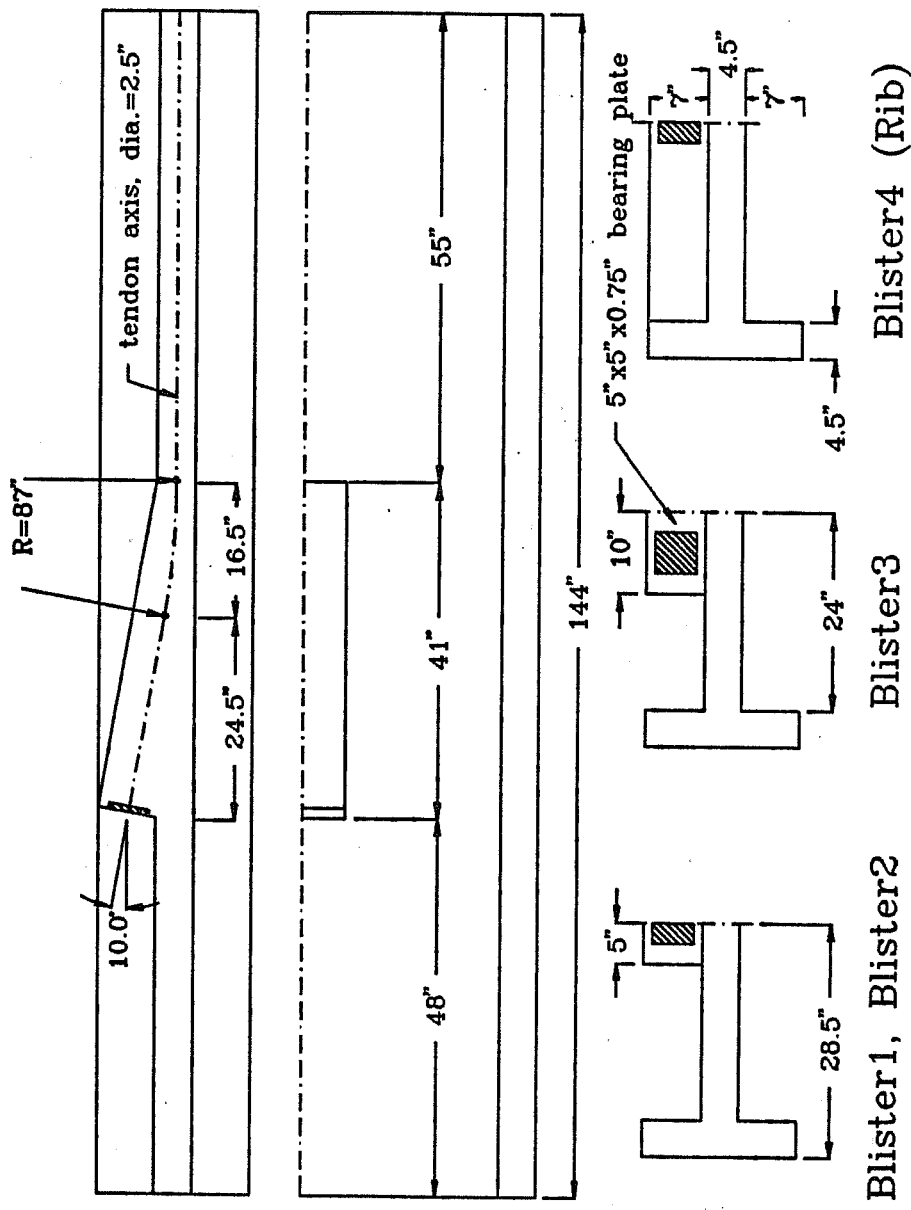


Figure 4.30 Geometry of Isolated Slab Blister and Rib Specimens

of 47 ksi. The yield strength for the #3 bars generally fell between 60 and 66 ksi.

Table 4.3 Concrete Strengths for Slab Blister Specimens

specimen	f'_{ci} (psi)
Blister1	4900
Blister2	4200
Blister3	4900
Blister4	4700

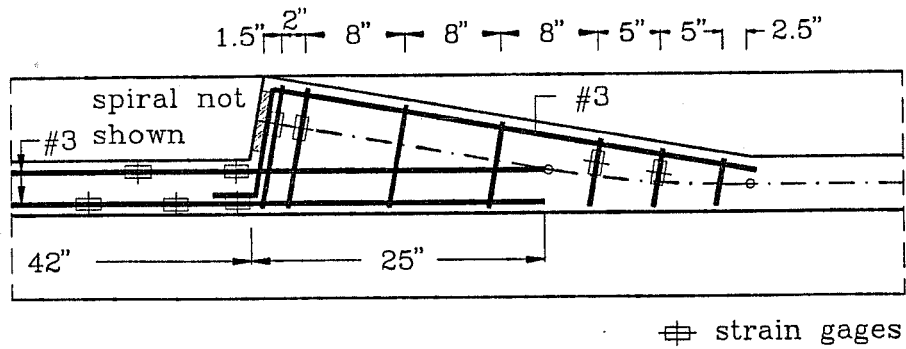
4.3.4.2 Specimen Design

The design load, F_{pu} , was 124 kips per tendon for all specimens. This load corresponds to the breaking strength of a 12-½ in. strand tendon, GR270, reduced by a factor of four for the half-scale model used ($\frac{1}{4} \times 12 \times 0.153 \text{ in}^2 \times 270 \text{ ksi} = 124 \text{ kips}$). Design was based on a combination of finite element analysis results, strut-and-tie models, and AASHTO specifications. Table 4.4 gives an overview of the tensile forces used for proportioning the reinforcement. The forces are expressed as a percentage of the design load, F_{pu} . Reinforcement was provided to resist these forces at yield. The design considerations for various regions in the specimens are discussed in more detail in the following paragraphs. Reinforcement details are shown in Figures 4.31 through 4.34.

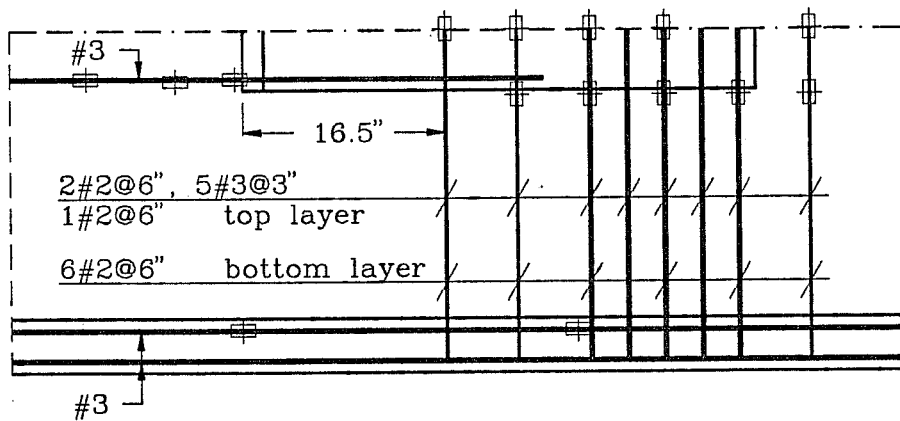
Table 4.4 Design Forces

specimen	F_{pu} (kips)	blister bursting* and corbel action (% F_{pu})	local bending (% F_{pu})	tension behind anchor (% F_{pu})	slab bursting (% F_{pu})	lateral bending (% F_{pu})
Blister1	124	0.12	0.11	0.20	0.28	0.25
Blister2	124	0.26	0.05	0.20	0.27	0.09
Blister3	2 x 124	0.17	0.09	0.15	0.24	0.09
Blister4	124	0.03	0.03	0.25	0.24	0.21

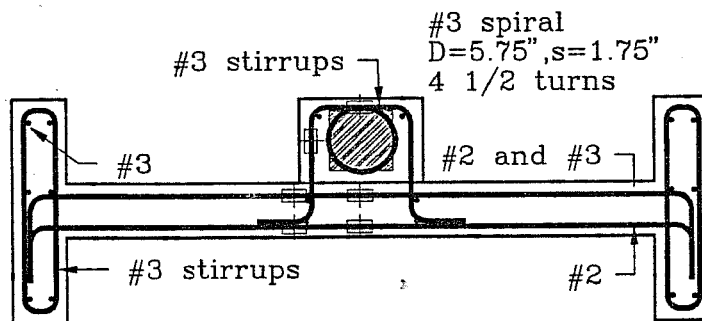
*) in addition to spiral



Elevation

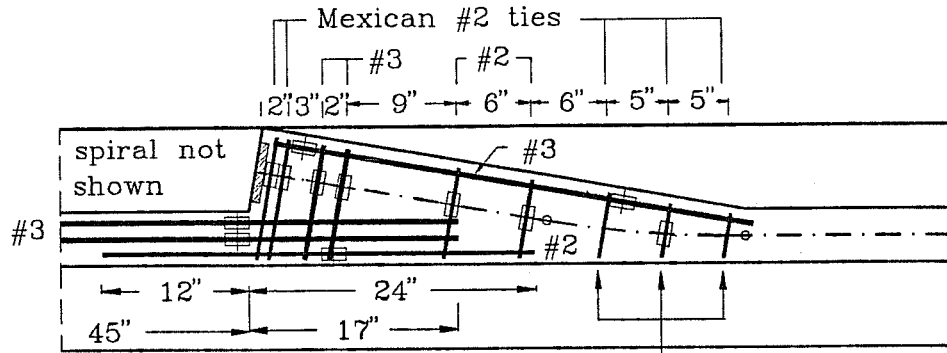


Plan

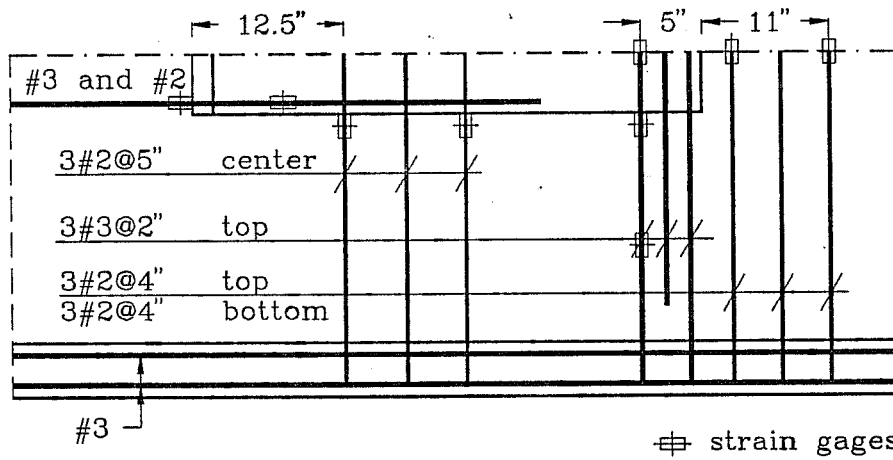
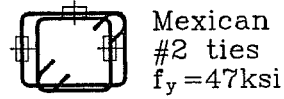


Cross Section

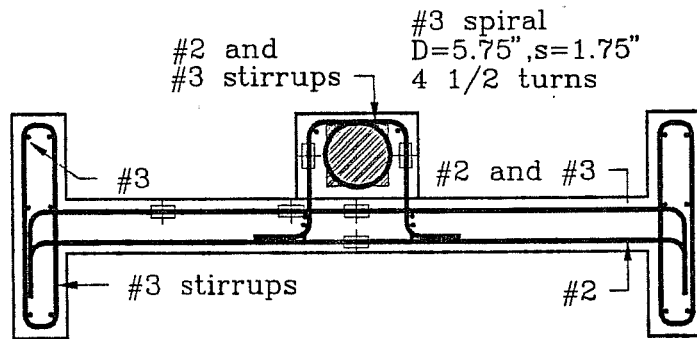
Figure 4.31 Reinforcement Details for Specimen Blister1



Elevation



Plan



Cross Section

Figure 4.32 Reinforcement Details for Specimen Blister2

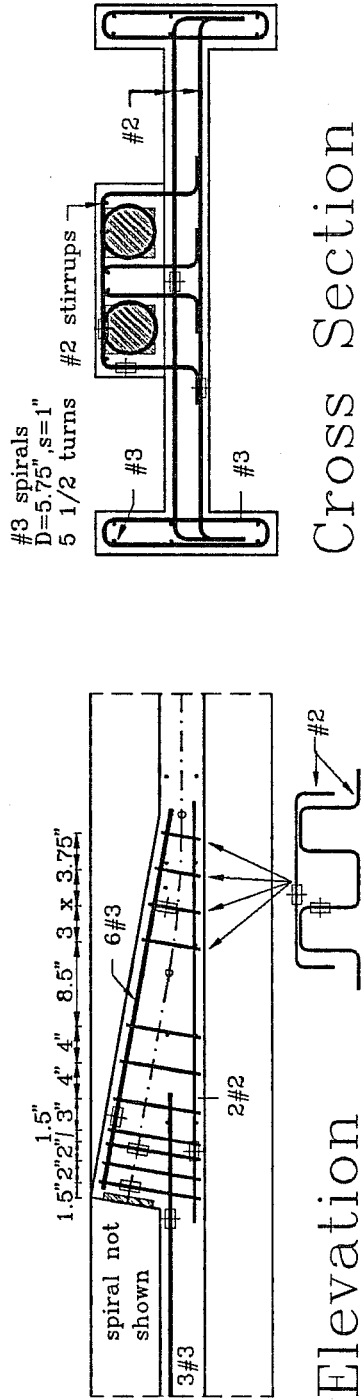
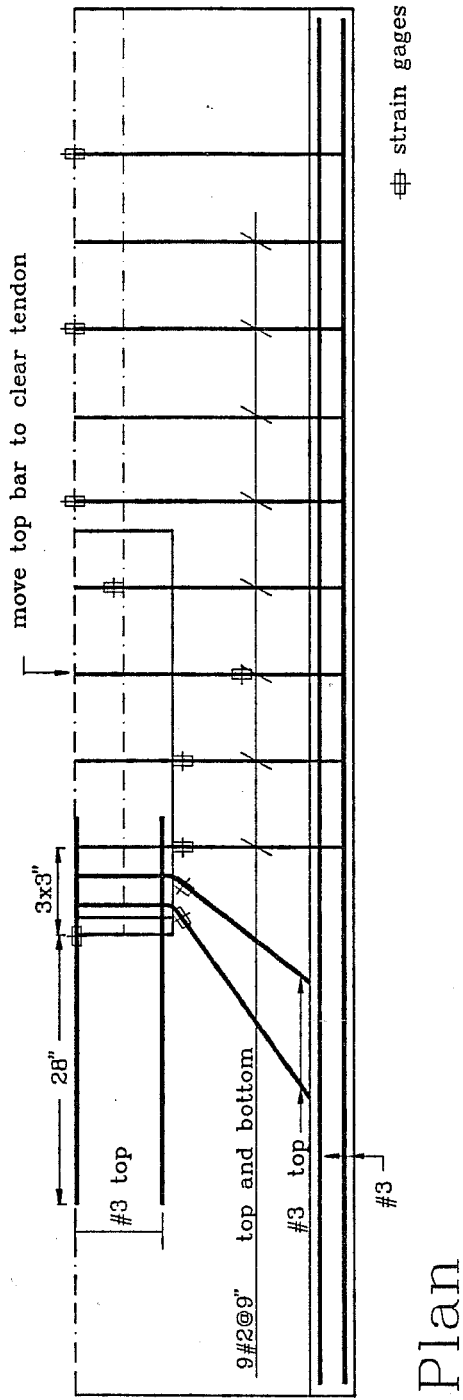
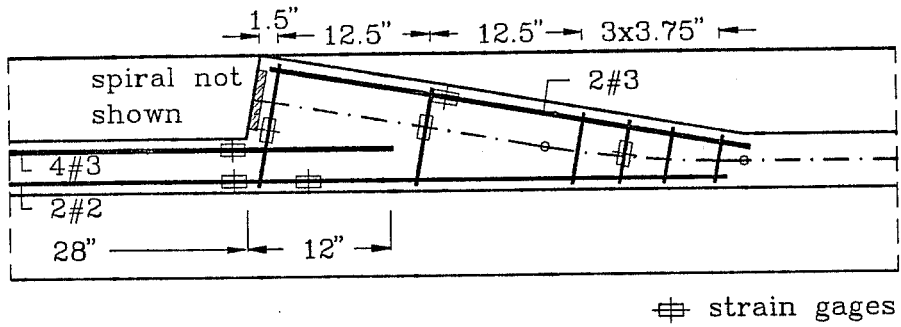
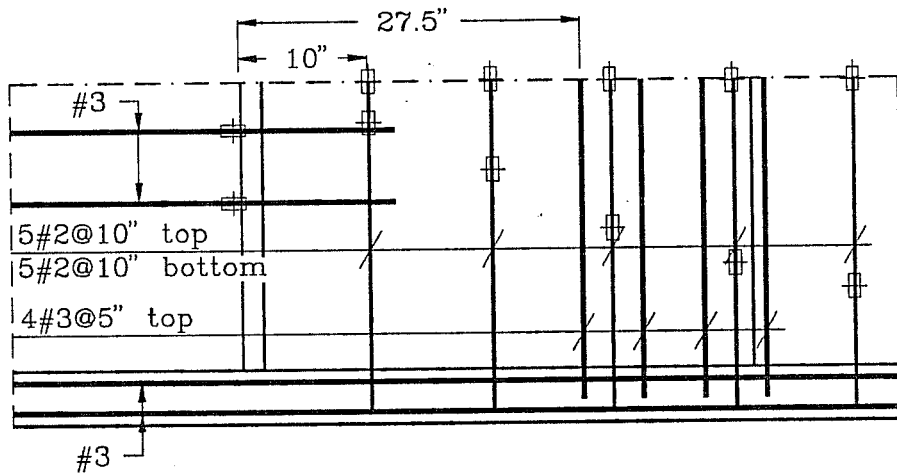


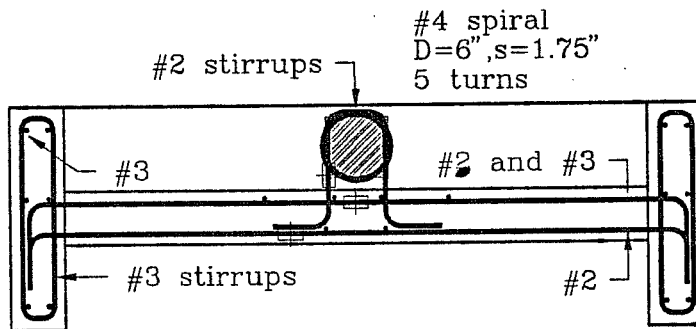
Figure 4.33 Reinforcement Details for Specimen Blister3



Elevation



Plan



Cross Section

Figure 4.34 Reinforcement Details for Specimen Blister4

1. Local zone confinement

Spiral reinforcement for confinement of the local zone was provided in all specimens. In specimens Blister1 and Blister2 anchor plate dimensions and spiral geometry were based on European manufacturers' information for three-strand tendons. With these dimensions and considering the additional ties in the local zone, the best fit equation proposed by Roberts (Equation 2.2) predicts a local zone capacity of 210 kips for specimen Blister1 and 188 kips for specimen Blister2. This is well above the design load of 124 kips and thus should preclude a local zone failure.

Because failure loads of the first two specimens exceeded the design loads significantly, in specimens Blister3 and Blister4 the amount of spiral reinforcement was increased and designed for a tendon force of 250 kips, using Roberts' equation and assuming a concrete strength of 4500 psi.

2. Blister bursting

In specimens Blister1 through Blister3 blister bursting reinforcement was provided in addition to the confining spiral reinforcement. In specimen Blister4 the spiral served as confinement reinforcement as well as blister bursting reinforcement and no additional tie reinforcement was provided.

The blister reinforcement in specimen Blister1 was based on the details in the prototype structure shown in Figure 4.9. In specimens Blister2 and Blister3 strut-and-tie models were used for design of the blister bursting reinforcement. As mentioned in Section 4.3.3.2, the blister bursting force is quite sensitive to the geometry of the strut-and-tie model, which is the reason for the fairly large differences of the design forces listed in Table 4.4.

3. Corbel action

Reinforcement for corbel action is placed immediately ahead of the anchor and should tie into the slab. The distinction between local zone confinement reinforcement, blister bursting reinforcement, and corbel action reinforcement is somewhat theoretical, since all of this reinforcement acts in all functions. Corbel action reinforcement is not essential for equilibrium and serves mostly for control of cracking at the reentrant corner behind the anchor.

4. Local Bending

Longitudinal local bending tensile stresses exist at the bottom of the slab due to eccentricity of the tendon. Similar to corbel action, local bending reinforcement is not essential for equilibrium. Nominal reinforcement (2#3 bars) was provided in specimen Blister1 (Figure 4.31). In the other specimens local bending reinforcement was based on integration of linear-elastic tensile stresses and on corresponding strut-and-tie models.

The local bending forces used in design have a magnitude of 3% to 11% of the anchor force (Table 4.4). This is lower than the 18% found in the strut-and-tie model shown in Figure 4.26. The difference is due to the sensitivity of these member forces to the geometry of the strut-and-tie model. This sensitivity is a consequence of the fact that local bending is induced by compatibility requirements but is not needed for equilibrium. The actual amount of reinforcement to resist these effects is secondary for the strength of the structure.

5. Tension behind the anchor

Nominal longitudinal reinforcement was provided in all specimens to control cracking behind the anchor. This reinforcement was proportioned to carry 15% to 25% of the anchor force. In specimen Blister1 equal amounts of reinforcement were arranged at top and bottom of the slab (2x2#3 in Figure 4.31). In specimen Blister2 all reinforcement was placed in the top half of the slab. In specimen Blister3 all reinforcement was placed close to the top face of the slab and followed the linear-elastic tensile stress trajectories (5#3 in Figure 4.33). In specimen Blister4 simple longitudinal reinforcement was provided (4#3 at top of slab, 2#2 at bottom, Figure 4.34).

6. Slab bursting

For specimen Blister1 design of the slab bursting reinforcement was based on Equation 14.2.2 in the AASHTO Segmental Bridge Guide Specifications [2] which is restated below in modified form.

$$T_{burst} = 0.3P_u \left(1 - \frac{a}{h}\right) \quad (4.2)$$

where T_{burst} is the slab bursting force;
 P is the anchor force;
 a is the anchor plate width;
 h is the slab width.

This equation is an approximation of Guyon's solution for a concentric end anchor in a rectangular section (see Chapter 2). For adaptation to the blister problem, the blister width was used instead of the anchor plate width ($a = 10$ in.) and the full width of the specimen was taken as slab width ($h = 57$ in.). The bursting reinforcement was centered at 31 in. ahead of the anchor, which is equal to $0.54h$, similar to the recommendation for end anchors (see Chapter 3).

In the remaining specimens the slab bursting reinforcement was based on strut-and-tie models similar to the models discussed in Section 4.3.3. The arrangement of the slab reinforcement was varied. The simplest and most practical arrangement was chosen for specimen Blister 3 where uniform reinforcement was provided throughout the anchorage zone (Figure 4.33)

7. Lateral bending

In the region of tendon curvature the tendon deviation force is balanced by the vertical components of the compression struts. In rib anchorages (specimen Blister4) the compression struts spread out immediately ahead of the anchor and carry a large portion of the shear force away from the tendon path. Hence significant lateral bending moments are generated in the region of tendon curvature (Figure 4.29). The lateral bending effect requires additional reinforcement at the top of the rib in this region (4#3 in Figure 4.34).

Incorrectly, the same approach was also used for design of the lateral bending reinforcement in specimen Blister1. Based on the recommendations in Reference 24 (see Section 4.2.2) the vertical forces generated by deviation of the compressive stresses were assumed as uniformly distributed over the slab width. In reality, in isolated slab blisters the shear force stays largely concentrated in the blister and the lateral bending effect is limited to this region (Figure 4.29e). This was recognized in the design of specimen Blister3 where

the horizontal legs of the ties in the region of tendon curvature were sufficient to carry the lateral bending forces and no additional slab reinforcement was needed.

In specimen Blister2 the lateral bending moment was determined from the linear-elastic distribution of vertical shear forces over the slab width. The analysis results indicated that 65% of the shear force is carried within the blister and another 21% within 5 in. (half the width of the blister) of the blister. Reinforcement was provided in the slab to carry the resultant lateral bending moment. Ties within the blister were not counted towards the reinforcement requirement.

8. Tendon curvature

In the region of tendon curvature reinforcement is required to tie back the radial tendon deviation forces into the portion of the blister outside the tendon curvature. Theoretically the required tie-back force is less than the full tendon deviation force, but practically it is best to tie back all of it. This approach was taken in specimens Blister2, Blister3, and Blister4. Reinforcement in specimen Blister1 was based on the prototype detail shown in Figure 4.9 and exceeded the required amount by about 30%.

4.3.4.3 Test Procedure and Measurements

All specimens were loaded by oversized tendons. The required duct diameter was kept to a minimum by tightly packing twelve strands into a 2½ in. diameter duct. The specimens were tested in an upright position as shown in Figure 4.36. Figure 4.35 further illustrates the test set-up. The tendons passed through an opening in the reaction floor and the dead end anchors were placed inside a tunnel under the floor. This arrangement was selected to ensure a uniform stress distribution at the base of the specimen. For stability the specimens were loosely connected to an adjacent steel column. Since the dimensions of the jack did not allow direct bearing on the anchor plate, a 14 in. long specially fabricated prestressing chair was used as transition link between the prestressing jack and the anchor plate.

All specimens were loaded monotonically to failure. In specimen Blister3 with two anchors both tendons were first consecutively loaded to their service loads (2 x 87 kips) and subsequently to their design loads (2 x 124 kips). One anchor was then loaded to failure while the second tendon force was kept constant at approximately 124 kips.

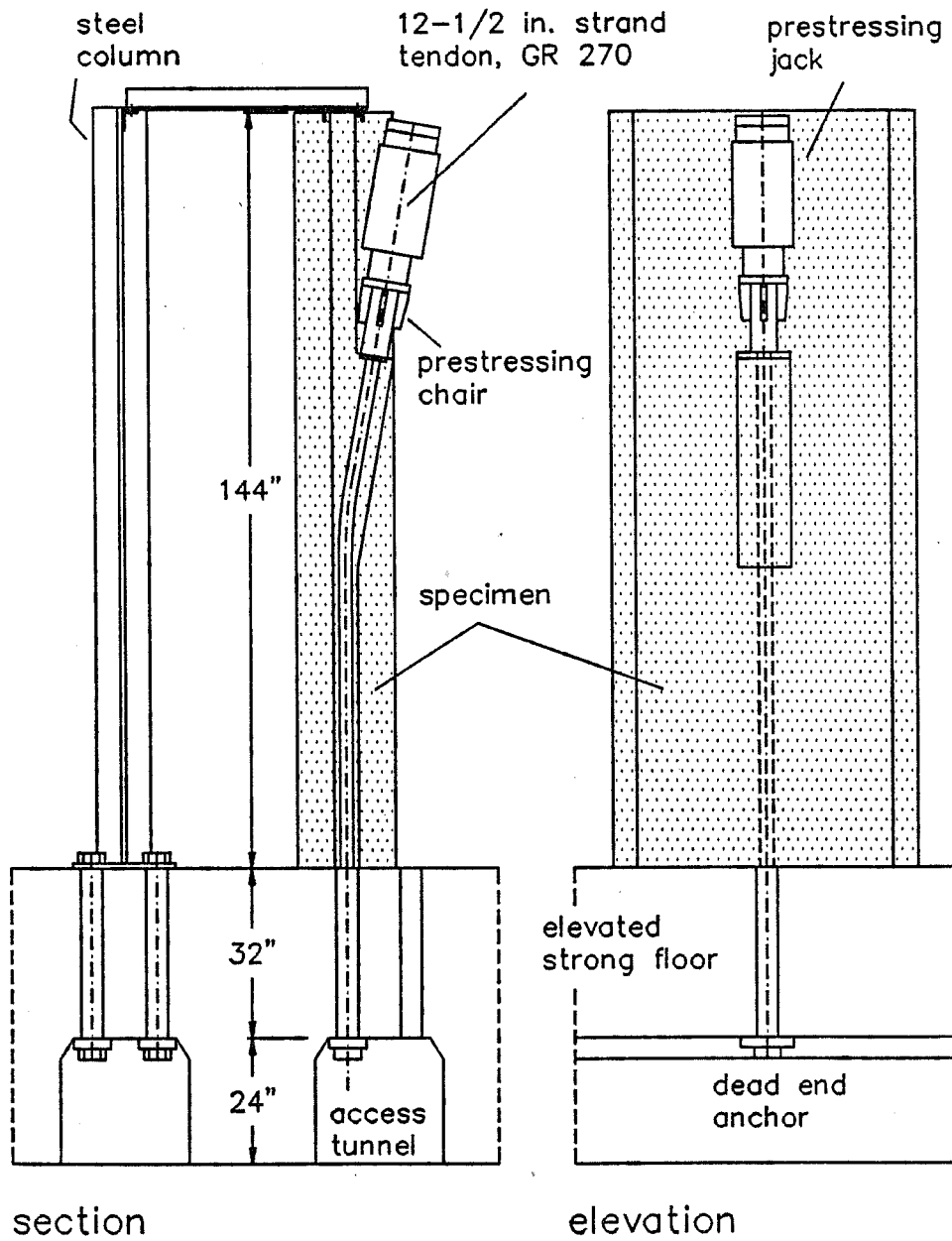


Figure 4.35 Test Set-Up for Blister Specimens

Reinforcement strains were measured with electronic resistance strain gages at critical locations (Figures 4.31 through 4.34). Typically, reinforcement strains were measured at 20 to 30 locations. In addition concrete surface strains were monitored using strain gages and DEMEC locator disks.

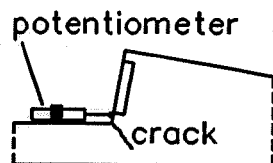


Fig. 4.37 Cracking Behind Anchor

Crack widths were measured with crack reading cards and a microscope. The cracks behind the anchor

occurred at the reentrant corner and were somewhat inaccessible. Crack reading cards were still very useful in this region. For more accurate readings linear potentiometers were used to measure the relative displacement between a point on the slab behind the anchor and the loaded face of the blister (Figure 4.37). This measurement should be indicative of the crack width behind the anchor, although it also includes distortions of the loaded face of the blister.

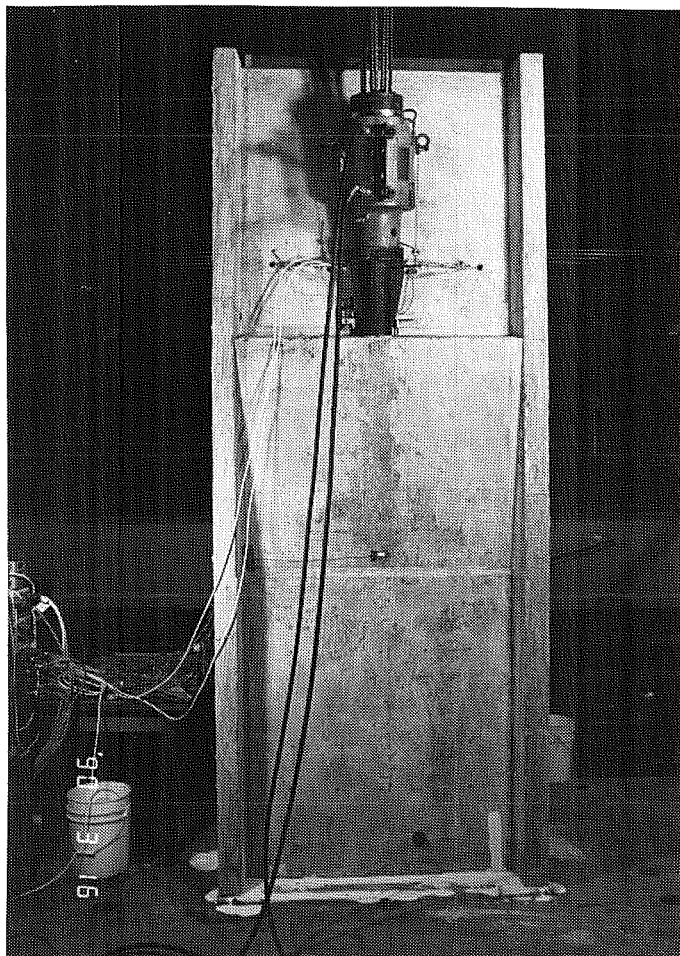


Figure 4.36 Specimen Blister4 Ready for Testing

4.3.5 Presentation of Test Results

4.3.5.1 Crack Development

In Table 4.6 first cracking, first yield, and ultimate loads are listed for the specimens of this series. All loads are expressed in terms of the design load, F_{pu} . Figure 4.38 shows the crack pattern for specimen Blister1 which is typical for all specimens. First cracking occurred at the reentrant

Table 4.5 Cracking Behind Anchor

specimen	initial		complete	
	kips	% F_{pu}	kips	% F_{pu}
Blister1	106	0.85	225	1.81
Blister2	90	0.73	190	1.53
Blister3*	95+0	0.77	165+124	1.33
Blister4	107	0.86	275	2.22

*) two anchors

corner behind the anchor and along the edges of the blister at 73% to 86% of the design load (cracks (1) in Figure 4.38). However, usually around twice the first cracking load had

Table 4.6 First Cracking, First Yield, and Ultimate Loads for Slab Blister Specimens

specimen	F_{pu} (kips)	1 st cracking load* (% F_{pu})	1 st yield load (% F_{pu})	ultimate load (% F_{pu})
Blister1	124	0.85 (1) 1.16 (2,3)	1.72 ² 1.92 ¹ 2.04 ³	2.04
Blister2	124	0.73 (1) 0.97 (2,3)	1.70 ²	1.90
Blister3	124 + 124	0.77 (1) 0.98 (2,3)	1.81 ²	1.91**
Blister4	124	0.86 (1) 1.38 (2,3)	1.68 ³ 2.06 ²	2.22

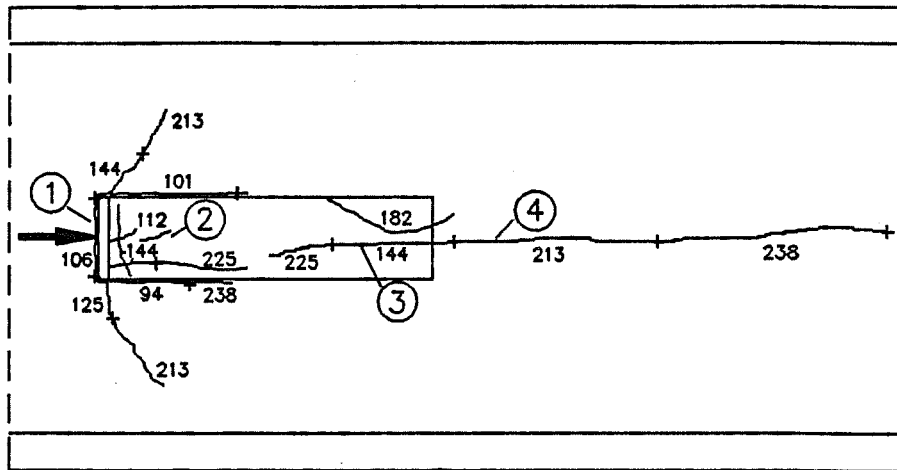
*) numbers in parenthesis correspond to cracks as labeled in Figure 4.38

**) (1.91 x 124) + 124 kips

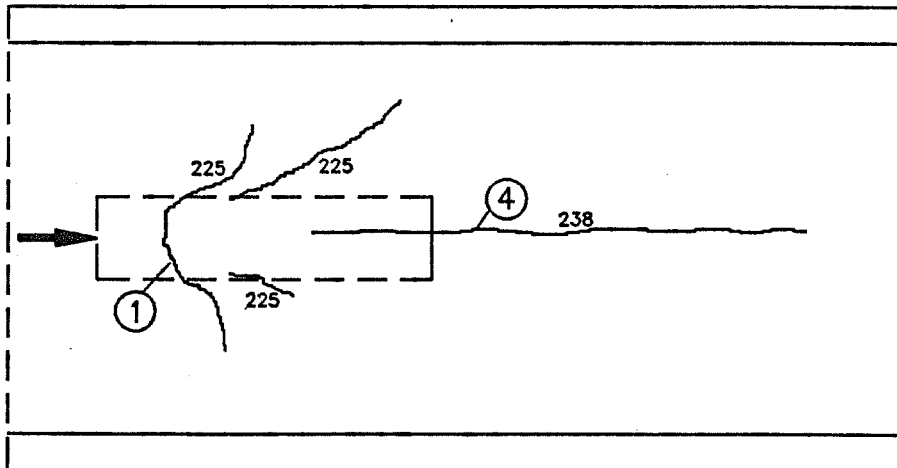
¹) tension behind anchor

²) local zone and corbel action

³) flange or rib bursting



top side



bottom side

Figure 4.38 Crack Pattern for Specimen Blister1

to be applied before these cracks propagated through the full slab thickness (Table 4.5) and could be detected on the bottom side of the slab. Subsequent cracking took place in the local zone region of the blister (cracks (2) in Figure 4.38) and at its toe where stresses due to slab bursting and due to lateral bending coincided (crack (3)). Crack (3) propagated towards the anchor and towards the base of the specimen. Slab bursting crack (4) followed

the tendon path on the top face of the slab. It extended through the full slab thickness only in specimens Blister1 and Blister4 and only in advanced load stages. In specimens Blister2 and Blister3 no tendon path cracking occurred at the bottom of the slab, but inclined slab bursting cracks similar to crack (5) in Figure 4.38 were observed.

The crack width behind the anchor stayed below 0.008 in. in all cases (Figures 4.39 and 4.40) and was less than 0.004 in. for rib specimen Blister4. Slab bursting cracks and particularly local zone cracks exhibited significantly larger crack widths. However, at service load levels no cracking was observed in these regions.

4.3.5.2 Ultimate Loads and Failure Mode

Failure loads exceeded the design loads roughly by a factor of two for the isolated blister specimens and by a factor of 2.2 for the rib specimen (Table 4.6). The failure mode involved crushing and spalling of the concrete ahead of and surrounding the confining spiral reinforcement in the local zone, similar to the failure mode observed for the beam specimens (Chapter 3).

Failures were preceded by wide cracking of the local zone region in the blister and by spalling of the concrete cover over the spiral (Figures 4.41 and 4.43). Yielding of the ties surrounding the local zone consistently occurred at 85% to 95% of the ultimate load and was an excellent indicator of impending failure.

Figure 4.42 and Figures 4.44 through 4.46 show the failed region of the specimens after removal of loose concrete. The spiral-confined plug with the concrete cone ahead of the spiral (Figure 4.44) is typical for failures at the transition from local zone to general zone. Figure 4.42 showing the double anchor specimen Blister3 illustrates clearly how localized this failure is. The anchor immediately adjacent to the failed anchor zone was completely unaffected. Closely spaced, well distributed ties provided throughout the local zone and ahead of the spiral were very effective in containing the damage (Figure 4.33).

4.3.5.3 Slab Bursting and Lateral Bending Strains

Figure 4.47 shows a comparison of the slab bursting strains for all specimens at a load of approximately 200 kips. In Figure 4.48 the same comparison is made at failure load levels. For specimen Blister3 with two tendons the indicated load refers to one tendon only. The second anchor force was held constant at approximately 120 kips.

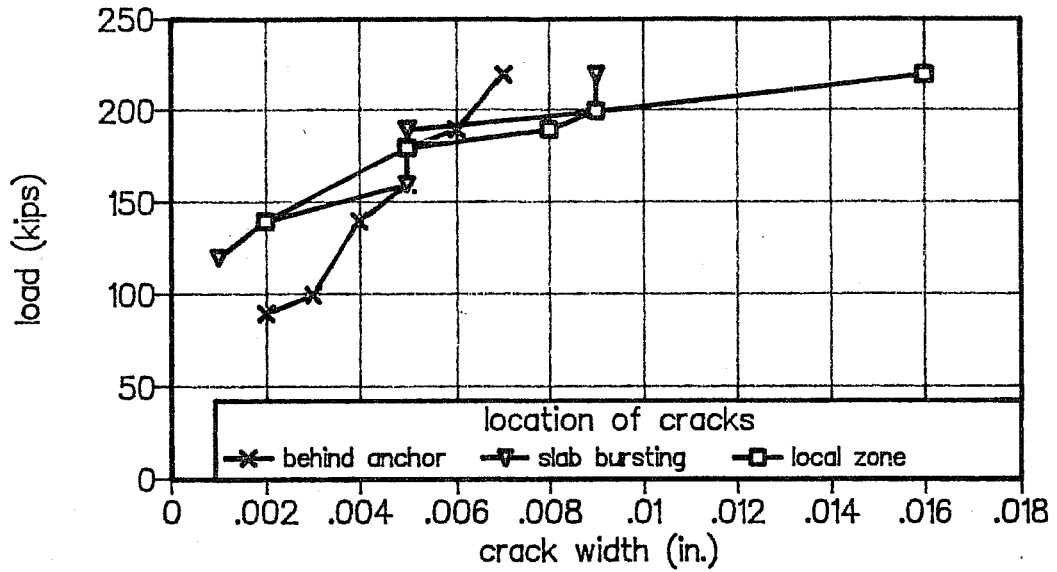


Figure 4.39 Crack Width Development for Specimen Blister2

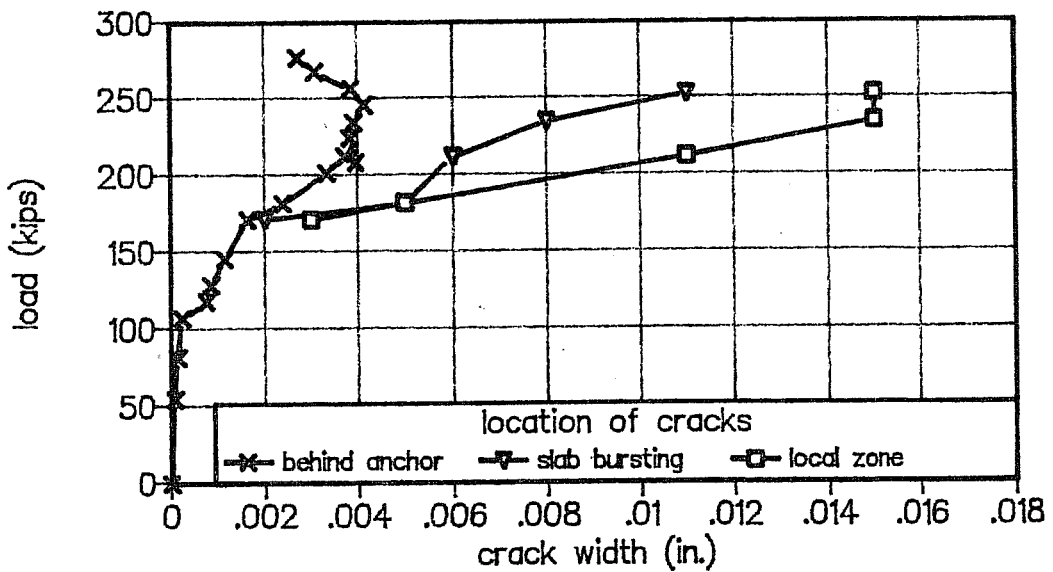


Figure 4.40 Crack Width Development for Specimen Blister4

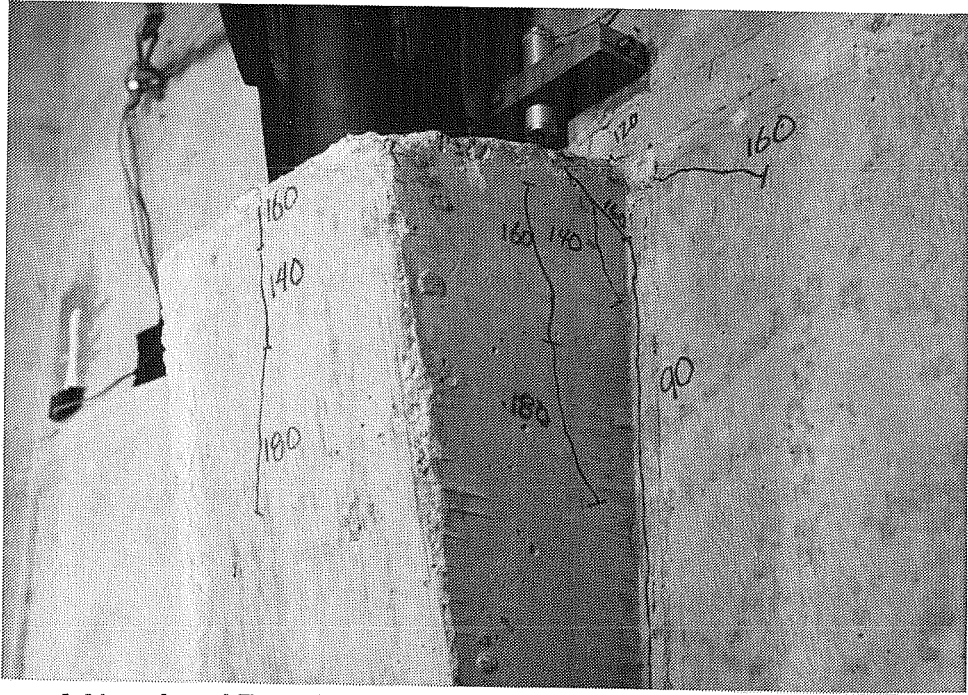


Figure 4.41 Local Zone Cracks in Specimen Blister2 at 75% of the Failure Load

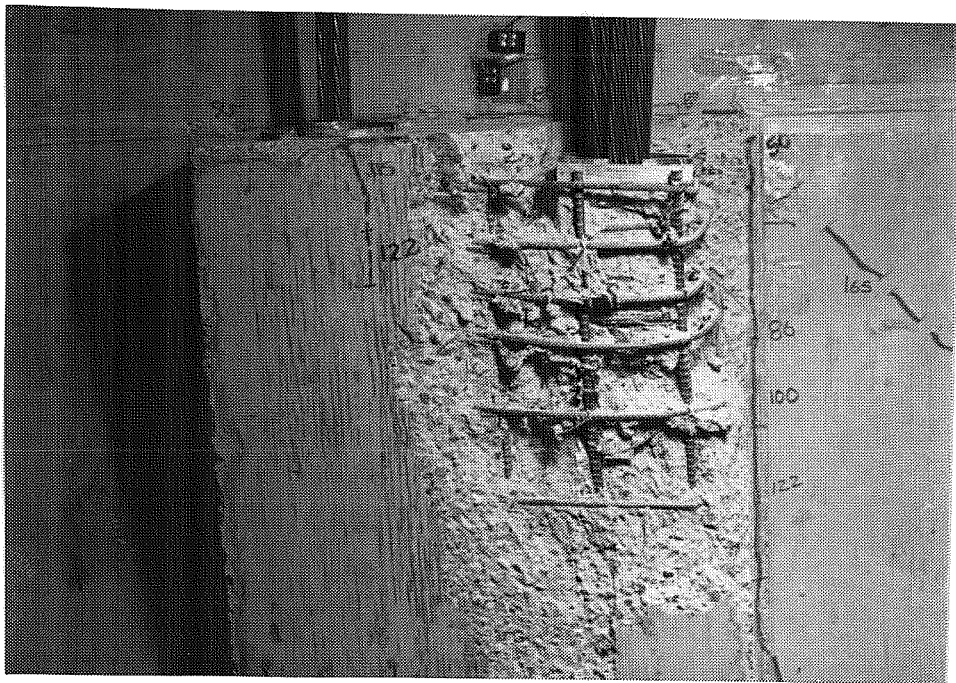


Figure 4.42 Specimen Blister3 After Failure

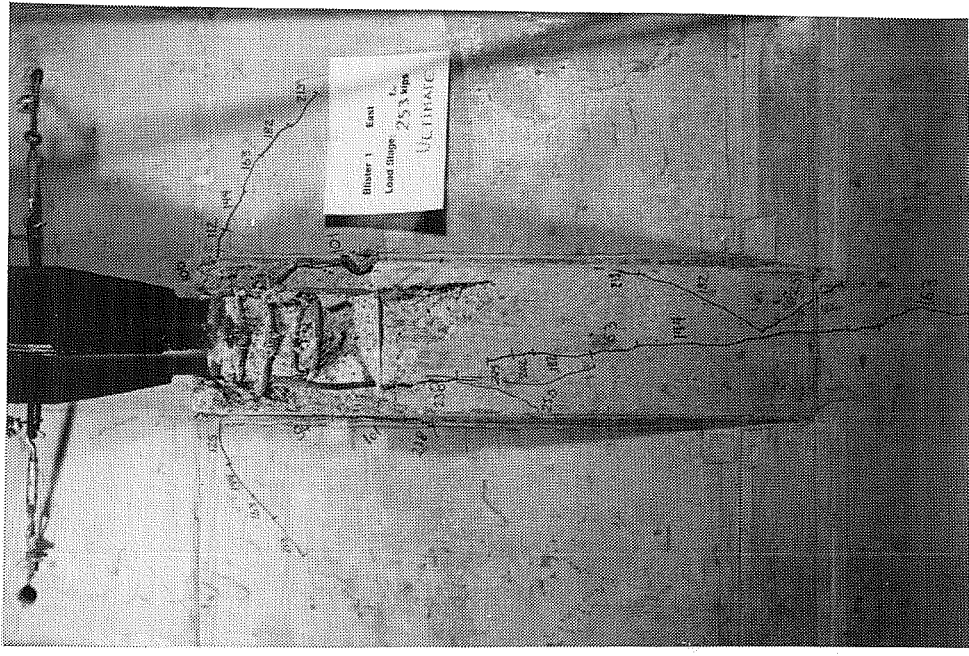


Figure 4.44 Specimen Blister1 After Failure

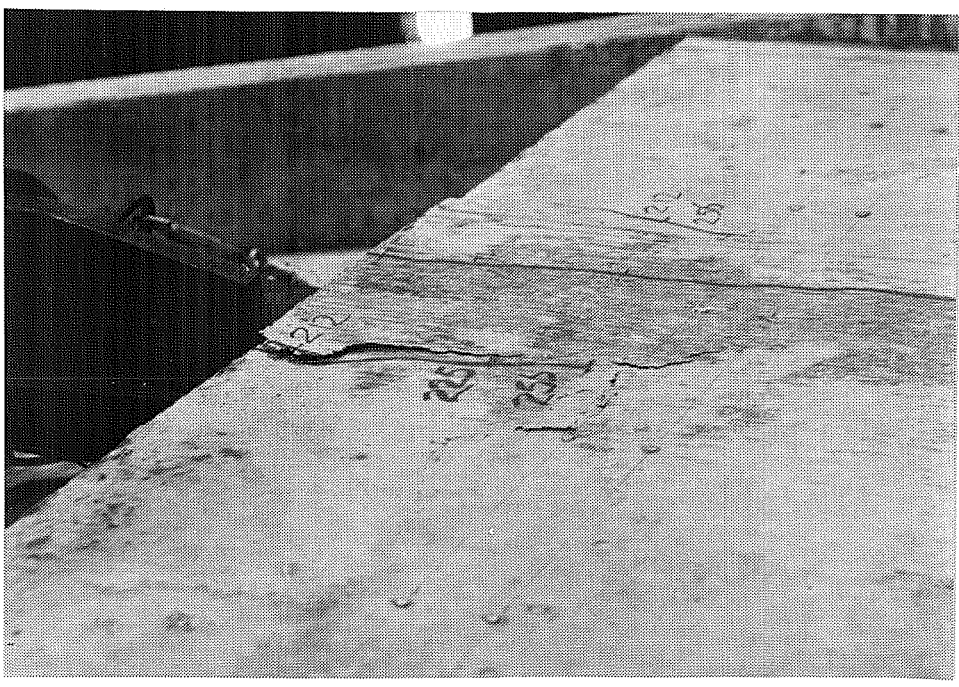


Figure 4.43 Local Zone Spalling in Specimen Blister4 at 90% of Failure Load

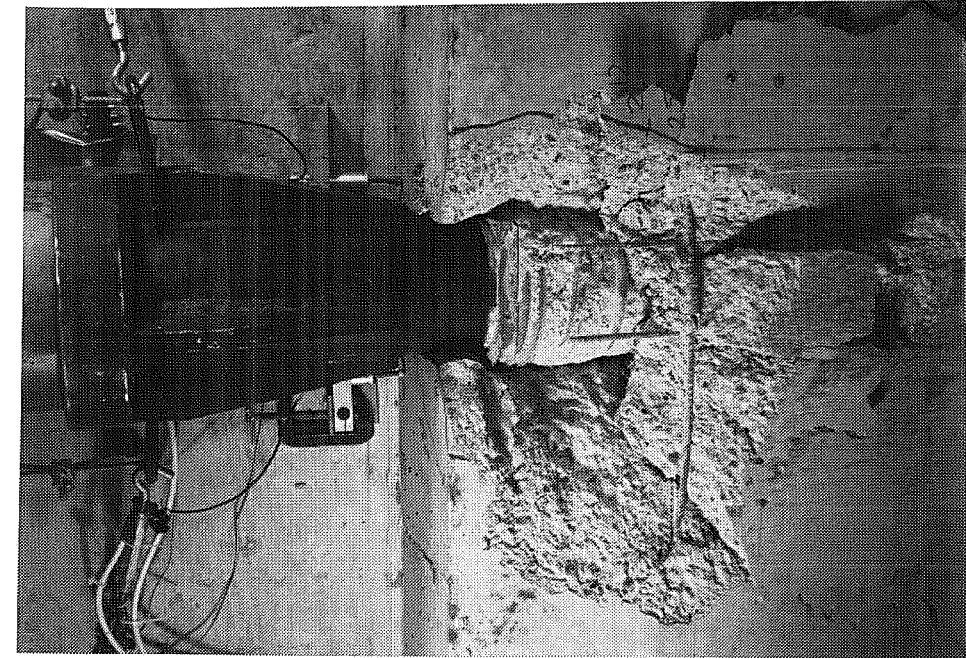


Figure 4.46 Specimen Blister4 After Failure

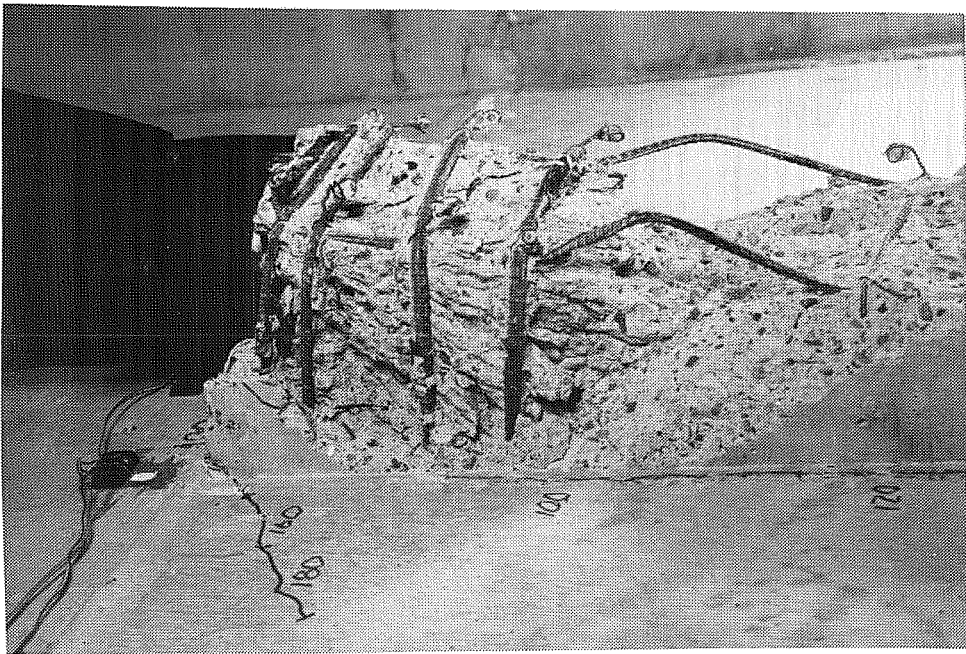


Figure 4.45 Specimen Blister2 After Failure

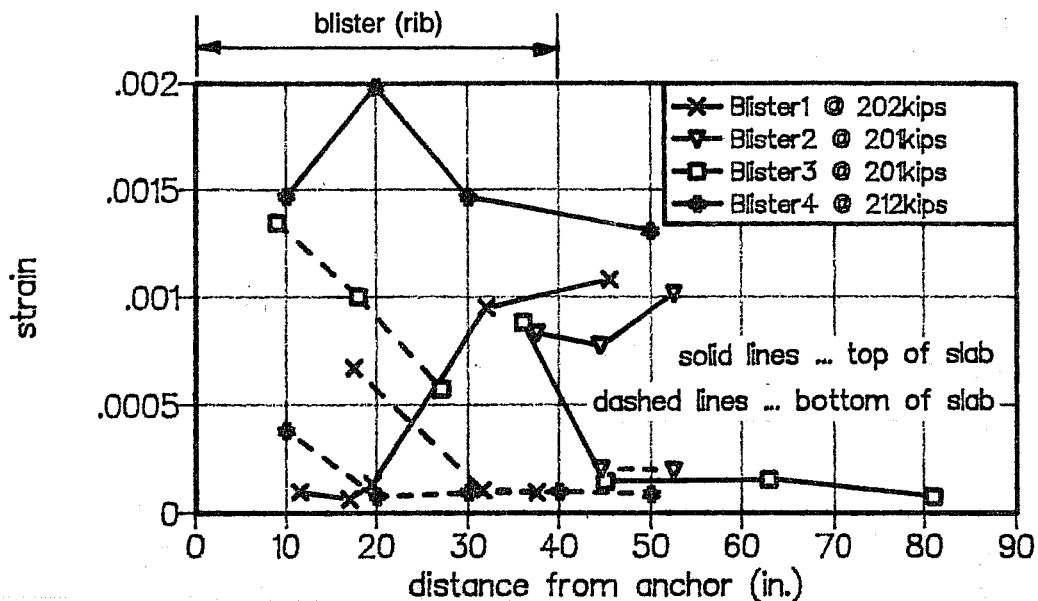


Figure 4.47 Slab Bursting Strains at 200 kips

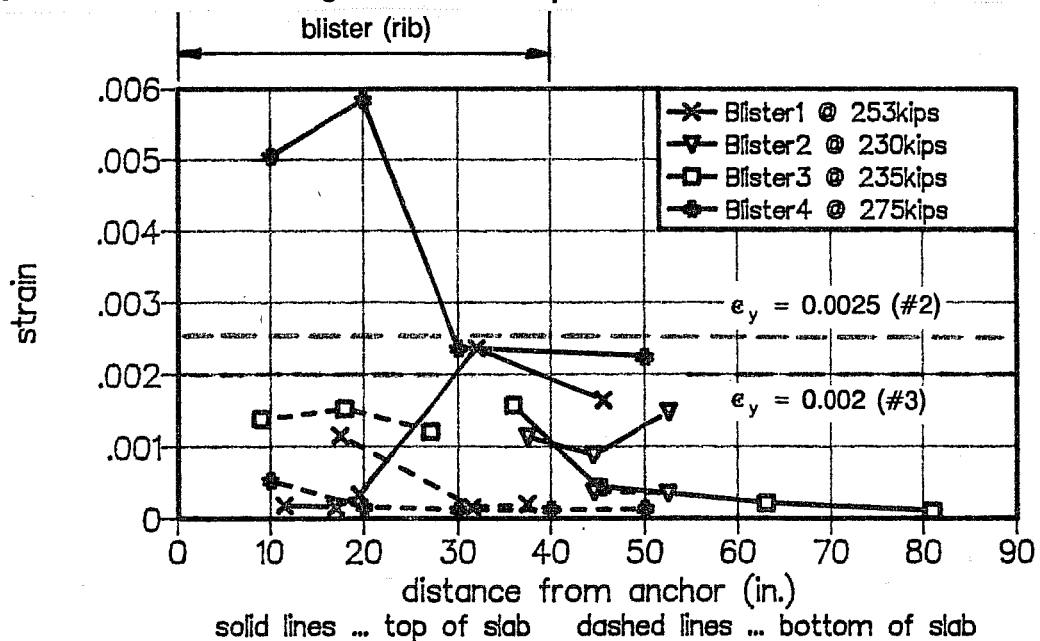


Figure 4.48 Slab Bursting Strains at Failure

The figures indicate that the slab bursting strains vary appreciably from top to bottom of the slab. Peak bursting strains in the top layer of reinforcement occur at the toe of the blister in the region of tendon curvature. For the rib specimen (Blister4) these strains were larger and more uniformly distributed throughout the rib. Bursting strains in the bottom

layer were small in the region of tendon curvature and were larger closer to the anchor. None of the bottom steel yielded at failure and yielding of the top steel was limited to a few bars except in the rib specimen. In the rib specimen all top bars reached their yield strain prior to failure. The larger strains in the rib specimen are partially a function of the location of the strain gages. In the rib specimen, strains were measured close to the top face of the rib, whereas in the blister specimens the strains were measured close to the top face of the slab but not at the top face of the blister.

Figure 4.49 shows lateral concrete surface strains measured in the region of tendon curvature of specimen Blister4. Due to lateral bending the bottom of the slab is actually subjected to compressive stresses. This explains the absence of tendon path cracks at the bottom of the slab in some of the specimens.

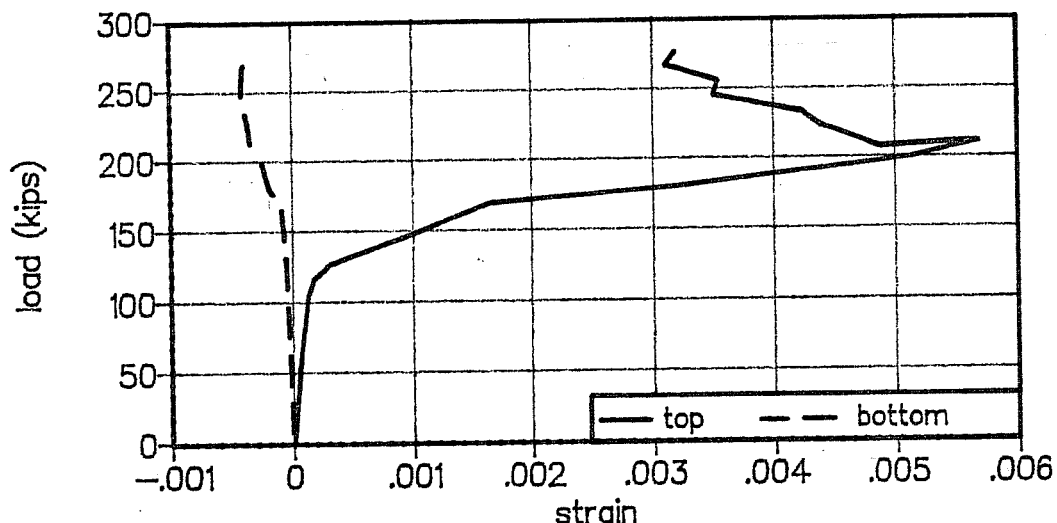


Figure 4.49 Lateral Bending Strains (Specimen Blister4)

4.3.5.4 Blister Tie Strains

Figure 4.50 shows the distribution of vertical tie strains throughout the blister of specimen Blister2. Peak strains were observed in the local zone region ahead of the anchor and in the region of tendon curvature. Yielding of the ties in the local zone was an excellent indicator of impending failure. The strains in the intermediate ties remained fairly small.

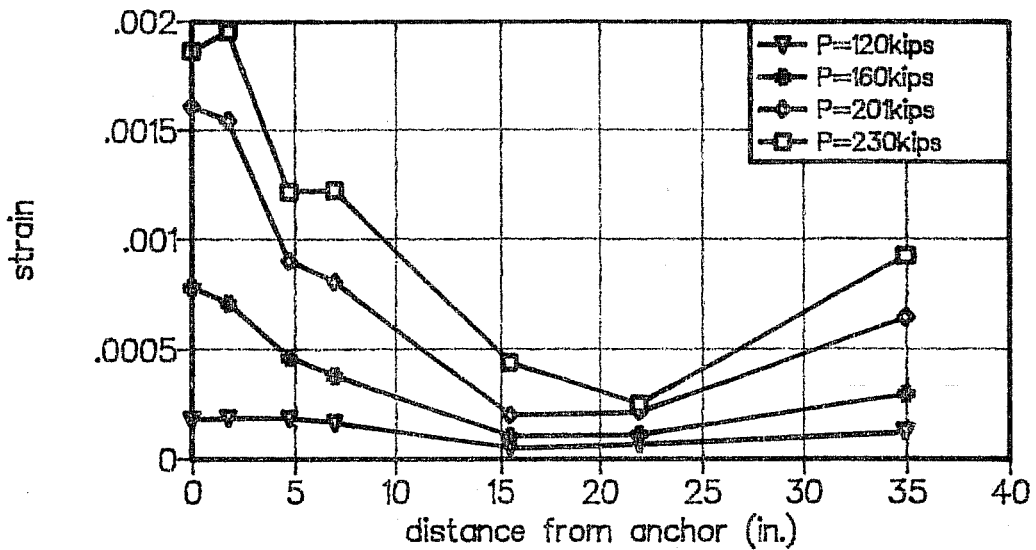


Figure 4.50 Blister Tie Strains (Specimen Blister2)

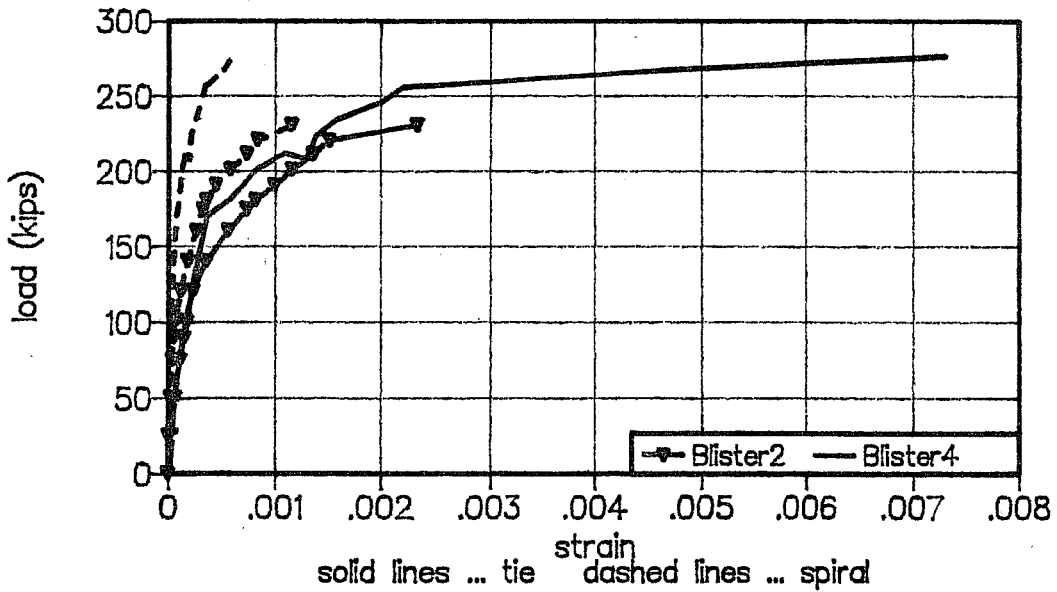


Figure 4.51 Local Zone Strains for Specimens Blister2 and Blister4

In Figure 4.51 spiral strains and tie strains in the local zone are compared. The spiral strains stayed consistently below the tie strains and developed less than half their yield strain at failure. In contrast, many of the ties in the local zone yielded just prior to failure. Specimen Blister4 had very little tie reinforcement, hence the large strain at failure.

Figure 4.52 shows the development of tie strains in the region of tendon curvature for specimen Blister1. The increase of the tie strains at a load of roughly 160 kips coincides fairly well with the first observation of lateral bending cracks at 144 kips (crack (3) in Figure 4.38). The dashed lines indicate the calculated strains, assuming that half the tendon deviation force and the entire tendon deviation force, respectively, have to be tied back by reinforcement.

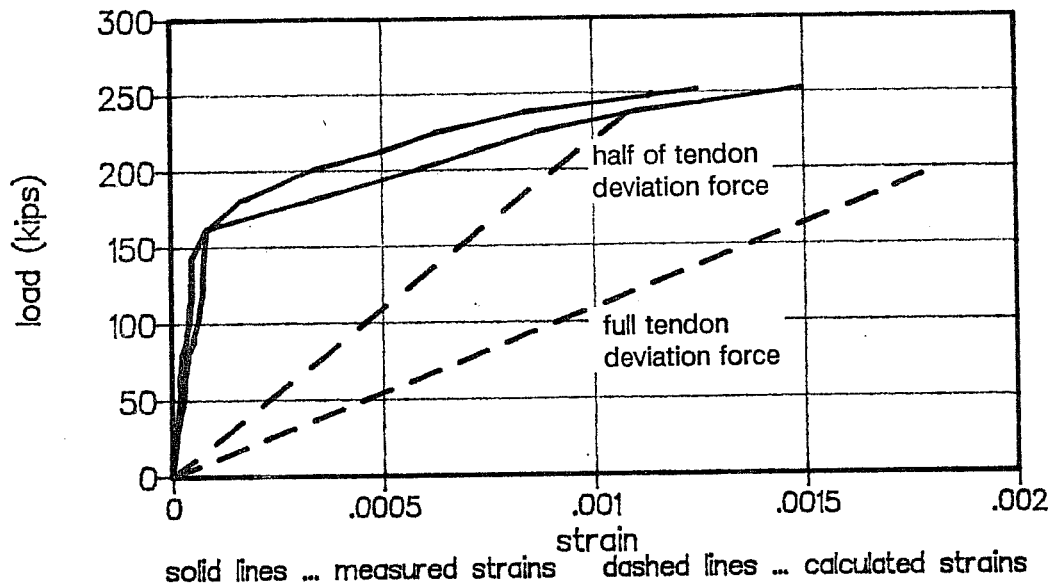


Figure 4.52 Tendon Deviation Strains (Specimen Blister1)

4.3.5.5 Strains Behind the Anchor

The strains in the slab reinforcement for control of cracking behind the anchor stayed fairly small in all tests. Figure 4.53 shows a comparison of isolated slab blister specimen Blister2 and rib specimen Blister4. The magnitude of the strains at failure is almost identical with roughly $800 \mu\epsilon$ measured closer to the top face of the slab and about $500 \mu\epsilon$ closer to the bottom face. With these strains the total tension force tied back into the portion of the slab behind the anchor is approximately 3.5% of the anchor force at failure for specimen Blister2 and 4.5% for specimen Blister4.

In the rib specimen cracking and crack propagation behind the anchor was substantially delayed. For specimen Blister2 the transition from the steep portion to the flat portion of the load-strain curve for the top reinforcement occurred at a load of roughly 50 kips. In rib specimen Blister4 the same transition occurred at 160 kips. Comparison of the

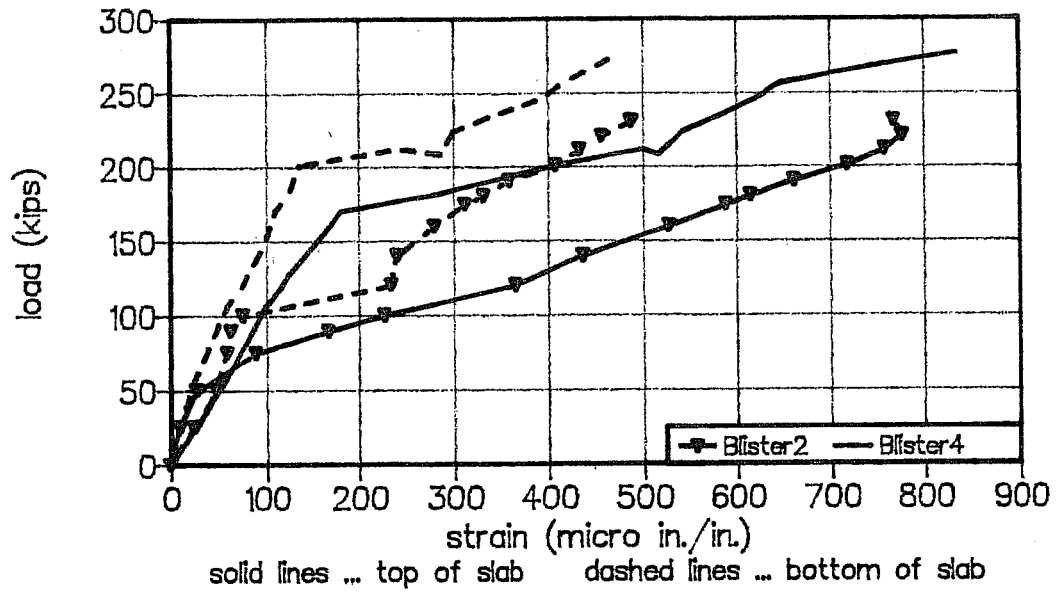


Figure 4.53 Strains Behind Anchor (Specimens Blister2 and Blister4)

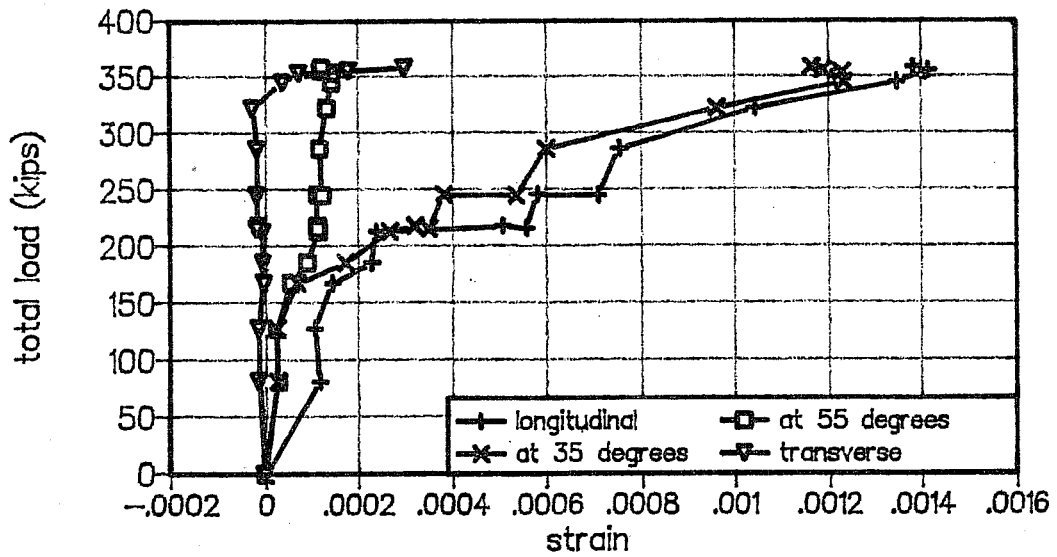


Figure 4.54 Strains Behind Anchor (Specimen Blister3)

strain development in top and bottom reinforcement layers confirm the observation made in Section 4.3.5.1, that cracking behind the anchor is more critical on the top side of the slab (the side which the blister projects from).

Figure 4.54 shows the strain development in the intermediate anchorage reinforcement in specimen Blister3. The sum of both tendon forces is plotted on the y-axis. One tendon load was held constant at roughly 120 kips while the other anchor was loaded to failure. All reinforcement was placed close to the top face of the slab and was arranged following the linear-elastic stress trajectories (Figure 4.33). The results shown in Figure 4.54 indicate that only the reinforcement close to the tendon axis and the reinforcement which was included within an angle of 35 degrees from the tendon axis developed significant strains. These strains are larger than for the other specimens. This is probably because less reinforcement was provided (Table 4.3) and because the bars arranged within an angle of 55 degrees with the tendon axis were not effective.

4.3.5.6 Local Bending Strains

Reinforcement strains due to local bending induced by the eccentricity of the tendon stayed below $500 \mu\epsilon$. Due to the combination of tensile stresses behind the anchor and of tensile stresses induced by local bending the cracks behind the anchor were inclined. The cracks originated at the reentrant corner behind the anchor and then propagated at an angle of approximately 45 degrees through the slab (Figure 4.37).

4.3.6 *Evaluation of Test Results*

4.3.6.1 Finite Element Analysis Predictions

Design based on the results of a finite element analysis corresponding to the proposed anchorage zone provisions (Appendix A) involves checking the linear-elastic compressive stresses in the concrete at a distance equal to one plate width ahead of the anchor and proportioning and detailing reinforcement to resist the resultant of the bursting stresses.

Table 4.7 Check of Compression Stresses

specimen	f'_c (ksi)	f_{ca} (ksi)	P_{calc} (kips)
Blister1	4.9	1.81	235
Blister2	4.2	1.81	201
Blister3	4.9	1.75	243
Blister4	4.7	1.58	258

Table 4.7 lists concrete compressive strengths, f'_c , critical compressive stresses, f_{ca} , ahead of the anchor as obtained from the finite element analysis, and the calculated

capacities, P_{calc} , of the specimens based on this check of compressive stresses. Stresses f_{ca} were calculated for an applied load of 124 kips. The effective concrete strength specified in the proposed anchorage zone specifications is $0.7f'_c$, hence

$$P_{calc} = 124 \times \frac{0.7f'_c}{f_{ca}} \quad (4.3)$$

In determining stresses f_{ca} , Section 9.21.5.2 of the proposed anchorage zone specifications allows peak stresses to be averaged over an area equal to the bearing plate area of the anchor. The presence of the tendon duct was ignored in the finite element analysis.

In addition to the check of the compression stresses ahead of the confined region (local zone-general zone interface) the capacity of the local zone has to be verified. The predictions for the local zone capacity are based on Roberts' best fit equation, which is restated below (see Section 2.2.2 for explanation of terminology).

$$P_n = 0.80 f'_c \sqrt{\frac{A}{A_b}} A_b + 4.1 f_{lat} A_{core} \left(1 - \frac{s}{D}\right)^2 \quad (4.4)$$

For calculation of the failure load controlled by slab bursting, the amount and arrangement of the slab bursting reinforcement must be compared to the magnitude and location of the bursting force found from the finite element analysis. Since the bursting reinforcement arrangement did not correspond to the finite element solution, the comparison of required bursting force to bursting reinforcement capacity has to be adjusted to reflect this difference. This is accomplished in Equation 4.5 by comparing the moments of the bursting force about the anchor:

$$P_{calc} = \frac{T_{act} \cdot d_{act}}{T_{FEM} \cdot d_{FEM}} \quad (4.5)$$

- where P_{calc} is the calculated anchor capacity;
 T_{act} is the bursting reinforcement capacity at yield;
 d_{act} is the distance of the centroid of the bursting reinforcement from the anchor;
 T_{FEM} is the resultant bursting force from finite element analysis for a 1 kip load;

d_{FEM} is the distance of resultant bursting force from anchor.

The results of these calculations are listed in Table 4.8.

Table 4.8 Check of Bursting Reinforcement

specimen	slab bursting reinforcement	T_{act} (kips)	d_{act} (in.)	T_{FEM} (kips)	d_{FEM} (in.)	P_{calc} (kips)
Blister1	9#2 + 5#3	62.2	38.0	0.24P	32.3	305
Blister2	9#2 + 3#3	49.0	37.1	0.24P	32.3	235
Blister3	18#2	58.3	44.6	0.17P	40.1	2x190
Blister4	10#2 + 4#3	58.8	32.3	0.40P	26.4	180

Table 4.9 Finite Element Analysis Predictions for Slab Blister Specimens

specimen	P_{test} (kips)	local zone (kips)	interface (kips)	slab bursting (kips)	P_{calc} (kips)	P_{test}/P_{calc}
Blister1	253	<u>210</u>	235	305	210	1.20
Blister2	235	<u>188</u>	201	235	188	1.25
Blister3	237 + 120	2 x 299	2 x 243	<u>2 x 190</u>	2 x 190	0.94
Blister4	275	240	258	<u>180</u>	180	1.53
average						1.23
standard deviation						0.21

Table 4.9 shows a comparison of the finite element analysis and local zone capacity predictions to the actual failure loads. The governing predictions are underlined. For specimen Blister3 with two tendons the prediction is controlled by the slab bursting reinforcement ($2 \times 190 = 380$ kips) and is compared to the total load at failure ($237 + 120 = 357$ kips). The predictions controlled by the capacity of the slab bursting reinforcement do not reflect the actual failure mode. Due to limited cracking and tensile strength contribution of the concrete most of the bursting reinforcement did not yield. This is reflected in Table 4.10 which shows a comparison of test results to predicted failure loads

ignoring the limiting capacity of the bursting reinforcement. For specimen Blister3 the prediction (243 kips per anchor) is compared to the ultimate load of the anchor that failed (237 kips). The predictions are more reliable than the predictions of Table 4.9 and reflect the actual failure mode.

4.3.6.2 Strut-and-Tie Model

Predictions

In Table 4.11 various predictions for the failure loads of the slab blister specimens based on strut-and-tie model procedures and on local zone capacities are listed. For the check of interface and blister compression stresses (columns (2) and (3) in Table 4.11) an effective concrete strength of $0.7 f'_c$ was used, as suggested in the proposed anchorage zone specifications. The determination of the critical section for the check of the interface stresses followed the procedure specified in Section 9.21.4 of the proposed specifications, which is explained in more detail in Section 3.7.2 in Chapter 3.

Table 4.11 Strut-and-Tie Model Predictions for Slab Blister Specimens

	1	2	3	4	5
specimen	local zone (kips)	interface (kips)	blister compression (kips)	slab bursting (kips)	tendon deviation (kips)
Blister1	<u>210</u>	245	244	249	226
Blister2	188	195	209	181	<u>161</u>
Blister3	2x299	2x255	2x244	<u>2x121</u>	2x148
Blister4	240	289	258	<u>131</u>	148

For the predictions based on slab bursting (column (4) in Table 4.11) the capacity of the slab bursting reinforcement at yield was compared to the requirements listed in

Table 4.10 Finite Element Analysis Predictions Assuming Compression Controls

specimen	P_{test} (kips)	P_{calc} (kips)	P_{test}/P_{calc}
Blister1	253	210	1.20
Blister2	235	188	1.25
Blister3	237 + 120	2 X 243	0.98
Blister4	275	240	1.15
	average		1.15
	standard deviation		0.10

Table 4.4. These predictions should be close to the design load of 124 kips, which is the case for specimens Blister3 and Blister4. In specimens Blister1 and Blister2 lateral bending reinforcement was present in the slab which was counted towards the slab bursting reinforcement requirements in Table 4.11. The predictions based on the capacity of the ties in the region of tendon curvature (column (5)) are based on the assumption that the full tendon deviation force has to be tied back.

Table 4.12 Evaluation of Strut-and-Tie Model Predictions

		including tension		assuming compression controls	
specimen	P_{test} (kips)	P_{calc} (kips)	P_{test}/P_{calc}	P_{calc} (kips)	P_{test}/P_{calc}
Blister1	253	210	1.20	210	1.20
Blister2	235	161	1.46	188	1.25
Blister3	237+120	2x121	1.48	244	0.97
Blister4	275	131	2.10	240	1.15
average			1.56		1.14
standard deviation			0.33		0.11

Table 4.12 shows the comparison of predicted to actual failure loads. Two comparisons are made: One considers the limiting capacity of slab bursting and tendon deviation reinforcement, while the other assumes that only compression failures control. For specimen Blister3 the sum of the tendon forces is compared to the predictions based on slab bursting, while individual anchors are compared for the predictions based on compression failure. Except for specimen Blister1, the lowest predictions are controlled by the capacity of the slab bursting or tendon deviation reinforcement (underlined in Table 4.11). The results indicate considerable conservatism for many specimens, as has generally been found with this lower bound approach which ignores the concrete tensile strength. If the limiting capacities of slab bursting and tendon deviation reinforcement are disregarded, the next lowest capacities are controlled by compression in the blister or by the local zone capacity. These predictions are still conservative for all specimens but the average is much closer to 1.0 and the standard deviation is significantly reduced.

4.3.6.3 General

The presentations in the preceding sections show that the capacities of slab bursting reinforcement and tendon deviation reinforcement are not good indicators of the failure loads. Predictions controlled by these capacities tend to be very conservative and do not reflect the actual failure mode. For example, yielding of the bursting reinforcement was limited to a few bars, whereas in the predictions yielding of all bars was assumed but the concrete tensile strength was neglected. Final failure of all specimens was caused by crushing of the concrete ahead of and surrounding the spiral in the local zone. Both FEM and STM predictions based on this failure mode are conservative and give predictions within 25% of the actual failure load. Failures were preceded by yielding of most of the ties providing confinement for the local zone. In no case did the spiral yield.

4.4 **Corner Blisters**

4.4.1 *Introduction*

In this section anchors located in a blister at the junction of flange and web of the cross section are discussed. Both anchorage of internal and external tendons are included in the study. Figures 4.2c and d show views of the specimens used in the experimental portion of the study. In these specimens the region affected by the introduction of the tendon force is isolated. The specimens essentially represent a web and flange of a box girder. However, for simplification of the experimental tests, in the specimens with internal tendons the web was extended below the flange to create an irregular T-shaped cross section. With this modification the cross section at the end of the anchorage zone is subject to compressive stresses only.

4.4.2 *Finite Element Analysis*

4.4.2.1 Corner Blister for Internal Tendons

Figure 4.55 shows geometry and loading conditions of the corner blister half-scale model used in the finite element analysis. For simplicity a regular T-shaped cross section was chosen with the tendon located at its centroid except in the blister region. The tendon force of 196 kips corresponds to the breaking strength of a 19-½ in. strand tendon in the full-scale structure. Figure 4.56 shows the 3D finite element mesh.

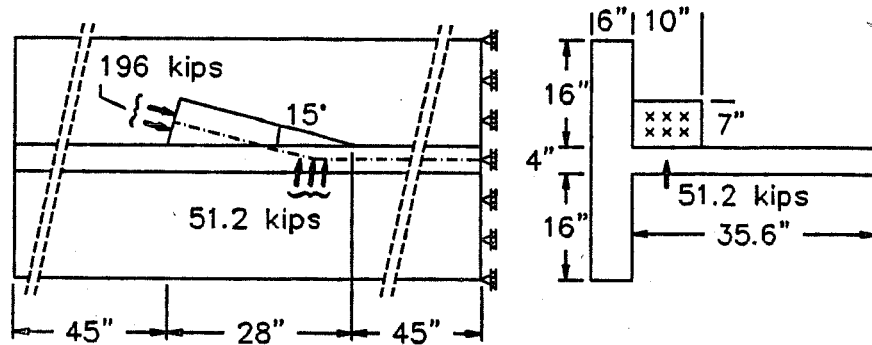


Figure 4.55 Dimensions and Loading Conditions for Finite Element Model of Corner Blister With Internal Tendon

The linear-elastic analysis indicates a distribution of principal stresses in a longitudinal section along the tendon path which is very similar to that in isolated slab blisters (Figure 4.57). Large tensile stresses exist behind the anchor, in the region immediately ahead of the anchor, and in the region of tendon curvature at the toe of the blister. In these regions typical concrete tensile strengths are exceeded and significant cracking must be expected. The dissipation of compression stresses occurs more rapidly in the corner blister than in the isolated slab blister (Figures 4.57b and 4.22a), because transfer of forces is possible from blister to flange and from blister to web.

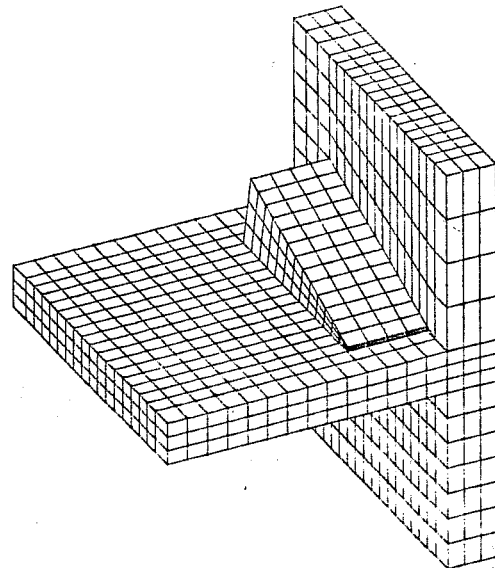


Fig. 4.56 Finite Element Mesh for Corner Blister Model With Internal Tendon

Evaluation of the complex state of stress in and around corner blisters in order to proportion the anchorage zone reinforcement is difficult. For example, integration of the principal tensile stresses shown in Figure 4.57a does not give any indication of the direction of the resultant force. On the other hand, integrating only the stress components perpendicular to the section is not adequate because shear stresses are ignored. This

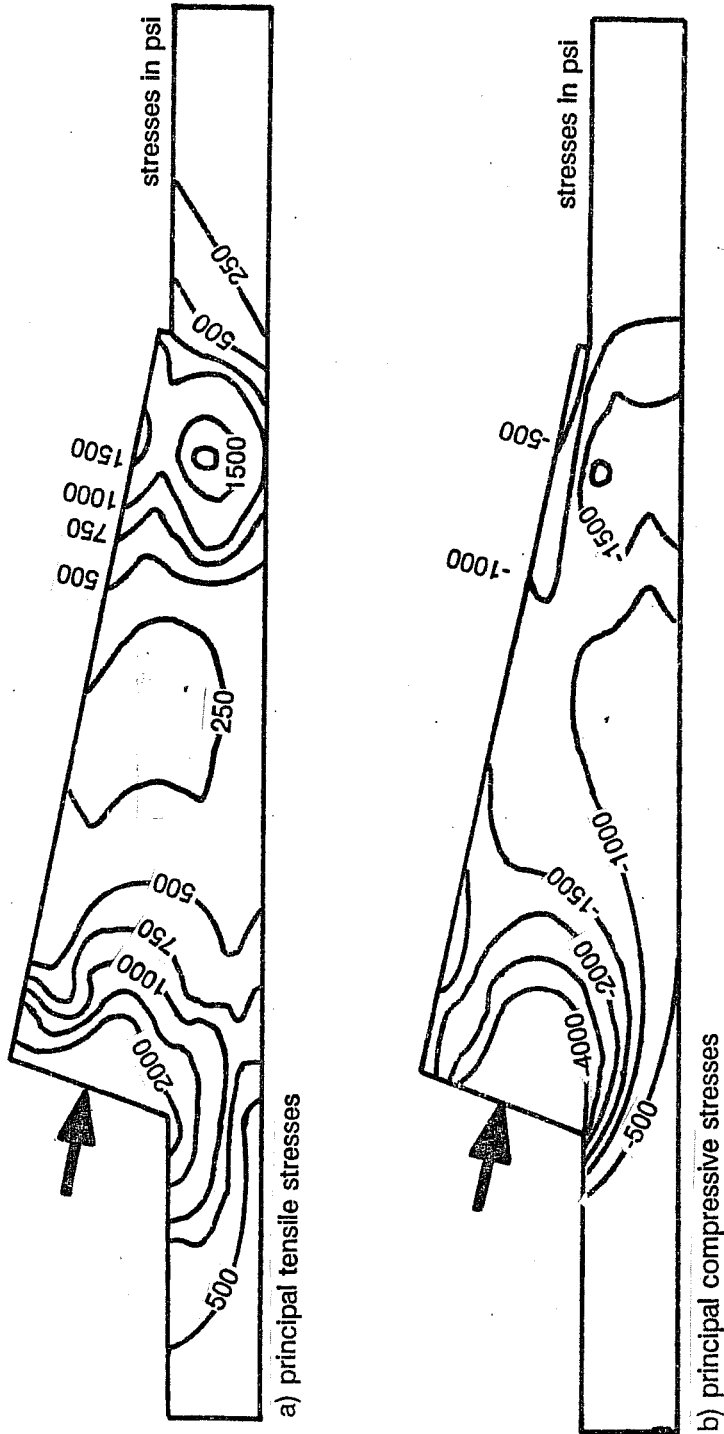


Figure 4.57 Principal Stresses in Section Along Tendon Path

problem did not occur in the analysis of the slab blisters in Section 4.3.2.2 because the linear-elastic stresses were evaluated at a plane of symmetry with no shear stresses.

In Table 4.13 two estimates for magnitude and location of the slab and web bursting forces are shown. In the column labeled "without shear" only the normal stress components perpendicular to the critical section were integrated. In the column labeled "including shear" the effect of the shear stresses in the plane of the slab was estimated by simply adding these stresses to the stresses perpendicular to the critical section. This approach is based on the assumption that after concrete cracking the shear stresses are carried by tension in the reinforcement perpendicular to the critical section and by compression stresses which include a 45 degree angle with the critical section. As shown in Table 4.13 accounting for the effect of shear in this manner nearly doubles the bursting reinforcement requirements for slab and web. However, the results are in good agreement with the strut-and-tie model results shown in Figures 4.63 and 4.65, whereas the bursting forces ignoring shear seem low.

Table 4.13 Linear-Elastic Bursting Forces for Corner Blisters

tendon	slab bursting		web bursting	
	without shear	including shear	without shear	including shear
internal	0.13 P @ 24.0"	0.23 P @ 23.7"	0.08 P @ 27.9"	0.17 P @ 23.5"
external	0.10 P @ 23.3"	0.15 P @ 20.9"	0.07 P @ 23.7"	0.17 P @ 17.0"

4.4.2.2 Corner Blister for External Tendon

Figures 4.58 and 4.59 show geometry, loading conditions, and finite element mesh for the half-scale model of a corner blister for anchorage of an external tendon. The tendon force is 196 kips, as before.

Figure 4.60 shows the principal stress contours in a longitudinal section along the tendon. Again, large tensile stresses occur at the reentrant corner behind the anchor and in the local zone ahead of the anchor. The principal tensile stress contours in a cross section immediately behind the anchor are shown in Figure 4.61.

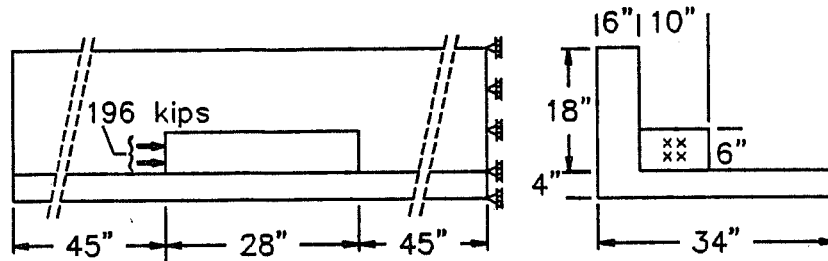


Figure 4.58 Dimensions and Loading Conditions for Finite Element Model of Corner Blister With External tendon

Since the tendon remains outside the cross section and is not deviated, no stresses induced by tendon curvature exist in this case. However, there are significant tensile stresses concentrated at the end of the blister, as shown in Figures 4.60a and 4.62. These tensile stresses increase with decreasing length of the blister. They are induced by "deep beam action" across the web-flange corner. Table 4.13 shows estimates for the bursting reinforcement requirements.

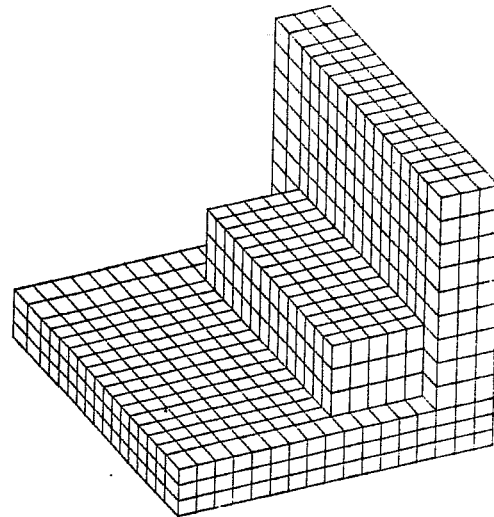


Fig. 4.59 Finite Element Mesh for Corner Blister Model With External Tendon

4.4.2.3 Discussion

The load-carrying mechanism of corner blisters for internal tendons and of those for external tendons is distinctly different. The corner blister for external tendons acts like a combination of corbel and deep beam. The principal load path in corner blisters for internal tendons is comparable to a curved, prestressed column that is embedded in the structure [43]. In both cases significant tensile stresses exist at the reentrant corner behind the anchor.

Design and detailing of the reinforcement based on this three-dimensional linear-elastic analysis is complex and not practical. Furthermore the level of tensile stresses indicates significant cracking of the structure which violates the assumption of a linear-

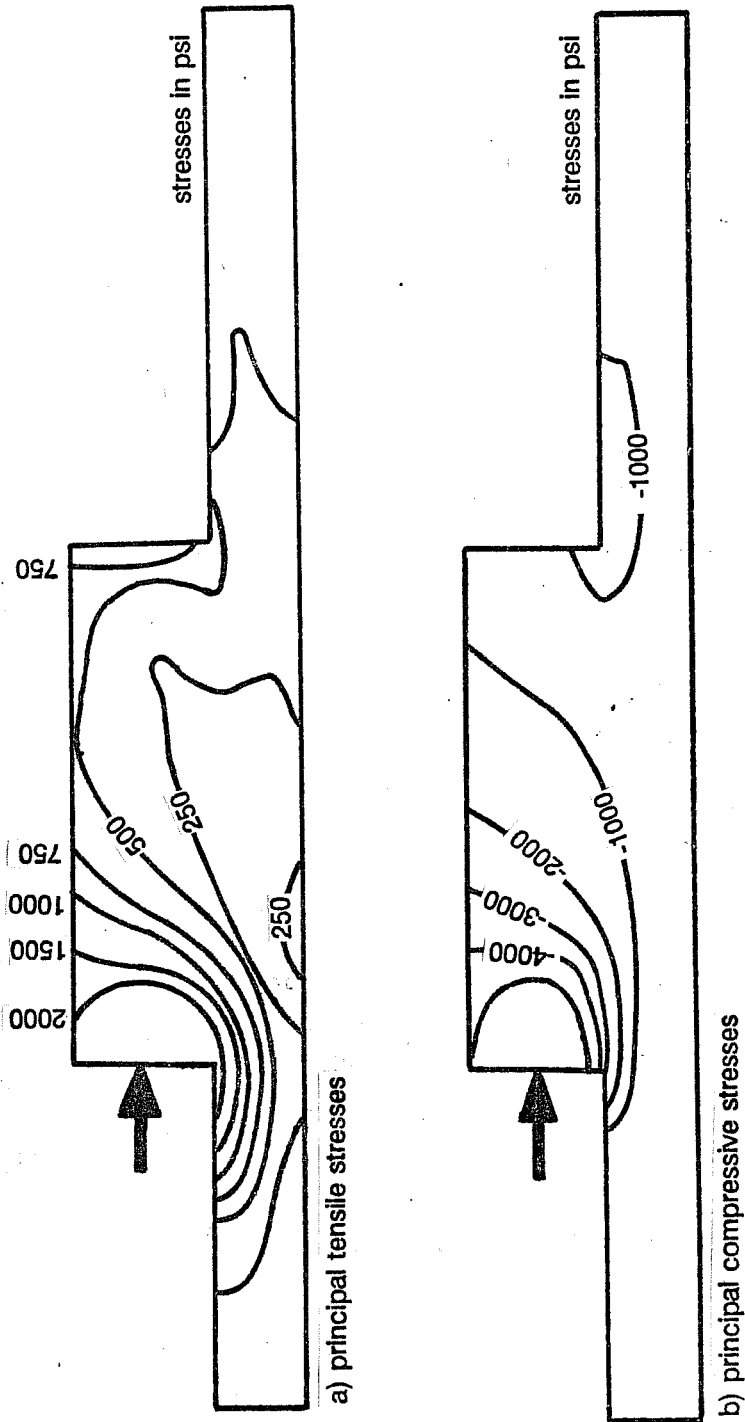


Figure 4.60 Principal Stresses in Section Along Tendon Path

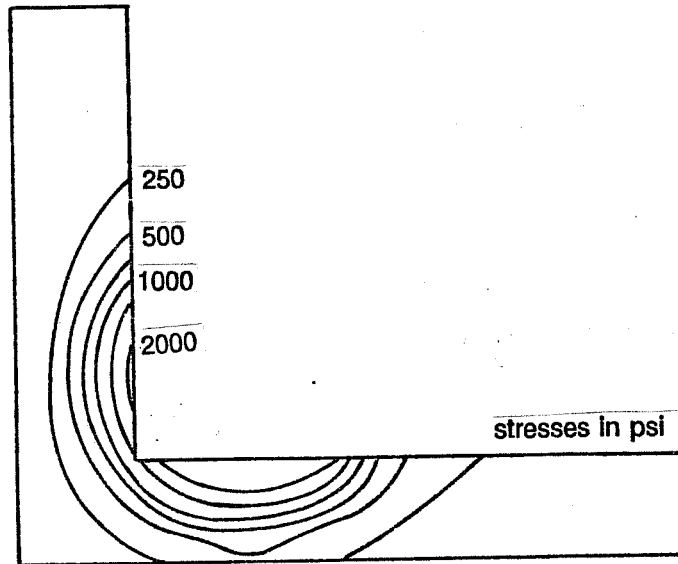


Figure 4.61 Principal Tensile Stresses in Cross Section Immediately Behind Blister

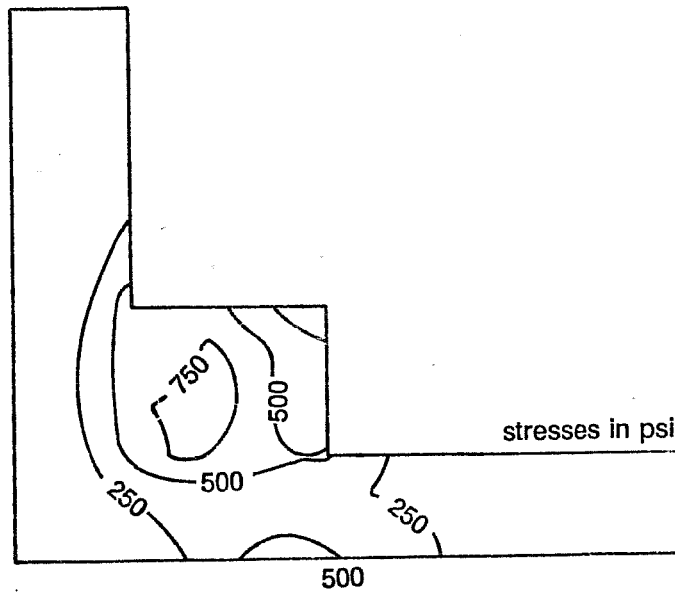


Figure 4.62 Principal Tensile Stresses in Cross Section Through End Face of Blister

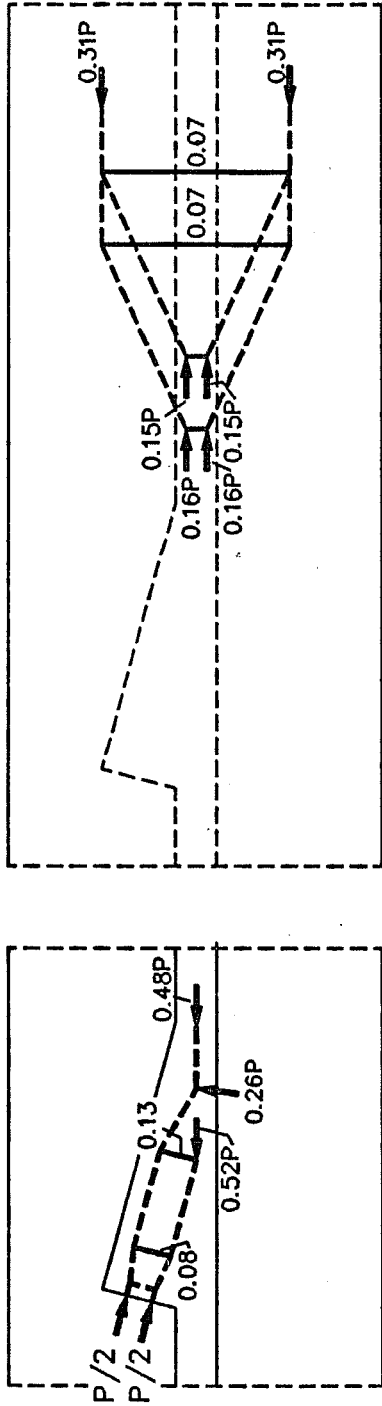
elastic, homogeneous, and isotropic material. The analysis results are useful to identify critical regions where cracking is likely and where large compression stresses occur, but other methods are needed for design and detailing.

4.4.3 *Development of Strut-and-Tie Models*

4.4.3.1 Corner Blisters for Internal Tendons

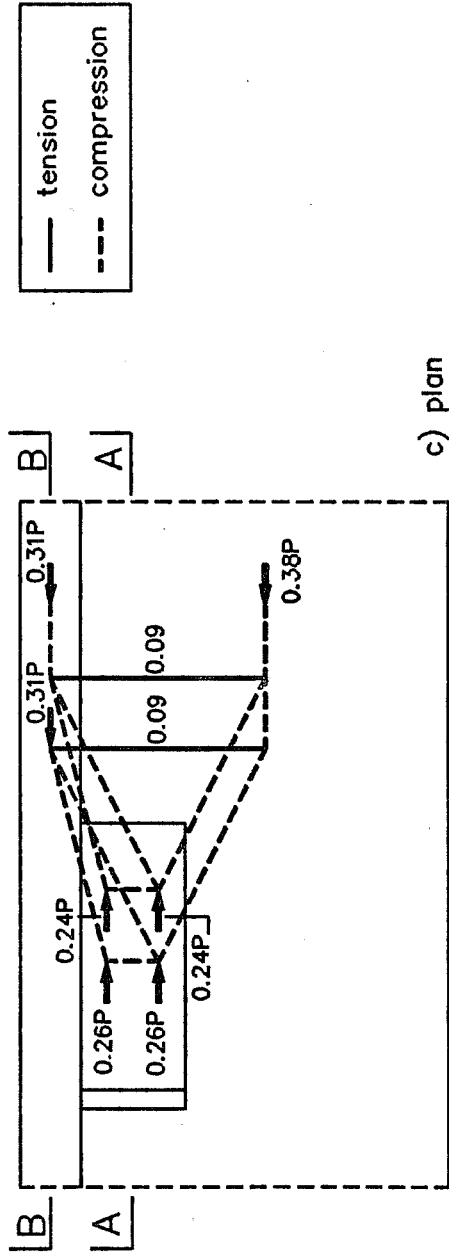
The most basic strut-and-tie models are identical to those for isolated slab blisters. They are labeled "concentrated strut model" and "split strut model" in Figure 4.24. Figure 4.63 shows a refined model for the corner blister specimen of Figure 4.55. In this model the anchor force is first transferred into the slab and from there into the flange of the T-section. Bursting forces are induced in both slab and flange. The load path shown in Figure 4.63a (section A-A) could be refined similarly to the refined model shown in Figure 4.24e. However, as pointed out in Section 4.3.3.2, equilibrium conditions alone are not sufficient to determine corbel action and local bending force of this refined load path. Neither force is essential for equilibrium, and hence the load path shown in Figure 4.63a is a valid lower bound to the plastic limit load. Of course, the finite element results indicate significant tensile stresses behind the anchor and some reinforcement should be provided for corbel action and local bending. However, the actual amount of this reinforcement is secondary for the strength of the structure.

The weakness of the model is that it does not account for the possibility of a direct load transfer from the blister into the flange of the T-section. As a consequence of the indirect load path described above the flange bursting force is located rather far ahead of the anchor (section B-B in Figure 4.63). A direct load path from blister to flange requires corbel action to pull a portion of the anchor force into the flange of the T-section, as indicated in Figure 4.64. This model represents the other extreme where the anchor force is first transferred into the flange and from there into the slab. The transfer of forces into the flange occurs much closer to the anchor, but slab bursting force and corbel force are quite large. Both load paths represent valid equilibrium solutions. The decision for one model or the other requires judgement, and still other models could be found. For this particular example a combination of the two load paths discussed above would probably be a better solution than the individual models by themselves. With these examples, it becomes quite



a) section A-A

b) section B-B



c) plan

Figure 4.63 Strut-and-Tie Model for a Corner Blister With Internal Tendon

apparent that the development of truly three-dimensional strut-and-tie models is certainly not an easy task.

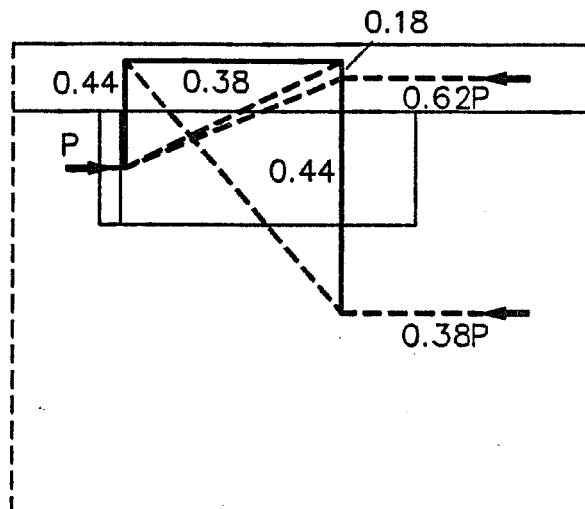
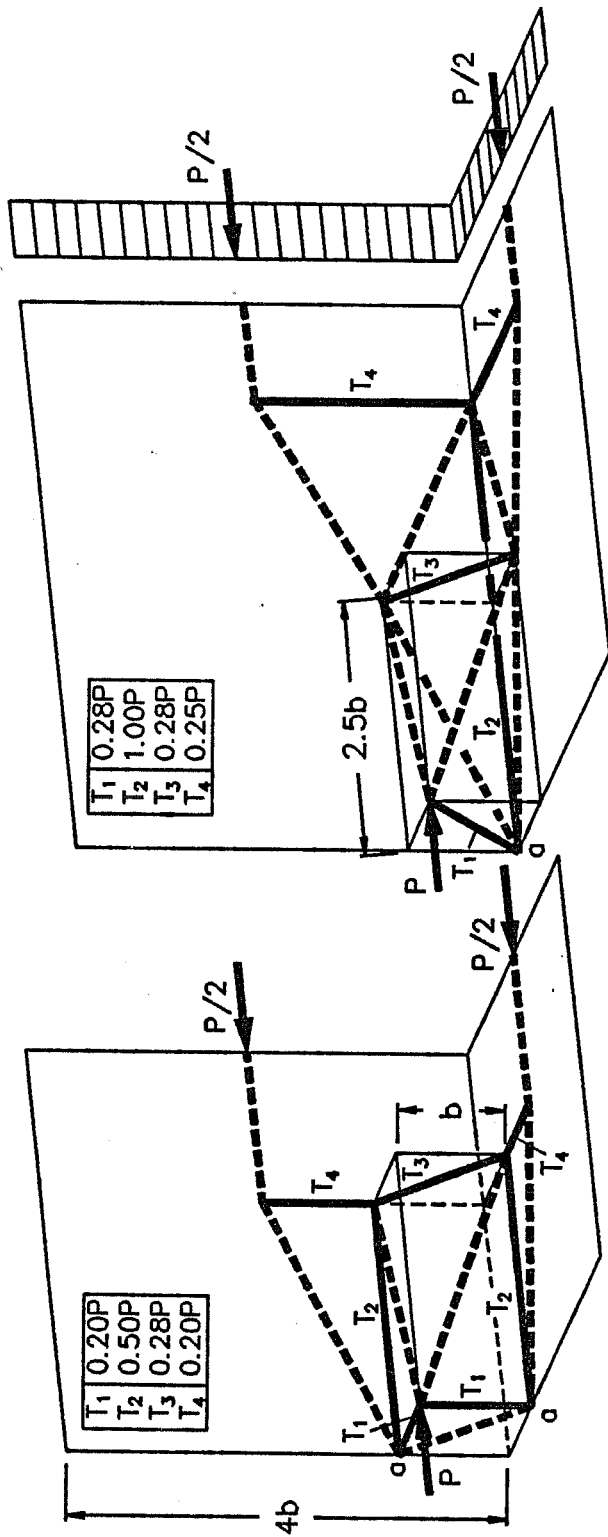


Figure 4.64 Alternative Strut-and-Tie Model

4.4.3.2 Corner Blisters for External Tendons

Figure 4.65 shows two different strut-and-tie models for the load path in a corner blister used for the anchorage of an external tendon. The anchorage zone extends for approximately one slab width ahead of the end of the blister. The portion of the slab behind the anchor is ignored for simplification of the problem. In both models corbel forces, T_1 , are required to deviate the anchor force towards web and flange. In contrast to blisters for internal tendons, these corbel forces are essential for equilibrium and hence for the strength of the structure. The corbel action induces local bending forces T_2 . These forces are necessary to satisfy equilibrium at nodes a. Deep beam action causes tensile force T_3 across the web-flange corner at the end face of the blister. Slab bursting forces T_4 are generated ahead of the blister due to spreading of the anchor force into flange and web of the cross section.

In both models the tensile forces T_2 are very large and the load path is not very effective. For example, in model A the anchor force is first transferred from the blister into web and flange, and is then tied back by forces T_2 before spreading out. A significant improvement of these load paths can be achieved by considering two resultant forces in



a) model A

b) model B

Figure 4.65 Strut-and-Tie Models for a Corner Blister With External Tendon

both web and flange instead of the single resultant forces shown in Figure 4.65. Such a refinement would cut the magnitude of tensile forces T_2 in half.

4.4.4 Experimental Program

4.4.4.1 General

The experimental program comprised tests of three half-scale corner blister specimens with internal tendons and one specimen modelling a corner blister for an external tendon. Figures 4.66 and 4.67 provide information on the geometry of these specimens. Concrete cylinder compressive strengths at time of testing are listed in Table 4.14. Specimen Corner22 was added to the experimental

Table 4.14 Concrete Strengths for Corner Blister Specimens

specimen	f'_{ci} (psi)
Corner1	4600
Corner21	2900
Corner22	4600
Corner3	4000

program because specimen Corner 21 fell well

short of the desired concrete strength. Test procedure and measurements were identical to those for the slab blisters (Section 4.3.4.3). Figures 4.68 through 4.70 indicate the location of the reinforcement strain gages.

4.4.4.2 Design of Corner Blister Specimens With Internal Tendons

Specimens Corner1, Corner21, and Corner22 modelled corner blisters for internal tendons. Specimens Corner21 and Corner22 were identical except for the concrete strength. Reinforcement details are shown in Figures 4.68 and 4.69. The design load, F_{pu} , was 196 kips, corresponding to the breaking strength of a 19-½ in. strand tendon in the full-scale structure ($\frac{1}{4} \times 19 \times 0.153 \text{ in}^2 \times 270 \text{ ksi} = 196 \text{ kips}$).

The dimensions of the spiral in the local zone were based on European product information for simple bearing plate anchors and were verified using Roberts' equation (Equation (2.2)).

The blister reinforcement in specimen Corner1 is an exact scaled-down replica of the details used in the prototype structure (Figure 4.10). This arrangement does not provide any reinforcement for the direct transfer of shear forces from the blister into the web. In specimens Corner21 and Corner22 the blister reinforcement was L-shaped and was anchored in both flange and web, except in the region of tendon curvature. In this region

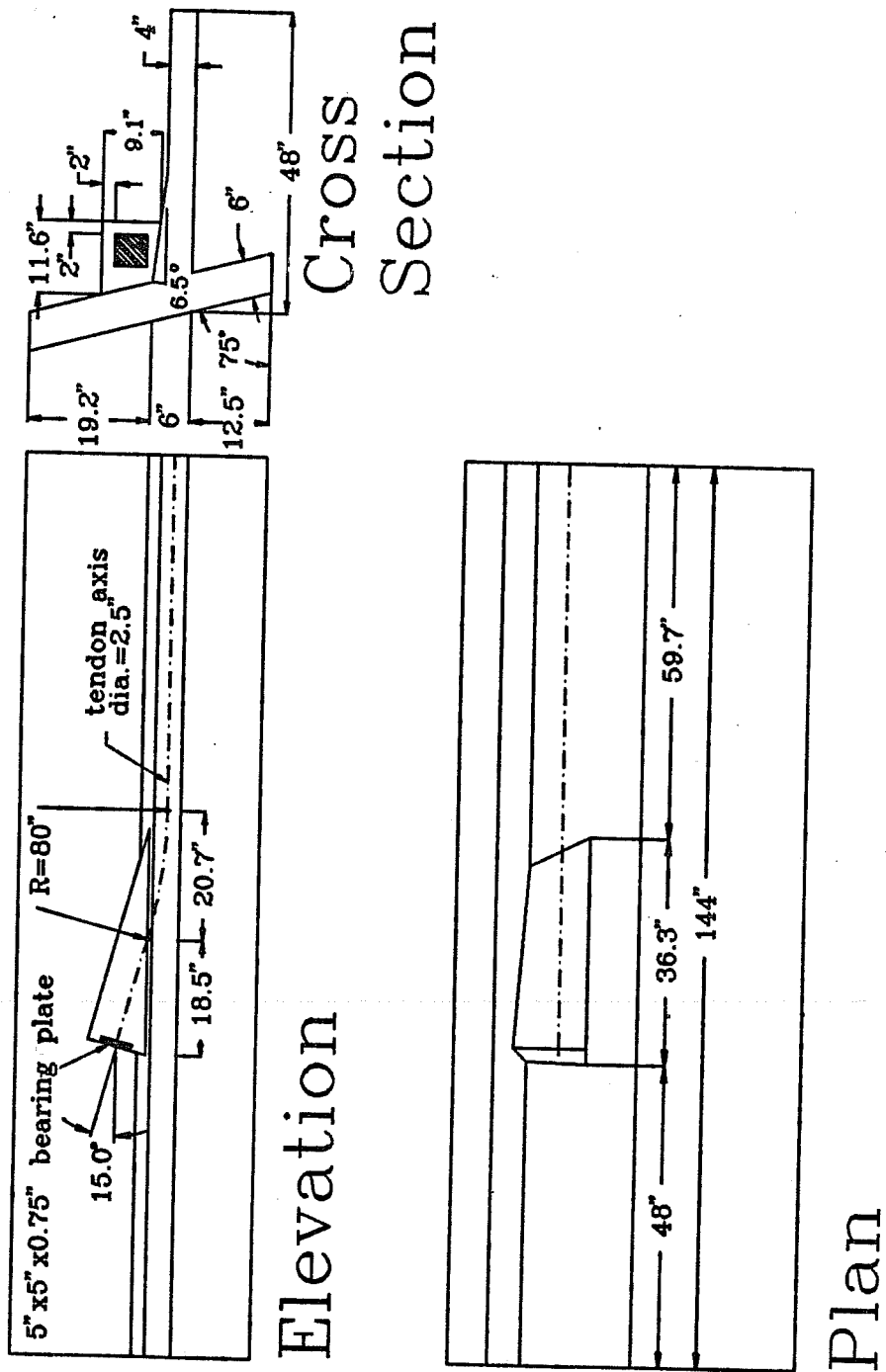
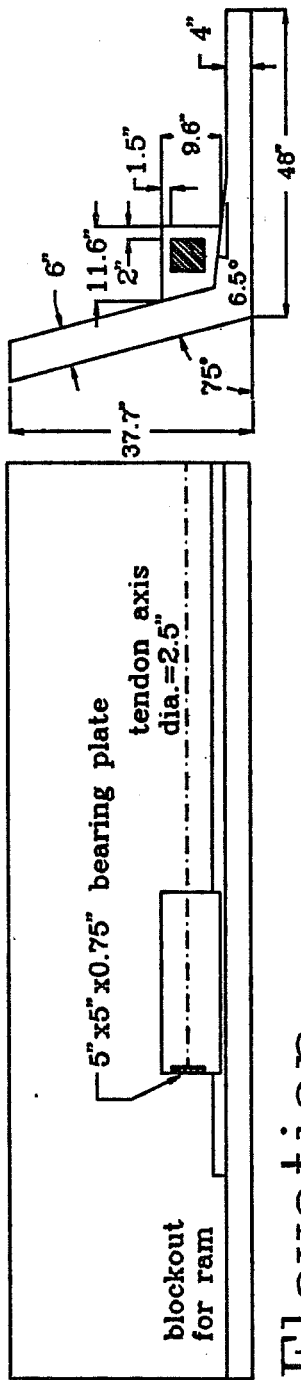
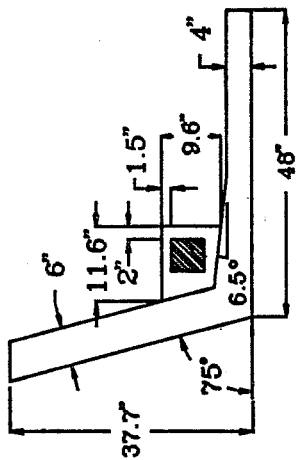


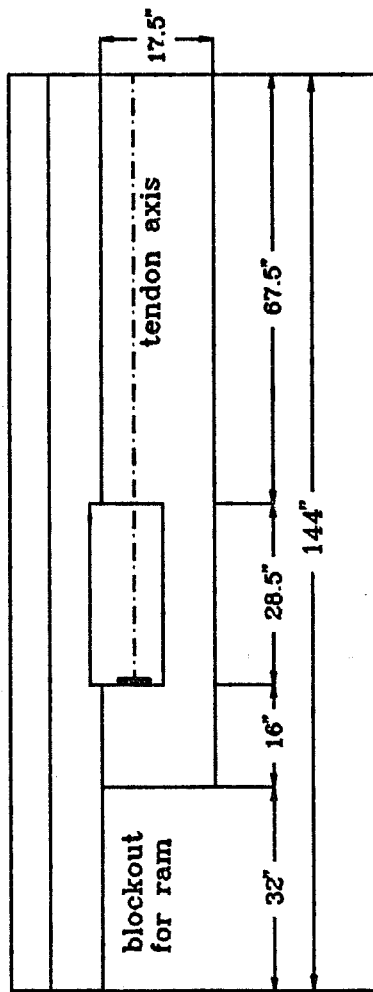
Figure 4.66 Geometry of Corner Blister Specimens With Internal Tendons



Elevation

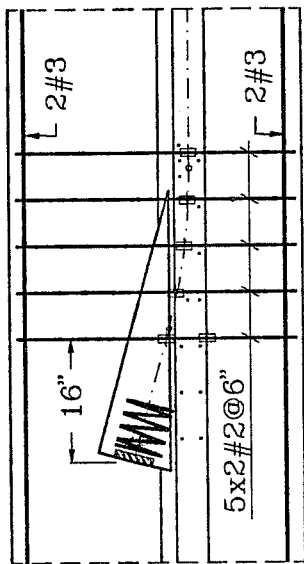


Cross
Section



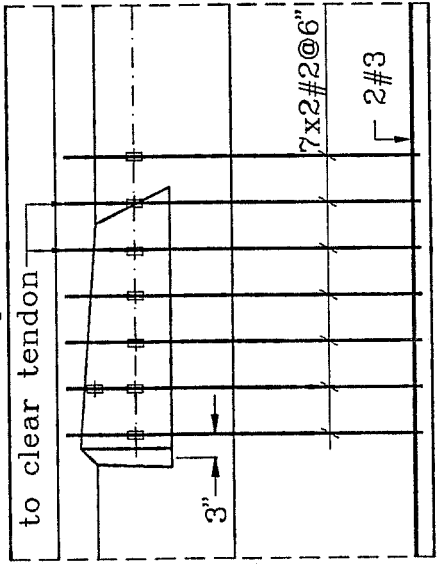
Plan

Figure 4.67 Geometry of Corner Blister Specimen With External Tendon

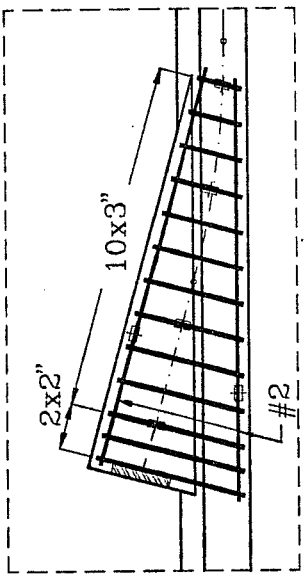


Elevation

move two top bars
to clear tendon

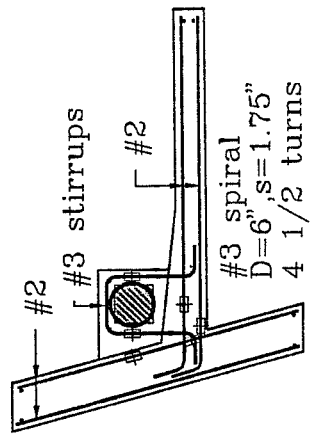


Plan



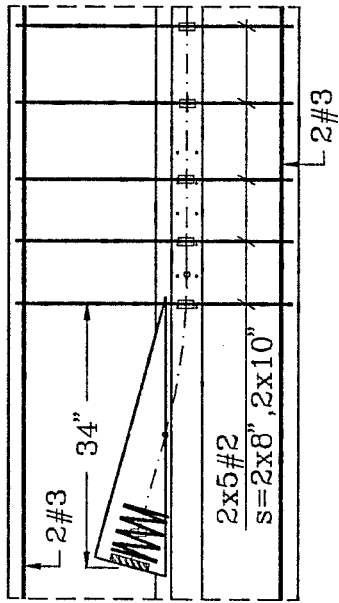
Blister Detail

⊕ strain gages

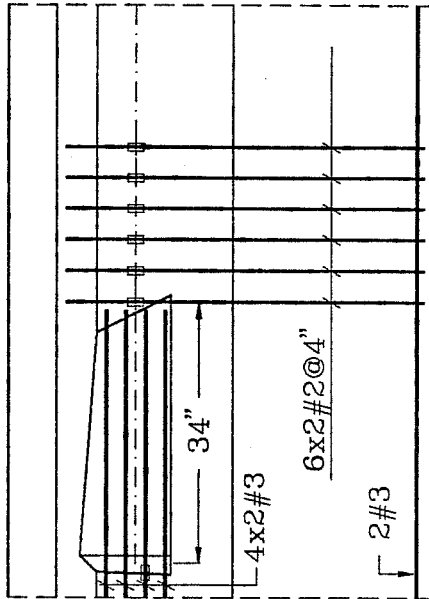


Cross Section

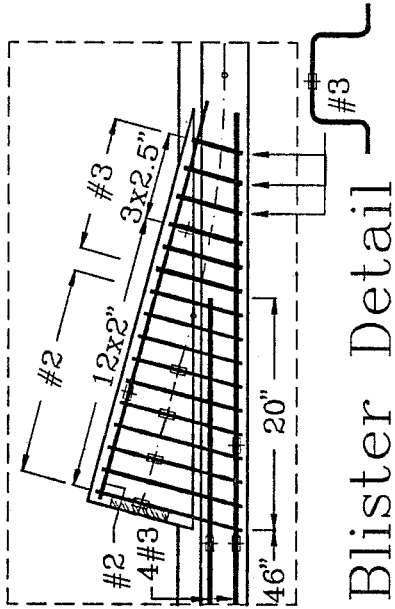
Figure 4.68 Reinforcement Details for Specimen Corner1



Elevation

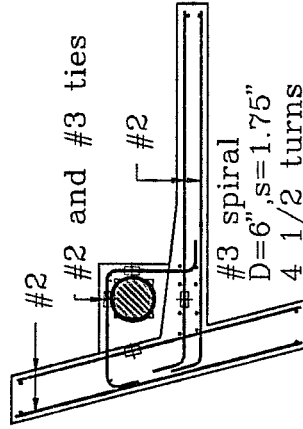


Plan



Blister Detail

strain gages



Cross Section

Figure 4.69 Reinforcement Details for Specimens Corner21 and Corner22

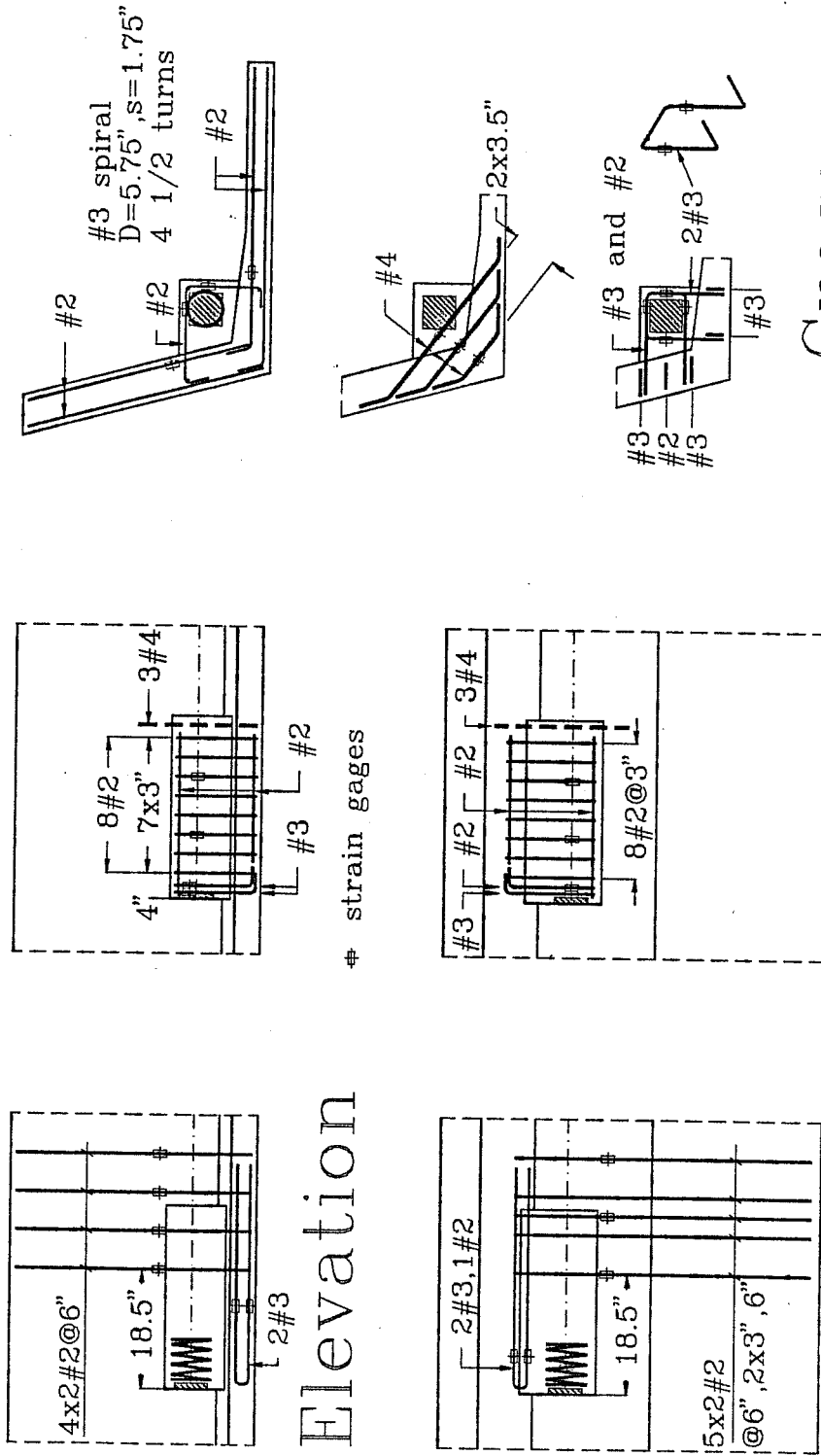


Figure 4.70 Reinforcement Details for Specimen Corners

U-ties were provided to tie back the tendon deviation force into the slab. The amount of blister reinforcement is based on shear-friction requirements and on requirements for tendon deviation. It is much lighter than for specimen Corner1 (#2 L-ties @ 2 in. (Figure 4.69) versus #3 U-ties @ 3 in. (Figure 4.68)).

The blister reinforcement arrangements in the corner blisters reflects an insight gained from the slab blister tests. Reinforcement requirements in the blister outside the region of tendon curvature are not so much determined by the need to carry direct tension forces but more by the necessity to provide good confinement around and ahead of the local zone. This reinforcement is needed to control crushing of the concrete and to increase ductility.

Independent simple strut-and-tie models, similar to Mörsh's basic model (Figure 2.5) were used for design of flange and web bursting reinforcement. Table 4.15 lists these bursting forces in terms of the anchor force, P . Two different bursting reinforcement arrangements were tested. In specimen Corner1 the bursting reinforcement was distributed mostly within the blister region. In specimens Corner21 and Corner22 this reinforcement was placed ahead of the blister at a larger distance from the anchor.

Table 4.15 Design Bursting Forces for Corner Blister Specimens

specimen	T_{slab}	T_{web}
Corner1	0.20P	0.14P
Corner21	0.17P	0.11P
Corner22	0.17P	0.11P
Corner3	0.22P	0.20P

Only specimens Corner21 and Corner22 had slab reinforcement for control of cracking behind the anchor. This reinforcement was proportioned to carry 25% of the design tendon force. Equal amounts of reinforcement were provided near the top and bottom face of the flange (2x4#3, Figure 4.69).

4.4.4.3 Design of Corner Blister Specimen With External Tendon

In specimen Corner3 anchorage of an external tendon in a corner blister was modelled. Reinforcement details are shown in Figure 4.70. The design load was 124 kips, corresponding to a 12-½ in. strand tendon in the full-scale structure.

The same spiral as for specimens Blister1 and Blister2 was used. Design of the general zone reinforcement was based on a strut-and-tie model similar to model A shown

in 4.65a. Model B is probably the better approximation of the actual load path in the structure, but it was only developed after testing of specimen Blister3. The strut-and-tie model calls for strong corbel reinforcement (2#3 U-ties into slab, 1#3 and 1#2 tie into the web, Figure 4.70). Inclined reinforcement was provided at the end of the blister across the web-flange corner (3#4). This deep beam reinforcement was proportioned to resist 28% of the design load at yield. Table 4.15 lists the flange and web bursting forces used in design. Closely spaced L-ties were placed throughout the blister (8#2) with the legs tying into adjacent web and flange. Design of this reinforcement was based on shear-friction requirements.

Reinforcement was provided in flange and web (2#3 hairpins in flange, 1#2 and 2#3 hairpins in web) to resist tensile forces T_2 as indicated by the strut-and-tie model (Figure 4.65a). There was no slab reinforcement for control of cracking behind the anchor in specimen Blister3.

4.4.5 *Presentation of Test Results*

4.4.5.1 Crack Development

First cracking loads, together with first yield and ultimate loads, are listed in Table 4.16. Typical crack patterns are shown in Figures 4.71 through 4.73. Crack patterns and crack development were very similar to those in the slab blister specimens. Cracking behind the anchor in both flange and web occurred first, but crack widths remained small. The cracks did not propagate through the web and propagated through the full slab thickness only late in the tests. Subsequent cracking occurred in the local zone region, in the region of tendon curvature, and along the tendon path (Figures 4.71 and 4.72).

The crack pattern in specimen Corner3 with an external tendon was somewhat different, reflecting the different behavior of this type of anchorage. As shown in Figure 4.73, the crack pattern followed the direction of the compression struts which are pulled towards flange and web by corbel action. The view of the end face of the blister shows cracking due to deep beam action. These cracks propagated ahead of the blister in the web-flange joint. The crack pattern confirms very well the load path envisioned in the development of the strut-and-tie models.

Figures 4.74 through 4.76 show the crack width development for specimens Corner1, Corner22, and Corner3. The crack widths behind the anchor stayed below

Table 4.16 First Cracking, First Yield, and Ultimate Loads for Corner Blister Specimens

specimen	F_{pu} (kips)	1 st cracking load* (% F_{pu})	1 st yield load (% F_{pu})	ultimate load (% F_{pu})
Corner1	196	0.51 (1) 0.91 (2,3)	1.34 ³	1.58
Corner21	196	0.51 (1) 0.69 (2) 0.91 (3)	0.91 ^{2,3}	1.05
Corner22	196	0.44 (1) 0.89 (2,3)	1.03 ²	1.17
Corner3	124	0.81 (1) 1.10 (2) 1.58 (3)	1.69 ¹	2.06

*) numbers in parenthesis correspond to cracks as labeled in Figure 4.38

¹) corbel/local zone ties

²) blister bursting/local zone ties

³) flange bursting reinforcement

0.005 in. in all cases. Cracking was much more critical in the local zone region and reached widths from 0.01 in. in specimen Corner1 to 0.03 in. in specimen Corner22. Comparison of Figures 4.74 and 4.75 shows that the heavier tie reinforcement in specimen Corner1 was effective in reducing the crack width in the local zone.

4.4.5.2 Ultimate Loads and Failure Mode

As in the slab blister series, failure was triggered by crushing of the concrete ahead of and surrounding the spiral confinement reinforcement (Figures 4.77 through 4.80). Except for specimen Corner1 all failures were preceded by yielding of most of the ties in the local zone at 82% to 88% of the failure load (Table 4.16). In specimen Corner1 the tie strains reached about 90% of yield.

The tie reinforcement in specimen Corner1 was much heavier than in the other specimens. Specimen Corner22 had the same concrete strength and the same spiral reinforcement but lighter tie reinforcement. The direct comparison of these specimens

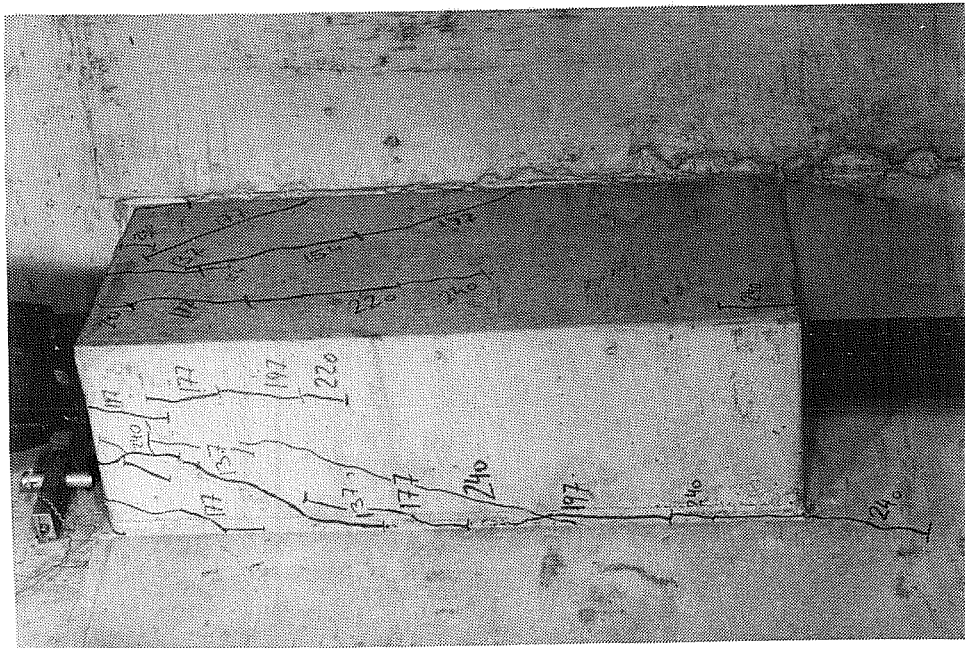


Figure 4.73 Crack Development In Specimen Corner3 at 94% of Failure Load

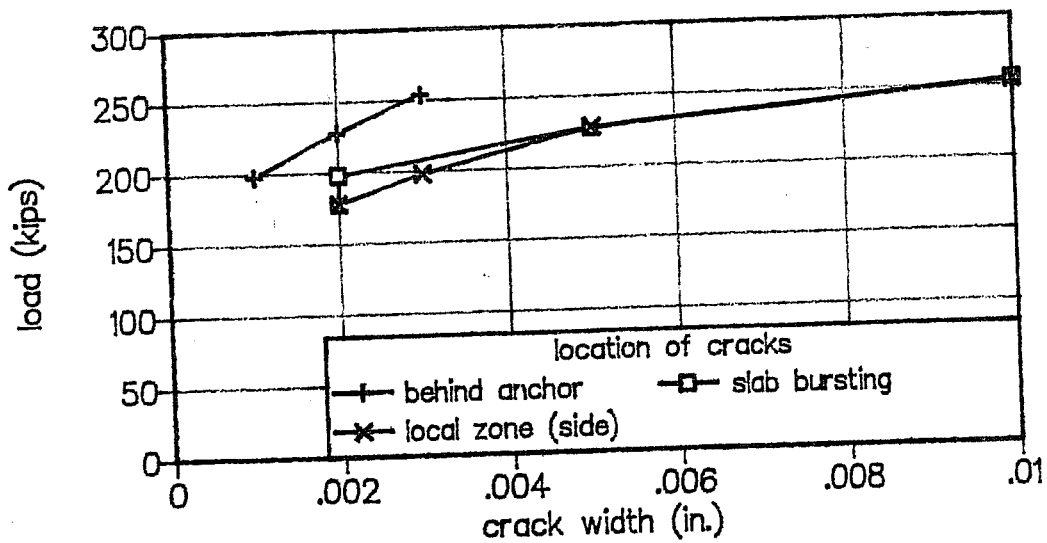


Figure 4.74 Crack Width Development for Specimen Corner1

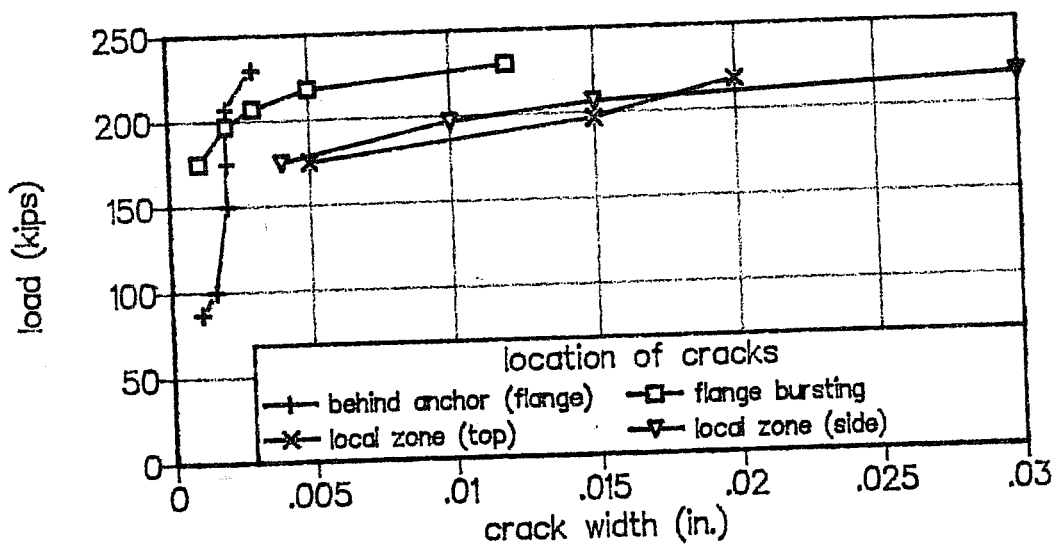


Figure 4.75 Crack Width Development for Specimen Corner22

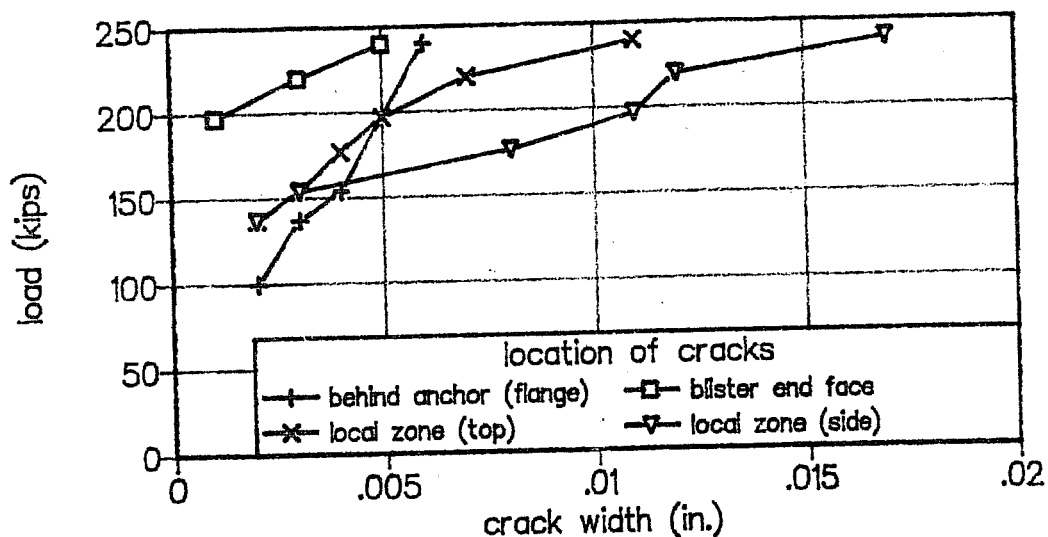


Figure 4.76 Crack Width Development for Specimen Corner3

shows that the extra tie reinforcement in specimen Corner1 had a beneficial effect on both crack widths in the local zone (Section 4.4.5.1) and on the failure load (Table 4.16).

4.4.5.3 Reinforcement Strains

Figure 4.81 shows a comparison of the flange bursting strains at failure. In the specimens with internal tendons stress peaks occurred in the region of tendon curvature close to the end of the blister due to the combined effect of slab bursting and lateral bending. Strains in specimen Corner3 were smaller because of the lack of a tendon path crack. However, significant strains were developed in the deep beam reinforcement across the web-flange corner, although it did not yield (Figure 4.83). The webs of the specimens did not crack, and consequently strains in the web bursting reinforcement were insignificant (Figure 4.82).

The distribution of tie strains throughout the blister was very similar to that of the isolated slab blister specimens (Figure 4.50). Most of the ties within 10 in. of the anchor yielded prior to failure, except in specimen Corner1. In specimen Corner1 these ties reached about 90% of yield. In the specimens with internal tendons peak tie strains were also observed in the region of tendon curvature, but did not exceed $800 \mu\epsilon$. Figure 4.84 shows the strain development for the corbel action reinforcement in specimen Corner3.

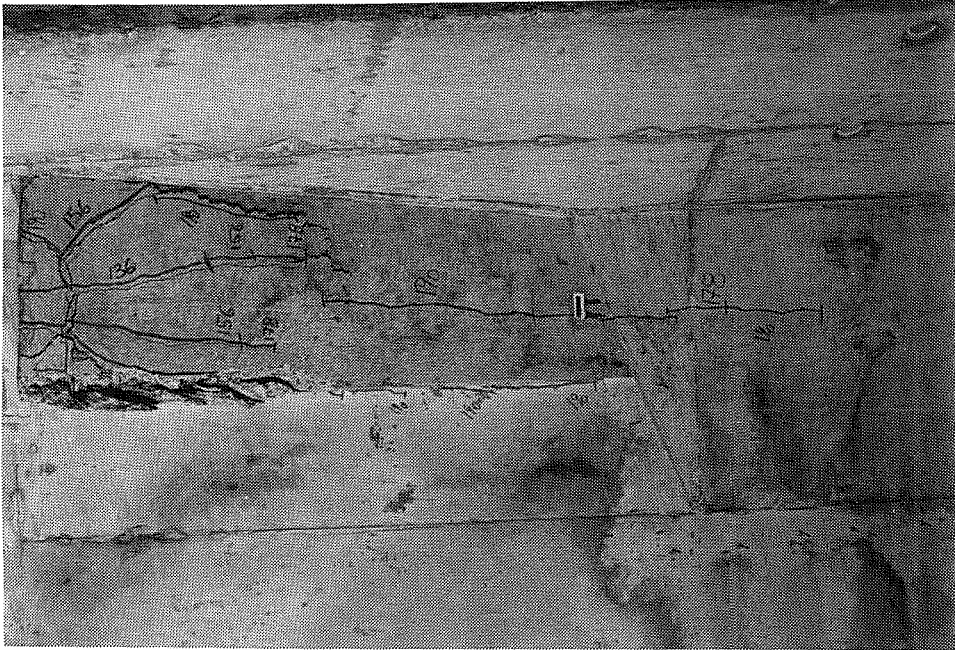


Figure 4.78 Local Zone Cracking and Concrete Spalling (SpecimenCorner21)

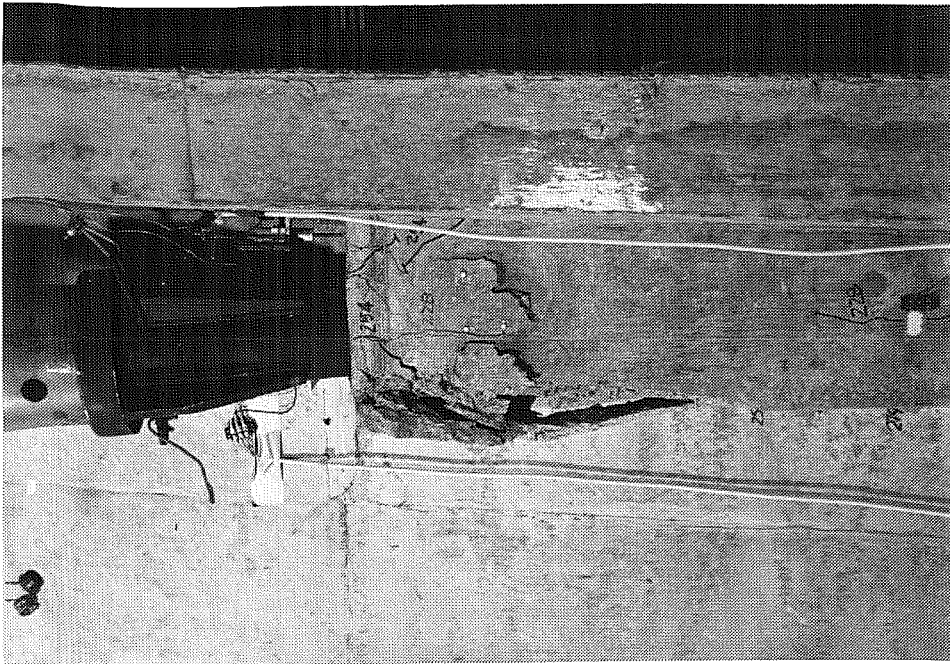


Figure 4.77 Specimen Corner1 at Failure

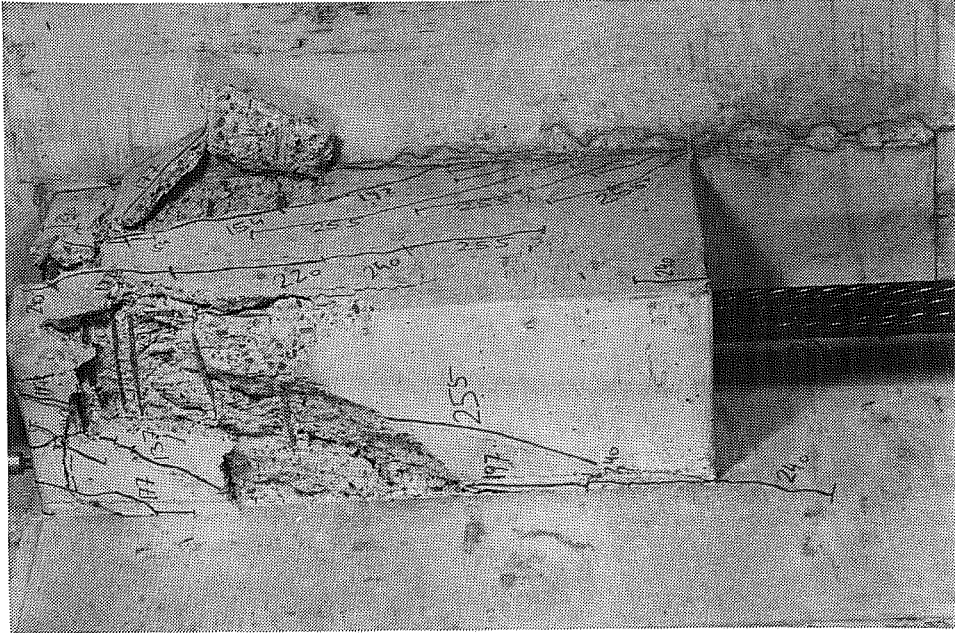


Figure 4.80 Specimen Corner3 at Failure

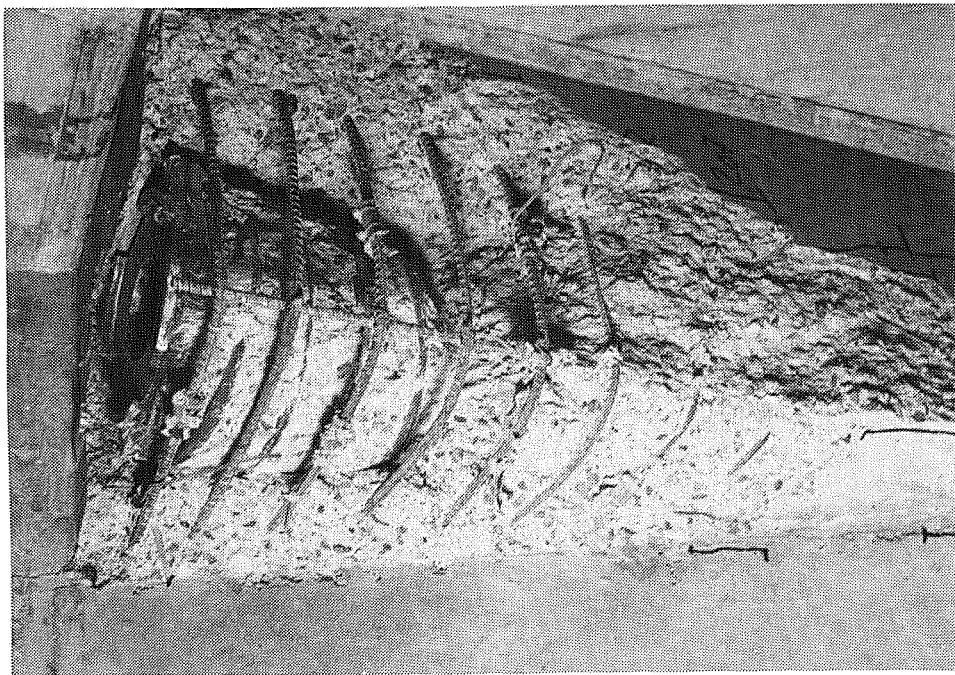


Figure 4.79 Specimen Corner22 After Removal of Loose Concrete

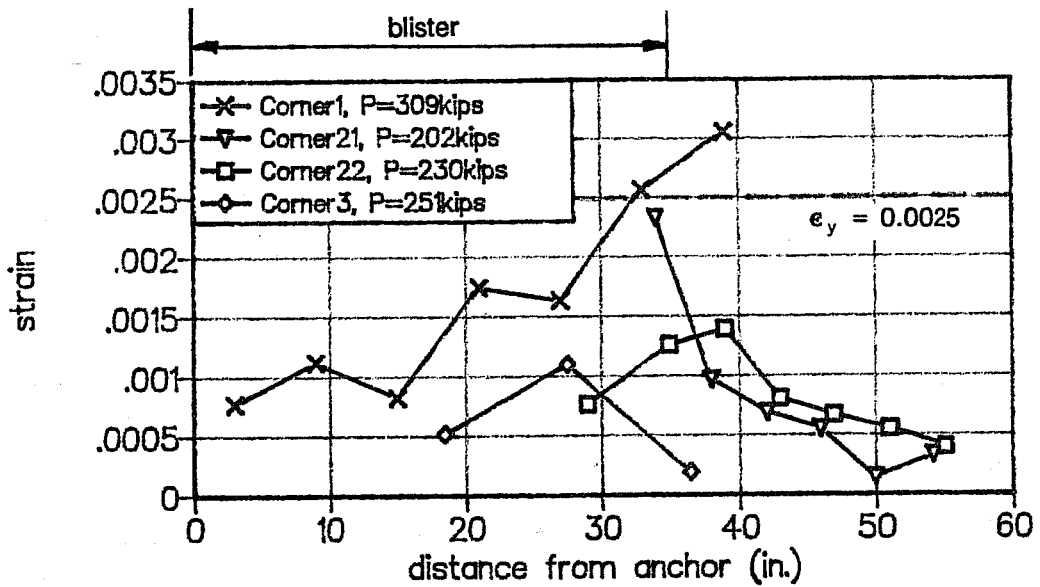


Figure 4.81 Flange Bursting Strains at Failure

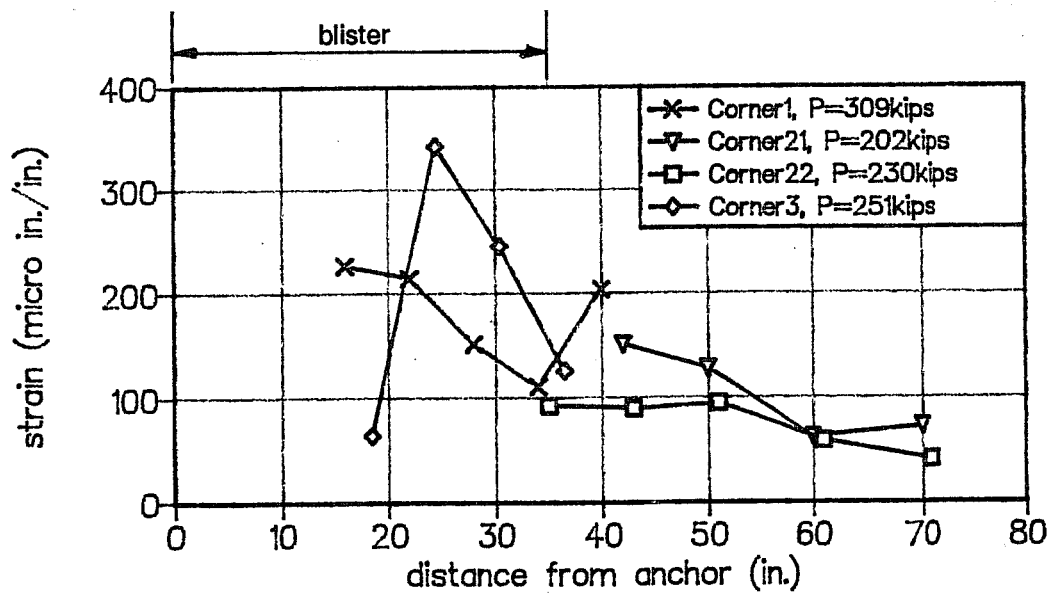


Figure 4.82 Web Bursting Strains at Failure

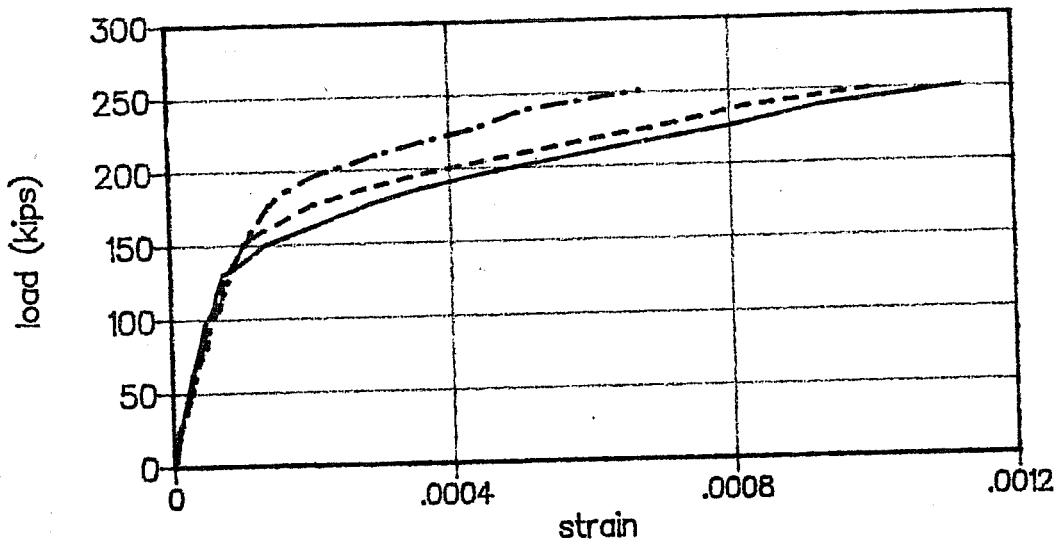


Figure 4.83 Deep Beam Action in Specimen Corner3

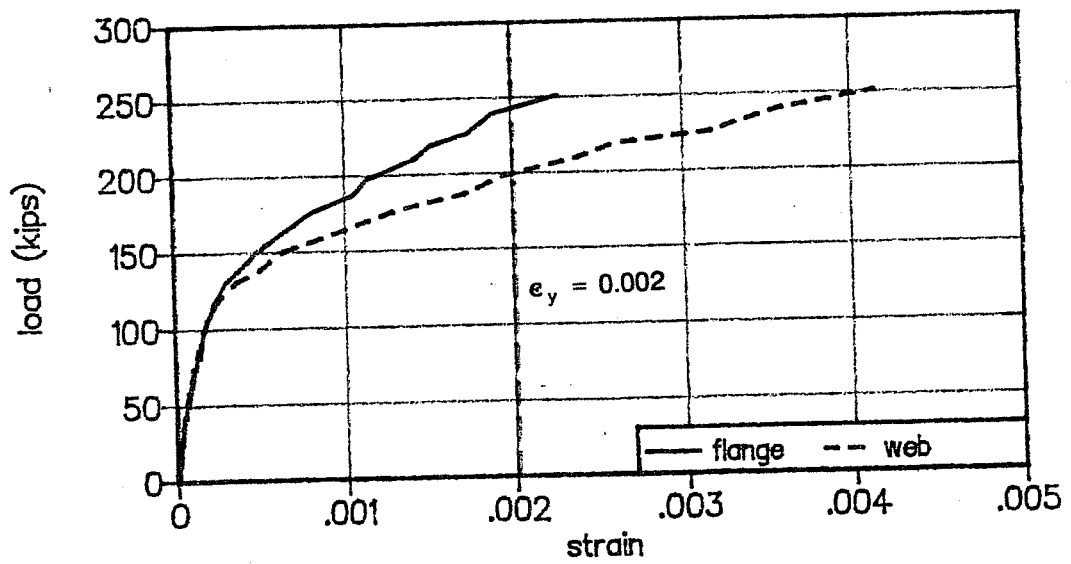


Figure 4.84 Corbel Action in Specimen Corner3

Strains in the slab reinforcement for control of cracking behind the anchor in specimens Corner21 and Corner22 reached about $900 \mu\epsilon$ in the top layer and about $500 \mu\epsilon$ in the bottom layer. Almost identical values were observed in the isolated slab blister specimens.

4.4.6 Evaluation of Test Results

Table 4.17 shows various failure load predictions based on Roberts' best fit equation for the capacity of the local zone (Equation (4.4)) and on the finite element analysis results (Section 4.4.2). The capacity at the local zone-general zone interface is determined by the linear-elastic compression stresses one plate width ahead of the anchor. The predictions controlled by slab bursting are based on the comparison of the bursting force, including the effects of shear (see Section 4.4.2), to the available reinforcement capacity at yield. No adjustment was made to account for the difference between actual reinforcement arrangement and the arrangement indicated by the finite element analysis. Table 4.18 shows similar predictions based on strut-and-tie model procedures and on local zone capacity. The predictions controlled by flange bursting are based on comparison of the available reinforcement capacity to the required bursting forces listed in Table 4.15.

The experimental program showed, that although some of the flange bursting reinforcement yielded prior to failure, capacity and arrangement of this reinforcement did not control the failure loads of the specimens due to limited concrete cracking. Therefore in Table 4.17 and in Table 4.18 the predictions controlled by flange bursting are put in parentheses and are not considered in the evaluation of the test results, although they would give the lowest prediction in most cases. The predictions assuming compression controls (underlined) give conservative results and have a fairly low standard deviation. Actual failure modes resembled very much the failures observed in the local zone tests by Roberts [41]. Clearly, compression of the blister region immediately ahead of the anchor was the dominant factor controlling the ultimate load of the corner blister specimens.

4.5 Summary and Conclusions

4.5.1 Summary of Study

In this chapter the anchorage of tendons in isolated slab blisters, ribs, corner blisters for internal tendons, and corner blisters for external tendons was investigated. The

Table 4.17 Evaluation of Finite Element Analysis Predictions for Corner Blister Specimens

specimen	P_{test} (kips)	local zone (kips)	interface (kips)	flange bursting (kips)	P_{calc} (kips)	$P_{test}/$ P_{calc}
Corner1	310	<u>236</u>	265	(193)	236	1.31
Corner21	206	172	<u>167</u>	(165)	167	1.23
Corner22	230	<u>221</u>	265	(165)	221	1.04
Corner3	255	<u>226</u>	231	(211)	226	1.13
average						1.18
standard deviation						0.10

Table 4.18 Evaluation of Strut-and-Tie Model Predictions for Corner Blister Specimens

specimen	P_{test} (kips)	local zone (kips)	interface (kips)	flange bursting (kips)	P_{calc} (kips)	$P_{test}/$ P_{calc}
Corner1	310	<u>236</u>	261	(222)	236	1.31
Corner21	206	172	<u>164</u>	(224)	164	1.26
Corner22	230	<u>221</u>	260	(224)	221	1.04
Corner3	255	<u>226</u>	231	(144)	226	1.13
average						1.19
standard deviation						0.11

research program included linear-elastic three-dimensional finite element analysis, development of strut-and-tie models, and physical tests of eight half-scale specimens. The study included investigation of the effects of tendon eccentricity (corbel action and local bending) and tendon curvature (tendon deviation force and lateral bending), of the introduction of the concentrated prestressing force (concrete crushing, blister bursting, slab bursting), and of compatibility induced tensile stresses behind intermediate anchorages.

4.5.2 Behavior of Intermediate Anchorages in Blisters or Ribs

The ultimate load of all specimens was clearly controlled by crushing and spalling of the concrete surrounding and ahead of the spiral in the local zone. This failure mode and crack patterns prior to failure were very similar to those observed in Roberts' local zone specimens [41]. Yielding of the ties surrounding the local zone region was a reliable indicator of impending failure in all specimens. Table 4.19 shows that the corner and rib specimens on average reached a higher ultimate bearing stress than the isolated slab blister specimens. This is explained by the slightly larger spiral in the corner blister specimens and by the better confinement provided by surrounding concrete in both rib and corner blister specimens.

Table 4.19 Comparison of Bearing Pressures at Failure

specimen	f'_{cl} (psi)	P_{test} (kips)	f_b (psi)*	f_b/f'_{cl}	average
Blister1	4900	253	12600	2.57	2.59
Blister2	4200	235	11700	2.79	
Blister3	4900	237	11800	2.41	
Blister4	4700	275	13700	2.91	2.91
Corner1	4600	310	15400	3.35	3.14
Corner21	2900	206	10300	3.55	
Corner22	4600	230	11400	2.48	
Corner3	4000	255	12700	3.18	

*) net bearing area $A_b = 20.1 \text{ in}^2$

Although the final failure mode observed in the tests was very similar for blisters with internal and with external tendons, there is a fundamental difference between these types of anchorages. In blisters with external tendons the tendon is eccentric and parallel to the slab. Corbel action is essential for equilibrium and hence reinforcement is needed to pull the anchor force into the slab. Blisters for external tendons removed from the web-flange junction of the cross section (isolated slab blisters) would introduce substantial bending moments into the slab, similar to the bending moments introduced by a corbel into a column. By arranging such blisters in the corner of the cross section these bending

moments can be much reduced. With internal tendons the tendon is eccentric only initially and is inclined with respect to the plane of the slab. Corbel action is not essential for equilibrium and may disappear after cracking in favor of the stiffer load path in direct compression. The distribution of the anchor force to the load path involving direct compression and to the load path involving corbel action and local bending depends on the relative stiffness of these load paths. Consequently, if more reinforcement is provided for corbel action and local bending, more of the anchor force will be attracted by this load path. If practical, blisters should be located in the web-flange corner of the cross section to minimize these local bending effects. However, there is no reason to make this requirement mandatory for blisters with internal tendons.

Curvature of the tendon creates deviation forces that need to be tied back into the structure. In rib anchorages this deviation force also induces a lateral bending moment in the slab. The concentrated deviation force is balanced by vertical shear stresses which are distributed over the slab width. In isolated slab blisters the shear force introduced by the vertical component of the tendon force remains concentrated within the blister, hence the lateral bending moment is much smaller.

Amount and arrangement of slab and web bursting reinforcement was of secondary importance in the specimens of this series and not a good predictor, albeit a conservative one, for the failure loads, due to limited concrete cracking. However, bursting reinforcement is essential to ensure transverse spreading of the concrete compression stresses after cracking of the slab. This was very obvious in Sanders' tests where anchorage failures were frequently preceded by yielding of the bursting reinforcement, although this occurred at much higher load levels than expected from the capacity of the bursting reinforcement [44]. Contrary to Sanders' tests, the flange bursting cracks in the blister specimens of this series did not extend all the way to the base of the specimens. In many cases they did not even extend through the full slab thickness, due to lateral compression stresses on the bottom side of the slab induced by lateral bending in the region of tendon curvature. No bursting cracks were observed in the webs of the corner blister specimens. Consequently much of the bursting reinforcement did not reach yield, except in the region of tendon curvature where tensile lateral bending stresses and slab bursting stresses coincided on the top side of the slab. However, it must be kept in mind that these tests modelled only the effect of

the anchor force. The role of the bursting reinforcement should be more significant if other loads or stresses increase the extent of cracking in the anchorage zone.

Linear-elastic analysis indicates very high tensile stresses in the reentrant corner behind the blister. These tensile stresses are induced by the requirement of compatibility of deformation ahead of and behind the anchor and cause early cracking behind the anchor. Such cracking does not affect the performance of the anchorage itself but it may have adverse effects on other requirements in the same region (watertightness, shear strength). In the experimental tests cracking behind the anchor was observed well below service loads but crack widths at service load levels were insignificant. The cracks initiated at the reentrant corner behind the blister and propagated slowly at an angle of approximately 45 degrees through the slab. Long term deformations tend to increase the crack width and some reinforcement should be provided across this crack. The purpose of this reinforcement is to control crack width and to arrest the crack, but it cannot delay cracking behind the anchor. The load path in tension behind the anchor is all but eliminated by this cracking in favor of the stiffer load path in compression ahead of the anchor. Provision of a rib reduces the linear-elastic tensile stresses behind the anchor, but not enough to prevent cracking. If cracking must be prevented it is necessary to precompress the critical section behind the anchor.

4.5.3 *Design Recommendations*

The following checks and design steps should be considered in the design of blister anchorages:

1. Bearing pressures immediately ahead of the anchor and concrete compression stresses ahead of the local zone confinement reinforcement should be checked. With blisters for external tendons concrete compressive stresses may also be critical immediately ahead of the blister, if flange and web of the section are thin compared to the dimensions of the blister.
2. Tie reinforcement within the blister has the following functions:
 - confinement of the local zone;
 - corbel action, particularly in blisters for external tendons;

- shear reinforcement, particularly in isolated slab blisters where the vertical component of the tendon force remains as shear force within the blister until it is balanced by the tendon deviation force;
 - tie-back reinforcement in the region of tendon curvature;
 - shear-friction.
3. Slab reinforcement perpendicular to the tendon is needed to carry bursting forces and, in rib anchorages, also to carry lateral bending forces. Slab reinforcement parallel to the tendon is needed to control cracking behind the anchor and to resist local bending forces due to tendon eccentricity.
4. Corner blisters for external tendons also require reinforcement across the web-flange corner at the end of the blister.

Linear-elastic finite element analysis is very useful to find the critical regions and to get an idea of the flow of forces in the structure. The method also worked well for the check of compression stresses ahead of the local zone reinforcement. However, particularly in 3D problems, such as the blister anchorages discussed in this chapter, it is very difficult to interpret the finite element analysis results with regard to reinforcement requirements. Non-linear analysis that accounts for concrete cracking and presence of reinforcement would be desirable but is not yet feasible for routine applications.

Strut-and-tie models are an excellent tool to find the most basic load path in the structure. This basic load path satisfies only equilibrium conditions and material strength limitations. In blisters with internal tendons it is a direct compression strut that is deviated in the region of tendon curvature. The only tensile force essential for equilibrium is needed to tie back the tendon deviation force (Figure 4.24a). With external tendons the basic load path requires tension forces for corbel action at the loaded face of the blister and for deep beam action at the end face of the blister (Figure 4.65). Additional information is needed to refine the basic load path if equilibrium conditions alone are not sufficient to arrive at a useful design model. For example, the need for slab bursting reinforcement becomes only apparent if a stress distribution based on simple beam theory is enforced at the end of the anchorage zone. Even with this additional information the magnitude of the bursting force is still very sensitive to the geometry of the strut-and-tie model. As another example, corbel action and local bending forces in blisters with internal tendons can be selected arbitrarily. This sensitivity is typical for members with strut-and-tie models that are not essential for

equilibrium because other load paths are available. Such members are less critical for the strength of the structure than the members of the basic load path.

Strut-and-tie models have the advantage that they give a clear indication of the basic load paths and of reinforcement requirements essential for the strength of the structure. Development of refined strut-and-tie models for design requires additional rules, which are summarized in Chapter 6. Design based on such models is conservative and satisfactory for strength considerations in simple cases. For three-dimensional problems the development of strut-and-tie models is quite feasible, if the problem can be approximated as a series of two-dimensional sub-problems. In this manner, a good model was found for the flow of forces in an isolated slab blister (Figure 4.24). However, for the corner blister problems fully three-dimensional solutions are required, which makes the development of satisfactory strut-and-tie models quite difficult. For such complex applications it is highly recommended to supplement strut-and-tie models with other design procedures, such as finite element methods, to identify critical regions of the structure, to determine areas requiring reinforcement for serviceability considerations, and in general to develop a better feel for the load path in the structure.

4.5.4 *Detailing Recommendations*

The tie reinforcement in blisters around and ahead of the local zone and in the region of tendon curvature is crucial for the performance of the anchorage zone. If an anchorage device is based on an acceptance test (special anchorage devices, Appendix A) similar reinforcement should be adequate in blisters. The ties do not have to be closed loops, but U-shaped ties should be fully developed at the interface between slab and blister. The ties in the region of tendon curvature should be conservatively dimensioned since this region is very susceptible to construction inaccuracies (kinks in the tendon instead of gradual curvature). On the other hand, overconservatism in the local zone leads to congested anchorage details and must be avoided. In blisters for external tendons the detailing rules for corbels should be observed.

Close spacing of the ties is recommended. The spacing should not exceed the smallest of width of the blister, height of the blister at the anchor, or 6 inches. Closer spacing of 1 to 3 in. is required if ties are used for concrete confinement around and ahead

of the local zone. The corner blister tests did not indicate any adverse effects from the use of U-ties which tied only into the flange but not into the web of the cross section.

Because of limited cracking, the tests did not give a good indication of the best arrangement of flange and web bursting reinforcement. If based on strut-and-tie models, the centroid of the bursting reinforcement should coincide with the corresponding force in the model. For practical purposes uniform arrangement of closely spaced bursting reinforcement throughout the anchorage zone is recommended. The anchorage zone extends from the loaded face of the blister to a section at a distance equal to one slab width ahead of the end of the blister. Additional reinforcement for lateral bending is required close to the top face of rib anchorages in the region of tendon curvature.

Reinforcement for control of cracking behind the anchor is only effective if arranged within the width of the blister. It should be placed close to the face of the slab where the blister is located. Yielding of this reinforcement is unlikely, but it is recommended that it be fully developed at the sections at one blister width or height behind and ahead of the anchor. Tie back reinforcement proportioned to carry 25% of the anchor force is adequate to control cracking behind the anchor, provided no tensile stresses from other loads or load effects exist in this region. The tie back reinforcement requirement can be expressed either in terms of service loads (25% of the unfactored tendon stressing force, with reinforcement stresses limited to 36 ksi) or in terms of ultimate loads (25% of the factored tendon stressing force, with reinforcement stresses limited by the nominal yield strength and the ϕ -factor). Because cracks behind blisters are usually inclined (approximately 45 degrees) tie reinforcement immediately ahead of the loaded face of the blister is also effective to control these cracks.

5 ANCHORAGE OF EXTERNAL POST-TENSIONING TENDONS IN DIAPHRAGMS

5.1 Introduction

5.1.1 General

Thin-walled cross sections must be stiffened at critical locations in order to maintain the section geometry. Such transverse stiffeners are called diaphragms (Figure 5.1). At the supports of the structure, a diaphragm facilitates the transfer of torsional moments and shear forces to the bearing pads. In externally post-tensioned structures the diaphragms also serve as reactions for anchorage of the prestressing tendons.

External post-tensioning, in particular in connection with precast segmental construction, has become very competitive in the United States in recent years and has been widely used in France for several decades. However, very little information is available on behavior and design of the diaphragms of such structures.

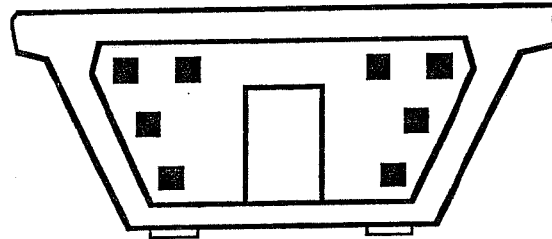


Figure 5.1 Diaphragm in Box Girder Bridge

5.1.2 Objectives

Diaphragms are very massive, and hence their behavior differs significantly from the lighter members discussed in the previous chapters. The main objective of this chapter is to gain insight into the behavior of diaphragms when used for anchorage of external tendons and to develop design and detailing recommendations. As in the preceding chapters the approach to the problem includes linear-elastic finite element analysis, strut-and-tie model considerations, and a verifying series of physical tests.

5.2 Background Information

5.2.1 Literature

A very good general overview of the state of the art of externally post-tensioned bridges with deviators is included in Reference 40. A number of papers discuss problems with diaphragms due to excessive cracking [16, 39, 56, 57], but very little information is available on behavior and design of diaphragms when used for the anchorage of external tendons.

Powell, et al. summarize a report by **Chatelain** on a number of externally post-tensioned bridges in France which were completed in the 1950's [40]. One of these bridges, the Can Bia Bridge, experienced cracks in the diaphragms which were attributed to transverse tensile forces induced by spreading of the concentrated tendon anchorage force.

Woodward describes diaphragm cracking in a concrete bridge which led to temporary closure of the structure to traffic after three years of service [57]. The problem was corrected by providing additional vertical prestressing in the diaphragm region and by grouting of the cracks.

Figure 5.2 shows typical crack patterns in the pier segments of a bridge structure of the Washington, D.C. rapid transit system [16, 26]. Vertical post-tensioning bars had to be added to control these cracks.

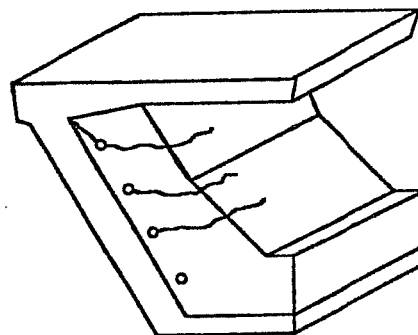


Figure 5.2 Diaphragm Cracking Due to Spreading of Tendon Forces

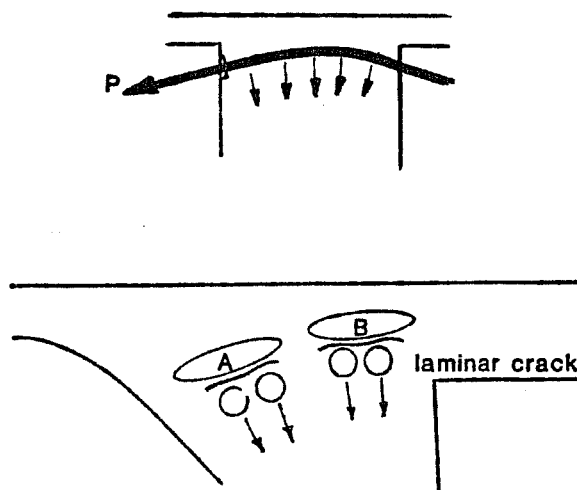


Figure 5.3 Diaphragm Cracking Due to Tendon Curvature (from [39])

Podolny describes in Reference 39 how diaphragm cracking may be induced by sharp tendon curvatures within the diaphragm region (Figure 5.3). A linear-elastic finite element study by **Wium and Buyukozturk** confirms the presence of tensile stress concentrations due to tendon curvature [56].

5.2.2 State of the Art

Current code provisions do not address the design of diaphragms and very little information is available in the literature. Hence, design procedures vary from office to office and include finite element analysis, rules of thumb, simple equilibrium considerations, and attempts to extend Guyon's solution which was developed for rectangular, prismatic members (Figure 2.7). In Reference 45 **Schlaich, et al.** present strut-and-tie models for the transfer of vertical shear forces through a diaphragm to the supports of the structure (Figure 5.4), but they are silent on the anchorage of external tendons in diaphragms.

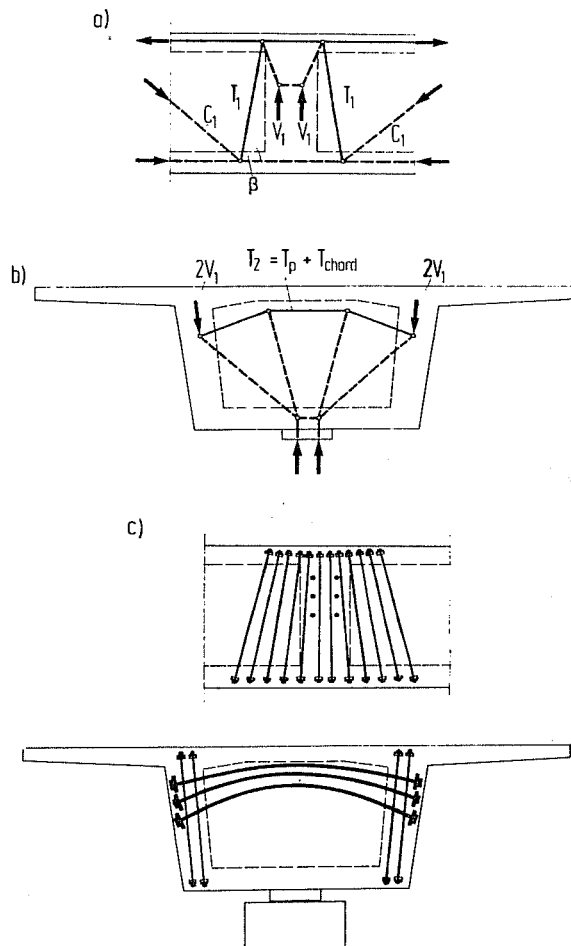


Figure 5.4 Transfer of Shear Forces to Supports Through Diaphragm (from [45])

Figures 5.5 through 5.8 [26] show design models used by one of the major externally post-tensioned segmental bridge designers in the United States. Figure 5.5 illustrates how the diaphragm has to span from flange to flange of a box girder, thus creating vertical tensile

forces due to deep beam action. Figure 5.6 shows a model for the flow of forces from the diaphragm into the web of the member. Behavior similar to a corbel is assumed. However, the model is incomplete and violates equilibrium conditions. No load path is provided to resist the applied couple $P_1 a$.

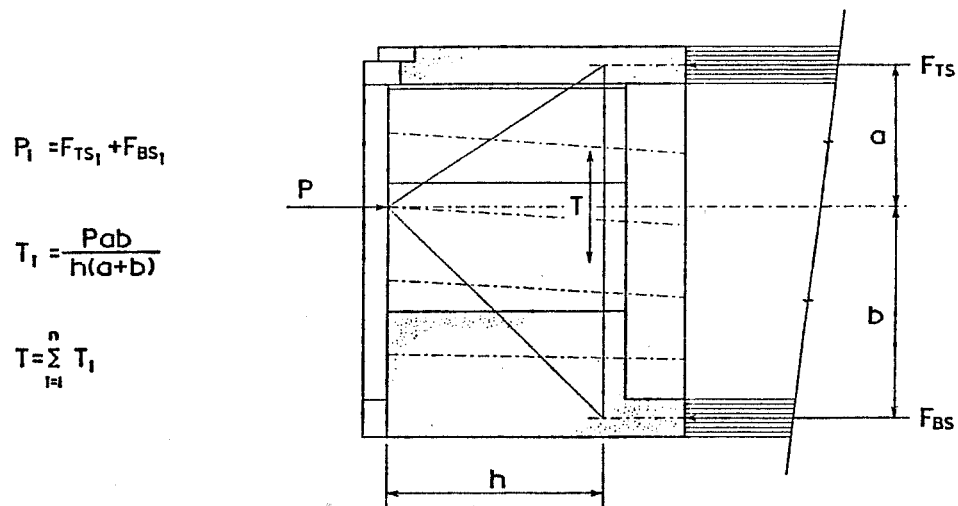


Figure 5.5 Design Model for Deep Beam Action

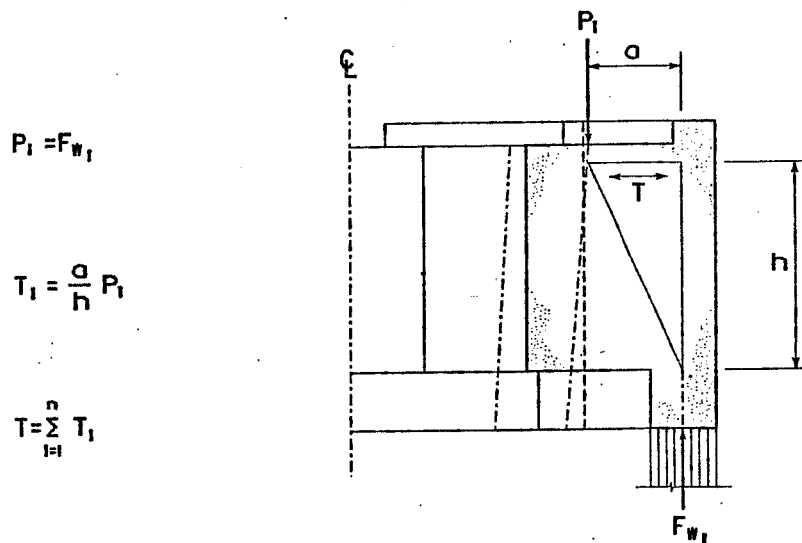


Figure 5.6 Design Model for Corbel Action

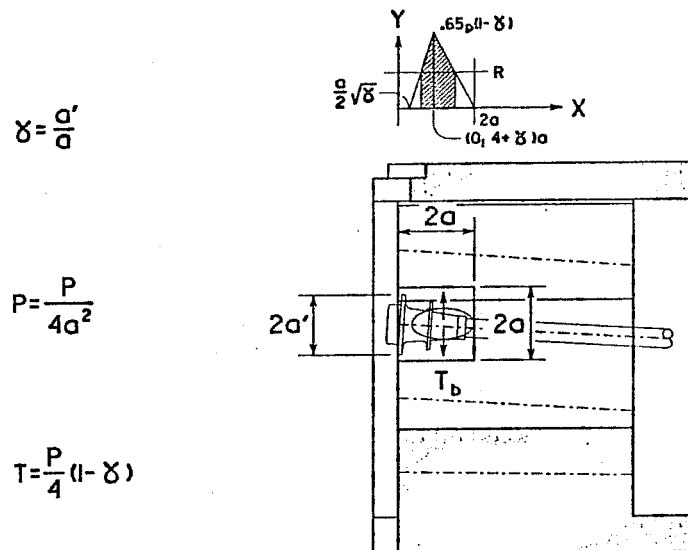


Figure 5.7 Design Model for Bursting Forces

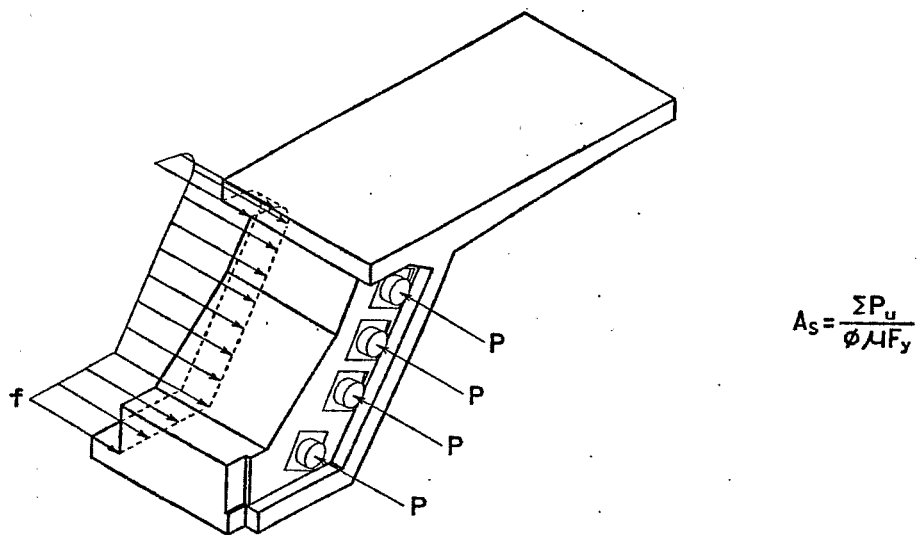


Figure 5.8 Design Model for Shear-Friction

Figure 5.7 addresses the "bursting forces" immediately ahead of the bearing plate. This reinforcement requirement is derived from Guyon's solution for a rectangular, prismatic member (Figure 2.7). The extension of his results to the diaphragm problem seems

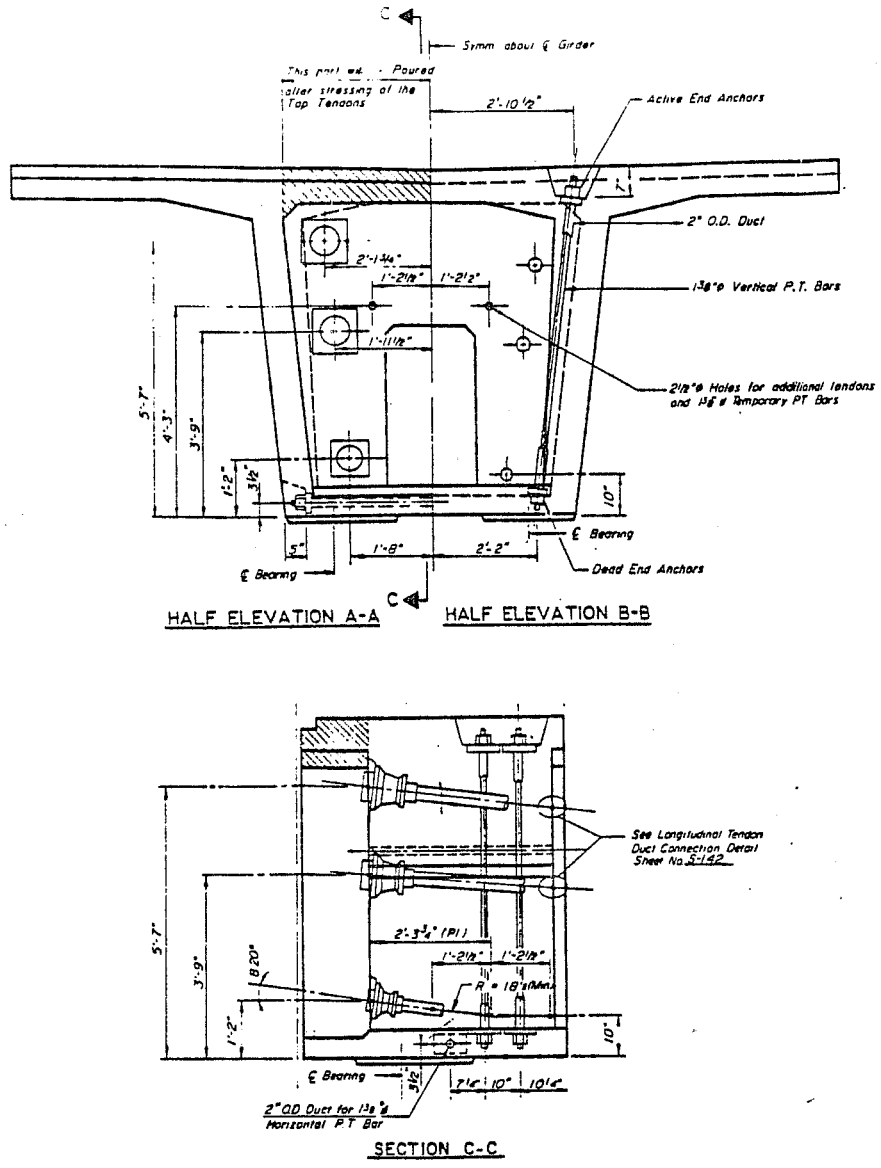


Figure 5.10 Typical Diaphragm Detail (from [27])

of the section. Neither detail satisfies the design model shown in Figure 5.5, since the tension tie provided by the transverse tendons does not adequately tie into the flanges.

The geometry of the diaphragm investigated in the following analytical and experimental studies is based on the structure shown in Figure 5.10. However, only two anchorage forces are applied so that advantage can be taken of symmetry. A half scale model was chosen to accommodate the capacities of the testing equipment available in the laboratory (Figures 5.12 and 5.43).

5.3 Finite Element Analysis

5.3.1 General

Linear-elastic, three-dimensional finite element analyses were conducted to gain insight into the stress distribution prior to cracking and to identify critical regions. Figure 5.12 shows dimensions and loading conditions of the model used in the analysis. This model is based on the structure shown in Figure 5.10. The wing portions of the top flange were clipped to be able to take advantage of symmetry about plane x-x (Figure 5.12). The tendon load used in the analysis of the half-scale model was 188 kips per anchor, corresponding to two 19-½ in. strand tendons, GR 270, in the full scale structure, stressed to $0.8f_{pu}$ with a load factor of 1.2 ($P_u = \frac{1}{4}(1.2)(0.8 \times 270 \text{ ksi})(19 \times 0.153 \text{ in}^2) = 188 \text{ kips}$).

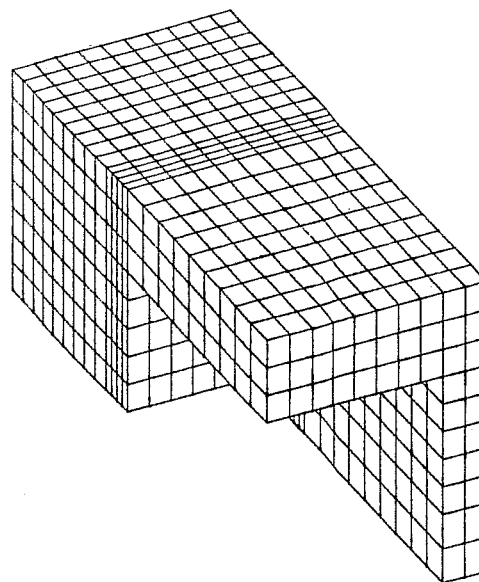


Figure 5.11 Finite Element Mesh

Two cases were investigated. Case A represents a load case where only one side of the diaphragm is loaded (a total of two anchor forces). The flange tips in plane y-y are free surfaces (Figure 5.12). In case B both sides of the diaphragm are loaded (a total of four anchor forces). Both plane x-x and y-y are planes of symmetry.

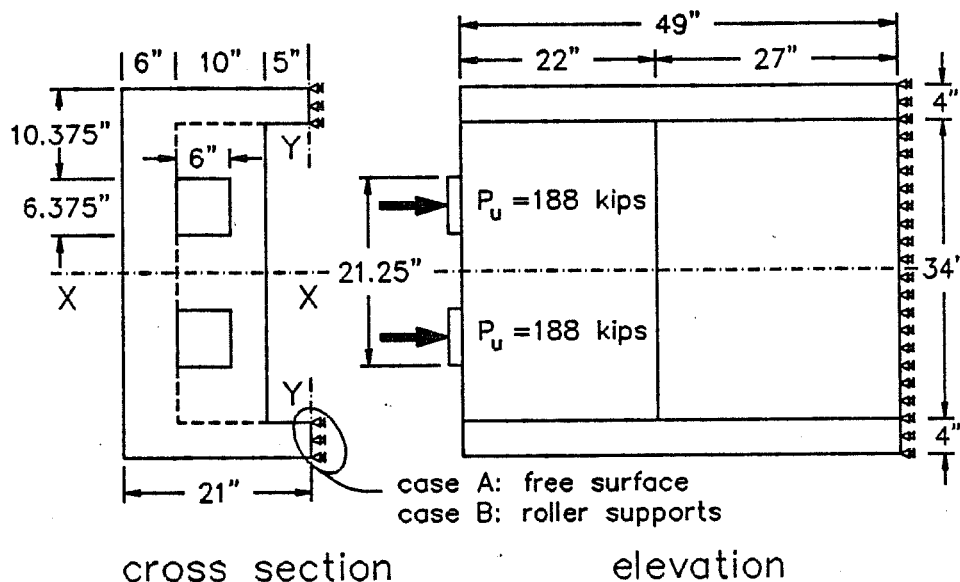


Figure 5.12 Dimensions and Loading of Diaphragm Finite Element Model

Figure 5.11 shows the finite element mesh. Eight-node brick elements were used. The tendon anchorage forces were applied as uniform pressure (4.92 ksi) over the bearing plate areas indicated in Figure 5.12. Poisson's ratio was taken as 0.16.

5.3.2 Analysis Results

Figure 5.13a shows the vertical stresses (perpendicular to plane x-x) in diaphragm and web for case B. Horizontal stresses (perpendicular to plane y-y) in the flanges are shown in Figure 5.13b. The stress distribution in web and flanges is similar to the stress distribution in rectangular, prismatic members under a concentrated axial load (Figure 2.6). Transverse compressive stresses occur immediately ahead of the anchor. At a larger distance, transverse tensile stresses exist which diminish with the distance from the anchor. The stress distribution in the diaphragm region resembles more the stress distribution found in deep beams, with maximum tensile stresses occurring at the end of the diaphragm.

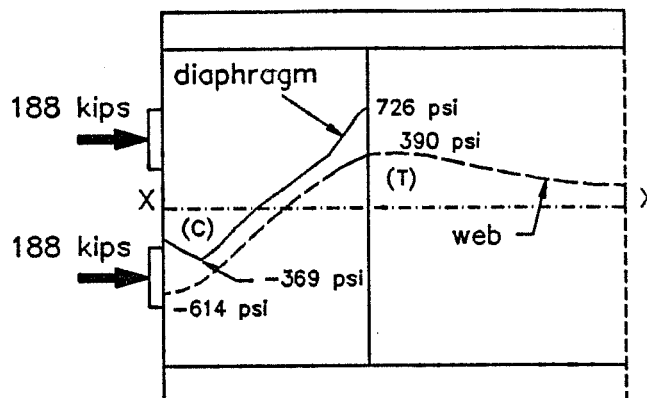
In Figure 5.14 the vertical stresses for case A and case B are compared. The maximum diaphragm bending stress is some 20% higher in case A. The web bursting stresses are virtually identical.

The following figures show stress contours from the analysis of case A. Figure 5.15 shows the principal tensile stresses in plane x-x and further illustrates diaphragm bending stresses and web bursting stresses. The distribution of web bursting stresses is also shown in Figure 5.16, which is a vertical section in the plane of the web of the structure.

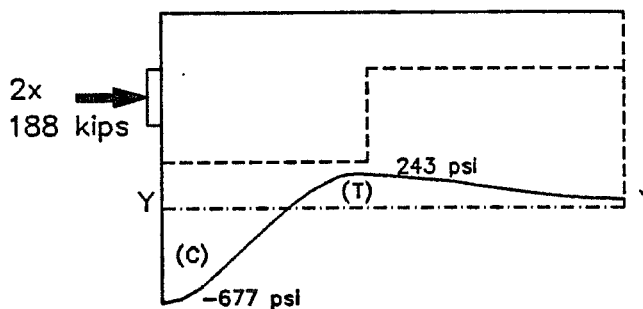
Due to the shear transfer from diaphragm to web large inclined principal tensile stresses occur at their interface. Figure 5.17 shows the corresponding stress contours, plotted in a

vertical section through the diaphragm, parallel to plane y-y. Finally, Figure 5.18 illustrates where critical compressive stresses occur. High compressive stresses are found in the region immediately ahead of the bearing plates. These stresses diminish rapidly as they spread out into the massive diaphragm. A second critical region exists at the end of the diaphragm, where the compressive stresses have to pass through a bottle neck as they enter the thin flanges ahead of the diaphragm section.

In Figure 5.19 location and magnitude of the resultant transverse tensile forces in diaphragm and web are shown for case A. They were obtained by integration of the elastic stresses perpendicular to plane x-x. The total vertical tensile force is 75 kips or 20% of the applied tendon anchorage forces. For case B the total vertical tensile force is about 15% smaller.



a) vertical stresses in diaphragm and web



b) horizontal stresses in flanges

Figure 5.13 Transverse Stresses

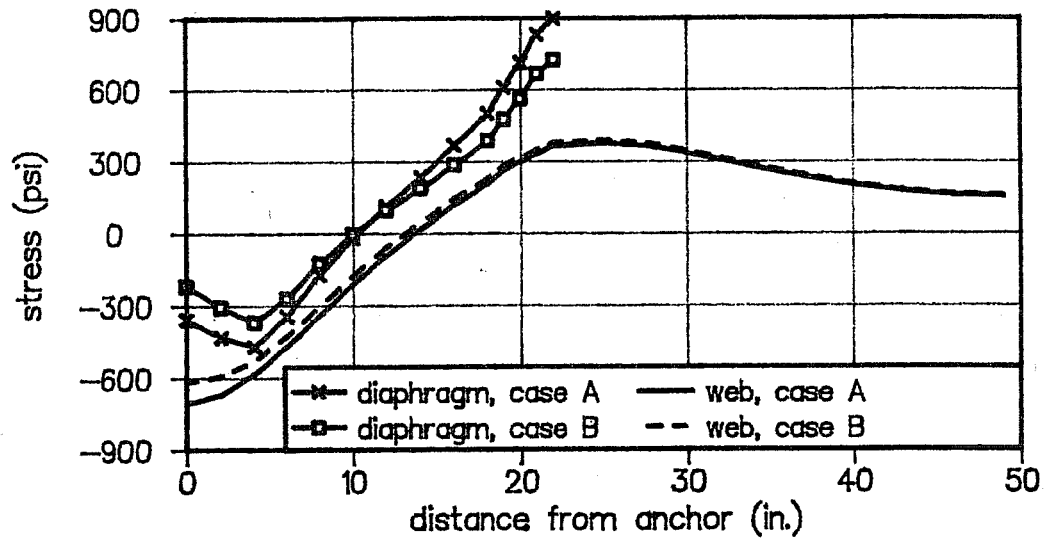


Figure 5.14 Comparison of Vertical Stresses

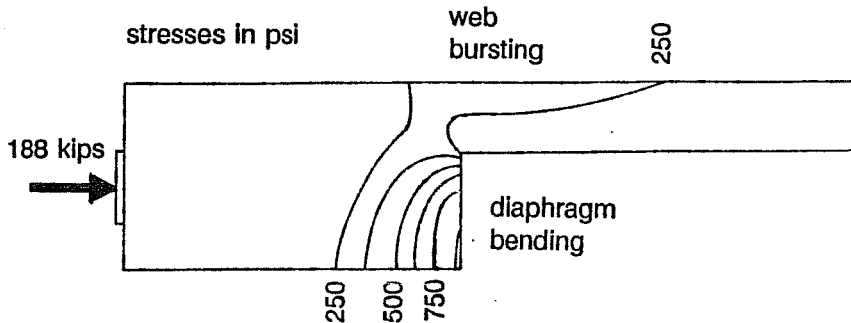


Figure 5.15 Principal Tensile Stresses in Plane X-X

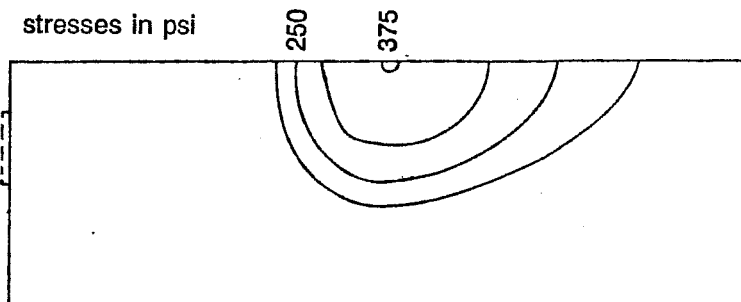


Figure 5.16 Principal Tensile Stresses in Web (Section Parallel to Plane Y-Y)

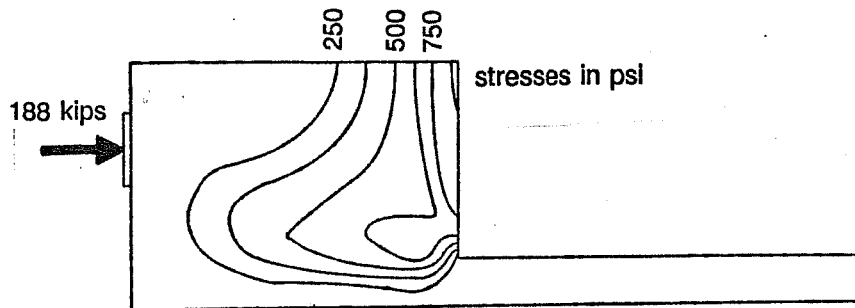


Figure 5.17 Principal Tensile Stresses in Diaphragm (Section Parallel to Plane Y-Y)

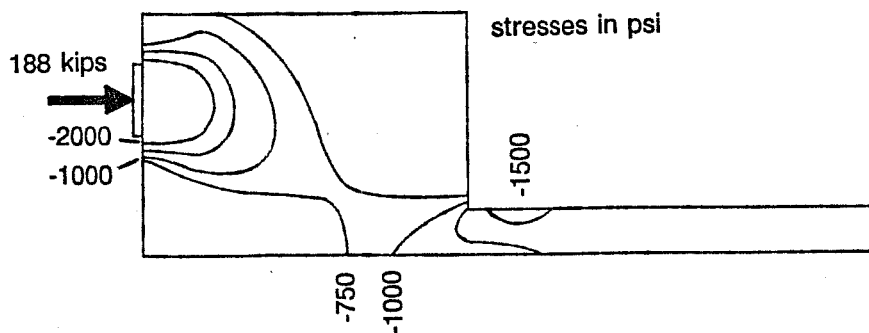


Figure 5.18 Principal Compressive Stresses in Diaphragm (Section Parallel to Plane Y-Y)

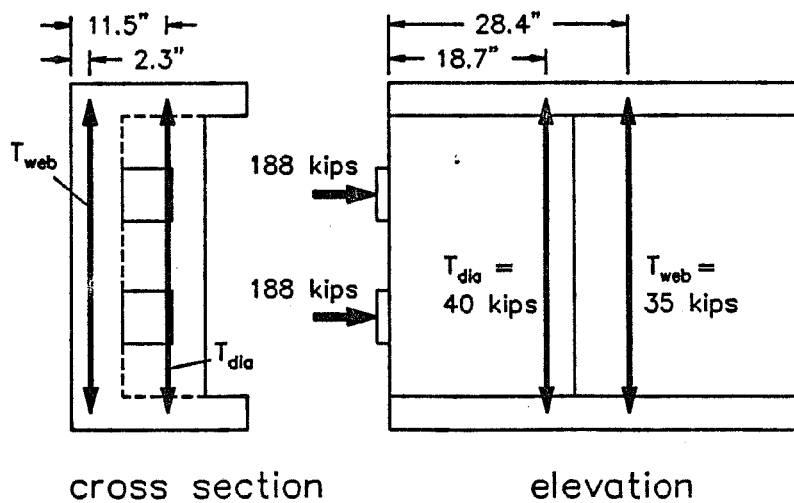


Figure 5.19 Location and Magnitude of Resultant Vertical Tensile Forces

5.3.3 Discussion

Critical regions with high compressive stresses are located immediately ahead of the anchor bearing plates and at the transition from the massive diaphragm section to the thin webs and flanges ahead. Peak tensile stresses occur in the end face of the diaphragm due to deep beam action. Tensile stresses are also critical at the interface between diaphragm and flanges where large shear stresses have to be transferred. Bursting tensile stresses occur in the flanges and webs of the structure. The effect of the different boundary conditions of case A and case B on the vertical tensile stresses is fairly small.

Guyon's solution was developed for prismatic members with rectangular cross section. It gives grossly erroneous results when applied to diaphragms. This is illustrated by the following calculations. Referring to Figure 2.6, dimension a_1 is taken as the distance between outside edges of the bearing plates, that is 21.25 in. (Figure 5.12). a_2 is the height of the cross section, equal to 42 in. Thus the a_1/a_2 ratio is 0.51. The vertical tensile force based on Guyon's solution would be 0.10 P or 37.6 kips (Figure 2.7). This is only half of the vertical tensile force calculated from the finite element analysis. Clearly, Guyon's solution is not valid for this case.

5.4 Development of Strut-and-Tie Models

5.4.1 General

For two-dimensional problems it is relatively easy to guess the flow of forces and to develop strut-and-tie models accordingly. Simple three-dimensional problems can be treated by considering a sufficient number of two-dimensional sub models. However, the complex geometry of the diaphragm problem requires a spatial strut-and-tie model solution. This introduces considerable complexity and makes it more difficult to find a solution that matches the finite element results closely. On the other hand, the strut-and-tie model procedure is much more convenient for the design of the reinforcement since the forces in the tension members can be translated directly into reinforcement requirements.

In the following sections load paths for the transfer of anchor loads from a diaphragm into webs and flanges of the continuing section are discussed and illustrated by strut-and-tie models. These load paths are referred to as tripod model, corbel action, and frame action. Subsequent sections discuss some details required for the development and refinement of these strut-and-tie models. Finally a complete example is presented in detail.

5.4.2 The Tripod Model

Figure 5.20 shows a load path where the anchorage force P is resisted by three inclined struts. This model is similar to the model shown in Figure 5.5, but also includes the transfer of forces from the diaphragm into the web. Deep beam action generates the tensile force T_1 . Additional tensile forces (T_2, T_3) are required across the flange-web corners for

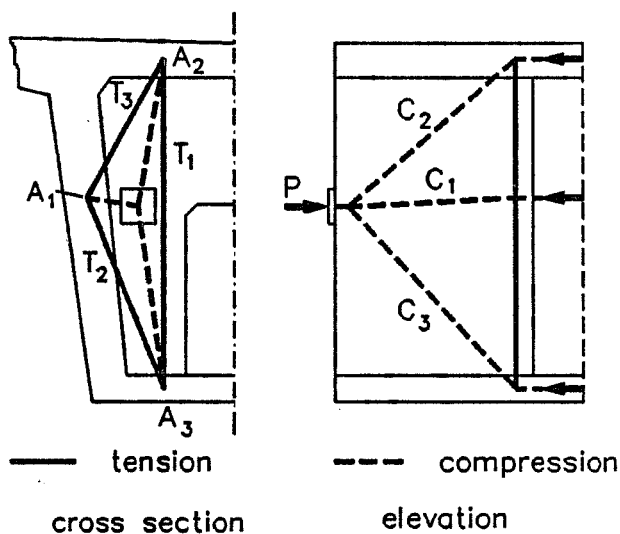


Figure 5.20 Tripod Model

equilibrium. A slightly more refined strut-and-tie model is necessary to capture the bursting force in the web (Figure 5.21).

It should be noted that anchorage of tensile force T_1 requires nodes in the flanges of the cross section (nodes A_2 and A_3 in Figure 5.20). Hence, reinforcement provided to resist this tensile force must tie into the flanges. This is frequently overlooked, particularly when transverse post-tensioning is applied (Figure 5.10). The result is comparable to a deep beam with the flexural reinforcement not anchored into the supports. Fortunately, significant concrete tensile strength contribution is available in these massive diaphragms, which often alleviates the problem.

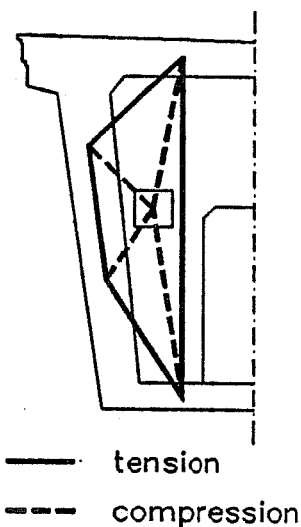


Fig. 5.21 Refined Model

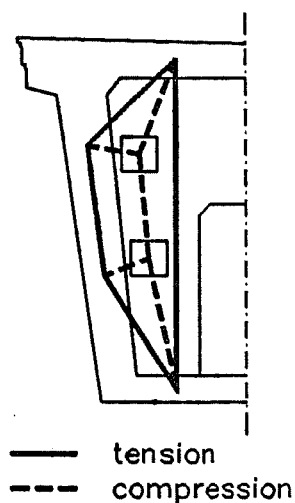


Figure 5.22 Multiple Anchors

If several anchor forces act on the diaphragm, either individual tripod models can be superimposed or an overall strut-and-tie model can be developed (Figure 5.22). In the latter case for computer analysis it is necessary to add a sufficient number of members to make the model statically determinate. Usually several iterations are required before a satisfactory strut-and-tie model is found.

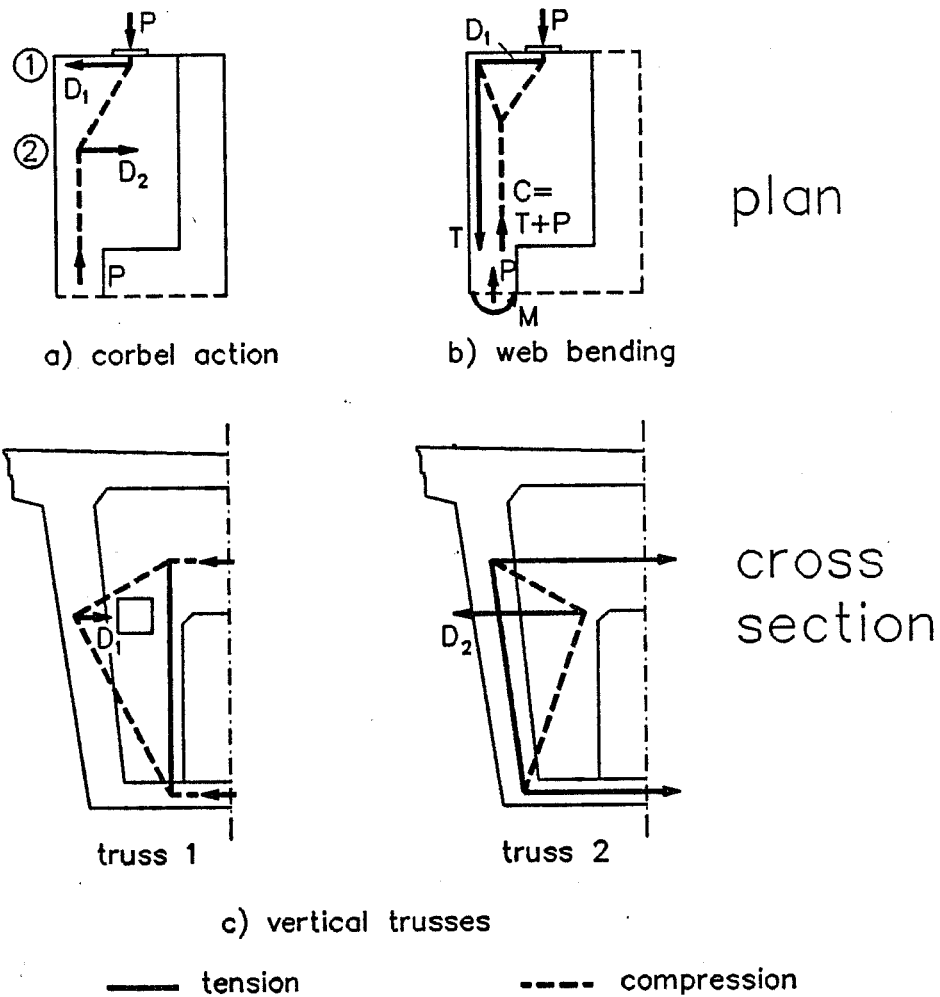


Figure 5.23 Corbel Action

5.4.3 Corbel Action

In Figure 5.6 the transfer of the anchor force from the diaphragm into the web is patterned after the flow of forces in a corbel. However, the load path shown in the figure must be completed to satisfy equilibrium conditions (Figure 5.23a). The tripod model discussed in Section 5.4.2 does not capture corbel action.

In columns the effect of a corbel is to introduce a bending moment into the column, as shown in Figure 5.23b. The corresponding effect in a diaphragm section is bending of the web in its thin direction. This bending moment is subsequently transferred to the flanges. An alternative and more efficient load path is shown in Figure 5.23c. The deviation forces D_1 and D_2 at levels 1 and 2 in Figure 5.23a are transferred by vertical trusses to the flanges (truss 1 at level 1, truss 2 at level 2). This load path does not require bending of the web.

5.4.4 Frame Action

The frame action load path is very similar to the tripod model (Figure 5.20). However, rather than providing ties between the base nodes (ties T_1 , T_2 , and T_3 in Figure 5.20), the transverse components of forces C_1 , C_2 , and C_3 are resisted by frame action of the flanges and webs ahead of the diaphragm (Figure 5.24). Obviously this load path is not very stiff compared to the other load

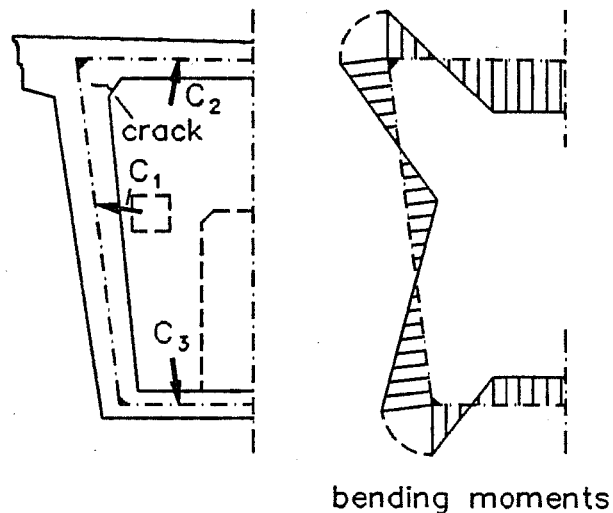


Figure 5.24 Frame Action

paths available, and only a small portion of the transverse tensile forces will be carried by frame action. However, it does explain cracks along the flange-web intersection ahead of the diaphragm which were observed in the structures discussed in Reference 26 and in the test specimens of this study.

5.4.5 Extent of the D-Region

The extent of the D-region can be taken as approximately equal to the largest cross-sectional dimension ahead of the end of the diaphragm [45]. Within the D-region the axial-flexural stress distribution is disturbed by the introduction of the concentrated tendon force and by the geometric discontinuities at the transition from diaphragm to continuous section. At the end of this region ordinary axial-flexural beam analysis can be used to establish boundary conditions for the development of a strut-and-tie model for the flow of forces within the D-region.

Unfortunately, these boundary conditions are not very helpful for the models discussed in the preceding sections where boundary conditions immediately ahead of the diaphragm are needed to establish the locations of nodes A_1 , A_2 , and A_3 (Figure 5.20). Simple beam theory is not valid at this location. Some guidance can be obtained from the following considerations. Spreading of the forces in flanges and web can only occur after these forces have actually reached flanges and web. Prior to this spreading only the portion of the cross section immediately adjacent to the diaphragm is effective in resisting the anchorage force (hatched area in Figure 5.25). A stress distribution based on simple beam theory for this effective cross section may be used as guidance to find the location of points A_1 , A_2 , and A_3 . Alternatively, the results of a finite element analysis or engineering judgement may be used to establish the location of tie force T_1 .

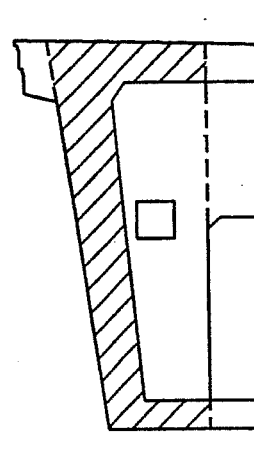


Fig. 5.25 Effective Cross Section Ahead of Diaphragm

The stress distribution at the end of the D-region will usually be different from the stress distribution immediately ahead of the diaphragm. Additional strut-and-tie models should be developed to track the flow of forces in the region between end face of diaphragm and end of anchorage zone as well.

5.4.6 The Local Zone Node

The massive diaphragm provides substantial confinement for the local zone and consequently the anchor bearing capacity is much increased. Equation (2.2) may be

applied, and frequently no local confinement reinforcement will be necessary. It should not be overlooked that this and similar equations were developed for blocks supported over their full bottom face, while the diaphragm has to span from flange to flange of the cross section. Therefore a limit should be placed on the

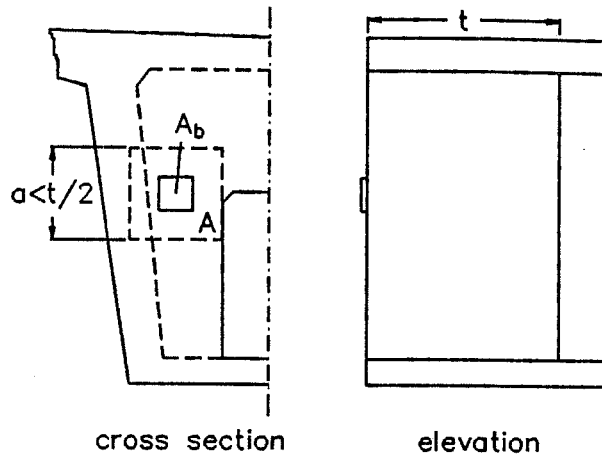


Figure 5.26 Bearing Strength

maximum dimensions of the supporting area A. Based on judgement and without the benefit of experimental data, it is suggested to limit these dimensions to half of the thickness of the diaphragm (Figure 5.26).

For the development of strut-and-tie models, the distance to the center of the local zone nodes from the bearing plates must be known. This distance depends on the state of stress at the node. In Chapter 2 procedures for checking two-dimensional local zone nodes were discussed. In plane problems the nodes are triangles with a biaxial state of stress. In the three-dimensional case the nodes are tetrahedra with a triaxial state of stress. Check of stresses at such nodes is extremely cumbersome and a simpler procedure is needed.

One method is to consider only the components of the forces joining at the local zone node which are parallel to the loaded face. Two checks in orthogonal directions parallel to the sides of the anchor bearing plate are required. The width of the strut is equal to the corresponding width of the bearing plate and the depth

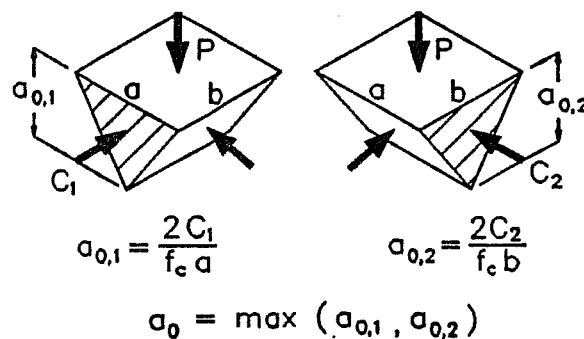


Figure 5.27 Location of Local Zone Nodes

of the local zone is determined by the strut force and the concrete strength (Figure 5.27). Note that no increase of the effective concrete strength due to confining concrete is available, since struts running along a free surface are considered. In the commentary to the proposed anchorage zone specifications a more pragmatic approach is taken by placing the local zone nodes at a distance equal to one fourth of the plate width ahead of the anchor plate, independent of the state of stress at the node (Appendix B, Section C.9.21.4.2).

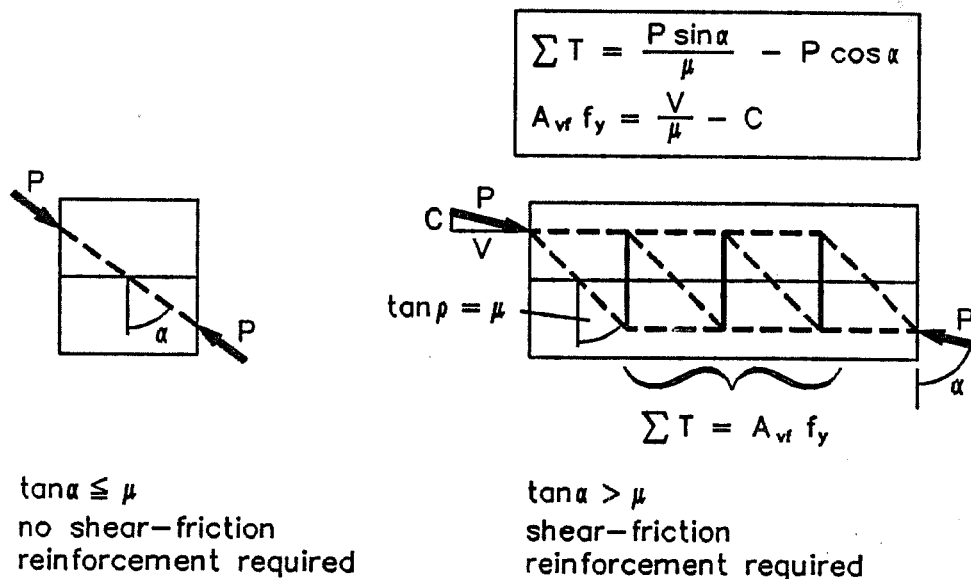


Figure 5.28 Shear-Friction

5.4.7 Shear-Friction

The finite element analysis indicates that large inclined tensile stresses exist at the interface of diaphragm and flanges due to shear transfer (Figure 5.17) and transfer of forces in shear-friction between diaphragm and adjacent web and flanges is a concern (Figure 5.8). In the development of strut-and-tie models shear-friction requirements can be considered by limiting the angle α between compression struts and the direction normal to the critical section for shear-friction (Figure 5.28). AASHTO provides values for the coefficient of friction, μ [1]. μ is equal to 1.4 for monolithically placed, normal-strength concrete. If $\tan \alpha$ is larger than μ shear-friction reinforcement is required. Figure 5.28 shows

a strut-and-tie model that satisfies shear-friction requirements and gives results identical to the code provisions.

5.4.8 Skew Reinforcement

A reinforcement arrangement following the tensile forces T_2 and T_3 of the tripod model (Figure 5.20) would require inclined reinforcement across the flange-web corners. However, usually a grid of horizontal reinforcement and of reinforcement parallel to the web is preferred. Figure 5.29 shows how a single tie can be replaced by a system of orthogonal

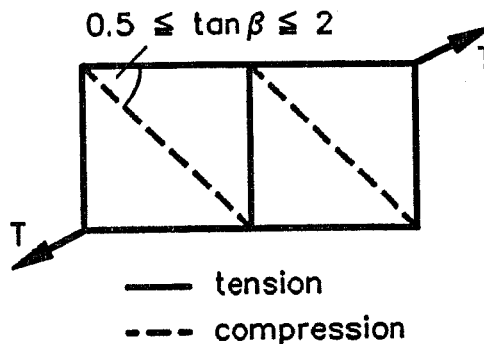


Figure 5.29 Skew Reinforcement

struts and ties. The angle between struts and ties should not be less than 25 to 30 degrees ($\tan \beta > 0.5$).

5.4.9 Example

A numerical example will be given in this section to illustrate the previously discussed concepts. The example illustrates the design of the specimens used in the experimental portion of this study (Figure 5.43). The conditions in an actual structure will be somewhat different, but the basic principles remain the same. A concrete strength of 5000 psi and a design load of 188 kips per anchor will be used in the following calculations. The ϕ -factor is taken as 1.0 for laboratory conditions. The geometry of the structure is shown in Figure 5.30.

1. Determine the stress distribution at the base of the specimen.

The stresses at the base of the specimen can be calculated using simple beam theory (Figure 5.31a). Location and magnitude of the resultant forces are obtained by integrating this stress distribution over the respective areas (Figure 5.31b).

2. Check the local zone node.

The net bearing plate area is

$$7 \times 7 - (2.5^2 \pi) / 4 = 44.1 \text{ in}^2.$$

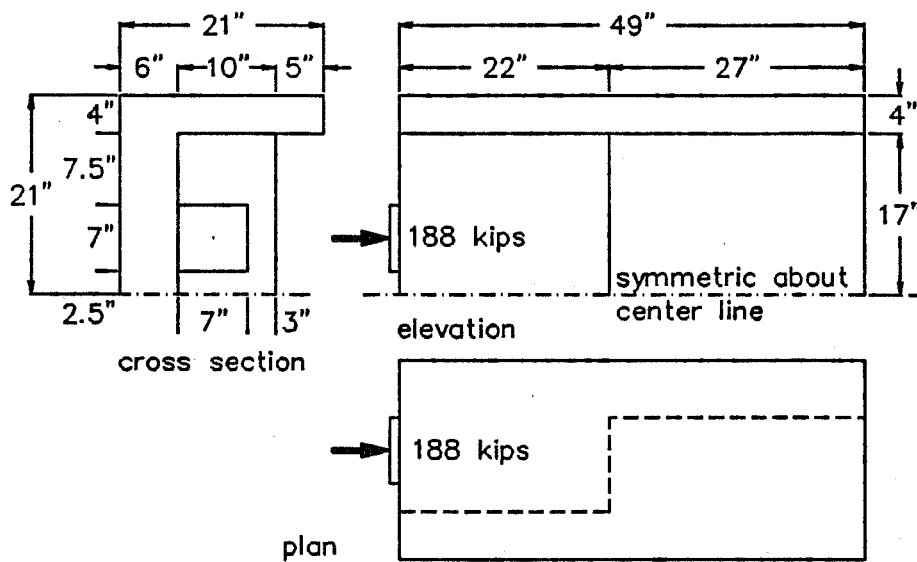


Figure 5.30 Diaphragm Design Example

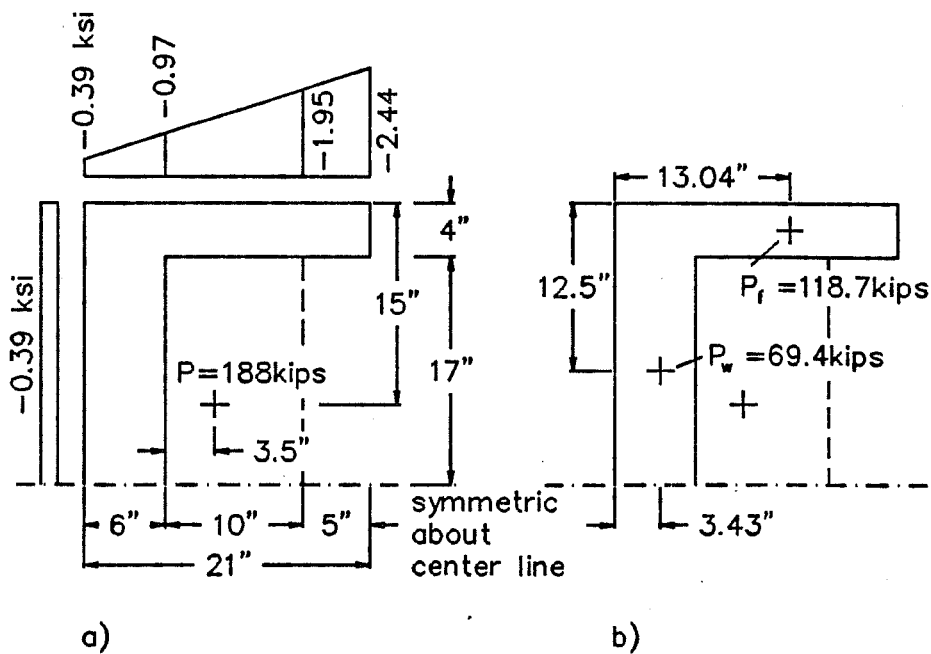


Figure 5.31 Stress Distribution at Base of Specimen

Hence the bearing pressure is

$$f_b = 188/44.1 = 4.26 \text{ ksi.}$$

Using Equation (9-39) from the proposed code specifications (Appendix A, Section 9.21.7.2) the effective bearing strength is (Figure 5.32)

$$0.7f_c \sqrt{A/A_g} = 0.7 \times 5 \times (11/7) = 5.5 \text{ ksi} > 4.26 \text{ ksi.} \therefore \text{OK.}$$

This is larger than the bearing pressure. The surrounding concrete provides sufficient confinement and no additional confinement reinforcement is needed in the local zone. Note that the dimensions of the supporting area A in Figure 5.32 are limited by the recommendations of Section 5.4.6 to restrict these dimensions to half the thickness of the diaphragm.

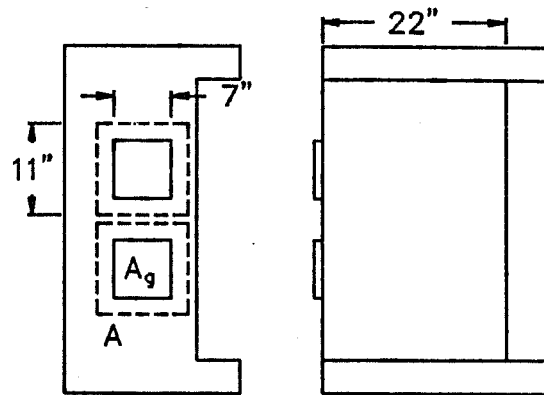


Figure 5.32 Check of Bearing Strength

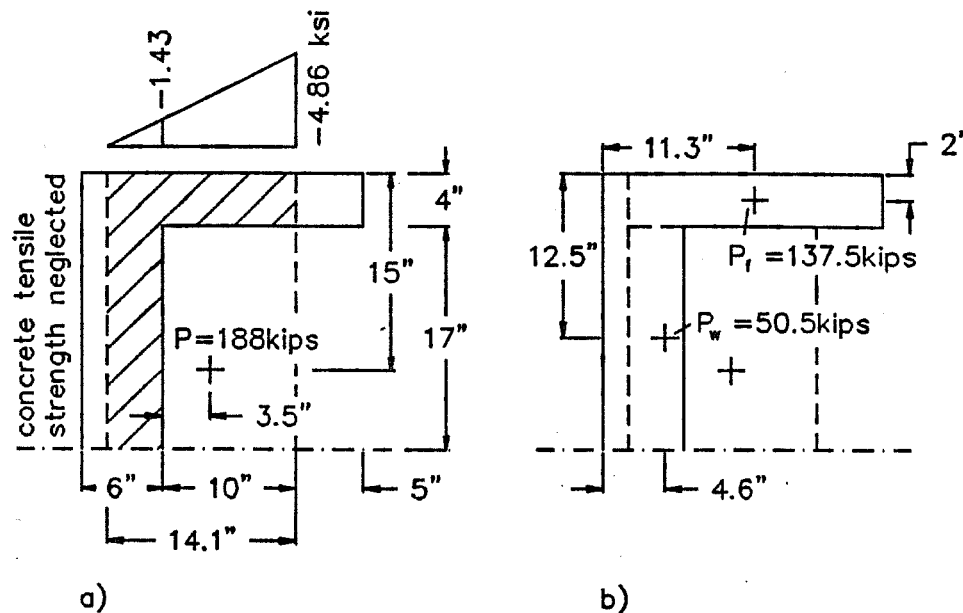


Figure 5.33 Resultant Forces Immediately Ahead of Diaphragm

3. Estimate the location of the resultant web and flange forces immediately ahead of the diaphragm.

As discussed in Section 5.4.5, an effective cross section outside the diaphragm region ignoring the flange tips will be used to estimate the location and magnitude of the resultant forces immediately ahead of the diaphragm. In Figure 5.33 a linear elastic stress distribution was assumed and the tensile strength of the concrete was neglected. Basically, any stress distribution that satisfies equilibrium conditions and material strength limitations is acceptable. Note that this stress distribution is used only to establish magnitude and location of the resultant forces. The check of stresses is discussed in Step 6.

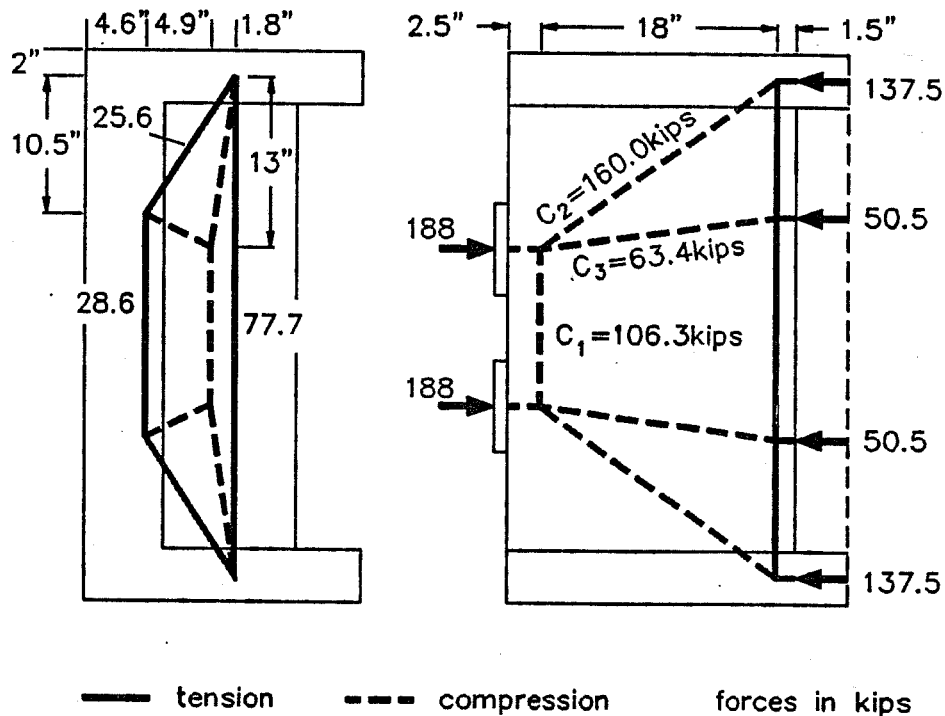


Figure 5.34 Basic Strut-and-Tie Model

4. Draw the basic strut-and-tie model and determine the critical member forces.

Figure 5.34 shows a basic model for the flow of forces from the diaphragm to the adjacent web and flanges. The location of the nodes at the end of the diaphragm section is based on the results found in Step 3. The depth of the center of the local zone nodes is

controlled by the required strut dimensions to accommodate force C_1 . Following the discussions in Section 5.4.6, the cross section of strut C_1 is assumed to be triangular with a base length equal to the plate width (7 in.). The effective concrete strength at this CCC node is taken as $0.85f'_c$, that is $0.85 \times 5 = 4.25$ ksi. The required strut area is

$$106.3/4.25 = 25.0 \text{ in}^2, \text{ hence}$$

$$a_o = 2 \times 25.0/7 = 7.14 \text{ in.}$$

The distance to the centroid of this triangle is $a_o/3 = 2.4$ in., which is less than the 2.5 in. assumed in the model shown in Figure 5.34, therefore the assumption is safe.

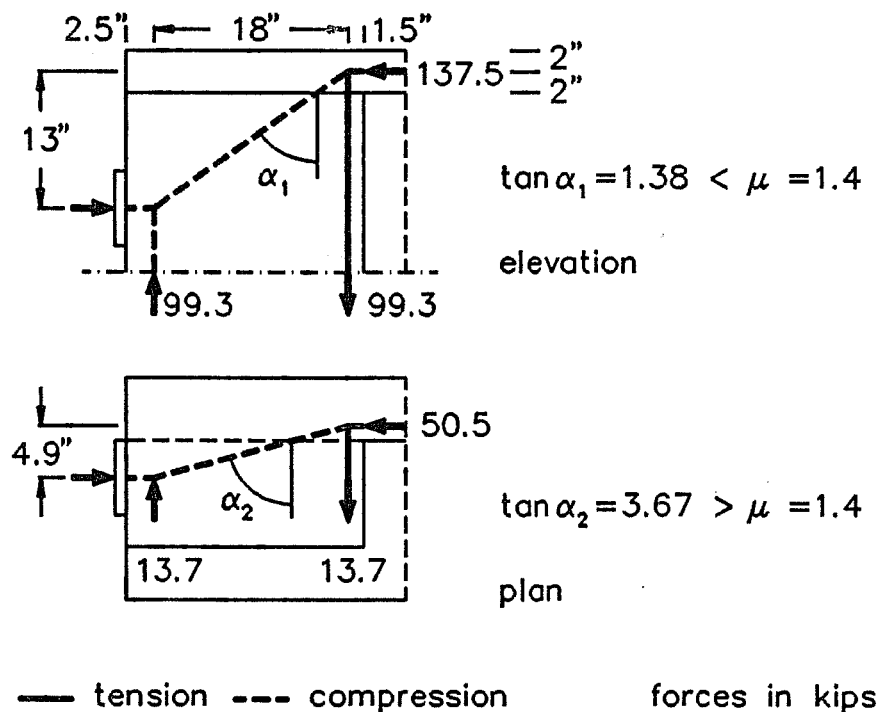


Figure 5.35 Shear-Friction Reinforcement Requirements

5. Design the shear-friction reinforcement.

Shear-friction reinforcement requirements between diaphragm and web and diaphragm and flanges should be checked. Figure 5.35 shows the angles included by the struts and the direction perpendicular to the corresponding critical sections. Shear-friction reinforcement is required if $\tan \alpha$ is larger than μ (Section 5.4.7). For monolithic, normal-strength concrete μ equal to 1.4 is used. As seen in Figure 5.35, shear-friction

reinforcement is required only for the transfer of shear forces to the web. The reinforcement requirement per anchor is:

$$A_{vf}f_y = P_w/\mu - C_2 = 50.5/1.4 - 13.7 = 22.4 \text{ kips.}$$

6. Check the compressive stresses at the end of the diaphragm.

The compressive stresses are also critical where the massive diaphragm section ends and all forces have to be carried by the thin flanges and web of the continuing section. Figure 5.36 illustrates the concrete area available for the struts at the end of the diaphragm. The area available for the strut in the web is

$2 \times 1.4'' \times 17'' = 47.6 \text{ in}^2$, and hence the compressive stress is

$$50.5/47.6 = 1.1 \text{ ksi.}$$

An effective concrete strength of $f_c = 0.70 f'_c$ will be used in the following calculations, as suggested in the proposed anchorage zone specifications (Appendix A). This value is also close to the recommendation for CTC nodes in 2D problems (Section 3.4.6).

$$f_c = 0.70f'_c = 0.70 \times 5 = 3.5 \text{ ksi} > 1.1 \text{ ksi} \therefore \text{web OK.}$$

The area available for the struts in the flanges (Figure 5.36) is

$$2 \times 4.7'' \times 4'' = 37.6 \text{ in}^2, \text{ hence the corresponding stress is}$$

$$137.5/37.6 = 3.65 \text{ ksi} > 3.5 \text{ ksi} \therefore \text{flange N.G.}$$

The calculated flange stresses are larger than the effective concrete strength. However, these stresses can be reduced if the compression struts from the anchor to the flanges are split as shown in Figure 5.37. This requires additional reinforcement (strut confinement reinforcement), but increases the capacity of the flanges in compression. The flange forces are now carried by two inclined struts, C_1 and C_2 (Figure 5.37). The area available for strut C_2 is still 37.6 in^2 , hence the corresponding stress is

$$99.3/37.6 = 2.6 \text{ ksi.}$$

However, the stresses introduced by strut C_1 must be added. These stresses are largest immediately at the location where strut C_1 enters the flange:

$$38.2/37.6 = 1.0 \text{ ksi.}$$

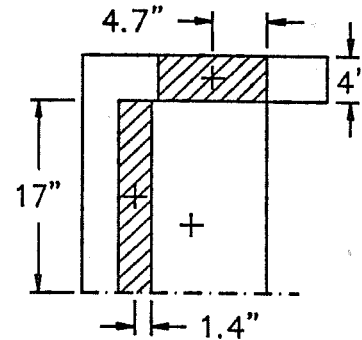


Figure 5.36 Concrete Area Available for Struts

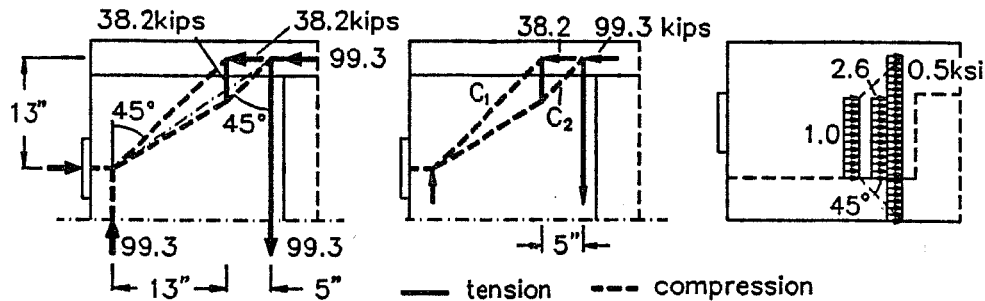


Figure 5.37 Check of Compression Stresses for Flange Struts

Assuming a 45 degree spreading angle, these stresses are reduced by half at the critical section where strut C_2 enters the flange (Figure 5.37). Superposition of all stresses at this section gives

$$2.6 + 0.5 = 3.1 \text{ ksi} < 0.70 f'_c = 3.5 \text{ ksi} \therefore \text{flange OK.}$$

7. Replace the inclined ties by orthogonal reinforcement.

Figure 5.38 shows how the inclined tie forces across the flange-web corners can be replaced by orthogonal reinforcement.

8. Trace the flow of forces from the end of the diaphragm to the base of the specimen.

Magnitude and location of the resultant forces immediately ahead of the diaphragm are different from those at the base of the specimen. Therefore

redirection of compressive forces and associated transverse compressive and tensile forces will occur in the region between the end of the diaphragm and the base of the specimen. In Figure 5.39 this flow of forces is modelled.

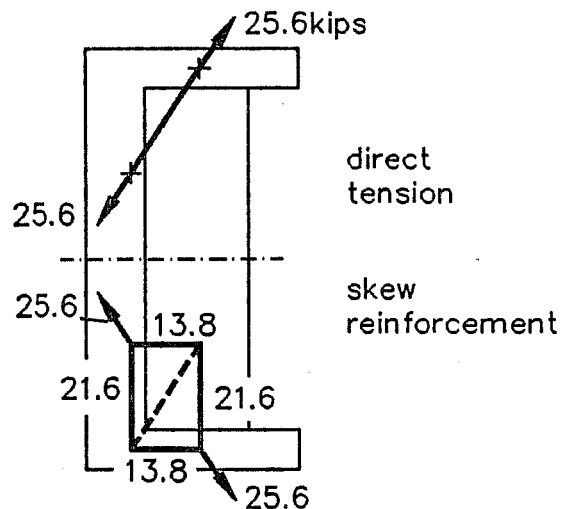


Figure 5.38 Skew Reinforcement

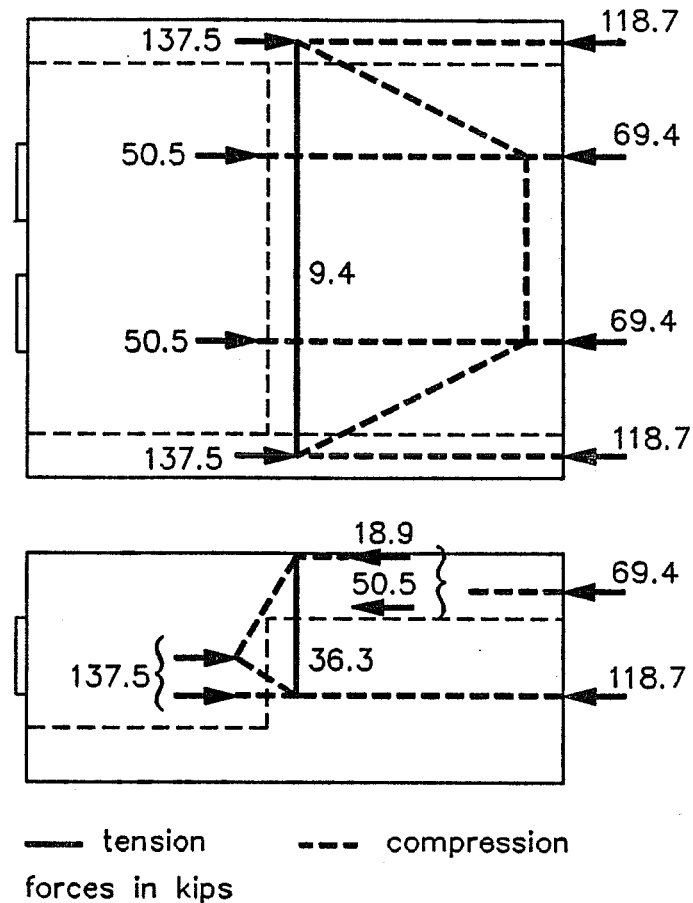


Figure 5.39 Load Path Ahead of Diaphragm

9. Summary of the primary reinforcement requirements.

Figure 5.40 and Table 5.1 summarize the reinforcement tensile force requirements determined above. Most of the reinforcement is concentrated at the end face of the diaphragm. The tensile force from diaphragm bending is quite large. Vertical post-tensioning would be effective to reduce congestion in this area.

10. Supplementary reinforcement requirements.

In addition to the primary reinforcement shown in Figure 5.40 supplementary reinforcement should be provided for serviceability. For instance, frame action and corbel action were ignored in the example because these load paths are inefficient in this case and require large reinforcement quantities. Figure 5.41 shows where nominal supplementary reinforcement should be provided to control cracking at unstressed corners, at the web-

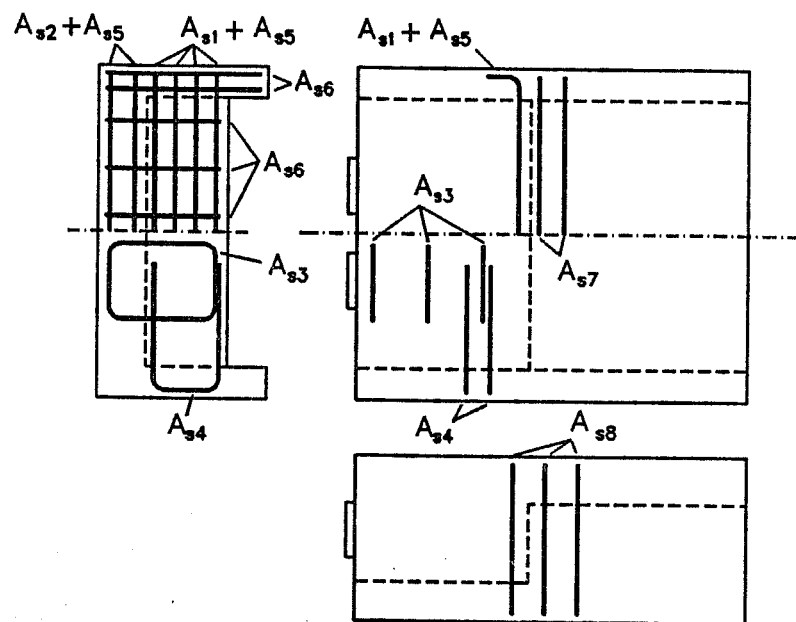


Figure 5.40 Primary Reinforcement Requirements

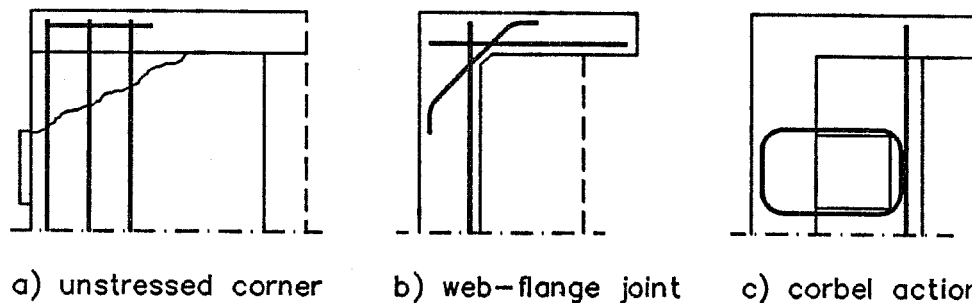


Figure 5.41 Supplementary Reinforcement Requirements

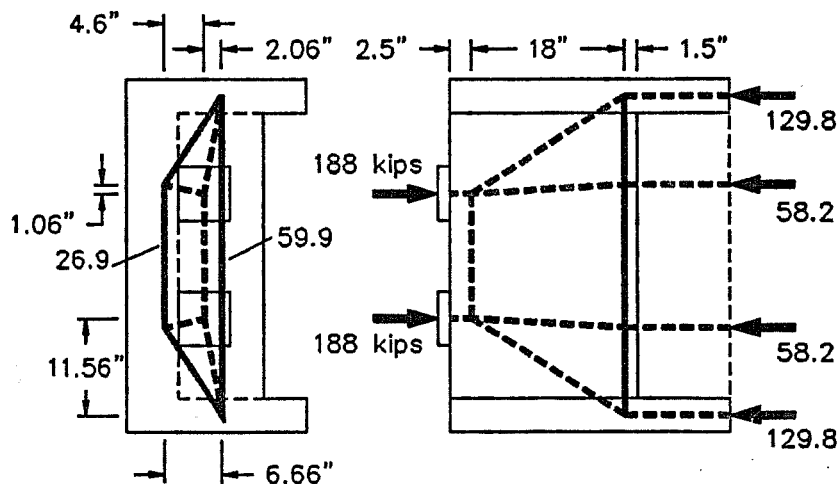
flange joint ahead of the diaphragm due to frame action, and at the loaded face due to corbel action.

5.4.10 Discussion

The example and the previous discussions clearly illustrate the complexity of three-dimensional strut-and-tie models. Development of such models requires excellent ability to envision spatial relationships. On the other hand, three dimensional strut-and-tie models offer a relatively quick method to approximate global load paths in the structure and to

Table 5.1 Reinforcement Requirements for Example Problem

reinf.	description	force (kips)
A_{s1}	diaphragm bending (Step 4, Figure 5.34)	77.7
A_{s2}	web bursting (Step 4, Figure 5.34)	28.6
A_{s3}	shear friction/web (Step 5, Figure 5.35)	44.8
A_{s4}	strut confinement (Step 5, Figure 5.37)	38.2
A_{s5}	orthogonal grid for inclined tensile forces (Step 7, Figure 5.37)	21.6
A_{s6}		13.8
A_{s7}	spreading of forces ahead of diaphragm (Step 8, Figure 5.39)	9.4
A_{s8}		36.3

**Figure 5.42 Strut-and-Tie Model for Comparison With Finite Element Analysis**

determine reinforcement requirements. Practically, a strut-and-tie model approach in conjunction with a finite element analysis to indicate possible areas where service load cracking needs controlling is probably the most viable technique for the design of such complex regions of a structure.

Table 5.2 Magnitude and Location of Vertical Tensile Forces in Diaphragm and Web

force (kips)	finite element solution	strut-and-tie model solution
diaphragm	40.0	59.4
web	35.0	26.7
total	75.0	86.1
distance from anchor (in.)	finite element solution	strut-and-tie model solution
diaphragm	18.7	20.5
web	28.4	20.5

Figure 5.42 shows a strut and-tie model for comparison with the finite element solution of Section 5.3. Linear-elastic finite element analysis results and strut-and-tie model results for the vertical tensile forces in web and diaphragm are listed in Table 5.2. The total tensile force compares very favorably, with the strut-and-tie model solution being about 15% higher. The location and distribution of web and diaphragm forces is somewhat different. Closer agreement could be achieved by refining the strut and tie model and by adjusting its geometry. However, this would be at the expense of the simplicity of the model and is not necessary for practical purposes.

5.5 Experimental Program

5.5.1 General

Three half-scale specimens modelling a diaphragm for the anchorage of external tendons in a box girder bridge were tested. Figure 5.43 shows the geometry of these specimens. The specimens were oriented such that the tendon forces could be applied as vertical loads. Table 5.3 lists the concrete cylinder compressive strengths at time of testing. Specimen Dia3 was added because of the excessively high concrete strength of

Table 5.3 Concrete Strengths for Diaphragm Specimens

specimen	f'_{cl} (psi)
Dia1	5900
Dia2	8100
Dia3	5200

testing. Specimen Dia3 was added because of the excessively high concrete strength of

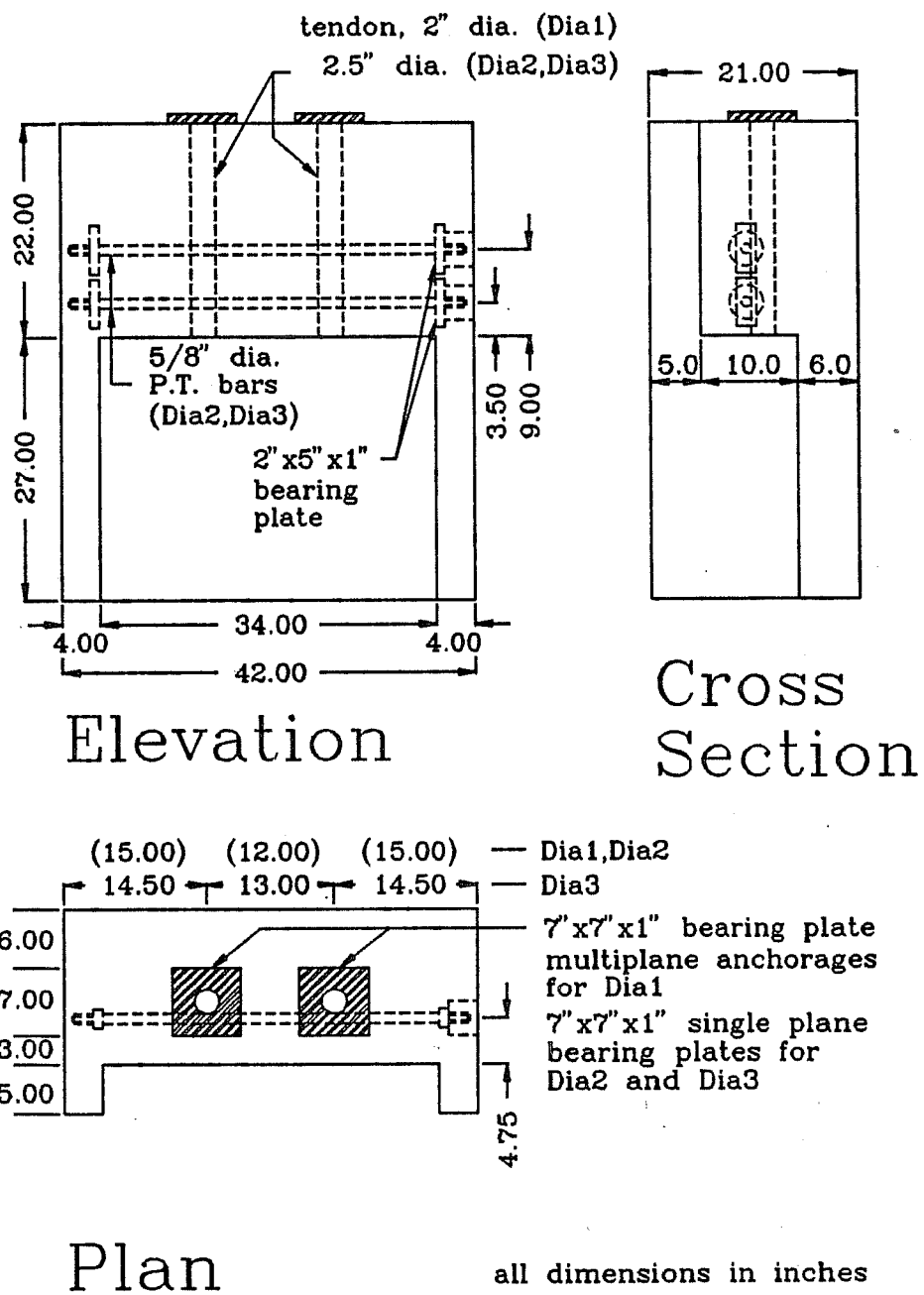


Figure 5.43 Geometry of Diaphragm Specimens

specimen Dia2. Reinforcement sizes #3 and larger were standard ASTM A615 GR60 steel with yield strengths between 60 and 66 ksi. Bars referred to as #2 bars are actually 6mm Swedish reinforcement bars with a yield strength of 72 ksi and a yield strain of 0.0025.

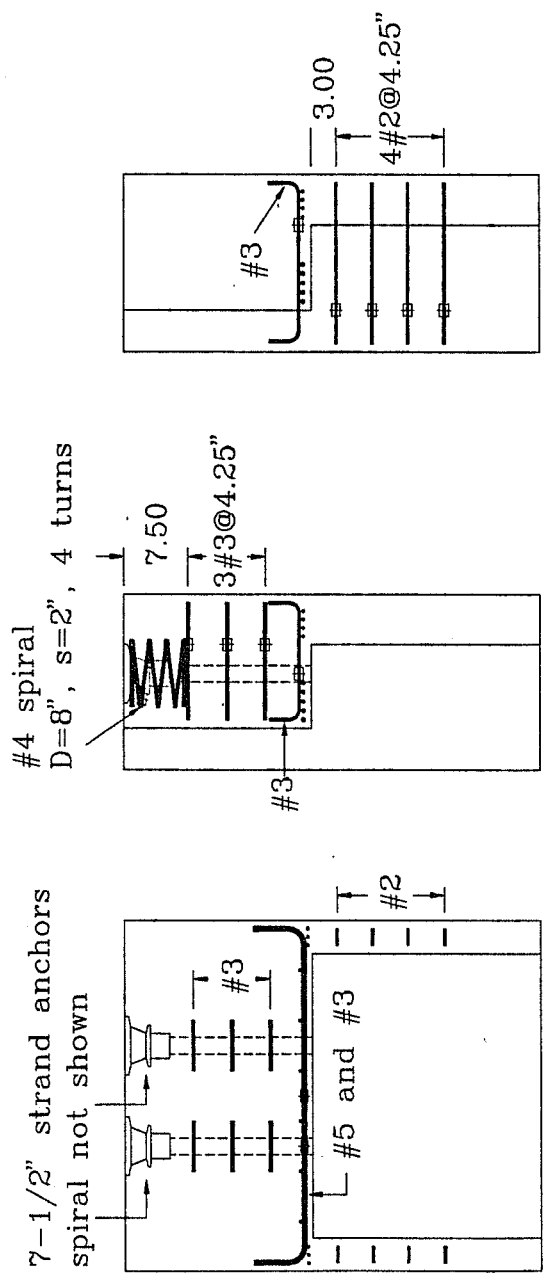
5.5.2 Specimen Design

Specimens Dia1 and Dia2 were designed for two loads of 188 kips each, representing half-scale models of two 19-½ in. strand tendons stressed to $0.8 f_{pu}$ with a load factor of 1.2 ($P_u = \frac{1}{4}(1.2)(0.8 \times 270 \text{ ksi})(19 \times 0.153 \text{ in}^2) = 188 \text{ kips}$). The design load for specimen Dia3 was increased to 2 x 215 kips after the previous diaphragm specimens exhibited considerable capacity beyond their design load due to the tensile strength of the concrete.

Design of all specimens was based on the procedures outlined in Section 5.4. Specimen Dia1 had heavy mild steel diaphragm bending and web bursting reinforcement concentrated at the end face of the diaphragm (5#5 and 4#3 bars)(Figure 5.44). Additional reinforcement was provided for flange bursting ahead of the diaphragm (4#2 stirrups) and for shear-friction between diaphragm and web (6#3 ties).

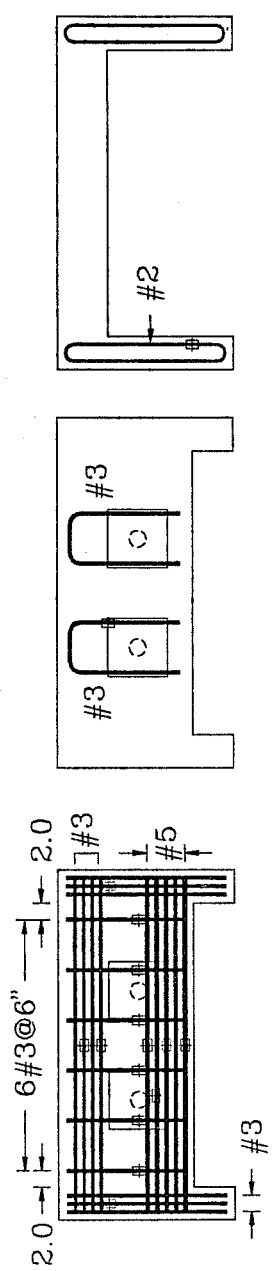
Commercially available 7-½ in. strand tendon anchor heads with confining spiral reinforcement as shown in Figure 5.44 were used in specimen Dia1. The spiral was eliminated and single plane bearing plates with the same outer dimensions were used in the subsequent tests.

In specimens Dia2 and Dia3 a combination of post-tensioned and mild steel reinforcement was provided to resist the diaphragm and web bursting forces (Figures 5.43, 5.45, and 5.46). Two unbonded 5/8 in. dia. threaded post-tensioning bars, GR 150, stressed to 105 ksi ($0.7 f_{pu}$) were used to apply a transverse prestressing force of 30.5 kips per bar. The additional stress developed in these bars under loading was taken as 15 ksi according to Section 9.21.3.2.1 in the proposed anchorage zone specifications (Appendix A). Mild reinforcement accounted for roughly 50% of the required diaphragm bending and web bursting force in both cases. This reinforcement was 4#4 and 4#3 in specimen Dia2 and 3#5 and 1#4 in specimen Dia3. In specimen Dia2 it was arranged so that its centroid coincided with the centroid of the prestressed reinforcement. In specimen Dia3 it was concentrated close to the end face of the diaphragm. Arrangement and detailing of the transverse post-tensioning bars were patterned after the prototype structure shown in



Elevation

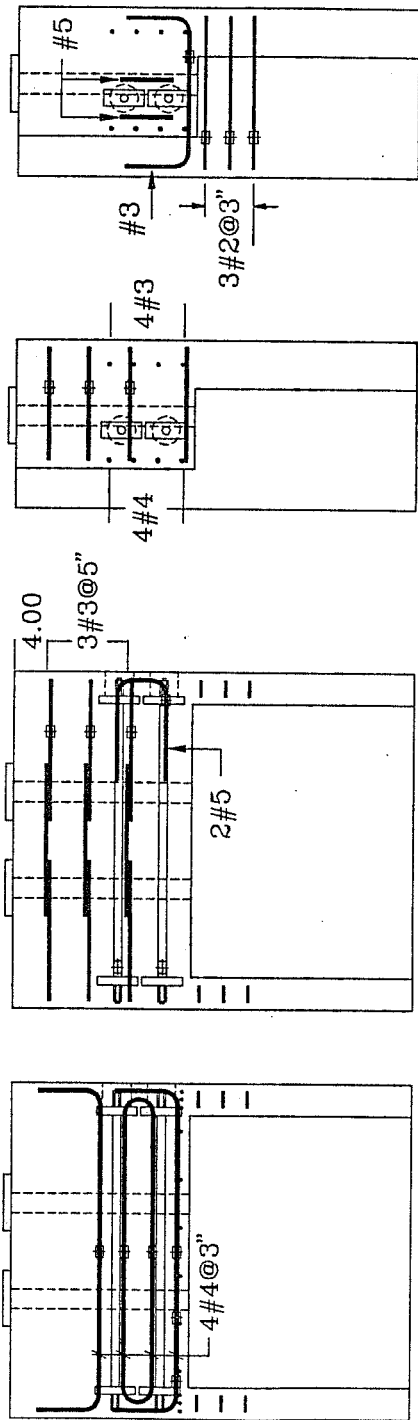
Cross Section



Plan

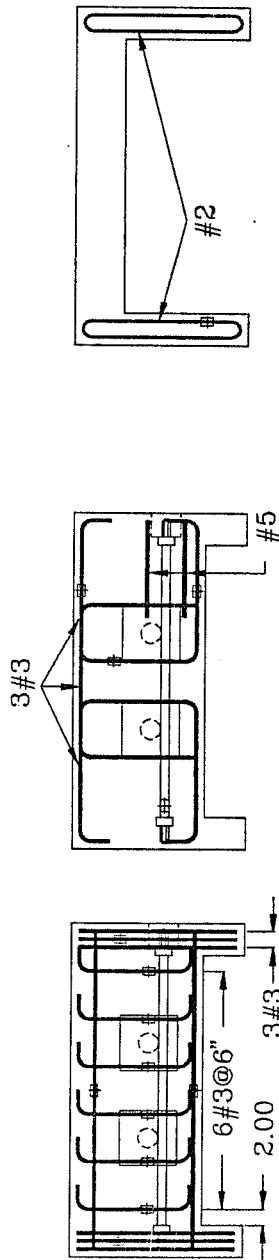
⊕ strain gages all dimensions in inches

Figure 5.44 Details for Specimen Dia1



Elevation

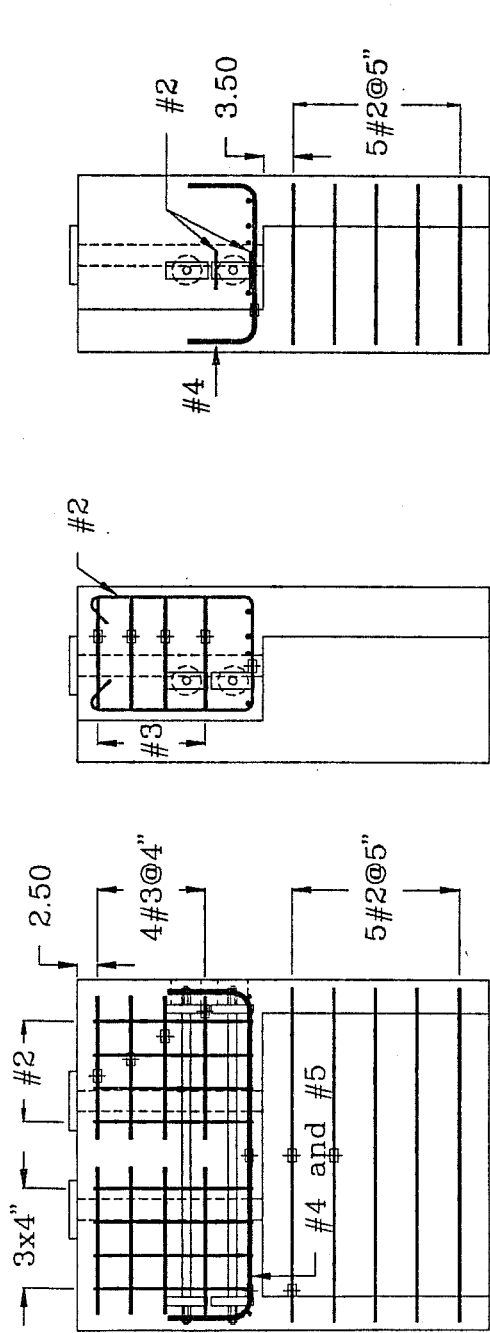
Cross Section



Plan

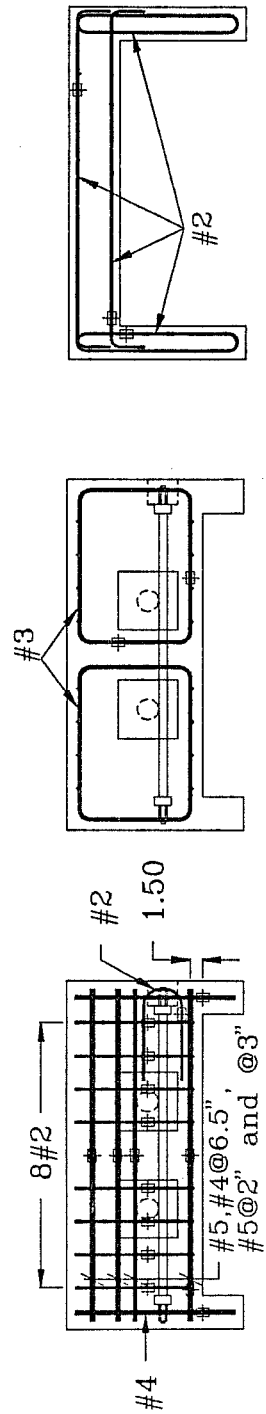
all dimensions in inches # strain gages

Figure 5.45 Details for Specimen Dia2



Elevation

Cross Section



Plan

strain gages all dimensions in inches

Figure 5.46 Details for Specimen Dia3

Figure 5.10. In particular, these bars were anchored before tying into the flanges. This is a commonly used detail but should be very detrimental to the behavior of diaphragms, if the concrete tensile strength is neglected. Reinforcement to tie the transverse post-tensioning force back into the flanges was provided only on one side of the specimens (2#5 U-ties in specimen Dia2, 2#2 U-ties in specimen Dia3).

Wide inclined cracks running from the anchor plates to the flanges were observed in the test of specimen Dia1 (cracks (1) in Figure 5.50). In specimens Dia2 and Dia3 "strut bursting reinforcement" was provided to control these cracks. In specimen Dia2 it consisted of 3#3 U-ties placed parallel to the loaded face of the diaphragm (Figure 5.45). Design was based on a strut-and-tie model in which the inclined compression struts from the anchor plates to the flanges were divided into two sub-struts. In specimen Dia3 design of the strut bursting reinforcement followed the provisions of ACI 318-89 [3] for the design of shear reinforcement in deep beams. A grid of ties parallel (2x4#3) and perpendicular to the loaded face (8#2) was provided.

Flange bursting and shear-friction reinforcement in specimens Dia2 and Dia3 were similar to the details used in specimen Dia1. Specimen Dia2 completely collapsed at failure. Light web and flange reinforcement (5#2) was added ahead of the diaphragm in specimen Dia3 to avoid a similar collapse.

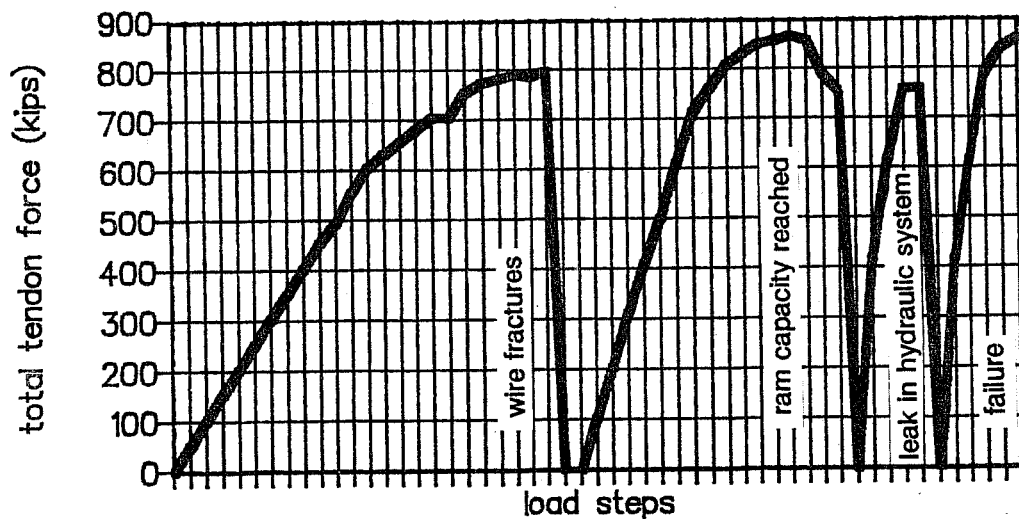


Figure 5.47 Load History for Specimen Dia2

5.5.3 Test Procedure and Measurements

All specimens were oriented such that the tendon forces could be applied vertically. Specimen Dia1 was loaded through a 600 kip testing machine. Problems with this machine limited the highest test load to 563 kips without achieving total failure of the specimen. However, the degrading stiffness of the load-displacement curve suggested that failure was imminent and 563 kips is used as failure load for the comparisons in the following sections. The specimen subsequently did resist ten load cycles to approximately 425 kips before finally failing at a load of 385 kips. Specimens Dia2 and Dia3 were loaded through oversize

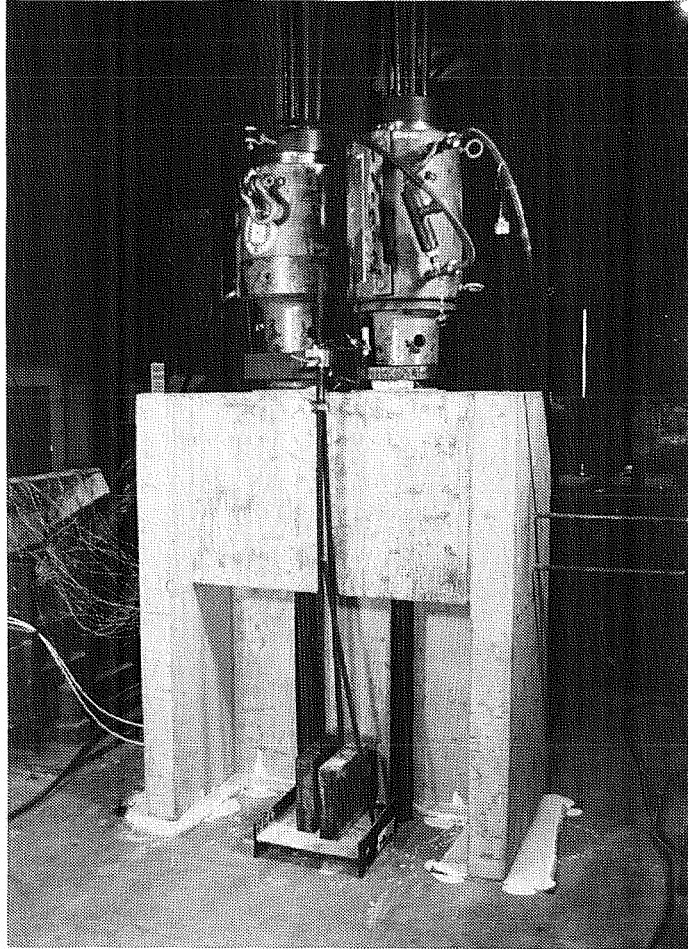


Figure 5.48 Diaphragm Specimen Ready for Testing

tendons (Figure 5.48 and 5.49). Specimen Dia3 failed under monotonic loading. Due to load system problems specimen Dia2 had to be unloaded three times before reaching its peak load and failure during the fourth load cycle (Figure 5.47).

Reinforcement strains were measured with electronic resistance strain gages. Their location is indicated in Figures 5.44 through 5.46. Additional measurements included concrete surface strains using electronic resistance strain gages and DEMEC locator disks, and horizontal and vertical anchor plate displacements using potentiometers.

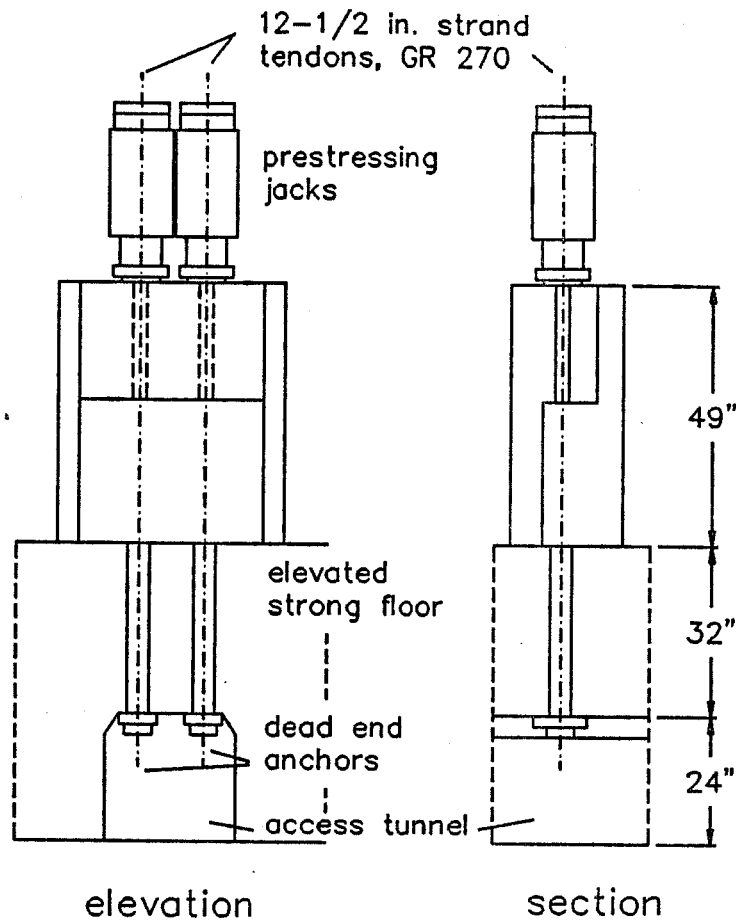


Figure 5.49 Test Set-Up for Diaphragm Specimens

5.6 Presentation of Test Results

5.6.1 General

The general behavior of all specimens was very similar, except that the various phenomena in specimen Dia2, which had much higher concrete strength, occurred at proportionally higher loads. Table 5.4 gives an overview of first cracking, first yield, and ultimate loads. These loads are expressed in terms of the breaking strength, F_{pu} , of the nominal tendons to be anchored in the structure.

Table 5.4 First Cracking, First Yield, and Ultimate Loads for Diaphragm Specimens

specimen	F_{pu} (kips)	P_{crack}/F_{pu}^*	P_{yield}/F_{pu}	P_{test}/F_{pu}
Dia1	2 x 196	0.73 (1) 0.89 (2,3,4,5) 1.28 (6)	1.38 ³ 1.44 ⁴	> 1.44
Dia2	2 x 196	1.03 (2,3) 1.16 (1,5) 1.26 (3,4) 1.42 (6)	1.98 ² 2.04 ¹	2.20
Dia3	2 x 215	0.66 (2) 0.71 (1) 0.95 (5) 1.04 (3,4) 1.14 (6)	1.14 ² 1.28 ¹ 1.43 ³	1.43

*) numbers in parentheses correspond to cracks as labeled in Figure 5.49

¹) diaphragm bending reinforcement

²) strut confinement reinforcement

³) flange bursting reinforcement

⁴) shear-friction reinforcement between diaphragm and web

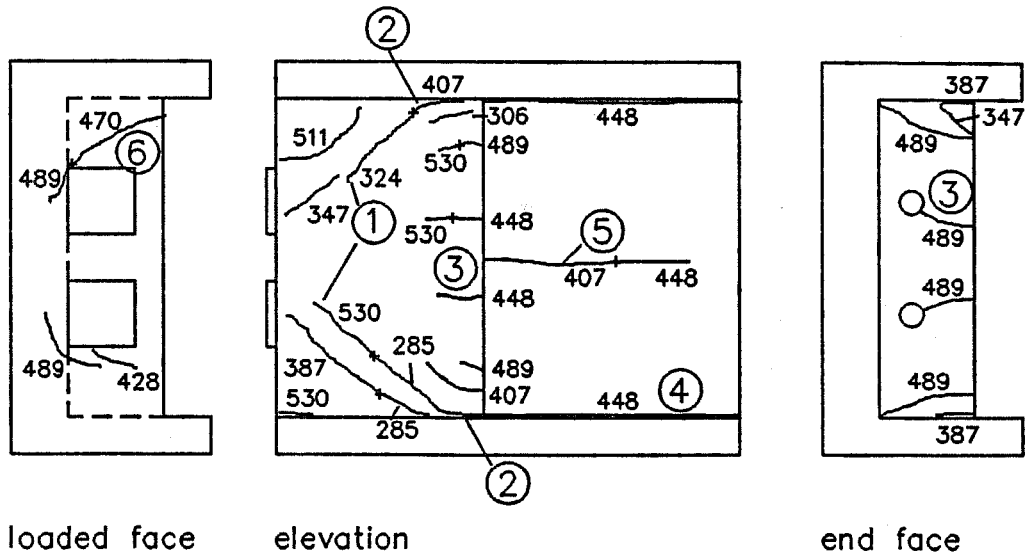


Figure 5.50 Typical Crack Pattern in Diaphragm Specimens (Dia3)

5.6.2 Crack Development

Figure 5.50 shows the typical crack pattern for the diaphragm specimens. The small numbers next to the cracks indicate the sum of both tendon forces when the crack was first noted. Cracks at the diaphragm-flange interface (cracks (2) in Figure 5.50) and diagonal cracks progressing towards the bearing plates (cracks (1) in Figure 5.50) occurred first in all tests. Subsequent cracks included web-flange junction cracks (4) ahead of the diaphragm, diaphragm bending cracks (3), web bursting cracks (5), and corbel action cracks in the loaded face (6). Table 5.4 lists the relative loads at which these cracks occurred.

Cracks (1) became very large with approaching failure. At about 90% of the failure load their width was about 0.06 in. for specimen Dia1 and approximately 0.02 in. for specimens Dia2 and Dia3 where crack controlling reinforcement was present. At design load crack widths were 0.02 in. for specimen Dia1 and 0.009 in. for specimen Dia3. Specimen Dia2 was uncracked at its design load. Figure 5.51 shows the crack width development for specimen Dia2. The numbers in parentheses in the legend correspond to the crack labels in Figure 5.50.

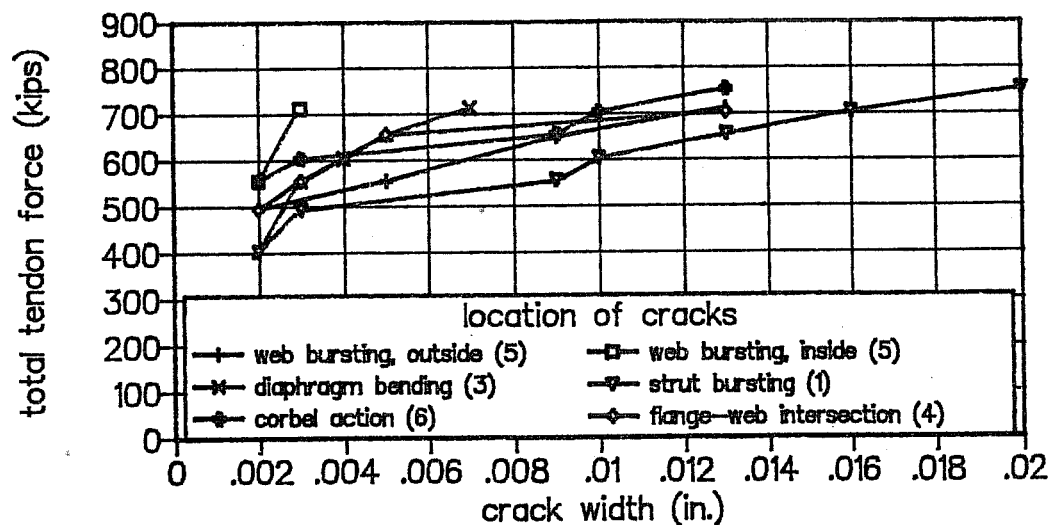


Figure 5.51 Crack Width Development for Specimen Dia2

5.6.3 Ultimate Loads and Failure Mode

All specimens exceeded their factored design load substantially (Table 5.4). The failure mode was characterized by the formation of a wedge bounded by cracks (1), (2), and (6) in Figure 5.50 (Figures 5.52, 5.53, and 5.60). Final failure of specimens Dia1 and Dia2 was induced by crushing of the inclined compression struts from the anchor plates to the flanges and of the flanges immediately ahead of the diaphragm (Figure 5.54). Figure 5.55 shows specimen Dia1 after removal of loose or crushed concrete. The large inclined gaps are due to removal of essentially sound pieces of concrete which were bounded by initially separate cracks that joined deeper inside the diaphragm. The large blocks above the wide gaps are unstressed corners and could be removed easily after completion of the test, revealing a crack between diaphragm and web over the full height of the diaphragm (Figure 5.57). Crushing on the inside of the web ahead of the diaphragm (Figure 5.54) and wide cracking on the other side (Figure 5.56) indicated substantial rotation of the failure wedge about its support along the web.

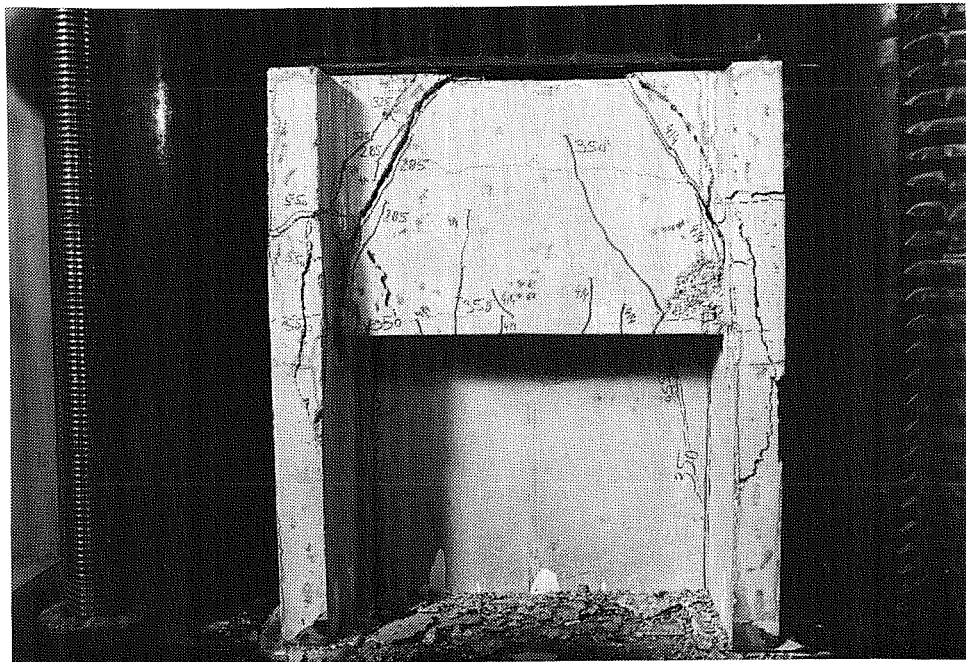


Figure 5.52 Specimen Dia1 After Failure

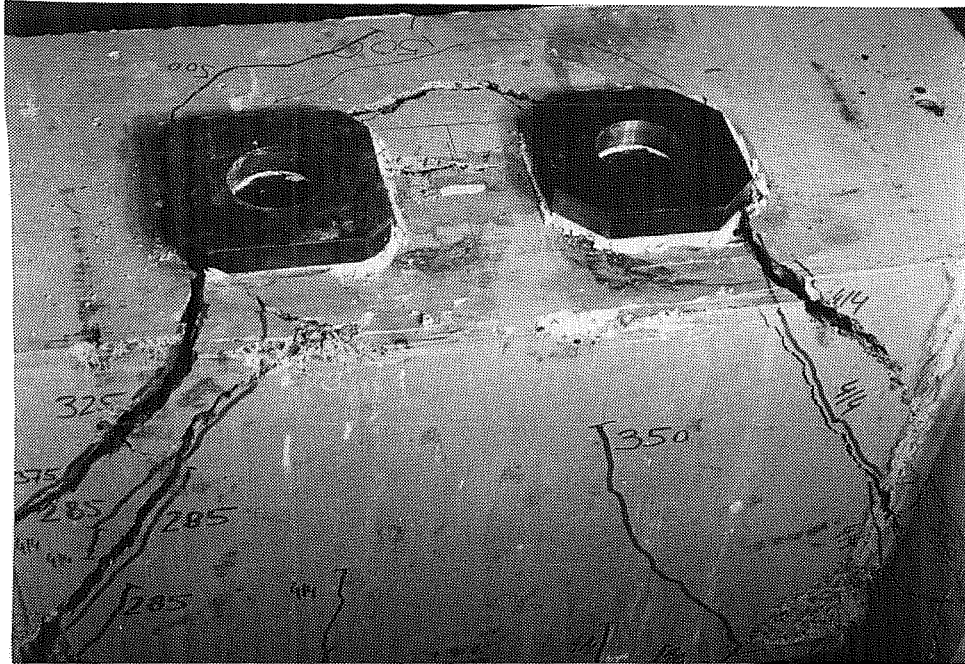


Figure 5.53 Failure Wedge in Specimen Dia1

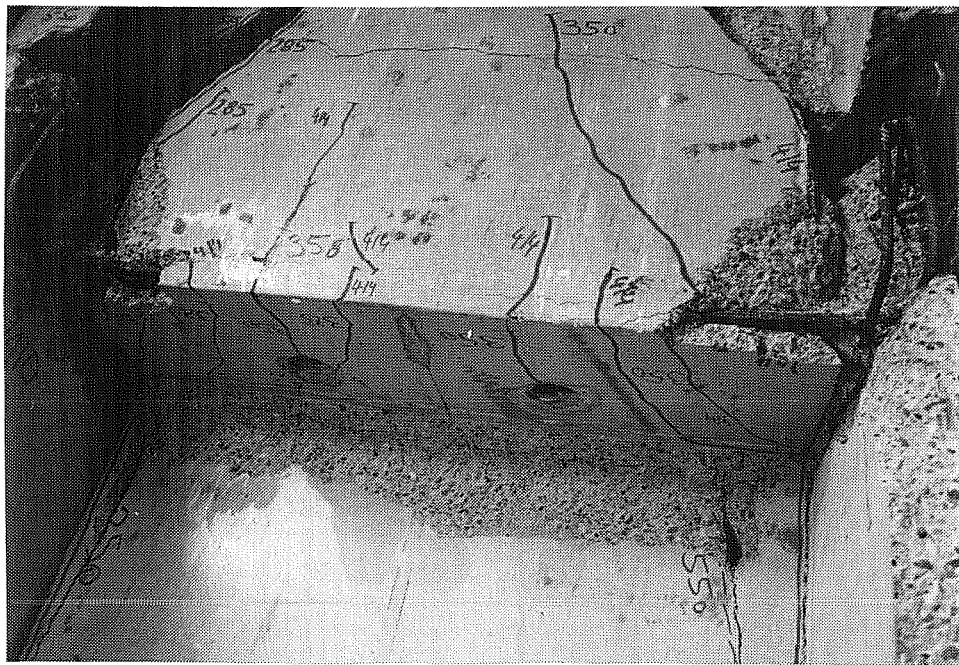


Figure 5.54 Crushing of Inclined Compression Struts and Flanges (Specimen Dia1)

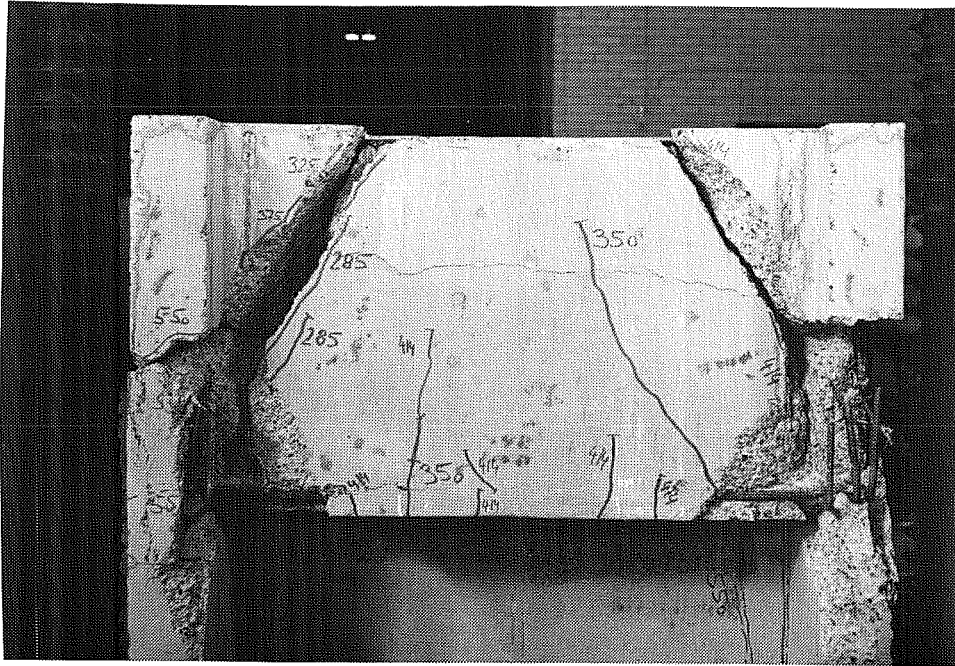


Figure 5.55 Specimen Dia1 After Removal of Loose Concrete

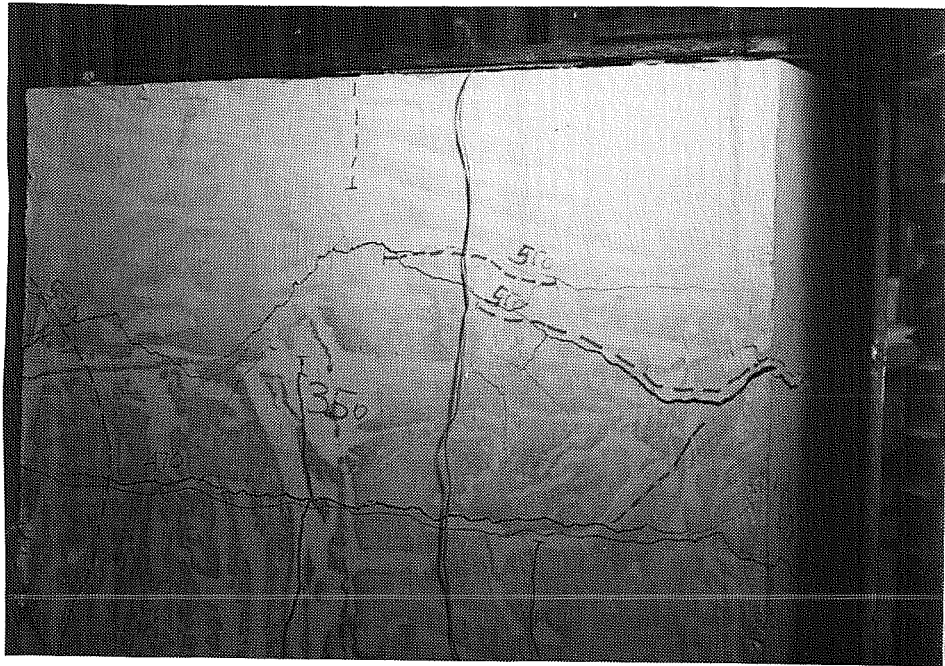


Figure 5.56 Cracking of Web Ahead of Diaphragm

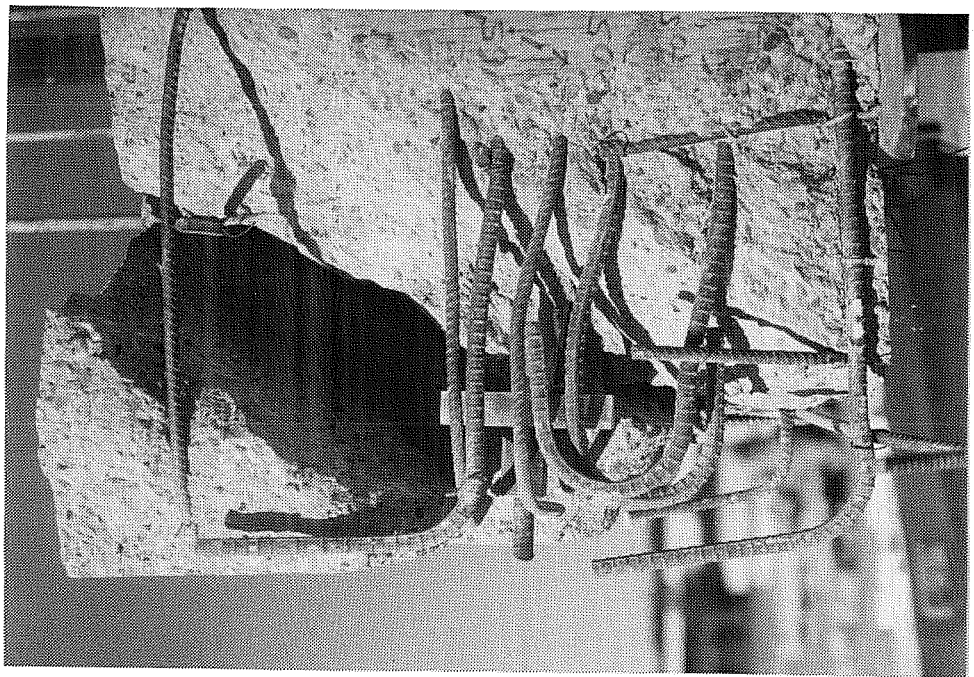


Figure 5.58 Distorted Reinforcement (Specimen Dia2)

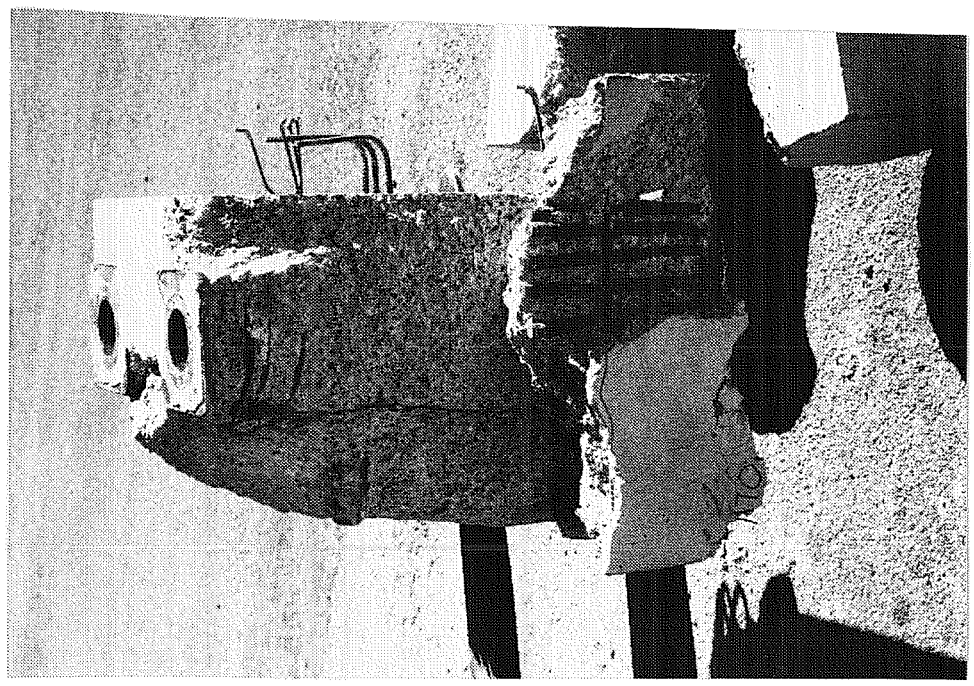


Figure 5.57 Cracking at Diaphragm-Web Interface (Specimen Dia1)

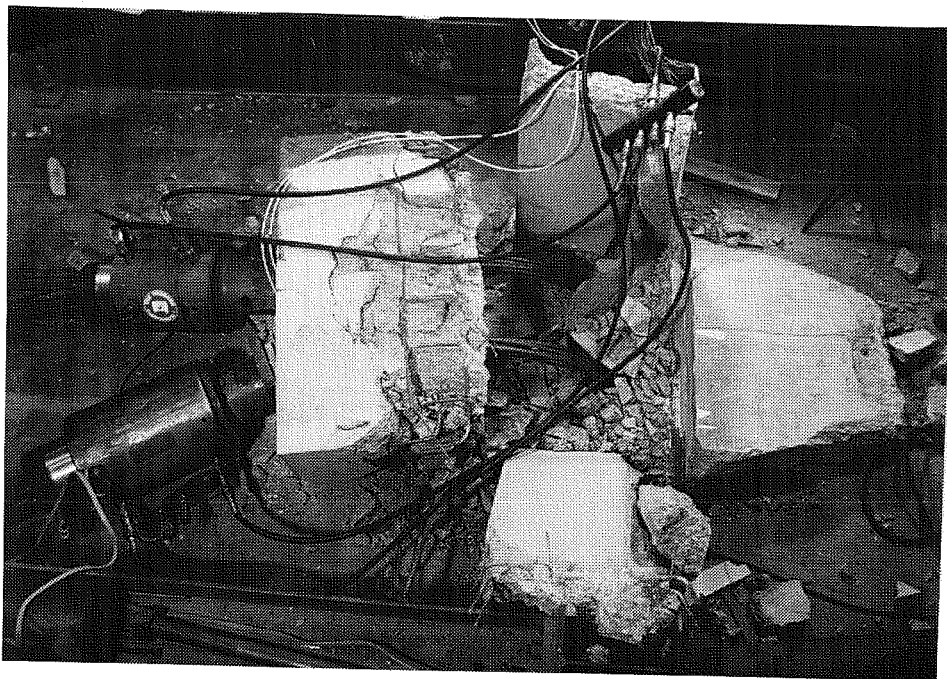


Figure 5.59 Collapse of Specimen Dia2 at Failure

Specimen Dia2 collapsed and broke into four parts at failure (Figure 5.59) with little warning, except for extensive cracking. Maximum crack widths of 0.02 in. at cracks (1) (Figure 5.50) were observed at 90% of the failure load. Failure was induced by crushing of the flanges immediately ahead of the diaphragm and of the inclined compression struts where they enter the flanges. When the diaphragm lost its support at the flanges it collapsed and pushed the flanges outwards. Flanges and web separated along cracks which had formed earlier in the test. Figure 5.58 shows the severely distorted diaphragm bending reinforcement at the interface between diaphragm and flange.

Failure of specimen Dia3 was more contained and involved a fairly uniform settlement of the entire failure wedge measuring $3/8$ to $1/2$ in. (Figure 5.60). It was initiated by collapse of the shear transfer between diaphragm and web and flanges. The crack widths of the wide inclined cracks seen in Figure 5.60 were some $3/8$ in. after failure but did not exceed 0.02 in. at 90% of the failure load. For safety reasons no crack width readings were taken after this level.

Displacement measurements close to the anchor plates indicated both vertical (parallel to the tendons) and horizontal (perpendicular to the tendons) displacements for

specimens Dia2 and Dia3 (Figure 5.61). No measurements were taken for specimen Dia1. The horizontal displacement component is caused by the rotation of the failure wedge about its support along the web and by separation of the diaphragm from the web due to the shear-friction mechanism.

5.6.4 *Diaphragm Bending and Web Bursting Strains*

Diaphragm bending and web bursting reinforcement were instrumented at midspan of the specimens. Additional strain measurements were available at the diaphragm-flange interface (strains across crack (2) in Figure 5.50) in specimens Dia2 and Dia3. These strains were measured on the diaphragm bending reinforcement in specimen Dia2 and on the tie-back reinforcement for the transverse post-tensioning bars in specimen Dia3. Figures 5.62 and 5.63 show that the strains at the diaphragm-flange interface were most critical. Reinforcement at this location yielded at 90% of the failure load. This is no surprise, since the transverse post-tensioning bars did not tie into the flanges and were not effective at the critical section.

Additional stresses developed by the unbonded transverse post-tensioning bars were approximately 30 ksi for the bar closer to the end face of the diaphragm and 15 ksi for the other bar (Figure 5.64). Figure 5.65 shows the distribution of diaphragm bending strains over the height of the diaphragm, measured at midspan. The initially linear distribution is affected by the increase of the transverse post-tensioning force at higher load stages.

No strain measurements at the diaphragm-flange interface were available for specimen Dia1. The strains at midspan did not reach yield (Figure 5.66). The strain development during cyclic loading after the peak load is interesting. While the diaphragm bending strains were reduced under the smaller loads after the first peak load, the web bursting strains continued to grow. This indicates a continuous loss of the concrete tensile strength contribution.

5.6.5 *Horizontal Bursting Strains*

The strut-and-tie model solution developed in Section 5.4 requires inclined tensile forces across the web-flange corners (forces T_2 and T_3 in Figure 5.20). If a grid of orthogonal bars is used, these inclined ties must be replaced by a corresponding system

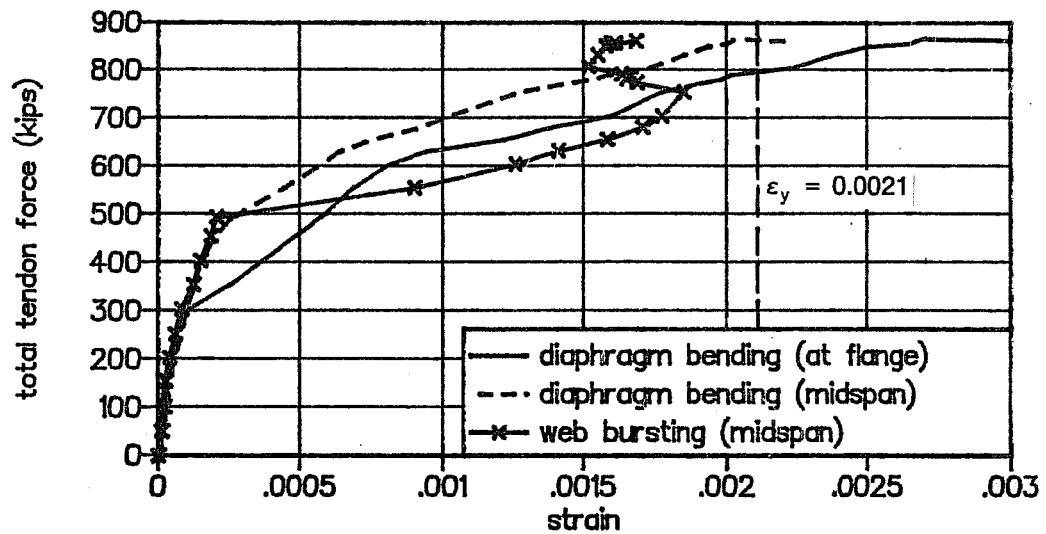


Figure 5.62 Diaphragm Bending and Web Bursting Strains in Specimen Dia2

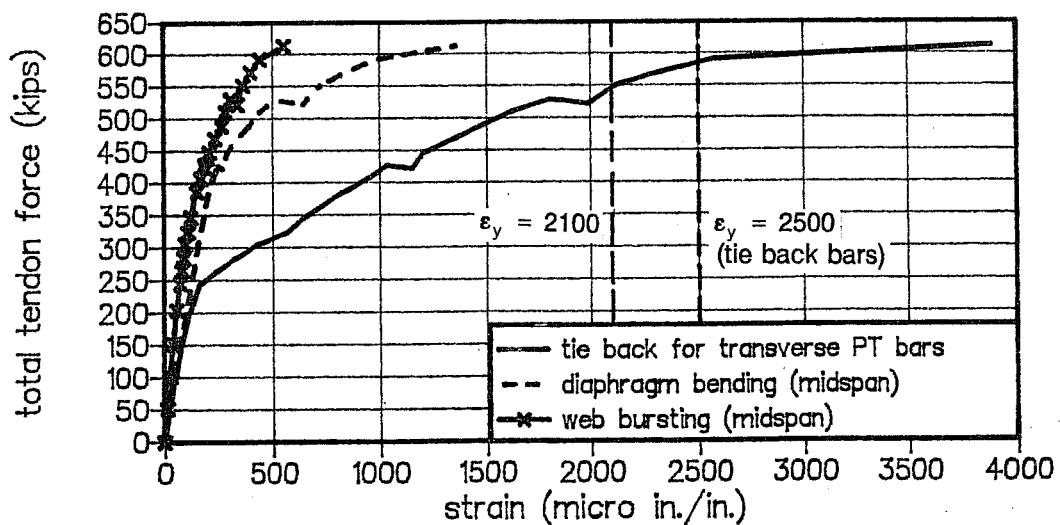


Figure 5.63 Diaphragm Bending and Web Bursting Strains in Specimen Dia3

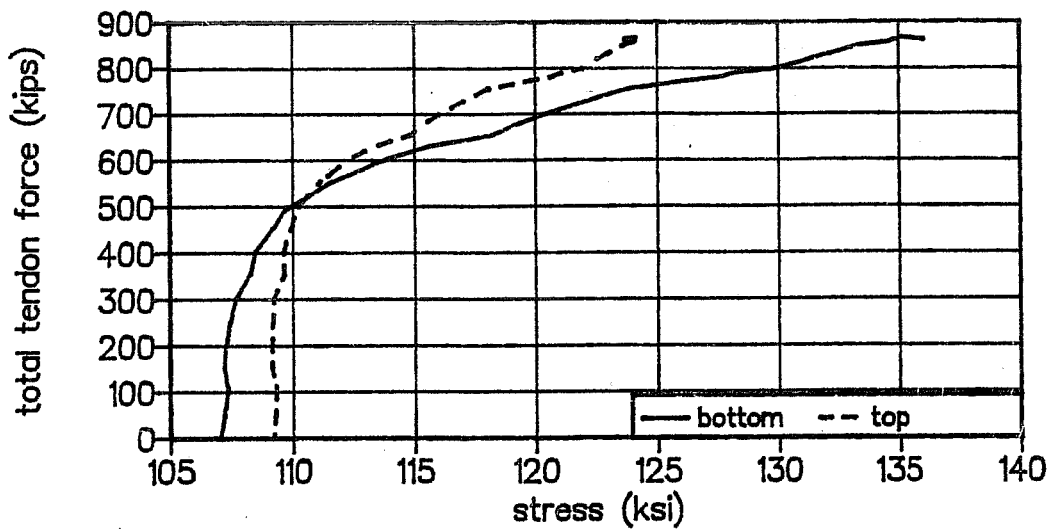


Figure 5.64 Stresses in Transverse Post-Tensioning Bars (Specimen Dia2)

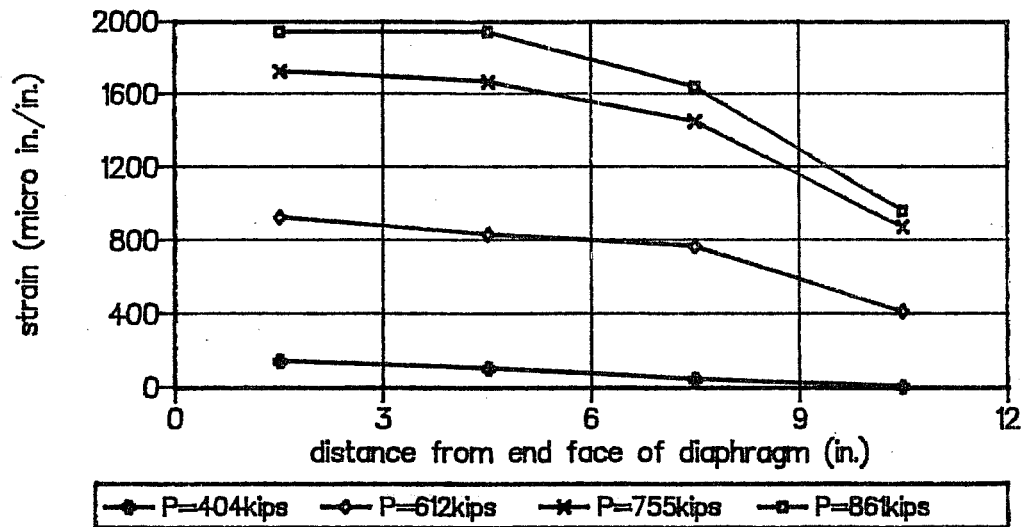


Figure 5.65 Distribution of Diaphragm Bending Strains (Specimen Dia2)

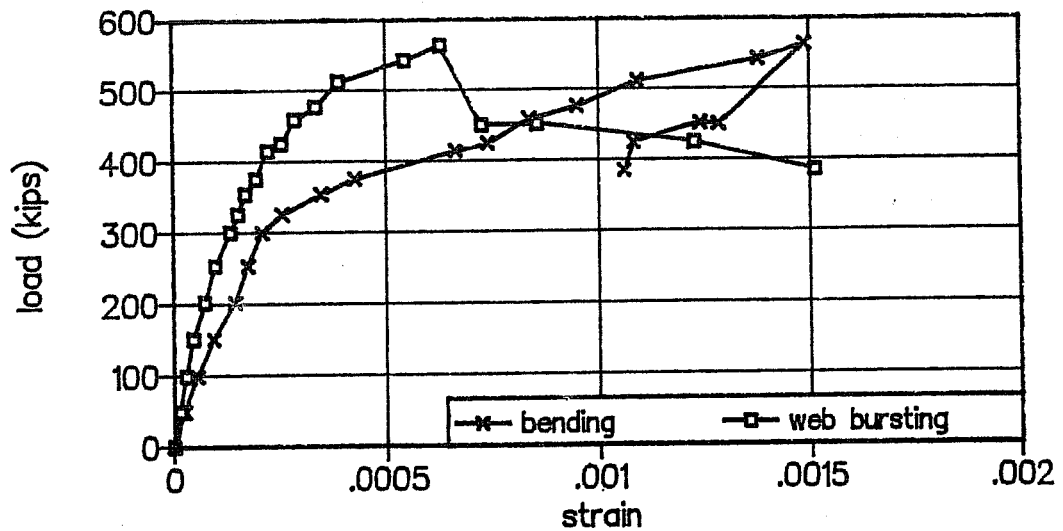


Figure 5.66 Bending and Web Bursting Strains in Specimen Dia1

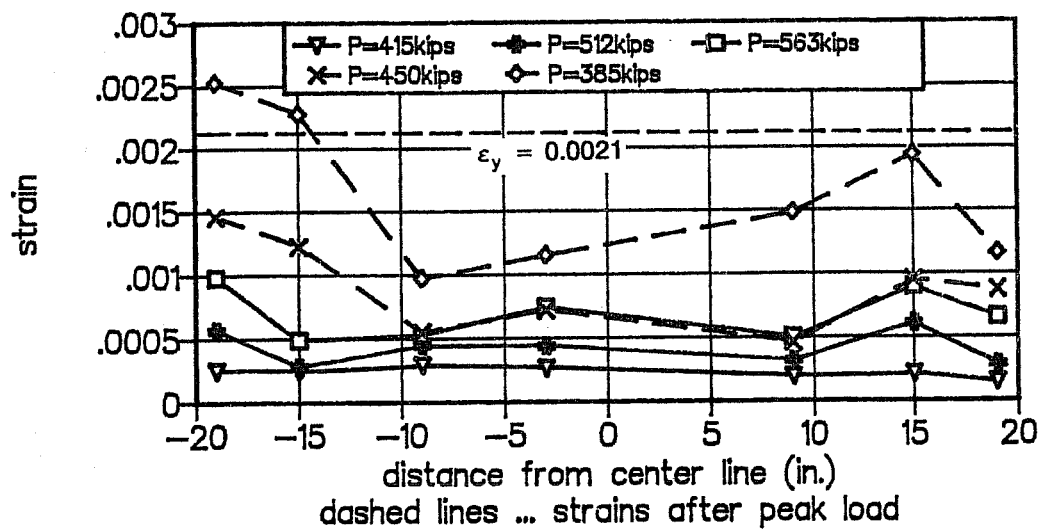


Figure 5.67 Horizontal Bursting Strains in Specimen Dia1

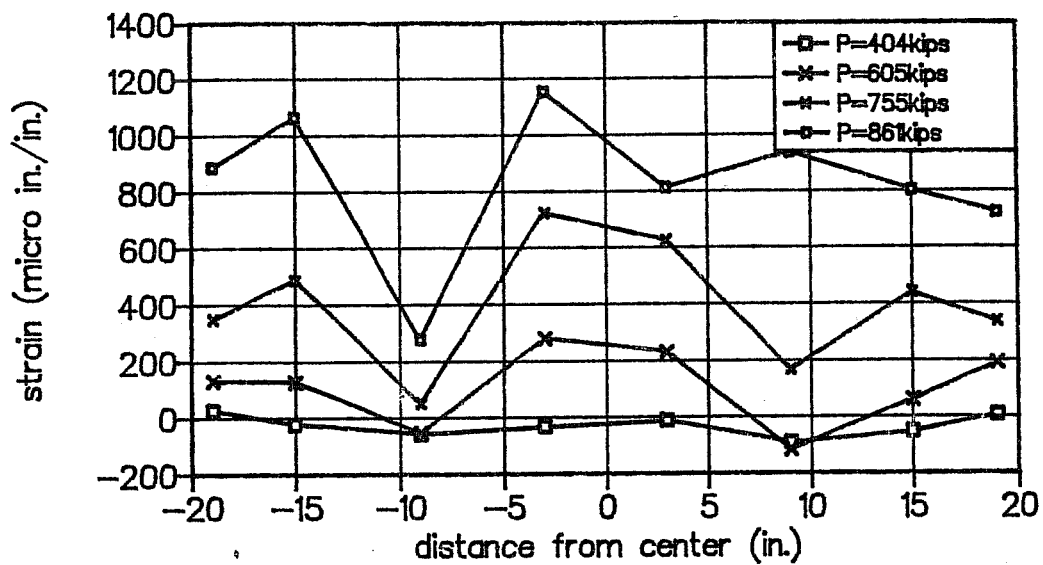


Figure 5.68 Horizontal Bursting Strains in Specimen Dia2

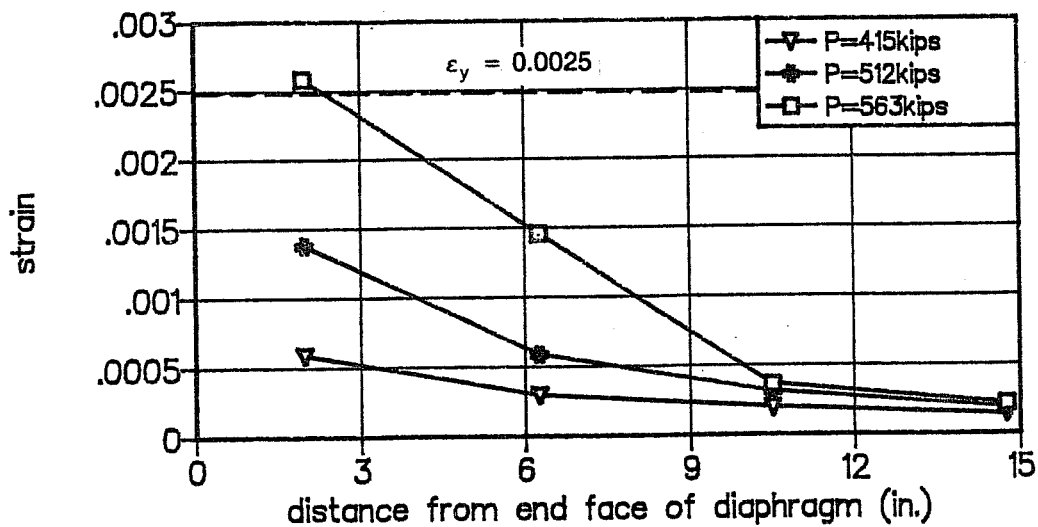


Figure 5.69 Flange Bursting Strains in Specimen Dia1

of strut and ties as shown in Section 5.4.8. This adds to the vertical tensile force (diaphragm bending and web bursting) and also generates "horizontal bursting forces" perpendicular to the web. Figures 5.67 and 5.68 show the horizontal bursting strains in specimens Dia1 and Dia2 at various load stages. Similar strain distributions were observed in specimen Dia3, with peak strains at failure at approximately 75% of yield. The horizontal bursting strains in specimen Dia1 continued to increase under cyclic loading, although subsequent peak loads were smaller than the first peak load. The figures indicate that horizontal bursting strains are significant, albeit smaller than would be expected from the strut-and-tie model solution.

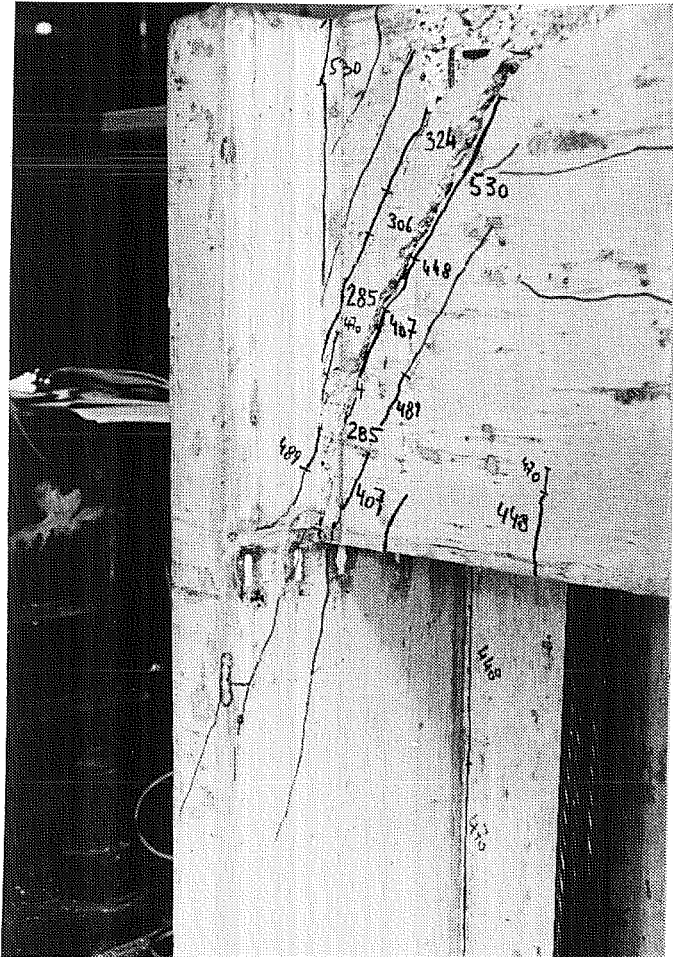


Figure 5.70 Flange Bursting Cracks Ahead of Diaphragm (Specimen Dia3)

5.6.6 Flange Bursting Strains

Strains in the flanges were critical immediately ahead of the diaphragm due to the transfer of compression stresses to the flange tips. These strains diminished rapidly with the distance from the diaphragm. Figure 5.69 shows these "flange bursting strains" for specimen Dia1. The strain distribution was similar for all specimens. The bar closest to the diaphragm yielded right at or shortly before failure (Table 5.4). Figure 5.70 shows cracking ahead of the diaphragm due to flange bursting in specimen Dia3.

5.6.7 *Strains in Shear-Friction Reinforcement*

Relatively substantial shear-friction reinforcement was required for the transfer of forces from the diaphragm to the web for all specimens. Figure 5.71 shows a comparison of the strains developed in this reinforcement. For specimens Dia1 and Dia3, which had similar concrete strengths but different reinforcement details, the strain development is almost identical initially. However, maximum strains are significantly higher in specimen Dia1. The curve for specimen Dia2 is similar in shape but affected by the higher concrete strength of this specimen (Table 5.3). The transition to the flat portion coincides approximately with cracking of the loaded face of the diaphragm (cracks (6) in Figure 5.50) (Table 5.4). The distribution of strains was fairly uniform over the height, as shown in Figure 5.72 for specimen Dia3.

5.6.8 *Strut Bursting Reinforcement*

In all specimens cracking parallel to the inclined compression struts from the anchor plates to the flanges of the section occurred early in the test. These cracks separated essentially unstressed corners from the highly stressed portion of the diaphragm (Figures 5.52 and 5.60) and became very large. Strut bursting reinforcement was provided in specimens Dia2 and Dia3 to confine the inclined compression struts and was effective in reducing the crack widths. Details of this reinforcement are described in Section 5.5.2. Figure 5.73 compares the strain development in the strut confinement reinforcement of specimens Dia2 and Dia3. The curves are similar, although inclined cracking and consequently flattening of the curve was delayed in specimen Dia2 due to its higher concrete strength. Maximum strains exceeded the yield strain significantly in both cases.

5.6.9 *Frame Action*

The vertical tensile forces due to diaphragm bending are not only resisted by tension in the diaphragm but also by flexure of flanges and web ahead of the diaphragm. This load path was described as "frame action" in Section 5.4.4. Strain measurements were taken at the web-flange joint immediately ahead of the diaphragm in specimen Dia3. Frame action has the effect of opening this joint (cracks (4) in Figure 5.50). Figure 5.74 shows that significant tensile stresses developed. The strains in the flanges are larger due to its smaller thickness of 4 in. compared to the web thickness of 6 in.

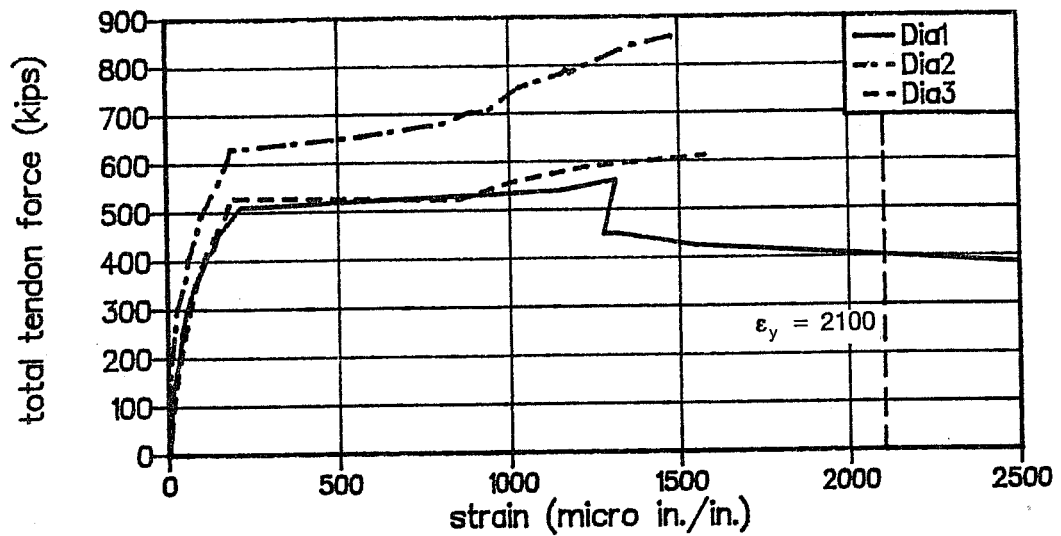


Figure 5.71 Strains in Shear-Friction Reinforcement

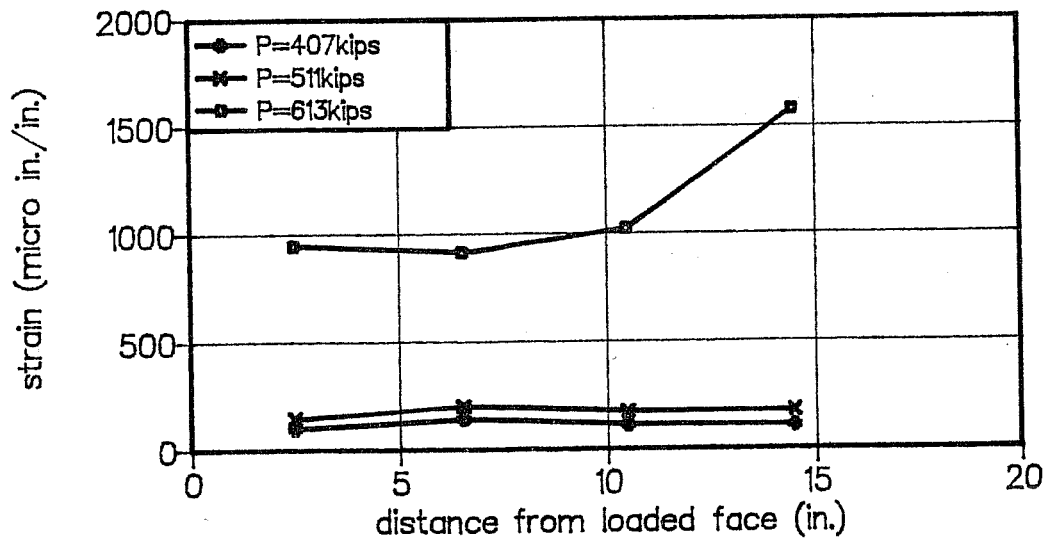


Figure 5.72 Strains in Shear-Friction Reinforcement in Specimen Dia3

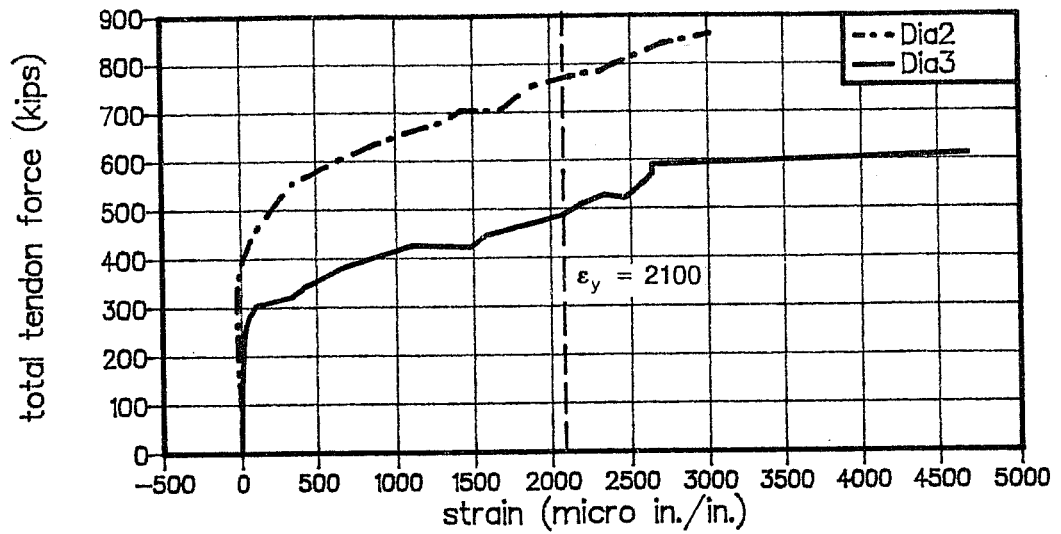


Figure 5.73 Strains in Strut Bursting Reinforcement

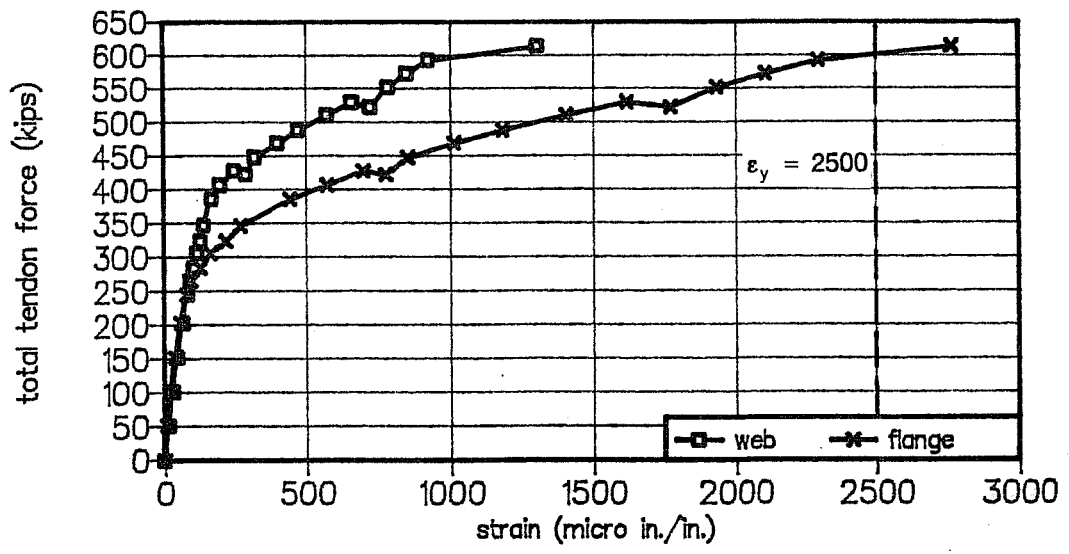


Figure 5.74 Strains at Web-Flange Junction Ahead of Diaphragm (Specimen Dia3)

5.6.10 Flange Compression Strains

In the development of the strut-and-tie model the distribution of compression stresses immediately ahead of the diaphragm was assumed as uniform over the flange thickness (Figure 5.37). The linear-elastic finite element analysis indicated a stress gradient over the flange thickness, with the stresses at the inside of the flange being about 60% higher than the outside stresses. Figure 5.75 shows the measured flange compression strains in specimen Dia3 at various load stages. The measurements indicate that the strain gradient was even more severe than predicted by the finite element analysis. Tensile stresses were observed on the outer face of the flange. A stress peak occurred at the inside of the flanges at a distance of approximately 11 in. from the outside face of the web. The transverse post-tensioning bars were located at the same distance. The stress peak indicates a local stress concentration due to dowel action of these post-tensioning bars.

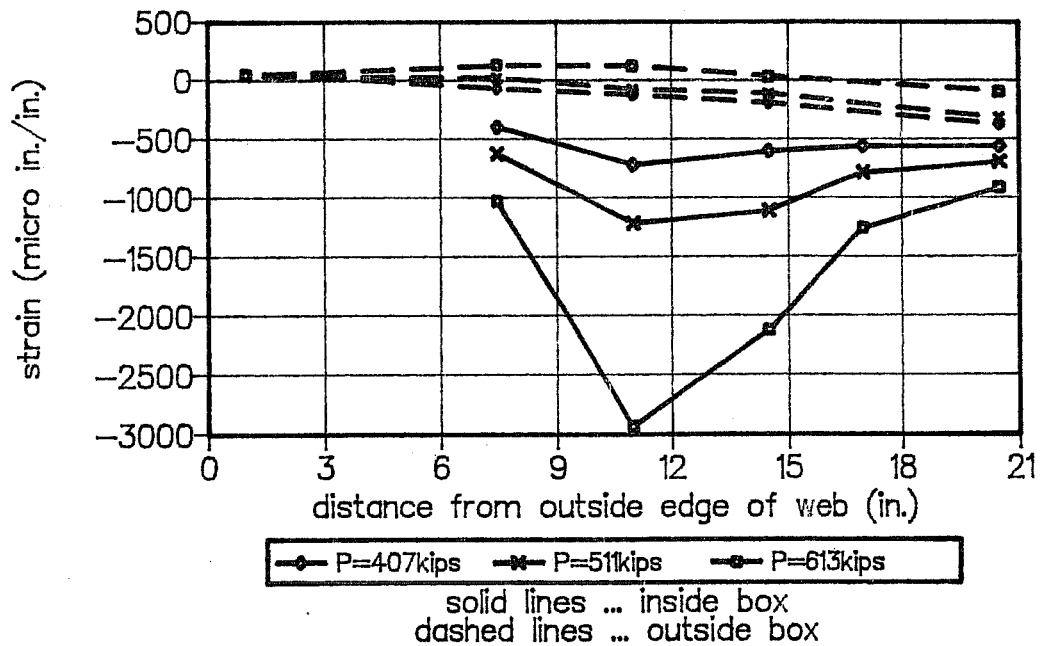


Figure 5.75 Flange Compression Strains Immediately Ahead of Diaphragm (Specimen Dia3)

5.7 Evaluation of Test Results

5.7.1 Finite Element Analysis Predictions

Table 5.5 shows a comparison of the test results to linear-elastic finite element analysis predictions. According to the finite element analysis, compressive stresses are critical in the flange tips at the base of the specimens. Following the proposed anchorage zone specifications, the predictions in the corresponding column of Table 5.5, labeled "base compression", are based on limiting the critical concrete compressive stresses to $0.7f_{ci}$. Averaged stresses over an area equal to the area of the bearing plates are considered. All predictions are controlled by the capacity of the web bursting and of the diaphragm bending reinforcement, labeled "vertical tension" in Table 5.5. These predictions are solely based on the reinforcement requirements in the plane of symmetry of the specimens. In particular, they ignore the large tensile stresses at the diaphragm-flange interface (Figure 5.17). At this location the three-dimensional state of stress makes it difficult to find magnitude and direction of a resultant force that could be used for proportioning the reinforcement. In contrast, in the plane of symmetry all stresses perpendicular to this plane are principal stresses and can be integrated relatively easily.

Table 5.5 Finite Element Analysis Predictions for Diaphragm Specimens

specimen	P_{test} (kips)	base compression		vertical tension	
		P_{calc} (kips)	$\frac{P_{test}}{P_{calc}}$	P_{calc} (kips)	$\frac{P_{test}}{P_{calc}}$
Dia1	563	813	0.69	472	1.19
Dia2	861	1116	0.77	352	2.45
Dia3	613	689	0.89	606	1.01
average			0.78		1.55
standard deviation			0.08		0.64

While the predictions assuming flange compression at the base controls have a low standard deviation, they are very unconservative and do not reflect the actual failure mode immediately ahead of the diaphragm. The predictions based on the capacity of the vertical tension reinforcement at midspan are conservative and quite good for specimens Dia1 and

Dia3. However, specimen Dia2, which had significantly higher concrete strength, exceeded the predicted failure loads by almost two and one-half times. Furthermore, the predictions do not reflect the actual failure mode, and the measured strains in the vertical tension reinforcement were significantly below the values expected from the analysis when the concrete tensile strength is neglected.

5.7.2 Strut-and-Tie Model Predictions

Table 5.6 lists a comparison of the strut-and-tie model predictions to the actual failure loads. The predictions are based on the provisions in the proposed anchorage zone specifications (Appendix A). In particular, the local zone nodes were placed at a distance equal to 1/4 of the plate width ahead of the anchor plates and the effective concrete compression strength was taken as $0.7\phi f'_{ci}$ throughout the structure.

Table 5.6 Strut-and-Tie Model Predictions for Diaphragm Specimens

specimen	P_{test} (kips)	flange compression		vertical tension	
		P_{calc} (kips)	P_{test} / P_{calc}	P_{calc} (kips)	P_{test} / P_{calc}
Dia1	563	459	1.23	360	1.56
Dia2	861	688	1.25	293 (372)	2.94
Dia3	613	494	1.24	388 (483)	1.58
average			1.24		2.03
standard deviation			0.01		0.65

The predictions based on the vertical tension capacity control. For specimen Dia1 this prediction is somewhat lower than the 376 kips design load because slightly different strut-and-tie models were used for initial design and for the prediction. Two values are given for specimens Dia2 and Dia3. The predictions in parentheses assume the transverse post-tensioning bars to be fully effective. However, since these bars did not adequately tie into the flanges (Section 5.5.2) the predictions were adjusted by discounting the vertical post-tensioning bar closer to the end face of the diaphragm. The second post-tensioning bar was considered effective. In this revised strut-and-tie model the compression struts are initially

deviated by the mild vertical tension reinforcement, and then an additional amount by the second post-tensioning bar. The strut-and-tie model predictions are even more conservative than the corresponding finite element analysis predictions. This is due to the fact that in the strut-and-tie model the overall load path is evaluated, actual reinforcement arrangement is considered, and concrete tensile strength is neglected. In contrast, the finite element predictions are based on a local check in the plane of symmetry of the specimens. Other load paths involving tensile strength of the concrete are easily overlooked, particularly in complex three-dimensional problems such as the present one.

The strut-and-tie model predicts a critical region in compression immediately ahead of the diaphragm, where inclined compression struts enter the thin flanges. Predictions based on this failure mode, using a nominal concrete strength of $0.7f'_{ci}$, are by far the best and are very consistent (Table 5.6). They also agree with the actual failure mode.

The predictions for the vertical tensile forces could be improved by refinement of the strut-and-tie model at cost of its simplicity. Possible refinements would include consideration of frame action and corbel action load paths. Another large source of conservatism is the treatment of the inclined tensile forces across the flange-web corner. The replacement of this force by orthogonal reinforcement as described in Section 5.4.8 increases the vertical tensile force reinforcement requirement by some 20%. Although cracking consistent with this inclined tensile force was observed in the experimental program, the extent of this cracking was limited and the remaining uncracked concrete provided sufficient tensile strength to prevent the load redistributions envisioned in the strut-and-tie model. The contribution of concrete tensile capacity could be recognized although the possibility of cracking from other load cases, restricted volume changes, and poor consolidation have led designers to avoid such reliance in important structural applications.

5.7.3 General

Both finite element analysis and strut-and-tie model predictions indicate failure would be controlled by the capacity of the diaphragm bending and web bursting reinforcement (vertical tension reinforcement). These predictions are inconsistent with the actual final failure mode which involved crushing of the flanges and of the inclined compression struts or collapse of the shear transfer from diaphragm to flanges. However, these final failures were preceded by yielding of the reinforcement crossing the interface

between diaphragm and flanges, which may have triggered failure. In general, all other reinforcement strains stayed below the values expected from the finite element analysis or the strut-and-tie model. The most obvious reason for this conservatism is the presence of uncracked concrete with a significant tensile strength contribution. In addition, reinforcement distortions noticed in the specimens after completion of the tests indicated substantial dowel action between diaphragm and flanges. Both contributions are difficult to assess and were not considered in the predictions.

The large width of the cracks parallel to the inclined compression struts (cracks (1) in Figure 5.50) are a consequence of the cracks at the diaphragm-flange interface (cracks (2) in Figure 5.50). After cracks (2) developed, transfer of forces into the flanges must have involved a shear-friction mechanism. The deformations required for shear-friction are reflected in the widths of cracks (1), which separated a highly stressed portion of the diaphragm from the dead corners closer to the loaded face.

5.8 Summary and Conclusions

5.8.1 Summary of Study

The behavior of diaphragms when used as reactions for the anchorage of external tendons in box girders was investigated. The study included linear-elastic finite element analysis, development of suitable strut-and-tie models, and physical tests of three half-scale diaphragm specimens. Particular attention was paid to giving a clear, comprehensive presentation of the procedures used in developing strut-and-tie models.

5.8.2 Behavior of Diaphragms for Anchorage of External Tendons

Linear-elastic finite element analysis results clearly indicate that the diaphragms investigated in this study act as a deep beam spanning between top flange and bottom flange of the section. This deep beam is additionally supported over its length at one side by the web. Substantial inclined tensile stresses exist where the diaphragm joins with the flanges due to the concentrated shear transfer at this location. The finite element analysis did not give any indication of corbel action for the transfer of forces into the web prior to cracking. In the corresponding strut-and-tie model the anchor forces are supported by inclined compression struts which extend from the anchor plates to web and flanges of the section. As these struts enter web and flanges tensile forces are required to redirect them.

The basic form of this load path is referred to as a "tripod model" and was discussed in Section 5.4.2. The crack pattern observed in the diaphragm specimens confirms this load path.

Actual failure loads exceeded the predicted failure loads substantially and reinforcement tensile stresses were lower than expected from the predictions. Failures occurred at the transition from the massive diaphragm section to the thin flanges ahead of the diaphragm. They involved either concrete crushing or collapse of the shear-transfer between diaphragm and flange and web. These failures were preceded by yielding of reinforcement crossing the interface between diaphragm and flanges in at least two of the three specimens. No corresponding measurements are available for specimen Dia1.

Local zone capacity had no impact on the behavior or final failure mode. In specimen Dia1 multiplane proprietary anchorage devices and confining spirals were used. Replacement by single plane bearing plates and elimination of the local zone confining spiral in the subsequent specimens had no adverse effect whatsoever. Sufficient confinement was provided by the concrete surrounding the anchorage devices. Bearing pressures from 2.1 to 2.7 f'_{ci} could be realized prior to failure elsewhere in the specimens.

Inclined cracks following the compression struts from the anchor plates to the flanges formed early in the tests and became very large subsequently. These cracks separated essentially unstressed corners closer to the loaded face of the diaphragms from a highly stressed wedge that transferred the anchor forces to flanges and web of the section. While this wedge experienced relatively large deflections, the unstressed "dead" corners essentially remained rigid and the difference in deformations accumulated at the inclined cracks.

Cracking of the web-flange junctions ahead of the diaphragm occurred in all specimens and was also observed in the structures shown in Figure 5.9. The joint between web and top flange is particularly susceptible to this type of cracking since this region is sometimes weakened or precracked due to settlement of the concrete in the web after casting.

5.8.3 *Design Recommendations*

A combination of finite element analysis and strut-and-tie model solution is recommended for design. The finite element solution is better suited for evaluation of the

behavior of the structure prior to cracking and for identification of regions with high potential for cracking. However, it is difficult to translate the linear-elastic stress distribution into reinforcement requirements and attention is focused on local stresses rather than the global load path. Furthermore, such linear-elastic solutions assuming a homogeneous, isotropic material become invalid with cracking of the structure. Hence the strut-and-tie model solution is more suitable for checking the overall load path and for design of the primary reinforcement. However, strut-and-tie models have only a limited capability to detect compatibility requirements. Therefore the geometry of such models should be based on a linear-elastic stress distribution in order to minimize stress redistributions, although some deviation is quite acceptable. It should not be overlooked that additional reinforcement is required for serviceability in regions where the finite element analysis indicates significant tensile stresses which are not captured by tie forces in the strut-and-tie model. For instance, in the experimental tests large inclined cracks opened due to the separation of stressed and unstressed portions of the diaphragm. Although not immediately detrimental to the strength of the structure these wide cracks may pose a long term problem. Reinforcement based on ACI provisions for shear in deep beams was effective in controlling these cracks.

The strut-and-tie model solution developed and discussed in this chapter is not a unique solution. Strut-and-tie models may be considered to be lower bound approaches to a plasticity solution and other possible solutions exist. Diaphragms take a wide variety of shapes and other geometries and loading conditions may require quite different solutions. The designer is free to experiment with various models to optimize the solution. Equilibrium conditions, material strength limitations, and some basic rules for the development of strut-and-tie models generally ensure that the solution is reasonable and safe. Both concrete compressive stresses and reinforcement requirements should be addressed. Unfortunately there are still open questions with regard to the effective concrete strength in strut-and-tie models and more research is needed in this area. In the proposed anchorage zone provisions (Appendix A) an effective strength of $0.7f_{ci}$ is suggested. This value gave conservative predictions for the capacity of the diaphragm specimens of this study.

5.8.4 *Detailing Recommendations*

The interface between diaphragm and flanges was a critical region in the specimens. It was subject to early cracking close to the end face of the diaphragm. Yielding of reinforcement across this crack was a good indicator of impending failure. In specimens Dia2 and Dia3 the transverse post-tensioning bars provided for deep beam action were deliberately anchored before tying into the flanges, which is a commonly used detail. With this arrangement, no prestressing force is available across the critical section described above. For deep beam action to develop, as envisioned in design, it is essential that both prestressed and non-prestressed reinforcement tie as deep into the flanges as possible. In specimens Dia2 and Dia3 reinforcement was provided to tie back the transverse post-tensioning forces into the flanges only at the live end of the bars. Although this reinforcement yielded prior to failure, the failure mode of the specimens appeared to be symmetric and unaffected by presence or lack of such tie-back reinforcement.

Inclined cracks following the compression struts from the anchor plates to the flanges became quite large. Closely spaced reinforcement is required to control these cracks. However, the best control is achieved by preventing cracking at the diaphragm-flange interface with well detailed transverse prestressing, as described above. Additional transverse prestressing closer to the loaded face should also be effective in controlling inclined cracking.

Cracking of the joint between web and flanges ahead of the diaphragm should be expected. Web and flange reinforcement located at the inside face of the section should be sufficient to control these cracks.

6 BEHAVIOR, DESIGN, AND DETAILING OF ANCHORAGE ZONES

6.1 Behavior of Anchorage Zones

6.1.1 Plain Concrete

A plain concrete cylinder or prism which is concentrically loaded over a portion of its cross section at one end and is fully supported at the other end fails either due to crushing of the concrete (Figure 6.1) or by splitting of the specimen (Figure 6.3). The failure mode is controlled by the ratio of supported area, A , to loaded area, A_b . If this ratio is close to one, crushing failure due to excessive lateral strains will occur. For larger A/A_b ratios the concrete surrounding the loaded area provides confinement and restrains the lateral strains. In this case failure is triggered by splitting of the specimen and is accompanied by formation of a cone ahead of the bearing plate. The failure load for both modes of failure can be predicted using Equation (6.1) [1].

$$f_b = 0.85 f'_c \sqrt{\frac{A}{A_b}} \quad (6.1)$$

For an A/A_b ratio equal to one the bearing pressure at failure in Equation (6.1) is $f_b = 0.85 f'_c$. This is less than the short-term cylinder compressive strength, $1.0 f'_c$, but is approximately equal to the concrete compressive strength under sustained loading [33].

The behavior of non-concentrically loaded members is quite similar. If none or little confining concrete is available, failure involves concrete crushing due to excessive lateral strains in the thin direction of the member (Figures 6.2 and 6.5), similar to the failure of the concrete cylinder shown in Figure 6.1. In thin slabs or thin rectangular members the crushing failure is often preceded by cracks which originate at the corners of the bearing plate and propagate at a rate of approximately 1:2 towards the surfaces of the slab (Figure 6.7). At failure portions of the slab surface spall off, as shown in Figures 6.5 and 6.7. Some designers consider this failure mode to be a consequence of bursting forces in the anchorage zone, but it is more a crushing failure due to excessive lateral strains.

If the member thickness is large compared to the corresponding dimension of the anchor plate, the failure mode changes from crushing to splitting (Figures 6.4 and 6.6). As

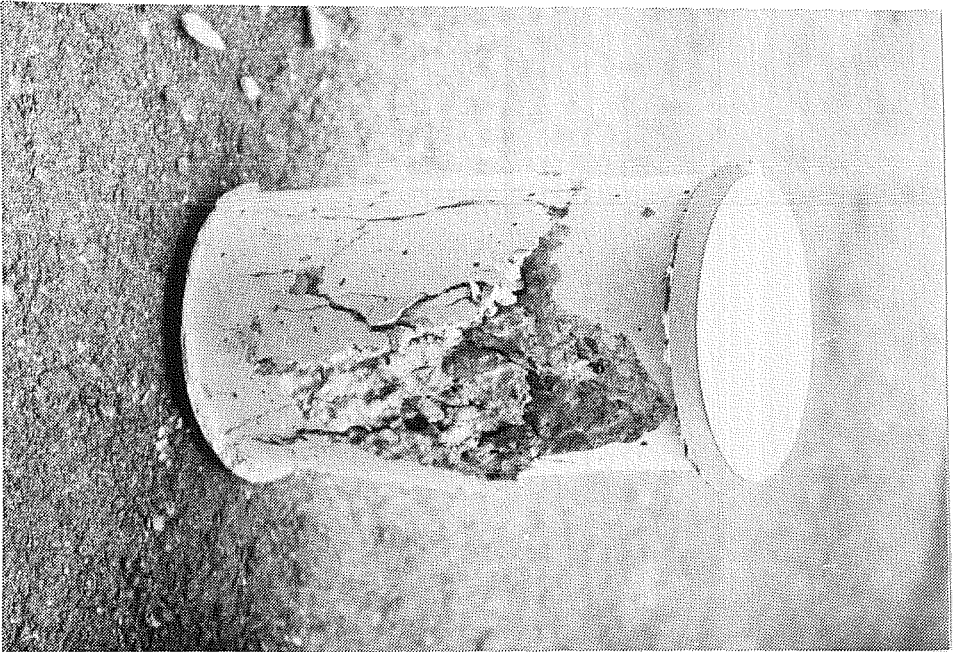


Figure 6.1 Crushing Failure of Cylinder Specimen



Figure 6.2 Failure of Sanders Specimen I1 [44]



Figure 6.3 Splitting Failure of Cylinder Specimens with Various A/A_b Ratios

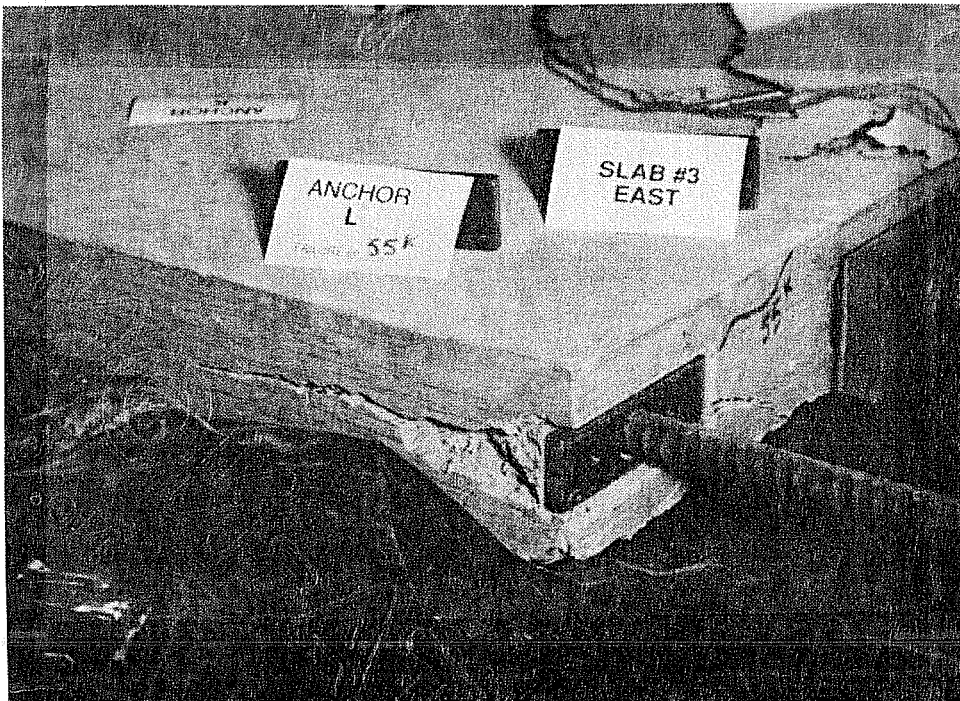


Figure 6.4 Splitting in Plane of Slab Close to Edge (from [17])

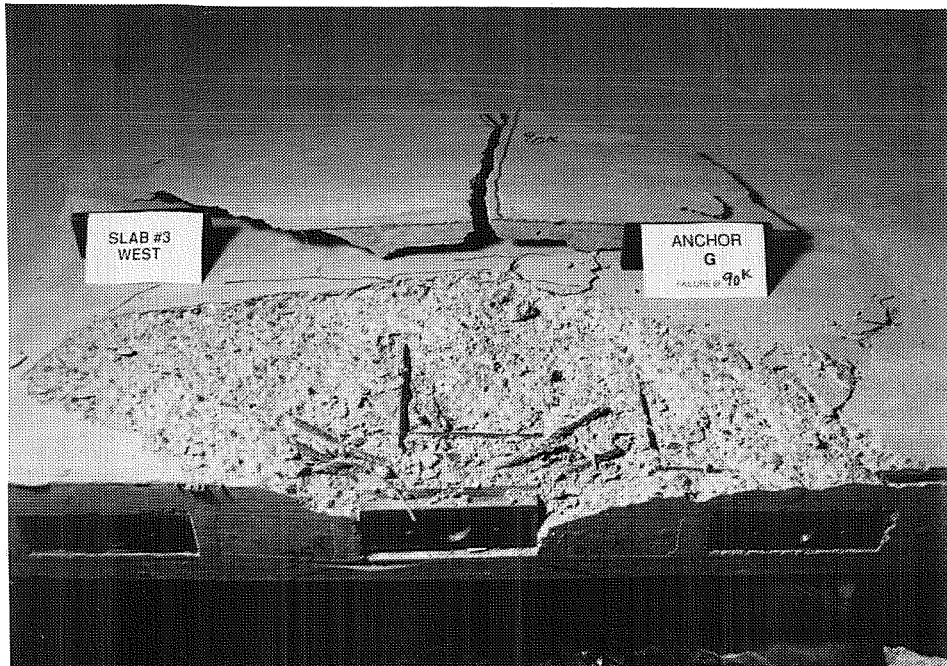


Figure 6.5 Crushing Failure of Slab Anchorage (from [17])

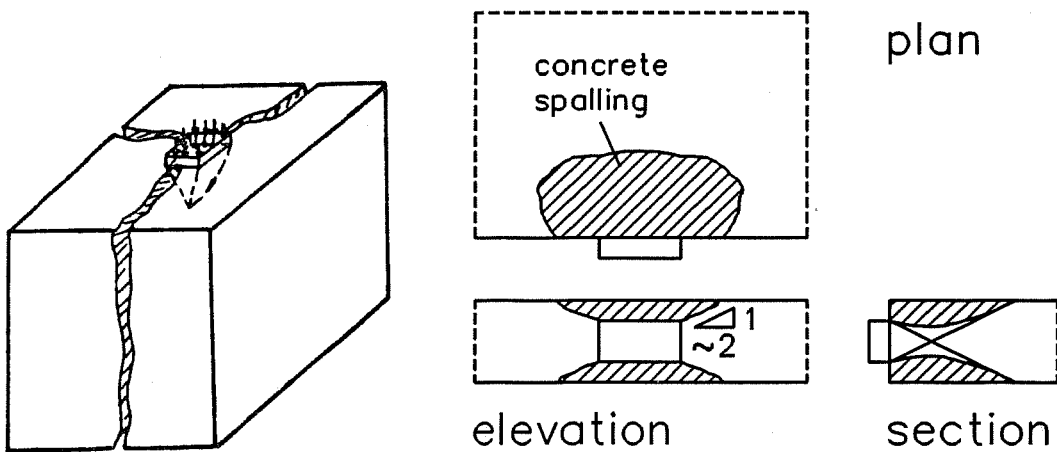


Figure 6.6 Splitting of Anchor Block (from [50])

Figure 6.7 Cracking and Spalling Due to Crushing Failure in Slabs

in the case of the cylinder specimens, this failure mode typically creates a concrete wedge ahead of the anchor plate. The splitting failure mode is particularly critical in slabs or rectangular members with closely spaced anchors (Figure 6.8) or with anchors close to the edge of the slab (Figures 6.4 and 6.9).

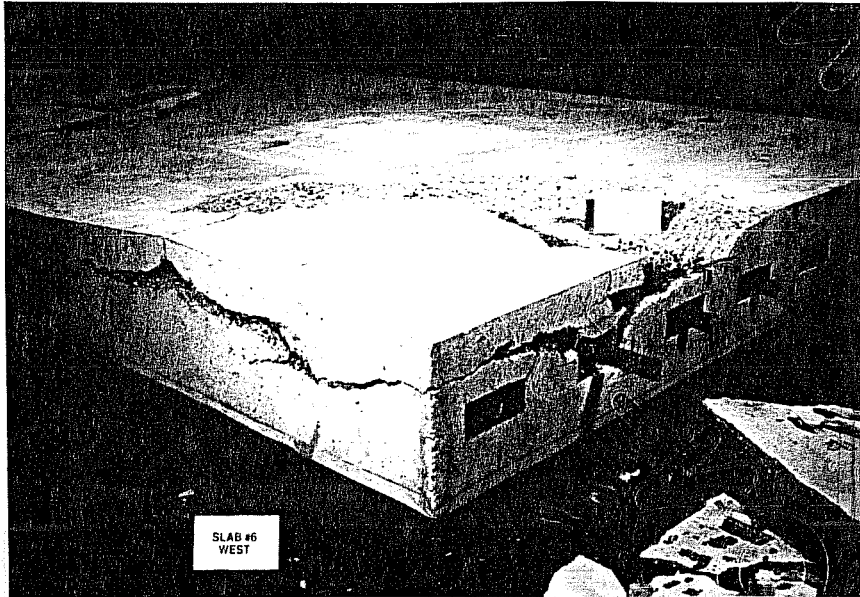


Figure 6.8 Slab Splitting Ahead of Closely Spaced Anchors (from [17])

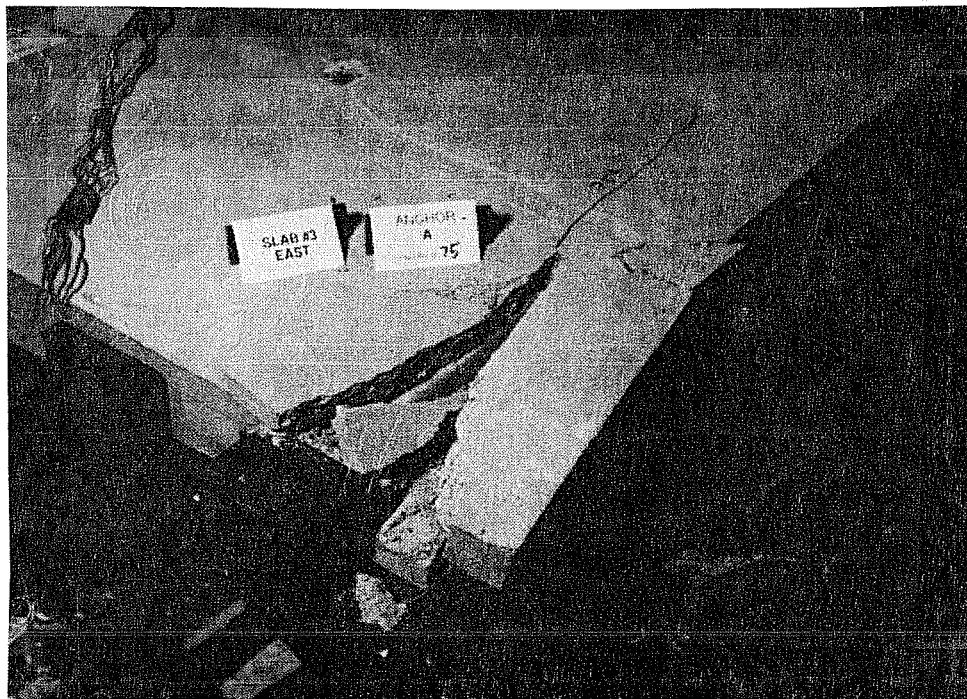


Figure 6.9 Splitting Perpendicular to Plane of Slab (from [17])

6.1.2 *Effect of Reinforcement*

6.1.2.1 Confinement Reinforcement

The compression strength of concrete can be enhanced if closely spaced reinforcement is provided to restrain the lateral strains. The most familiar application of this observation is in spiral reinforced columns. The improved performance of such columns is reflected by the increased ϕ -factor and the increased nominal capacity in the AASHTO specifications [1].

In anchorage zones for post-tensioning tendons confinement reinforcement ahead of the anchorage device plays exactly the same role as it does in spiral reinforced columns. However, since in anchorage zones the compression stresses spread out rapidly, such confinement reinforcement is needed only in a small region ahead of the anchor. This region is the "local zone" (Section 2.1.4). Failure of thin members with local zone confinement reinforcement usually involves concrete crushing ahead of the local zone and spalling of the concrete cover over the confinement reinforcement.

If the area of the anchor bearing plate is much smaller than the supporting concrete area, confinement is provided by the surrounding concrete and no confinement reinforcement is needed. However, in such cases the splitting failure mode is critical and reinforcement must be provided to resist the splitting forces (better known as bursting forces).

In summary, confinement reinforcement is useful and necessary where the concrete surrounding the anchorage device does not provide sufficient confinement. For example, in thin slabs, compared to the width of the anchor plate, reinforcement is needed to provide confinement in the thin direction of the slab. In blisters confinement reinforcement is needed to restrain the lateral strains perpendicular to the free surfaces of the blister.

6.1.2.2 Bursting Reinforcement

In contrast to confinement reinforcement, the role of bursting reinforcement is to resist direct tensile stresses, rather than to increase the effective concrete strength in compression. Typically such reinforcement is designed based on the bursting stresses obtained from a linear-elastic analysis. This approach is safe but not entirely logical. Prior to cracking of the concrete the bursting reinforcement is not very effective. After cracking the anchorage zone loses most of its transverse stiffness along the crack. Consequently the

compression stresses take a stiffer load path in more direct compression and spread at a slower rate, which reduces the bursting stresses. In order to maintain the elastic stress distribution bursting reinforcement would be needed to replace the stiffness of the cracked concrete. As shown in Equation (6.2), this requirement leads to a reinforcement ratio of some 15% which is absolutely not feasible.

$$\begin{aligned}
 A_s E_s &= A_c E_c \\
 \rho A_c E_s &= A_c E_c \\
 \rho &= \frac{A_c E_c}{A_c E_s} = \frac{E_c}{E_s} \sim \frac{4000}{29000} = 0.14
 \end{aligned}
 \tag{6.2}$$

Thus, for typical and practical reinforcement ratios, the effect of bursting cracks in the anchorage zone is to reduce the magnitude of the transverse tensile stresses, as well as the rate of dispersal of the compression stresses introduced by the anchor. The latter is of concern, if confinement reinforcement is provided only locally ahead of the anchor and a certain rate of dispersal of the compression stresses is relied on. It is pointed out that the stress redistribution after cracking in the anchorage zone does not require any plastic deformations but simply is a consequence of the loss of the transverse stiffness provided by uncracked concrete in tension.

If no confinement reinforcement is provided in the local zone, the splitting failure is usually accompanied by formation of a concrete cone ahead of the anchor plate (Figures 6.3, 6.4, and 6.6). In this case the stress redistribution described above is limited by the requirements for the transfer of shear stresses across the surface of the concrete cone.

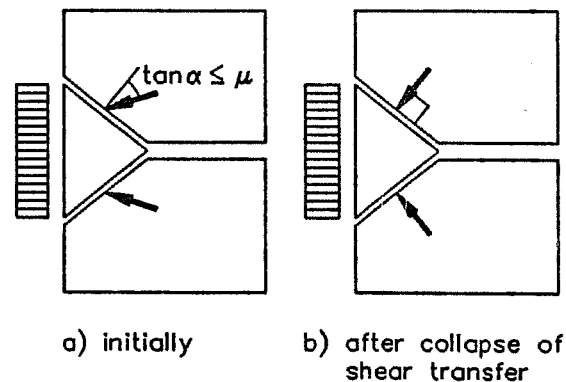


Fig. 6.10 Concrete Cone Ahead of Bearing Plate

Initially the stresses can be transferred in shear-friction. However, with increasing anchor load the shear-friction mechanism deteriorates, because a layer of pulverized concrete is created along the surface of the cone, which reduces the coefficient of friction.

Consequently the anchor force is forced to spread out at a flatter angle (Figure 6.10)[50]. This failure mode is typical for members with large concrete confinement around the anchor, so that concrete crushing does not control.

6.1.3 General

The observations made so far apply to prismatic concrete members. In non-prismatic members regions with critical compression and tensile stresses may also exist at geometric or loading discontinuities. Geometric discontinuities may also prevent the stress redistribution described in Section 6.1.2.2.

6.2 Design of Anchorage Zones

6.2.1 Limit States

6.2.1.1 Ultimate Limit State

The ultimate limit state is characterized by collapse of part or all of a structure. In ultimate strength design the resistance, R , of a member is compared to the load effects, L (Equation (6.3)).

$$\phi R > \gamma L \quad (6.3)$$

ϕ is a strength reduction factor ($\phi \leq 1.0$) which accounts for [33]:

- The variability of the material strengths;
- Geometric variabilities of as-built dimensions;
- Accuracy of the member resistance calculations;
- Type of failure and warning before failure;
- Consequences of failure.

γ is a load factor ($\gamma \geq 1.0$) which accounts for the variability of loadings.

In the proposed anchorage zone specifications a load factor $\gamma = 1.2$ is proposed for the tendon stressing force and the proposed resistance factor ϕ is 0.85. The basis for these proposals is discussed herein. In post-tensioned concrete structures usually the highest anchor load is applied during stressing of the tendon. In the United States tendon stresses after lock-off are limited to 70% of the guaranteed ultimate tensile strength of the tendon, f_{pu} . However, during the stressing operation short overstressing to $0.8 f_{pu}$ is permitted.

Arguments for a low load factor include [43]:

- The tendon load is monitored during stressing by measuring both the hydraulic pressure in the stressing jack and the elongations of the tendon. Therefore the variability of the applied load should be low.
- The anchor load is limited by the capacity of the tendon and of the stressing equipment. The tendon capacity is controlled by the anchor efficiency. Typical anchorage devices have an anchor efficiency factor of at least 0.95, which means an unbonded tendon will fail at the anchorage at about 95% of its breaking strength.
- Overstressing of the tendon is accompanied by large tendon elongations. For example, low relaxation strand, GR 270, stressed to $0.95 f_{pu}$ would experience strains of more than 2% or 24 inches per 100 feet of strand [10].
- The stressing load is a very short term load. After seating and lock-off the anchor force is reduced by 10 to 15%.

Arguments for a higher load factor include:

- The pressure gauge in the stressing equipment may be faulty or the operator may blunder.
- An oversized tendon or stressing jack may be used. Use of an oversized tendon would eliminate all warnings that come with overstressing of a tendon.
- Actual tendon strengths are usually 10% to 20% higher than nominal strengths.

The load factor selected for the proposed anchorage zone specifications is 1.2. This load factor is to be applied to the maximum stressing force. This is equivalent to a load factor of 1.3 to 1.35 on the tendon force after seating and lock-off, which is consistent with other AASHTO load factors for well defined loads (dead load, buoyancy). The load factor of 1.2 applied to the maximum stressing force, $0.8F_{pu}$, results in design load of $0.96F_{pu}$. This load compares well to the maximum attainable tendon force if excess tendon strength above its nominal strength is discounted.

On the resistance side initially a strength reduction factor $\phi = 0.75$ was specified in the proposed anchorage zone specifications [8, 44]. This low ϕ -factor reflected the brittle failure mode that was observed in the anchorage zone tests of this study, the wide scatter of the test results, and the consideration that it is easier to replace the tendon than to repair the anchorage zone. However, there are several arguments [43] that have led to an

increase of the ϕ -factor to $\phi = 0.85$ in the final version of the proposed anchorage zone specifications (Appendix A).

- The concrete strength is verified prior to stressing of the tendon.
- The stressing operation is a very short-term load, and in fact represents a load test for the anchorage zone.
- Failure is preceded by concrete spalling and formation of wide cracks, which gives ample warning to the construction crew.
- In general consequences of failure are less severe. Usually the construction site is closed to the public and the construction crew is more aware of the risks on the site. In most cases the stressing operation takes place when the member is still supported on falsework. Failure of the anchorage zone would not cause collapse of the member and would not affect other portions of the structure.
- Frequently the tendons are stressed at an early concrete age, typically when the concrete has reached 80% of its cylinder compressive strength. The subsequent increase in concrete strength gives additional safety.
- It is difficult to separate the effects of tendon anchorage forces and shear forces in the anchorage zone. Therefore it is desirable to use the same ϕ -factor for both load effects.
- Comparison with the extensive test results in this overall study, showed the expressions chosen for determining the resistance, R , are lower bounds with substantial conservatism.

6.2.1.2 Serviceability Limit State

When a high ϕ -factor and a low load factor are used for checking the ultimate limit state, serviceability requirements become particularly important.

There are significant tensile stresses in the anchorage zone and some cracking under service loads should be expected. With adequate reinforcement such cracks do not affect the strength of the structure immediately, but may become a long-term concern due to the increased potential for corrosion. Crack widths are best controlled by providing closely spaced reinforcement close to the surfaces of the member and by limiting the reinforcement strain and stress under service loads. Linear-elastic analysis is useful to identify regions where cracking is likely.

If the same model is used for ultimate load design and for service load design, with a load factor of 1.2 and a ϕ -factor of 0.85, the stresses in GR60 reinforcement steel are

$$f_s = (0.85/1.2) \times 60 = 42.5 \text{ ksi temporarily during stressing and are}$$

$$f_s \sim (0.7/0.8) \times 42.5 = 37.2 \text{ ksi after seating and lock-off.}$$

This is slightly high but acceptable in most cases, since concrete tensile strength contribution and stress redistributions after cracking tend to reduce the reinforcement stresses. Hence the load and resistance factors proposed in Section 6.2.1.1 also ensure sufficiently low reinforcement strains under service loads in most cases.

The compressive stresses in unconfined concrete under service loads should be limited to $0.6 f'_{ci}$, even under short term temporary loads. This stress level marks the onset of localized mortar cracking in concrete cylinder compression tests [33]. Stressing beyond this level causes permanent damage to the concrete. For local peak stresses, such as extreme fiber stresses, the limit may be somewhat relaxed. For example, for post-tensioned concrete girders AASHTO limits the extreme fiber stresses in compression to $0.55 f'_{ci}$ after seating and lock-off, which is equivalent to up to $0.63 f'_{ci}$ during the stressing operation [1]. The ACI code effectively allows extreme concrete fiber stresses as high as $0.69 f'_{ci}$ during stressing of the tendons [3].

In the proposed anchorage zone specifications an effective concrete strength of $0.7 f'_{ci}$ is proposed. Hence using a load factor of 1.2 and a ϕ -factor of 0.85, the concrete stresses under service loads are

$$f_c = (0.85/1.2) \times 0.7 f'_{ci} = 0.5 f'_{ci} \text{ temporarily during stressing and are}$$

$$f_c \sim (0.7/0.8) \times 0.5 f'_{ci} = 0.43 f'_{ci} \text{ after seating and lock-off.}$$

This is higher than the bearing stress limit stipulated by AASHTO [1] for allowable stress design of reinforced concrete ($0.3 f'_{ci}$), but is well below the critical stress of $0.6 f'_{ci}$ discussed above.

6.2.2 *Design of the Local Zone*

6.2.2.1 Introduction

The introduction of the concentrated post-tensioning force causes very large compression stresses immediately ahead of the anchorage device. These stresses usually decrease rapidly with the distance from the anchor. The region subjected to high local compression stresses is the local zone (Section 2.2). The bearing strength of concrete can

be increased above its uniaxial strength if some form of confinement for the local zone is available. This confinement may be provided by surrounding concrete, special confinement reinforcement, or other loads (Figure 6.11).

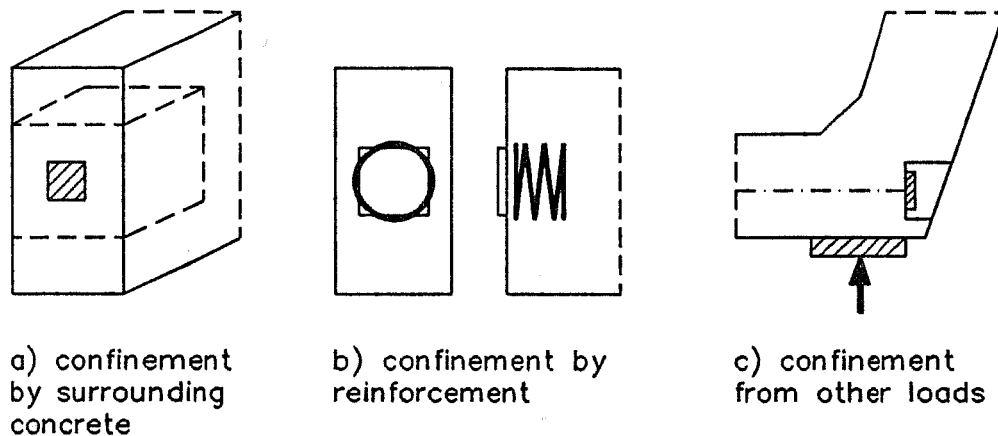


Figure 6.11 Confinement of the Local Zone

In the proposed anchorage zone specifications anchorage devices are classified as either **basic anchorage devices** or as **special anchorage devices**. Basic anchorage devices have to satisfy certain bearing stress limitations and stiffness requirements (Appendix A, Section 9.21.7.2). Special anchorage devices may violate these requirements but their adequacy must have been verified in a standardized acceptance test (Appendix A, Section 9.21.7.3). This division is merely concerned with the transfer of the anchor force from the anchorage device into the surrounding concrete. For both types of anchor the transfer of the anchor force from the tendon to the anchorage device must also be ensured. This is usually ascertained by both static and dynamic acceptance tests of the anchorage device proper.

6.2.2.2 Basic Anchorage Devices

The provisions for basic anchorage devices in the proposed anchorage zone provisions are intended for simple bearing plate anchors. Such anchors qualify as basic anchorage device if the bearing pressure under factored tendon load satisfies Equation (6.4) and if certain limits on the minimum stiffness of the bearing plate are adhered to (Appendix A, Section 9.21.7.2).

$$f_b \leq 0.7 \phi f'_{ci} \sqrt{\frac{A}{A_b}} \quad (6.4)$$

where f_b is the bearing pressure;

ϕ is the strength reduction factor;

f'_{ci} is the concrete strength at time of stressing;

A is the supporting area;

A_b is the bearing area.

Basic anchorage devices do not require any special confinement reinforcement in the local zone, provided adequate general zone reinforcement is available. It is noted that the bearing pressure limit depends on the concrete confinement available. This implies that some anchorage devices may qualify as basic anchorage device in some applications but may fail to do so in other cases.

6.2.2.3 Special Anchorage Devices

Anchorage devices which violate the restrictions for basic anchorage devices may still be used, if they can pass a standardized acceptance test. The proposed code specifications include provisions for such a special anchorage device acceptance test (Appendix A, Section 10.3.2.3). The acceptance test essentially simulates the most severe application the anchorage device is intended for. For acceptance of the anchorage device the test specimen must sustain a minimum failure load and must satisfy crack width limitations at various load levels.

If local confinement reinforcement is used to increase the concrete compressive strength ahead of special anchorage devices, concrete stresses may become critical immediately outside this confined region. In principle the acceptance test for the anchorage device represents the most critical application and therefore is also a test of the critical section immediately ahead of the confined region. However, in the acceptance test the concrete strength may be as high as the minimum specified concrete strength at time of stressing, f'_{ci} , for the particular anchorage device, or 85% of the specified 28-day strength, f'_c . In contrast, the effective concrete strength for design of the general zone is limited to $0.7 f'_{ci}$ in the proposed anchorage zone specifications. Therefore the capacity of the local

zone-general zone interface may control the maximum tendon force that can be anchored and must be checked.

6.2.2.4 Responsibilities

There has been considerable confusion about the responsibilities of the parties involved in the design and construction of anchorage zones [44]. To alleviate this confusion Section 9.21.2.3 of the proposed anchorage zone provisions defines the responsibilities of anchorage device supplier, engineer of record, and constructor. The responsibilities of the anchorage device supplier include:

- To provide an anchorage device that can pass all required acceptance tests for both the transfer of the anchor force from the tendon to the anchorage device and from the anchorage device to the concrete. It is not necessary to actually test each and every anchorage device. For special anchorage devices the proposed specifications only require testing of representative samples for a series of similar anchorage devices.
- To provide information on all requirements necessary for the special anchorage device to pass the acceptance test. This includes information on the confinement reinforcement for the local zone (usually a spiral or closely spaced ties surrounding the anchorage device), auxiliary reinforcement provided throughout the specimen, minimum edge distance, minimum anchor spacing, and minimum concrete strength at time of stressing.
- To provide records of the acceptance test for the particular type of anchorage device used in the structure.

Unless otherwise agreed upon by the parties involved, the responsibilities of the anchorage device supplier do not include:

- To provide or pay for any reinforcement in the anchorage zone.
- To design any reinforcement, other than that required for the anchorage device to pass the acceptance test.

The engineer of record is responsible for the integration of the information provided by the anchorage device supplier into the design of the actual structure and to adapt the details of the acceptance test specimen to the conditions of the specific application. In general, the contractor should not have any final responsibility for design of any portions of the anchorage zone.

6.2.3 Design of the General Zone

6.2.3.1 Introduction

The major concerns in design of the local zone are the high bearing pressure and compressive stresses immediately ahead of the anchor. The main concerns in general zone design are to determine the reinforcement requirements to resist the tensile forces in the anchorage zone and to check the

concrete compressive stresses. The compressive stresses may be critical at the interface with the local zone and at geometric discontinuities, for example at the transition from an end block to the regular section (Figure 6.12).

Traditionally design of the anchorage zone reinforcement is based on linear-elastic solutions, particularly on Guyon's results for a prismatic member under a concentric load (Section 2.1.2.2). With the advancement of finite element methods linear-elastic analysis even of complicated problems has become quite feasible. In this study an alternative approach, the application of strut-and-tie model procedures, was explored for a wide range of anchorage zone problems.

6.2.3.2 Elastic Analysis

Analytical solutions for anchorage zone problems are available for only a few special cases. Hence for most practical problems numerical procedures, most notably the finite element method, are required to perform the analysis. Amount and arrangement of the anchorage zone reinforcement are then determined by integrating the linear-elastic tensile stresses in the anchorage zone. The advantages of this procedure are:

- The analysis results give a very good indication of the state of stress in the structure prior to cracking. Thus the method is useful to identify critical regions with great potential for cracking or with high compressive stresses.
- A reinforcement arrangement based on the linear-elastic tensile stress trajectories helps to reduce stress redistributions after cracking of the structure.

Some of the disadvantages are:

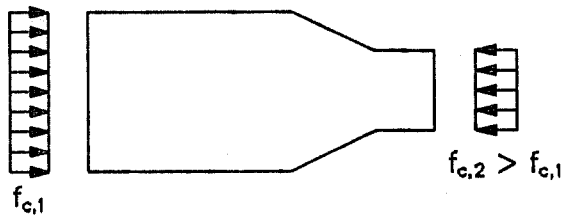


Fig. 6.12 Critical Compression Stresses at Geometric Discontinuities

- The analysis is based on the assumption of a homogeneous, isotropic material. It cannot take into account concrete cracking and effects of the reinforcement. With modern finite element methods these shortcomings can be overcome, but only with large computational efforts.
- It is very difficult to translate the analysis results into reinforcement requirements.
- Attention is focused on local stresses rather than global load paths.
- The numerical procedure requires access to a computer and generally is not suitable for hand calculations.

6.2.3.3 Strut-and-Tie Models

With strut-and-tie models the flow of forces in a structure is approximated by a system of straight compression members (struts) and tension members (ties) which are connected at nodes (Section 2.3.2). In general, different loads on the same structure will require different models.

Table 6.1 shows a set of rules that should be observed when developing strut-and-tie models. It is helpful to make a distinction between **basic** and **refined strut-and-tie models**. The basic load path satisfies only equilibrium conditions and material strength limitations. Such load paths are easy to find, even in three-dimensional problems. They represent a lower bound solution to the failure load for a structure made of perfectly plastic

material. Of course, reinforced concrete is not a perfectly plastic material and some concessions must be made to its limited ductility. This is done by applying Rules 3 to 6 in Table 6.1 which are measures to capture the effects of compatibility requirements in the strut-and-tie model. Rules 7 and 8 account for the state of stress in the structure after cracking of the concrete: Only reinforcement can transfer tensile forces (Rule 7), and load paths in compression are stiffer than load paths in tension (Rule 8, Figure 6.13). With the additions of Rules 3 to 8 the strut-and-tie model becomes a better approximation to the

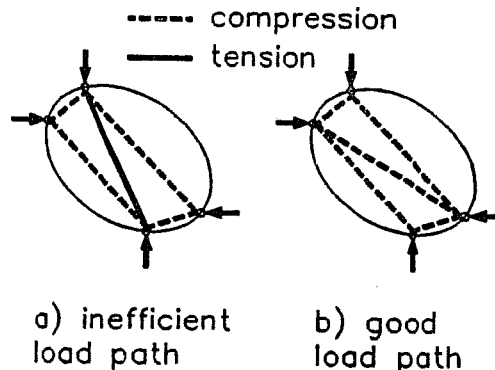


Fig. 6.13 Efficient and Inefficient Load Paths in Struts-and-Tie Models

Table 6.1 Rules for the Development of Strut-and-Tie Models

rule	requirement	
1	satisfy equilibrium conditions	basic STM
2	satisfy material strength limitations	
3	satisfy simple beam theory at the boundaries of the anchorage zone	refined STM
4	select angle between struts and ties larger than 25 degrees	
5	orient the geometry of the strut-and-tie model on the linear-elastic stress trajectories	
6	split struts carrying large compression forces into a number of sub-struts	
7	keep practical reinforcement arrangements in mind when selecting the orientation of the ties	
8	avoid inefficient load paths	

actual state of stress in the structure and the procedure is more independent from the assumption of a perfectly plastic material.

Figure 6.14 shows a series of examples for basic and refined strut-and-tie models. The first example in Figure 6.14a shows basic and refined load paths for an anchorage zone with a concentric end anchor and a basic anchorage device. The basic strut-and-tie model is a single compression strut with the same width as the anchor plate. Application of Rules 3, 5, and 6 leads to the refined model which indicates the need for bursting reinforcement.

Figure 6.14b also shows a strut-and-tie model for a concentric end anchor, but this time with a special anchorage device. Because the bearing pressure ahead of the anchor plate is larger than the effective concrete strength outside the local zone, a single compression strut with constant width is no longer possible. Instead spreading of the compression stresses and consequently a bursting force are required even for the basic strut-and-tie model when special anchorage devices are used.

The next example (Figure 6.14c) shows an anchorage zone with two anchors. In the basic model the anchor forces are carried by two isolated struts. Enforcement of Rule 3 reveals the presence of the tie force between the anchors in the refined model.

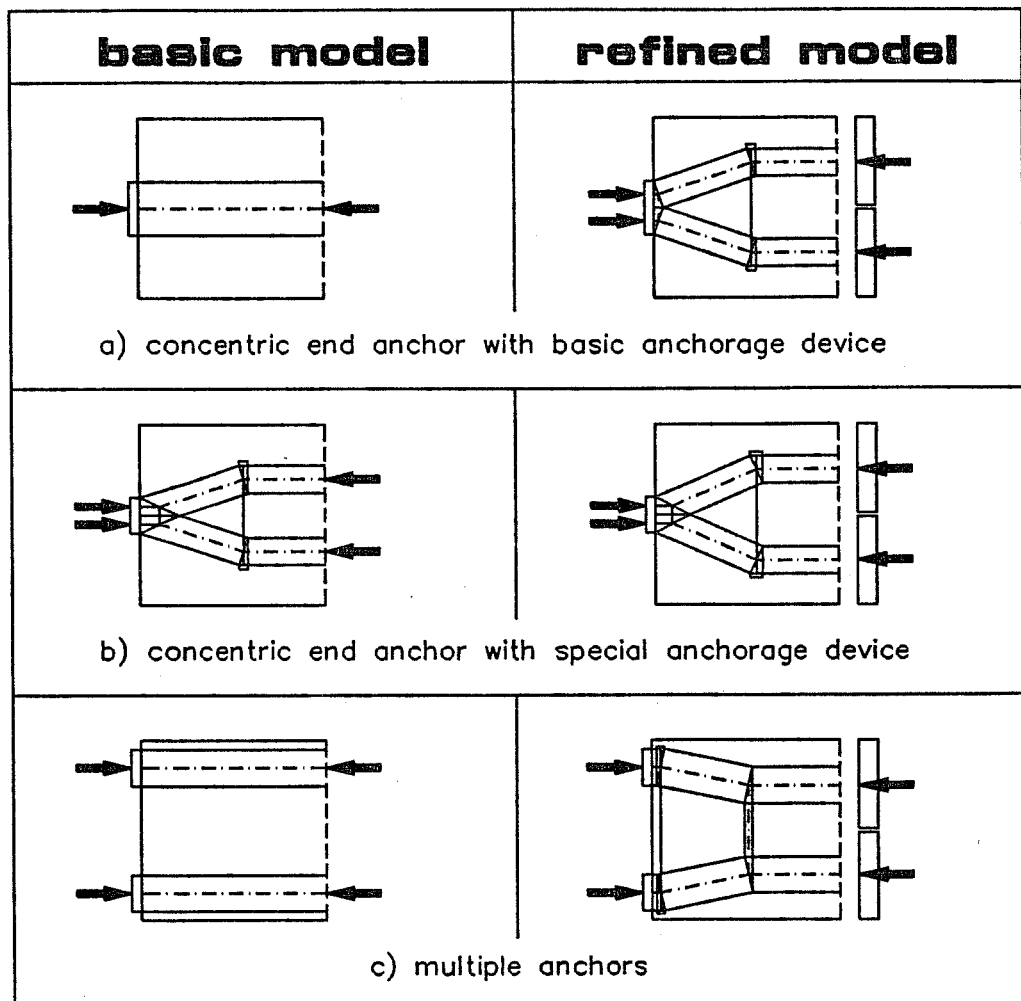


Figure 6.14 Examples for Basic and Refined Strut-and-Tie Models

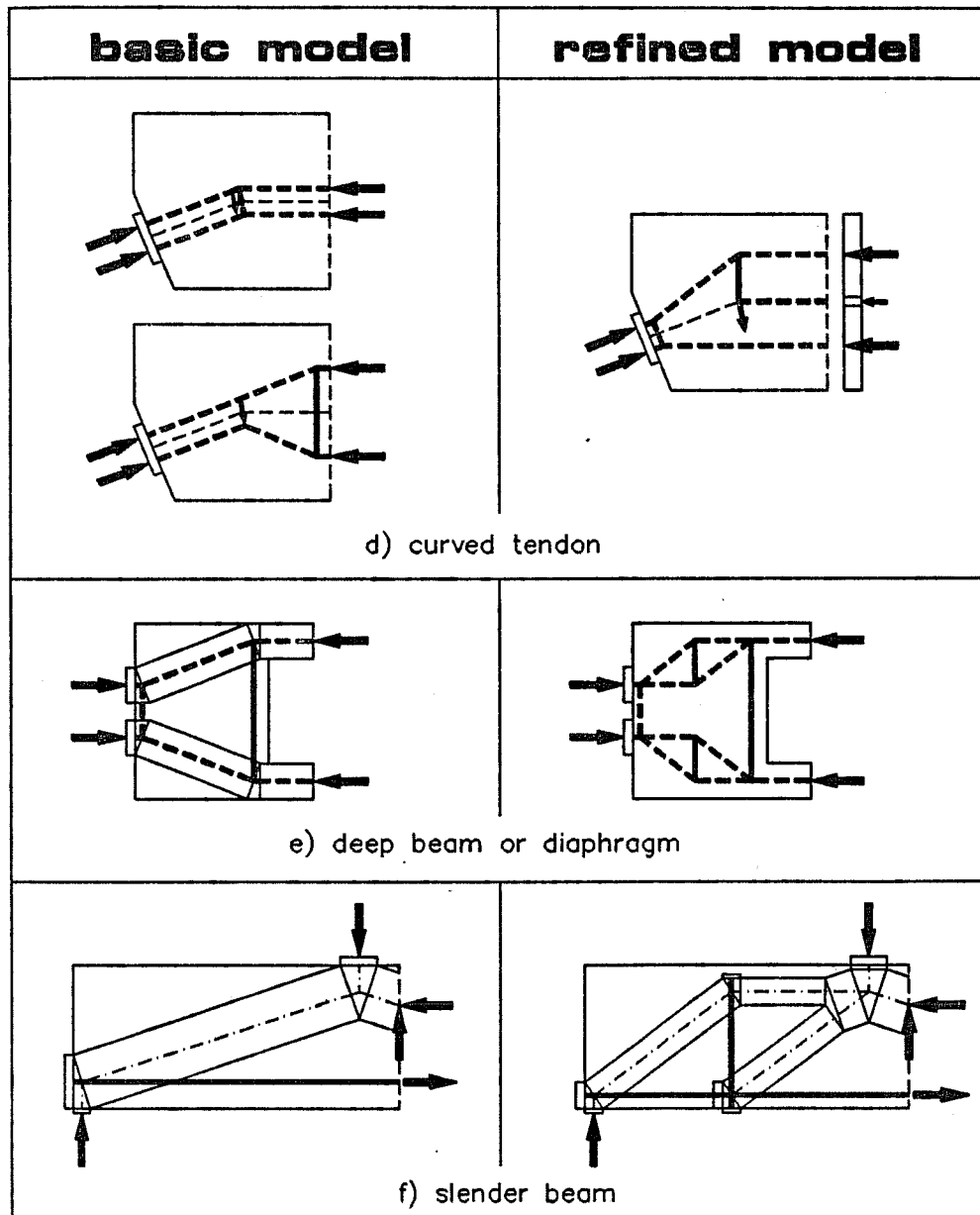


Figure 6.14 (cont.) Examples for Basic and Refined Strut-and-Tie Models

Figure 6.14d shows two different basic load paths in an anchorage zone with a single curved tendon. Both models require tensile forces to tie back a portion of the tendon deviation force but the location of the ties is quite different. The refined model illustrates the application of Rule 7. The tie in the model is oriented to reflect a practical reinforcement arrangement.

In a deep beam (or diaphragm) both basic and refined model yield the same tensile force at the tension side of the beam (Figure 6.14e). In the refined model Rule 6 is applied to find the tensile forces due to spreading of the inclined compression struts.

As a last example Figure 6.14f illustrates the application of Rule 4. The refined strut-and-tie model for a slender flexural beam shows the need for stirrups (if the concrete tensile strength is ignored).

There is a fundamental difference between the examples shown in Figures 6.14a and c and the examples of Figures 6.14b, d, e, and f. In the first group no tensile force is required in the basic strut-and-tie model to find a solution that satisfies equilibrium and concrete strength limitations. In the second group tensile forces are essential to satisfy these requirements. In the first group the behavior of the anchorage zone is less sensitive to amount and distribution of the reinforcement. Cracking will reduce the stiffness in the direction of the tension force and induce stress redistributions in favor of the stiffer load path in more direct compression. In the second group a similar stress redistribution is not possible because no other load path without tension is available.

These observations have an interesting impact on ductility considerations. Enforcement of a ductile failure by limiting the amount of reinforcement (to ensure yielding of the steel prior to crushing of the concrete) is only possible, if the tension force carried by this reinforcement is essential for equilibrium. It is not possible with reinforcement for non-essential forces or if a significant portion of the tension force is carried by concrete tensile stresses. In most anchorage zone problems the bursting force is not essential for equilibrium and significant concrete tensile strength contribution is available. Hence in general failure of anchorage zones is not ductile, independent of the amount of bursting reinforcement.

Strut-and-tie model procedures were used extensively in this study to describe and predict the behavior of a wide range of different anchorage zone problems. In many ways

the method is superior to traditional design methods, but it also has its shortcomings. Some of the advantages and disadvantages are listed below.

Advantages:

- The tie forces in the strut-and-tie model can be directly translated into reinforcement requirements.
- The actual reinforcement arrangement is reflected in the model.
- Strut-and-tie models direct the attention to global load paths.
- The nodal concept emphasizes good detailing.
- Essential (required by equilibrium) and non-essential (required by compatibility) load paths are easily detected.
- Strut-and-tie models are suitable for hand calculations.

Disadvantages:

- Strut-and-tie models have only a limited capacity to predict compatibility induced forces. Hence they do not necessarily detect all regions where reinforcement is required for serviceability considerations.
- The concrete tensile strength is neglected. Sometimes it is difficult to find load paths without relying on concrete tensile strength (for example shear in slabs).
- The choice of the effective concrete compressive strength is somewhat arbitrary and is affected by a large number of variables.
- Strut-and-tie model solutions often are not unique. This is particularly true for refined models, but is not so much the case for basic strut-and-tie models. Often engineering judgement is required to select a suitable model for design.
- High demands are put on the designer's abilities to visualize spatial relationships.

6.2.3.4 Conclusions

With linear-elastic solutions compatibility requirements for an isotropic, homogeneous material are satisfied. With strut-and-tie models compatibility requirements can only be considered indirectly. Hence the choice between finite element analysis and strut-and-tie model procedure is a choice between a method that satisfies the incorrect compatibility conditions accurately (in the case of cracked concrete structures) and a method that uses educated guesses and rules of thumb to consider compatibility

requirements. Although neither method is entirely satisfactory to provide very accurate solutions, they both satisfy equilibrium conditions and are safe for design if applied properly.

Due to the limitations of either method it appears to be best to combine finite element analysis and strut-and-tie model procedures, at least for design of very complex problems. The finite element analysis results serve to identify critical regions. In two-dimensional problems linear-elastic stress trajectories can be used to get rough guidelines for the selection of the geometry of the strut-and-tie model. Check of concrete compressive stresses and design of the primary reinforcement can then be based on the member forces of this model. Additional nominal reinforcement may be necessary for crack control in regions where the elastic analysis indicates tensile stresses which are not captured by the strut-and-tie model.

6.3 Detailing of Anchorage Zones

6.3.1 Local Zone

The local zone details are most critical in members which are thin compared to the anchor plate dimensions. Failures have been reported which were caused by congested details, inadequate concrete compaction, and insufficient tolerances [44]. Local zone confinement reinforcement needs a small pitch or tie spacing to increase the confinement effect, but it should not obstruct concrete placement and concrete consolidation. A clear spacing of 1 in. should be the minimum. Some responders to Sanders' survey recommended even larger clear spacings for spirals in the local zone.

Local zone confinement reinforcement must be placed coaxially with the tendon. This is extremely important for the performance of the anchorage device but easily disregarded during construction, particularly with congested details. Of course it must be ensured that the entire local zone can actually be accommodated within the boundaries of the structure. Figure 6.15 shows an example where disregarding this requirement may have contributed to serious concrete spalling ahead of the anchor [16].

With special anchorage devices in thin members the local zone reinforcement should be similar and equivalent to the reinforcement recommended by the anchorage device supplier and verified in the acceptance test (Figure 6.16). In thick members it may be possible to eliminate the confinement reinforcement if the concrete surrounding the anchorage device can provide sufficient confinement. With basic anchorage devices in thin

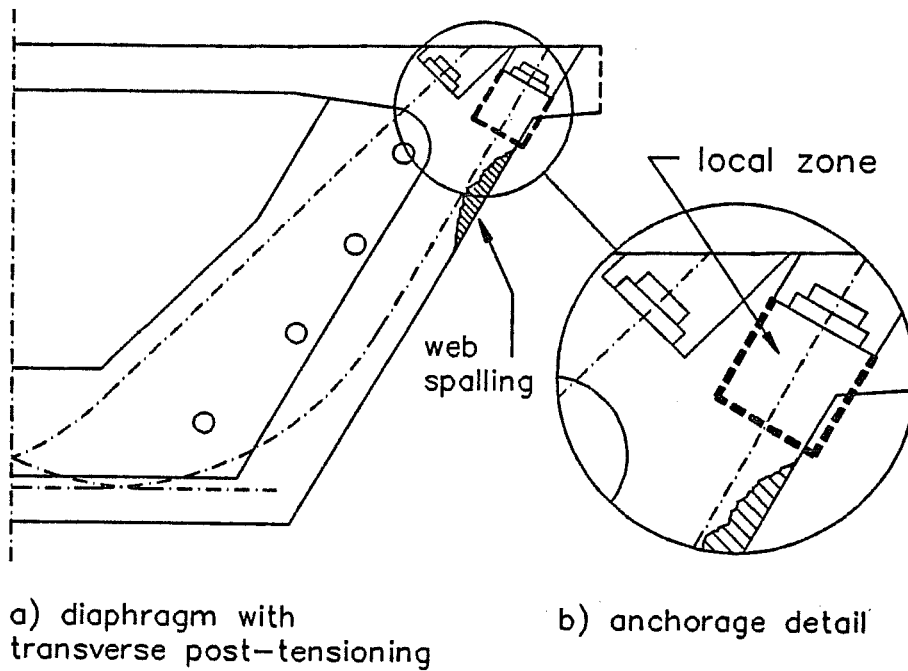


Figure 6.15 Concrete Spalling Due to Insufficient Attention to Local Zone Details

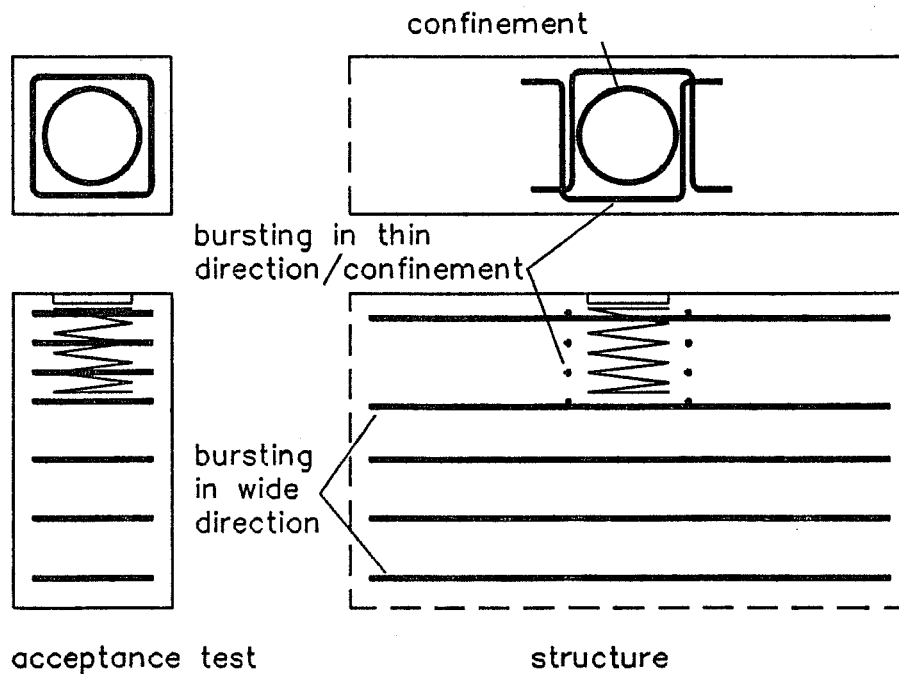


Figure 6.16 Local Zone Details in Acceptance Test and in Actual Structure

members no confinement reinforcement is needed, but bursting reinforcement should be provided in the thin direction of the member which in fact will also serve as confinement reinforcement (Figure 6.16).

6.3.2 *General Zone*

General zone reinforcement, such as the bursting reinforcement, serves to resist direct tensile forces in the anchorage zone. In contrast, the confinement reinforcement in the local zone serves to increase the concrete compression strength locally by restraining lateral strains due to Poisson's effect. For example, the primary purpose of a spiral ahead of an anchorage device is to provide confinement. Although a spiral may also be effective as bursting reinforcement, tie reinforcement is better suited for this purpose (Figure 6.16).

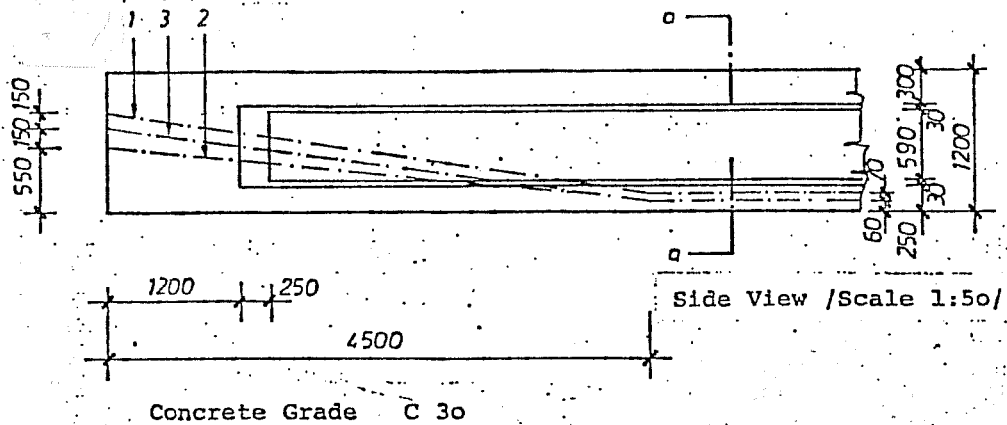
The arrangement of the general zone reinforcement should coincide with the design assumptions. For example the centroid of the bursting reinforcement should coincide with the location of the centroid of the corresponding stress field in the finite element analysis or with the location of the corresponding tie in strut-and-tie models. As a consequence of the assumption of zero concrete tensile strength anchorage zone reinforcement may be stressed very non-uniformly, depending on the extent of cracking in the anchorage zone. However, in general this assumption is necessary because of the low tensile strength of concrete and the potential for cracking from unforeseen loads.

Reinforcement based on refined strut-and-tie models which also satisfy rules to approximate compatibility requirements should give satisfactory reinforcement arrangements and details. Nominal reinforcement should be added where the finite element analysis indicates tensile stresses which are not represented by ties in the corresponding strut-and-tie model. The amount of such reinforcement cannot be determined from equilibrium conditions alone but is not critical for the strength of the structure. In general engineering judgement should suffice to size this reinforcement. A typical example is the unstressed corner problem mentioned in Section 2.1.3.1.

6.4 **Design Example**

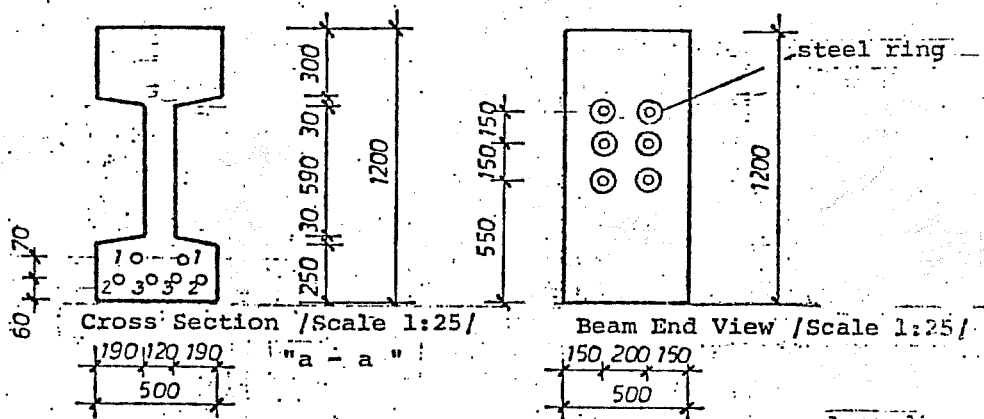
6.4.1 *Introduction*

Figure 6.17 shows an anchorage zone design problem which was sent out to European designers in a 1987 CEB survey [6]. This problem is used as a design example



Prestressing force: 450 kN/ tendon

The anchorage device is a 120 mm steel ring placed on the beam end surface.



According to NC HB

The calculated transverse tensile force kN

distributed at a length of mm

The required cross section of TR mm²

this is a calculated TR

minimum TR

Supplementary LR needed ; not needed

Supplementary bearing device needed ; not needed

Supplementary reinforcement /spirals etc./ under the anchorage device needed ; not needed

Figure 6.17 CEB Survey Problem (from [8])

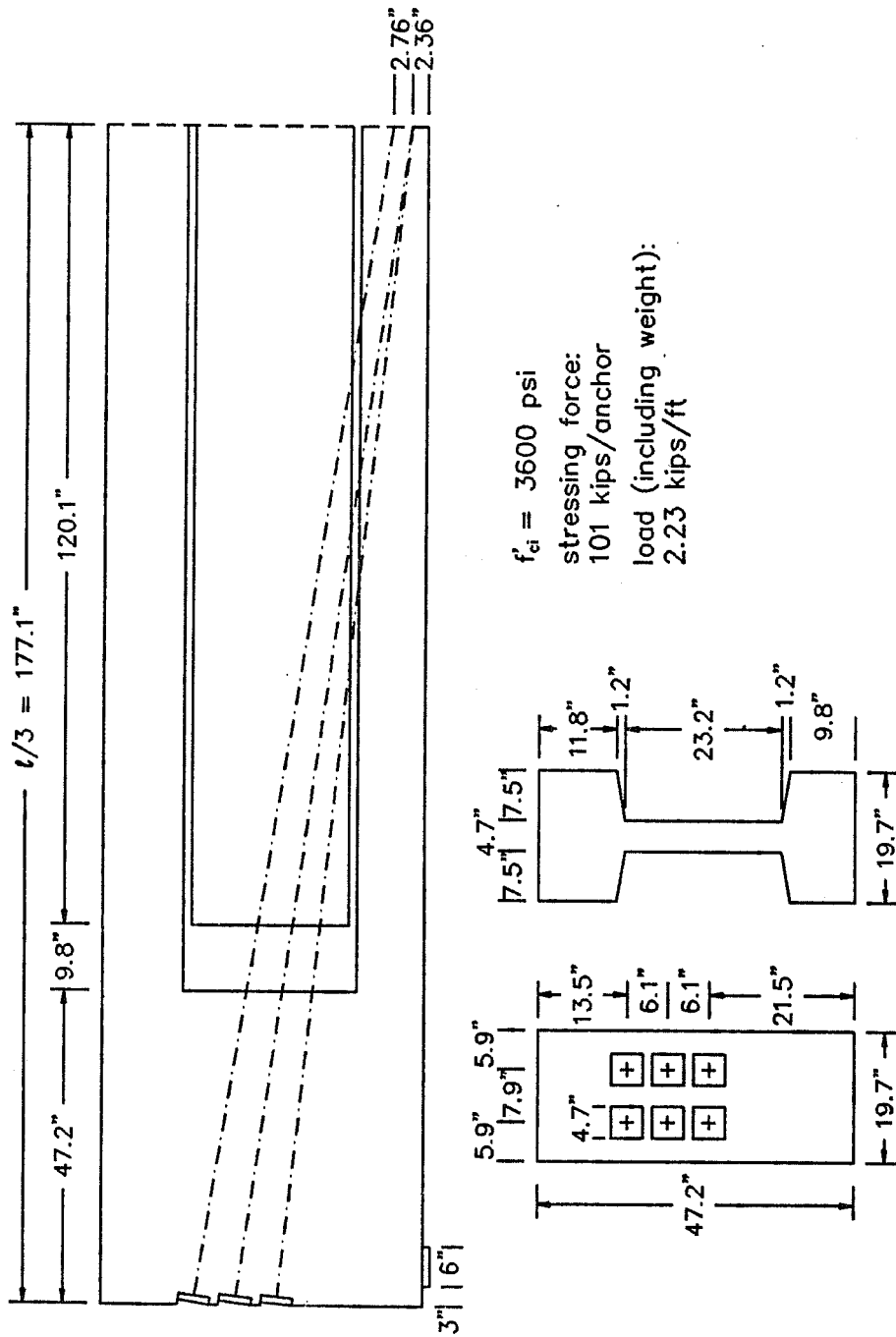


Figure 6.18 Revised CEB Problem With Customary Units

in this section. Figure 6.18 shows the same problem with customary units. Some revisions and additional assumptions are necessary to make the design example workable:

- To avoid exceeding allowable extreme fiber concrete stresses some load has to be present on the girder in addition to its weight. Assuming that the tendons are draped at the 1/3 points of the girder, a uniform load of 2.23 kips/ft is needed.
- The girder is supported on 6 in. wide bearings with their center 6 in. from the end faces of the girder.
- As shown in Section 6.4.2 the "anchorage steel rings" in the original problem statement (Figure 6.17) do not qualify as basic anchorage devices, and special anchorage devices are needed.
- The web of the I-section is too thin to accommodate two tendons in the same layer. However, this problem does not affect the procedures that are to be demonstrated with this design example and is ignored.

A load factor of 1.2 and a ϕ -factor of 0.85 will be used, as specified in the proposed anchorage zone specifications. For convenience in calculations, the ϕ -factor is included on the load side. Hence the tendon force used in the design problem is $(1.2/0.85) \times 101 = 142.6$ kips per anchor or a total force of 855.5 kips. The uniform load and the reaction force tend to reduce the bursting force and a load factor of 1.0 is used for these loads.

6.4.2 Local Zone Design

This section leads step by step through the design of the local zone.

1. Check if the anchors qualify as basic anchorage devices.

In the original problem statement circular anchor plates with a diameter $D = 120$ mm (4.7 in.) and a minimum spacing of 150 mm (5.9 in.) are used. The concrete cube strength is 30 MPa, corresponding to a cylinder strength of 25 Mpa or 3600 psi.

The area of the bearing plate is

$$A_b = 4.7^2 \pi / 4 = 17.3 \text{ in}^2,$$

and thus the bearing pressure is

$$f_b = 142.6 / 17.3 = 8.24 \text{ ksi.}$$

The maximum bearing pressure to qualify as a basic anchorage device is (Equation (6.4))

$$f_{b,\max} = 0.7 f'_{ci} \sqrt{A/A_b} = 0.7 \times 3.6 \times 5.9 / 4.7 = 3.16 \text{ ksi} < 8.24 \text{ ksi.}$$

Hence the anchors do not qualify as basic anchorage device and special anchorage devices are needed. Information on required edge distance, minimum anchor spacing, confinement and auxiliary reinforcement, and concrete strength should be provided by the anchorage device supplier.

2. Select a special anchorage device.

In this example the VSL EC 5-3 anchor is used. This anchor can accommodate three ½ in. strands, GR 270, with a maximum stressing force of $0.8 \times 0.153 \text{ in}^2 \times 270 \text{ ksi} \times 3 = 99 \text{ kips}$. This is close enough to the specified stressing force of 101 kips in the design problem.

Figure 6.19 shows manufacturer's specifications for the anchorage device [55]. The EC 5-3 anchor is a square anchor with bearing plate widths of 120 mm (4.7 in.). The minimum spacing is 155 mm (6.1 in.). The minimum edge distance is one-half the spiral diameter plus required cover ($5.1/2 + 1.5 = 4.1 \text{ in.}$). The anchor spacing in the original problem is 150 mm or 5.9 in. which has to be slightly increased to 6.1 in. to satisfy the manufacturers specifications.

Roberts' design equation for the capacity of the local zone (Equation (6.5), Reference 41) is used to find a spiral equivalent to the spiral specified in the manufacturer's information.

$$P_n = 0.7 f'_c \sqrt{\frac{A}{A_g}} A_b + 4 \frac{2 A_{sp} f_y}{D s} \left(1 - \frac{s}{D}\right)^2 A_{core} \quad (6.5)$$

The spiral specified by the manufacturer has a pitch, s , of $150/3 = 50 \text{ mm}$ (1.97 in.), an outside diameter, D , of 130 mm (5.1 in.), and a yield strength of 420 Mpa (~ 60 ksi). The cross sectional area of the bar is $10^2 \pi / 4 = 78.5 \text{ mm}^2$ or 0.12 in^2 . Hence the second term of Equation (6.5) divided by $4 A_{core}$ is

$$2 \times 0.12 \times 60 / (5.1 \times 1.97) \times (1 - 1.97/5.1)^2 = 0.54 \text{ ksi.}$$

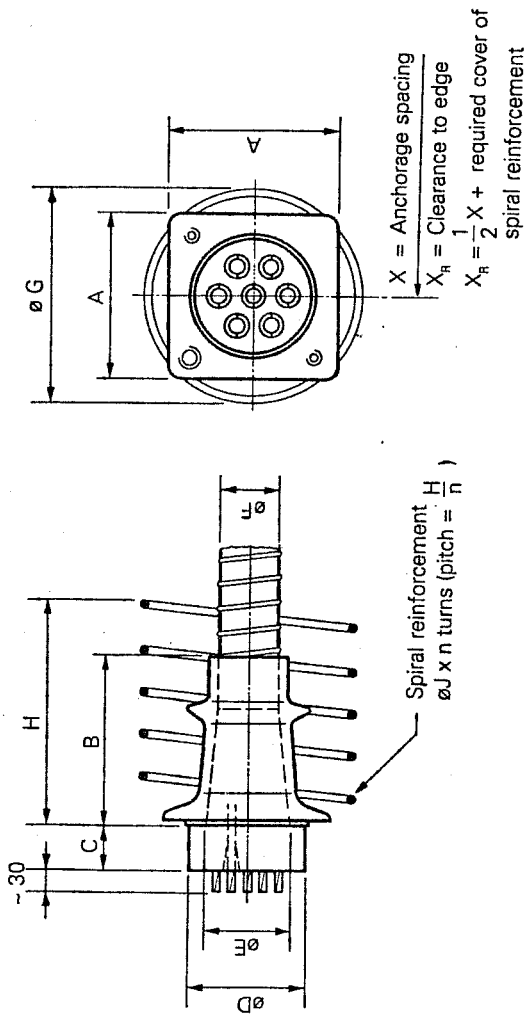
Try a #4 spiral, GR60, with a 2¼ in. pitch as equivalent spiral:

$$2 \times 0.20 \times 60 / (5.1 \times 2.25) \times (1 - 2.25/5.1)^2 = 0.65 \text{ ksi} > 0.54 \text{ ksi.}$$

∴ USE #4 spiral, $s=2\frac{1}{4}\text{in.}$, $D=5\frac{1}{8}\text{in.}$

3. Design the auxiliary reinforcement.

Ordinarily in the acceptance test of special anchorage devices auxiliary reinforcement is provided in addition to the local zone confinement reinforcement.



Tendon unit	A	B	C	ØD	ØE	ØF ¹⁾ internal/external	ØG	H	ØJ	n	X ²⁾
5-3	120	130	50	90	50	40/45	130	150	10	3	155

Dimensions in mm

- 1) Standard diameter for corrugated steel duct. For polyethylene ducts PT-PLUS™ see page 6.
 - 2) Anchorage spacings are in accordance with test requirements of CEB/FIP (Recommendations for acceptance and application of post-tensioning systems, March 1981). Modifications to these values may be possible.
- Dimensions are valid for:
- Nominal concrete strength at 28 days: 35 MPa (cube), 28 MPa (cylinder).
 - Yield strength of spiral reinforcement: ≥ 420 MPa.
 - Spirals may be replaced by suitable orthogonal reinforcement.
- Maximum prestressing force may be applied when concrete reaches 80 % of its nominal strength.
 Max. prestressing force is 75 % of min. tendon breaking load (temporary overstressing to 80 %).
 Dimensions for other concrete strengths on request.

Fig. 6.19 Manufacturer's Specifications for Special Anchorage Device (from [55])

Equivalent reinforcement should also be provided in the actual structure, according to the manufacturers specifications. Since no pertinent information is available in Figure 6.19, Equation (6.5) is used for design of the auxiliary reinforcement.

The supporting area, A , is 6.1^2 in^2 , the gross bearing plate area, A_g , is 4.7^2 in^2 .

The net bearing plate area is

$$A_b = 4.7^2 - 1.8^2 \pi / 4 = 19.6 \text{ in}^2.$$

The area of the concrete core confined by the spiral is

$$A_{\text{core}} = 5.1^2 \pi / 4 = 20.4 \text{ in}^2.$$

Thus the nominal capacity of the local zone is

$$\begin{aligned} P_n &= 0.7 \times 3.6 \times (6.1/4.7) \times 19.6 + 4 \times 0.65 \times 20.4 \\ &= 64.1 + 53.3 = 117.4 \text{ kips} < 142.6 \text{ kips}. \end{aligned}$$

The difference to the required capacity of 142.6 kips has to be made up by the auxiliary tie reinforcement. With tie reinforcement, dimension D is the length of the legs of the ties.

Try #3 ties spaced at 1.75 in.:

$$\begin{aligned} P_n &= 117.4 + 4 \times (0.11 \times 60) / (6.1 \times 1.75) \times (1 - 1.75/6.1)^2 \times 20.4 \\ &= 117.4 + 25.7 = 143.1 \text{ kips} > 142.6 \text{ kips} \end{aligned}$$

∴ USE #3 ties @ 1¾ in.

Following Roberts' recommendations the tie reinforcement is considered to be only half as effective as spirals, and for A_{core} the area confined by the spiral is used if both spiral and ties are available for confinement of the local zone. This approach is quite conservative resulting in a somewhat crowded detail (Figure 6.20). The spacing of the ties could be increased by increasing the concrete strength or by decreasing the pitch of the spiral. Ordinarily manufacturer's information should be available on the auxiliary reinforcement used in the acceptance test. This reinforcement should also be adequate for the actual application, and there would be no need to check Equation (6.5).

4. Investigate an alternative local zone detail.

Another method to reduce crowding of the local zone is to replace the spirals by closely spaced orthogonal ties. Such ties are roughly only half as effective as spirals, but the confined area, A_{core} , becomes larger if no spiral is used for confinement (D^2 versus $D^2 \pi / 4$).

Try #4 ties spaced at 1½ in.:

$$D = 6.1 - 0.5 = 5.6 \text{ in.}$$

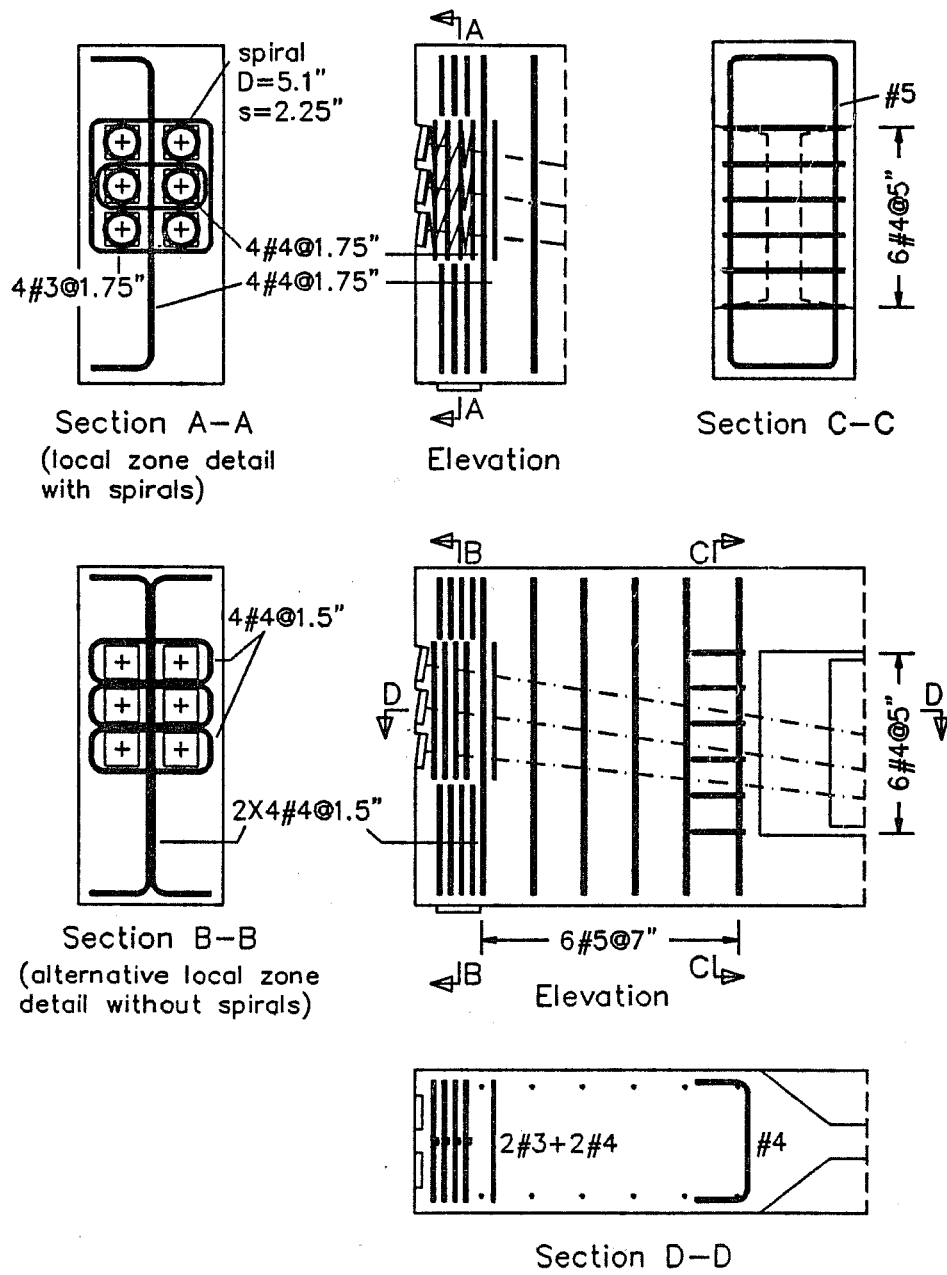


Figure 6.20 Reinforcement Details for CEB Problem

$$\begin{aligned}
 P_n &= 64.1 + 4 \times (0.20 \times 60) / (5.6 \times 1.5) \times (1 - 1.5/5.6)^2 \times 5.6^2 \\
 &= 64.1 + 96.1 = 160.2 \text{ kips} > 142.6 \text{ kips}
 \end{aligned}$$

∴ USE #4 ties @ 1½ in. (alternative detail).

Section B-B in Figure 6.20 shows this detail. The ties have to be bundled where they run adjacent to each other between the anchor plates. Alternatively, two overlapping #6 ties might be used. However, this is not a good detail, because the required center-to-center spacing of 1½ in. would violate the minimum clear spacing requirement of 1 in. and, more seriously, a solid wall of reinforcement would be created where the ties overlap.

6.4.3 General Zone Design

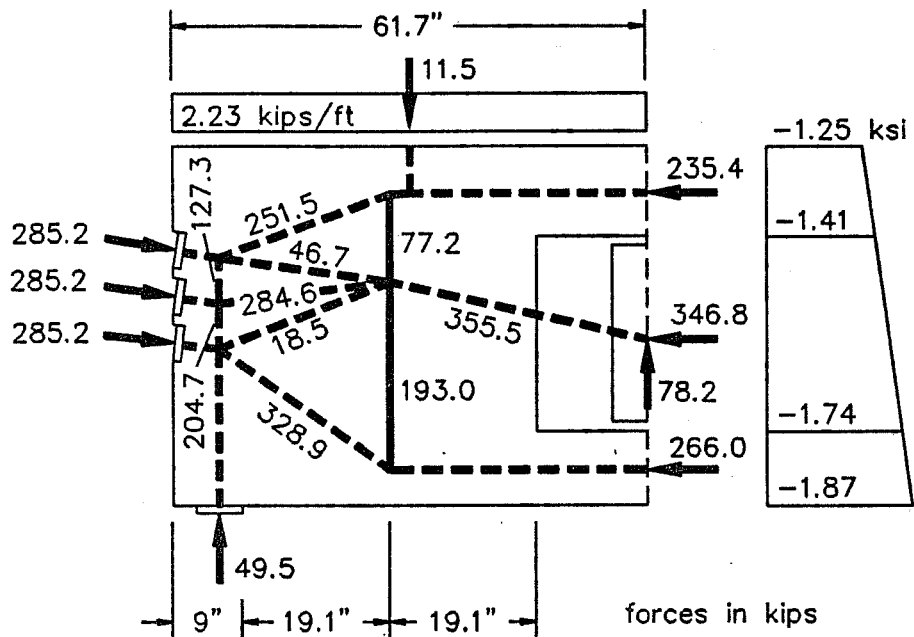
The approximate equations in the proposed anchorage zone specifications are limited to rectangular prismatic members and do not apply to the present problem. The following paragraphs lead step by step through the design of the general zone using strut-and-tie model procedures.

1. Determine the extent of the D-region.

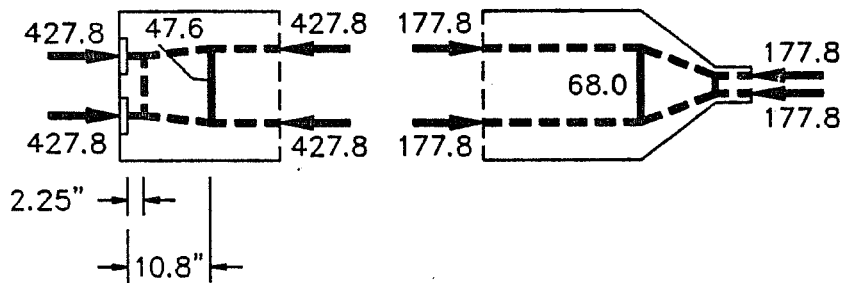
There are several discontinuities in the end region of the girder which disturb the stress distribution based on simple beam theory. The concentrated post-tensioning force and the reaction force are loading discontinuities, and the transition from the end block to the regular I-section is a geometric discontinuity. The region affected by these discontinuities extends approximately one girder height from the end of the reaction force bearing plate ($9 + 47.2 = 56.2$ in.) or one web width ahead of the end of the end block ($47.2 + 9.8 + 4.7 = 61.7$ in.). The second requirement controls and defines the end of the D-region.

2. Determine stress distribution and resultant forces at the end of the D-region.

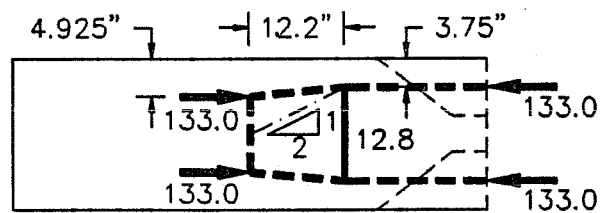
Simple beam theory is employed to find the stress distribution at the end of the D-region (Figure 6.21a). The resultant axial force in the web (346.8 kips) is determined by integrating the flexural stresses over the full girder height and the thickness of the web. The resultant forces in the flanges are determined by integrating over the flange areas outside the web. Resultant shear forces could be assigned based on the shear stress distribution (Section 3.4.7.2), but it is simpler and sufficiently accurate to assign all of the shear force to the web.



a) longitudinal section



b) horizontal section through web



c) horizontal section through bottom flange

Figure 6.21 Strut-and-Tie Model for CEB Problem

3. Select the location of the local zone nodes and of the bursting tie.

For simplicity the local zone nodes are selected 6 in. ahead of the anchor bearing plates, coinciding with the distance of the reaction force from the anchors. The closer to the anchors the local zone nodes are located, the smaller is the bursting force. However, the local zone nodes have to be far enough to accommodate the compression forces between the anchors.

For the bursting reinforcement a uniform arrangement of reinforcement between the end of the bearing plate for the reaction force and the begin of the transition from the end block to the regular section is envisioned. This fixes the location of the bursting tie midway between these points. Thus the distance from the end face of the girder is $9 + 19.1 = 28.1$ in. or 60% of the girder height (Figure 6.21a).

4. Draw the strut-and-tie model and determine the member forces.

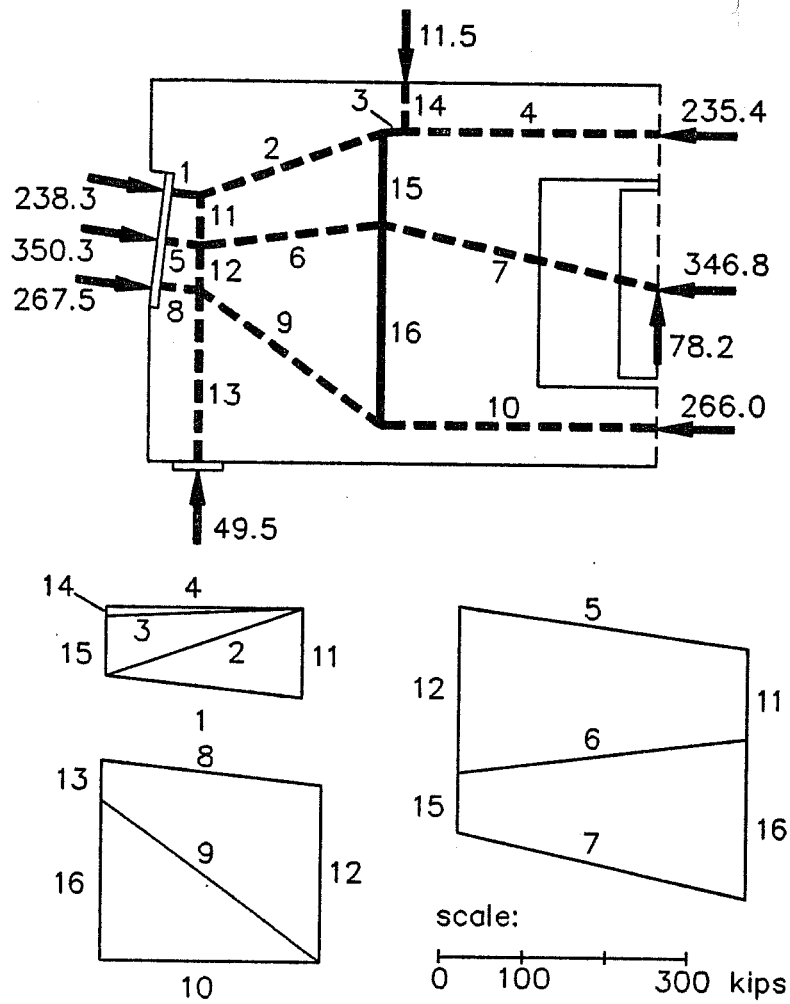
With the information found in the previous steps the strut-and-tie model for a longitudinal section through the girder is defined (Figure 6.21a). The member forces can be determined with sufficient accuracy by graphic procedures. Figure 6.22 shows a slightly different strut-and-tie model solution where force vector polygons for each node were used to construct the geometry of the strut-and-tie model and to determine the member forces graphically. Note that this is a kinematic model which is stable only for this particular load configuration.

5. Develop strut-and-tie models in the thin direction of the girder.

Figure 6.21b shows that tensile forces in the thin direction of the end block exist ahead of the anchor and at the transition from the end block to the thin web from the regular I-section. Small tensile forces are also found in the flanges of the I-section due to spreading of the compression stresses into the flanges (Figure 6.21c). Additional tensile forces in the thin direction of the member are induced by horizontal curvature of the tendons. This curvature is necessary because the tendons have to flare out from the thin web of the I-section to their final position at the loaded face of the end block.

6. Check the compression stresses.

Compression stresses may be critical immediately ahead of the anchor plates (bearing pressure), immediately outside the locally confined region (local zone-general zone interface), and at the transition from the end block to the thin web of the I-girder. Following Section 9.21.3.2.2 of the proposed specifications, the effective compression strength for



member forces (kips)			
1	-238.3	9	-331.2
2	-252.1	10	-266.0
3	-235.7	11	-111.7
4	-235.4	12	-206.2
5	-350.3	13	-49.5
6	-349.7	14	-11.5
7	-355.5	15	74.0
8	-267.5	16	197.3

Fig. 6.22 Graphical Determination of Member Forces

unconfined concrete is taken as

$$f_c = 0.7 f_{cl} = 0.7 \times 3.6 = 2.52 \text{ ksi.}$$

The adequacy of the confinement reinforcement to increase the bearing pressure sufficiently was already checked in Section 6.4.2. The stresses immediately ahead of the transition from end block to I-section are less than 1.87 ksi, which is below the effective concrete strength (Figure 6.21a).

The only remaining critical region is the local zone-general zone interface. Two checks are necessary:

1. The distance of the local zone nodes from the anchor plates, d_o , must be large enough to accommodate the vertical compression force between the anchors (204.7 kips, Figure 6.21a)
2. The compression stresses at the end of the confined region must be smaller than the effective concrete strength.

From the first requirement the minimum distance of the local zone nodes from the anchor plates is found to be

$$d_{o,\min} = \frac{1}{2} \times 204.7 \text{ kips} / (2 \times 4.7 \text{ in.} \times 2.52 \text{ ksi}) = 4.32 \text{ in.} < 6 \text{ in.}$$

In the calculation of $d_{o,\min}$ the strut area is taken as $(2 \times a) \times (2 \times d_{o,\min})$, where a is the side length of the anchor plates (4.7 in.). The minimum required distance is less than the actual distance, $d_o = 6$ in., and hence the first requirement is satisfied. The bursting force could be slightly reduced by moving the local zone nodes somewhat closer to the anchor plates.

For the second check information on the rate of spreading of the compression stresses is needed. Burdet observed that in two-dimensional problems the linear-elastic peak compression stress at a distance equal to one plate width ahead of the anchor is approximately 60% of the bearing pressure immediately ahead of the anchor plate [8]. Figure 6.23 shows that this relation is equivalent to assuming spreading of the compression stresses at a 1:3 ratio.

The anchorage devices used in this problem have local confinement reinforcement extending for 5.9 in. However, in Section 3.4.5 it is recommended to check the concrete compressive stresses at a distance not more than

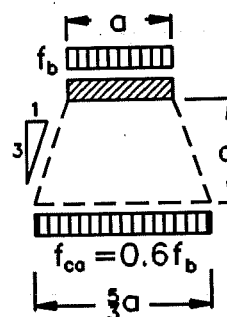


Fig. 6.23 Spreading of Compression Stresses

1.15 plate widths ahead of the anchors, which controls in this case ($1.15 \times 4.7 = 5.4$). Figure 6.24 shows the effective concrete area ahead of the locally confined region, assuming a 1:3 spreading of compression stresses in all directions, as discussed above. This area has to resist the total anchor force, hence

$$f_{ca} = (6 \times 142.6)/(16.2 \times 20.5) = 2.58 \text{ ksi.}$$

The effective concrete strength is

$$f_c = 0.7 f'_{cl} = 0.7 \times 3.6 = 2.52 \text{ ksi} \sim 2.58 \text{ ksi} \therefore \text{OK (2\% short).}$$

For practical purposes these two checks are sufficient to examine the local zone-general zone capacity. Figure 6.25 shows the more rigorous strut-and-tie model procedure to check the compression stresses. All compression struts are drawn with their minimum width so that the effective concrete compressive strength is nowhere exceeded. The effective concrete strength is $0.7 f'_{cl}$, except immediately ahead of the bearing plates, where local zone confinement enhances the effective concrete strength.

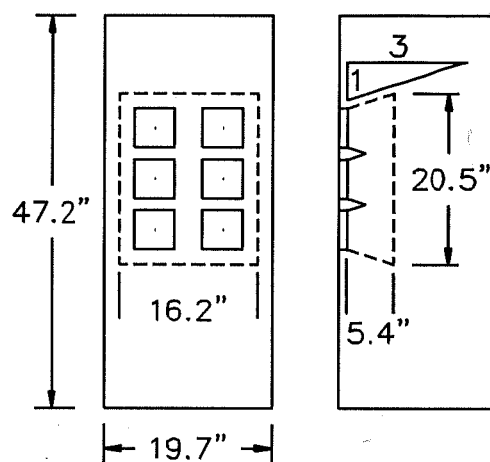
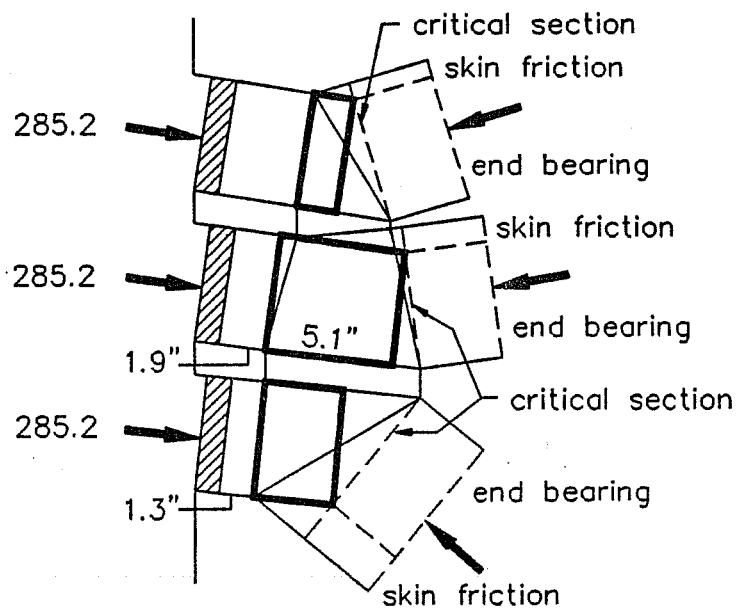
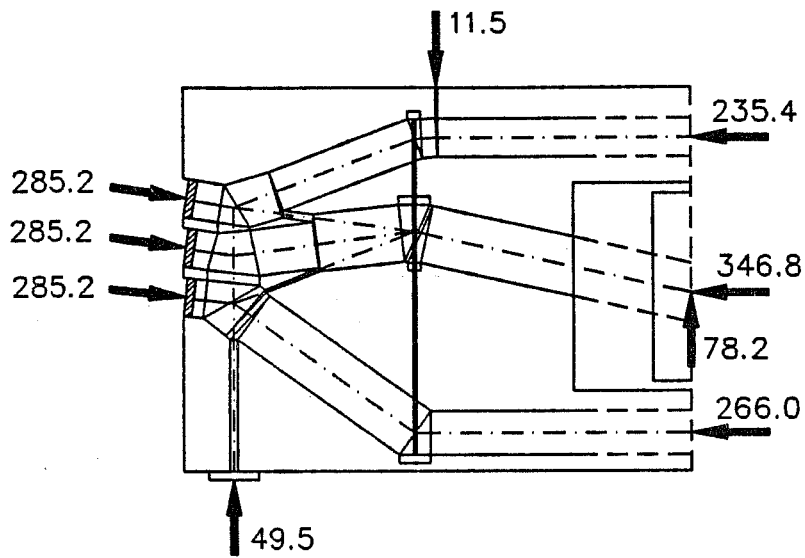


Fig. 6.24 Effective Concrete Area Ahead of Local Confinement Reinforcement

As pointed out in Sections 3.4.5 and 3.7.4 the full thickness of the end block (19.7 in.) may be used as effective thickness for the struts within the end block. The effective thickness in the I-region should be reduced to $19.7 - 4.7 = 15$ in. for the flange forces and to 4.7 in. for the web force (dashed strut portions in Figure 6.25). For simplicity the same effective thickness is used in the entire model, since the stresses in the I-section immediately ahead of the end block do not exceed the effective concrete strength (Figure 6.21a).

All nodes in the strut-and-tie model are hydrostatic nodes, except for the three nodes immediately ahead of the anchor plates. At hydrostatic nodes all struts are stressed to the same level and the boundaries of the nodes are perpendicular to the corresponding struts. Reference 48 includes an algorithm for the construction of hydrostatic nodes. The local zone node is the region within which the transition from the high bearing pressure to the lower effective concrete strength outside the confined region occurs. Hence hydrostatic



local zone detail

Figure 6.25 Check of Compression Stresses in Strut-and-Tie Model

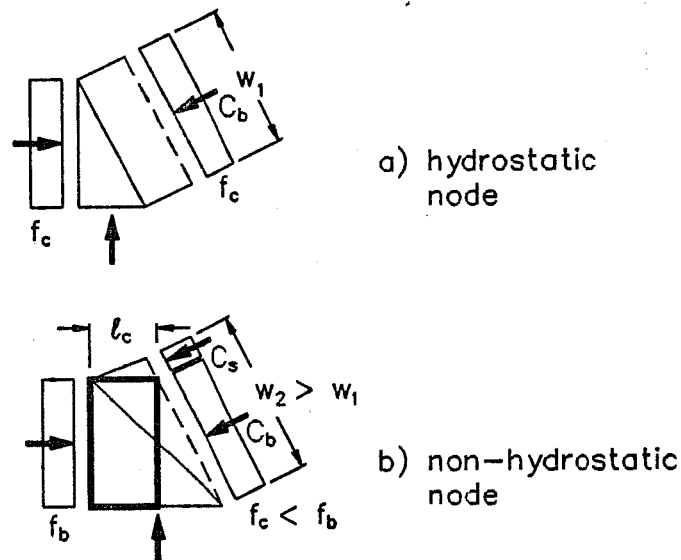


Figure 6.26 Local Zone Node

nodes are not possible at the local zone, when special anchorage devices are used. This is illustrated in Figure 6.26. The non-hydrostatic node in Figure 6.26b allows the strut width to increase from width w_1 to width w_2 . Part of the anchor force is transferred in end bearing (force C_b) as for the hydrostatic node. Additional capacity comes from the inclined compression strut C_s along the skin of the confined region ("skin friction", see Section 3.4.5). This concept is useful to estimate the required extent of the local zone confinement reinforcement (dimension l_c in Figure 6.26b).

The detail in Figure 6.25 shows the local zone nodes for the example problem. The fat lines indicate the minimum extent of the local confinement reinforcement for each anchor. As seen in the figure, the local zone nodes could be moved about 1.3 in. closer to the anchor plates. With this adjustment the required length of confinement is controlled by the center anchor and is

$$l_c = 5.1 + 1.9 - 1.3 = 5.7 \text{ in.} < 5.9 \text{ in.} \therefore \text{OK.}$$

The bursting force is reduced by approximately the same ratio as the distance from the local zone nodes to the bursting tie increases:

$$T_{\text{burst}} = 193.0 \times (28.1 - 1.3)/28.1 = 184.7 \text{ kips.}$$

This is a 4% decrease and quite negligible.

7. Select the reinforcement.

Table 6.2 lists the tensile forces in the anchorage zone, the corresponding reinforcement requirements, and the bars selected. Figure 6.20 shows all local and general zone details for the design problem.

Table 6.2 General Zone Reinforcement for Example Design Problem

action	force (kips)	reinforcement (in ²)	
		required	selected
transverse bursting	193.0	3.22	3.72 (12#5)
bursting in thin direction	47.6	0.79	1.24 (4#3+4#4) [*]
transition to I-section	68.0	1.13	1.20 (6#4)
flange bursting	12.8	0.21	0.93 (3#5) ^{**}

^{*}) partially provided by ties around local zone

^{**}) horizontal legs of transverse bursting reinforcement

#5 ties are selected for the bursting reinforcement for ease of construction. The spacing limitation of 12 in. (Appendix A, Section 9.21.3.4.5) would also allow the use of #6 ties. An extra closed tie close to the loaded face of the girder would be desirable but is not possible due to conflicts with the local zone reinforcement. Instead some of the bars provided for confinement of the local zone are extended over the full height of the girder (Figure 6.20, Section A-A, Section B-B). The primary purpose of this reinforcement is to tie into the "unstressed corners" of the girder. At the same time it satisfies Section 9.21.3.4.8 in the proposed anchorage zone specifications, which requires spalling reinforcement for 2% of the anchor force:

$$0.02 \times 855.5/60 = 0.29 \text{ in}^2 < 0.40 \text{ in}^2 \text{ (2#4)}.$$

The ties in the local zone are also effective to resist the bursting forces in the thin direction of the member. However, extra bursting reinforcement is added to achieve better agreement with the location of the tie used in the design model (Figure 6.20, section D-D, and Figure 6.21b).

Although much attention was paid to proper detailing, it is very difficult to avoid congestion of the local zone for the given problem due to the presence of six closely spaced anchors. This problem could be eliminated by using larger tendons (for example

three 6-½ in. strand tendons) and by distributing the anchors better over the height of the girder.

6.4.4 Discussion

The design example worked in this section is based on a design problem used in a 1987 CEB survey among European designers (Figure 6.17). Designers were asked to calculate among other things the transverse tensile force in the anchorage zone and the required area of transverse reinforcement. Six responses were received. The range of solutions varied almost by a factor of ten, as shown in Table 6.3 [8].

Table 6.3 Range of Results for CEB Problem

	CEB survey results		example problem
	minimum	maximum	
bursting force (kips)	11	99	137
bursting reinforcement (in ²)	0.32	3.1	3.22

Table 6.3 also includes the results found in the previous section. The bursting force of 193 kips (Figure 6.21) includes load and ϕ -factors and was readjusted in the table ($193 \times 0.85/1.2 = 137$ kips). Bursting force and required bursting reinforcement are slightly higher than the high-end responses to the CEB survey. It is noted that Guyon's solution (Section 2.1.2.2) to this problem gives a bursting force of

$$T_{burst} = \frac{1}{4}P(1-a/h) = (6 \times 101)/4 \times (1-16.9/47.2) = 97 \text{ kips.}$$

This is very close to the maximum bursting force found in the CEB survey. In fact, many code provisions for bursting reinforcement requirements are based on Guyon's solution and it is quite surprising that many respondents to the CEB survey indicated a significantly lower bursting force. Actually Guyon's solution is limited to rectangular, prismatic members, and hence does not apply to the I-girder in the CEB problem. In I-girders, the compression stresses have to spread out further, and consequently the bursting force should be even larger (Section 2.1.2.2). This is reflected by the results obtained in the design example.

7 SUMMARY AND CONCLUSIONS

7.1 Summary of Overall Study

In this study and its companion investigations (References 8, 17, 41, and 44) a synthesis of evaluation of literature, linear-elastic analysis, strut-and-tie model procedures, and experimental tests was used to accomplish the following objectives:

- To increase the understanding of a wide range of specific anchorage zone problems.
- To derive general and logical procedures for the design of anchorage zones.
- To develop provisions for a standardized acceptance test for anchorage devices.
- To implement all findings in a proposal for anchorage zone specifications and commentary, suitable for inclusion in current AASHTO specifications.

The specific anchorage zone problems investigated in the overall study included:

- Study of the isolated region surrounding and immediately ahead of anchorage devices (local zone) [41].
 - Anchorage zones at the end of girders. Variables included tendon eccentricity, tendon curvature, number of tendons, arrangement of multiple anchors, shape of cross section [8, 44], and presence of a reaction force in the anchorage zone (Chapter 3 of this study).
 - Intermediate anchors in isolated slab blisters, in corner blisters, and in ribs (Chapter 4 of this study).
 - Anchorage of closely spaced anchors in slabs [17].
 - Anchorage of external tendons in diaphragms (Chapter 5 of present study).

Based on the study of these specific anchorage zone problems general recommendations for design and detailing of anchorage zones were derived. They are discussed in Chapters 2 and 6 of this study and are implemented in the proposed anchorage zone specifications (Appendices A and B). The main concerns in the design of anchorage zones are the high compression stresses immediately ahead of the anchorage device and tensile stresses in the remainder of the anchorage zone. These tensile stresses are induced by spreading of the concentrated tendon force into the overall structure. Failure

of unreinforced anchorage zones is controlled by either crushing of the concrete due to excessive lateral strains or by splitting due to excessive lateral tensile stresses. Confinement reinforcement is effective to delay the crushing failure mode, while bursting reinforcement is needed to carry the tensile stresses in the anchorage zone after splitting cracks have occurred.

Two key concepts were formulated and tested in this study:

- The division of the anchorage zone into a local zone and a general zone, to clarify the responsibilities of anchorage device supplier, engineer of record, and constructor.
- The use of strut-and-tie models for the design of anchorage zones as a quick practical design method.

7.2 Local Zone and General Zone Concept

Because high compressive stresses occur only locally ahead of the anchorage device, it is useful to provide local confinement reinforcement to delay the crushing failure and to enhance the bearing capacity. In European practice such reinforcement, together with other requirements for the performance of the anchorage device, are specified by the anchorage device supplier and are verified in a standardized acceptance test. In US practice no such procedure exists and there has been considerable confusion about the responsibilities for design and payment of the reinforcement in anchorage zones [6].

The division of the anchorage zone into a local zone and a general zone is an attempt to alleviate this confusion. The local zone is the region immediately ahead of the anchorage device subject to high compression stresses. For simplicity, in the proposed anchorage zone specifications the local zone is defined geometrically, although a definition based on the compressive stress levels in the concrete ahead of the anchorage device may be more logical [42]. The performance of the local zone is the responsibility of the anchorage device supplier. Adequate performance may be proven by a standardized acceptance test. The responsibilities of the supplier are limited to providing the anchorage device proper and information on the requirements for the anchorage device to pass the acceptance test.

The general zone is a larger region ahead of and behind anchorage devices, within which the concentrated compression stresses ahead of the anchor spread out over the

cross section of the member. Design of the general zone is the responsibility of the engineer of record. Originally a strict separation of local zone and general zone was envisioned. However, when the anchor plate is large compared to the thickness of the member, local zone effects (high compressive stresses) and general zone effects (bursting stresses) occur in the same region. For this reason in the final version of the proposed anchorage zone provisions the general zone includes the local zone and is identical to the overall anchorage zone (Appendix A, Section 9.21.2.1).

The acceptance test is in fact a test of the isolated local zone of an anchorage device. Thus the information provided by the anchorage device supplier is independent from the specific application. It is the responsibility of the engineer of record to evaluate the applicability of the anchorage device for the actual structure and to adapt the details of the acceptance test for the particular application.

It should be recognized that the local zone is inherently a region susceptible to congestion, due to the presence of confinement reinforcement which has to be closely spaced to be effective. Extra attention should be paid to this fact in design and construction. This is probably the most important and most effective measure to avoid anchorage zone problems.

7.3 Use of Strut-and-Tie Models for the Design of Anchorage Zones

Traditionally the design of anchorage zones is based on linear-elastic solutions. However, classical analytical solutions are sorely limited in their applicability. Modern numerical procedures (finite element analysis) require access to a computer and considerable efforts for the interpretation of the analysis results.

Strut-and-tie models offer an attractive alternative. By concentrating on equilibrium conditions alone strut-and-tie models offer a quick method to model primary load paths in the structure and to proportion the reinforcement with adequate accuracy for design purposes. In fact, this approach has been used for almost 100 years, beginning in 1899 with Ritter's truss model for shear in beams. Modern strut-and-tie models extend this approach to include the check of critical compression stresses in the structure.

One of the major advantages of strut-and-tie models is that the designer is led to visualize a global load path. The structure is idealized as a truss. Familiar truss analysis procedures can be employed to find the member forces which are then used to proportion

the reinforcement and to check the concrete dimensions.

One of the more delicate problems with strut-and-tie models is the choice of the effective concrete compressive strength, $f_c = \nu_e f'_c$. The effectiveness factor, ν_e , depends on a large number of variables and is generally in the range from 0.35 to 0.85. Efforts to establish general guidelines for the choice of the effectiveness factor have been made only in recent years and much more research is needed in this area. In this study an effectiveness factor of 0.7 was used and gave conservative failure load predictions for all test specimens .

Another problem with strut-and-tie models is the lack of compatibility requirements. This problem can be eliminated by following a set of simple rules for the development of strut-and-tie models (see Chapter 6). However, with more complex problems it is recommended to complement strut-and-tie models with finite element analysis.

7.4 Conclusions

7.4.1 General Conclusions

Figures 7.1 and 7.2 show comparisons of the finite element predictions and the strut-and-tie model predictions to the actual failure loads of the specimens investigated in this study. A few predictions are controlled by the capacity of the local zone which was determined from Roberts' best fit equation [41]. The calculated failure loads are conservative in most cases and are unconservative by less than 5% otherwise. The finite element analysis and strut-and-tie model predictions are based on the procedures specified in the proposed code provisions (Appendices A and B). In particular, the effective concrete strength was taken as $0.7 f'_{cl}$ and the concrete tensile strength was disregarded. As indicated in the figures, significant conservatism is introduced by neglecting the concrete tensile strength. However, in general, this approach is necessary due to the non ductile behavior of concrete in tension and its unreliable tensile strength.

Both procedures are safe and are recommended for design of anchorage zones in the proposed specifications. Practically, a combination of strut-and-tie model procedure and finite element analysis may be most useful in complicated cases. The finite element analysis results can be used to find critical regions in the structure and to serve as guidance for the selection of the geometry of the strut-and-tie model. Strut-and-tie model procedures are then employed to proportion the primary reinforcement and to check the

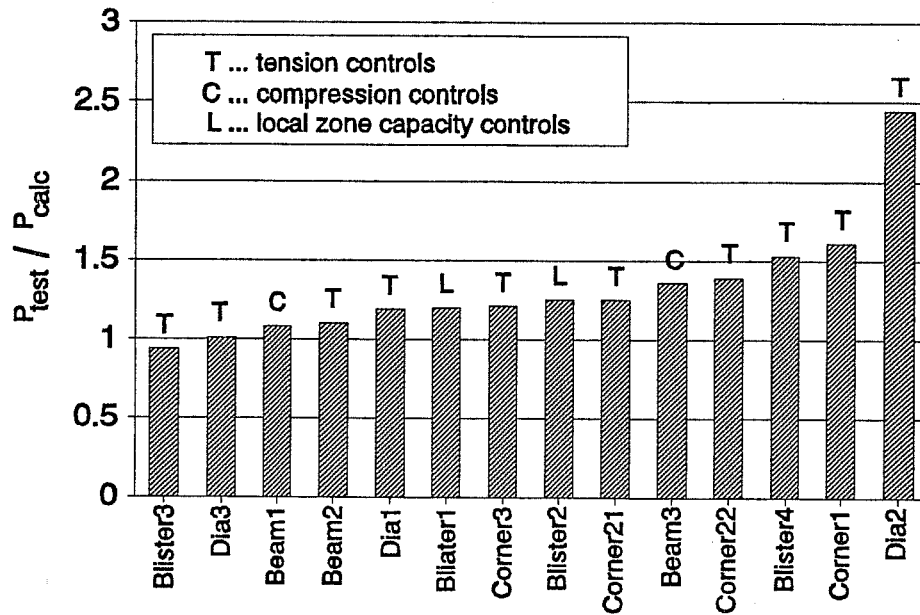


Figure 7.1 Finite Element Analysis Predictions

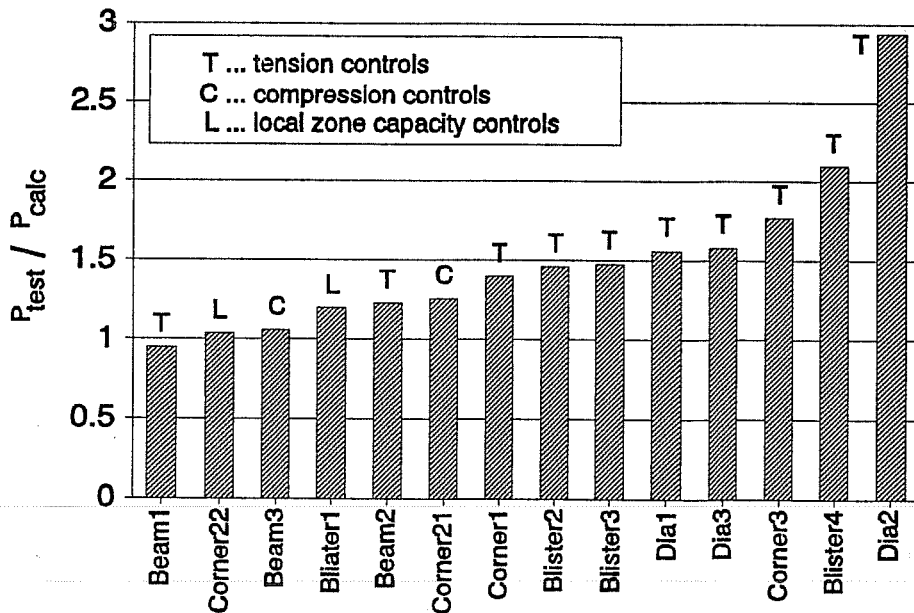


Figure 7.2 Strut-and-Tie Model Predictions

member dimensions. Additional nominal reinforcement may be required where the finite element solution indicates tensile stresses which are not captured by the strut-and-tie model.

Neither method is suitable for recipe-type solutions or black box procedures. Engineering judgement is required for the interpretation of linear-elastic finite element analysis results as well as for the development of good strut-and-tie models.

7.4.2 End Anchorages and the Influence of Support Reactions

This portion of the study included analytical studies and three experimental tests of concentrically post-tensioned members with and without a reaction force in the anchorage zone. The primary conclusions are summarized below. A more detailed discussion is included in Chapter 3.

1.) Magnitude and location of the linear-elastic bursting stresses and the resulting bursting force in the wide direction of a girder (transverse bursting) are affected by the presence of a reaction force in the anchorage zone. For small tendon eccentricity and if no flexural tensile stresses exist at the end of the anchorage zone, this influence is conservative and can be neglected. For example, a reaction force between 8% and 20% of a concentric tendon force reduces the maximum transverse bursting stress by some 20%, independent of the magnitude of the reaction force.

2.) Failure of thin members is controlled by concrete crushing due to excessive lateral strains in the thin direction of the member. Failures in the experimental program were explosive and occurred with little warning. The influence of a reaction force in the anchorage zone on this failure mode is small. Hence, confinement reinforcement in the thin direction of the member is more critical than bursting reinforcement in the wide direction. However, in the experimental program all failures were preceded by yielding of at least one or two ties of the bursting reinforcement at 83% to 94% of the failure load. Tie strains were largest about one plate width ahead of the anchor and diminished rapidly with the distance from the anchor due to the contribution of uncracked concrete in tension.

3.) The presence of bursting stresses makes cracking in the anchorage zone, particularly along the tendon path, a very real possibility. Such cracking is harmless if properly designed and detailed bursting reinforcement is present in the anchorage zone. In the experimental program first cracking occurred as low as 5% above the service load.

Maximum crack widths at first yield (1.2 to 1.6 service loads) were 0.01 in. to 0.02 in.

4.) Spalling stresses along the loaded edge of a member may be induced by local compatibility requirements (for example in concentrically loaded members). Spalling stresses may also be required for equilibrium in order to satisfy a linear strain distribution and the corresponding stress distribution at the end of the anchorage zone (for example the tie force between widely spaced multiple anchors (Figure 6.14c)). Only compatibility induced spalling stresses are relieved upon concrete cracking.

7.4.3 *Intermediate Anchorages in Blisters and Ribs*

This portion of the study included the anchorage of internal tendons in isolated slab blisters, corner blisters, and ribs, and the anchorage of external tendons in corner blisters. The experimental program included three isolated slab blisters and one rib anchorage with internal tendons, three corner blisters with internal tendons, and one corner blister with an external tendon (Chapter 4). The most important conclusions are:

1.) In the experimental program failure of all specimens was controlled by crushing of the concrete surrounding and ahead of the local zone confinement reinforcement. Failures were preceded by yielding of the ties surrounding the local zone.

2.) The region of tendon curvature was another critical region in the structure. Deviation forces induced by the curvature of the tendon must be tied back. This region is particularly sensitive, because frequently a gradual curvature is envisioned in design, but the tendon is sharply kinked in the field.

3.) Cracking behind the anchor is virtually unavoidable due to the presence of stress concentrations at the reentrant corner behind the blister or rib. In the experimental program cracks occurred at load levels as low as 60% of the service load. However the cracks propagated very slowly through the thickness of the slab and crack widths at service load were below 0.004 in. in all cases. For both blister anchorages and embedded anchors reinforcement proportioned to carry 25% of the tendon force is quite adequate to control cracking behind the anchor. In addition, intermediate anchorages should not be placed in regions where tensile stresses from other loads exist behind the anchor.

4.) Based on finite element analysis results and strut-and-tie model results, as a rule of thumb the slab bursting force can generally be taken as 20 to 25% of the anchor force. Additional reinforcement is required for lateral bending effects in the region of tendon

curvature. In this region the concentrated tendon deviation force is balanced by shear stresses which are distributed over the slab width. In the experimental program the capacity of the slab bursting reinforcement was of secondary importance due to limited concrete cracking.

5.) Anchorage in a rib rather than an isolated slab blister reduces the linear-elastic tensile stresses behind the anchor. A rib also provides better confinement for the local zone and facilitates faster dispersal of the concentrated compressive stresses ahead of the anchor. A disadvantage of rib anchorages is the larger lateral bending moment in the region of tendon curvature.

6.) Local bending moments and corbel action introduced by the eccentricity of the tendon are reduced if the anchorage blister is located in the web-flange junction of the cross section. However, for blisters with internal tendons these local effects are not critical because a load path in more direct compression is available. Hence, properly designed isolated slab blisters are quite acceptable. In contrast, for blisters with external tendons, corbel action forces and local bending moments are significantly greater and are essential for equilibrium. Therefore such anchors should always be placed in the web-flange junction of the cross section to minimize local bending effects. An additional advantage of corner blisters over isolated slab blisters is the better confinement of the local zone provided by the concrete in the adjacent portions of web and flange.

7.4.4 *Diaphragms for the Anchorage of External Tendons*

This portion of the study investigated the behavior of end diaphragms when used as reactions for the anchorage of external tendons (Chapter 5). The experimental program included three tests. The main conclusions are:

1.) Diaphragms for the anchorage of external tendons act to a large degree as deep beams spanning between the flanges of the cross section and across the flange-web corners. Hence, classical solutions which were developed for prismatic members (Guyon [22]) are not applicable and are unsafe.

2.) Critical compression stresses occur ahead of the anchor plate and at the transition from the massive diaphragm to the thin members of the regular section. Critical tensile stresses are induced by deep beam action. In the experimental program all failures involved either concrete crushing in the flanges immediately ahead of the diaphragm or

collapse of the shear transfer across the diaphragm-flange interface. These failures were preceded by yielding of the reinforcement across the diaphragm-flange interface. The behavior of the local zone was not critical due to the presence of substantial confining concrete in the massive diaphragm.

3.) Both finite element analysis predictions and strut-and-tie model predictions were controlled by the capacity of the bursting reinforcement and were very conservative in some cases. Significant contributions of reinforcement dowel action and of uncracked concrete in tension are believed to be the reasons for this conservatism.

7.5 Proposed Anchorage Zone Specifications

7.5.1 General

Appendices A and B include proposals for anchorage zone specifications and commentary, respectively, suitable for inclusion in the current AASHTO code [1]. The objectives of the proposed specifications are:

- To increase the awareness of design engineers and constructors of the special requirements in anchorage zones.
- To specify load and resistance factors for the design of anchorage zones.
- To define local zone and general zone and the related responsibilities.
- To specify general procedures for the design of anchorage zones.
- To specify simplified methods for the design of anchorage zones in simple cases.
- To delineate basic and special anchorage devices and to specify an acceptance test procedure for special anchorage devices.

The proposed code is quite a comprehensive document. Most codes only give recommendations on the bursting reinforcement which are (or should be) constricted to rectangular, prismatic members. In the proposed specifications all efforts were made to cover a wider range of applications, on one hand by defining other forces besides the bursting force in the anchorage zone, such as spalling and edge tension forces, on the other hand by providing general procedures for the design of anchorage zones. The objective of the proposed specifications is not only to regulate but also to educate. It may be questionable how much a code is the proper place to educate the engineering community, but this approach was deemed necessary, because a large number of

anchorage zone problems is due to the lack of such education. However, the code proposal could be significantly abridged by eliminating some of the very specific provisions in favor of more general language. Specific guidelines could be included in handbooks, together with design examples. Thus the tasks of education and of regulation could be separated, which would allow for much sleeker anchorage zone specifications. The proposed specifications comprise six major sections which are discussed below.

7.5.2 Load and Resistance Factors

A load factor of 1.2 applied to the tendon force during the stressing operation and a ϕ -factor of 0.85 are specified. These proposals are the result of engineering judgement and much industry input. They compare well with current code provisions for other loads and load effects and also ensure that reinforcement and concrete stresses under service load do not control.

7.5.3 Definition of the Anchorage Zone Geometry

Section 9.21.1 of the proposed specifications includes very precise definitions of the anchorage zone. However, its main purpose is more educational. It is intended to alert the user of the code to the existence of a region ahead and behind the anchor where simple beam theory is not valid.

7.5.4 Responsibilities

Section 9.21.2 of the proposed specifications defines the responsibilities of engineer of record, anchorage device supplier, and constructor. For this purpose the anchorage zone is divided into the local zone and the general zone. In general, the only concern of the anchorage device supplier is the local zone. The supplier's responsibilities are limited to furnish anchorage devices which can pass certain acceptance tests and to provide all information necessary for the proper performance of the anchorage device in the acceptance test. Basis for the division into a local zone and a general zone are tests by Roberts [41] which indicated that anchorage devices and local zone details that can pass an isolated local zone test perform equally well or better when used in an actual structure.

7.5.5 Design of the General Zone

Section 9.21.3 of the proposed specifications includes general design principles and detailing requirements. It focuses mainly on identifying the critical regions and critical force effects in the anchorage zone. These are the high compressive stresses immediately ahead of the anchorage device, ahead of local confinement reinforcement, and at geometric or loading discontinuities. Critical tensile forces include the bursting force and the edge tension forces. These general specifications are supplemented by provisions for some special cases (intermediate anchorages, diaphragms, and multiple slab anchors).

Provisions for design procedures are included in Sections 9.21.4 through 9.21.6. Both finite element analysis and strut-and-tie model procedures are addressed in the code. Section 9.21.6 describes approximate methods which apply in simple cases. These methods are essentially based on the evaluation of linear-elastic finite element analysis results [8].

7.5.6 Design of the Local Zone

Section 9.21.7 of the proposed specifications includes precise geometric definitions of the local zone and defines basic anchorage devices and conditions for which no acceptance test for the transfer of the anchor force to the concrete is required. These provisions and the provisions discussed in the next section are based on the study by Roberts [41].

7.5.7 Special Anchorage Device Acceptance Test

Division II, Section 10.3.2.3 of the proposed code provides specifications for a standardized acceptance test for special anchorage devices. This test is to verify the transfer of the post-tensioning force from the anchor to the surrounding concrete for anchors that do not qualify as basic anchorage device. Both special and basic anchorage devices have to pass an acceptance test for the transfer of the post-tensioning force from the tendon to the anchor.

7.6 Recommendations for Further Research

7.6.1 Variability of Concrete Strength

The experimental portion of this study was limited to a small number of tests for each specific anchorage zone problems. The failure mode of the specimens was very much

influenced by concrete tensile and compressive strength and consequently the test results had a fairly large scatter. It would be desirable to perform a large number of systematic tests with a minimum of variables and measurements to gain a better understanding of the influence of the variability of the concrete strength.

7.6.2 Local Zone-General Zone Interaction

Roberts' study showed that details that perform well in an isolated local zone test usually perform even better when used in the overall anchorage zone [41]. However, the number of local zone-general zone interaction tests was limited. Additional experimental investigations should provide quantitative expressions to estimate the beneficial effects of the interaction between general zone and local zone. Such expressions could be used to justify reducing the amount of confinement reinforcement in the local zone and consequently to relieve congestion in this region.

7.6.3 Extent of Cracking in the Anchorage Zone

The contribution of uncracked concrete in tension was an important factor for the behavior of the specimens of this study. In actual applications it is conceivable that the anchorage zone is precracked from other load effects or constraints which would eliminate the concrete tensile strength contributions. More research is needed to estimate the potential for such cracking and its ramifications for design and detailing of anchorage zones.

7.6.4 Effective Concrete Compressive Strength for Strut-and-Tie Models

The failure load of anchorage zones is controlled to a large extent by the compressive strength of concrete and careful selection of the effective concrete strength is particularly important. Current recommendations in the literature are not sufficiently supported by experimental evidence and more experimental research is needed to establish general guidelines for the selection of the effectiveness factor for a wide variety of applications.

7.6.5 Development of Interactive Design Programs for D-Regions

Although strut-and-tie model procedures are quite suitable for hand calculations

their power can be much increased by implementation into a computer program [48]. Such programs should provide an interactive procedure for the development of the geometry of the strut-and-tie model and should automate the determination of member forces, minimum strut widths, and reinforcement requirements. With modern hardware and graphics capabilities the strut-and-tie model can be made a very powerful method to visualize and check the flow of forces in a structure, when more conventional design methods do not apply.

APPENDIX A PROPOSED POST-TENSIONED ANCHORAGE ZONE PROVISIONS FOR INCLUSION IN THE AASHTO BRIDGE SPECIFICATIONS

DIVISION I - DESIGN

9.1.2 Notations [add to current Section 9.1.2]

F_{pu} = guaranteed ultimate strength of the prestressing tendon, $A_s^* f_s$

P_u = factored tendon force

9.1.3 Definitions [add to current Section 9.1.3]

Anchorage Device - The hardware assembly used for transferring a post-tensioning force from the tendon wires, strands or bars to the concrete.

Anchorage Spacing - Center-to-center spacing of anchorage devices.

Anchorage Zone - The portion of the structure in which the concentrated prestressing force is transferred from the anchorage device onto the concrete (Local Zone), and then distributed more widely into the structure (General Zone)(Section 9.21.1).

Basic Anchorage Device - Anchorage device meeting the restricted bearing stress and minimum plate stiffness requirements of Sections 9.21.7.2.2 through 9.21.7.2.4; no acceptance test is required for Basic Anchorage Devices.

Diaphragm - Transverse stiffener in girders to maintain section geometry.

Edge Distance - Distance from the center of the anchorage device to the edge of the concrete member.

End Anchorage - Length of reinforcement, or mechanical anchor, or hook, or combination thereof, beyond point of zero stress in reinforcement. [Delete remainder of current definition]

General Zone - Region within which the concentrated prestressing force spreads out to a more linear stress distribution over the cross section of the member (Saint Venant Region)(Section 9.21.2.1).

Intermediate Anchorage - Anchorage not located at the end surface of a member or

segment; usually in the form of embedded anchors, blisters, ribs, or recess pockets.

Local Zone - The volume of concrete surrounding and immediately ahead of the anchorage device, subjected to high local bearing stresses (Section 9.21.2.2).

Special Anchorage Device - Anchorage device whose adequacy must be proven experimentally in the standardized acceptance tests of Division II, Section 10.3.2.3. Most multi-plane anchorages and all bond anchorages are Special Anchorage Devices.

9.14 LOAD FACTORS [add underlined to current Section 9.14]

The computed strength capacity shall not be less than the largest value from load factor design in Section 3.22. For the design of anchorage zones a load factor of 1.2 shall be applied to the maximum tendon jacking force.

The following strength capacity reduction factors shall be used:

For factory produced precast prestressed concrete members $\phi = 1.0$

For post-tensioned cast-in-place concrete members $\phi = 0.95$

For shear $\phi = 0.90$

For anchorage zones $\phi = 0.85$ for normalweight concrete
and $\phi = 0.70$ for lightweight concrete.

9.21 POST-TENSIONED ANCHORAGE ZONES

9.21.1 Geometry of the Anchorage Zone

9.21.1.1 The anchorage zone is geometrically defined as the volume of concrete through which the concentrated prestressing force at the anchorage device spreads transversely to a linear stress distribution across the entire cross section.

9.21.1.2 For anchorage zones at the end of a member or segment, the transverse dimensions may be taken as the depth and width of the section. The longitudinal extent of the anchorage zone in the direction of the tendon (ahead of the anchorage) shall be taken as not less than the larger transverse dimension but not more than one and one-half times that dimension.

9.21.1.3 For intermediate anchorages in addition to the length of Section 9.21.1.2 the anchorage zone shall be considered to also extend in the opposite direction for a distance

not less than the larger transverse dimension.

9.21.1.4 For multiple slab anchorages, both width and length of the anchorage zone shall be taken as equal to the center-to-center spacing between stressed tendons, but not more the length of the slab in the direction of the tendon axis. The thickness of the anchorage zone shall be taken equal to the thickness of the slab.

9.21.1.5 For design purposes, the anchorage zone shall be considered as comprised of two regions; the *general zone* as defined in Section 9.21.2.1 and the *local zone* as defined in Section 9.21.2.2.

9.21.2 General Zone and Local Zone

9.21.2.1 General Zone

9.21.2.1.1 The geometric extent of the general zone is identical to that of the overall anchorage zone as defined in Section 9.21.1 and includes the local zone.

9.21.2.1.2 Design of general zones shall meet the requirements of Sections 9.14 and 9.21.3.

9.21.2.2 Local Zone

9.21.2.2.1 The local zone is defined as the rectangular prism (or equivalent rectangular prism for circular or oval anchorages) of concrete surrounding and immediately ahead of the anchorage device and any integral confining reinforcement. The dimensions of the local zone are defined in Section 9.21.7.

9.21.2.2.2 Design of local zones shall meet the requirements of Sections 9.14 and 9.21.7 or shall be based on the results of experimental tests required in Section 9.21.7.3 and described in Section 10.3.2.3 of Division II. Anchorage devices based on the acceptance test of Division II, Section 10.3.2.3, are referred to as *special anchorage devices*.

9.21.2.3 Responsibilities

9.21.2.3.1 The engineer of record is responsible for the overall design and approval of

working drawings for the general zone, including the specific location of the tendons and anchorage devices, general zone reinforcement, and the specific stressing sequence. The engineer of record is also responsible for the design of local zones based on Section 9.21.7.2 and for the approval of special anchorage devices used under the provisions of Section 9.21.7.3. All working drawings for the local zone must be approved by the engineer of record.

9.21.2.3.2 Anchorage device suppliers are responsible for furnishing anchorage devices which satisfy the anchor efficiency requirements of Division II, Section 10.3.2. In addition, if special anchorage devices are used, the anchorage device supplier is responsible for furnishing anchorage devices that satisfy the acceptance test requirements of Section 9.21.7.3 and of Division II, Section 10.3.2.3. This acceptance test and the anchor efficiency test shall be conducted by an independent testing agency acceptable to the engineer of record. The anchorage device supplier shall provide records of the acceptance test in conformance with Division II, Section 10.3.2.3.12 to the engineer of record and to the constructor and shall specify auxiliary and confining reinforcement, minimum edge distance, minimum anchor spacing, and minimum concrete strength at time of stressing required for proper performance of the local zone.

9.21.2.3.3 The responsibilities of the constructor are specified in Division II, Section 10.4.

9.21.3 Design of the General Zone

9.21.3.1 Design Methods

The following methods may be used for the design of general zones:

- (1) Equilibrium based plasticity models (strut-and-tie models) (see Section 9.21.4)
- (2) Elastic stress analysis (finite element analysis or equivalent) (see Section 9.21.5)
- (3) Approximate methods for determining the compression and tension forces, where applicable (see Section 9.21.6).

Regardless of the design method used, all designs shall conform to the requirements of Section 9.21.3.4.

The effects of stressing sequence and three-dimensional effects shall be considered in the design. When these three dimensional effects appear significant, they may be analyzed using three-dimensional analysis procedures or may be approximated by considering two or more planes. However, in these approximations the interaction of the planes' models must be considered, and the model loadings and results must be consistent.

9.21.3.2 Nominal Material Strengths

9.21.3.2.1 The nominal tensile strength of bonded reinforcement is limited to f_{sy} for non-prestressed reinforcement and to f_y for prestressed reinforcement. The nominal tensile strength of unbonded prestressed reinforcement is limited to $f_{se} + 15,000$ psi.

9.21.3.2.2 The effective nominal compressive strength of the concrete of the general zone, exclusive of confined concrete, is limited to $0.7f'_c$. The tensile strength of the concrete shall be neglected.

9.21.3.2.3 The compressive strength of concrete at transfer of prestressing shall be specified on the construction drawings. If not otherwise specified, stress shall not be transferred to concrete until the compressive strength of the concrete as indicated by test cylinders, cured by methods identical with the curing of the member, is at least 3,500 psi.

9.21.3.3 Use of Special Anchorage Devices

Whenever special anchorage devices which do not meet the requirements of Section 9.21.7.2 are to be used, reinforcement similar in configuration and at least equivalent in volumetric ratio to the supplementary skin reinforcement permitted under the provisions of Division II, Section 10.3.2.3.4 shall be furnished in the corresponding regions of the anchorage zone.

9.21.3.4 General Design Principles and Detailing Requirements

Detailing and quality workmanship are essential for the satisfactory performance of anchorage zones. Sizes and details for anchorage zones should respect the

need for tolerances on the bending, fabrication, and placement of reinforcement, the size of the aggregate, and the need for placement and sound consolidation of the concrete.

9.21.3.4.1 Compressive stresses in the concrete ahead of basic anchorage devices shall meet the requirements of Section 9.21.7.2.

9.21.3.4.2 Compressive stresses in the concrete ahead of special anchorage devices shall be checked at a distance measured from the concrete bearing surface equal to the smaller of:

- (1) The depth to the end of the local confinement reinforcement.
- (2) The smaller lateral dimension of the anchorage device.

These compressive stresses may be determined according to the strut-and-tie model procedures of Section 9.21.4, from an elastic stress analysis according to Section 9.21.5.2, or by the approximate method outlined in Section 9.21.6.2. These compressive stresses shall not exceed $0.7\phi f_{ci}$.

9.21.3.4.3 Compressive stresses shall also be checked where geometry or loading discontinuities within or ahead of the anchorage zone may cause stress concentrations.

9.21.3.4.4 The bursting force is the tensile force in the anchorage zone acting ahead of the anchorage device and transverse to the tendon axis. The magnitude of the bursting force, T_{burst} , and its corresponding distance from the loaded surface, d_{burst} , can be determined using the strut-and-tie model procedures of Section 9.21.4, from an elastic stress analysis according to Section 9.21.5.3, or by the approximate method outlined in Section 9.21.6.3. Three-dimensional effects shall be considered for the determination of the bursting reinforcement requirements.

9.21.3.4.5 Resistance to bursting forces, $\phi A_s f_{sy}$ and/or $\phi A_s^* f_y$, shall be provided by non-prestressed or prestressed reinforcement, in the form of spirals, closed hoops, or well anchored transverse ties. This reinforcement is to be proportioned to resist the total factored bursting force. Arrangement and anchorage of bursting reinforcement shall satisfy the following:

- (1) Bursting reinforcement shall extend over the full width of the member and must be anchored as close to the outer faces of the member as cover permits.
- (2) Bursting reinforcement shall be distributed ahead of the loaded surface along both sides of the tendon throughout a distance of $2.5 d_{burst}$ for the plane considered, but not to exceed 1.5 times the corresponding lateral dimension of the section. The centroid of the bursting reinforcement shall coincide with the distance d_{burst} used for the design.
- (3) Spacing of bursting reinforcement shall exceed neither 24 bar diameters nor 12 inches.

9.21.3.4.6 Edge tension forces are tensile forces in the anchorage zone acting parallel and close to the transverse edge and longitudinal edges of the member. The transverse edge is the surface loaded by the anchors. The tensile force along the transverse edge is referred to as *spalling force*. The tensile force along the longitudinal edge is referred to as *longitudinal edge tension force*.

9.21.3.4.7 Spalling forces are induced in concentrically loaded anchorage zones, eccentrically loaded anchorage zones, and anchorage zones for multiple anchors. Longitudinal edge tension forces are induced when the resultant of the anchorage forces considered causes eccentric loading of the anchorage zone. The edge tension forces can be determined from an elastic stress analysis, strut-and-tie models, or in accordance with the approximate methods of Section 9.21.6.4.

9.21.3.4.8 In no case shall the spalling force be taken as less than two percent of the total factored tendon force.

9.21.3.4.9 Resistance to edge tension forces, $\phi A_s f_{sy}$ and/or $\phi A_s^* f_y$, shall be provided in the form of non-prestressed or prestressed reinforcement located close to the longitudinal and transverse edge of the concrete. Arrangement and anchorage of the edge tension reinforcement shall satisfy the following:

- (1) Minimum spalling reinforcement satisfying Section 9.21.3.4.8 shall extend over

the full width of the member.

- (2) Spalling reinforcement between multiple anchorage devices shall effectively tie these anchorage devices together.
- (3) Longitudinal edge tension reinforcement and spalling reinforcement for eccentric anchorage devices shall be continuous. The reinforcement shall extend along the tension face over the full length of the anchorage zone and shall extend along the loaded face from the longitudinal edge to the other side of the eccentric anchorage device or group of anchorage devices.

9.21.3.5 Intermediate Anchorages

9.21.3.5.1 Intermediate anchorages shall not be used in regions where significant tension is generated behind the anchor from other loads. Whenever practical, blisters shall be located in the corner between flange and webs, or shall be extended over the full flange width or web height to form a continuous rib. If isolated slab blisters must be used on a flange or web, local shear, bending, and direct force effects shall be considered in the design.

9.21.3.5.2 Bonded reinforcement shall be provided to tie back at least 25 percent of the intermediate anchorage unfactored stressing force into the concrete section behind the anchor. Stresses in this bonded reinforcement are limited to a maximum of $0.6f_{sy}$ or 36 ksi. The amount of tie back reinforcement may be reduced using Equation (9-32), if permanent compressive stresses are generated behind the anchor from other loads.

$$T_{ia} = 0.25P_s - f_{cb} A_{cb} \quad (9-32)$$

where T_{ia} is the tie back tension force at the intermediate anchorage;
 P_s is the maximum unfactored anchorage stressing force;
 f_{cb} is the compressive stress in the region behind the anchor;
 A_{cb} is the area of the continuing cross section within the extensions of the sides of the anchor plate or blister. The area of the blister or rib shall not be taken as part of the cross section.

9.21.3.5.3 Tie back reinforcement satisfying Section 9.21.3.5.2 shall be placed no further

than one plate width from the tendon axis. It shall be fully anchored so that the yield strength can be developed at a distance of one plate width or half the length of the blister or rib ahead of the anchor as well as at the same distance behind the anchor. The centroid of this reinforcement shall coincide with the tendon axis, where possible. For blisters and ribs, the reinforcement shall be placed in the continuing section near that face of the flange or web from which the blister or rib is projecting.

9.21.3.5.4 Reinforcement shall be provided throughout blisters or ribs as required for shear friction, corbel action, bursting forces, and deviation forces due to tendon curvature. This reinforcement shall be in the form of ties or U-stirrups which encase the anchorage and tie it effectively into the adjacent web and flange. This reinforcement shall extend as far as possible into the flange or web and be developed by standard hooks bent around transverse bars or equivalent. Spacing shall not exceed the smallest of blister or rib height at anchor, blister width, or 6 inches.

9.21.3.5.5 Reinforcement shall be provided to resist local bending in blisters and ribs due to eccentricity of the tendon force and to resist lateral bending in ribs due to tendon deviation forces.

9.21.3.5.6 Reinforcement required by Sections 9.21.3.4.4 through 9.21.3.4.9 shall be provided to resist tensile forces due to transfer of the anchorage force from the blister or rib into the overall structure.

9.21.3.6 Diaphragms

9.21.3.6.1 For tendons anchored in diaphragms, concrete compressive stresses shall be limited within the diaphragm in accordance with Sections 9.21.3.4.1 through 9.21.3.4.3. Compressive stresses shall also be checked at the transition from the diaphragm to webs and flanges of the member.

9.21.3.6.2 Reinforcement shall be provided to ensure full transfer of diaphragm anchor loads into the flanges and webs of the girder. The more general methods of Section 9.21.4 or 9.21.5 shall be used to determine this reinforcement. Reinforcement shall also be

provided to tie back deviation forces due to tendon curvature.

9.21.3.7 Multiple Slab Anchorages

9.21.3.7.1 Minimum reinforcement meeting the requirements of Sections 9.21.3.7.2 through 9.21.3.7.4 shall be provided unless a more detailed analysis is made.

9.21.3.7.2 Reinforcement shall be provided for the bursting force in the direction of the thickness of the slab and normal to the tendon axis in accordance with Sections 9.21.3.4.4 and 9.21.3.4.5. This reinforcement shall be anchored close to the faces of the slab with standard hooks bent around horizontal bars, or equivalent. Minimum reinforcement is two #3 bars per anchor located at a distance equal to one-half the slab thickness ahead of the anchor.

9.21.3.7.3 Reinforcement in the plane of the slab and normal to the tendon axis shall be provided to resist edge tension forces, T_1 , between anchorages (Equation (9-33)) and bursting forces, T_2 , ahead of the anchorages (Equation (9-34)). Edge tension reinforcement shall be placed immediately ahead of the anchors and shall effectively tie adjacent anchors together. Bursting reinforcement shall be distributed over the length of the anchorage zones (see Section 9.21.1.4).

$$T_1 = 0.10 P_u \left(1 - \frac{a}{s}\right) \quad (9-33)$$

$$T_2 = 0.20 P_u \left(1 - \frac{a}{s}\right) \quad (9-34)$$

where T_1 is the edge tension force;
 T_2 is the bursting force;
 P_u is the factored tendon load on an individual anchor;
 a is the anchor plate width;
 s is the anchorage spacing.

9.21.3.7.4 For slab anchors with an edge distance of less than two plate widths or one

slab thickness, the edge tension reinforcement shall be proportioned to resist 25 percent of the factored tendon load. This reinforcement shall preferably be in the form of hairpins and shall be distributed within one plate width ahead of the anchor. The legs of the hairpin bars shall extend from the edge of the slab past the adjacent anchor but not less than a distance equal to two plate widths plus development length.

9.21.4 Application of Strut-and-Tie Models to the Design of Anchorage Zones

9.21.4.1 General

9.21.4.1.1 The flow of forces in the anchorage zone may be approximated by a series of straight compression members (struts) and straight tension members (ties) that are connected at discrete points (nodes). Compression forces are carried by concrete compression struts and tension forces are carried by non-prestressed or prestressed reinforcement.

9.21.4.1.2 The selected strut-and-tie model shall follow a load path from the anchorages to the end of the anchorage zone. Other forces acting on the anchorage zone, such as reaction forces, tendon deviation forces, and applied loads, shall be considered in the selection of the strut-and-tie model. The forces at the end of the anchorage zone can be obtained from an axial-flexural beam analysis.

9.21.4.2 Nodes

Local zones which meet the provisions of Section 9.21.7 or Division II, Section 10.3.2.3 are considered as properly detailed, adequate nodes. The other nodes in the anchorage zone are adequate if the effective concrete stresses in the struts meet the requirements of Section 9.21.4.3 and the tension ties are properly detailed to develop the full yield strength of the reinforcement.

9.21.4.3 Struts

9.21.4.3.1 The effective concrete compressive strength for the general zone shall usually be limited to $0.7\phi f'_{ci}$. In areas where the concrete may be extensively cracked at ultimate due to other load effects, or if large plastic rotations are required, the effective compressive strength shall be limited to $0.6\phi f'_{ci}$.

9.21.4.3.2 In anchorage zones the critical section for compression struts is ordinarily located at the interface with the local zone node. If special anchorage devices are used, the critical section of the strut can be taken as that section whose extension intersects the axis of the tendon at a depth equal to the smaller of the depth of the local confinement reinforcement or the lateral dimension of the anchorage device.

9.21.4.3.3 For thin members with a ratio of member thickness to anchorage width of no more than three, the dimension of the strut in the direction of the thickness of the member can be approximated by assuming that the thickness of the compression strut varies linearly from the transverse lateral dimension of the anchor at the surface of the concrete to the total thickness of the section at a depth equal to the thickness of the section.

9.21.4.3.4 The compression stresses can be assumed as acting parallel to the axis of the strut and as uniformly distributed over its cross section.

9.21.4.4 Ties

9.21.4.4.1 Tension forces in the strut-and-tie model shall be assumed to be carried completely by non-prestressed or prestressed reinforcement. Tensile strength of the concrete shall be neglected.

9.21.4.4.2 Tension ties shall be properly detailed and shall extend beyond the nodes to develop the full tension tie force at the node. The reinforcement layout must closely follow the directions of the ties in the strut-and-tie model.

9.21.5 Elastic Stress Analysis

9.21.5.1 Analyses based on assumed elastic material properties, equilibrium, and compatibility of strains are acceptable for analysis and design of anchorage zones.

9.21.5.2 If the compressive stresses in the concrete ahead of the anchorage device are determined from a linear-elastic stress analysis, local stress maxima may be averaged over an area equal to the bearing area of the anchorage device.

9.21.5.3 Location and magnitude of the bursting force may be obtained by integration of the corresponding tensile bursting stresses along the tendon path.

9.21.6 Approximate Methods

9.21.6.1 Limitations

In the absence of a more accurate analysis, concrete compressive stresses ahead of the anchorage device, location and magnitude of the bursting force, and edge tension forces may be estimated by Equations (9-35) through (9-38), provided that:

- (1) The member has a rectangular cross section and its longitudinal extent is at least equal to the largest transverse dimension of the cross section.
- (2) The member has no discontinuities within or ahead of the anchorage zone.
- (3) The minimum edge distance of the anchorage in the main plane of the member is at least one and one-half times the corresponding lateral dimension, a , of the anchorage device.
- (4) Only one anchorage device or one group of closely spaced anchorage devices is located in the anchorage zone. Anchorage devices can be treated as closely spaced if their center-to-center spacing does not exceed one and one-half times the width of the anchorage devices in the direction considered.
- (5) The angle of inclination of the tendon with respect to the center line of the member is not larger than 20 degrees if the anchor force points toward the centroid of the section and for concentric anchors, and is not larger than 5 degrees if the anchor force points away from the centroid of the section.

9.21.6.2 Compressive Stresses

9.21.6.2.1 No additional check of concrete compressive stresses is necessary for basic anchorage devices satisfying Section 9.21.7.2.

9.21.6.2.2 The concrete compressive stresses ahead of special anchorage devices at the interface between local zone and general zone shall be approximated by Equations (9-35) and (9-36).

$$f_{ca} = \kappa \frac{0.6P_u}{A_b} \frac{1}{1 + \ell_c \left(\frac{1}{b_{eff}} - \frac{1}{t} \right)} \quad (9-35)$$

$$\kappa = 1 + \left(2 - \frac{s}{a_{eff}} \right) \left(0.3 + \frac{n}{15} \right) \quad \text{for } s < 2a_{eff} \quad (9-36)$$

$$\kappa = 1 \quad \text{for } s \geq 2a_{eff}$$

- where f_{ca} is the concrete compressive stress ahead of the anchorage device;
- κ is a correction factor for closely spaced anchorages;
- A_b is an effective bearing area as defined in Section 9.21.6.2.3;
- a_{eff} is the lateral dimension of the effective bearing area measured parallel to the larger dimension of the cross section or in the direction of closely spaced anchors;
- b_{eff} is the lateral dimension of the effective bearing area measured parallel to the smaller dimension of the cross section;
- ℓ_c is the longitudinal extent of confining reinforcement for the local zone, but not more than the larger of $1.15 a_{eff}$ or $1.15 b_{eff}$;
- P_u is the factored tendon load;
- t is the thickness of the section;
- s is the center-to-center spacing of multiple anchorages;
- n is the number of anchorages in a row.

If a group of anchorages is closely spaced in two directions, the product of the correction factors, κ , for each direction is used in Equation (9-36).

9.21.6.2.3 Effective bearing area, A_b , in Equation (9-35) shall be taken as the larger of the anchor bearing plate area, A_{plate} , or the bearing area of the confined concrete in the local zone, A_{conf} , with the following limitations:

- (1) If A_{plate} controls, A_{plate} shall not be taken larger than $4/\pi A_{conf}$.
- (2) If A_{conf} controls, the maximum dimension of A_{conf} shall not be more than twice the maximum dimension of A_{plate} or three times the minimum dimension

of A_{plate} . If any of these limits is violated the effective bearing area, A_b , shall be based on A_{plate} .

- (3) Deductions shall be made for the area of the duct in the determination of A_b .

9.21.6.3 Bursting Forces

Values for the magnitude of the bursting force, T_{burst} , and for its distance from the loaded surface, d_{burst} , shall be estimated by Equations (9-37) and (9-38), respectively. In the application of Equations (9-37) and (9-38) the specified stressing sequence shall be considered if more than one tendon is present.

$$T_{burst} = 0.25 \sum P_u \left(1 - \frac{a}{h} \right) + 0.5 P_u \sin \alpha \quad (9-37)$$

$$d_{burst} = 0.5(h - 2e) + 5e \sin \alpha \quad (9-38)$$

where $\sum P_u$ is the sum of the total factored tendon loads for the stressing arrangement considered;

- a is the lateral dimension of the anchorage device or group of devices in the direction considered;
- e is the eccentricity (always taken as positive) of the anchorage device or group of devices with respect to the centroid of the cross section;
- h is the lateral dimension of the cross section in the direction considered;
- α is the angle of inclination of the resultant of the tendon forces with respect to the centerline of the member.

9.21.6.4 Edge Tension Forces

9.21.6.4.1 For multiple anchorages with a center-to-center spacing of less than 0.4 times the depth of the section, the spalling forces shall be given by Section 9.21.3.4.8. For larger spacings, the spalling forces shall be determined from a more detailed analysis, such as strut-and-tie models or other analytical procedures.

9.21.6.4.2 If the centroid of all tendons considered is located outside of the kern of the section both spalling forces and longitudinal edge tension forces are induced. The

longitudinal edge tension force shall be determined from an axial-flexural beam analysis at a section located at one half the depth of the section away from the loaded surface. The spalling force shall be taken as equal to the longitudinal edge tension force but not less than specified in Section 9.21.3.4.8.

9.21.7 Design of the Local Zone

9.21.7.1 Dimensions of the Local Zone

9.21.7.1.1 When no independently verified manufacturer's edge distance recommendations for a particular anchorage device are available, the transverse dimensions of the local zone in each direction shall be taken as the larger of:

- (1) The corresponding bearing plate size plus twice the minimum concrete cover required for the particular application and environment.
- (2) The outer dimension of any required confining reinforcement plus the required concrete cover over the confining reinforcing steel for the particular application and environment.

9.21.7.1.2 When independently verified manufacturer's recommendations for minimum cover, spacing and edge distances for a particular anchorage device are available, the transverse dimensions of the local zone in each direction shall be taken as the smaller of:

- (1) Twice the edge distance specified by the anchorage device supplier.
- (2) The center-to-center spacing specified by the anchorage device supplier.

The manufacturer's recommendations for spacing and edge distance of anchorages shall be considered minimum values.

9.21.7.1.3 The length of the local zone along the tendon axis shall be taken as the greater of:

- (1) The maximum width of the local zone.
- (2) The length of the anchorage device confining reinforcement.
- (3) For anchorage devices with multiple bearing surfaces, the distance from the loaded concrete surface to the bottom of each bearing surface plus the maximum dimension of that bearing surface.

In no case shall the length of the local zone be taken as greater than one and one-half

times the width of the local zone.

9.21.7.1.4 For closely spaced anchorages an enlarged local zone enclosing all individual anchorages shall also be considered.

9.21.7.2 Bearing Strength

9.21.7.2.1 Anchorage devices may be either basic anchorage devices meeting the bearing compressive strength limits of Sections 9.21.7.2.2 through 9.21.7.2.4 or special anchorage devices meeting the requirements of Section 9.21.7.3.

9.21.7.2.2 The effective concrete bearing compressive strength f_b used for design shall not exceed that of Equations (9-39) or (9-40).

$$f_b \leq 0.7\phi f'_{ci} \sqrt{A/A_g} \quad (9-39)$$

$$\text{but } f_b \leq 2.25\phi f'_{ci} \quad (9-40)$$

where f_b is the maximum factored tendon load, P_u , divided by the effective bearing area A_b ;

f'_{ci} is the concrete compressive strength at stressing;

A is the maximum area of the portion of the supporting surface that is geometrically similar to the loaded area and concentric with it;

A_g is the gross area of the bearing plate if the requirements of Section 9.21.7.2.3 are met, or is the area calculated in accordance with Section 9.21.7.2.4;

A_b is the effective net area of the bearing plate calculated as the area A_g minus the area of openings in the bearing plate.

Equations (9-39) and (9-40) are only valid if general zone reinforcement satisfying Section 9.21.3.4 is provided and if the extent of the concrete along the tendon axis ahead of the anchorage device is at least twice the length of the local zone as defined in Section 9.21.7.1.3.

9.21.7.2.3 The full bearing plate area may be used for A_g and the calculation of A_b if the

anchorage device is sufficiently rigid. To be considered sufficiently rigid, the slenderness of the bearing plate (n/t) must not exceed the value given in Equation (9-41). The plate must also be checked to ensure that the plate material does not yield.

$$n/t \leq 0.08 \sqrt[3]{E_b/f_b} \quad (9-41)$$

where n is the largest distance from the outer edge of the wedge plate to the outer edge of the bearing plate. For rectangular bearing plates this distance is measured parallel to the edges of the bearing plate. If the anchorage has no separate wedge plate, the size of the wedge plate shall be taken as the distance between the extreme wedge holes in the corresponding direction.

t is the average thickness of the bearing plate.

E_b is the modulus of elasticity of the bearing plate material.

9.21.7.2.4 For bearing plates that do not meet the stiffness requirements of Section 9.21.7.2.3, the effective gross bearing area, A_g , shall be taken as the area geometrically similar to the wedge plate (or to the outer perimeter of the wedge hole pattern for plates without separate wedge plate) with dimensions increased by assuming load spreading at a 45 degree angle. A larger effective bearing area may be calculated by assuming an effective area and checking the new f_b and n/t values for conformance with Sections 9.21.7.2.2 and 9.21.7.2.3.

9.21.7.3 Special Anchorage Devices

Special anchorage devices that do not meet the requirements of Section 9.21.7.2 may be used provided that they have been tested by an independent testing agency acceptable to the engineer of record according to the procedures described in Division II, Section 10.3.2 (or equivalent) and meet the acceptance criteria specified in Division II, Section 10.3.2.3.10. For a series of similar special anchorage devices, tests are only required for representative samples.

9.22 PRETENSIONED ANCHORAGE ZONES

9.22.1 Vertical stirrups resisting at least two percent of the total factored prestressing

force, P_u , shall be placed within the distance $d/4$ of the end of the beam, the end stirrups to be as close to the end of the beam as practicable.

9.22.2 For at least the distance d from the end of the beam, nominal reinforcement shall be placed to enclose the prestressing steel in the bottom flange.

9.22.3 For box girders, transverse reinforcement shall be provided and anchored by extending the leg into the web of the girder.

9.22.4 Unless otherwise specified, stress shall not be transferred to concrete until the compressive strength of the concrete as indicated by test cylinders, cured by methods identical with the curing of the member, is at least 4,000 psi.

DIVISION II - CONSTRUCTION

10.3 MATERIALS

10.3.1 Prestressing Steel

[Split current Section 10.3.1 into two sections to reduce number of sub levels]

10.3.2 Post-Tensioning Anchorages and Couplers

[same as first paragraph in current Section 10.3.1.4 except for underlined.]

All anchorages and couplers shall develop at least 95 percent of the actual ultimate strength of the prestressing steel,

10.3.2.1 Bonded Systems

[same as current Section 10.3.1.4.1]

10.3.2.2 Unbonded Systems

[same as current Section 10.3.1.4.2]

10.3.2.3 Special Anchorage Device Acceptance Test

[replaces current Sections 10.3.1.4.3, 10.3.1.4.4, and 10.3.1.4.5]

10.3.2.3.1 The test block shall be a rectangular prism. It shall contain those anchorage components which will also be embedded in the structure's concrete. Their arrangement has to comply with the practical application and the suppliers specifications. The test block shall contain an empty duct of size appropriate for the maximum tendon size which can be accommodated by the anchorage device.

10.3.2.3.2 The dimensions of the test block perpendicular to the tendon in each direction shall be the smaller of the minimum edge distance or the minimum spacing specified by the anchorage device supplier, with the stipulation that the cover over any confining reinforcing steel or supplementary skin reinforcement be appropriate for the particular application and environment. The length of the block along the axis of the tendon shall be at least two times the larger of the cross-sectional dimensions.

10.3.2.3.3 The confining reinforcing steel in the local zone shall be the same as that specified by the anchorage device supplier for the particular system.

10.3.2.3.4 In addition to the anchorage device and its specified confining reinforcement steel, supplementary skin reinforcement may be provided throughout the specimen. This supplementary skin reinforcement shall be specified by the anchorage device supplier but shall not exceed a volumetric ratio of 0.01.

10.3.2.3.5 The concrete strength at the time of testing shall be not more than the minimum specified concrete strength at time of tensioning, f'_{ci} , or $0.85 f'_c$.

10.3.2.3.6 Either of three test procedures is acceptable: cyclic loading described in Section 10.3.2.3.7, sustained loading described in Section 10.3.2.3.8, or monotonic loading described in Section 10.3.2.3.9. The loads specified for the tests are given in fractions of the ultimate load F_{pu} of the largest tendon that the anchorage device is designed to accommodate. The specimen shall be loaded in accordance with normal usage of the

device in post-tensioning applications.

10.3.2.3.7 Cyclic Loading Test

10.3.2.3.7.1 In a cyclic loading test, the load shall be increased to $0.8F_{pu}$. The load shall then be cycled between $0.1F_{pu}$ and $0.8F_{pu}$ until crack widths stabilize, but for not less than 10 cycles. Crack widths are considered stabilized if they do not change by more than 0.001 in. over the last three readings. Upon completion of the cyclic loading the specimen shall be preferably loaded to failure or, if limited by the capacity of the loading equipment, to at least $1.1F_{pu}$.

10.3.2.3.7.2 Crack widths and crack patterns shall be recorded at the initial load of $0.8F_{pu}$, at least at the last three consecutive peak loadings before termination of the cyclic loading, and during loading to failure at $0.9F_{pu}$. The maximum load shall also be reported.

10.3.2.3.8 Sustained Loading Test

10.3.2.3.8.1 In a sustained loading test, the load shall be increased to $0.8F_{pu}$ and held constant until crack widths stabilize but for not less than 48 hours. Crack widths are considered stabilized if they do not change by more than 0.001 in. over the last three readings. After sustained loading is completed, the specimen shall be preferably loaded to failure or, if limited by the capacity of the loading equipment, to at least $1.1F_{pu}$.

10.3.2.3.8.2 Crack widths and crack patterns shall be recorded at the initial load of $0.8F_{pu}$, at least three times at intervals of not less than four hours during the last twelve hours before termination of the sustained loading, and during loading to failure at $0.9F_{pu}$. The maximum load shall also be reported.

10.3.2.3.9 Monotonic Loading Test

10.3.2.3.9.1 In a monotonic loading test, the load shall be increased to $0.9F_{pu}$ and held constant for 1 hour. The specimen shall then be preferably loaded to failure or, if limited by the capacity of the loading equipment, to at least $1.2F_{pu}$.

10.3.2.3.9.2 Crack widths and crack patterns shall be recorded at $0.9F_{pu}$ after the one hour

period, and at $1.0F_{pu}$. The maximum load shall also be reported.

10.3.2.3.10 The strength of the anchorage zone must exceed:

Specimens tested under cyclic or sustained loading... $1.1F_{pu}$

Specimens tested under monotonic loading... $1.2F_{pu}$

The maximum crack width criteria specified below must be met for moderately aggressive environments. For higher aggressivity environments the crack width criteria shall be reduced by at least 50 percent.

- (1) No cracks greater than 0.010 in.
at $0.8F_{pu}$ after completion of the cyclic or sustained loading, or at $0.9F_{pu}$ after the 1 hour period for monotonic loading.
- (2) No cracks greater than 0.016 in.
at $0.9F_{pu}$ for cyclic or sustained loading, or at $1.0F_{pu}$ for monotonic loading.

10.3.2.3.11 A test series shall consist of three test specimens. Each one of the tested specimens must meet the acceptance criteria. If one of the three specimens fails to pass the test, a supplementary test of three additional specimens is allowed. The three additional test specimen results must meet all acceptance criteria of Section 10.3.2.3.10. For a series of similar special anchorage devices, tests are only required for representative samples.

10.3.2.3.12 Records of the anchorage device acceptance test shall include:

- (1) Dimensions of the test specimen.
- (2) Drawings and dimensions of the anchorage device, including all confining reinforcing steel.
- (3) Amount and arrangement of supplementary skin reinforcement.
- (4) Type and yield strength of reinforcing steel.
- (5) Type and compressive strength at time of testing of concrete.
- (6) Type of testing procedure and all measurements required in Sections 10.3.2.3.7 through 10.3.2.3.10 for each specimen.

10.4 PLACEMENT OF DUCTS, STEEL, AND ANCHORAGE HARDWARE**10.4.1 Placement of Ducts**

[same as current Section 10.4.1]

10.4.2 Placement of Prestressing Steel

[same as current Section 10.4.2]

10.4.3 Placement of Anchorage Hardware

[add to current Section 10.4]

The constructor is responsible for the proper placement of all materials according to the design documents of the engineer of record and the requirements stipulated by the anchorage device supplier. The constructor shall exercise all due care and attention in the placement of anchorage hardware, reinforcement, concrete, and consolidation of concrete in anchorage zones. Modifications to the local zone details verified under provisions of Section 9.21.7.3 in Division I and Section 10.3.2.3 in Division II shall be approved by both the engineer of record and the anchorage device supplier.

APPENDIX B COMMENTARY TO THE PROPOSED ANCHORAGE ZONE SPECIFICATIONS

C.9.1.2 Notations

The factored tendon force P_u is the product of the load factor (1.2 from Section 9.14) and the maximum tendon force. Under AASHTO Section 9.15.1 this is usually overstressing to $0.9F_y^*$ which is permitted for short periods of time. ASTM Specifications A 416-90 provides that minimum yield strength be 85% of specified minimum breaking strength for stress relieved strand and 90% for the widely used low relaxation strand. Thus typically

$$\begin{aligned} P_u &= (\text{L.F.}) 0.90f_y^* A_y^* = (1.2)(0.90)(0.90)f_s^* A_s^* \\ &= (1.2)(0.81)f_s^* A_s^* = 0.972 f_s^* A_s^*. \end{aligned}$$

C.9.14 LOAD FACTORS

The load factor of 1.2 applied to the maximum tendon jacking force results in a design load of about 96% of the nominal ultimate strength of the tendon. This compares well with the maximum attainable jacking force which is limited by the anchor efficiency factor.

The ϕ -factor of 0.85 reflects the importance of the anchorage zone, the brittle failure mode for compression struts in the anchorage zone, and the relatively wide scatter of results of experimental anchorage zone studies. The ϕ -factor of 0.70 for lightweight concrete reflects its often lower tensile strength and is based on a reduction of the normalweight concrete value using the multiplier for lightweight concrete given in ACI 318-89, Section 11.2.1.2.

C.9.21 POST-TENSIONED ANCHORAGE ZONES

Article 9.21 applies to anchorage zones for post-tensioned tendons only. Provisions for anchorage zones in pretensioned concrete are included in Article 9.22.

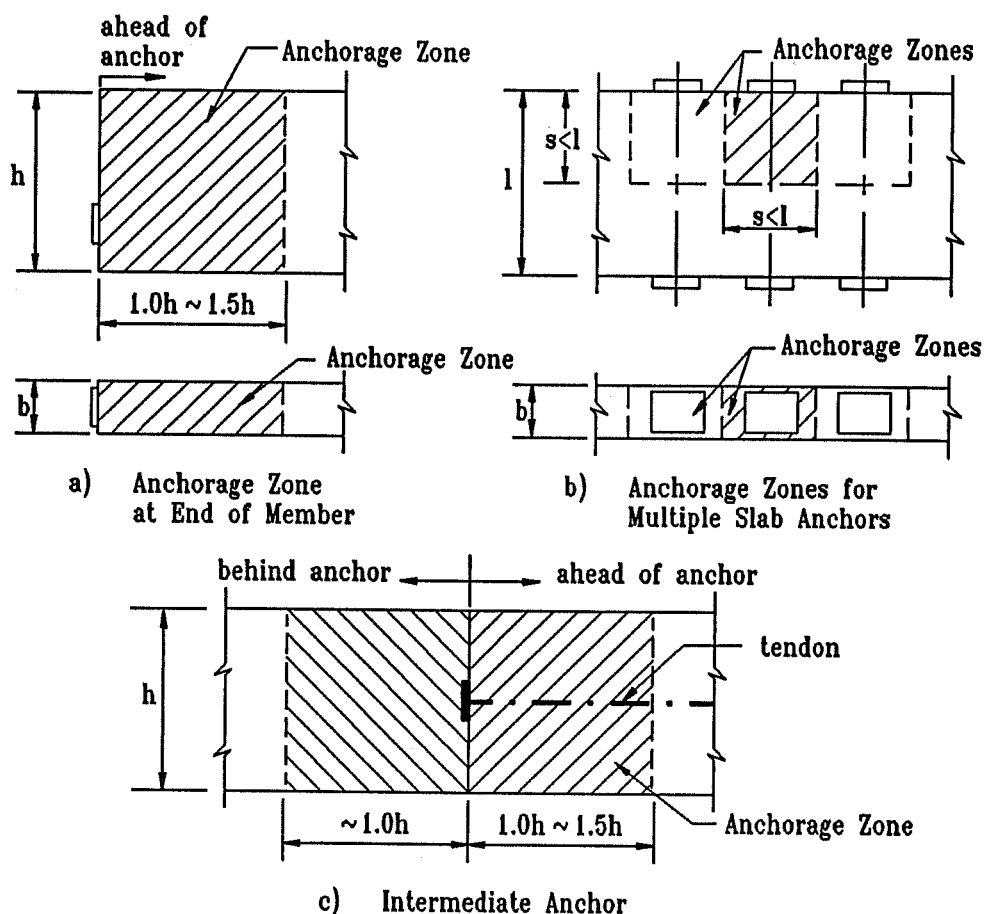


Figure 1 Geometry of the Anchorage Zone

C.9.21.1 Geometry of the Anchorage Zone

C.9.21.1.1 Within the anchorage zone the usual assumption of beam theory that plane sections remain plane is not valid.

C.9.21.1.2 The definitions of Section 9.21.1.2 through 9.21.1.4 are based on the Principle of Saint Venant and are illustrated in Figure 1.

C.9.21.1.3 For intermediate anchorages large tensile stresses exist locally behind the anchor. These tensile stresses are induced by incompatibility of deformations ahead of and behind the anchorage. The entire region must be considered (Figure 1c).

Figure 1c also clarifies the terminology used to address the regions around intermediate anchorages. Locations at the rear of the anchorage (the direction opposite to the prestressing force) are referred to as "behind the anchor", while locations in front of the anchor (same direction as the prestressing force) are referred to as "ahead of the anchor". Such terminology is essential for intermediate anchorages. For consistency, it is very useful to use the same terminology for end anchors as shown in Figure 1a.

C.9.21.1.4 For multiple slab anchorages the dimensions of the anchorage zone are determined by the anchorage spacing. For very widely spaced anchors the transverse dimension of the anchorage zone does not have to exceed the slab length in the direction of the tendon (Figure 1b). Anchorage zones for anchors on opposite sides of the slab may overlap.

C.9.21.1.5 Figure 2 illustrates the distinction between the local zone and the general zone. The region of very high compressive stresses immediately ahead of the anchorage device is the local zone. The region subjected to tensile stresses due to spreading of the concentrated tendon force into the structure is the general zone.

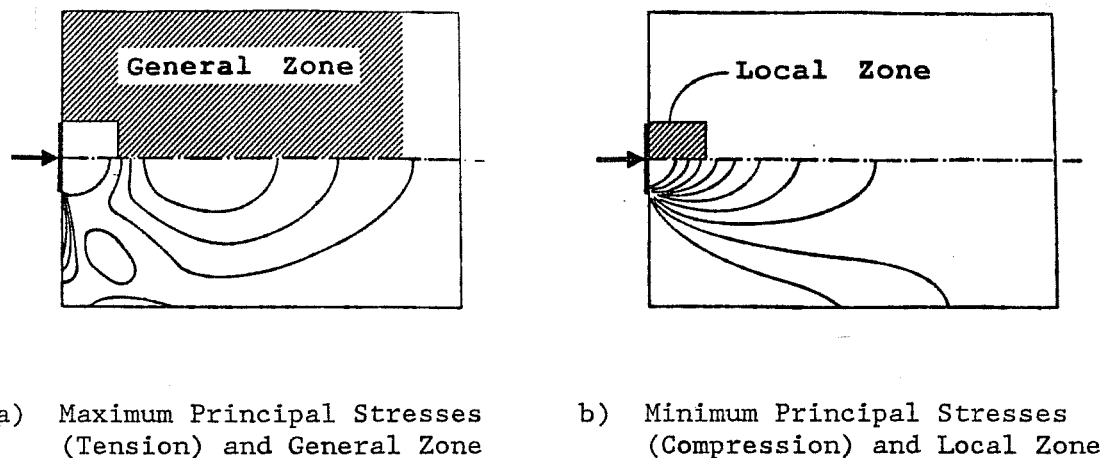


Figure 2 Local Zone and General Zone

C.9.21.2 General Zone and Local Zone**C.9.21.2.1 General Zone**

C.9.21.2.1.1 In many cases the general zone and the local zone can be treated separately. However, for small anchorage zones, such as in slab anchorages, local zone effects (high bearing and confining stresses) and general zone effects (tensile stresses due to spreading of the tendon force) may occur in the same region.

C.9.21.2.1.2 The main considerations in general zone design are the determination of the reinforcement requirements for the tensile forces in the anchorage zone (such as bursting forces and spalling forces) and the check of the compressive stresses at the interface with the local zone.

C.9.21.2.2 Local Zone

C.9.21.2.2.1 The local zone must resist the very high local stresses introduced by the anchorage device and transfer them to the remainder of the anchorage zone. The behavior of the local zone is strongly influenced by the specific characteristics of the anchorage device and its confining reinforcement, and less influenced by the geometry and loading of the overall structure.

C.9.21.2.2.2 The main considerations in local zone design are the effects of the high bearing pressure and the adequacy of any confining reinforcement to increase the bearing strength. Anchorage devices either are basic anchorage devices which have to satisfy the bearing pressure limitations and stiffness requirements of Section 9.21.7 or are special anchorage devices which have to pass an acceptance test by an independent testing agency as described in Division II, Section 10.3.2.3.

C.9.21.2.3 Responsibilities

C.9.21.2.3.1 The engineer of record has the responsibility for the location of individual tendons and anchorage devices. Should the plans show only total tendon force and eccentricity the engineer of record is responsible for approval of the specific tendon layout and anchorage arrangement submitted by the post-tensioning specialist or the contractor. The engineer of record is responsible for the proper design of general zone reinforcement

required by the approved tendon layout and anchorage device arrangement.

If basic anchorage devices are used, the engineer of record is responsible for the design of the local zone in accordance with Section 9.21.7. If special anchorage devices are used, the anchorage device supplier assumes certain responsibilities as specified in Section 9.21.2.3.2. However, use of special anchorage devices does not relieve the engineer of record from the responsibility of approving the design and working drawings for the anchorage zone to ensure compliance with the anchorage device supplier's specifications.

C.9.21.2.3.2 The responsibility of demonstrating the adequacy of special anchorage devices and specifying the proper reinforcement of the local zone is assigned to the supplier of the anchorage device. The anchorage device supplier has to provide information on all requirements necessary for the satisfactory performance of the local zone to the engineer of record and to the constructor. The supplier is also responsible for furnishing the anchorage device proper. Necessary local zone confinement reinforcement has to be specified by the supplier. Contractual documents should make clear the responsibility of furnishing and the method of payment for the additional local zone reinforcement needed for special anchorage devices, above the indicated general zone plan quantity.

Design of the general zone reinforcement is the responsibility of the engineer of record. Usually general zone reinforcement should not have to be furnished by the anchorage device supplier.

C.9.21.2.3.3 The constructor is responsible for the proper execution of the instructions of both the engineer of record and the anchorage device supplier.

C.9.21.3 Design of the General Zone

C.9.21.3.1 Design Methods

The list of design methods in Section 9.21.3.1 is not meant to preclude other recognized and verified procedures but includes some methods that have been found acceptable and useful for general zone design. In many anchorage applications where substantial or massive concrete regions surround the anchorages and where the members are essentially rectangular without substantial deviations in the force flow path (see Section C.9.21.6.1), the approximate procedures of Section 9.21.6 can generally be used. However,

in the post-tensioning of thin sections, flanged sections, irregular sections, or when the tendons have appreciable curvature, the more general procedures of Section 9.21.4 and 9.21.5 will be required.

Different anchorage force arrangements have a significant effect on the general zone stresses. Therefore it is important to consider not only the final stage of a stressing sequence with all tendons stressed but also intermediate stages during construction.

The provision for three-dimensional effects was included to alert the designer to effects perpendicular to the main plane of the member, such as bursting forces in the thin direction of webs or slabs. In many cases these effects can be determined independently for each directions, but some applications require a fully three-dimensional analysis (for example diaphragms for the anchorage of external tendons).

C.9.21.3.2 Nominal Material Strengths

Since anchorage zone design is based on an ultimate load approach some plastic concrete deformation is expected. The low value for the nominal concrete compressive strength for unconfined concrete reflects this possibility. For well confined concrete the effective compressive strength could be increased. The values for nominal tensile strength of bonded and unbonded prestressed reinforcement are based on the general AASHTO values of Section 9.17.4

C.9.21.3.3 Use of Special Anchorage Devices

For the acceptance test of special anchorage devices, supplementary skin reinforcement in addition to any required confining reinforcement is permitted (Division II, Section 10.3.2.3.4). Equivalent reinforcement should also be placed in the actual structure. Other general zone reinforcement in the corresponding portion of the anchorage zone may be counted towards this reinforcement requirement.

C.9.21.3.4 General Design Principles and Detailing Requirements

The provisions of this section include requirements that apply to all design methods, while Sections 9.21.4 through 9.21.6 address specific requirements for the various methods listed in Section 9.21.3.1.

C.9.21.3.4.1 With basic anchorage devices meeting the provisions of Section 9.21.7.2, concrete stresses are critical immediately ahead of the anchor plate.

C.9.21.3.4.2 With special anchorage devices, the interface between the confined concrete of the local zone and the usually unconfined concrete of the general zone is most critical. The provisions of Section 9.21.3.4.2 define the location where concrete stresses should be checked and apply the compressive stress limits of Section 9.21.3.2.2.

C.9.21.3.4.3 Stress concentrations may occur away from the critical regions defined in Sections 9.21.3.4.1 and 9.21.3.4.2 at locations of loading or geometry discontinuities. An example is the transition from a diaphragm to flanges and webs of a member.

C.9.21.3.4.4 Bursting forces are caused by the lateral spreading of the concentrated prestressing forces. The emphasis on the three-dimensional nature of the spreading of the forces is important, because it was observed that out of major plane transverse reinforcement is often neglected in design. For example, in members with thin rectangular cross sections bursting forces not only exist in the major plane of the member, but also perpendicular to it.

C.9.21.3.4.5 The guidelines for the arrangement of the bursting reinforcement attempt to direct the designer towards reinforcement patterns which are relatively close to the elastic stress distribution. The experimental test results show that this leads to a satisfactory behavior under service loads by limiting the extent and opening of cracks, and at ultimate by limiting the required amount of redistribution of forces in the anchorage zone (Reference 4). A uniform distribution of the bursting reinforcement with its centroid at d_{burst} is acceptable (Figure 3).

C.9.21.3.4.6 Figure 4 illustrates the location of the edge tension forces. The term "spalling forces" to address the tensile forces along the transverse edge of the member is not really accurate since spalling tends to imply a compression type failure. It is used for historic reasons.

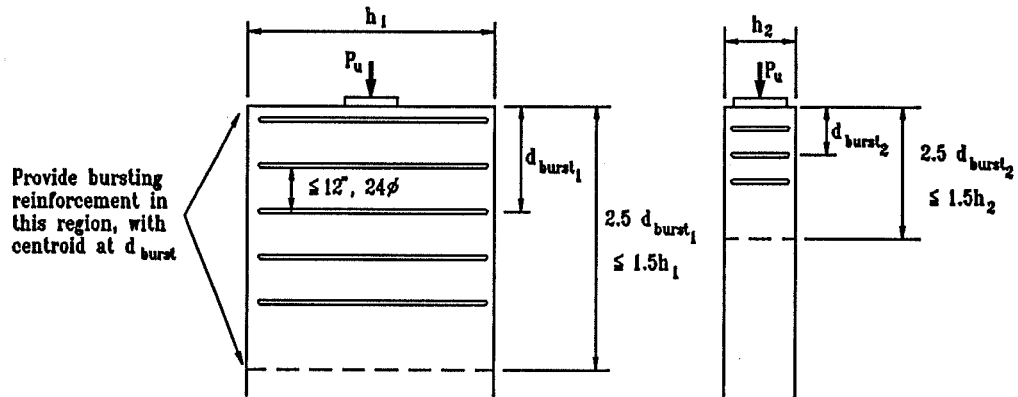


Figure 3 Bursting Reinforcement Arrangement

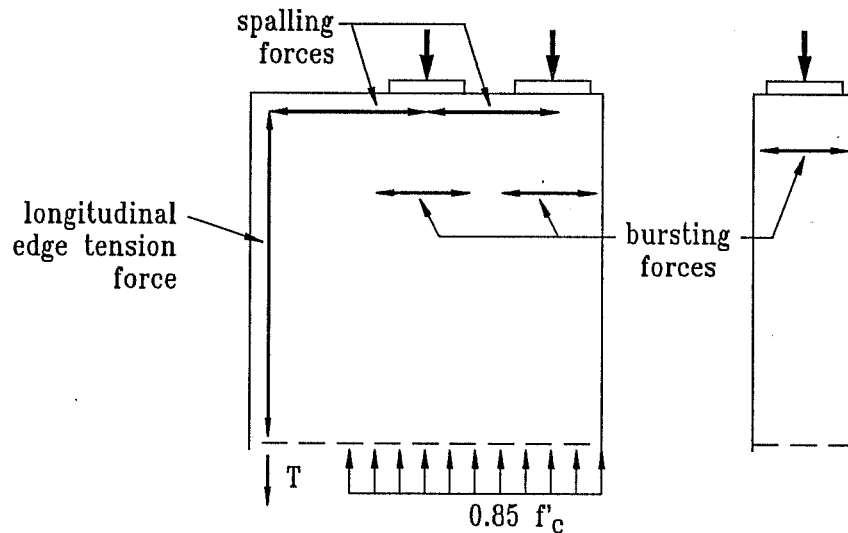


Figure 4 Edge Tension Forces

C.9.21.3.4.8 The minimum spalling force for design is two percent of the total post-tensioning force. This value is smaller than the four percent proposed by Guyon (Reference 3), and reflects both analytical and experimental findings which show that Guyon's values for spalling forces are rather high and that spalling cracks are very rarely observed in experimental studies (References 1, 4).

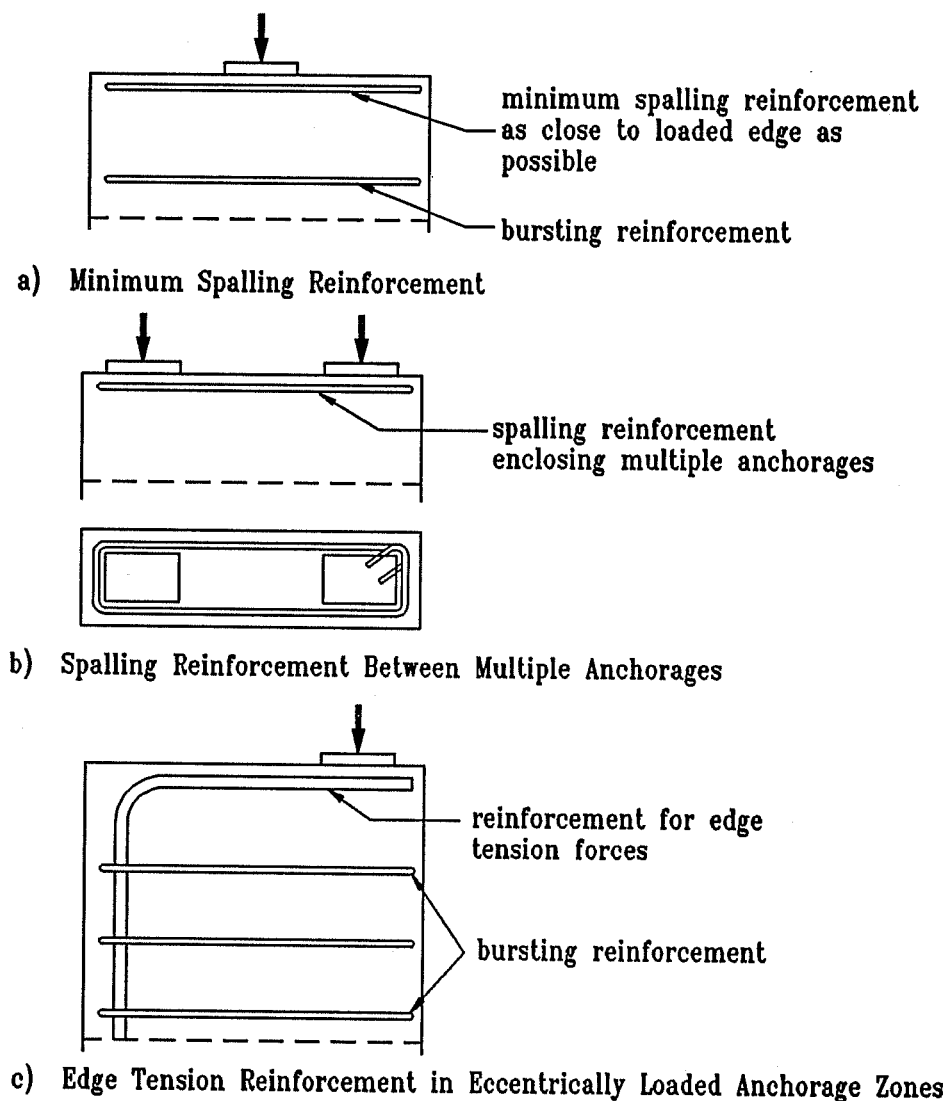


Figure 5 Arrangement of Spalling Reinforcement

C.9.21.3.4.9 Figure 5 illustrates the reinforcement requirements of Section 9.21.3.4.9.

C.9.21.3.5 Intermediate Anchorages

Intermediate anchorages are used for anchorage of tendons that do not extend over the full length of a member or segment. They are usually in the form of blisters, ribs, embedded anchors, or recess pockets. Local tensile stresses are generated behind

intermediate anchorages due to compatibility requirements for deformations ahead of and behind the anchor. Arrangement of intermediate anchors in the junction of flange and web or in continuous ribs over the full slab width helps to reduce these stress concentrations.

Bonded reinforcement is required in the immediate vicinity of the anchorage to control cracking behind the anchor. In Equation (9-32) the beneficial effect of compression behind the anchor from other loads is considered. Should an intermediate anchorage be located in regions with moderate tension behind the anchor, additional reinforcement must be provided to carry these tensile forces. Figure 6 illustrates the definition of area A_{cb} for use in Equation (9-32).

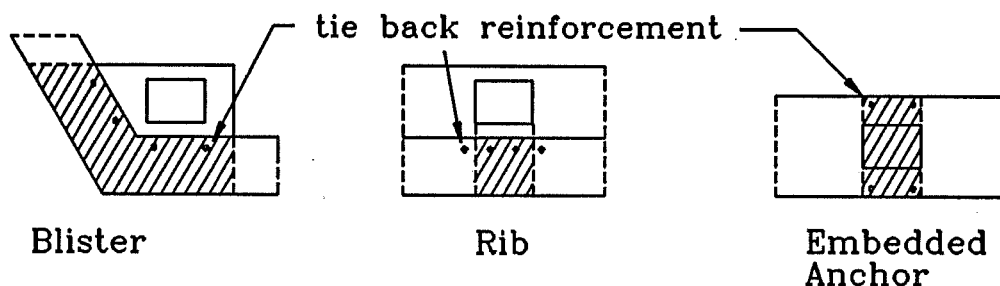


Figure 6 Area A_{cb} Behind Intermediate Anchorages

Tie back reinforcement is also required where tendon curvature generates deviation forces. Problems have occurred in blisters where such tie back reinforcement was designed for a gradual tendon curvature but the tendons were actually kinked at the toe of the blister. These problems can be avoided by either ensuring the envisioned gradual tendon curvature is actually provided during construction or, more realistically, by providing additional tie back reinforcement to compensate for accidental kinking of the tendon.

C.9.21.3.6 Diaphragms

In diaphragms, compressive stresses may become critical not only immediately ahead of the anchorages, but also at the transition from the massive diaphragm to the relatively thin flanges and webs of the cross section.

Bursting reinforcement requirements in diaphragms may be significantly larger than for beams with a continuous rectangular section (Figure 11). In particular, the approximate equations of Section 9.21.6 or Guyon's symmetrical prism (Reference 3)

should not be used to determine these reinforcement requirements.

C.9.21.3.7 Multiple Slab Anchorages

Edge tension forces and bursting forces in slabs with multiple anchors along an edge can be visualized as the tie forces existing in an inverted uniformly loaded continuous deep beam supported at the locations of the anchorages. Figure 7 illustrates the requirements of Section 9.21.3.7.

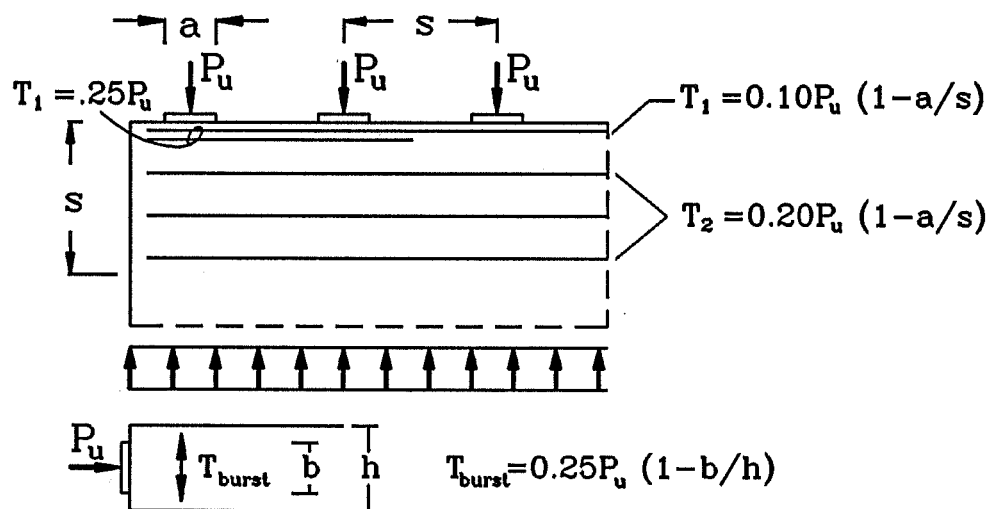


Figure 7 Reinforcement Requirements for Multiple Slab Anchorages

The bursting reinforcement in the thin direction of the slab is frequently omitted. This may be acceptable and approved by the engineer of record for large anchorage spacing if indicated as satisfactory by well documented past experience or more detailed analysis, provided that anchorage failures would cause only local damage. For more closely spaced anchors the full bursting reinforcement as required in Section 9.21.3.7.2 should always be provided.

The bursting reinforcement in the plane of the slab can often be provided by slab reinforcement which is present for thermal, shrinkage, or load distribution requirements. The engineer is always free to make a more detailed analysis as per 9.21.3.7.1.

C.9.21.4 Application of Strut-and-Tie Models to the Design of Anchorage Zones

C.9.21.4.1 General

C.9.21.4.1.1 A lower bound of the ultimate load that a given concrete structure or member can carry can be obtained by application of the lower bound theorem of the theory of plasticity of structures. Models in which the actual flow of forces in a structure is approximated by a series of straight compression members (struts), and straight tension members (ties) which are connected at discrete points (nodes) are called strut-and-tie models. If sufficient ductility (rotation capacity) is present in the system, strut-and-tie models fulfill the conditions for the application of the above mentioned theorem, and the ultimate load predicted on the basis of a strut-and-tie model will be a conservative estimate of the actual ultimate load of the structure or member. Figure 8 shows the linear elastic stress field and a corresponding strut-and-tie model for the case of an anchorage zone with two eccentric anchors (Reference 5).

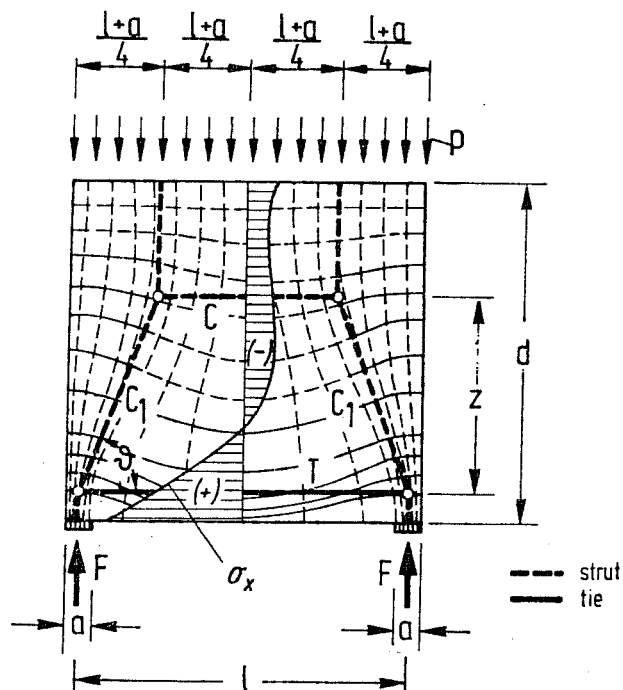


Figure 8 Stress Field and Strut-and-Tie Model (from Reference 4)

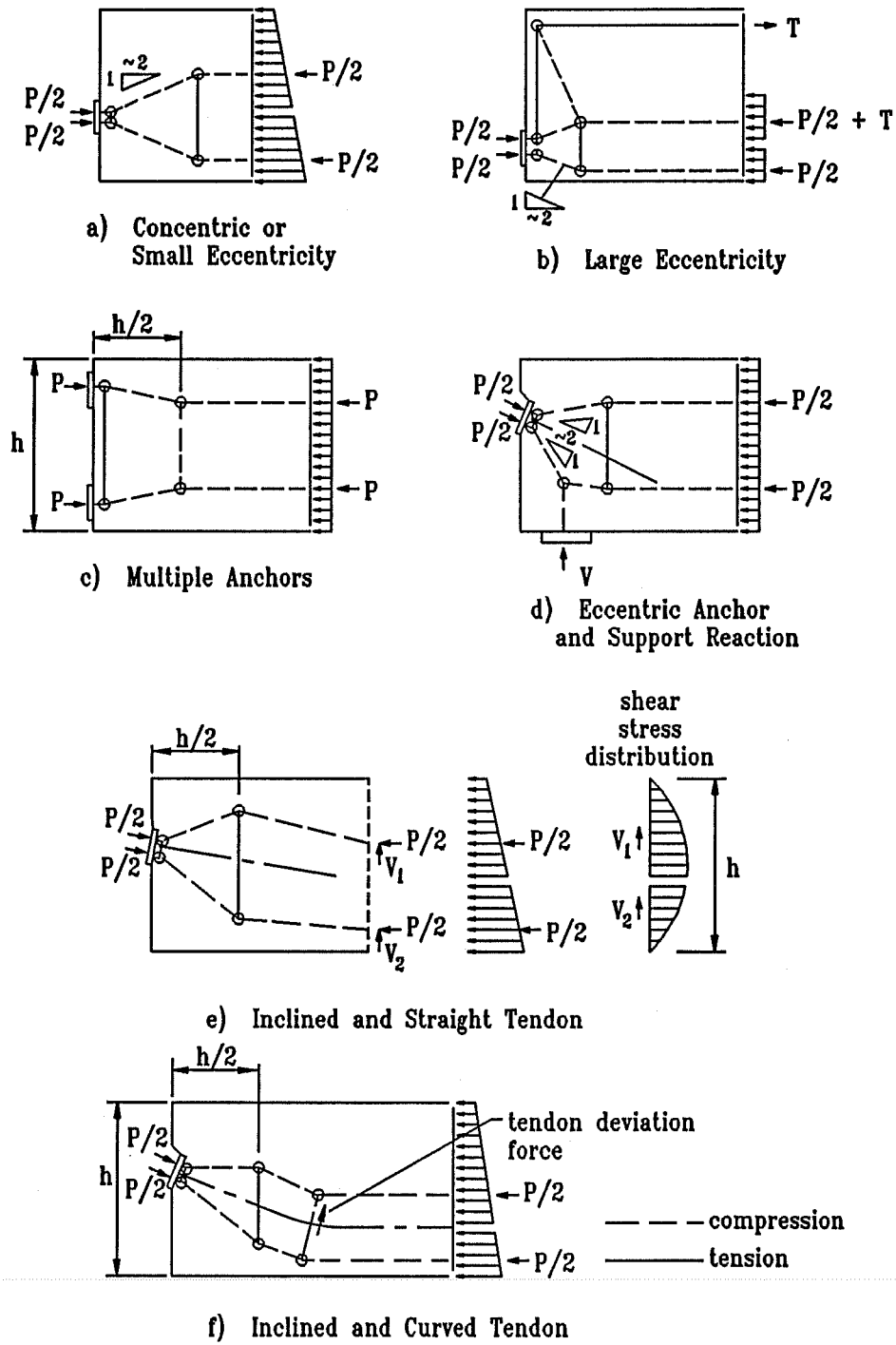


Figure 9 Typical Strut-and-Tie Models for Anchorage Zones

C.9.21.4.1.2 Because of the limited ductility of concrete, strut-and-tie models not greatly different from the elastic solution should be selected. This procedure will limit the required stress redistributions in the anchorage zone, and will also ensure that crack control reinforcement is provided where cracks are most likely to occur. In Figure 9 strut-and-tie models for some typical load cases for anchorage zones are shown.

C.9.21.4.2 Nodes

Nodes are critical elements of the strut-and-tie model. The entire local zone constitutes the most critical node (or group of nodes) for anchorage zones. In Section 9.21.7 the adequacy of the local zone is ensured by limiting the bearing pressure ahead of the anchorage device. Alternatively, this limitation may be exceeded if the adequacy of the anchorage device is proven by the acceptance test of Division II, Section 10.3.2.3.

The local zone nodes for the development of a strut-and-tie model may be selected at a depth of $a/4$ ahead of the anchorage plate (Figure 10).

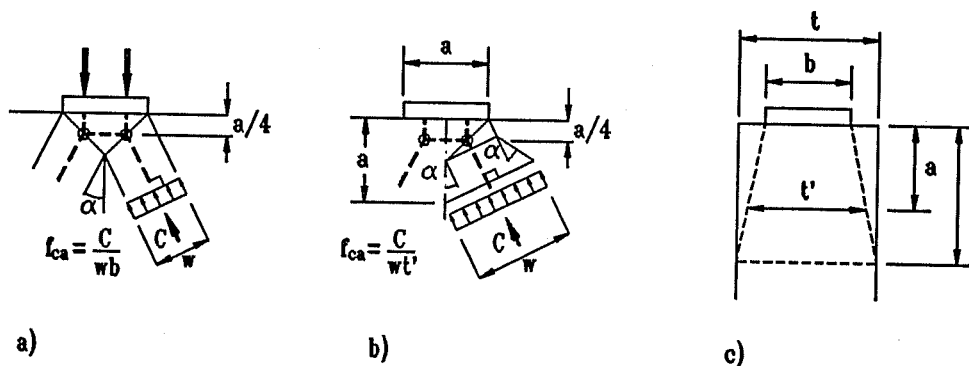


Figure 10 Critical Section for Compression Struts in Anchorage Zones

C.9.21.4.3 Struts

C.9.21.4.3.1 For strut-and-tie models oriented on the elastic stress distribution the nominal concrete strength specified in Section 9.21.3.2 is adequate. However, if the selected strut-and-tie model deviates considerably from the elastic stress distribution, large plastic deformations are required and the concrete strength should be reduced. The concrete strength should also be reduced if the concrete is cracked due to other load effects.

C.9.21.4.3.2 Ordinarily the geometry of the local zone node and thus of the interface between strut and local zone is determined by the size of the bearing plate and the selected strut-and-tie model, as indicated in Figure 10a. For special anchorage devices based on the acceptance test of Division II, Section 10.3.2.3, it is suggested (Reference 1) that stresses be checked at a larger distance from the node, assuming that the width of the strut increases with the distance from the local zone (Figure 10b).

C.9.21.4.3.3 The determination of the dimension of the strut in the direction of the thickness of the member is illustrated in Figure 10c. For members with a ratio of member thickness to anchorage width of more than three, strut-and-tie models for each direction should be considered.

C.9.21.4.4 Ties

C.9.21.4.4.1 Because of the unreliable strength of concrete in direct tension, it is prudent to neglect it entirely.

C.9.21.4.4.2 It is important that the reinforcement layout is in agreement with the selected strut-and-tie model. In the selection of a strut-and-tie model practical reinforcement arrangements should be considered.

C.9.21.5 Elastic Stress Analysis

C.9.21.5.1 Although the development of cracks in the anchorage zone causes stress redistributions, elastic analysis of anchorage zone problems has been found acceptable and useful (Reference 1).

C.9.21.5.2 Results of a linear-elastic analysis can be adjusted by smoothing out local stress maxima to reflect the non-linear behavior of concrete at higher stresses.

C.9.21.5.3 This procedure gives a conservative estimate of the reinforcement required in the anchorage zone. A reinforcement arrangement deviating from the elastic stress

distribution is acceptable (for example uniform distribution of bursting reinforcement), as long as the centroid of the bursting reinforcement coincides with the location of the bursting force.

C.9.21.6 Approximate Methods

C.9.21.6.1 Limitations

(1) The equations in this section are based on the analysis of members with a rectangular cross section and an anchorage zone at least as long as the largest dimension of that cross section. For cross sections that deviate significantly from a rectangular shape, for example I-girders with wide flanges, the approximate equations should not be used.

(2) Discontinuities, such as web openings, disturb the flow of forces and may cause higher compressive stresses, bursting forces, or edge tension forces in the anchorage zone. Figure 11 compares the bursting forces for a member with a continuous rectangular cross section and for a member with a non-continuous rectangular cross section.

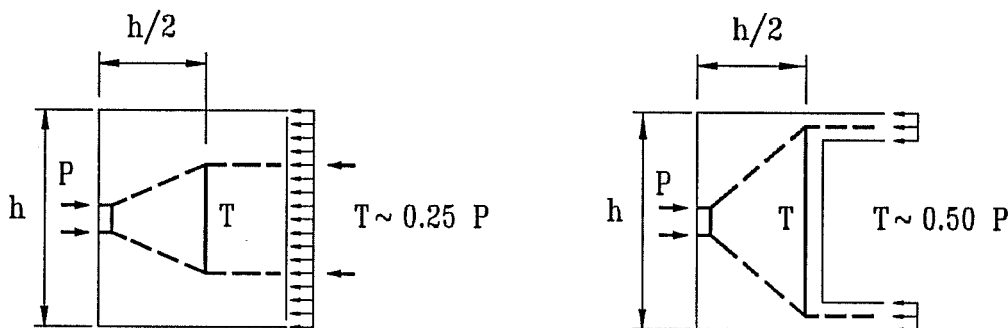


Figure 11 Effect of Discontinuity in Anchorage Zone

(3) The approximate equations for the concrete compressive stresses are

based on the assumption that the anchor force can spread in all directions. Requirement 3 ensures this assumption and is illustrated in Figure 12.

(4) The approximate equations for bursting forces are based on finite element analyses for a single anchor acting on a rectangular cross section. Equation (9-37) gives conservative results for the bursting reinforcement even if limitation (4) is violated and the anchors are not closely spaced, but the resultant of the bursting force is located closer to the anchor than indicated by Equation (9-38).

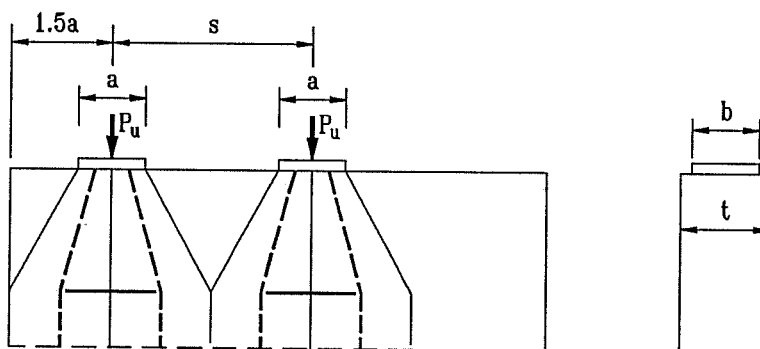


Figure 12 Notations for Equations (9-35) and (9-36)

C.9.21.6.2 Compressive Stresses

Equations (9-35) and (9-36) are based on linear-elastic finite element analysis for a single concentric anchor and a rectangular cross section of the member. In a plane stress analysis, the compressive stresses at a distance equal to one plate width ahead of the anchor are not more than 60% of the bearing pressure (Reference 1). Equation (9-35) was modified to approximate dispersal of compressive stresses in the thin direction of the member (Figure 10c) and to account for the beneficial effect of a larger spiral.

For multiple anchorages spaced closer than $2a$, a correction factor κ is necessary. This factor is based on an assumed stress distribution at a distance of one anchor plate width ahead of the anchorage device (Figure 13). Figure 14 illustrates the definition of A_b and ℓ_c .

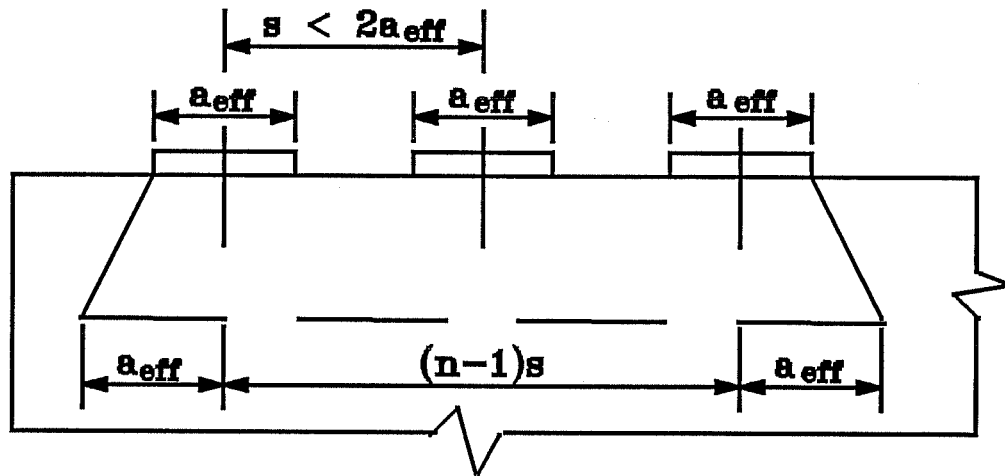


Figure 13 Closely Spaced Multiple Anchorages

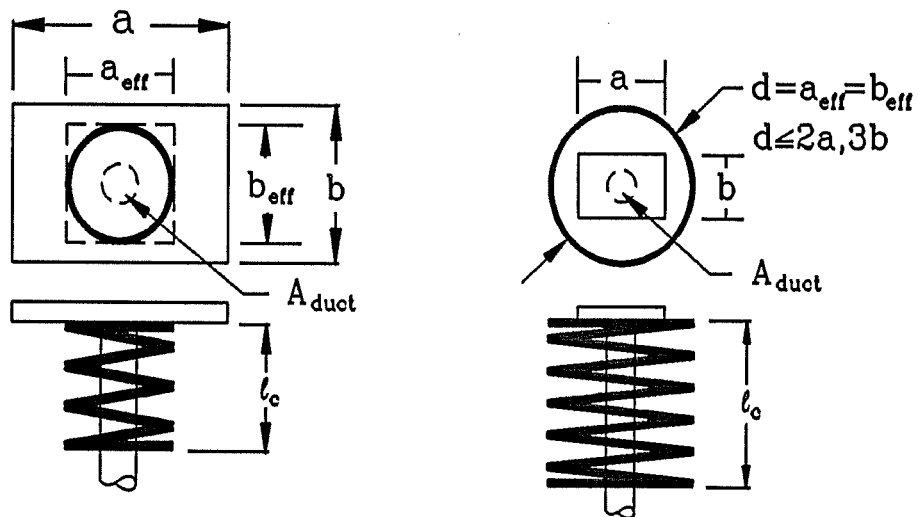


Figure 14 Effective Bearing Area in Equation (9-35)

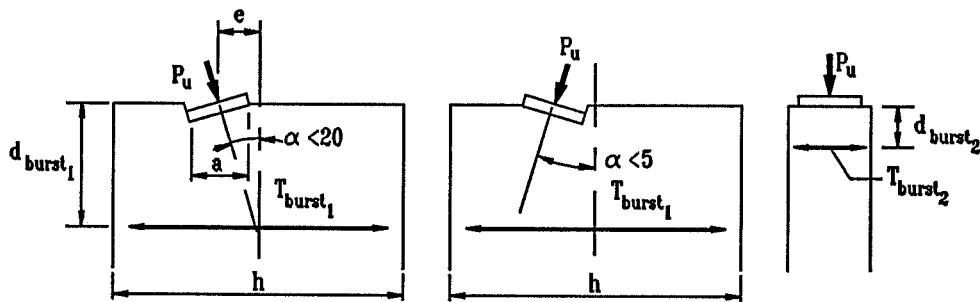
C.9.21.6.3 Bursting Forces

Equations (9-37) and (9-38) are based on the results of linear-elastic stress analyses (Reference 1). Shear reinforcement in the anchorage zone may be counted towards the requirement of Equation (9-37). Figure 15 illustrates the terms used in the equations.

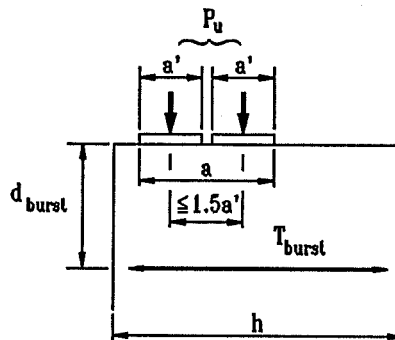
Equations (9-37) and (9-38) may also be used if a reaction force is present

in the anchorage zone, provided that

- 1) the eccentricity of the tendon is small,
- 2) the reaction force is applied at the bottom of the beam,
- 3) no flexural tensile stresses due to the combined effect of reaction force and tendon force exist at the end of the anchorage zone.



a) Inclined Tendons



b) Closely Spaced Anchorage Devices

Figure 15 Notations in Equations (9-37) and (9-38)

C.9.21.6.4 Edge Tension Forces

C.9.21.6.4.1 For multiple anchorages the spalling forces are required for equilibrium and provision of adequate reinforcement is essential for the ultimate load capacity of the anchorage zone (Figure 16). These tension forces are similar to the tensile tie forces existing between footings in deep walls supported on individual footings. In most cases the minimum spalling reinforcement of Section 9.21.3.4.8 will control.

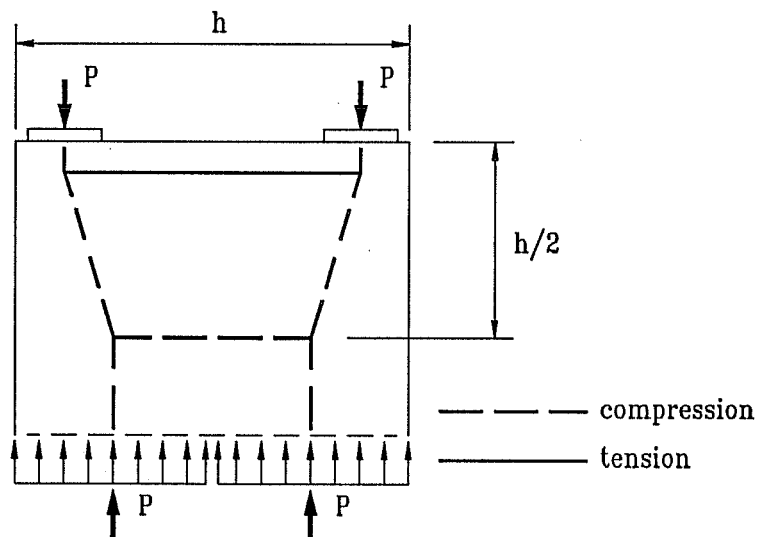


Figure 16 Spalling Forces Between Multiple Anchorages

C.9.21.6.4.2 The determination of the edge tension forces for eccentric anchorages is illustrated in Figure 17. Either type of axial-flexural beam analysis is acceptable. As in the case for multiple anchorages this reinforcement is essential for equilibrium of the anchorage zone. It is important to consider stressing sequences that may cause temporary eccentric loadings of the anchorage zone.

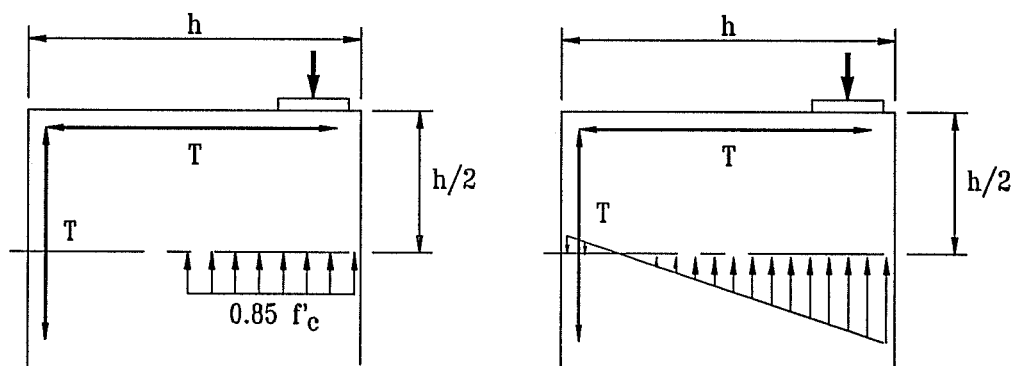


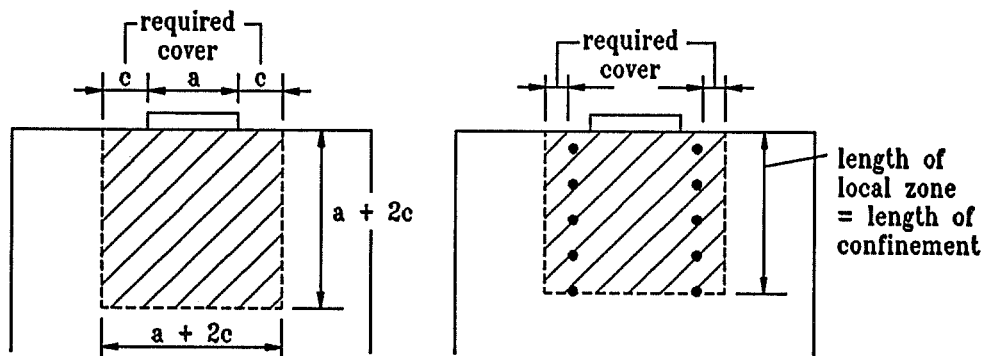
Figure 17 Determination of Edge Tension Forces for Eccentric Anchorages

C.9.21.7 Design of the Local Zone

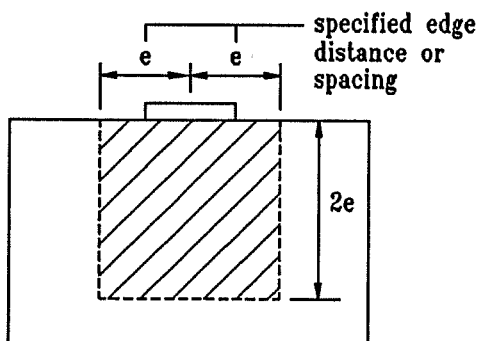
The specifications of Section 9.21.7 were provided to ensure adequate concrete strength in the local zone. They are not intended to give guidelines for the design of the actual anchorage hardware.

C.9.21.7.1 Dimensions of the Local Zone

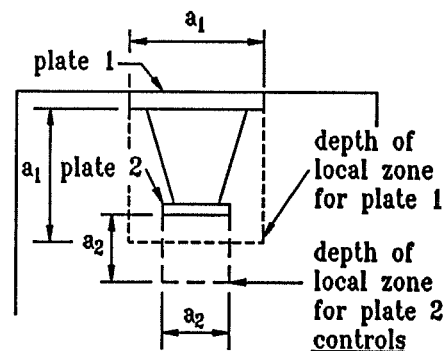
The local zone is the highly stressed region immediately surrounding the anchorage device. It is convenient to define this region geometrically, rather than by stress levels. Figure 18 illustrates the local zone definitions of Sections 9.21.7.1.1 to 9.21.7.1.3.



a) Manufacturer's Recommendations Not Available



b) Manufacturer's Recommendations Available



c) Length of Local Zone for Multiple Bearing Surfaces

Figure 18 Geometry of the Local Zone

In Section 9.21.7.1.1 knowledge of a minimum cover requirement over the anchorage bearing plate is needed. AASHTO does not specify any particular concrete cover required for corrosion protection of anchorage devices. In ACI 318-89, Section 6.3.10 a cover of not less than 1-1/2 in. for pipes, conduits, and fittings in concrete exposed to earth and weather is specified. It is recommended to use this value with Section 9.21.7.1.1 of the proposed specification.

C.9.21.7.2 Bearing Strength

Section 9.21.7.2 provides bearing pressure limits for anchorage devices that need not be tested in accordance with the acceptance test of Division II, Section 10.3.2.3. Alternatively, these limits may be exceeded if an anchorage system passes the acceptance test. Figures 19, 20, and 21 illustrate the specifications of Sections 9.21.7.2.2 to 9.21.7.2.4 (Reference 6).

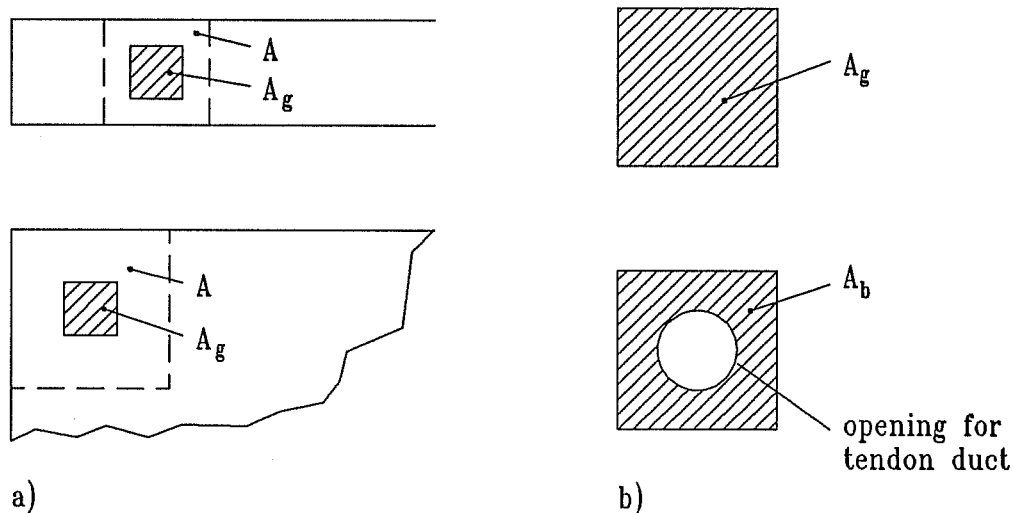


Figure 19 Area of Supporting Concrete Surface in Equation (9-39)

C.9.21.7.3 Special Anchorage Devices

Most proprietary anchorage devices fall in this category and have to pass the acceptance test of Division II, Section 10.3.2.3. However, many of the anchorage systems currently available in the United States have passed equivalent acceptance tests. The results

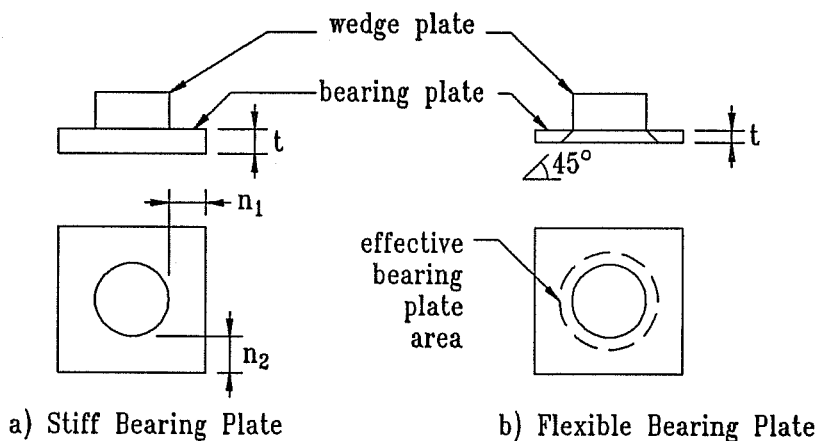


Figure 20 Effective bearing Plate Area for Anchorage Devices With Separate Wedge Plate

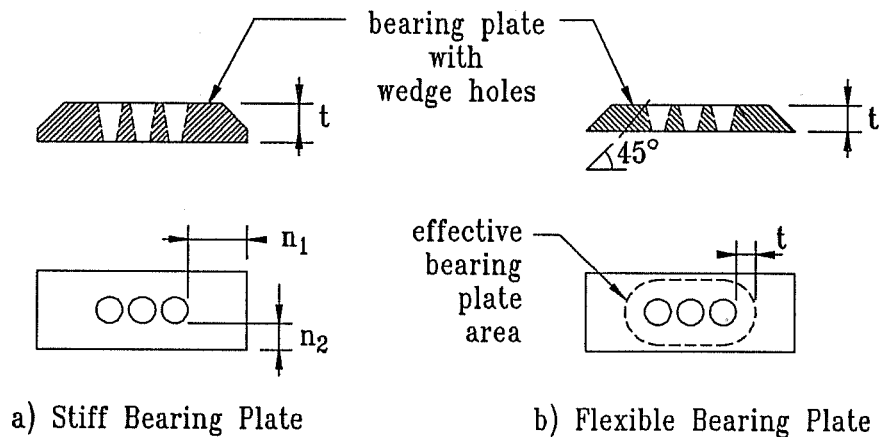


Figure 21 Effective Bearing Plate Area for Anchorage Device Without Separate Wedge Plate

of these tests may be acceptable if the test procedure is generally similar to that specified in Division II, Section 10.3.2.3.

C.9.22 PRETENSIONED ANCHORAGE ZONES

Provisions for pretensioned anchorage zones were beyond the scope of Project NCHRP 10-29, therefore the current AASHTO Standard Specifications for

pretensioned concrete were included in this section. Many results for post-tensioned concrete are also applicable to anchorage zones in pretensioned concrete, but some differences exist due to the more gradual force transfer of pretensioning tendons.

C.9.22.1 This provision is roughly equivalent to the provisions of Section 9.21.3 in the current AASHTO specifications, except that the requirements were adjusted for the application of factored load design. Section 9.22.1 of the proposed specifications for pretensioned concrete corresponds to the spalling force provisions in Section 9.21.3.4.7 for post-tensioned anchorage zones.

C.9.22.2 This provision corresponds to the bursting force requirements of Sections 9.21.3.4.4 and 9.21.3.4.5.

DIVISION II - CONSTRUCTION

C.10.3.2 Post-Tensioning Anchorages and Couplers

The anchorage efficiency test requirement that devices develop 95% of the ultimate strength of the prestressing steel has been expressed as actual ultimate strength rather than guaranteed ultimate strength. The reason for this is that the test requirement is to make sure that effects from the hardware used for gripping do not reduce the capacity of the tendon more than five percent. This can only be measured in reference to the actual strength of the particular prestressing steel used in the test.

C.10.3.2.3 Special Anchorage Device Acceptance Test

C.10.3.2.3.1 Figure 22 shows a local zone specimen with the local zone confining reinforcement in the upper portion of the specimen and the optional supplementary reinforcement of Section 10.3.2.3.4 over the full length of the specimen. However, an anchorage device supplier could also choose to eliminate such reinforcement in either or both portions of the block.

C.10.3.2.3.4 The supplementary reinforcement in the specimen is specified by the anchorage device supplier within the limits of Section 10.3.2.3.4. The same amount of

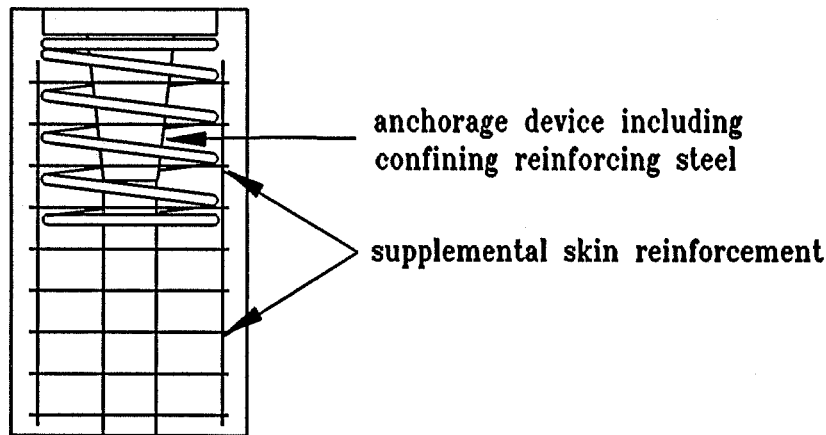


Figure 22 Special Anchorage Device Acceptance Test Specimen

reinforcement is also required in the actual structure, as stipulated in Section 9.21.3.3. However, other reinforcement in the corresponding portion of the structure (such as minimum reinforcement for creep and shrinkage or bursting reinforcement) may be counted towards this requirement. Since the confinement and supplementary reinforcement in the test specimens will generally be provided in orthogonal directions, similar reinforcement in the actual structure must be furnished to achieve an equivalent orthogonal action.

C.10.3.2.3.6 Long term loading has been found to be more critical for the behavior of the local zone than short term loading. A cyclic loading test gives comparable results to sustained loading tests, but is less time consuming than the sustained loading test (Reference 6). A monotonic short term loading test procedure is also included in the provisions. Stricter acceptance criteria are necessary to make the short term loading test comparable to the other test methods.

Loading in accordance with normal usage of the anchorage device in post-tensioning applications means loading through the wedge plate if available, or over an area formed by the perimeter of the wedge hole pattern. It is not required to load the specimen through the tendon.

C.10.3.2.3.7 The required minimum failure load of $1.1F_{pu}$ for cyclic and sustained loading tests reflects the incorporation of the maximum allowable stressing level of $0.8F_{pu}$ with a

load factor of 1.2 and a ϕ -factor of 0.85. Alternatively, if limited by test equipment capacity, a minimum failure load of $0.95F_{pu}$ can be specified, provided the actual concrete strength of the specimen is reduced proportionately.

C.10.3.2.3.9 In the monotonic loading test the required minimum failure load is increased to $1.2F_{pu}$, reflecting comparative test experience with monotonic, sustained, and cyclic loading procedures. Alternatively, if limited by test equipment capacity, a minimum failure load of $1.0F_{pu}$ can be specified, provided the actual concrete strength of the specimen is reduced proportionately.

C.10.3.2.3.10 The crack width requirements of Section 10.3.2.3.10 are based on recommendations in Reference 9. A moderately aggressive environment is characterized by moist environments where deicing or sea salts may be present in mists, but where direct exposure to corrosive agents is prevented (Reference 6). This should include most bridge applications.

C.10.3.2.3.11 If representative samples out of a series of similar anchorage devices pass the acceptance test, the anchorage device supplier may elect not to test the other anchorage devices in the series. However, the responsibility for the proper performance of such untested anchorage devices remains with the supplier.

C.10.3.2.3.12 Records of the anchorage device acceptance test have to be provided by the anchorage device supplier to the engineer of record and to the constructor. These records must include all the necessary information for proper installation of the anchorage device including all confining and supplementary reinforcement.

C.10.4.3 Placement of Anchorage Hardware

Anchorage zones are very critical regions of a structure. Therefore construction should follow exactly the specifications by the engineer of record and the anchorage device supplier. Change of anchorage zone details have to be approved by the engineer of record and the anchorage device supplier.

REFERENCES

- (1) Burdet, O.L., "Analysis and Design of Anchorage Zones in Post-Tensioned Concrete Bridges", Ph.D. Dissertation, The University of Texas at Austin, May 1990.
- (2) Falconer, B.A., "Post-Tensioning Anchorage Zones in Bridge Decks", M.S. Thesis, The University of Texas at Austin, May 1990.
- (3) Guyon, Y., "Prestressed Concrete", John Wiley and Sons, New York, 1953.
- (4) Sanders, D.H., "Design and Behavior of Post-Tensioned Concrete Anchorage Zones", Ph.D. Dissertation, The University of Texas at Austin, August 1990.
- (5) Schlaich, J., Schäfer, K., Jennewein, M., "Towards a Consistent Design of Structural Concrete", PCI Journal, Vol.32, No.3, May-June 1987, pp.74 - 151.
- (6) Roberts, C.L., "Behavior and Design of the Local Anchorage Zone in Post-Tensioned Concrete", M.S. Thesis, The University of Texas at Austin, May 1990.
- (7) Stone, W.C., Breen, J.E., "Behavior of Post-Tensioned Girder Anchorage Zones", PCI Journal, Vol.29, No.1, January-February 1984, pp.64-109.
- (8) Stone, W.C., Breen, J.E., "Design of Post-Tensioned Girder Anchorage Zones", PCI Journal, Vol.29, No.1, January-February 1984, pp.64-109.
- 9) Leonhardt, F., "Cracks and Crack Control in Concrete Structures", IABSE Proceedings, P109/87, 1987, pp.25-44.
- (10) Wollmann, G.P., "Anchorage Zones in Post-Tensioned Concrete Structures", Ph.D. Dissertation, The University of Texas at Austin, Mai 1992.

REFERENCES

1. American Association of State Highway Transportation Officials (AASHTO), "Standard Specifications for Highway Bridges", Fourteenth Edition, 1989.
2. American Association of State Highway Transportation Officials (AASHTO), "Guide Specifications for Design and Construction of Segmental Concrete Bridges", Washington, D.C., 1989.
3. ACI Committee 318, "Building Code Requirements for Reinforced Concrete (ACI 318-89) and Commentary - ACI 318R-89", First Printing, November 1989.
4. Adeghe, L.N., Collins, M.P., "A Finite Element Model for Studying Reinforced Concrete Detailing Problems", Publication No. 86-12, Department of Civil Engineering, University of Toronto, October 1986.
5. Bergmeister, K., Breen, J.E., Jirsa, J.O., "Dimensioning of Nodes and Development of Reinforcement", IABSE Colloquium Stuttgart 1991, IABSE Report, Vol. 62, April 1991, pp. 551-556.
6. Breen, J.E., Fenves, G., Sanders, D.H., Burdet, O.L., "Anchorage Zone Reinforcement for Post-Tensioned Concrete Girders", National Cooperative Highway Research Program Interim Report 10-29, University of Texas at Austin, August 1987.
7. Breen, J.E., "Why Structural Concrete", IABSE Colloquium Stuttgart 1991, IABSE Report, Vol. 62, April 1991, pp. 15-26.
8. Burdet, O.L., "Analysis and Design of Post-Tensioned Anchorage Zones in Concrete Bridges", Ph.D. Dissertation, The University of Texas at Austin, May 1990.

9. Chen, W.F., "Plasticity in Reinforced Concrete", McGraw-Hill, New York, 1982.
10. Collins, M.P., Mitchell, D., "Prestressed Concrete Structures", Prentice Hall, Englewood Cliffs, New Jersey, 1990.
11. DIN 4227, Teil 1, "Spannbeton; Bauteile aus Normalbeton mit beschränkter oder voller Vorspannung", July 1988.
12. Drucker, D.C., "On Structural Concrete and the Theorems of Limit Analysis", IABSE Proceedings, Vol. 21, 1961, pp. 49-59.
13. Dywidag Systems International Catalogue, "Dywidag Précontrainte", Munich.
14. Eibl, J., Iványi, G., "Innenverankerungen im Spannbetonbau", Deutscher Ausschluß für Stahlbeton, Heft 223, Berlin, 1973, pp. 1-46.
15. Eibl, J., Iványi, G., "Innenverankerungen von Spanngliedern", Beton- und Stahlbetonbau, Vol. 2, 1973, pp. 35-39.
16. Anonymus, "Girder Defects Raise Controversy", Engineering News Record, September 7, 1989, pp. 11-12.
17. Falconer, B.A., "Post-Tensioning Anchorage Zones in Bridge Decks", M.S.Thesis, The University of Texas at Austin, May 1990.
18. Fenwick, R.C., Lee, S.C., "Anchorage Zones in Prestressed Concrete Members", Magazine of Concrete Research, Vol. 38, No. 135, June 1986, pp.77-89.
19. Figg, E.C., Jr., "Segmental Bridge Design in the Florida Keys", Concrete International, Vol. 2, No. 8, August 1980, pp. 17-22.

20. Fédération Internationale de la Précontrainte (FIP), "Recommendations for Acceptance and Application of Post-Tensioning Systems", March 1981.
21. Fujii, M., Miyamoto, A., Kajimura, Y., "Crack Control Design of Intermediate Anchorage Zone in Prestressed Concrete", FIP Symposium on Partial Prestressing and Practical Construction in Prestressed and Reinforced Concrete, Proceedings Part One, Romania, September 1980, pp. 44-51.
22. Guyon, Y., "Prestressed Concrete", John Wiley and Sons Inc., New York, 1953.
23. International Association of Bridge and Structural Engineers (IABSE), Colloquium on "Structural Concrete", IABSE Report Vol. 62, Stuttgart, 1991.
24. Kammenhuber, J., Schneider, J., "Arbeitsunterlagen für die Berechnung vorgespannter Konstruktionen", Stahlton AG, Zürich, 1974.
25. Koutsoukos, D.P., "Finite Element Analysis of Anchorage Zones in Reinforced Concrete Structures Using a Damage Model", Ph.D. Dissertation under Preparation, The University of Texas at Austin, December 1992.
26. Kreger, M.E., "Evaluation of Distress in J-2e Bridge Structures", Final Report Submitted to the Washington Metropolitan Area Transit Authority, Austin, November 1989.
27. Kreger, M.E., "Evaluation of E-6f Bridge Structures", Final Report Submitted to the Washington Metropolitan Area Transit Authority, Austin, February 1990.
28. Leonhardt, F., "Prestressed Concrete - Design and Construction", Wilhelm Ernst und Sohn, Berlin, 1964.
29. Leonhardt, F., "Vorlesungen über Massivbau", Part Two, Third Edition, Springer Verlag, Berlin, 1986.

30. Libby, J.R., "Critique of a Post-Tensioned Roof Slab Failure", *Concrete International*, Vol. 7, No. 10, October 1985, pp. 28-32.
31. Libby, J.R., "Modern Prestressed Concrete", Van Nostrand Reinhold Inc., New York, 1984.
32. Macchi, A.J., "Roof Slab Failure", Letter to the Editor, *Concrete International*, Vol. 9, No. 1, January 1987, pp. 7-8.
33. MacGregor, J.G., "Reinforced Concrete - Mechanics and Design", Prentice Hall Inc., Englewood Cliffs, New Jersey, 1988.
34. Marti, P., "Basic Tools of Reinforced Concrete Beam Design", *ACI Journal*, Vol. 82, No. 1, January-February 1985, pp. 46-56.
35. Marti, P., "Truss Models in Detailing", *Concrete International*, Vol. 7, No. 12, December 1985, pp. 66-73.
36. Mörsch, E., "Über die Berechnung der Gelenkquader", *Beton und Eisen*, No. 12, 1924, pp. 156-161.
37. Nielsen, M.P., "Limit Analysis and Concrete Plasticity", Prentice Hall Inc., Englewood Cliffs, New Jersey, 1984.
38. Post-Tensioning Institute (PTI), "Post-Tensioning Manual", Fourth Edition, PTI, 1986.
39. Podolny, W., Jr., "The Cause of Cracking in Post-Tensioned Concrete Box Girder Bridges and Retrofit Procedures", *PCI Journal*, Vol. 30, No. 2, March - April 1985, pp. 82-139.

40. Powell, L.C., Breen, J.E., Kreger, M.E., "State-of-the-Art Externally Post-Tensioned Bridges with Deviators", Research Report 365-1, Center for Transportation Research, The University of Texas at Austin, June 1988.
41. Roberts, C.L., "Behavior and Design of the Local Anchorage Zone in Post-Tensioned Concrete", M.S. Thesis, The University of Texas at Austin, May 1990.
42. Rogowsky, D.M., MacGregor, J.G., "Design of Reinforced Concrete Deep Beams", Concrete International, Vol. 8, No. 8, August 1986, pp. 49-58.
43. Rogowsky, D.M., Marti, P., "Detailing for Post-Tensioning", VSL International, Berne, 1991.
44. Sanders, D.H., "Design and Behavior of Anchorage Zones in Post-Tensioned Concrete Members", Ph.D. Dissertation, The University of Texas at Austin, August 1990.
45. Schlaich, J., Schäfer, K., Jennewein, M., "Toward a Consistent Design of Structural Concrete", PCI Journal, Vol. 32, No. 3, May - June 1987, pp. 74-151.
46. Schlaich, J., Schäfer, K., "Konstruieren im Stahlbetonbau", Betonkalender 1989, Part Two, Ernst und Sohn, Berlin 1989, pp. 563-715.
47. Schlaich, J., Scheef, M., "Concrete Box Girder Bridges", Structural Engineering Documents 1e. International Association for Bridge and Structural Engineering (IABSE), Zürich, 1982.
48. Schlaich, M., Anagnostou, G., "Stress Fields for Nodes of Strut-and-Tie Models", Journal of Structural Engineering, ASCE, Vol. 116, No. 1, January 1990, pp. 13-23.
49. Seible, F., Libby, D.R., Chai, Y.H., "Coupling Joint Behavior in Segmental Post-Tensioned Bridges", Structural Systems Research Report No. 88/07, Department

of Applied Mechanics and Engineering Sciences, University of California, San Diego, September 1988.

50. Soroushian, P., Ahmadi, P., Navas, F., Haji, M.N., "Transfer of Column Pressure to Concrete Footings", *Concrete International*, Vol. 8, No. 12, December 1986, pp. 38-42.
51. Stone, W.C., Breen, J.E., "Behavior of Post-Tensioned Girder Anchorage Zones", *PCI Journal*, Vol. 29, No. 1, January - February 1984.
52. Stone, W.C., Breen, J.E., "Design of Post-Tensioned Girder Anchorage Zones", *PCI Journal*, Vol. 29, No. 2, March - April 1984.
53. Thürlimann, B., Marti, P., Pralong, J., Ritz, P., Zimmerli, B., "Anwendung der Plastizitätstheorie auf Stahlbeton", Seminar for Structural Engineers, Swiss Federal Institute of Technology, April 13-15, 1983.
54. Timoshenko, S., "Theory of Elasticity", McGraw-Hill Book Company, Inc., New York and London, 1934.
55. VSL International Catalogue, "Post-Tensioning Systems, Berne, 1990.
56. Wium, D.J.W., Buyukozturk, O., "Problems in Designing Prestressed Segmental Concrete Bridges", National Academy of Sciences, Transportation Research Record No. 950, Second Bridge Engineering Conference, Vol. 2, pp. 68-75, March 1984.
57. Woodward, R.J., "Cracks in a Concrete Bridge", *Concrete*, Vol. 17, No. 7, 1983, pp. 40-45.
58. Yong, Y.-K., Gadegbeku, C.B.K., Nawy, E.G., "Anchorage Zone Stresses of Beams Subjected to Shear Forces", *Journal of Structural Engineering*, ASCE, Vol. 113, No. 8, August 1987, pp. 1789-1805.

VITA

Gregor Peter Wollmann was born in Hamburg, Germany, on May 3, 1962, the son of Gerhard Erich Wollmann and Anngrit Wollmann, nee Bäurle. After completing his work at Bundesgymnasium and Bundesrealgymnasium Baden, in Baden, Austria, in 1980, he entered the Technical University of Vienna. He graduated in June 1986 with highest honors and received the degree of Diplomingenieur für Bauingenieurwesen. In September, 1986 he entered the Graduate School of the University of Texas at Austin on a Fulbright Scholarship. He received the degree of Master of Science in December of 1988.

Permanent Address: Langäckergasse 10
A-2345 Brunn/Gebirge
Austria

This dissertation was typed by the author.